RTR 213-01

SRB ENVIRONMENT EVALUATION AND ANALYSIS

FINAL REPORT

VOLUME I: REDESIGNED SRB FLIGHT HEATING EVALUATION

September 1991

Prepared by:

William K. Crain

Contract:

NAS8-37891

For:

Induced Environments Branch (ED33)
onal Aeronautics and Space Administration
George C. Marshall Space Flight Center
Marshall Space Flight Center, AL 35812

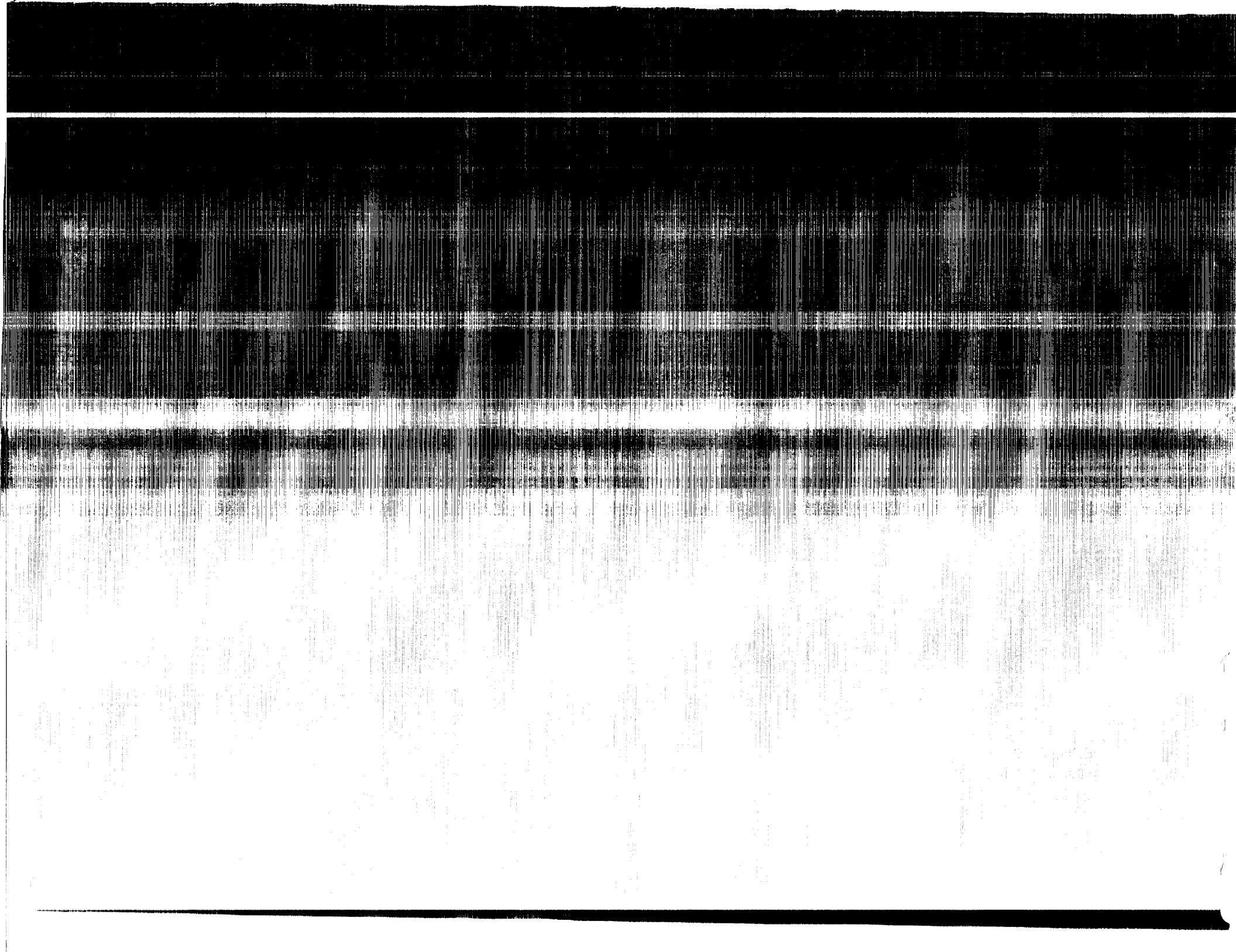

ABSTRACT

Following the Space Shuttle STS-51L disaster on January 28, 1986, a considerable redesign effort was launched on the Solid Rocket Booster. This effort culminated in three instrumented flights, STS-26R, 27R and 29R, beginning in September of 1989. Aeroheating data were obtained on these flights in the form of pressure, heat flux and gas temperature probe measurements. These data were analyzed from an ascent and reentry heating point of view. The flight data were verified, compared with historic and theoretical results and scaled to design. Impact of these results on the current design environment set was assessed and recommendations made. This report documents this effort.

FOREWORD

This Technical Report documents the results of the analyses done on the redesigned Solid Rocket Booster (SRB) and advanced SRB performed by REMTECH inc., under NASA/MSFC Contract NAS8-37891, Mr. L. D. Foster, ED33, COTR. This report is presented in three volumes:

Volume I: Redesigned SRB Flight Heating Evaluation
Volume II: RSRB Joint Filling Test/Analysis Improvements
Volume III: ASRB Plume Induced Environment Studies

This Volume I documents the ascent and reentry heating analysis on the redesigned SRBs for flights STS-26R, 27R and 29R.

Contents

ACKNOWLEDGMENT

During the course of this contract many people contributed to the analysis of the flight data. The author wishes to acknowledge their direct support, and without whose help, successful completion of the project could not have been possible. Thanks are due Mr. Robert Kirchner for the SRB reentry trajectory reconstruction, ascent and reentry heating calculations; Messrs. Steve Bancroft and Terry McLean for the frustum venting calculations; Mr. Maurice Prendergast for the plume heating analysis and Mr. David Hollman and Mrs. Cynthia Frost for acquiring the data base for the three flights as well as support on the ascent and reentry heating analysis. A debt of gratitude is owed to Mr. Hamilton Woods for his consultation and help in debugging the STATE and BATER codes; Mr. Bob Bender for plume consultation, and Dr. Carl D. Engel for his overall technical direction of the project. Last, thanks are extended to Mrs. Kim Alford and Joan Skoglund for their graciousness, flexibility and willingness in preparing the progress reports and technical documentation for the project, as well as Mrs. Linda Styles for preparing all figures and artwork.

List of Figures

List of Tables

Section 1
INTRODUCTION

Following the Space Shuttle STS-51L disaster on January 28, 1986, a considerable redesign effort was begun on the Solid Rocket Booster. This effort culminated in three (DFI) instrumented flights: STS-26R, 27R, and 29R, beginning September 29, 1989. Aeroheating data in the form of pressure, heat flux and gas temperature probe measurements were acquired on the SRB external skin and internal aft skirt. These data were analyzed from an ascent and reentry point of view. In this analysis, ascent convection, plume convection and plume impingement at SRB separation, reentry trajectory reconstruction, reentry heating as well as frustum venting were considered. The data were verified, compared with historic data from previous instrumented flights as well as semi-empirical and theoretical calculations. These results were then scaled to design, and impact assessments on the current design environment set made. The individual aerothermal analyses, i.e., ascent, reentry and plume heating evaluation, etc., were completed and documented in Refs. [1–5].

The purpose of this report is to address the current flight data from a design point of view and document its impact on the current design environment set. Many of the measurements were made at locations where previous flight data did not exist or were very sparse. Consequently, the current data set was invaluable in defining heating in these areas. For the sake of completeness, so that the work will be under one cover, the individual evaluations from Refs. [1–5] are presented as appendices to this report.

Last, by way of reference, the raw flight data from STS-26R, 27R and 29R were acquired along with the ascent and reentry trajectories. These data are presented in plotted and tabular form in Refs. [6–8].

Section 2
ASCENT HEATING ASSESSMENT

Three areas of the redesigned SRB were instrumented for external ascent flight definition. These included three gages on the nose cone THETA-B = 90 deg ray, the inboard side of the attach ring and the outboard side of the aft skirt, Fig. 1. The nose cone instrumentation was located for the purpose of clarifying the discrepancy between the Rockwell IVBC-3 design environments and the REMTECH design environments, Fig. 1a. Gages on the front face of the attach ring, Fig. 1b, were located at positions thought to have the highest heating on the ring. These positions represented locations which did not have previous wind tunnel or flight data. In like manner, the THETA-B = 180 and 270 deg positions on the aft skirt were instrumented since very limited flight data existed at these locations, Fig. 1c, and plume recirculation and flow separation information were needed in these locations.

In the methodology used to calculate the design heating environment at a particular location, interference heating data obtained from scaled model wind tunnel tests are multiplied by the tunnel to flight scaling factor [9]. These are then flown along the design trajectory and the design heating rate and integrated heat load calculated. The wind tunnel data are assumed to account for the heating variation with pitch and yaw, while the tunnel to flight factors give the appropriate magnitude of heating. The tunnel to flight factors are derived from the flight measured interference heating data and are defined as the heating difference between tunnel and flight heat transfer coefficient at the flight angle of attack and yaw.

$$\text{Tunnel to Flight Factor} = \frac{(H_i/H_u)_{\text{flight}}}{(H_i/H_u)_{\text{tunnel at flight}_{\alpha,\beta}}}$$

In performing the design evaluation and impact of the DFI data from STS-26R, 27R, and 29R on the current design environment set, flight factors for each gage on the external skin were calculated and compared with the flight factors used in the design calculations. Impact was then assessed on this basis.

2.1 Nose Cone

Wind tunnel to flight scaling factors for the three gages on the nose cone were calculated and summarized along with the values used for design. These are presented in Table 1. In general, flight factors based on the current data from STS-26R, 27R, and 29R are lower than the design values by about 60 percent. This is mainly at the M = 4.00 condition (Gages 7700 and 7701), although the M = 3.00 flight factor for Gage 7702 is the one that is low. The effect of this is to lower the REMTECH calculated design heating rates [9] in the direction of the Rockwell IVBC-3 [10] calculations, Fig. 1a. The lower flight factors from the current flights are not expected to impact the design environments on the nose cone, since the integrated heat loads for both the IVBC-3 and REMTECH environments are low.

2.2 Attach Ring

As previously stated, design environments at the THETA-B = 27.5 and 55.0 deg position on the forward face of the attach ring were generated without a previous wind tunnel or flight test data base. These were calculated using the nearest skin point for which tunnel data existed, and an amplification factor to get from the skin to the forward face of the ring which was calculated based on available attach ring flight data. Flight factors for Gages 7703 and 7704 were calculated using the wind tunnel data base body points used for the design environments. These flight factors are summarized in Table 2 along with the factors used for design. In this table the reference body point for each gage location is also listed. The first number, 1369 and 1384, pertains to the wind tunnel body point, and the last number, 53, 54, pertains to the REMTECH design body point from Ref. [9]. As seen in Table 2, the flight data from STS-26R, 27R, and 29R represent a considerable increase over the design factors. This could represent a design impact since the integrated heat loads are already in the 500-600 BTU/ft^2 range (Fig.1b) in this area of the attach ring.

2.3 Aft Skirt

Aft skirt factors for the current flights are summarized in Table 3. Along with these data are the factors used to calculate the design environments, and flight factor data from STS-1 and 2 (Body Points 8435 and 8443). As can be seen, the flight factors used for design are considerably lower than the current results or the STS-1 and 2 results. The reason for this is that prior to the current DFI flights, the only flight data that existed at the THETA-B = 180 and 270 deg position were the STS-1 and 2 data. Since the flight data were limited and the flight factors unusually high, it was felt that the data were possibly erroneous and judgment toward a lower factor chosen. This yielded design heating rates of 1-2 BTU/ft^2-sec, which was in general agreement with the Rockwell IVBC-3 design values (Figs. 2,3). In light of the current DFI results and their agreement with the previous data, it is felt that the higher flight factors are correct. This represents a design impact for the environments on the aft skirt, since not only those at the THETA-B = 180 and 270 deg positions were generated with the lower flight factors, but other locations also. Evidence of this is presented in Figs. 4 and 5, which is a comparison of calculated and flight measured (STS-27R) heating rates. These results were generated during the flight verification phase of the project [1]. Actual flight trajectory heating rates were calculated using the design scale factors (Fig. 4), and scale factors from STS-1 and 2 (Fig. 5). Using the higher scale factors from STS-1 and 2, brings the calculated results in agreement with the measurements from STS-27R. In this light, it is recommended that the design environments on the aft skirt be regenerated.

Section 3
PLUME HEATING

3.1 Plume Convection

Part of the reason for instrumenting the aft skirt in the THETA-B = 180 and 270 deg positions, was to help define plume recirculation heating in this region of the SRB. Previous data in this area were very limited. Analysis of the data from the aft skirt gages on the current flights [1] showed that plume recirculation heating was at an extremely low level (~0.5 BTU/ft^2-sec) over the circumferential range 180 > THETA-B > 270 deg. In fact, a reexamination of the data shows that the level is ~0.5 BTU/ft^2-sec at the THETA-B = 180 deg position, and ~0 BTU/ft^2-sec at the THETA-B = 270 deg position. Examples of this are shown in Figs. 6–8. Plume recirculation heating manifests itself as an abrupt increase in heating rate beginning around an altitude of 84,000 feet ($t \sim$ 94-100 sec). A good example of this is shown in Fig. 6. These data were obtained on STS-5, and correspond to a gage on the aft face of the kick ring on the left hand booster (B07R7674). Note the increase in heating at t = 96 seconds. In like manner, an example of a gage which did not experience plume recirculation heating is B07R8665 on the right hand SRB located outboard at the THETA-B = 34 deg position, Fig. 7. Comparison of these data with typical results from the current DFI flights, Fig. 8 STS-27R, shows a maximum plume effect of ~0.5 BTU/ft^2-sec at the THETA-B = 180 deg position, and no measurable effect at the THETA-B = 270 deg position. These observations confirm the limited results obtained on the first six DFI flights. The current ground rule observed at REMTECH in applying design environments to the aft skirt, is to cut off the aeroheating component at t = 96 seconds and apply the plume recirculation heating environment as defined in the data book [11]. In light of these current results, consideration should be given to continuing the aeroheating component out to SSME plume impingement and applying the greater of the two.

Comparisons of the aft skirt flight measured heating rates and base gas recovery temperature with the operational design envelopes [11] are shown in Figs. 9 and 10. Since the flight calorimeter temperature was generally below 150°F, the heating rates were considered to be cold wall values and were compared directly to design. Trends and magnitudes of the flight measured heating rates at the THETA-B = 180 deg position (Figs. 9 and 9a) are well within the design envelope. The same is true for flight measurements at the THETA-B = 270 deg position on STS 26R and 27R, (Figs. 9b, c). The flight data for 7706 and 7707 on STS-29R at this location, however, agree fairly well with design. Since the design curve represents an envelope of previous flight data, increasing this level by some magnitude should be considered. The design impact is not considered to be a crucial issue in this area of the SRB since the heating rates are generally low (≤2 BTU/ft^2-sec).

Base gas recovery temperature for the current DFI flights is presented in Fig. 10 along with the design curve. Based on the current data, the design appears to be

fairly conservative at this circumferential location (THETA-B = 45 deg). However, the gas temperature probes have several error sources which produce lower readings than expected. Consequently, there is no design impact even though the magnitude of the design could possibly be lowered to a less conservative level.

3.2 Plume Impingement

Following separation, the SRB undergoes a slow inboard roll into the SSME plumes. This is depicted by SRB aft skirt pressure coefficient data shown in Fig. 11. The sector from THETA-B = 90-180-270 deg rolls outboard, and consequently sees very little of the plume impingement heating. DFI flight heating rates due to the SSME plume impingement on the SRB aft skirt are presented in Figs. 12–14. These data are compared with the operational design environment from Ref. [11]. From the current flight data, the THETA-B = 180 deg position (Gage B07R7705) sees virtually no heating from the SSME plumes. Similarly, the THETA-B = 270 deg position is fairly benign compared to the operational environment for the first 5 seconds or so. Since the operational environment, Fig. 15, is applied to the SRB aft skirt uniformly, consideration should be given to reducing the design environment over the THETA-B = 180 to 270 deg sector.

Section 4
SRB REENTRY TRAJECTORIES

The left hand SRB was instrumented with 12 external circumferential static pressures on flights STS-27R and 29R. These pressures were located on the forward motor case (XB = 763), and from these measurements SRB reentry angle of attack and roll were calculated. Definition of the instrumentation location as well as angle of attack and roll are shown in Fig. 16. These calculations are described in Ref. [2] and are presented in Appendix III of this report. Comparisons of the reentry angle of attack with the lofted and non-lofted design Monte Carlo trajectory set [12] are presented in Fig. 17. The reentry trajectories from the current flights are seen to be within the design set. Comparisons of the individual flight reentry velocity and altitude with the design envelope is shown in Fig. 18. The SRB velocities were obtained from Cape-based radar measurements, consequently they are erratic. Reentry of the SRB's on flights STS-26R and STS-27R exceeded the design boundary during the latter phase of the aeroheating and subsonic portion of the flight. Since the these flights did not represent an unusually hot reentry, consideration should be given to the components which define the design boundary with a view of increasing this somewhat.

Section 5
REENTRY HEATING

5.1 SRB External Reentry Heating

Analysis of the external reentry heating data from STS-27R and 29R [3] showed that the data base was very adequate for predicting reentry heating rates to the vehicle in the forward areas. An example of this is shown in Fig. 19 for an instrumented point on the nose cone and attach ring. However, when it came to calculating the aft skirt heating, the data base at the THETA-B = 180 and 270 deg positions was able to predict the general magnitude only. Some peaks and most peak rates were missed. An example of this is shown in Fig. 20. These plots compare the measured and predicted heating rates on the aft skirt at the three gage locations for STS-27R. The reason for the disparity is due to the limited data from the historic flights, STS 1-3,5 and 6. Consequently, the aft skirt interference heating factor data base should be updated based on the current results.

5.2 Internal Aft Skirt Reentry Heating

Analysis of the reentry flight data [3] showed that the STATE code [13] did a very good job in predicting the internal aft skirt reentry gas temperature and a fair job in predicting reentry heating rates for the case of reentry aerodynamic heating only i.e., no nozzle flame entrainment. An example of this is shown in Figs. 21 and 22. Figure. 21 is a comparison of STATE predicted and flight measured internal aft skirt reentry gas temperature, and Fig. 22 is a comparison of predicted and measured heating rates for a gage near the TVC fuel isolation valve. Some adjustment to the reentry data base might improve the agreement in heating rate prediction at the later time points ($t >$ 300 sec). However, the main impact on design of the current data is in the area of nozzle flame heating during the reentry process. Significant nozzle flame heating was experienced by both boosters on STS-29R. Peak gas temperatures of 2800-3000°R and maximum heating rates of 30 BTU/ft^2-sec were experienced, as shown in Figs. 23 and 24. This was mainly due to severing the nozzle extension at apogee for STS-29R. This action exposed the internal components to longer periods of flame heating than has been experienced with the nozzle extension on. As a consequence, high heat loads were experienced by the left hand booster and the design load was exceeded on the right hand booster, Fig. 25. (The vehicle is designed to the 95 percentile reentry trajectory). Using the gas temperature algorithm in the STATE code to calculate reentry heating for this case severely underpredicts the heating rate, Fig. 26a. However, if the measured internal aft skirt gas temperature is used to determine the recovery enthalpy used in the heating predictions, the STATE code does a very good job of calculating the reentry heating, Fig. 26b. The practical significance of this is that the increase in heating is primarily due to the increase in gas temperature, as opposed to an increase in internal aft skirt heat transfer coefficient. Application of the nozzle flame to the design model

is depicted in Fig. 27. It is added as a radiant heat flux source during the subsonic portion of the reentry. Contrasting this model to the heating observed on STS-29R (Figs. 24 and 26b), the nozzle flame heating distribution is much wider spread and occurs during the supersonic reentry phase of flight. Also, by virture of the agreement between the calculated and measured heating rates in Fig. 26b, the nozzle flame heating responds well if treated as a convective source. Consequently, a new nozzle flame model is needed to adequately predict the internal aft skirt reentry heating and design environments. This should be done for both nozzle extension-on and off, since flame heating was observed during the STS-27R nozzle extension-on reentry (Appendix IV) also.

An estimate of the increase in the design environments for several of the TVC components was calculated by enveloping the nozzle flame gas temperature in Fig. 23a. This was then used to calculate the enthalpy with time and applied to the 95 percentile design trajectory for the TVC body points in question. A sketch defining the TVC body points and application of the resulting environments is presented in Fig. 28. The enthalpy profile with time for two of the body points is shown in Fig. 29. The results in the form of integrated heat load are presented in Table 4. These represent cold wall (T_w = 460°R) conditions, and are compared to the current design numbers. Increases in design load of from 116 to 160 BTU/ft^2 are observed. Heating rate versus time for Body Points 163 and 164 are plotted in Figs. 30 and 31. These results graphically show where the increase comes from. (The nozzle flame component in the design environment for t > 340 seconds was also used in the STS-29R derived design environments).

Section 6
FRUSTUM VENTING

Prior to the redesigned SRB flights, frustum venting design environments were calculated and applied without the benefit of supporting flight data. Consequently, the validity of the environments could not be verified. However, on STS-26R, 27R, and 29R, frustum internal gas temperature and pressure measurements were made for the first time in Shuttle history. These measurements, when compared with the design calculations, made it clear that revisions to the math model needed to be made, (Fig. 32). In this comparison, some of the ascent measurements were above the design curve, Fig. 32a, while the reentry measurements were considerably below design, Fig. 32b, and did not show the oscillatory motion resulting from the coning of the SRB during reentry.

The current DFI flight measurements were used to upgrade the frustum ascent and reentry venting math models, such that they would predict the individual flight ascent and reentry gas temperature histories. This work is documented in Appendix V of this report. The resulting math models were then used to generate a "new" design environment for both ascent and reentry. This is shown in Fig. 33. The ascent portion is composed of one environment based on the Light Weight Tank Design Trajectory [9]. The reentry results are composed of an environment for the 0, 50, 95, and 100 percent integrated heat load reentry trajectory from the design Monte Carlo set of Ref. [12]. Frustum gas temperature encounters a 20°R drop during ascent and a maximum 70°R rise during reentry. Since the vehicle is designed to the 95 percentile load reentry trajectory, this environment was plotted along with the "new" ascent design and compared to the existing frustum venting design environment set. These comparisons are presented in Fig. 34. The "new" environments are seen to be approximately 50°R hotter during ascent, and a minimum of 90-150°R cooler during reentry. (The existing reentry design is shown as an envelope of the maximum and minimum values. For the original calculations, the Booster was allowed to pitch and roll, thereby giving an oscillating temperature history. For the current calculations, the SRB was assumed to be trimmed at α = 170 deg). The lowering of the gas temperature environment during reentry, for the present calculations, is due to the assumption that the gas temperature at the beginning of reentry was the same as the gas temperature at the end of ascent instead of the 660°R minimum limit imposed on the existing design. Consequently, the "new" calculations represent a significant impact on the existing frustum design environment set, and recommendations are made to adopt the STS-26R, 27R and 29R derived environments as the official set.

One final aspect covered in the venting analysis [5] is worthy of mention here since it affects the design environment calculation. In an effort to define a more accurate venting model, a considerable amount of effort was expended in defining the temperature of the gas entering the vent holes during reentry. The MSA-2 surface temperature was felt to be the dominant level, and calculations of this were made and used in the determination of the "new" environments. This was based on the view that only a certain percentage of the boundary layer flow enters the vent holes, and use of the free-stream total temperature

was considered to be too high. (Up to this point, all the design venting environments were calculated using the free-stream total temperature.) Flight data analyses indicated that the theoretical models could not be made to agree with flight data if total temperature was used as input. The use of the MSA surface temperature as the input made reasonable comparisons possible. As a check to see what type differences existed between the two philosophies, design calculations were made using the free-stream total temperature. These results in the form of frustum internal reentry gas temperature and internal heat transfer coefficient are presented in Figs. 35 and 36. By way of illustration, the MSA-2 surface temperature and free-stream total are plotted in Fig. 35. Although a large difference exists between the MSA-2 surface temperature and the free-stream total, the effect on the frustum internal gas temperature is small compared with total or surface temperature. However, the internal gas temperature change produced by using total or MSA surface is significant compared with the value of the internal temperature. The large heat transfer surface area of the compartment and parachutes produce the nonadiabatic effect of reducing the gas temperature to near the internal structural temperature. Other compartments usually do not have this large an internal heat transfer area to volume ratio as does the frustum.

Section 7
OUTSTANDING ISSUES

7.1 Calorimeter Wall Temperature Measurement

Use of the flight measured heating rates in aerothermal analysis involves converting them to a heat transfer coefficient form so that they will be independent of the ambient conditions and may be scaled to various flight conditions. This action requires the use of a corresponding calorimeter wall temperature. Historically, this value was calculated through a one dimensional conduction math model. The current DFI flights provided the first opportunity to obtain flight measured calorimeter temperature measurements. Comparison of the calorimeter temperature response with that calculated by the conduction math model showed that the previous results from STS-1 through STS-6 were anywhere from 20 to 200°F off. This issue was addressed in Ref. [1]. The data are presented as Figs. 37 and 38 for reference. These data are for a calorimeter in an essentially undisturbed heating area (Fig. 37) and for one located in a shock impingement area i.e., high heating (Fig. 38). Location of these gages may be found in Fig.1. Resulting errors in the flight derived heat transfer coefficient, shown in Fig. 39, can be as much as 20 percent or greater. As part of this analysis, two one-dimensional models of the nose cone gage (Fig. 40) were generated. Gage thermal response at a depth corresponding to the thermocouple location was calculated and compared with flight measurements for Gage 7701 on STS-27R. The results are presented in Fig. 41. This represents a location of low to moderate heating. Model 1 was generated considering the volume of the flange. It was treated as an extension of the gage length. Model 2 did not consider the flange material for a diameter greater than the gage . These represent two scenarios which might be used to model the gage from a one- dimensional point of view. As can be seen, there is approximately a 40°F difference between the two. The thermal response of the DFI calorimeters on the first six flights was provided by Lockheed conduction models. Consequently, the philosophy of modeling the gages is not known as is the calculation uncertainties. The problem is clearly a two-dimensional case, though. The point of revisiting this aspect of the analysis is to highlight the need for a corresponding calorimeter wall thermocouple at each gage location, or at least on gages located in areas of areas of similar heating, i.e., high, low, etc. In closing this discussion, it was found from the conduction models that location of the thermocouple was not of major significance, since the axial gradient in gage temperature was virtually nonexistent. The reason for this was because the gage was made primarily of copper.

7.2 SRB DFI Flight Heating Trend Uncertainty

As part of the earlier analysis on the flight data from STS 1-3,5 and 6, the DFI heating measurements were put in the form of Stanton number versus Reynolds number. These were based on free-stream conditions. It was later found that basing the measurements

on free-stream conditions did not correlate the data well, as might be expected, and that local conditions should be used. The results were still useful in comparing flight to flight trends. Consequently, these results are presented in Appendix VI of this report so that they will be documented. Nose cone data in this form for the current DFI flights were presented in Appendix I of this report. Concerning the validity and use of the data in this form, one aspect remains to be investigated. Comparisons of the data with the classical turbulent and laminar slopes show that the data have more of a laminar trend than a turbulent one. This is demonstrated in Figs. 42 and 43. Figure 42 pertains to Gage 7660 (STS 1-6) and Gage 7701 (STS 26R-29R). Both are located midway up the nose cone on the THETA-B = 90 deg ray. This gage is in a relatively undisturbed region, except for the angularity of the flow coming off of the External Tank. Figure 43 pertains to Gage 7657 (STS 1-6) and Gage 7702 (STS 26R-29R), both located on the THETA-B = 90 deg ray behind the SRB reflected shock impingement on the nose cone. In both cases, the experimental data exhibit a strong laminar trend. The SRB is designed to a turbulent heating level, and predictions generally agree with the experimental flight data. So the observed trend of Figs. 42 and 43 is somewhat puzzling and needs to be put to rest. It should be pointed out that these measurements as well as those presented in Appendix VI represent areas on the forward end of the SRB. In addressing this issue, measurements taken further back on the booster should be included in the analysis.

Section 8
SUMMARY AND CONCLUSIONS

Flight heating data from the redesigned Solid Rocket Booster DFI instrumented flights STS-26R, 27R and 29R, were analyzed from a design environment point of view. Design impact was assessed for the following areas: ascent convection, plume convection and plume impingement at SRB separation, reentry heating, reentry trajectories, as well as frustum internal ascent and reentry venting. Instrumentation for the redesigned SRB flights were located, for the most part, in areas which had not previously been instrumented. Consequently, acquisition of this data was invaluable in defining the heating environments on the SRB, and analysis of these measurements resulted in a direct impact on the current design environment set. Areas affected are:

1. The existing heat loads for the inboard sector of the attach ring are already in the 500-600 BTU/ft^2 range. The flight derived scaling factors from the current data represent a significant increase over the factors used to calculate the current design.

2. The external aft skirt ascent aeroheating environments, especially in the THETA-B = 180-270 deg range, are low. The tunnel to flight scaling factors represent a factor of 3-4 over those currently used for design.

3. Plume convection measurements on the aft skirt at THETA-B = 180 and 270 deg confirm measurements made on STS-1 and 2. Based on this, the design environment applied over this sector could be reduced. In addition, the method in which the environment is applied needs to be reconsidered, i.e., aeroheating is considered to end at t = 95 seconds and the plume convection environment is then applied out to SRB separation. Since the plume component in this sector amounts to about 0.5 BTU/ft^2-sec, the aeroheating component past t = 95 seconds may be greater.

4. SSME plume impingement heating in the 15 seconds following SRB separation is virtually nonexistent at the THETA-B = 180 deg location, and 0.5 BTU/ft^2-sec at the THETA-B = 270 deg position. Since the operational environment is applied uniformly over the aft skirt, and is of a large magnitude, reduction of the design over the THETA-B = 180-270 deg segment of the aft skirt could be made.

5. The design model for the nozzle flame heating to the internal aft skirt during reentry needs to be completely updated. This is for both the case of the nozzle extension-off and nozzle extension-on. The design is currently applied as a radiant source during the subsonic portion of flight. Results from the current DFI flights clearly show that the mechanism is largely convective in nature and that the increase in heating in the presence of the nozzle flame is mainly due to the increase in internal aft skirt gas temperature. The current DFI flight data showed that the nozzle flame heating was substantially more severe with the

nozzle extension off, and that the distribution dominated the supersonic phase of the reentry. Estimated increases in cold wall design load to the internal aft skirt components is in the 120-160 BTU/ft^{2}range.

6. The STATE code did a very good job in predicting the internal aft skirt reentry gas temperature for the case of no nozzle flame heating. The interference factor data base for both internal and external aft skirt needs to be updated based on the current DFI flights. For the external case, the STATE code could predict general magnitude only for heating in the THETA-B = 180-270 deg sector. Many of the peaks and peak heating rates were missed. It did a better job in predicting the internal aft skirt heating although some improvement could be made.

7. The existing frustum venting design environment for both ascent and reentry was seen to be inadequate when compared to the flight data from STS-26R, 27R and 29R. A "new" design environment based on the current DFI flight data was calculated for the frustum internal components. It was seen to be approximately 50°R hotter than the existing design during ascent, and 90-150 °R cooler than the existing design during reentry.

8. Flight data evaluation indicated that in ingested air, total temperature was controlled by the external wall surface temperature. The ingested air temperature was reduced substantially by the large heat transfer surface area within the frustum. The effects of the wall temperature on ingested air temperature should be analyzed and studied for future venting applications.

9. Provision of a thermocouple on the redesigned flight calorimeters was invaluable in reducing the data to heat transfer coefficient form and alleviating conduction model uncertainties. For future flight test programs involving the acquisition of heat transfer data, strong consideration should be given to making simultaneous heating rate and gage temperature measurements. One cannot be divorced from the other in the engineering use of the data, and a heating rate without a valid gage temperature reduces the use of the heating rate to speculation.

10. In the analysis of the reentry heating data from the redesigned SRB flights, it was found that only when the external pressures on the motor case were provided could good engineering use be made of the reentry heating data. That is, the pressures provided a means of determining the SRB orientation during reentry. Consequently, the data from STS-26R could be used only from a supportive role since confirming heating calculations could not be made.

Section 9
REFERENCES

[1] Crain, William K. and Kirchner, Robert D., "SRB Ascent Flight Heating Analysis of STS-26R, 27R and 29R," REMTECH Report RTN 213–14, May 1991.

[2] Kirchner, Robert D. and Crain, William K., "Calculations of SRB Pitch and Roll Characteristics During Reentry for Flights STS-27R and STS-29R," REMTECH Report RTN 213–05, May 1991.

[3] Crain, William K. and Kirchner, Robert D., "SRB Reentry Flight Heating Analysis of STS–26R, 27R and 29R," REMTECH Report RTN 213–15, June 1991.

[4] Prendergast, Maurice J., "Solid Rocket Booster (SRB) Ascent Base Heating Flight Evaluation for Flights STS-26R, STS-27R and STS-29R," REMTECH Report RTN 213–12, Feb. 7, 1991.

[5] Crain, William K., "SRB Ascent and Reentry Frustum Venting Analysis and Design Update (STS-26R, 27R and 29R)" REMTECH Report RTN 213–16, June 1991.

[6] Crain, William K., "Raw Flight Data Report — STS-26R," REMTECH Report RTN 213–01, Dec. 1988.

[7] Frost, Cynthia L. and Crain, W. K., "Raw Flight Data Report — STS-27R," REMTECH Report RTN 213–02, Oct. 1989.

[8] Frost, Cynthia L. and Crain, W. K, "Raw Flight Data Report — STS-29R," REMTECH Report RTN 213–03, Sep. 1989.

[9] Crain, W. K., Frost, C. L., and Engel, C. D., "Final Report SRB Ascent Aerodynamic Heating Design Criteria Reduction Study," Vol. I, REMTECH Report RTR 090–01, Jan. 8, 1989.

[10] "Space Shuttle IVBC-3 Aerodynamic Heating Data Book SRB-Ascent," Rockwell International Report STS 84–0575 (Change Notice 3), Oct. 30, 1987.

[11] "IVBC-3 SRB Plume Heating Data Book," Rockwell International Report STS84–0259, (Change Notice 1), Oct. 1984.

[12] Engel, C., Hulsey, D., and Brewer, E., "The Steel Case SRB Reentry Thermal Environment Data Book," REMTECH Report RTR 039–13, June 1984.

[13] Kirchner, Robert D. and Hollman, David, "User's Guide for Program STATE," REMTECH Report RTN 213–07, Dec. 1990.

Section 10

FIGURES

NOSE CONE/FRUSTUM CALORIMETERS

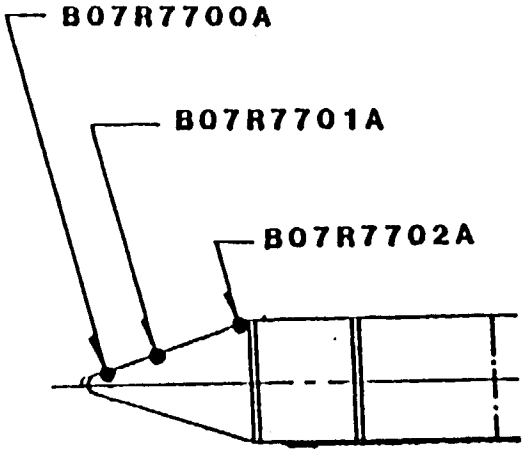

- RESOLVE 90 DEG. RAY HEATING DISCREPANCY
- RESOLVE HIGH HEATING FROM SRB/ET SHOCK IMPINGEMENT ON 90 DEG. RAY

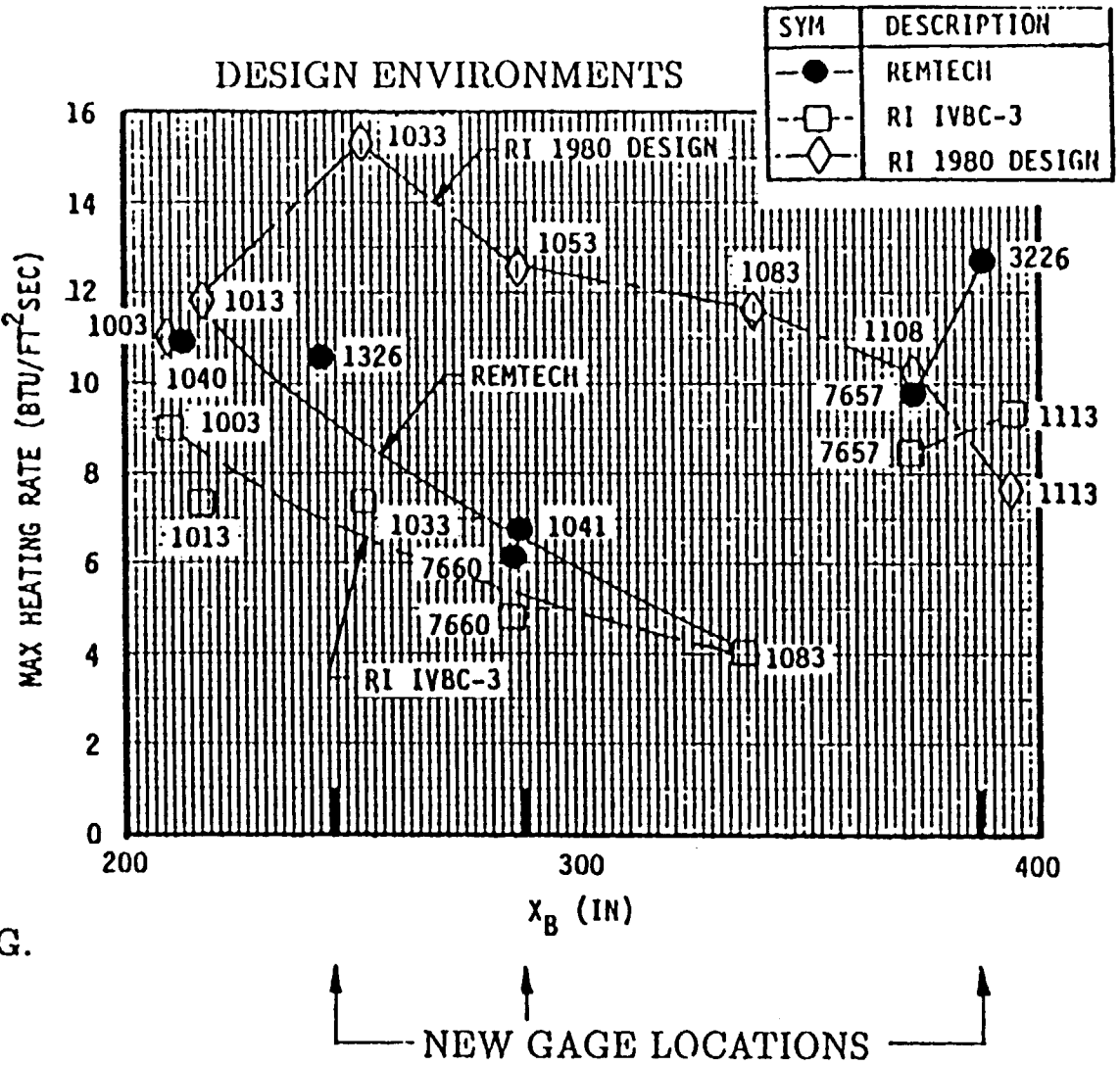

(a) Nose Cone/Frustum Calorimeters

Figure 1: Instrumentation Location and Objective

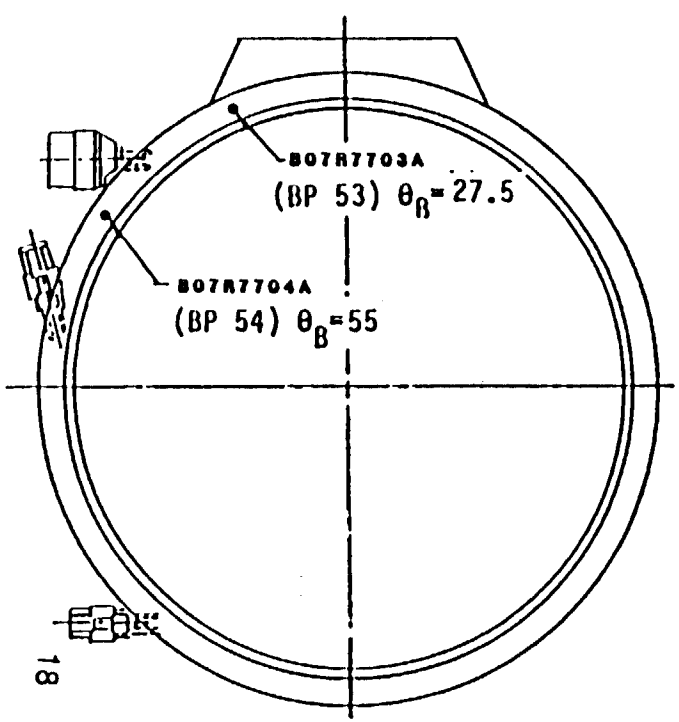

- NO PREVIOUS FLIGHT DATA
- DEFINE HIGH HEATING REGION ON ATTACH RING

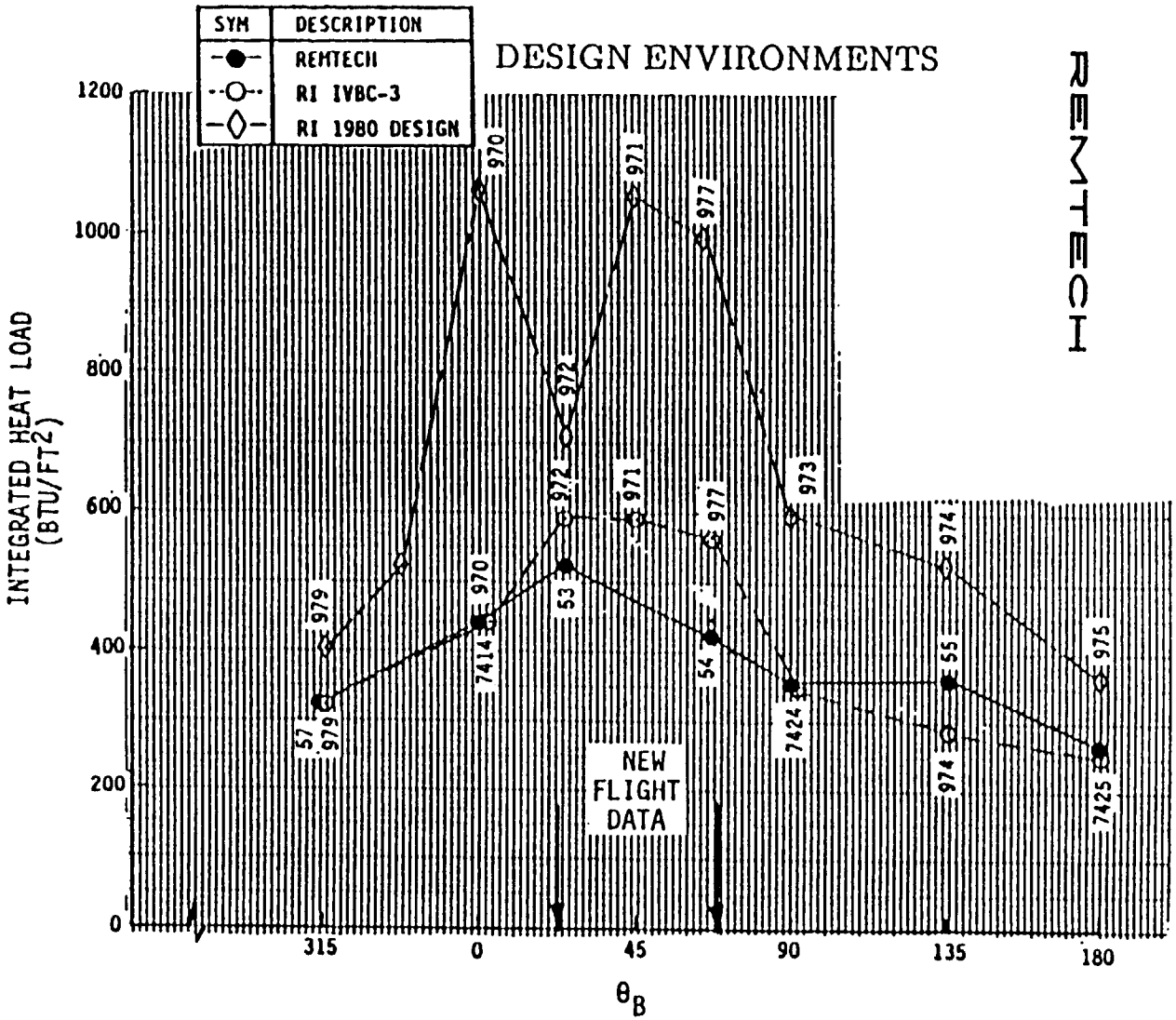

(b) Attach Ring

Figure 1: Instrumentation Location and Objective (Continued)

REMTECH

RTR 213-01

- NO PREVIOUS FLIGHT DATA IN THESE UNDISTURBED AREAS
- FLIGHT HEATING DETERMINATION OF
  - PLUME RECIRCULATION
  - REENTRY HEATING
- HELP DEFINE FLOW SEPARATION ZONE

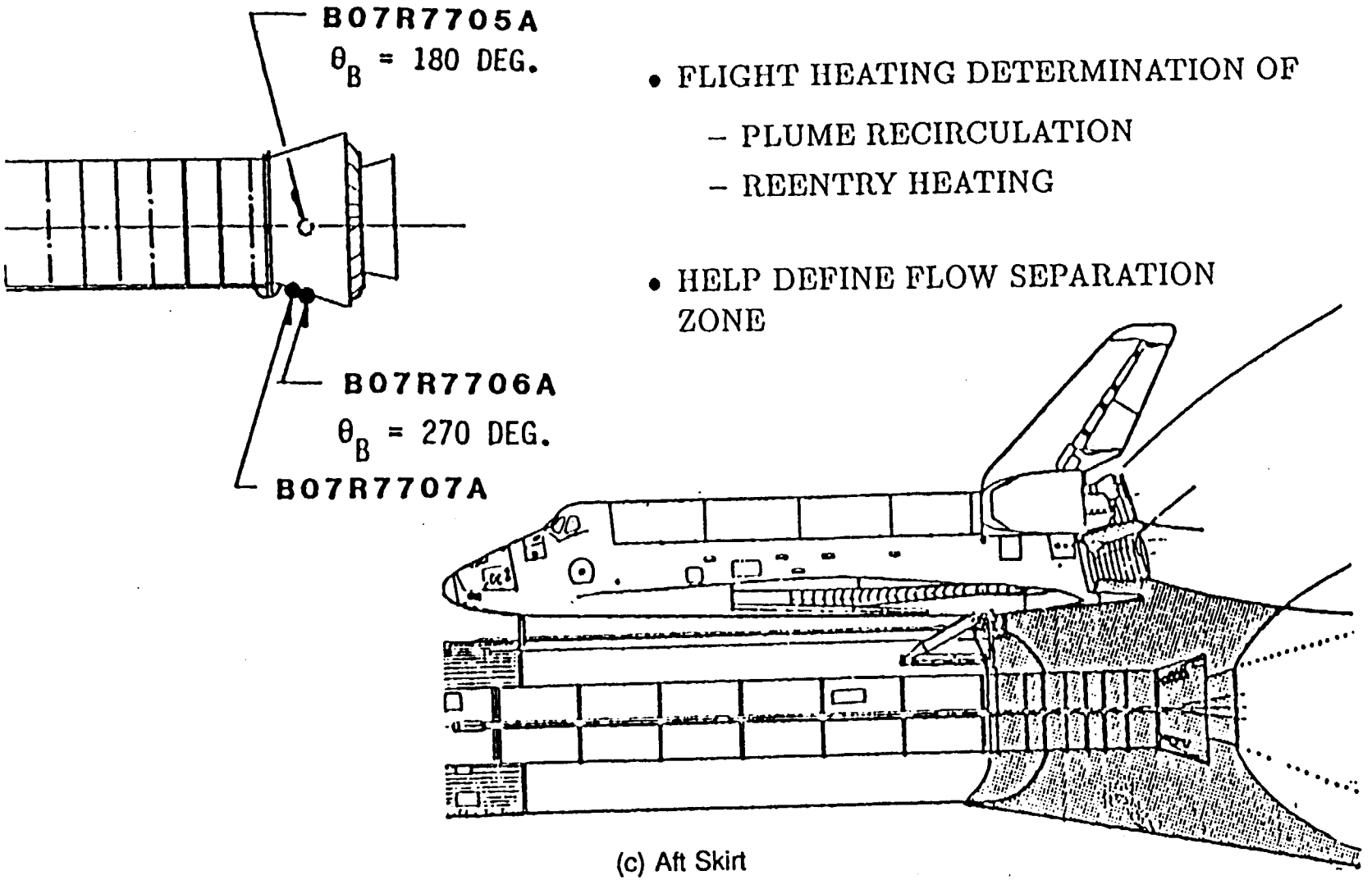

(c) Aft Skirt

Figure 1: Instrumentation Location and Objective (Concluded)

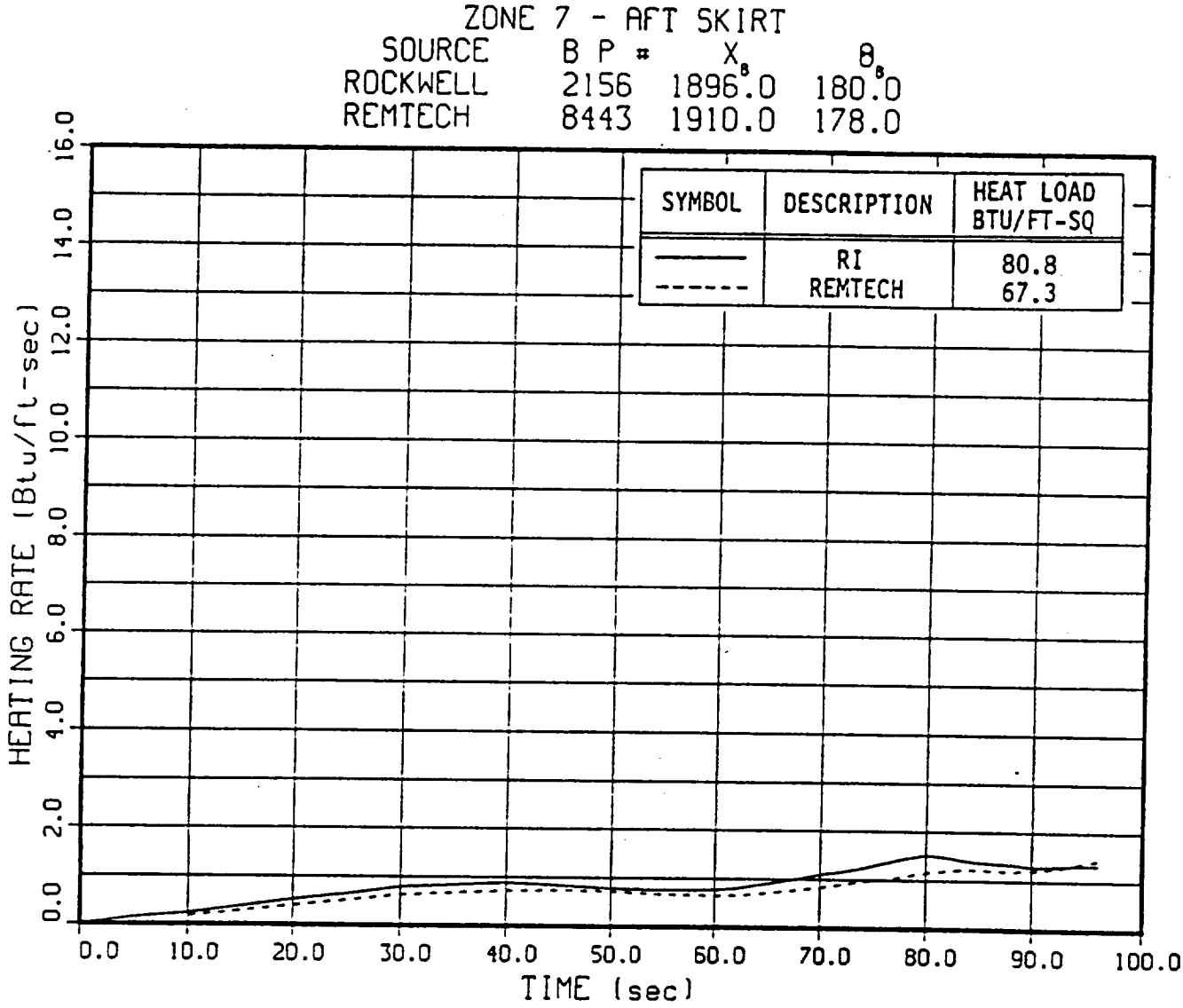

Figure 2: Comparison of Rockwell IVBC-3 and REMTECH Design Heating Rates on Aft Skirt at θ_B = 178 Deg

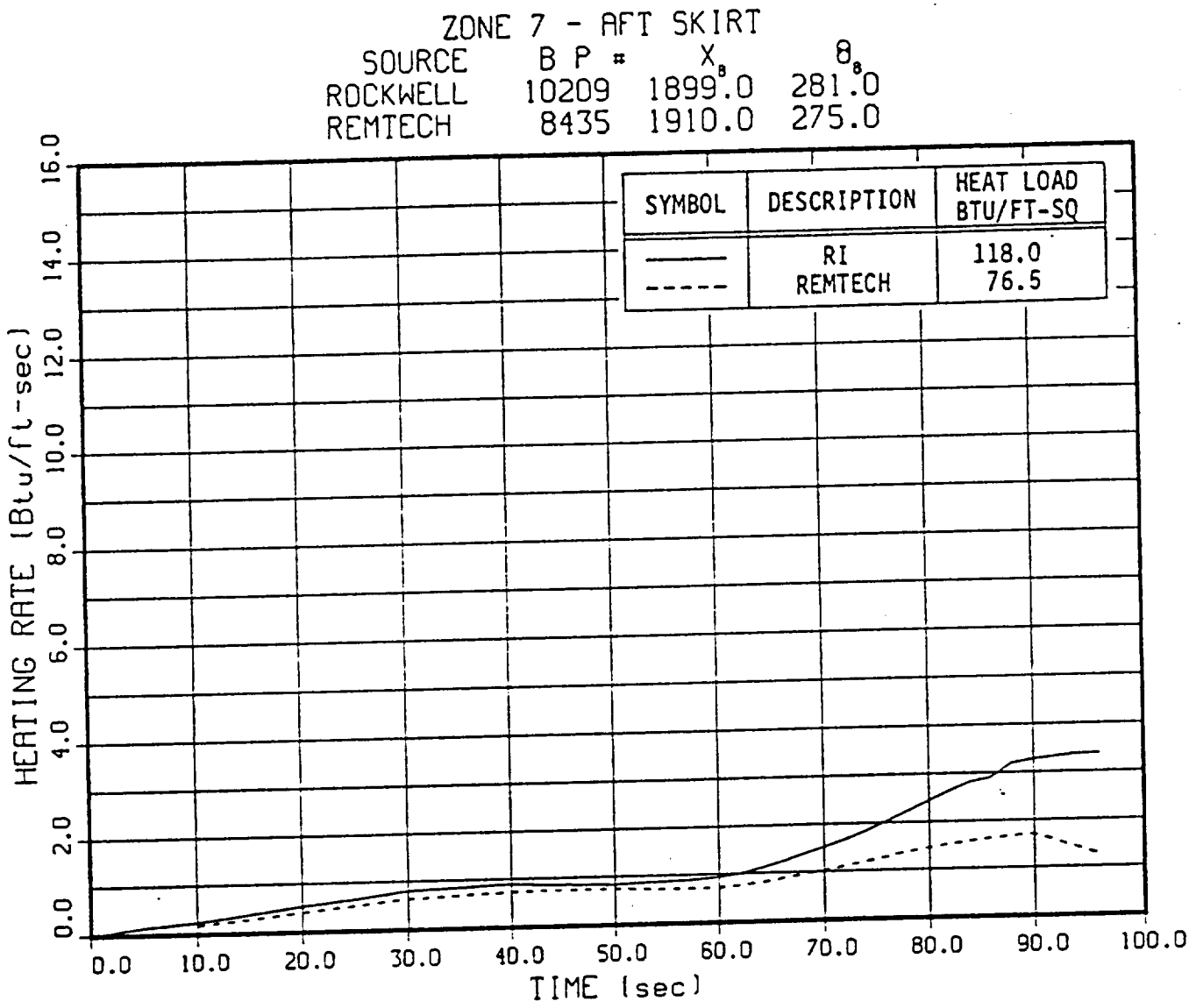

Figure 3: Comparison of Rockwell IVBC-3 and REMTECH Design Heating Rates on Aft Skirt at θ_B = 275 Deg

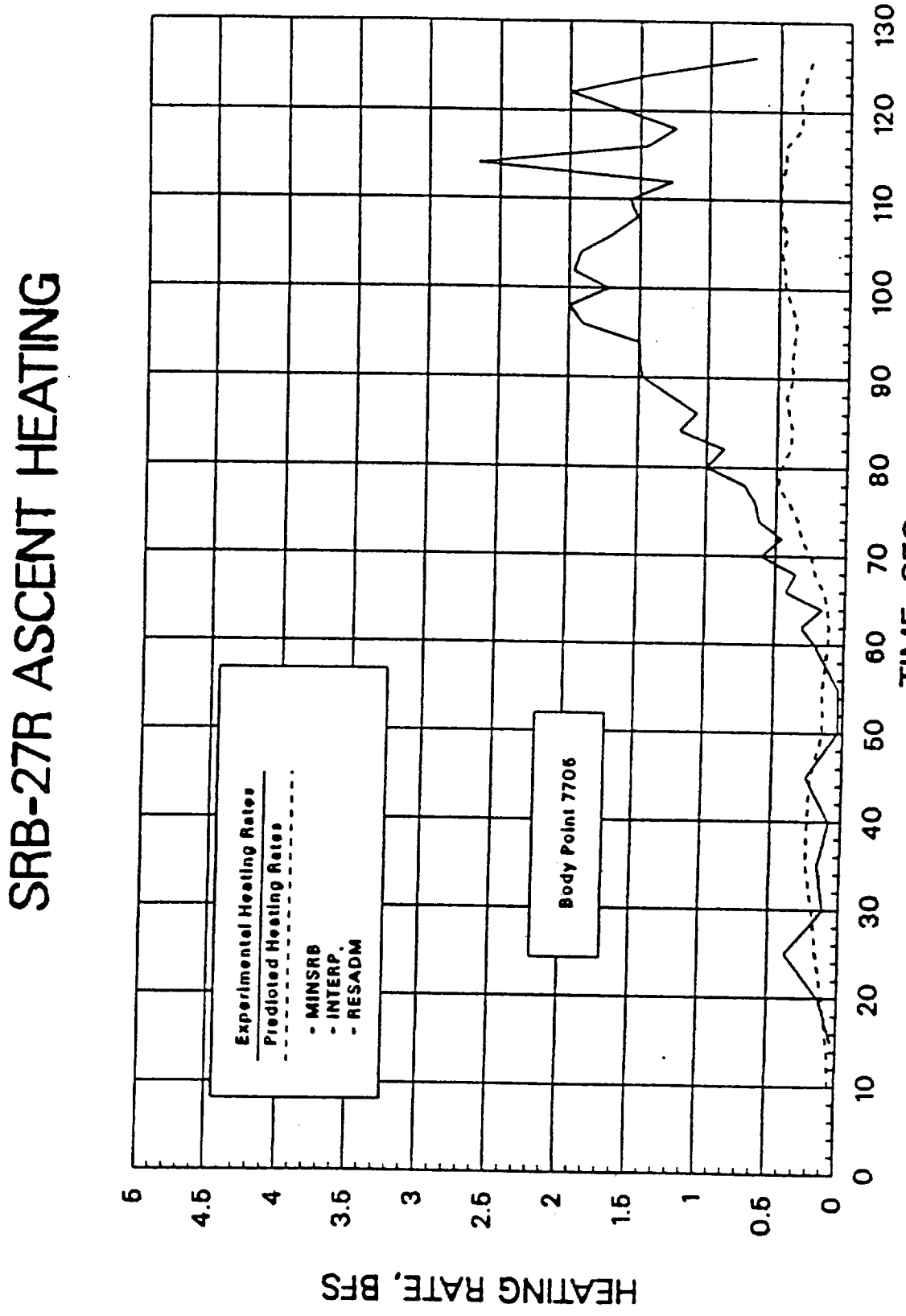

Figure 4: Comparison of Heating Predictions Using "Design" Flight Factors with Flight Measured Heating Rates for STS-27R

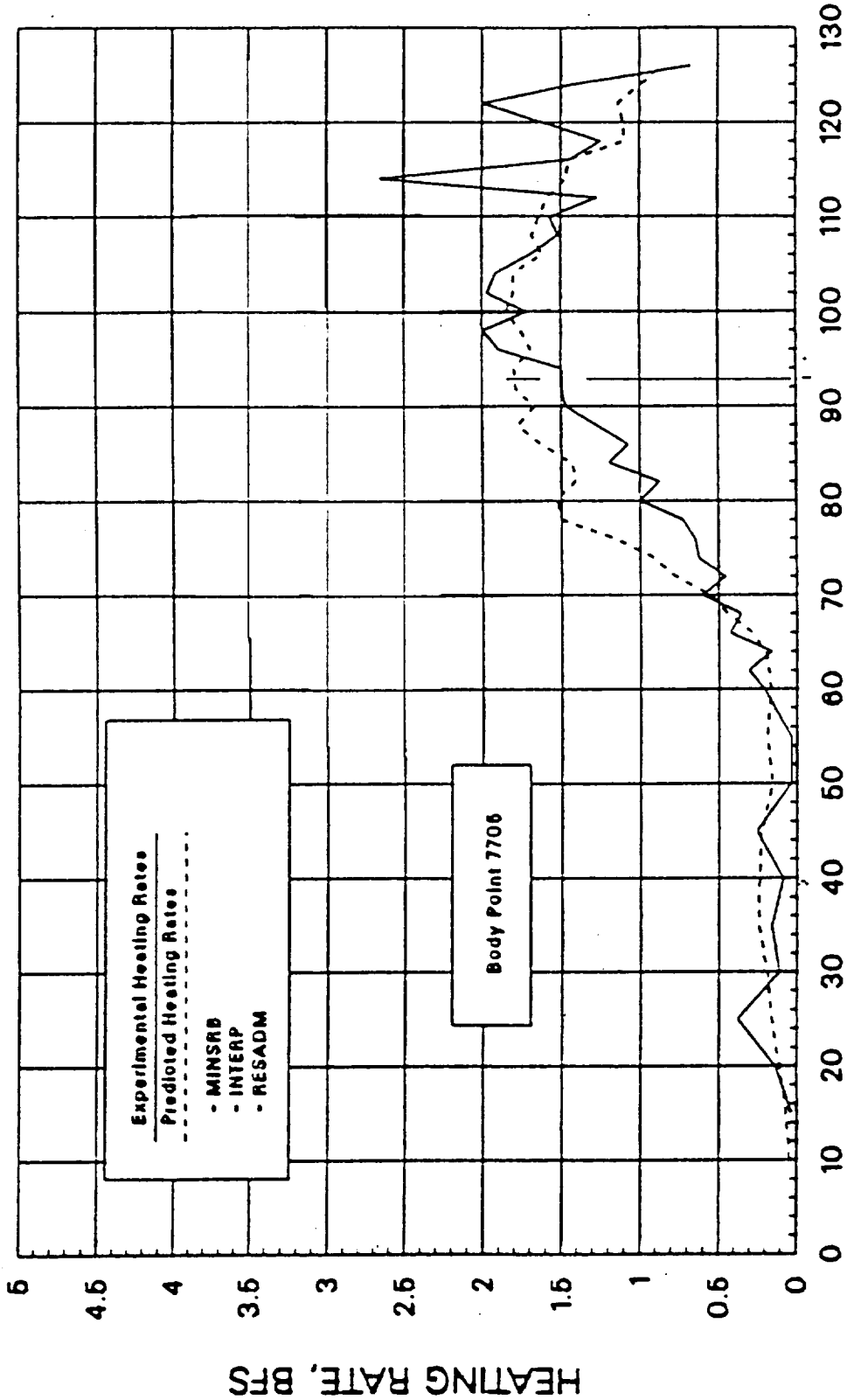

Figure 5: Comparison of Heating Predictions Using STS-1, 2 Flight Factors with Flight Measured Heating Rates for STS-27R

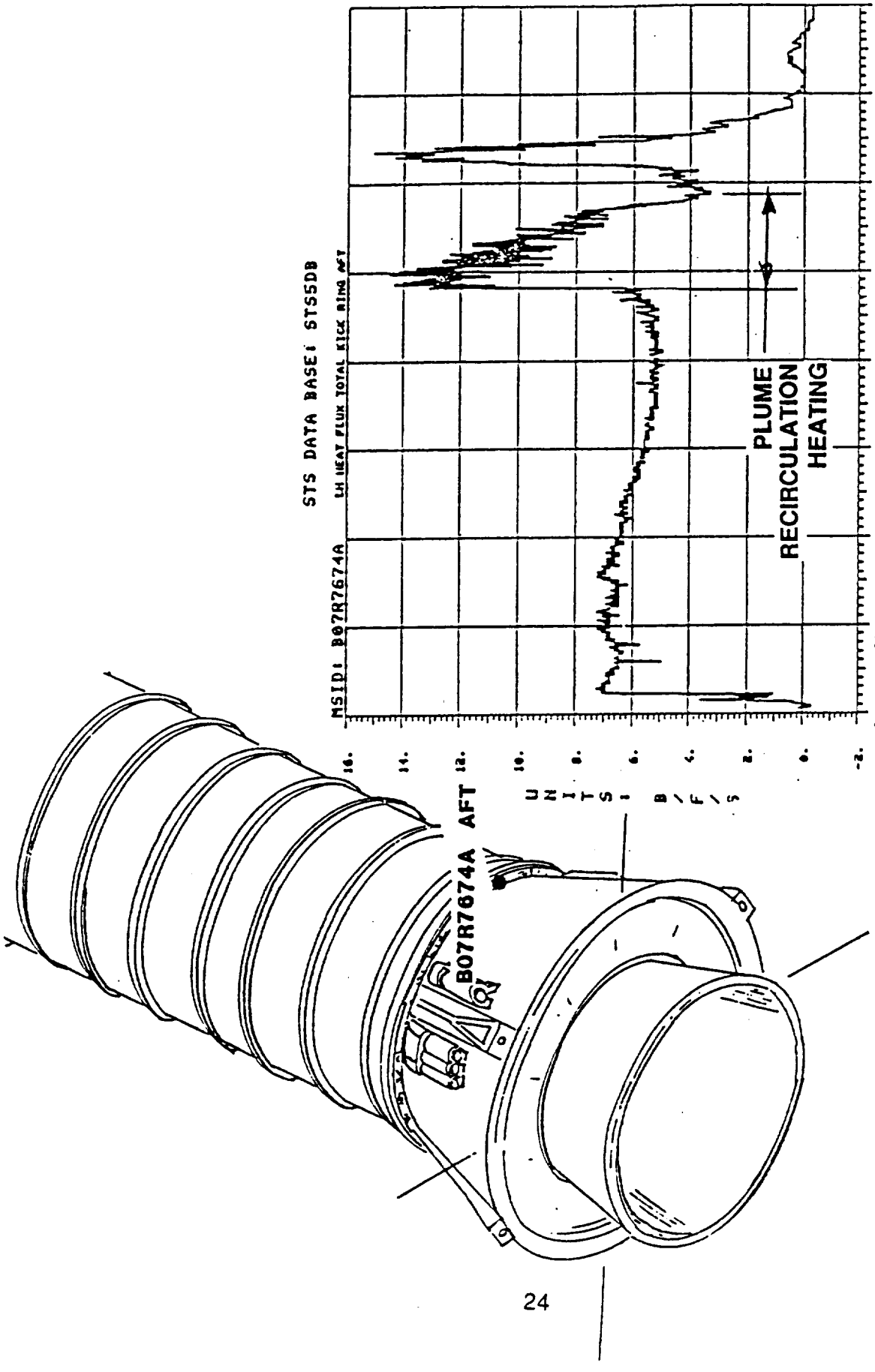

Figure 6: Example of Aft Skirt Gage With Plume Recirculation

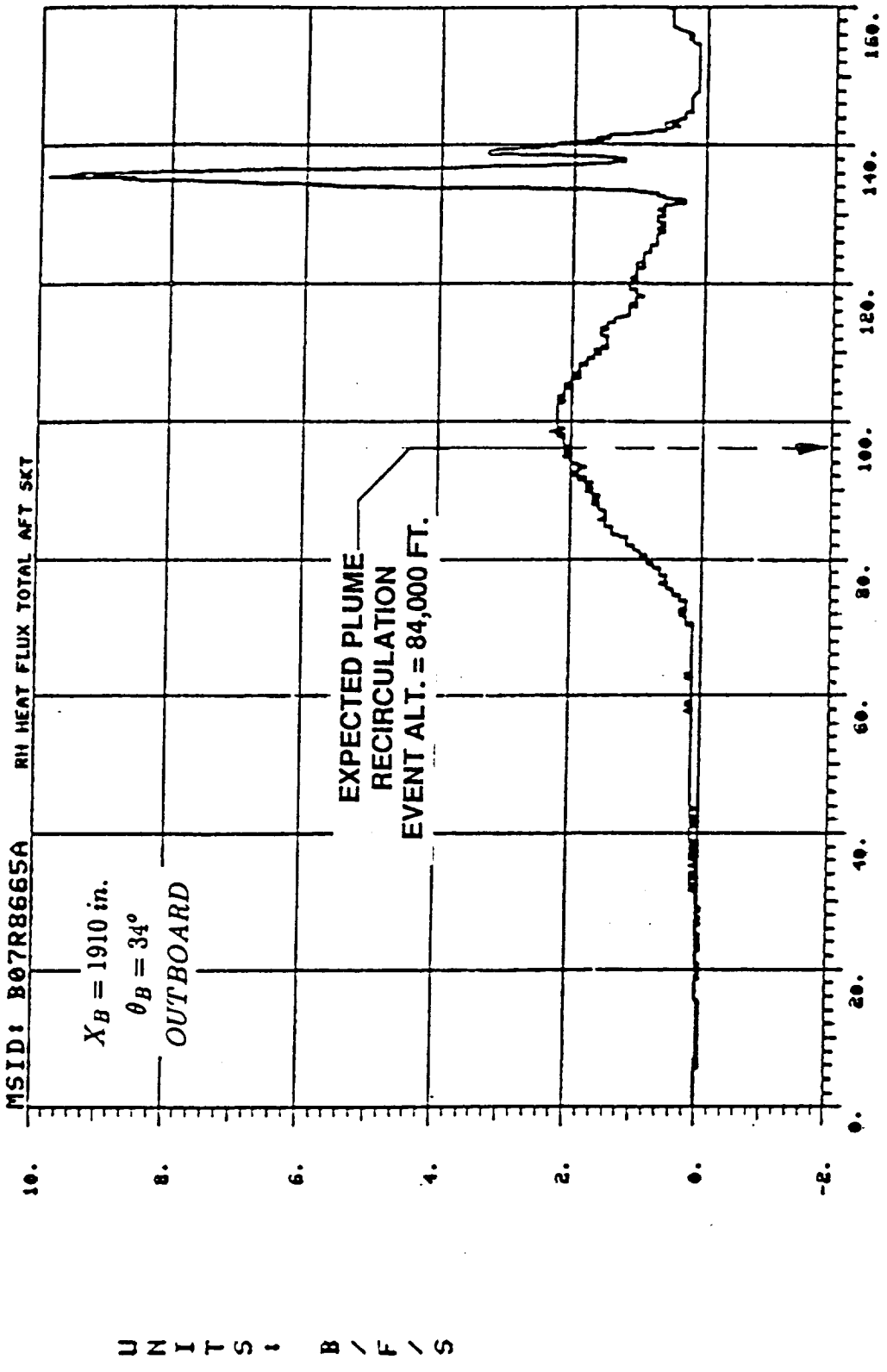

Figure 7: Example of Aft Skirt Gage With No Plume Recirculation (STS-5)

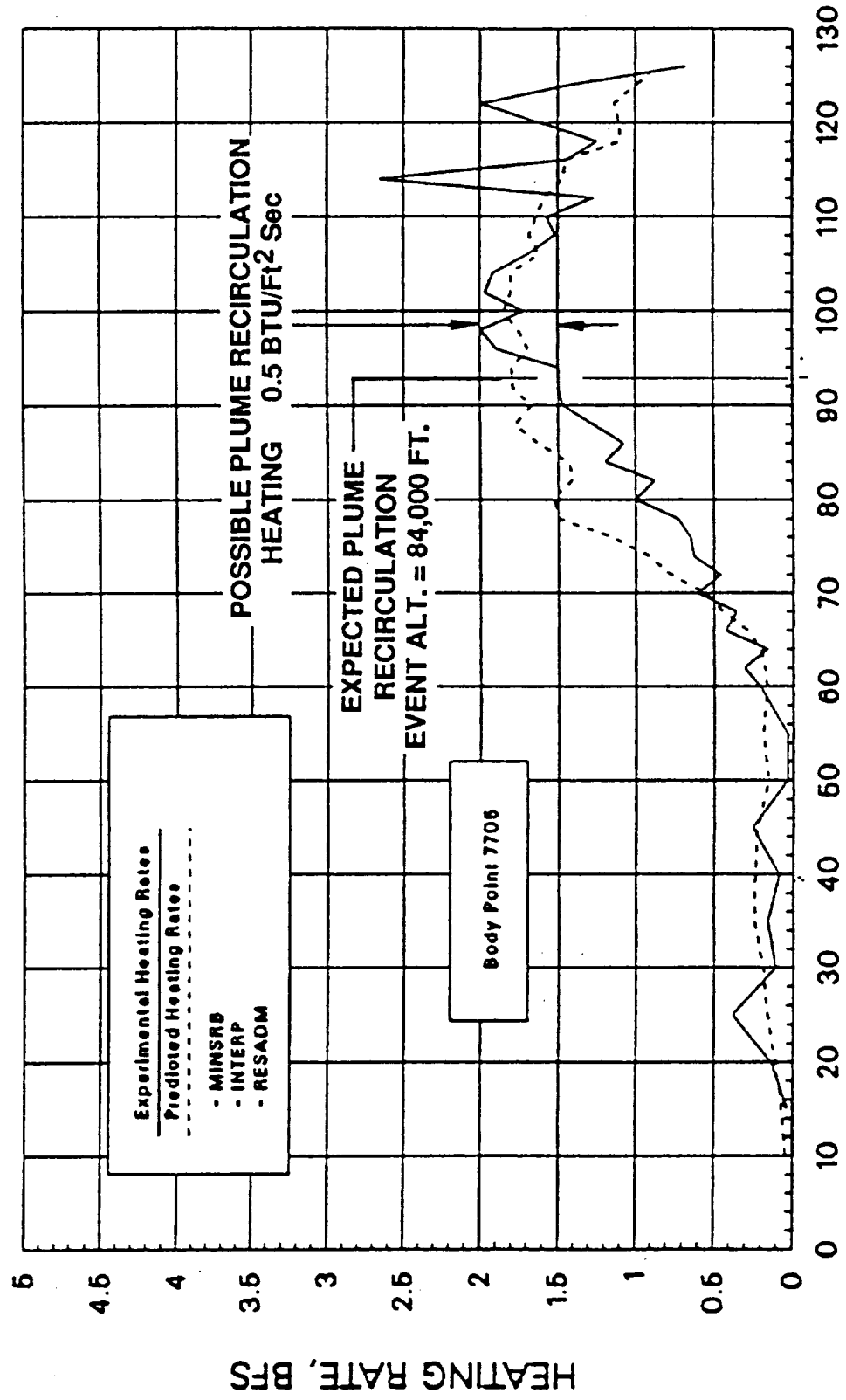

(a) B07R7705 $X_B = 1880, \theta_B = 180deg$

Figure 8: Aft Skirt Heating (STS-27R)

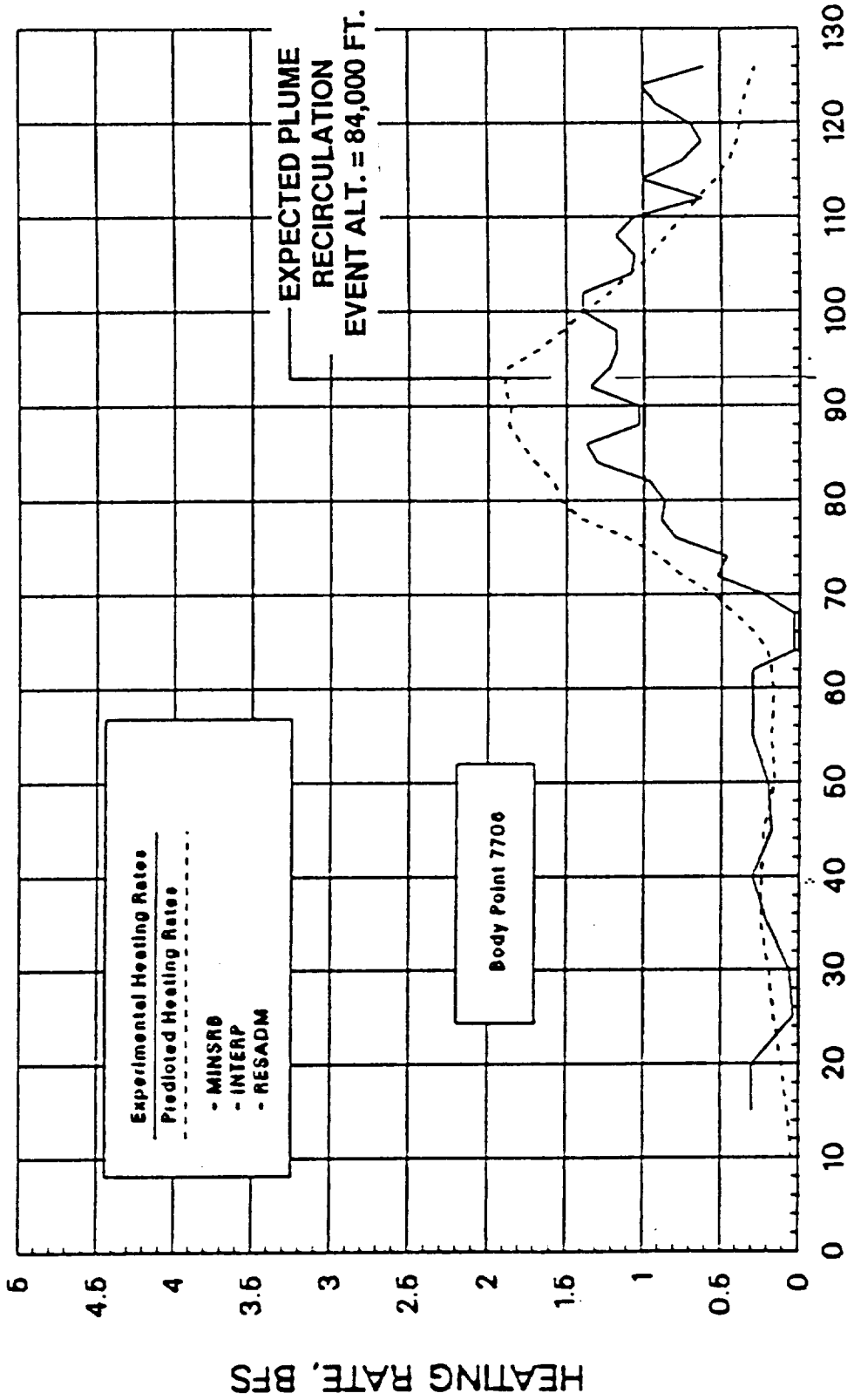

(b) B07R7706 $X_B = 1880, \theta_B = 270deg$

Figure 8: Aft Skirt Heating (STS-27R)

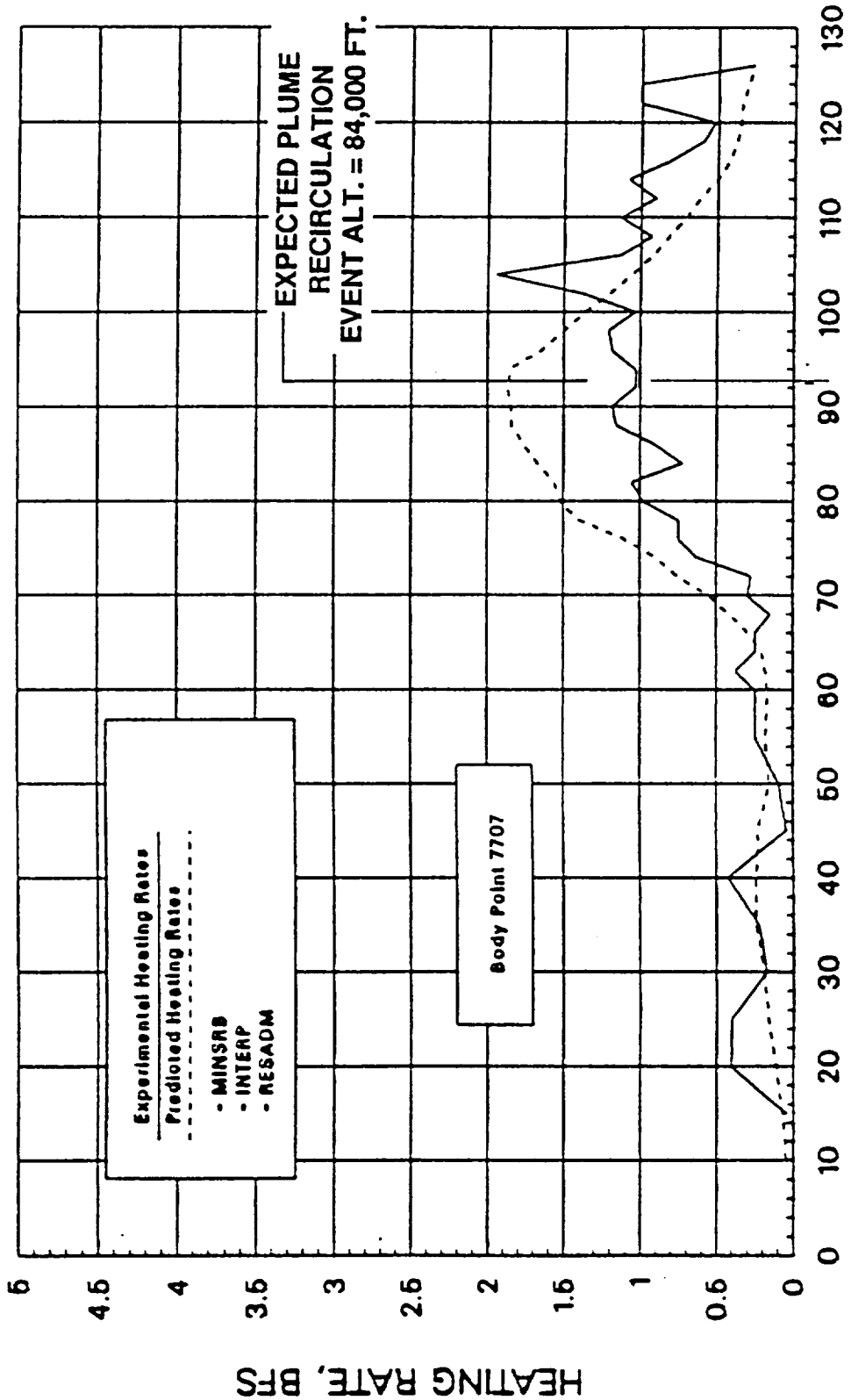

(c) B07R7707 $X_B = 1870, \theta_B = 270deg$

Figure 8: Aft Skirt Heating (STS-27R)

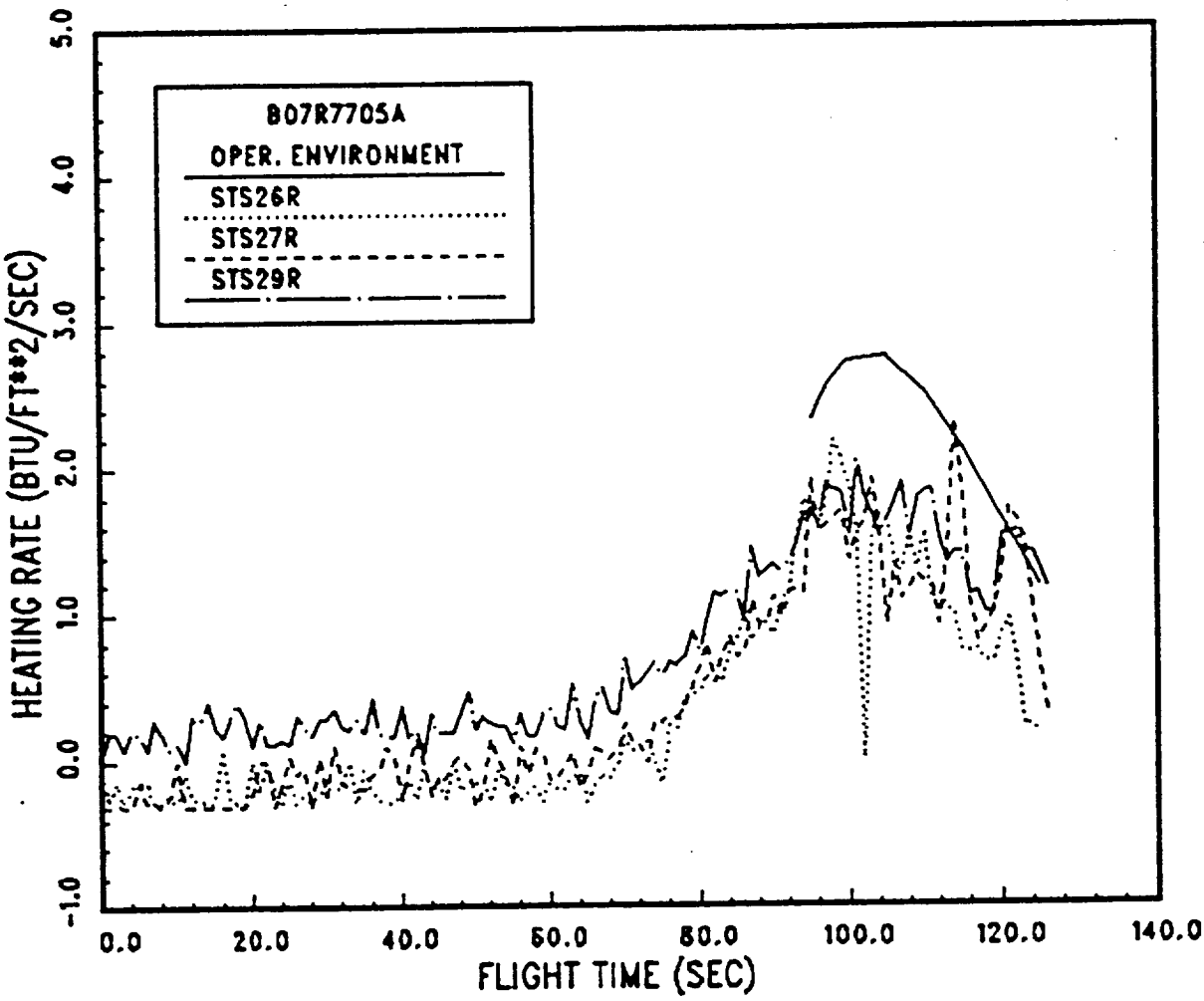

a) B07R7705 θ_B = 180 Deg

Figure 9: SRB Base Heating Environment — Q_c vs. Time — Aft Skirt

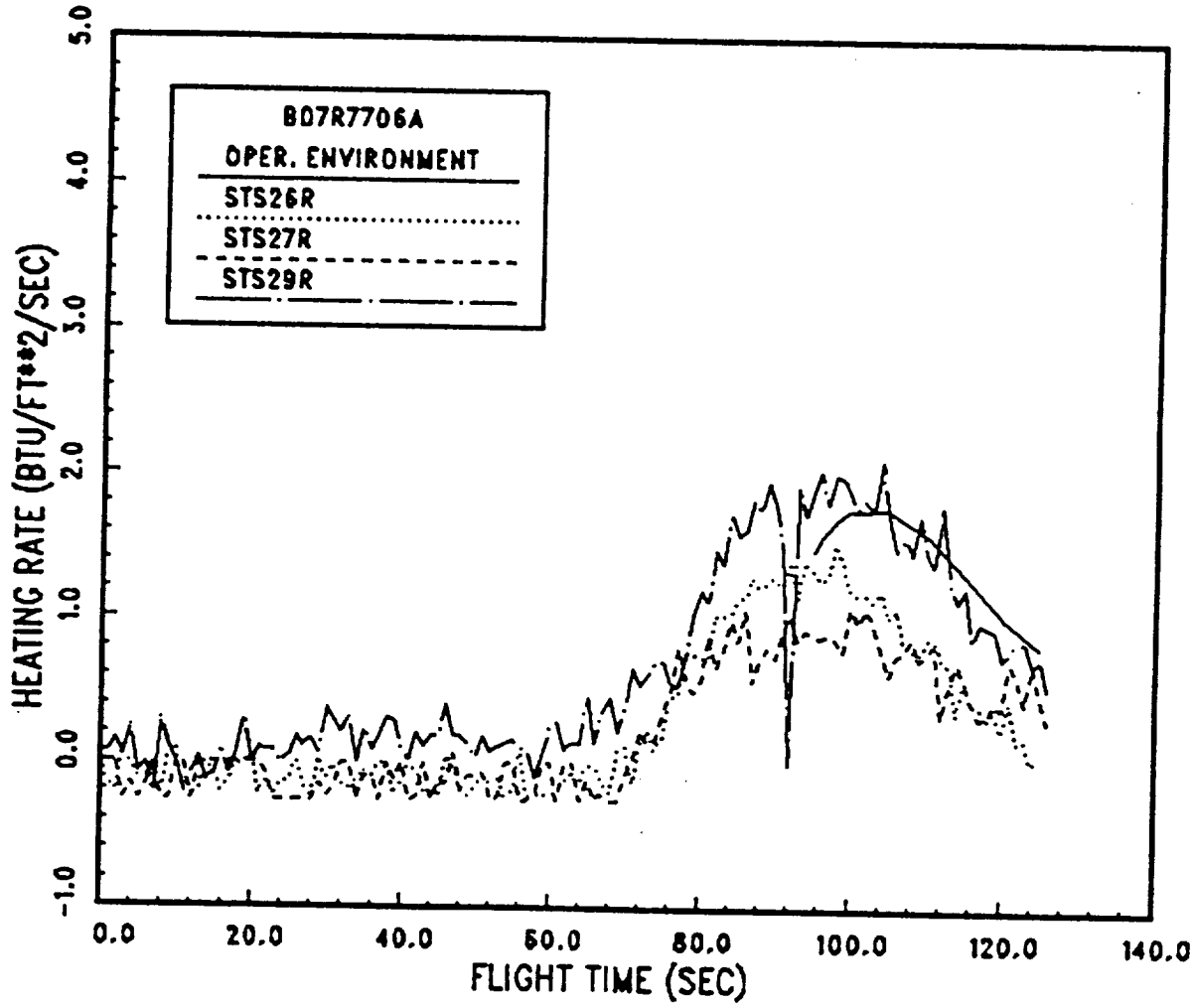

b) B07R7706 θ_B = 270 Deg

Figure 9: SRB Base Heating Environment — Q_c vs. Time — Aft Skirt (Continued)

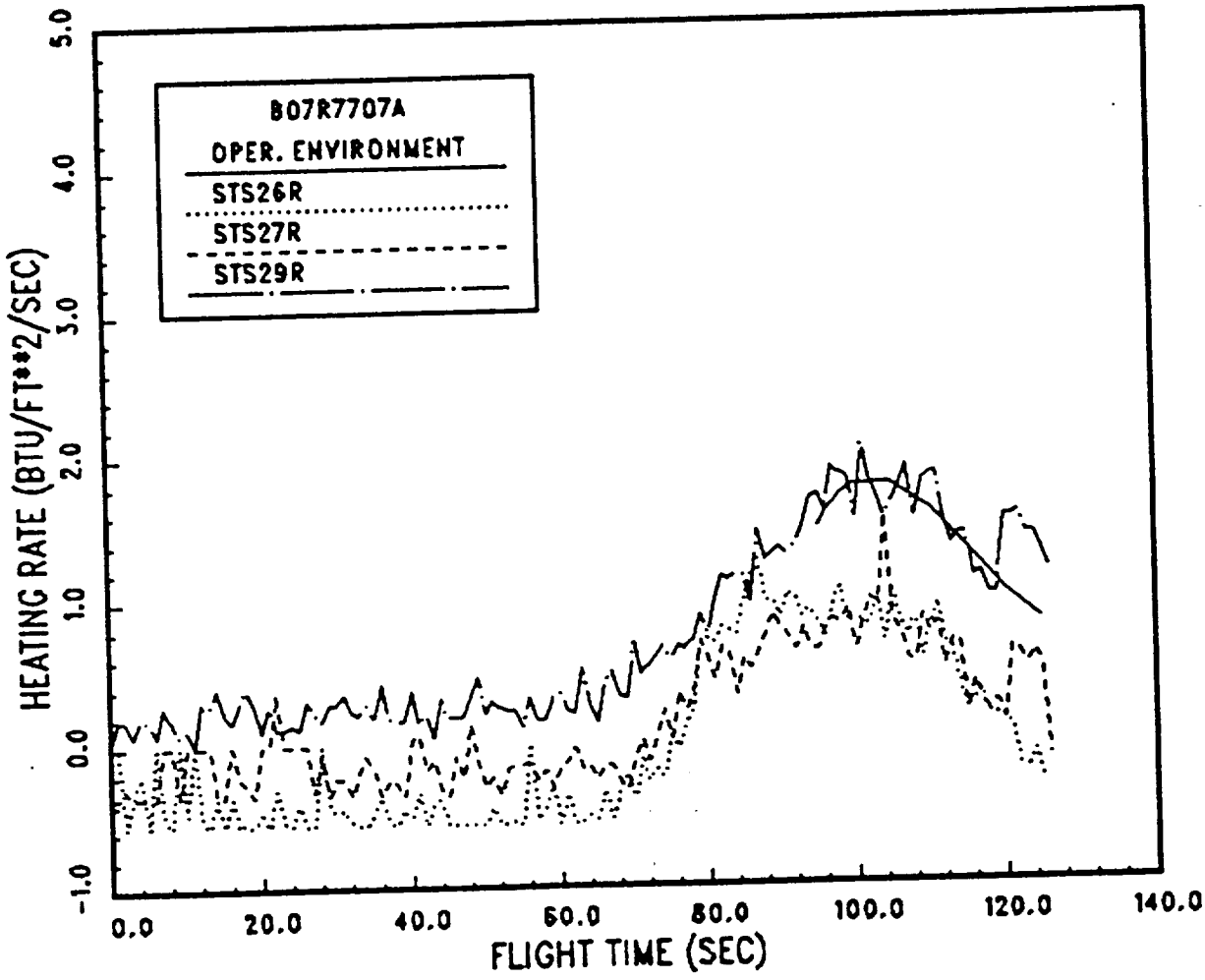

c) B07R7707 θ_B = 270 Deg

Figure 9: SRB Base Heating Environment — Q_c vs. Time — Aft Skirt (Concluded)

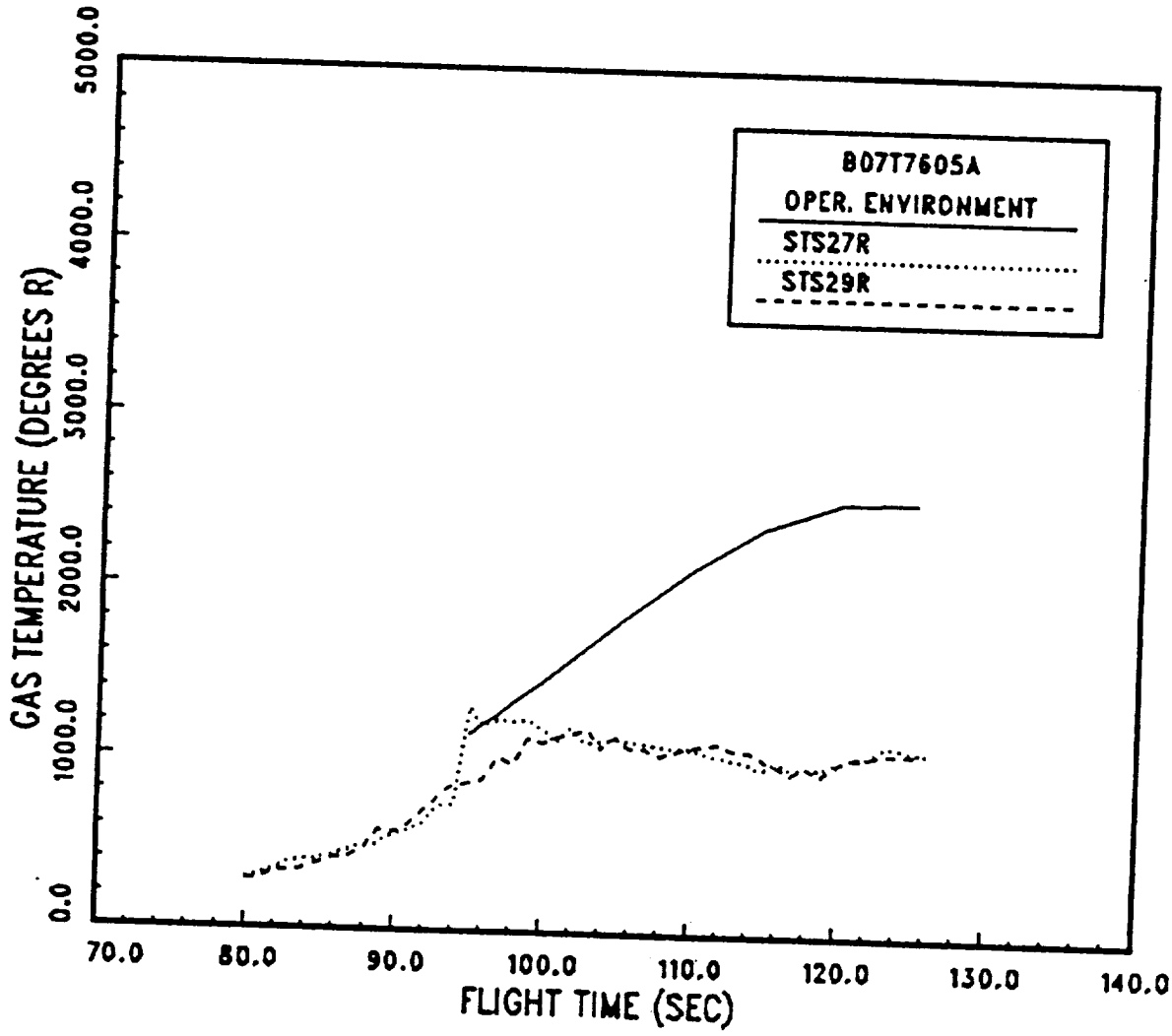

Figure 10: SRB Base Heating Environment — Base Gas Recovery Temperature vs. Time — Aft Skirt

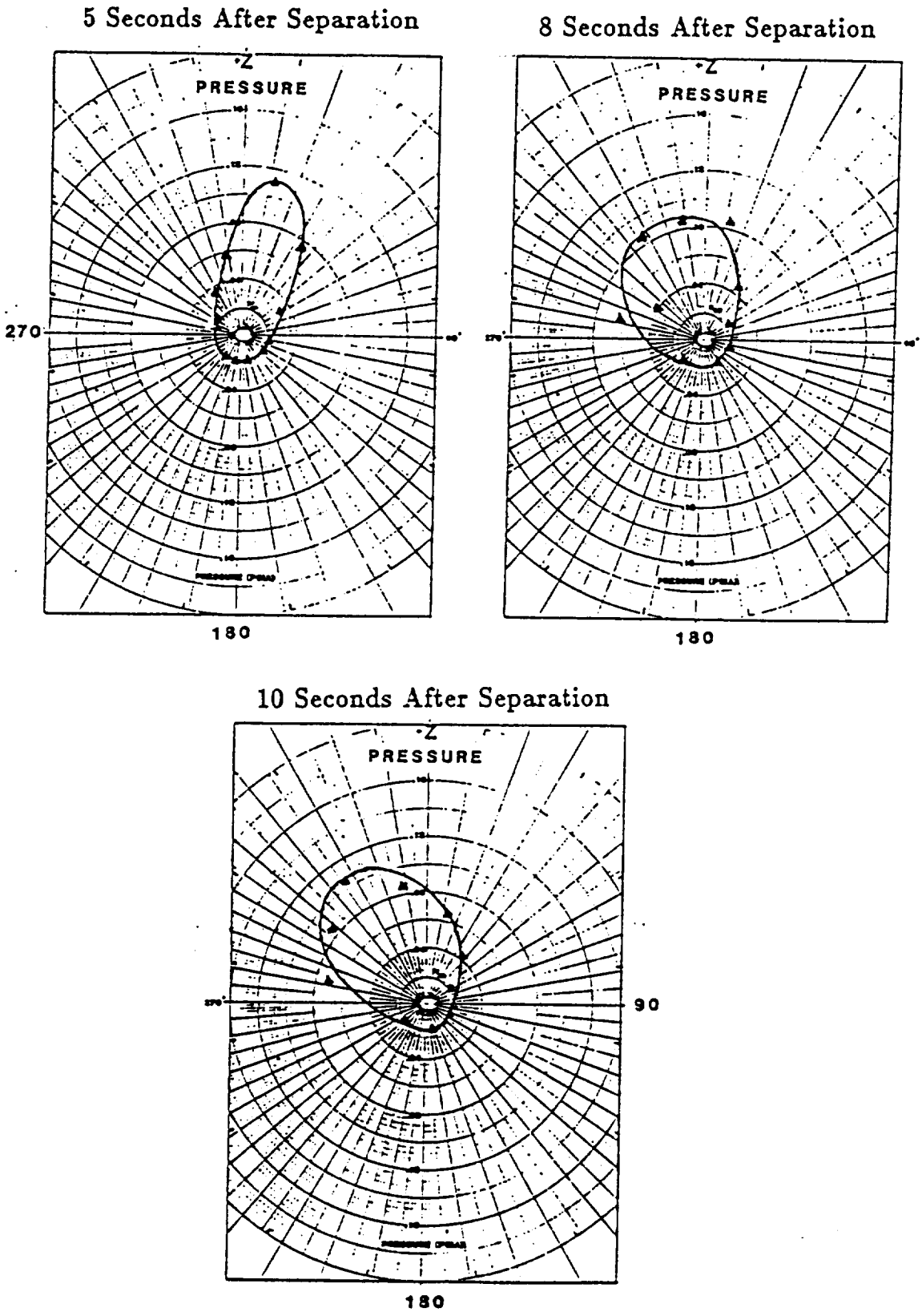

Figure 11: Roll Effect on Plume Impingement
Heating of the SRB Aft Skirt Following Separation

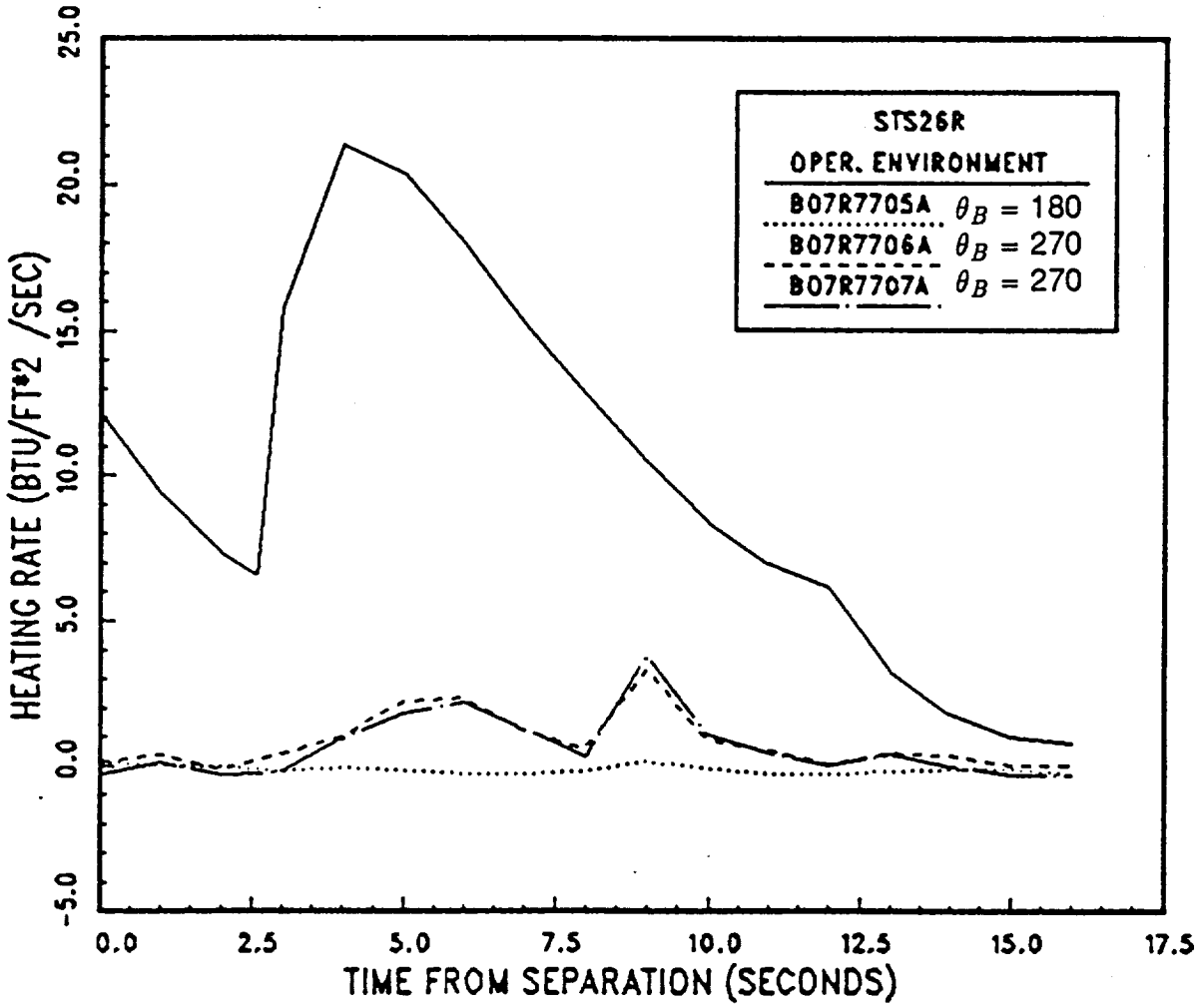

Figure 12: STS-26R Convective Heating Environment to SRB Aft Skirt for 16 Seconds Following Separation

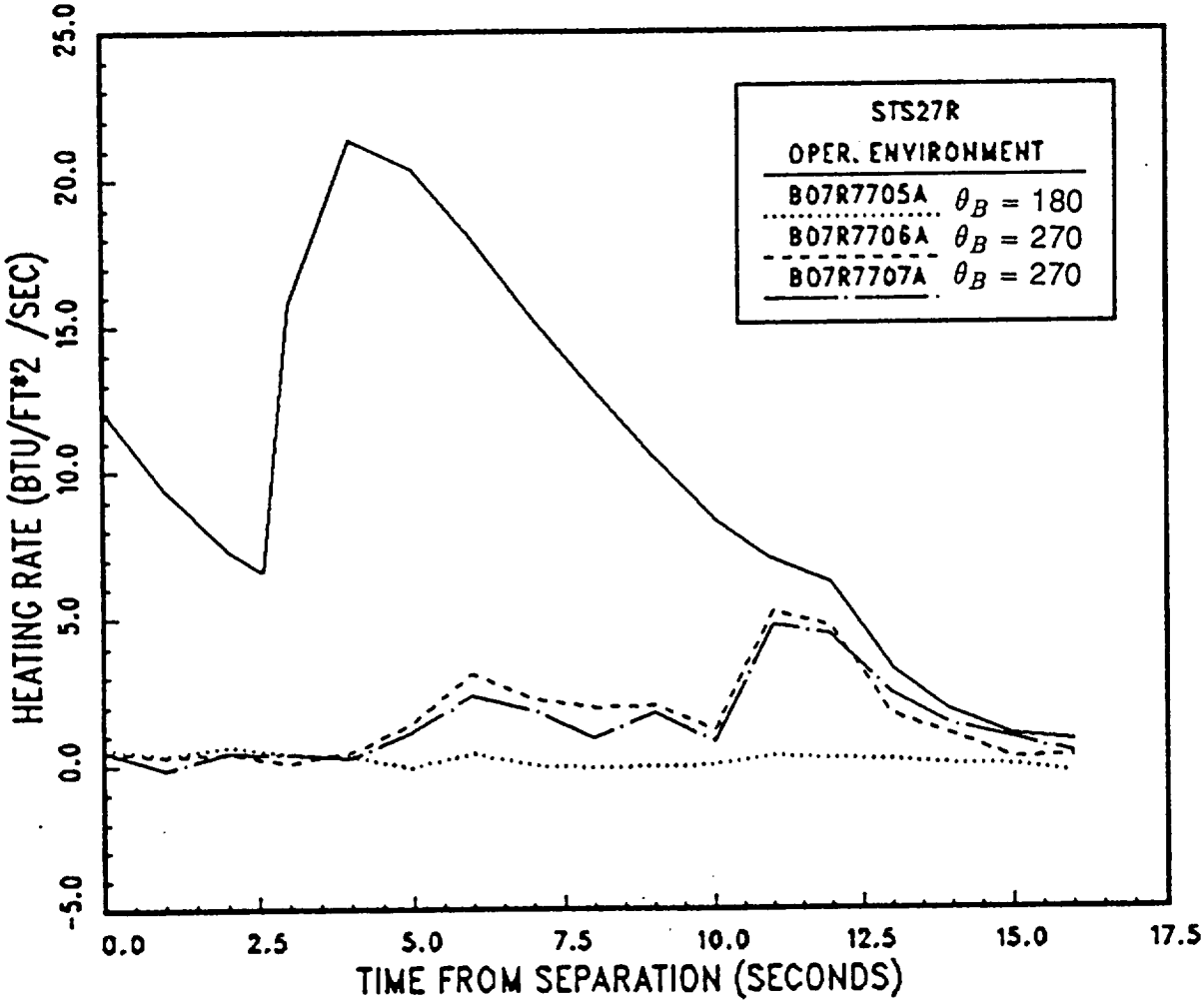

Figure 13: STS-27R Convective Heating Environment to SRB Aft Skirt for 16 Seconds Following Separation

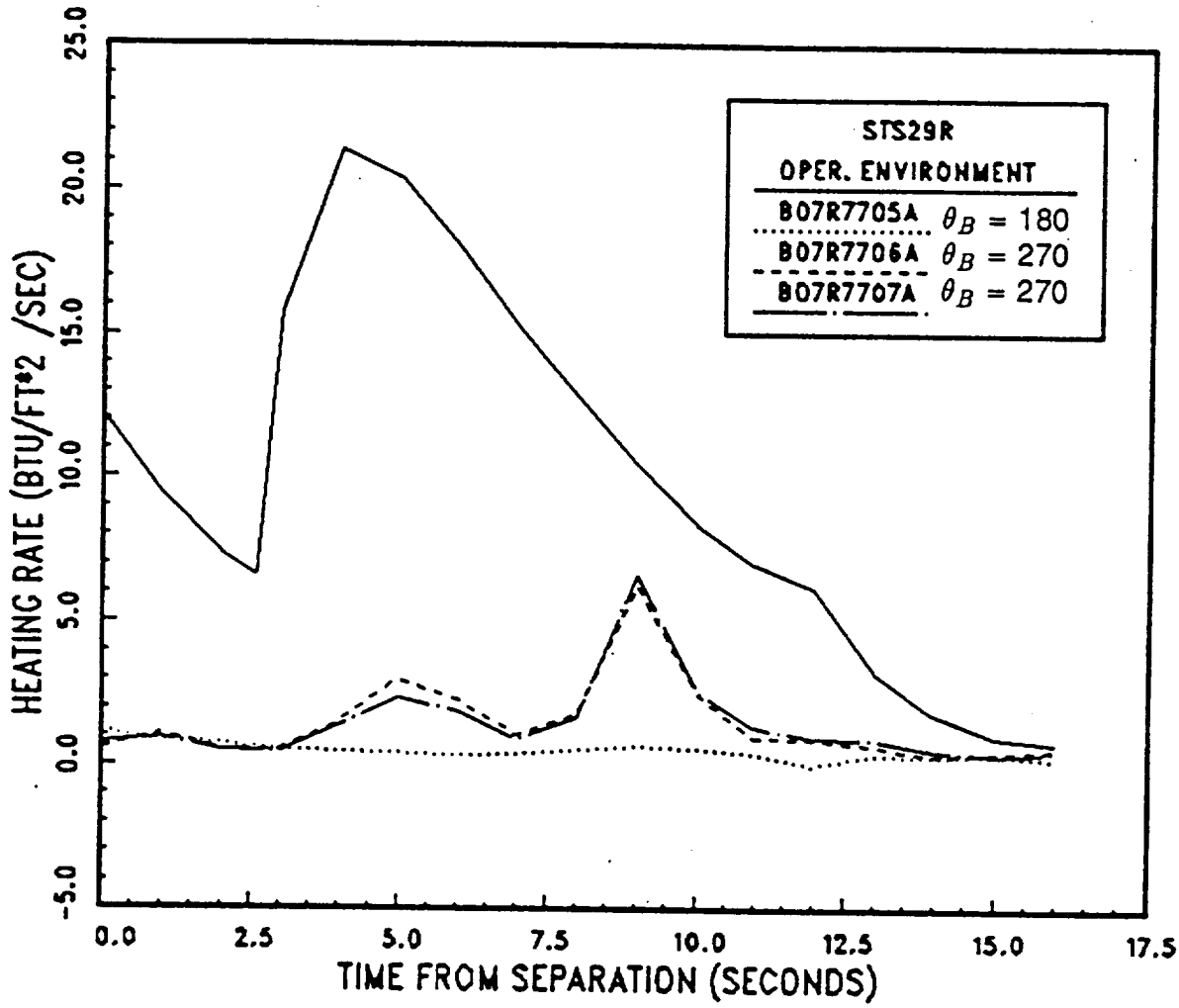

Figure 14: STS-29R Convective Heating Environment to SRB Aft Skirt for 16 Seconds Following Separation

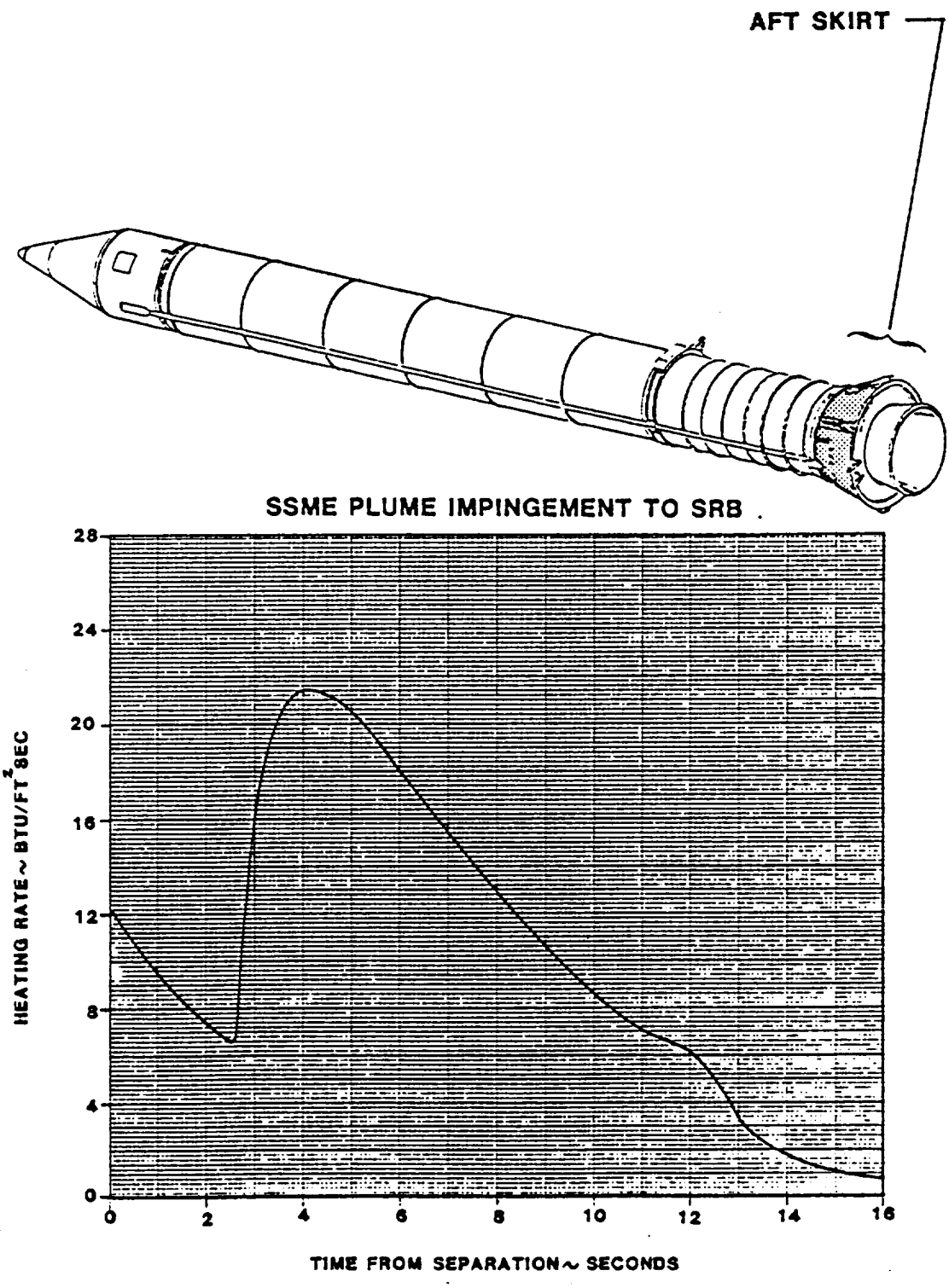

Figure 15: Convective Heating Environment to SRB Aft Skirt for 16 Seconds Following Separation

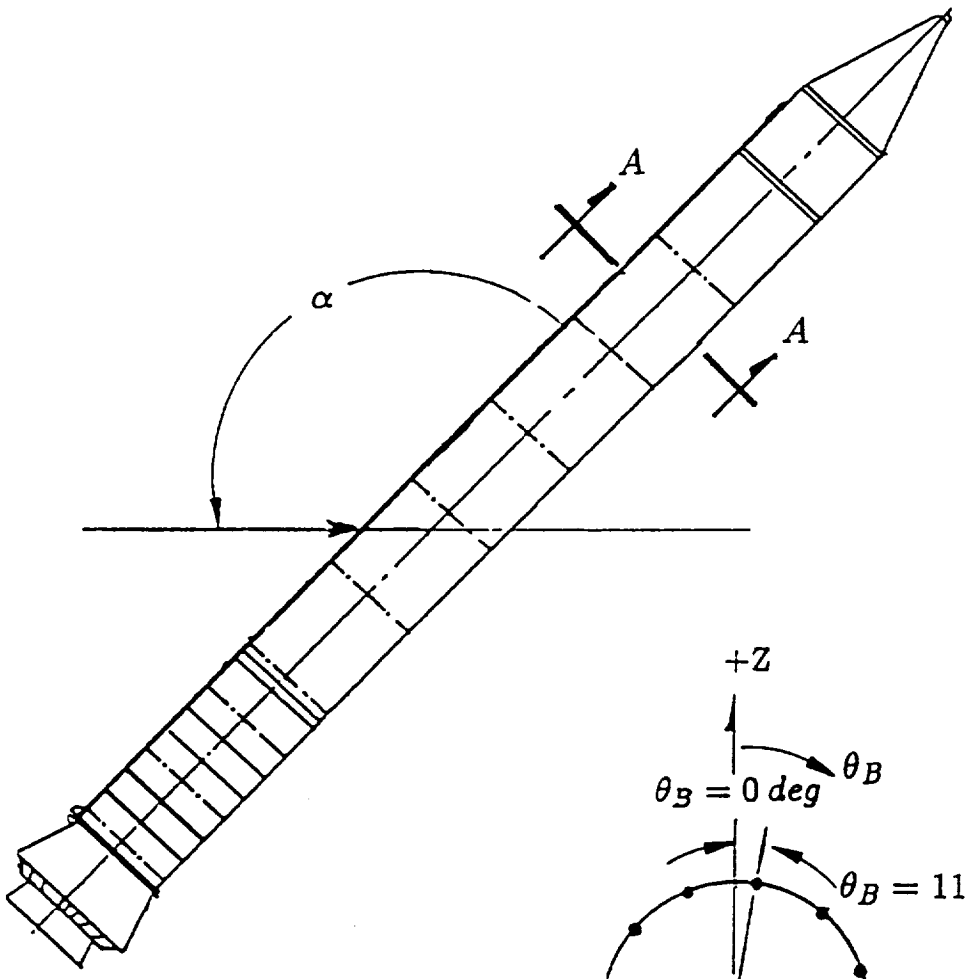

a) Angle-of-Attack

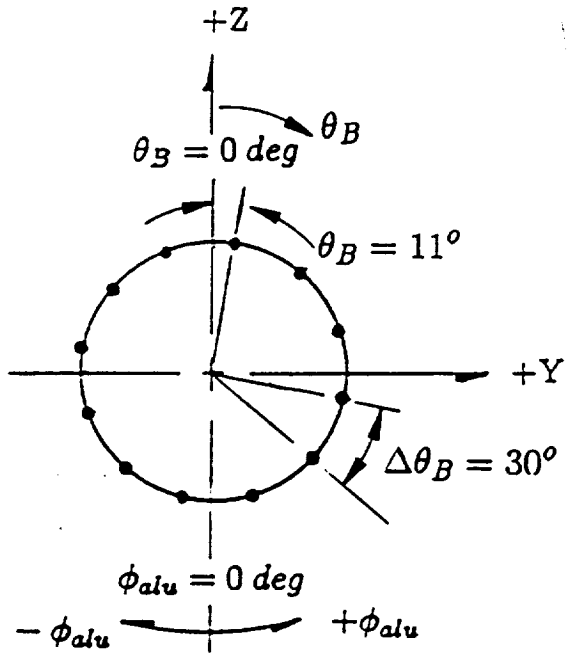

Section A – A
$X_B = 763in$

b) Roll Angle

Figure 16: Angle-of-Attack and Roll Definition

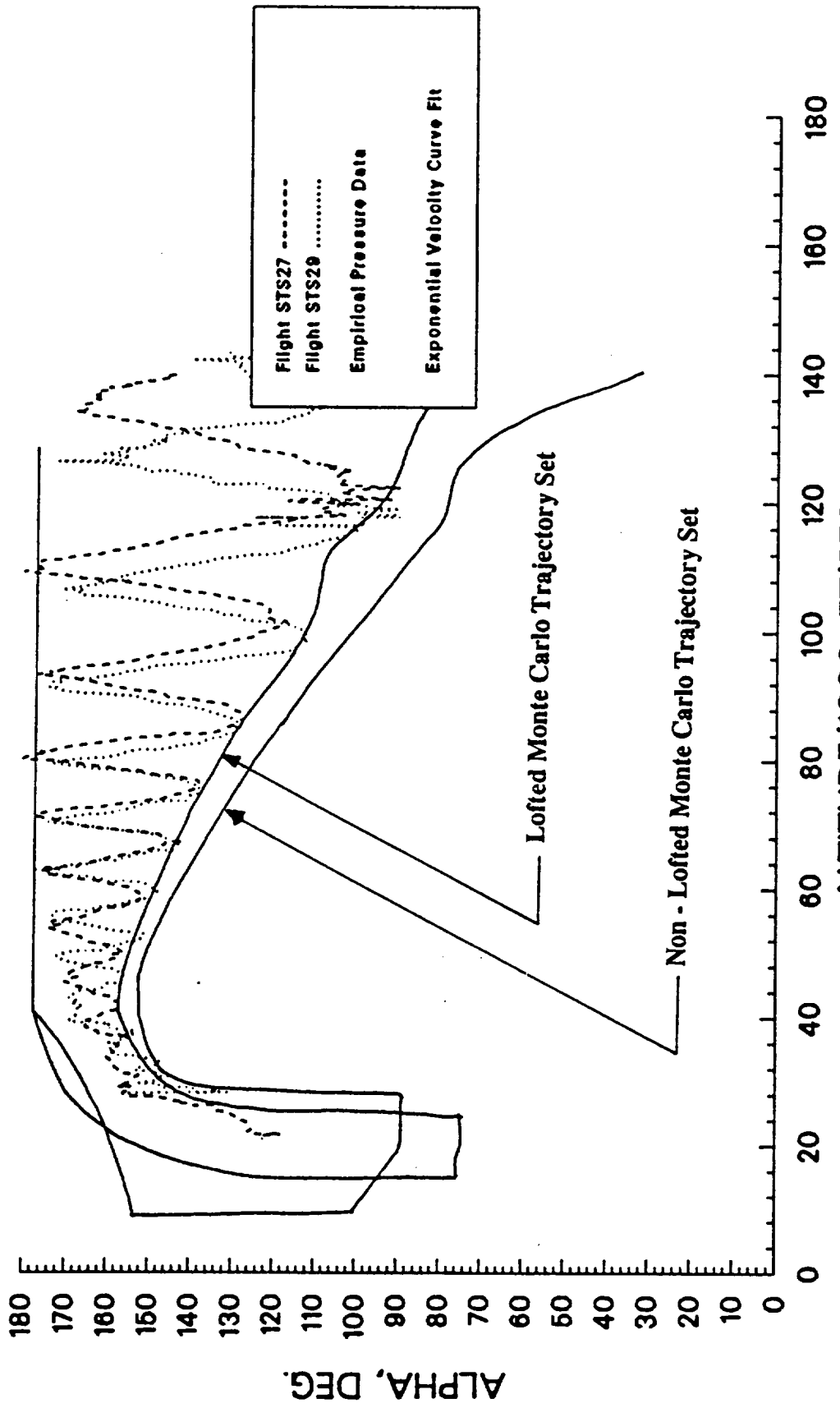

Figure 17: Comparison of STS-27R and 29R Reentry Angle-of-Attack with the Design Trajectory Set

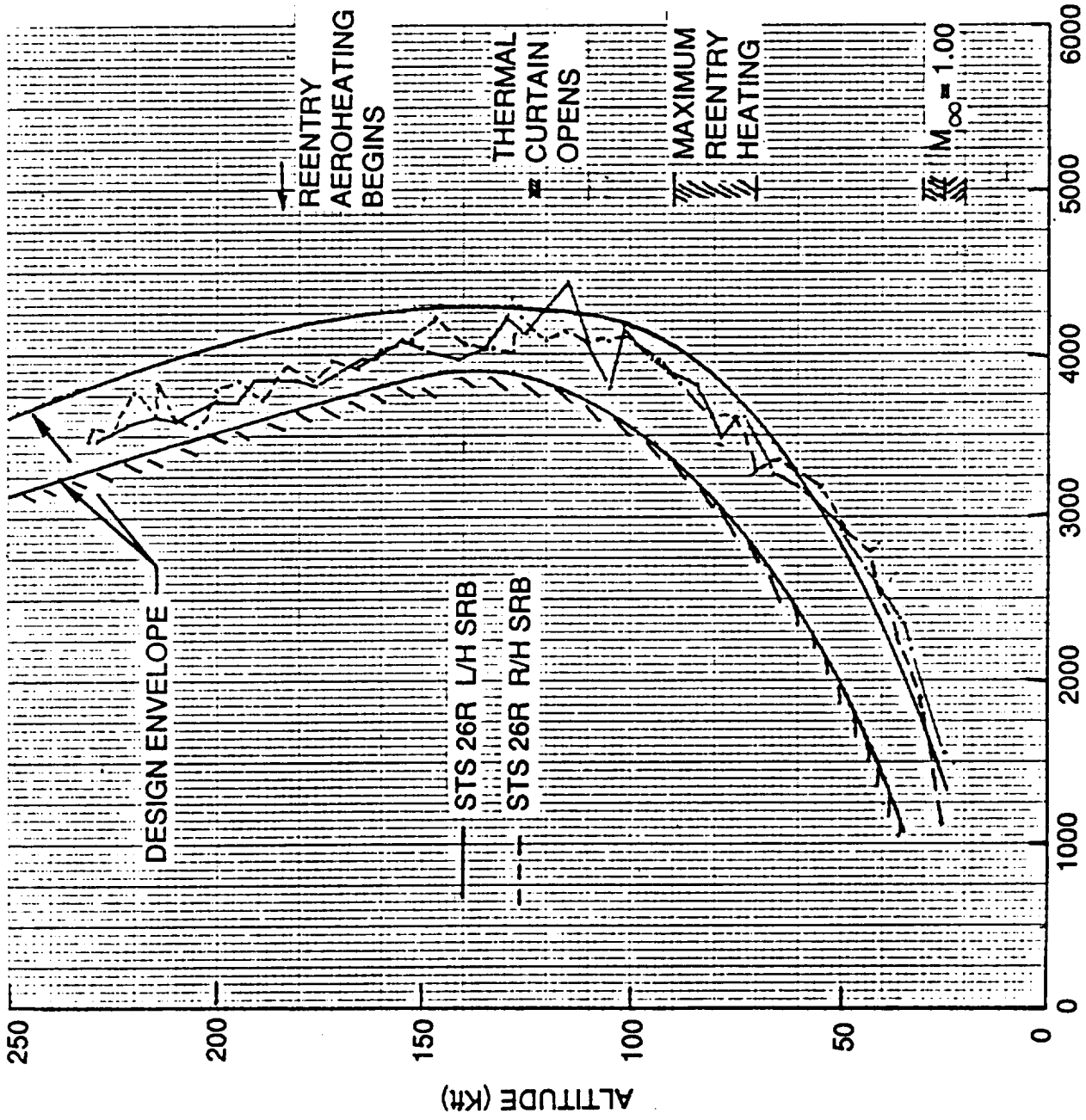

a) STS-26R

Figure 18: Reentry Trajectory Summary

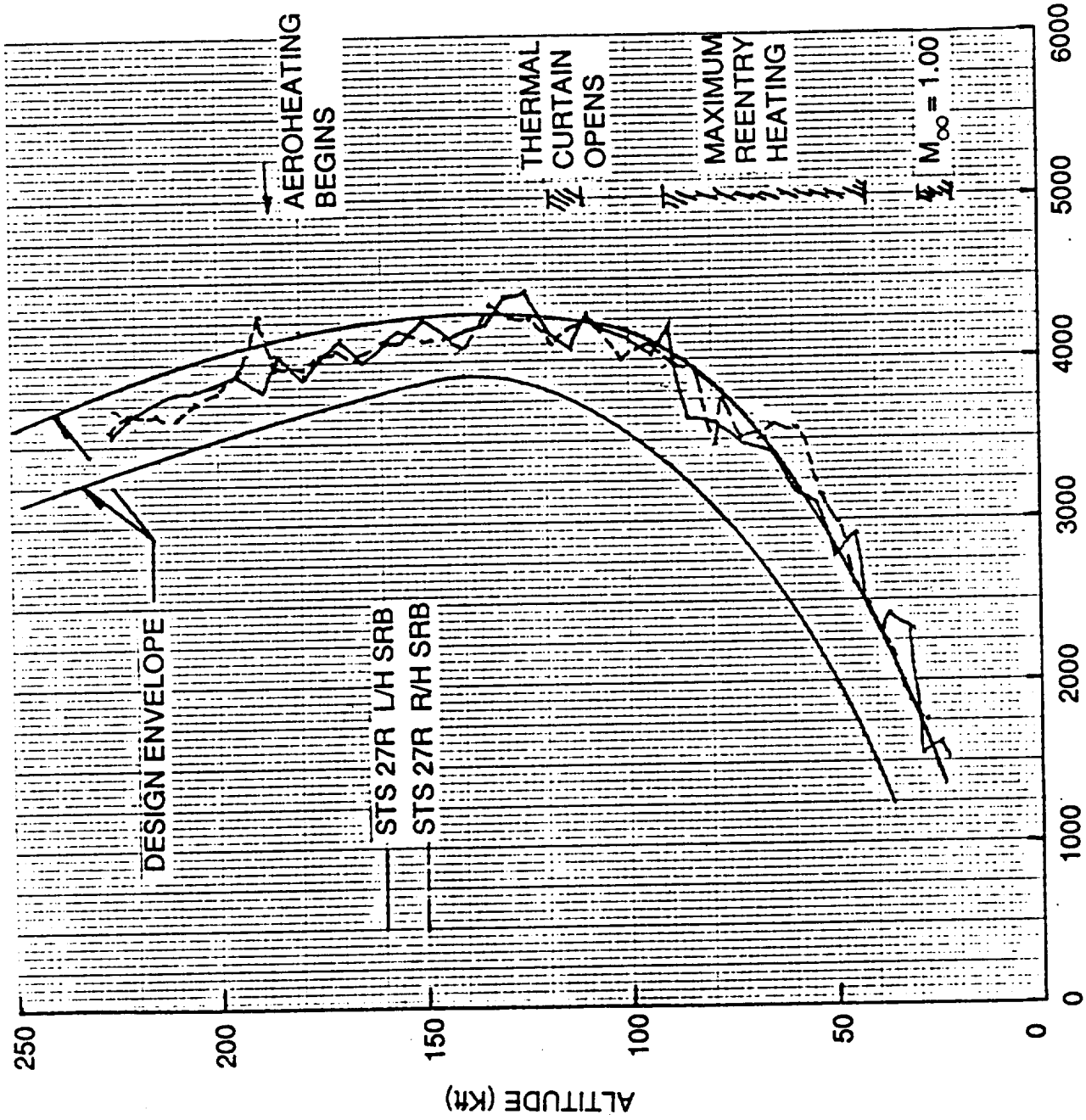

b) STS-27R

Figure 18: Reentry Trajectory Summary (Continued)

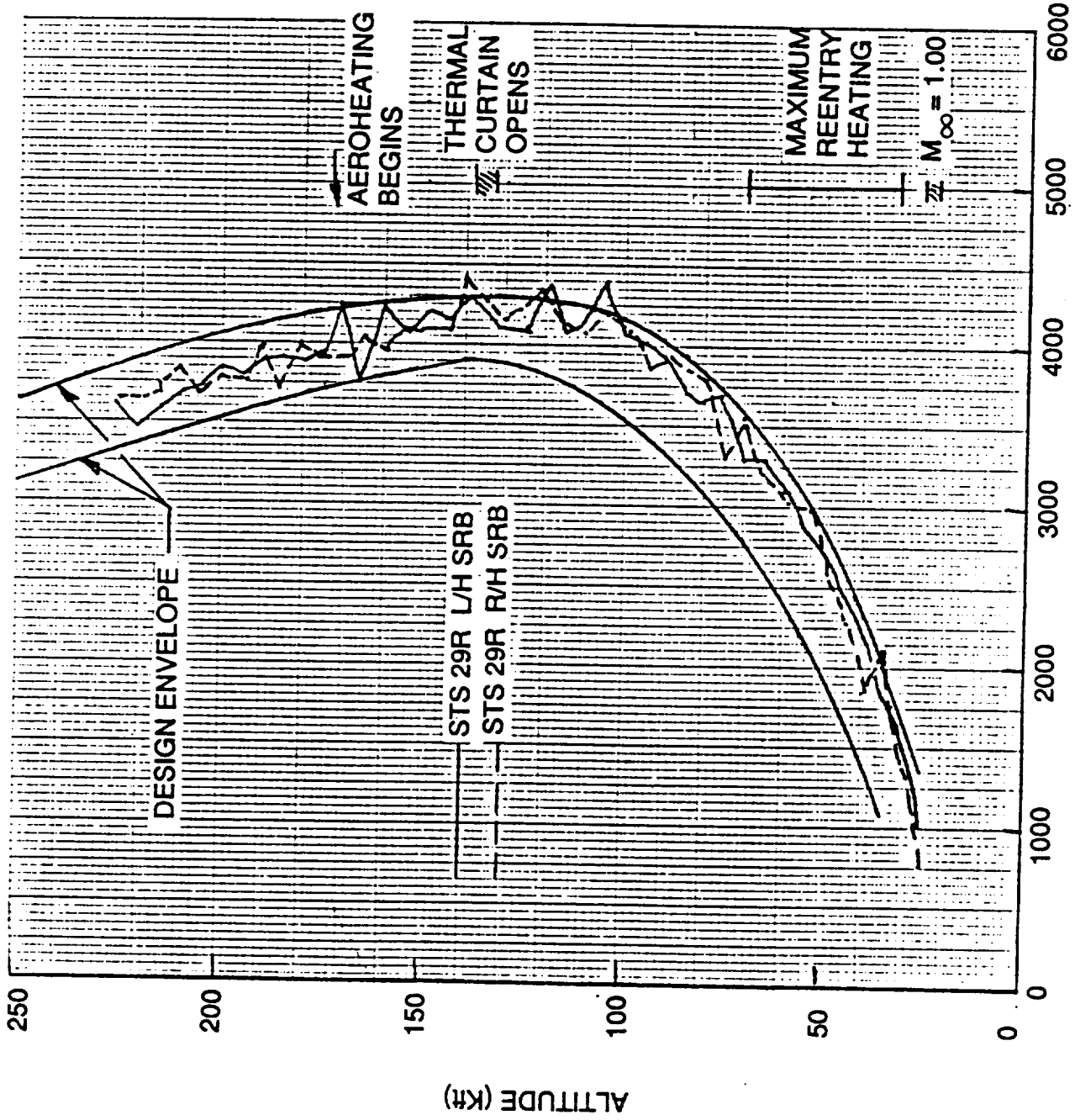

c) STS-29R

Figure 18: Reentry Trajectory Summary (Concluded)

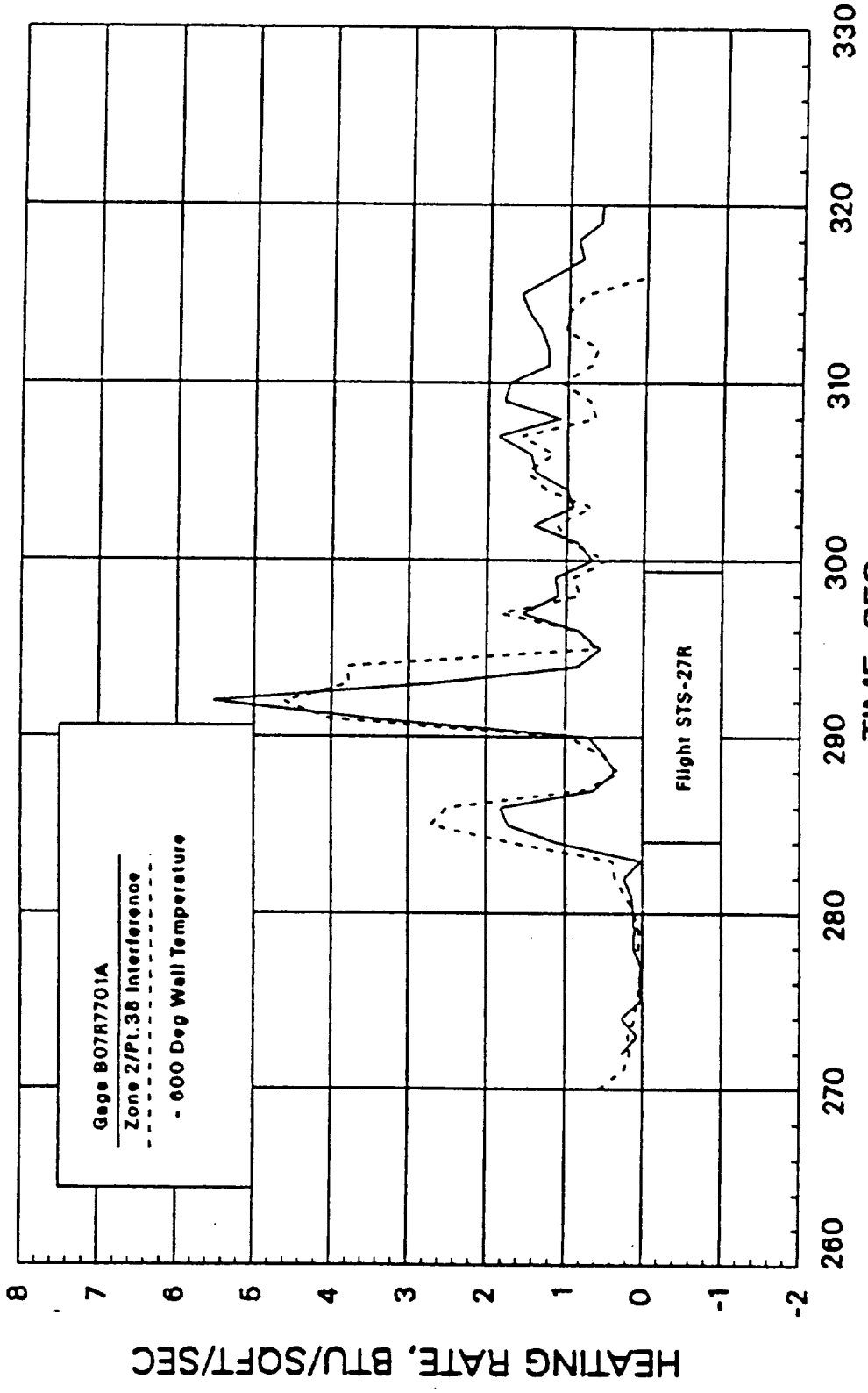

a) B07R7701 — Nose Cone

Figure 19: External Reentry Flight Heating Validation STS-27R

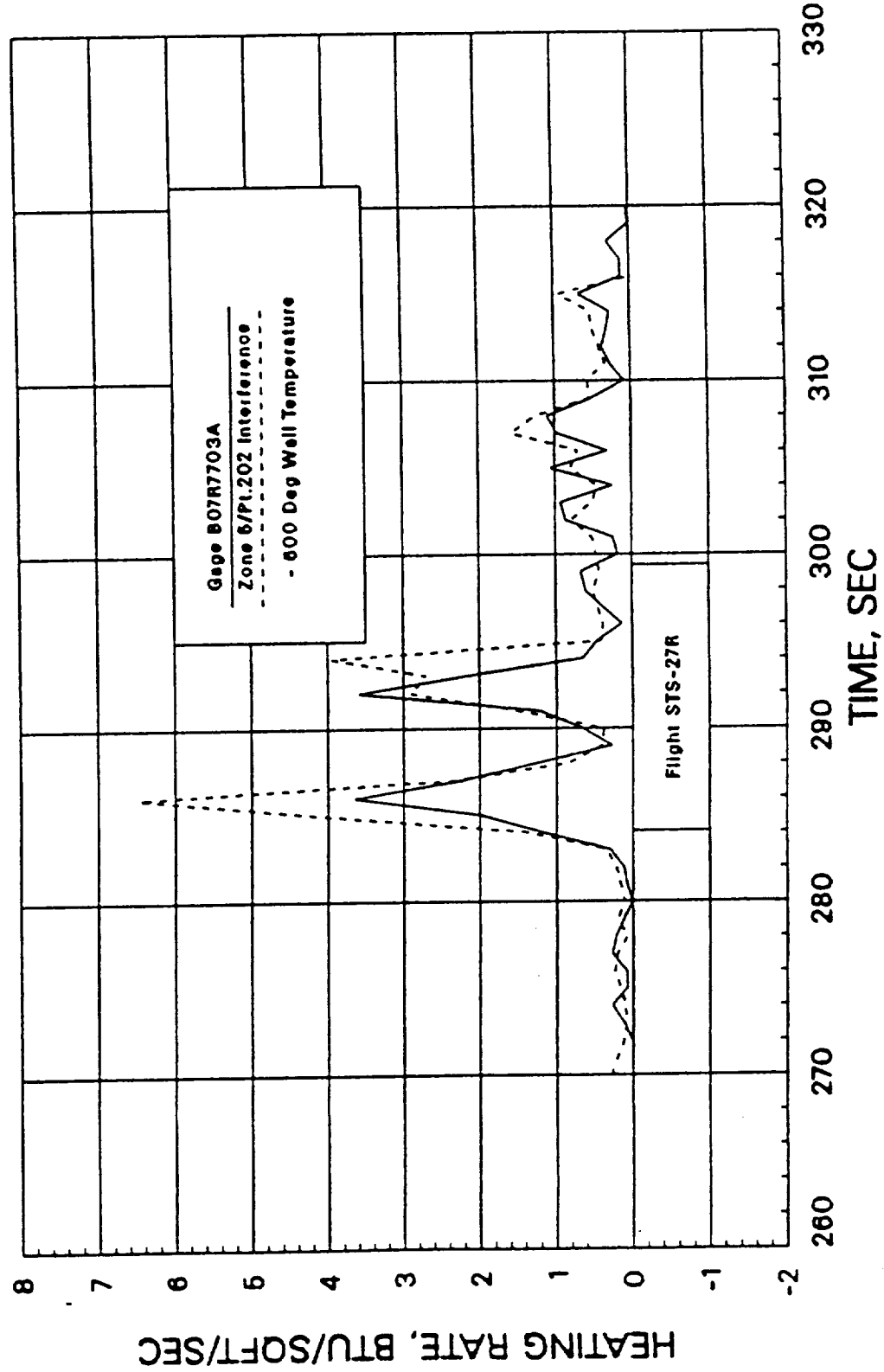

b) B07R7703 — Attach Ring

Figure 19: External Reentry Flight Heating Validation STS-27R (Concluded)

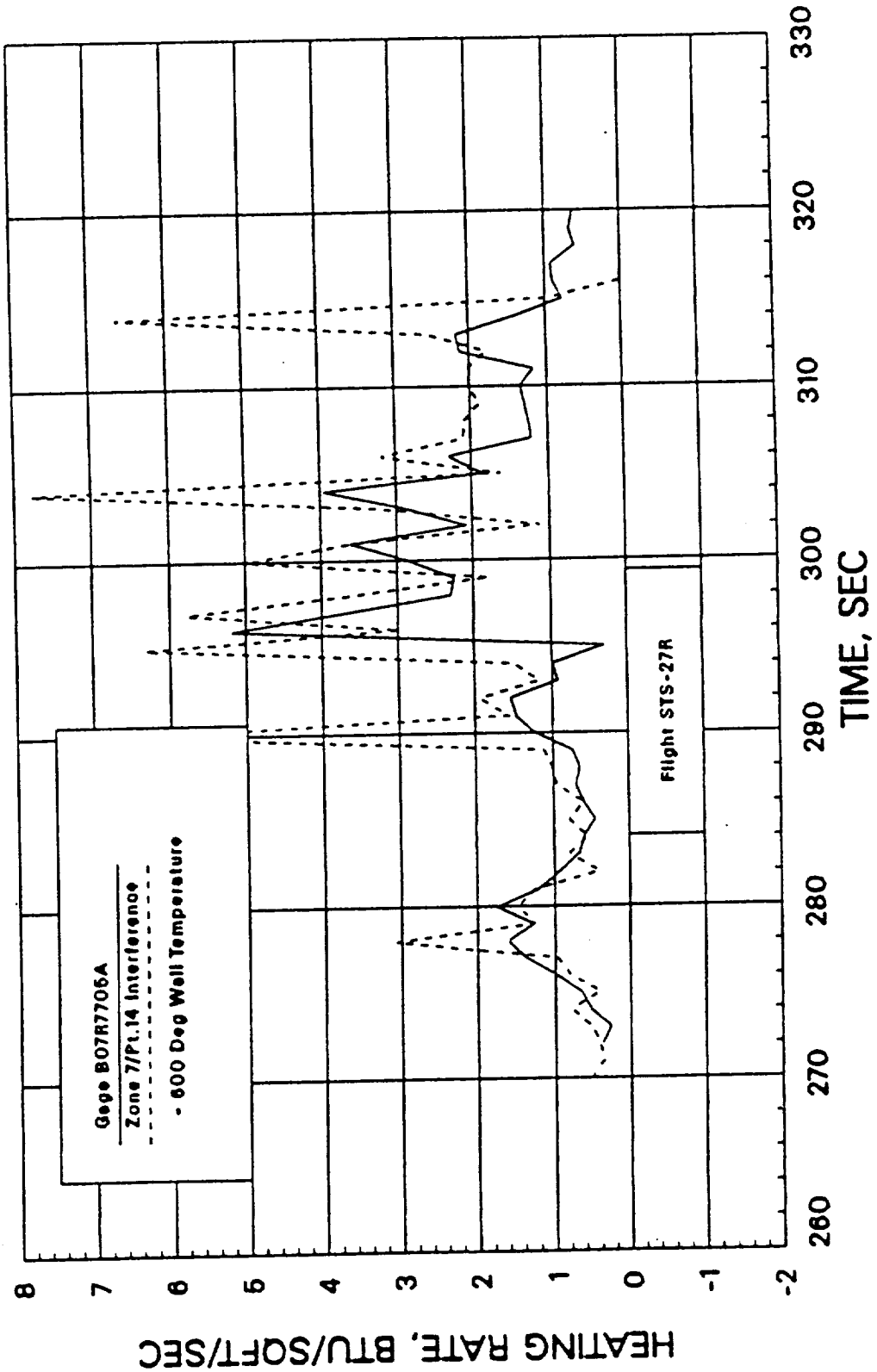

a) B07R7705 — Aft Skirt θ_B = 180 Deg

Figure 20: External Reentry Flight Heating Validation STS-27R

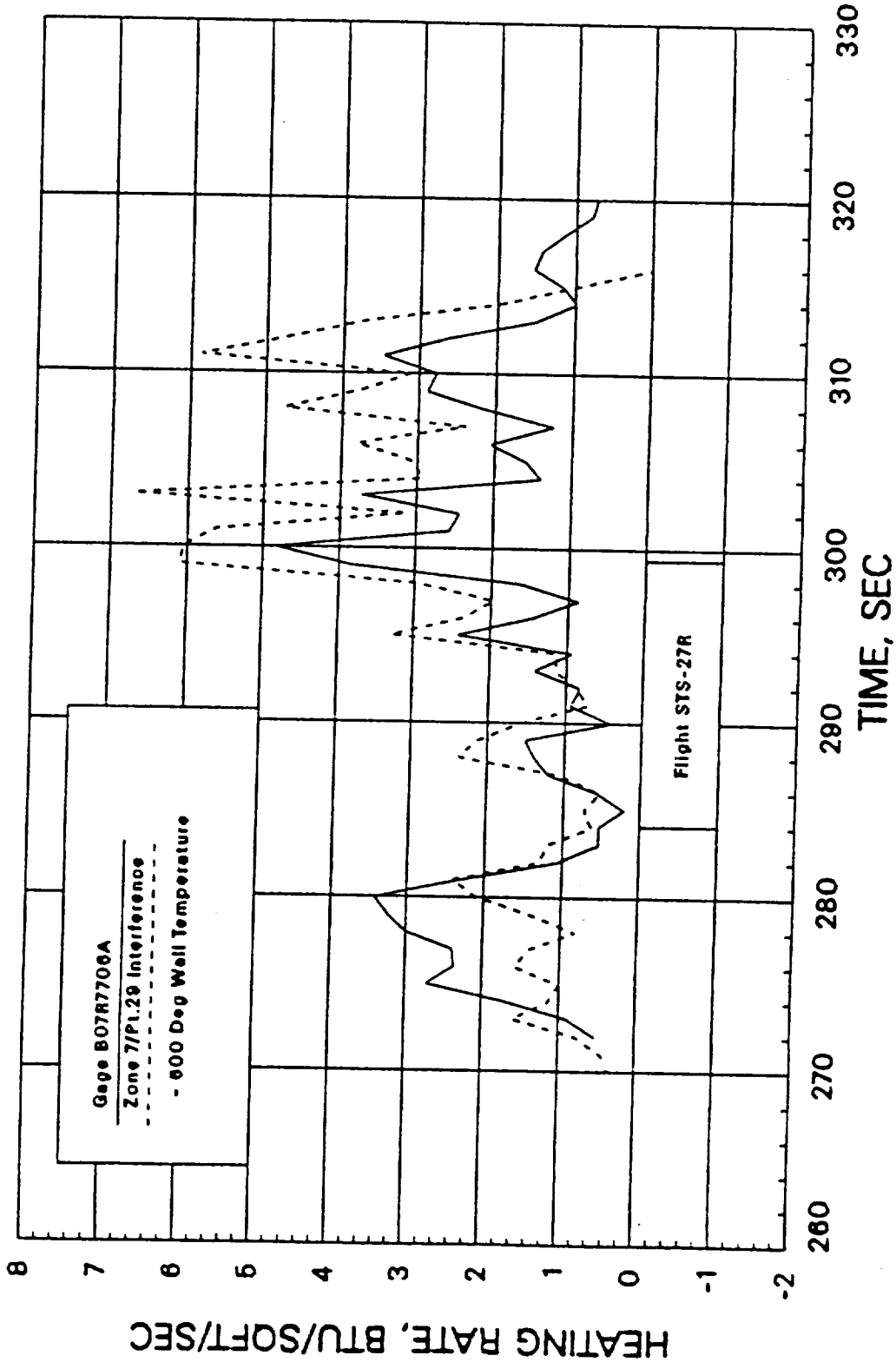

b) B07R7706 — Aft Skirt θ_B = 270 Deg

Figure 20: External Reentry Flight Heating Validation STS-27R (Continued)

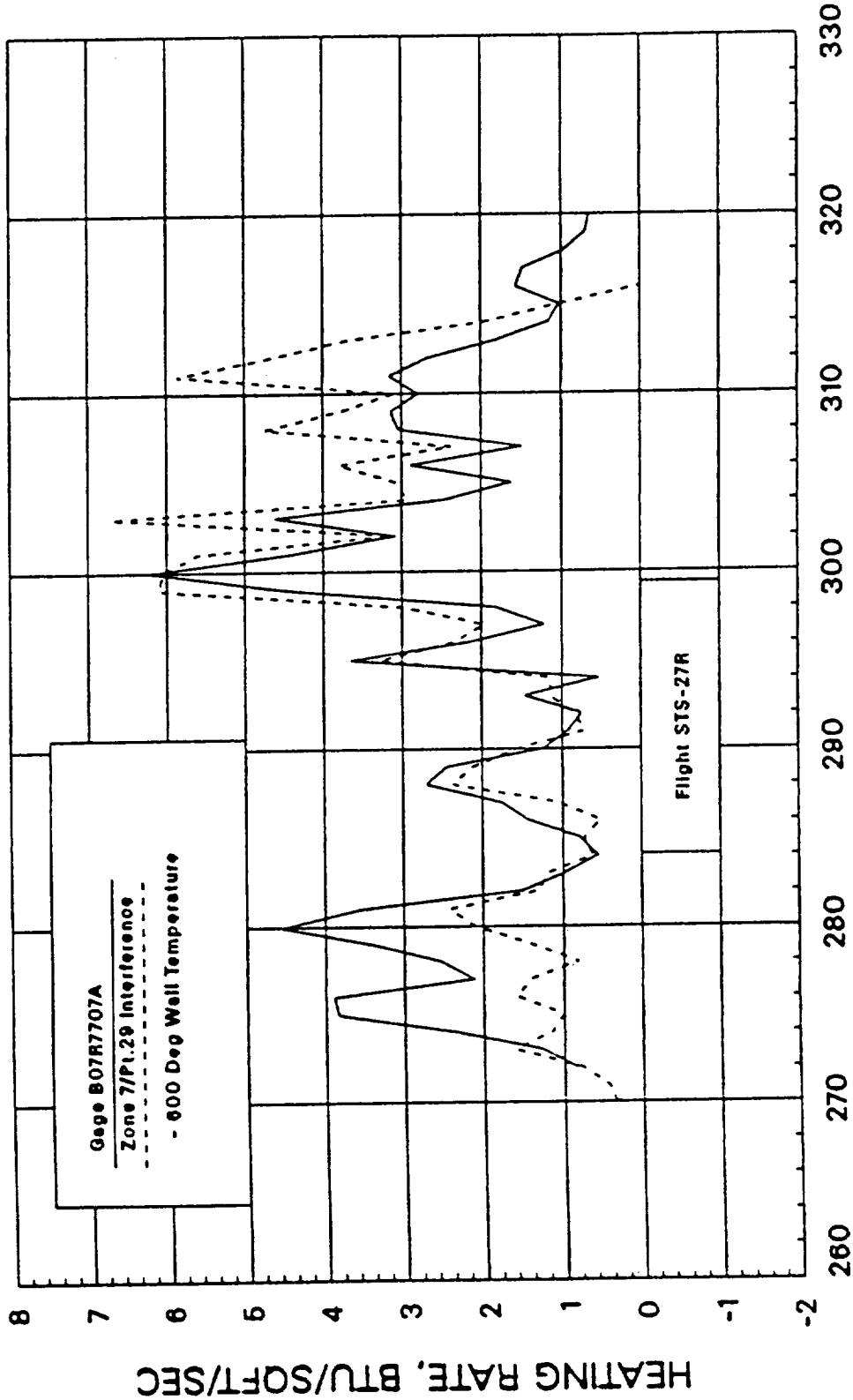

c) B07R7707 — Aft Skirt θ_B = 270 Deg

Figure 20: External Reentry Flight Heating Validation STS-27R (Concluded)

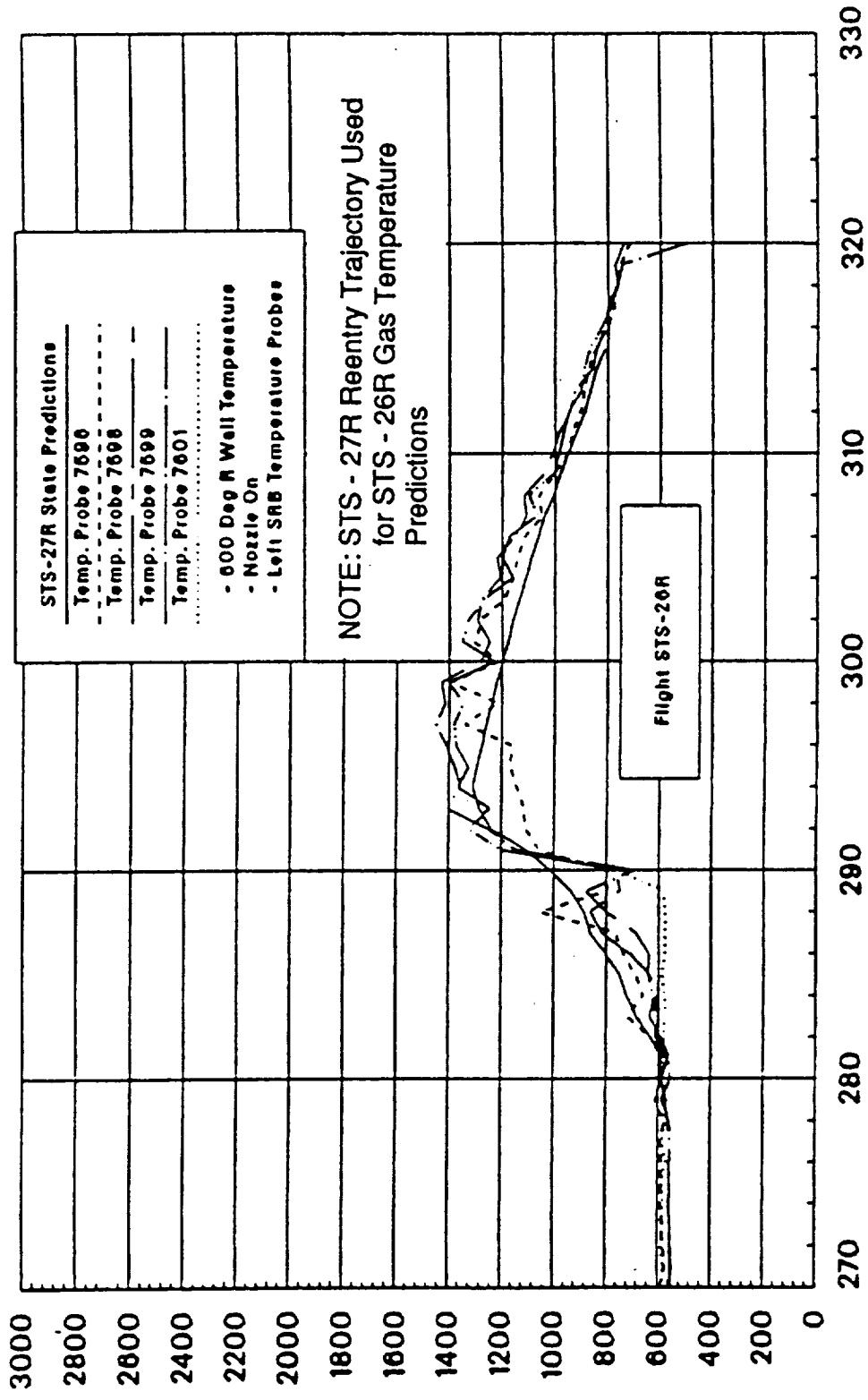

a) Left Hand SRB — STS 26R

Figure 21: SRB Internal Aft Skirt Gas Temperature Comparison

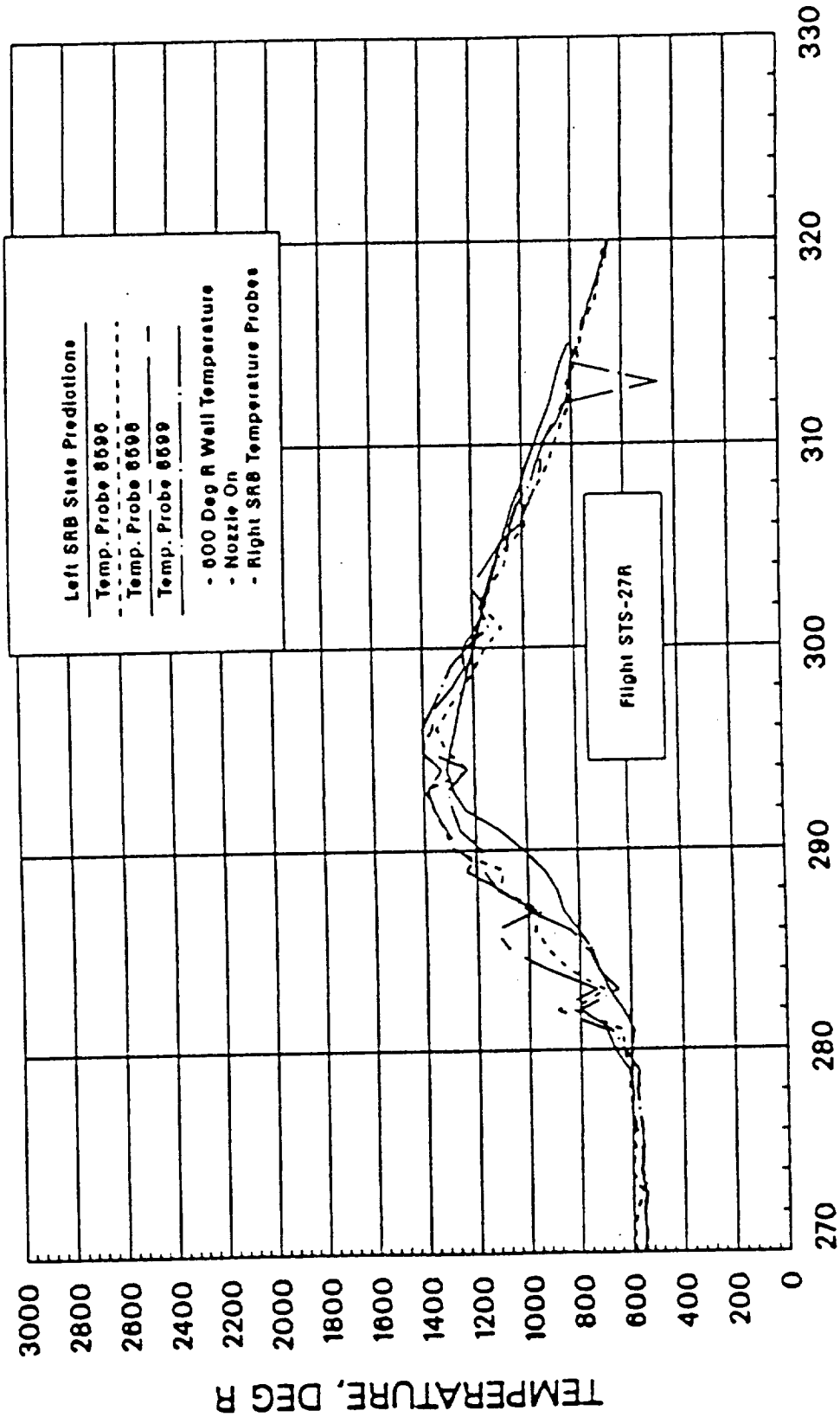

b) Right Hand SRB — STS 27R

Figure 21: SRB Internal Aft Skirt Gas Temperature Comparison (Concluded)

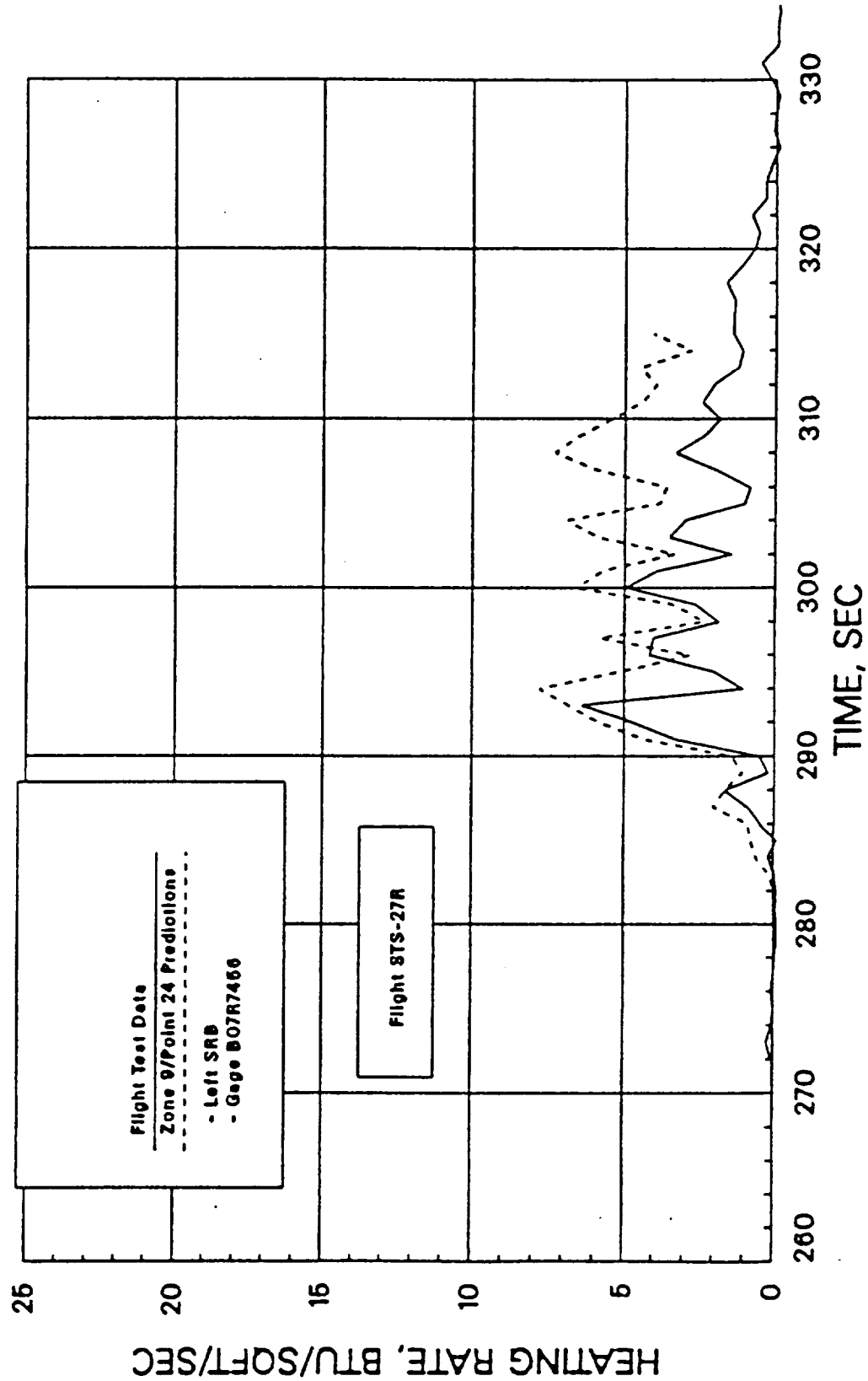

Figure 22: Internal Aft Skirt Heating Rate Validation (B07R7456 STS-27R) Using the STATE Gas Temperature Algorithm

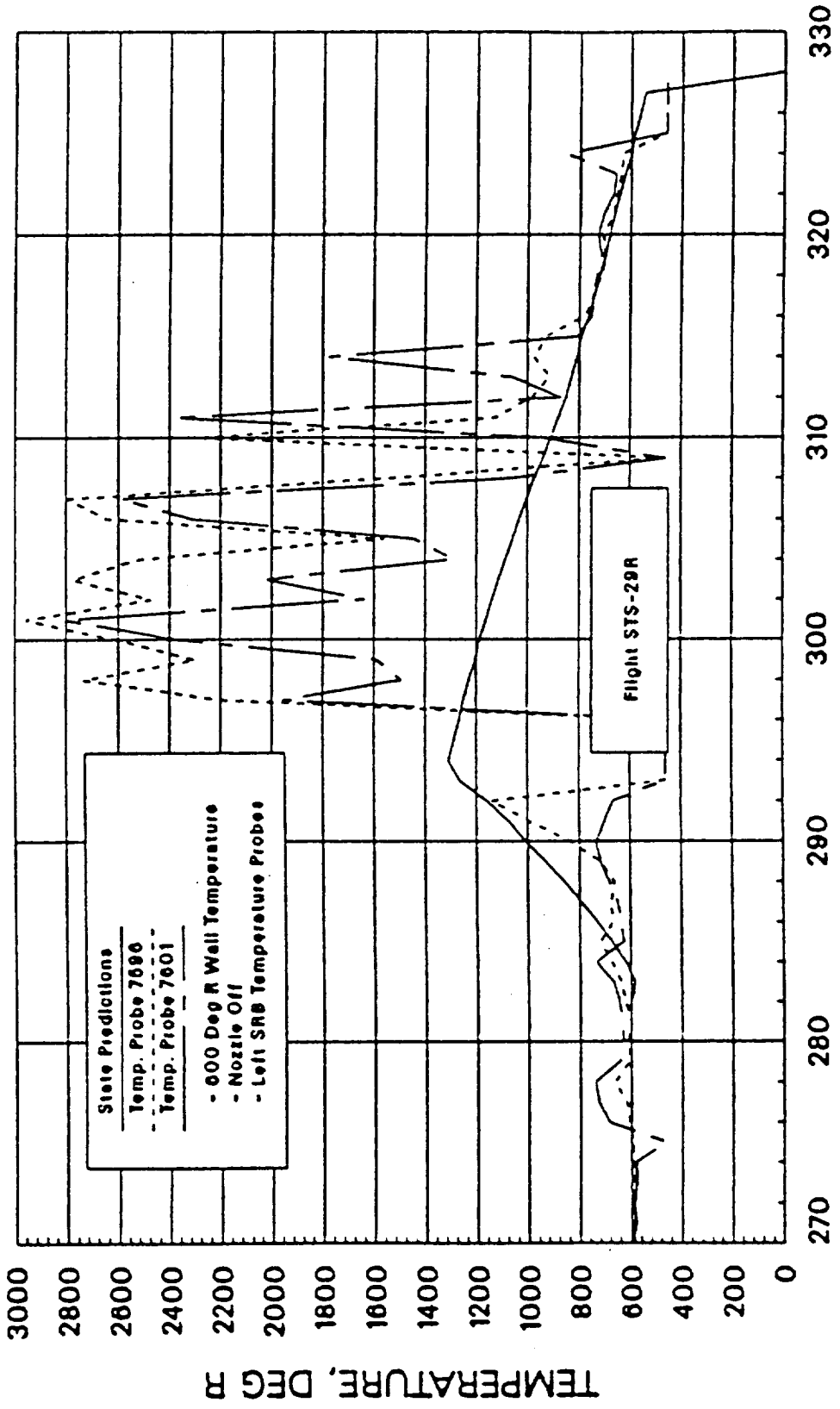

a) Left Hand SRB

Figure 23: SRB Internal Aft Skirt Gas Temperature STS-29R

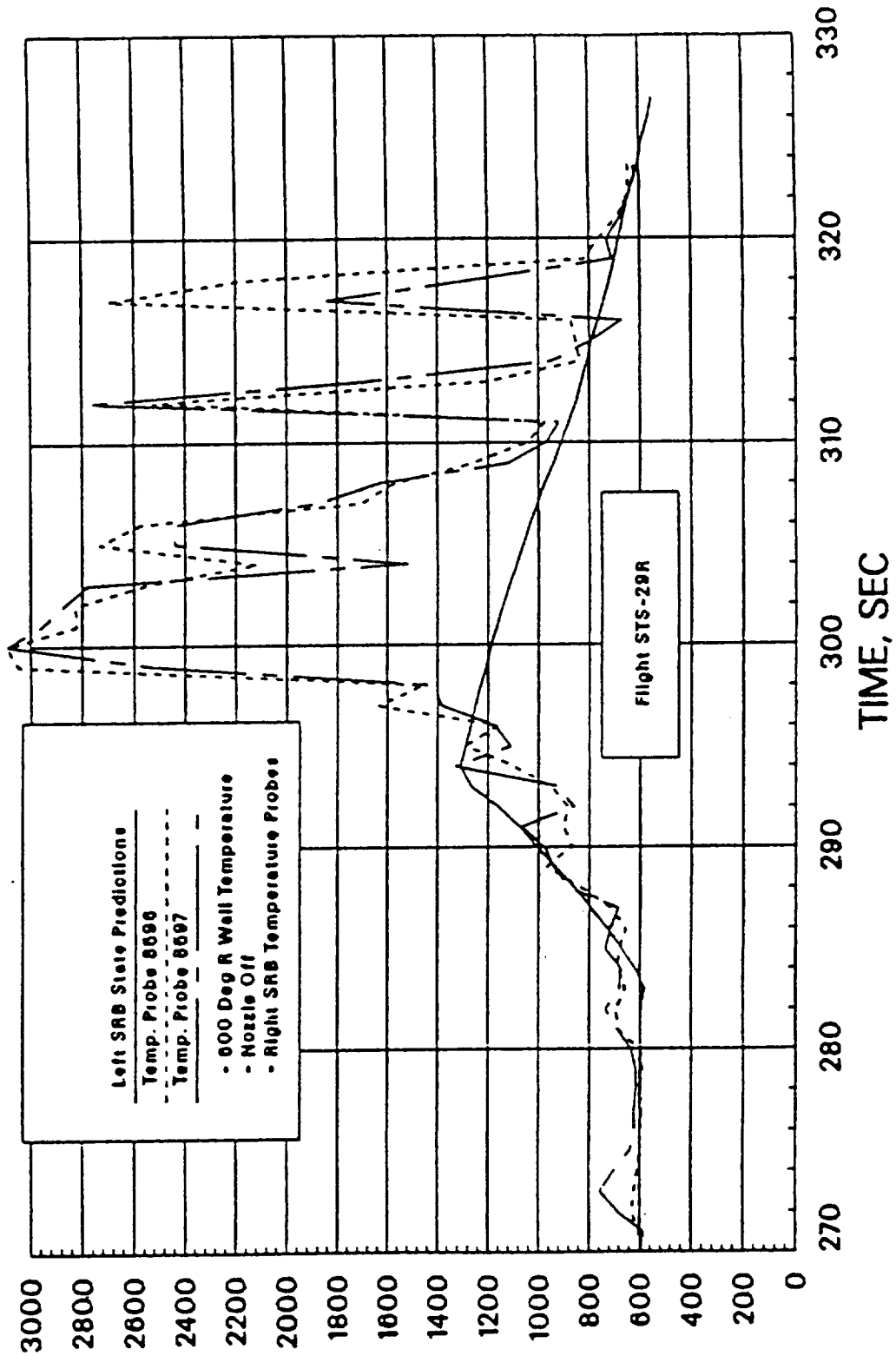

b) Right Hand SRB

Figure 23: SRB Internal Aft Skirt Gas Temperature STS—29R (Concluded)

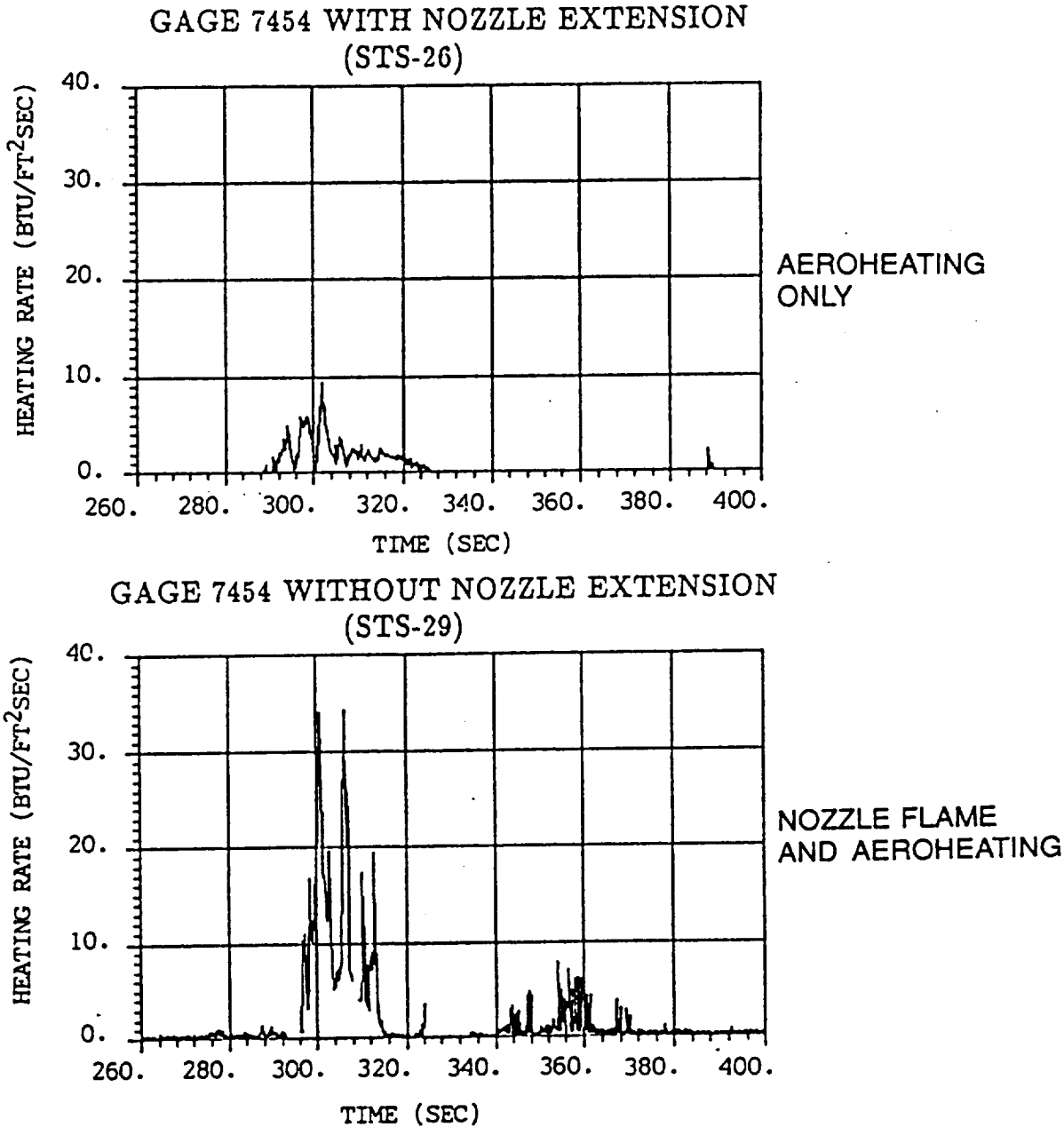

Figure 24: STS-29R Flame Entrainment Contribution to Internal Aft Skirt Reentry Heating Rates

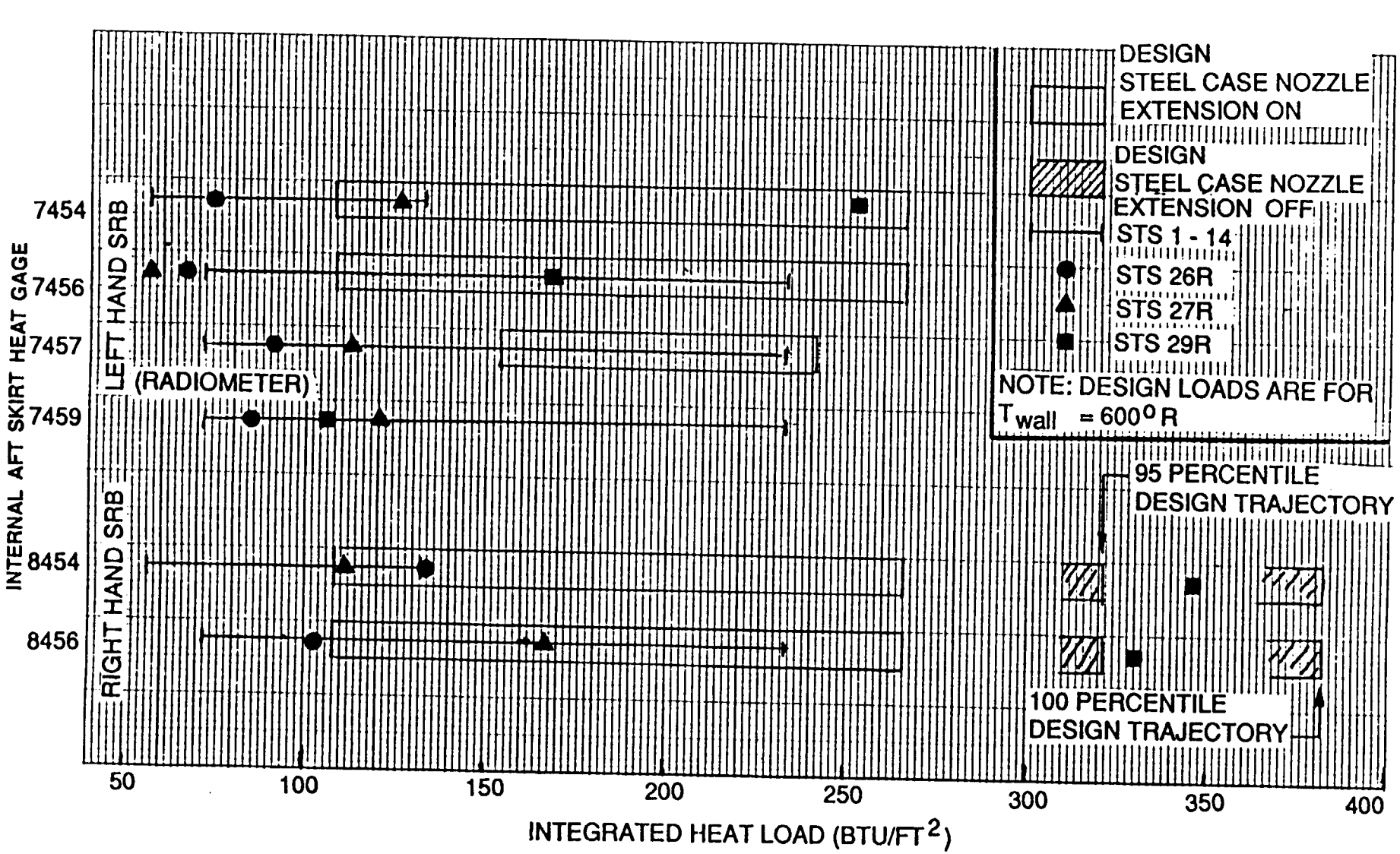

Figure 25: Internal Aft Skirt Heat Load Summary

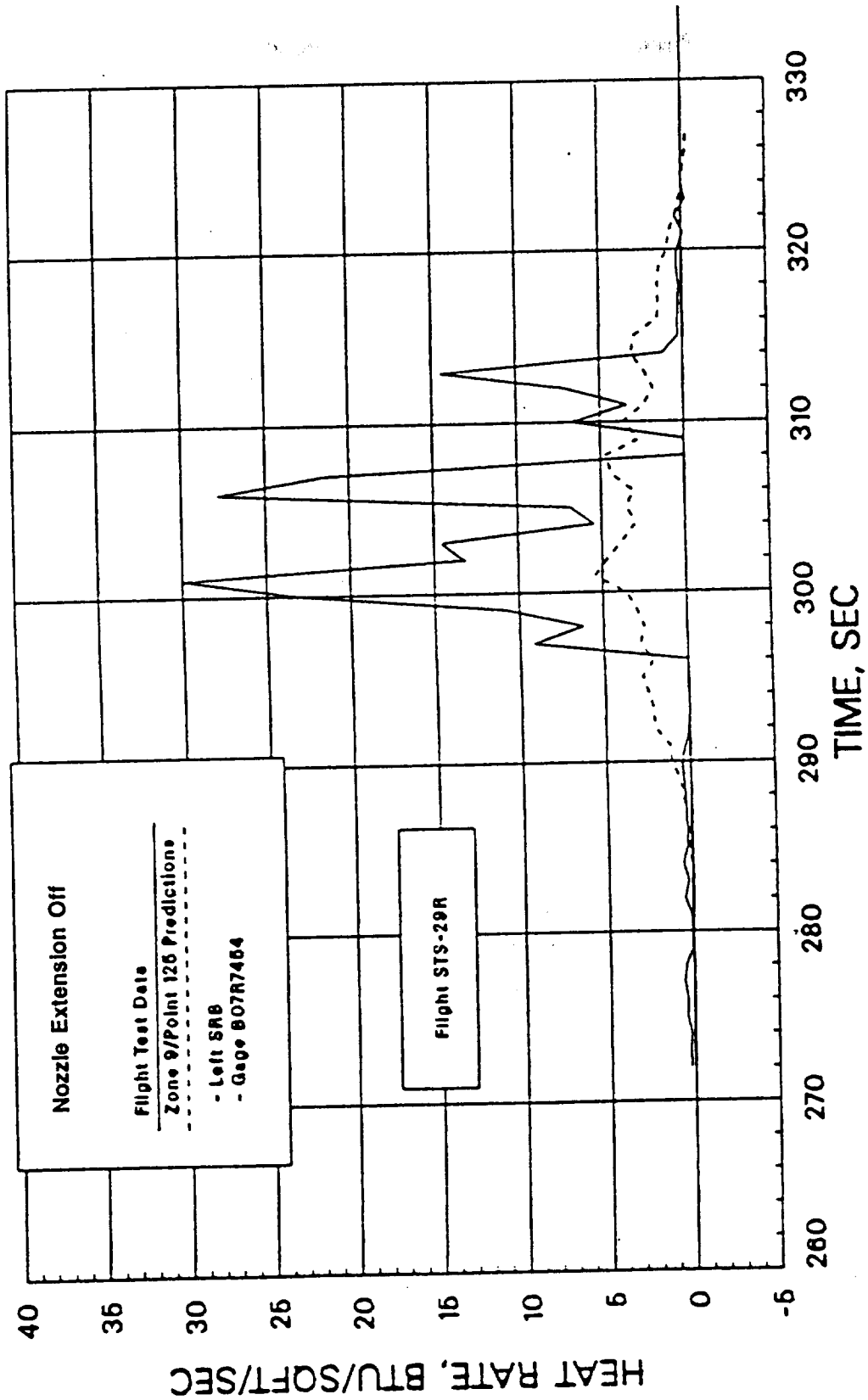

a) Using STATE Gas Temperature Algorithm

Figure 26: Internal Aft Skirt Heating Rate Validation B07R7454 STS-29R

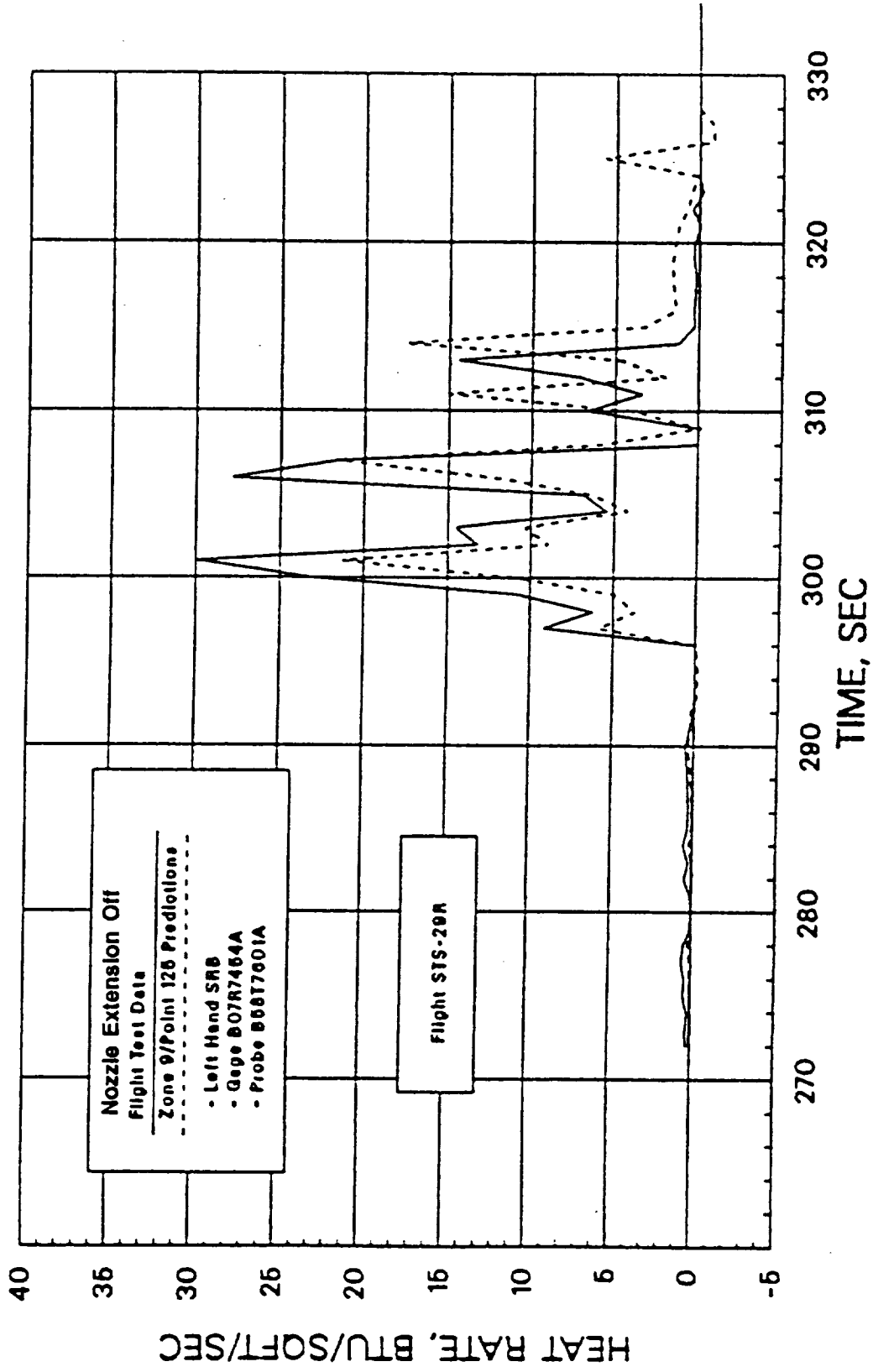

b) Using Flight Gas Temperature Measurement (B07T7601)

Figure 26: Internal Aft Skirt Heating Rate Validation B07R7454 STS-29R (Concluded)

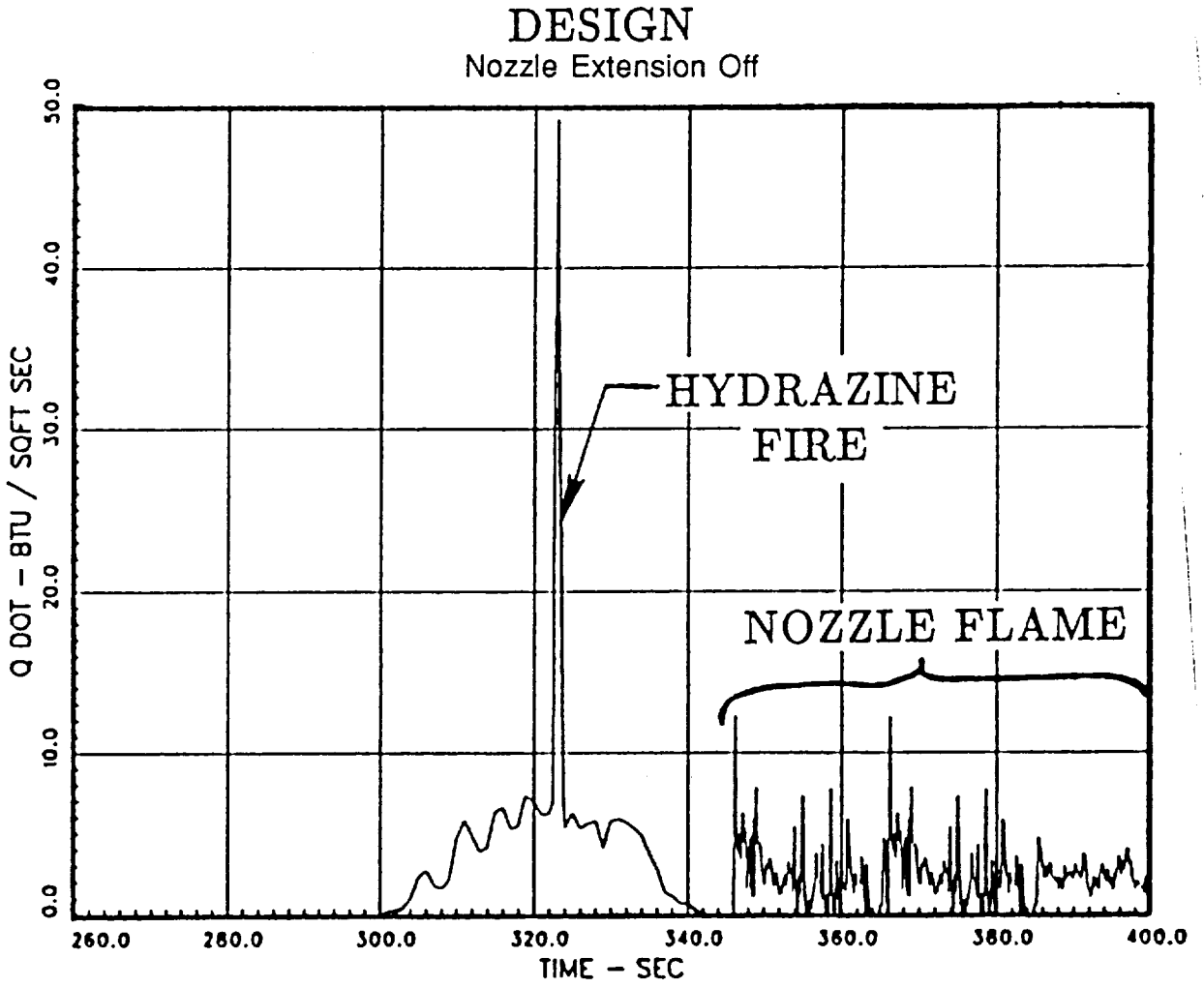

Figure 27: Current Application of Nozzle Flame Heating to Design (BP 9–164)

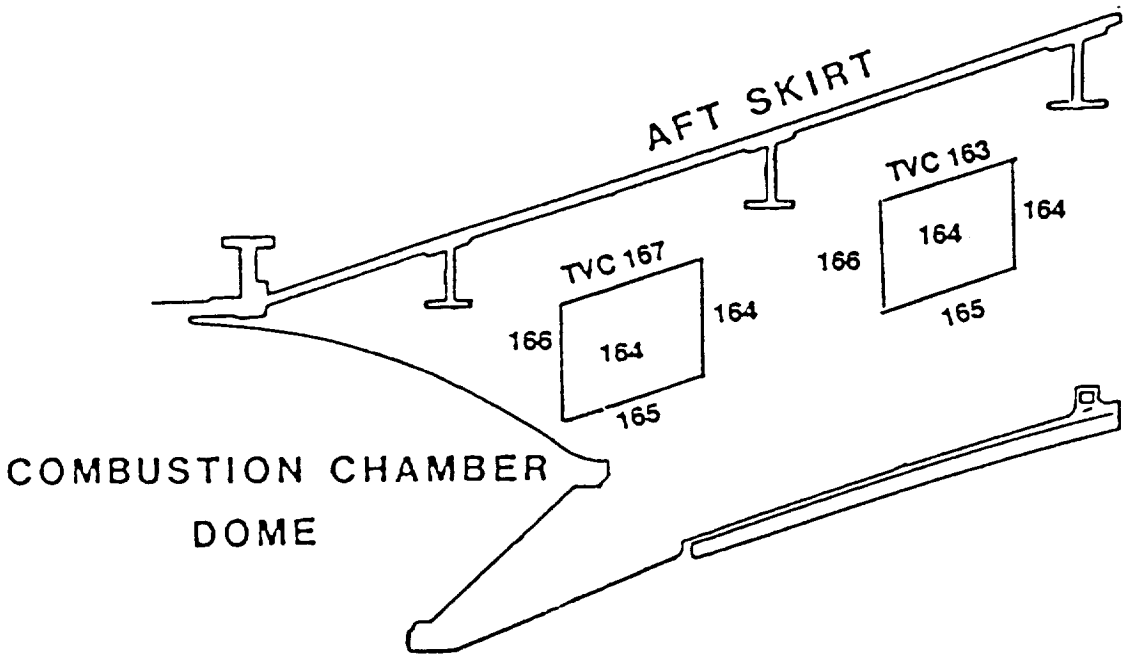

Figure 28: Environment Application

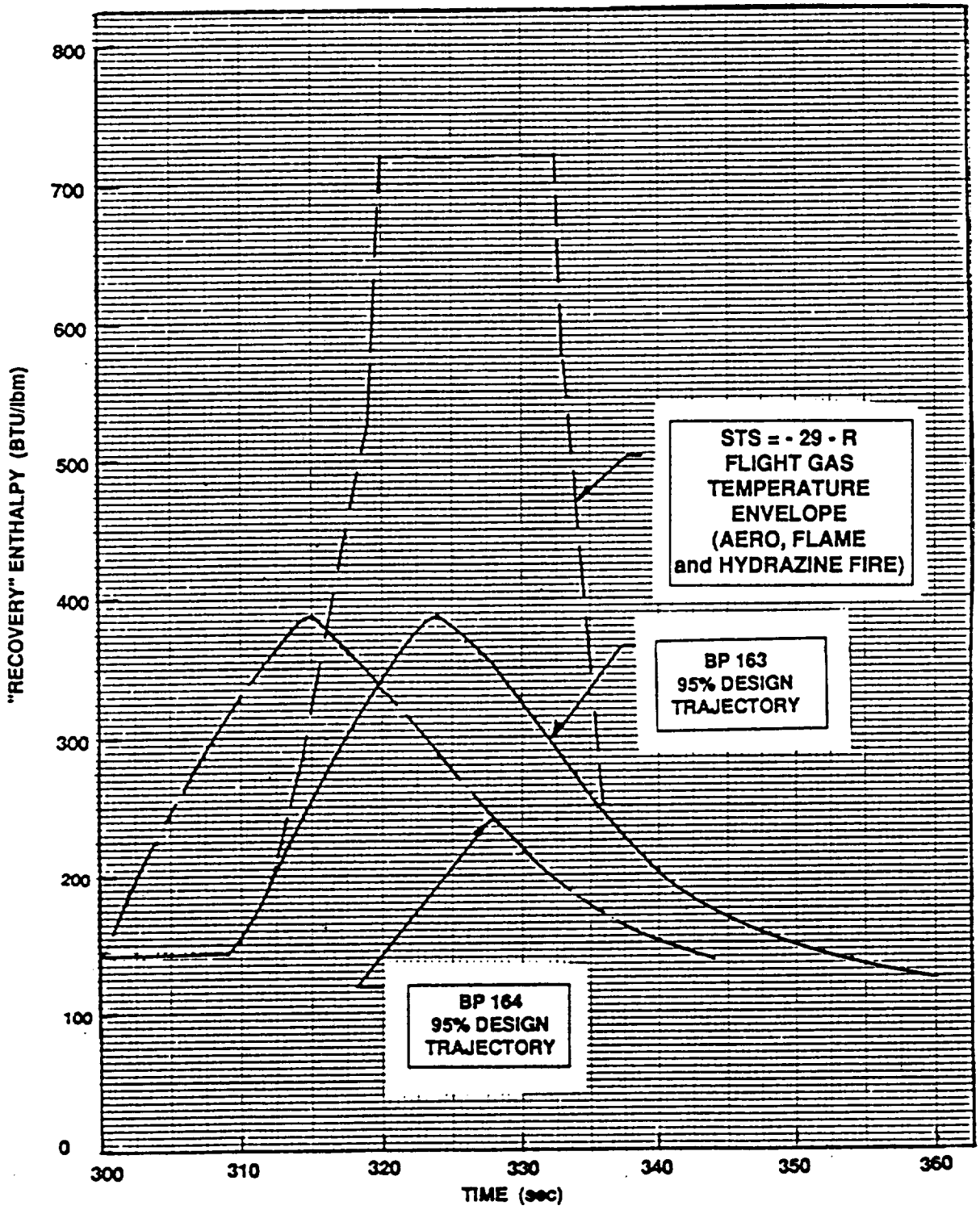

Figure 29: Recovery Enthalpy Used for TVC Assessment (Nozzle Extension-Off)

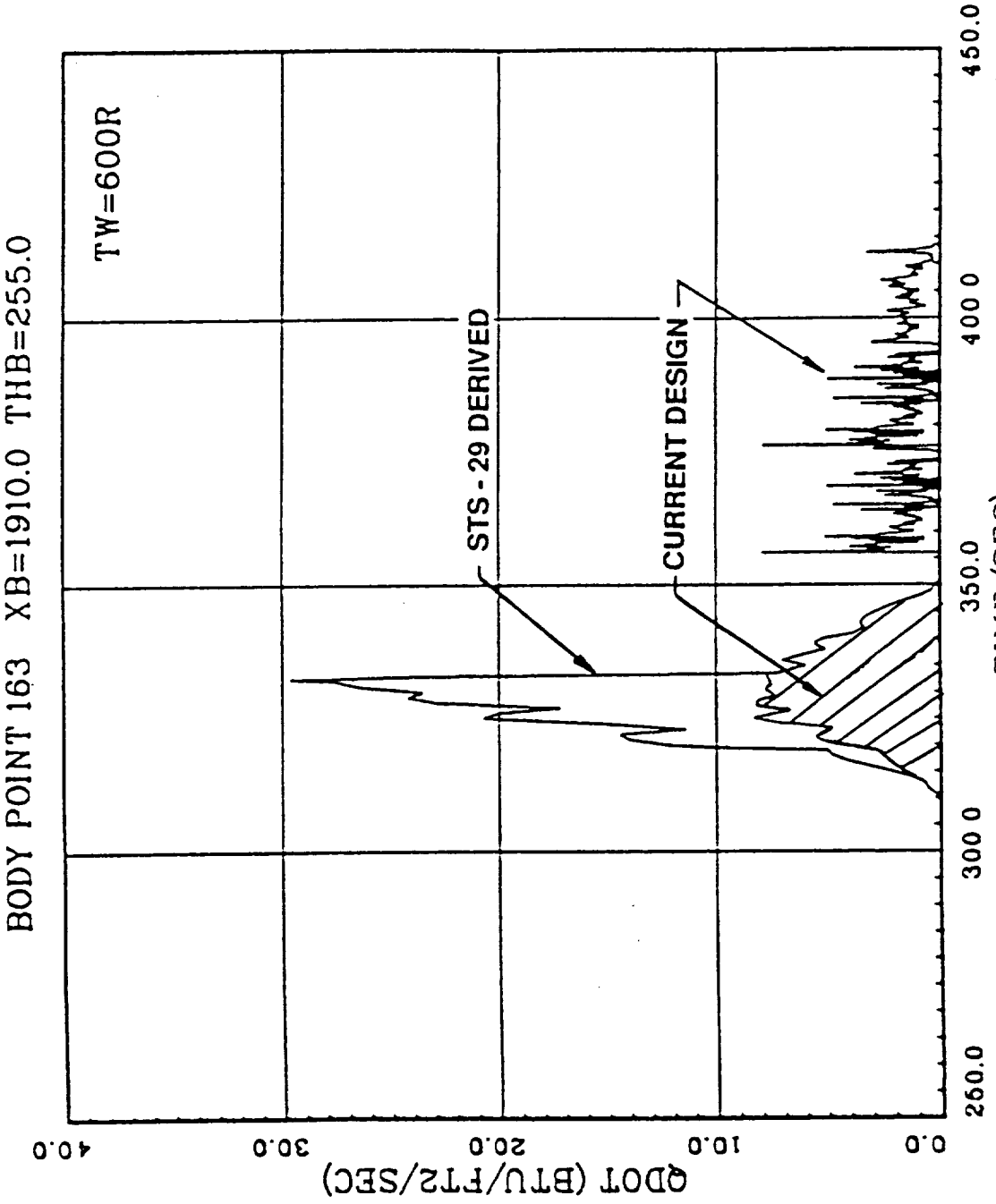

Figure 30: TVC (STS-29R Derived) Design Environment, B. P. 163 (Nozzle Extension-Off)

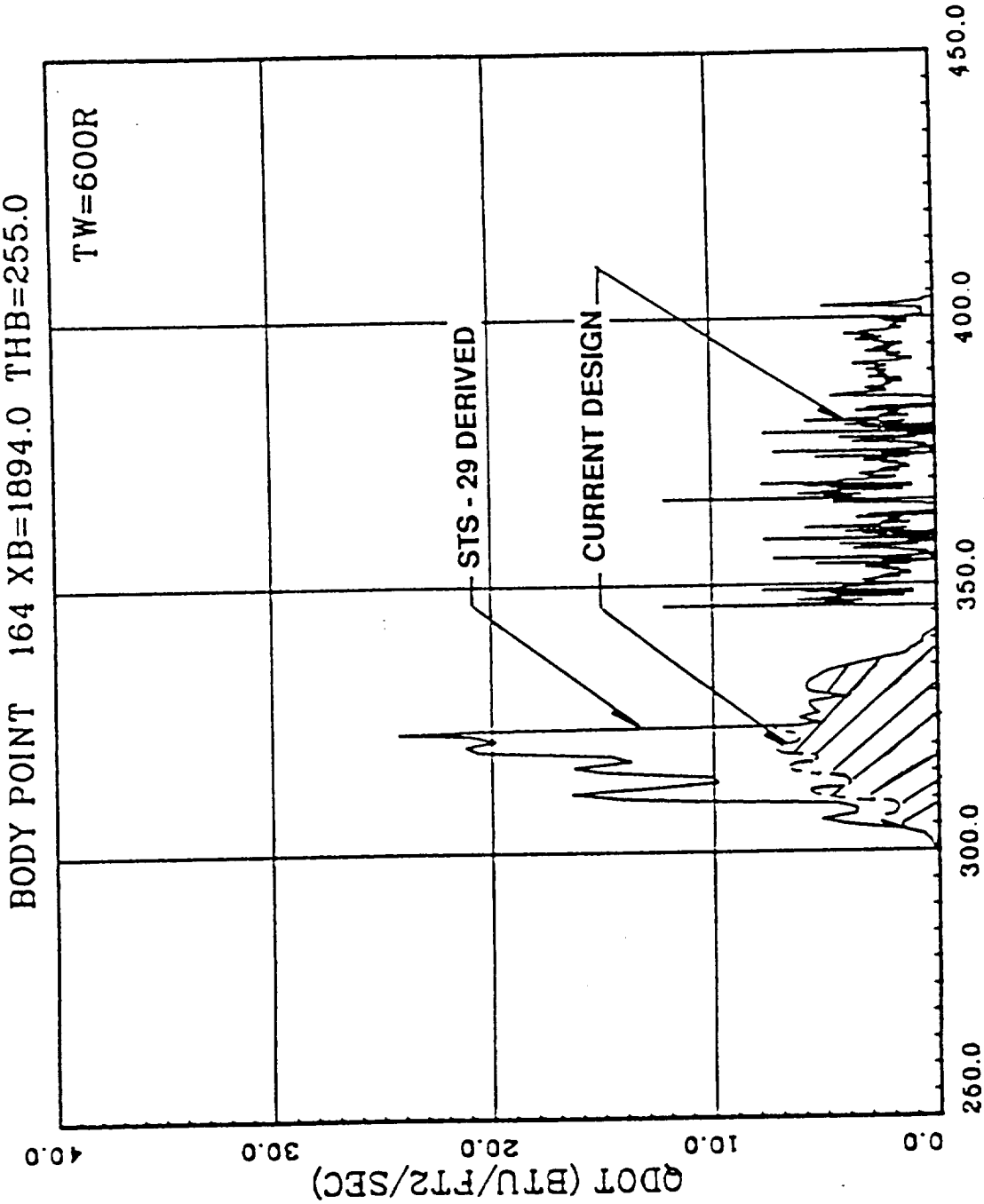

Figure 31: TVC (STS-29R Derived) Design Environment, B. P. 164 (Nozzle Extension-Off)

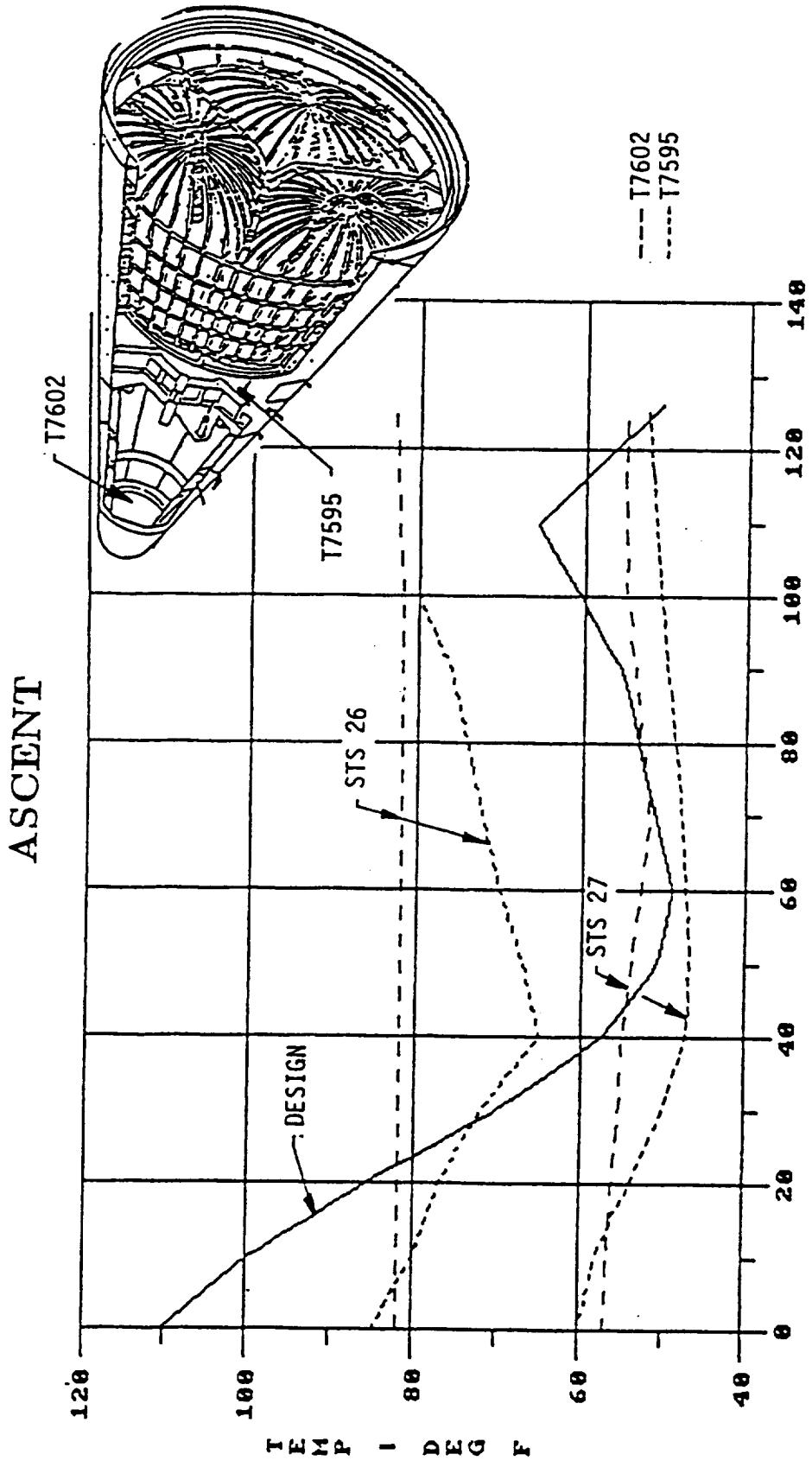

a) Ascent

Figure 32: Frustum Design Gas Temperature Compared with Current DFI Flights

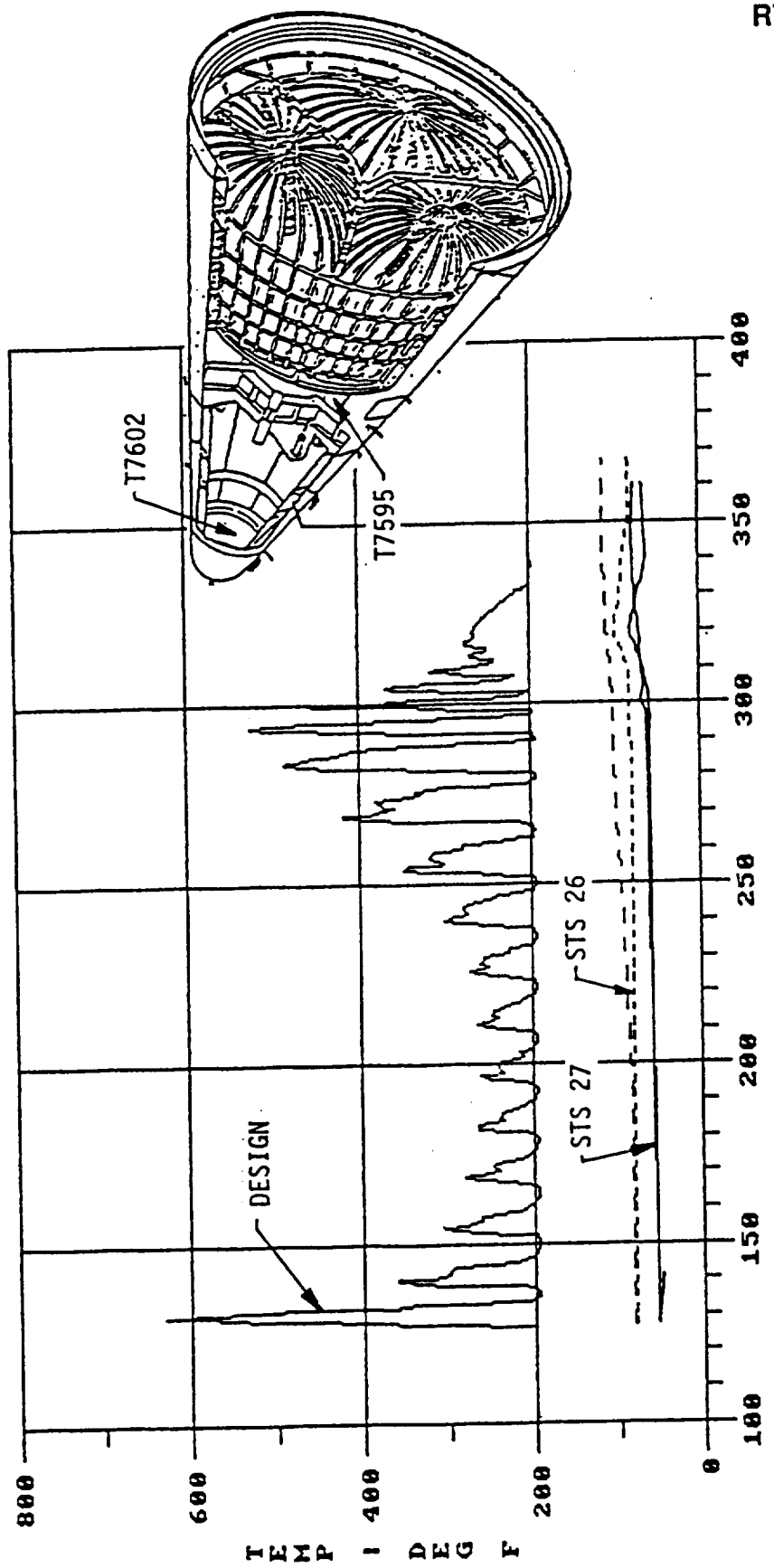

Figure 32: Frustum Design Gas Temperature Compared with Current DFI Flights (Concluded)

Figure 33: Frustum Combined Ascent and Reentry
Design Internal Gas Temperature Summary — B. P. 401

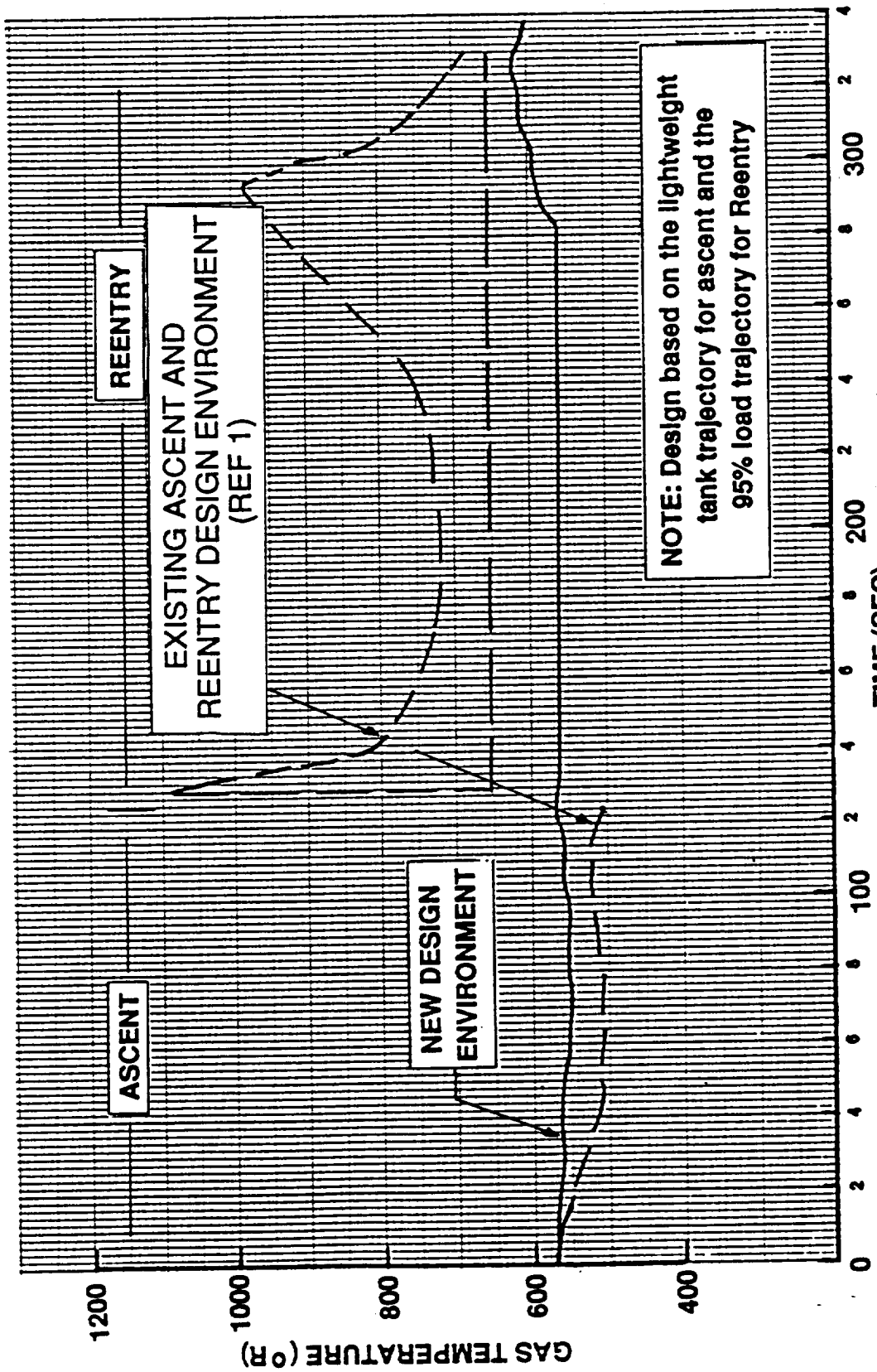

Figure 34: Comparison of Existing and New Frustum Internal Gas Temperature Design Environments

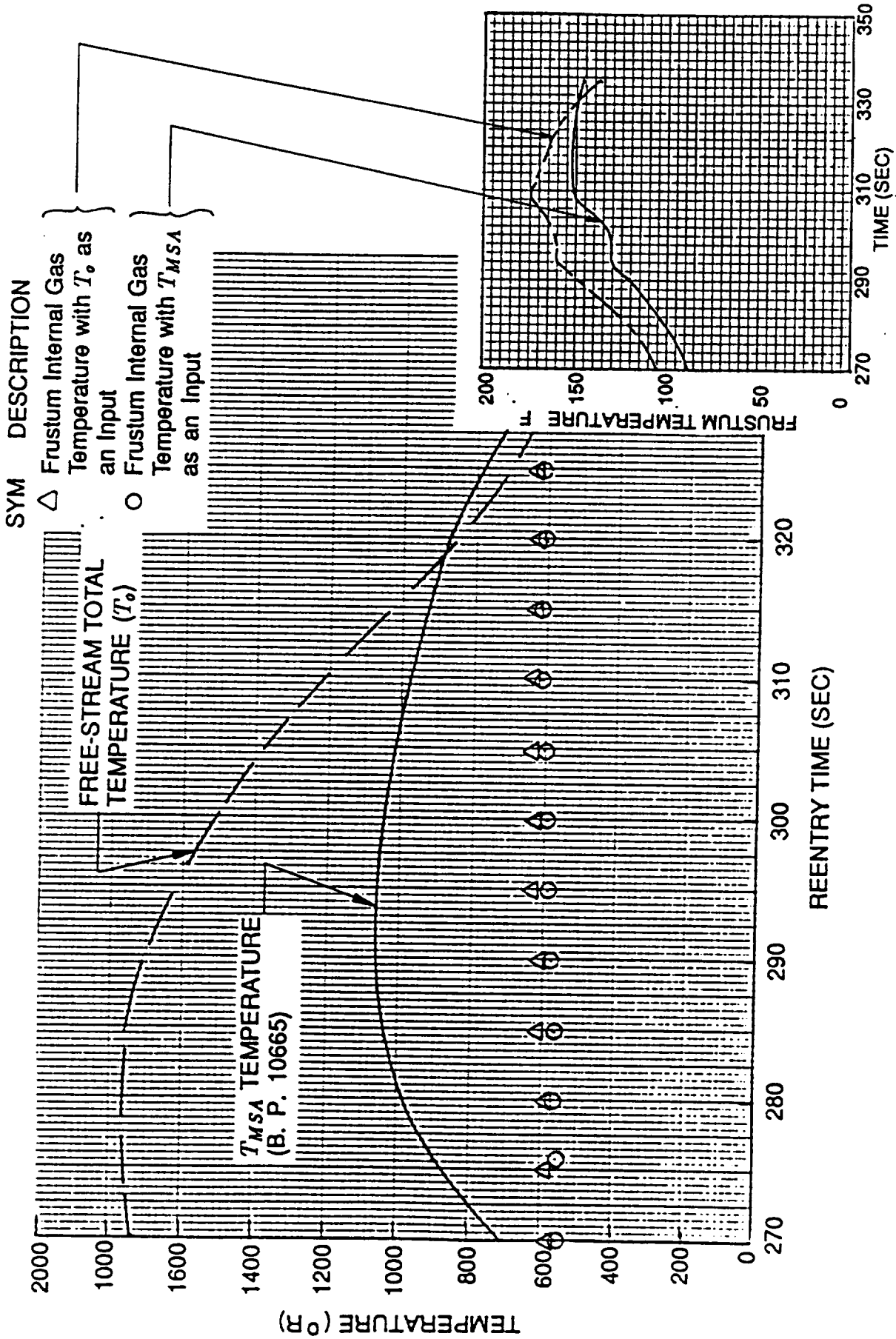

Figure 35: Effect of Using T_o and T_{MSA} as Entry Conditions on Frustum Reentry Calculated Internal Gas Temperature

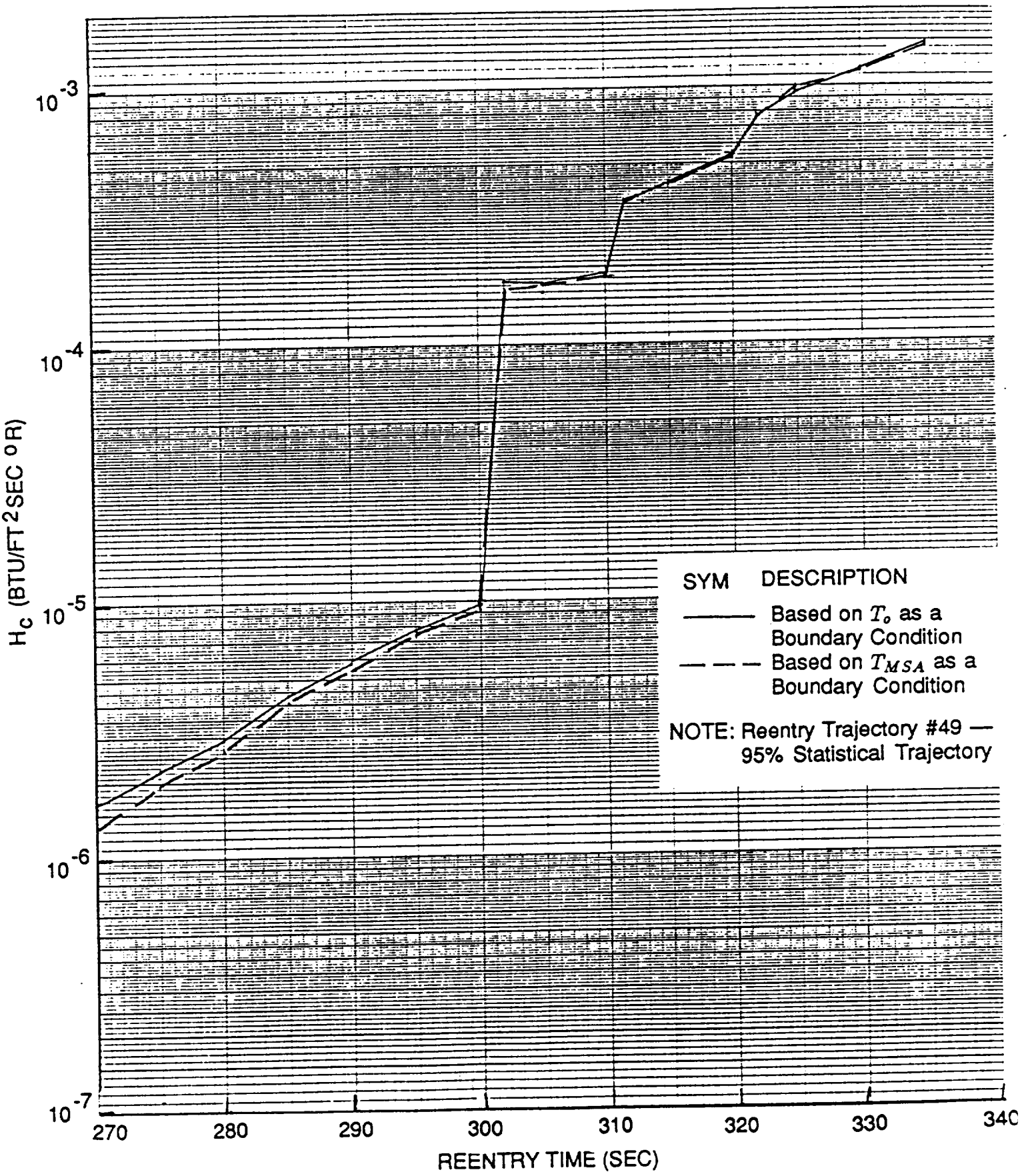

Figure 36: Effect of Using T_o and T_{MSA} as Entry Conditions on Frustum Reentry Internal Heat Transfer Coefficient

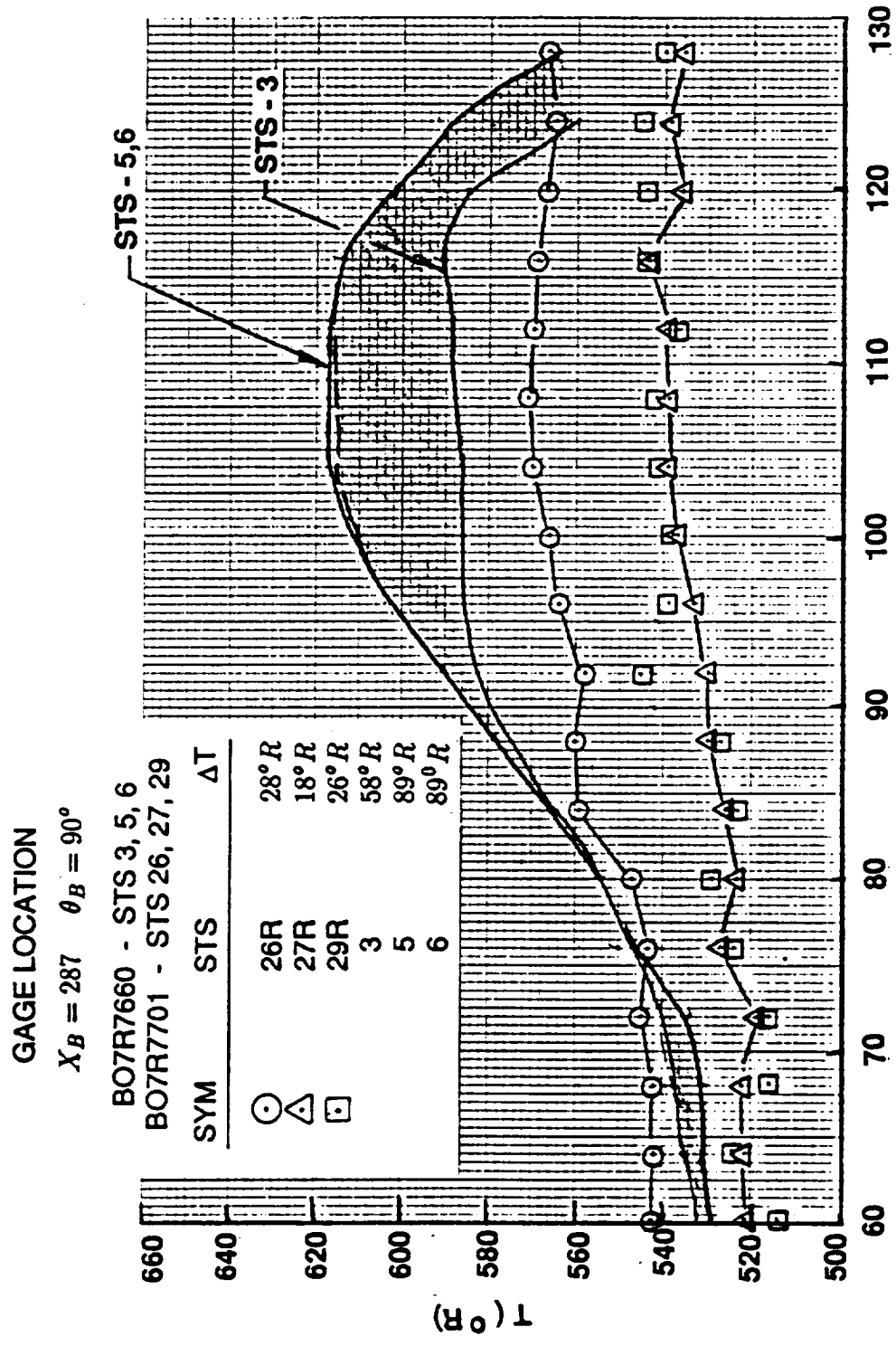

Figure 37: Heat Gage Wall Temperature Rise Comparison (Low to Moderate Heating)

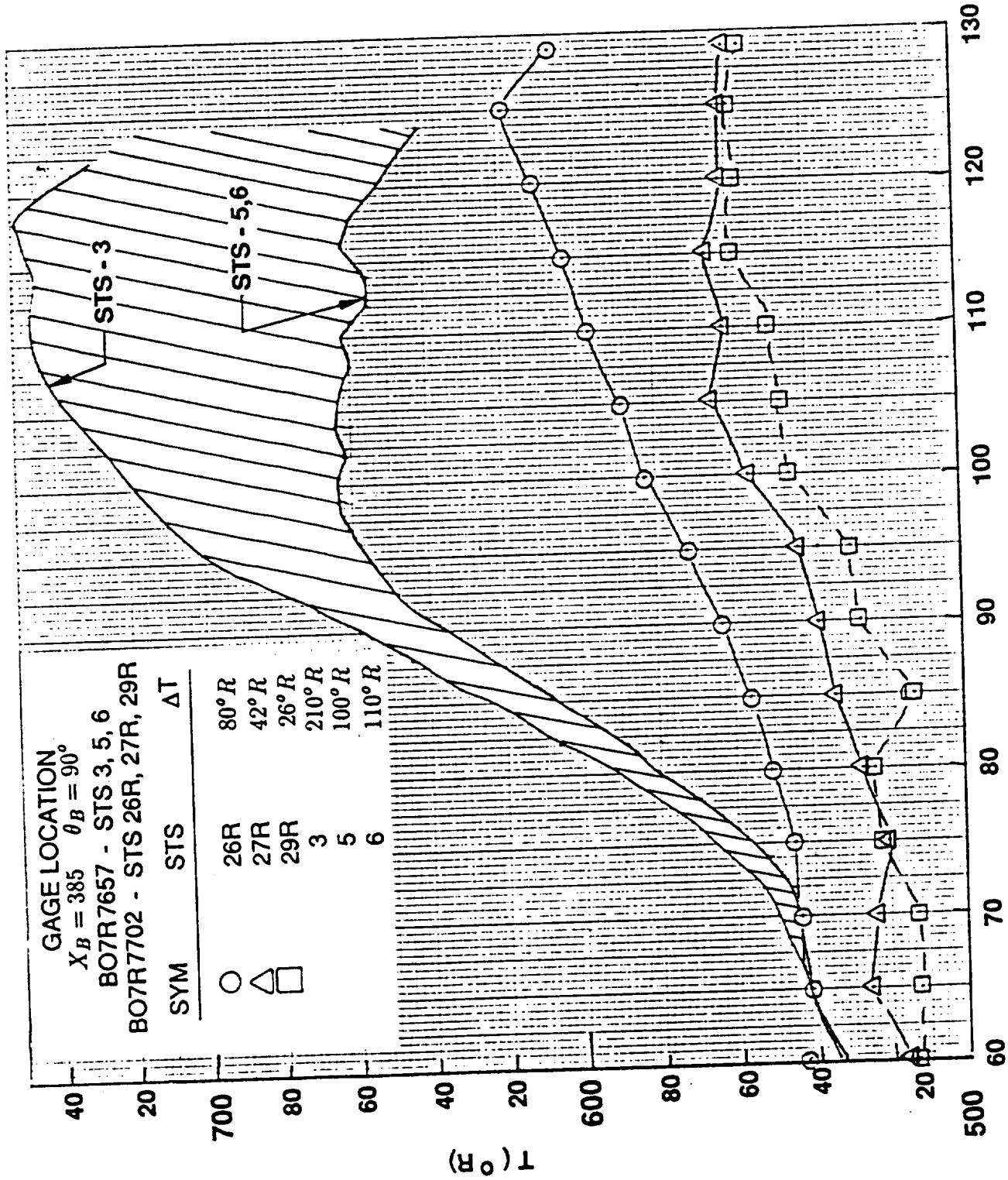

Figure 38: Heat Gage Wall Temperature Rise Comparison
(High Heating — Shock Interference or Stagnation Regions)

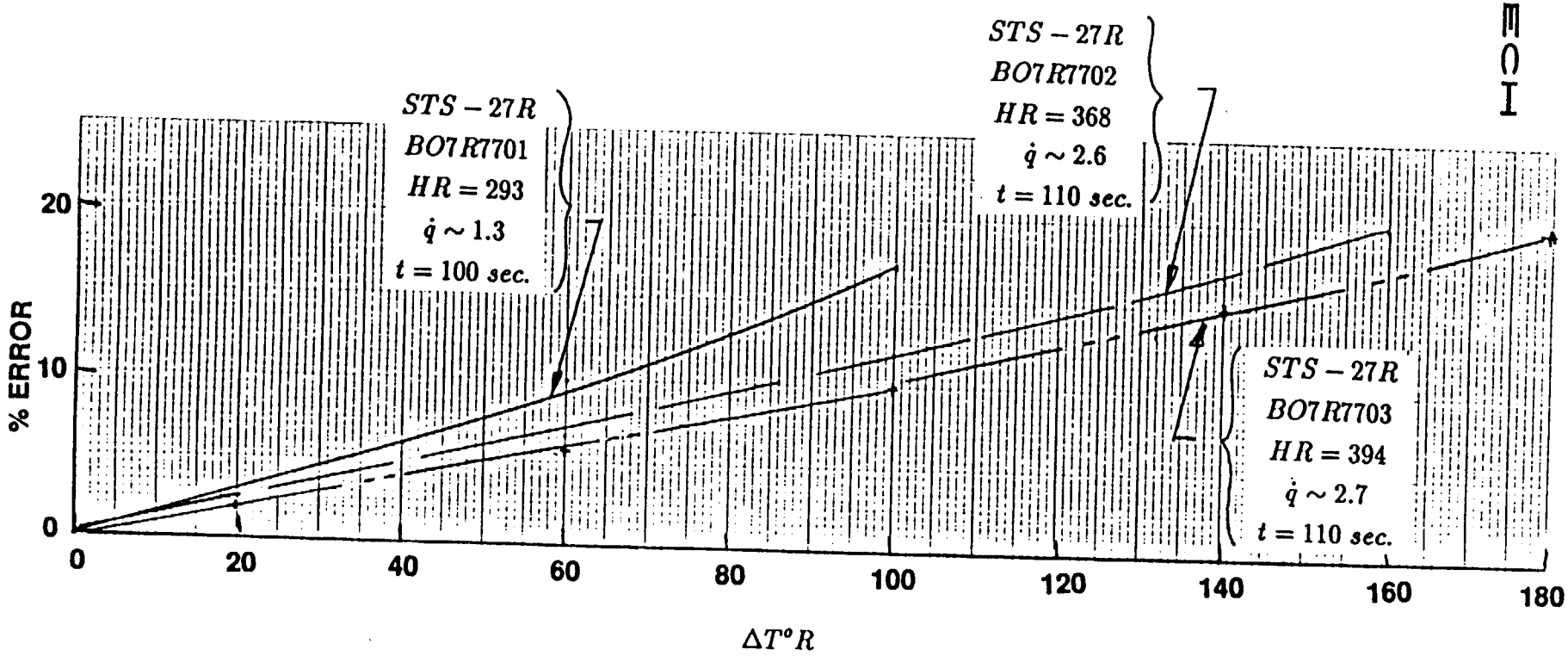

Figure 39: Impact on Typical Flight Heat Transfer Coefficients Due to Erroneous Wall Temperature

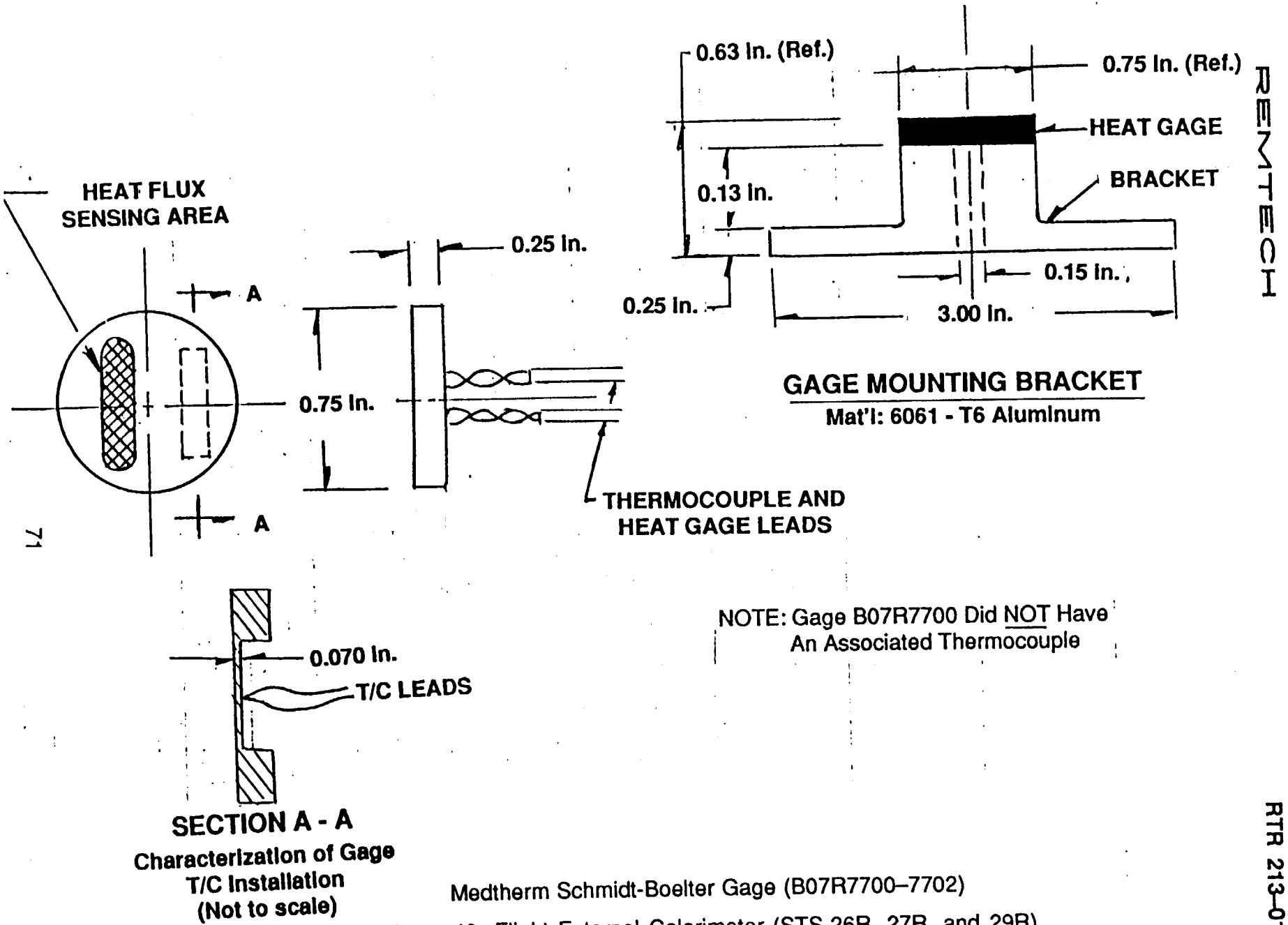

NOTE: Gage B07R7700 Did NOT Have An Associated Thermocouple

Medtherm Schmidt-Boelter Gage (B07R7700–7702)

Figure 40: Flight External Calorimeter (STS-26R, 27R, and 29R)

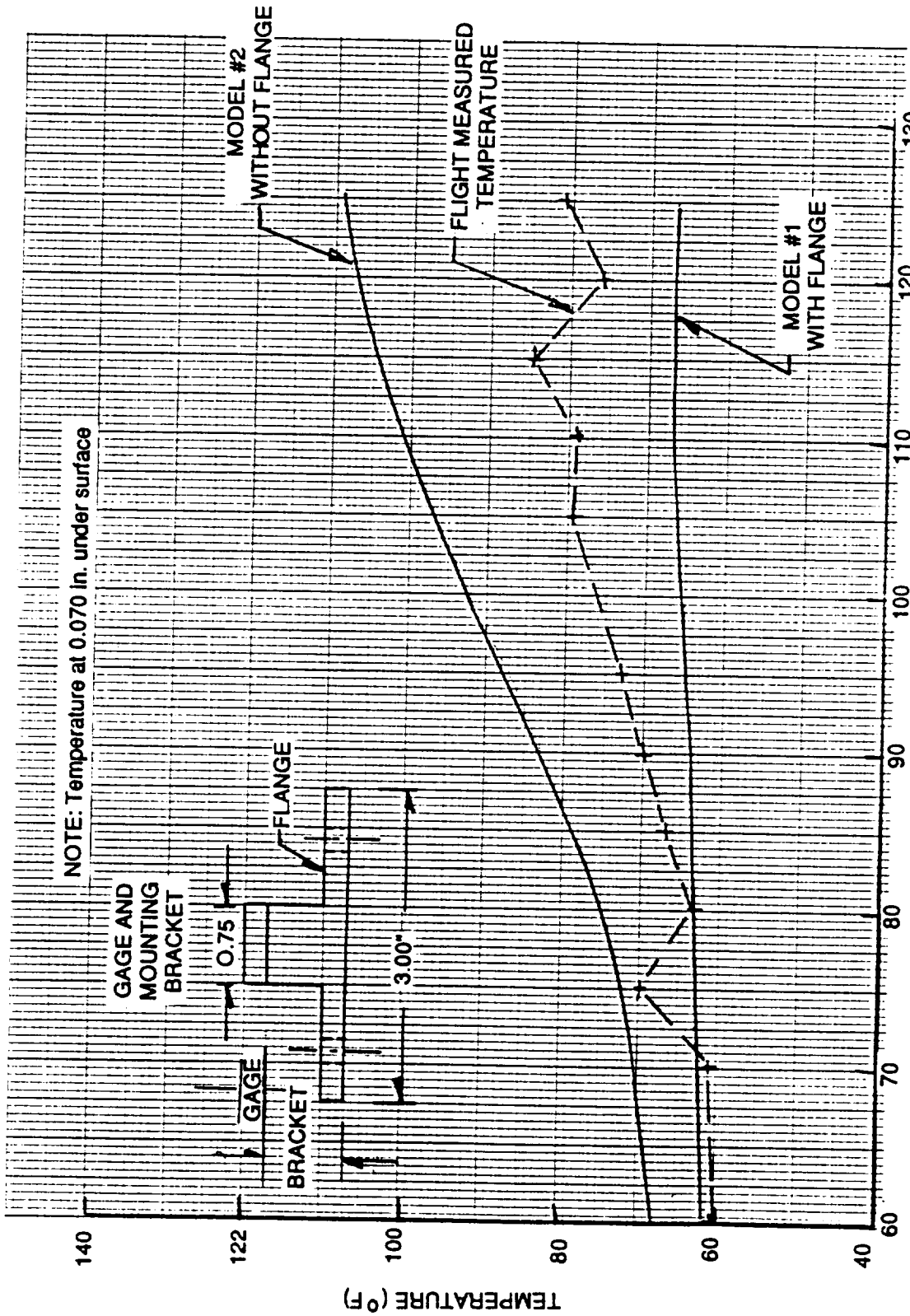

Figure 41: Schmidt-Boelter Case Thermal Response Comparison — Exits Calculated vs. Measured

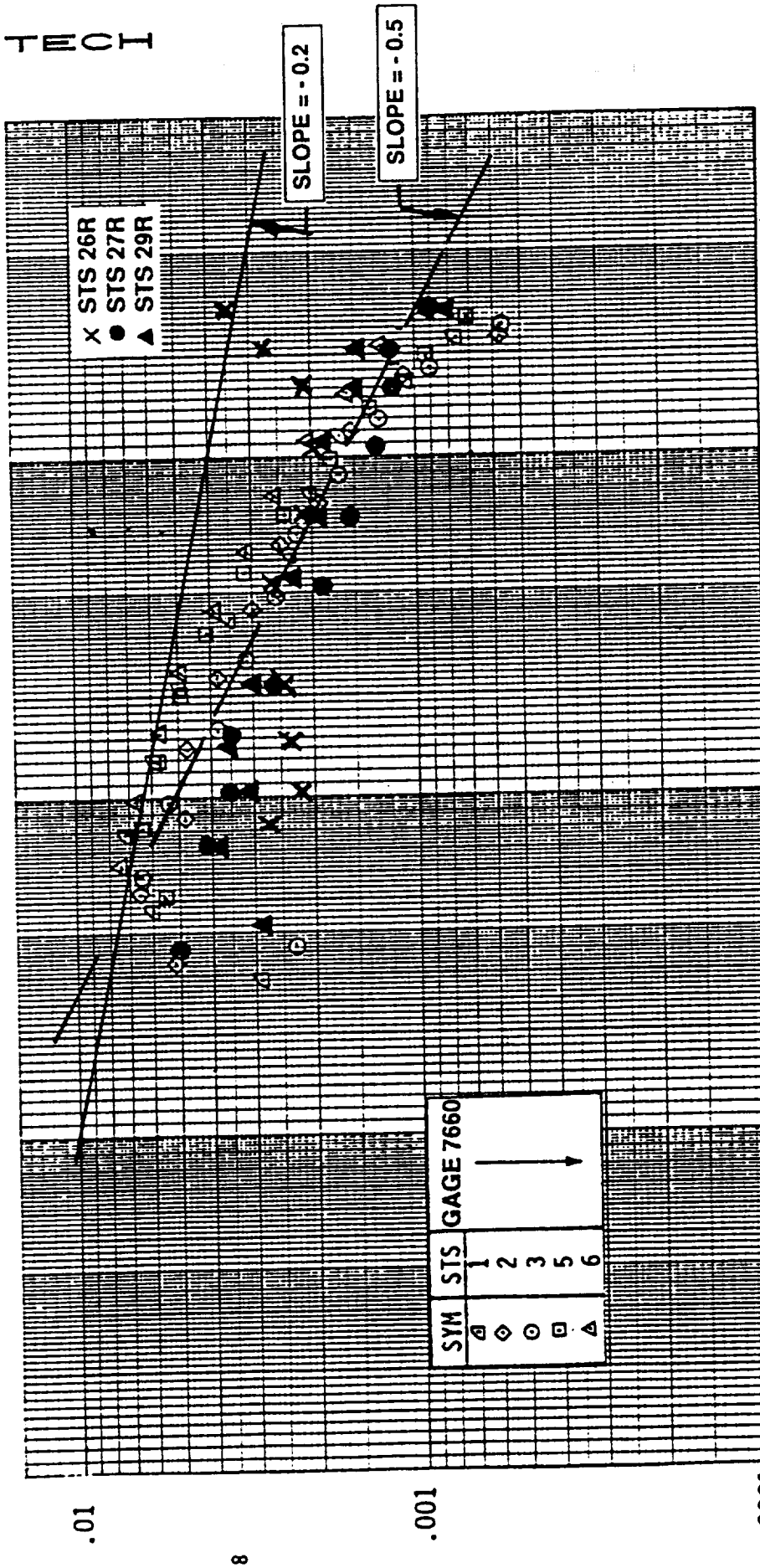

Figure 42: Comparison of Current Flight Data for Gage B07R7701 with Historic Flight Heating Data from STS 1–3, 5, 6

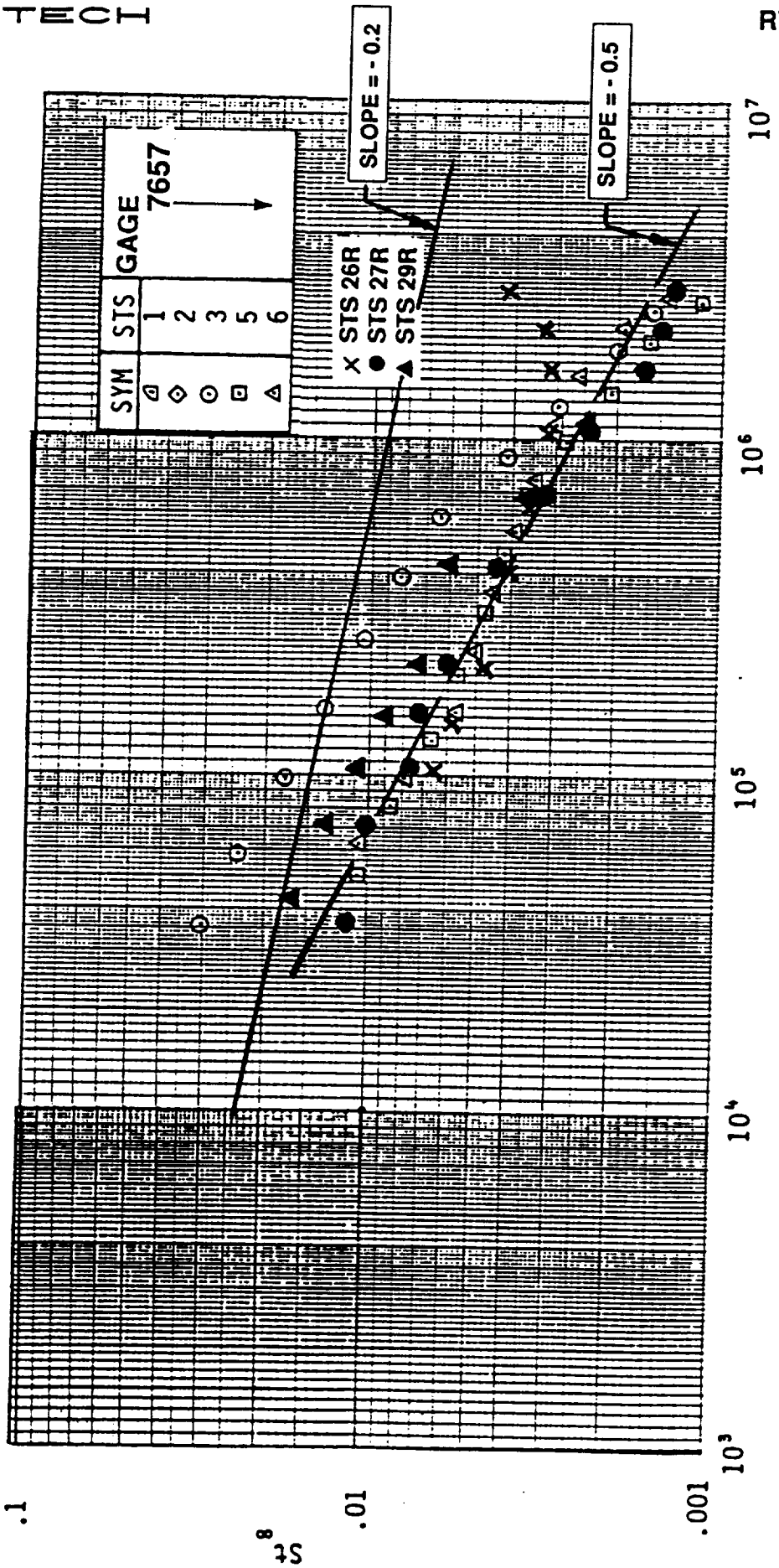

Figure 43: Comparison of Current Flight Data for Gage B07R7702 with Historic Flight Heating Data from STS 1–3, 5, 6

Section 11
TABLES

Table 1: SRB Nose Cone Flight Factor Summary

GAGE	X_B (IN)	θ_B (DEG)	FLIGHT FACTOR FROM CURRENT DATA		FLIGHT FACTOR USED FOR DESIGN	
			f_3	f_4	f_3	f_4
7700	243	90	0.76	0.98	1.00	1.65
7701	285	90	0.83	0.99	1.00	1.63
7702	385	90	1.31	2.57	2.11	2.39

NOTES:

(1) Tunnel to Flight Factor $= \frac{(H_i/H_u)_{\text{flight}}}{(H_i/H_u)_{\text{tunnel at flight}_{\alpha,\beta}}}$

(2) f_3 = Flight Factor Calculated with the M = 3.00 Wind Tunnel H_i/H_u Data Base.

f_4 = Flight Factor Calculated with the M = 4.00 Wind Tunnel H_i/H_u Data Base.

(3) The flight factors for the current data represent an average of the individual flight factors from STS-26R, 27R and 29R.

The design flight factors represent an average of the STS 1-3, 5, 6 flght factors.

Table 2: SRB Attach Ring Flight Factor Summary

GAGE	X_B (IN)	θ_B (DEG)	FLIGHT FACTOR FROM CURRENT DATA		FLIGHT FACTOR USED FOR DESIGN		REFERENCE BODY POINT (Ref. 9)
			f_3	f_4	f_3	f_4	
7703	1504	27.5	1.07	4.46	1.68	1.84	1369(53)
7704	1504	55.0	1.29	3.08	1.20	1.20	1384(54)

Table 3: SRB Aft Skirt Flight Factor Summary

GAGE	X_B (IN)	θ_B (DEG)	FLIGHT FACTOR FROM CURRENT DATA		FLIGHT FACTOR USED FOR DESIGN		STS 1, 2 FLIGHT FACTORS	
			f_3	f_4	f_3	f_4	f_3	f_4
7705	1880	180	3.57	4.94	1.00	1.60	4.69	7.69
7706	1880	270	1.95	4.85	1.00	1.00	2.57	11.98
7707	1870	270	1.91	5.08	1.00	1.00	2.57	11.98

NOTE: f_3 = Flight Factor Calculated with the M = 3.00 Wind Tunnel H_i/H_u Data Base.
f_4 = Flight Factor Calculated with the M = 4.00 Wind Tunnel H_i/H_u Data Base.

Table 4: TVC Integrated Heat Load Environment Summary (Nozzle Extension-Off)

COMPONENT	B. P.	X_B (IN)	θ_B (DEG)	COLD WALL DESIGN*	
				CURRENT DESIGN (RTN 163-55) (BTU/ft^2)	STS-29R MODIFIED DESIGN (BTU/ft^2)
TVC-AFT	9-164	1894	255	419	535
TVC FWD	9-166	1894	255	333	453
TVC INBD	9-165	1894	255	434	592
TVC OUTBD: AFT BAY	TVC 9-163	1910	255	291	451
FWD BAY	TVC 9-167	1876	255	230	351
TVC SIDES	9-164	1894	255	419	535

* @ T_W = 460°R

Appendix I

SRB Ascent Flight Heating Analysis of STS-26R, 27R and 29R (RTN 213-14)

REMTECH TECHNICAL NOTE

SUBJECT: SRB Ascent Flight Heating Analysis of STS-26R, 27R, AND 29R

DATE: May 1991

AUTHORS: William K. Crain and Robert D. Kirchner

CONTRACT NO.: NAS8-37891

PREPARED FOR: Induced Environments Branch (ED-33), George C. Marshall Space Flight Center

INTRODUCTION

The left hand SRB was instrumented externally with DFI calorimeters on flights STS-26R, STS-27R, and STS-29R, Fig. 1. Many of these measurements were made at locations where previous DFI measurements did not exist and, consequently, would contribute significantly to the overall understanding of the thermal environments in these areas. The basic flight data from these flights have been compiled and are presented in plotted and tabular form in Refs. [1–3]. Subsequently, the measurements were analyzed from an ascent heating point of view. The purpose of the analysis was to assess the quality of the individual measurements. If judged acceptable, they would be incorporated into the ascent heating data base and be used for ascent design environment impact assessment. It is the purpose of this report to document the results of this analysis, and to describe the methodology used.

INSTRUMENTATION AND LOCATION

Heat gages used on the SRB were a combination of MEDTHERM Schmidt-Boelter gages and HY-CAL asymptotic calorimeters. A sketch of these is shown in Fig. 2. The Schmidt-Boelter gages were used on the nose cap and forward frustum. The remainder were HY-CAL calorimeters. Gage ranges used were 0-15 BTU/ft^2-sec on the nose cap, forward frustum, and attach ring, and 0-20 BTU/ft^2-sec on the aft skirt. Uncertainty of the gages alone is quoted to be ±3 percent of full scale. Two of the calorimeters on the nose, B07R7701 and B07R7702, had thermocouples attached to the body of the gage, so that an idea of gage surface temperature could be inferred. This measurement was then used to define a flight heat transfer coefficient and thermal mismatch correction factor.

General location of the gages is shown pictorially in Fig. 1. Specific location is given in Table 1 in terms of gage number, SRB axial station (XB), and circumferential coordinate (THETA-B). The gages on the nose were located on the THETA-B = 90 deg ray for the purpose of clarifying the discrepancy between the Rockwell IVBC-3 design environments and the REMTECH design environments as illustrated in Fig. 3a. Gages on the front face

of the attach ring were located at positions thought to have the highest heating (Fig. 3b). These positions represented locations which did not have previous wind tunnel or flight test data. The three gages on the aft skirt were to be located at THETA-B = 0, 180, and 270 deg to define the ascent heating in the vicinity of the THETA-B = 270 deg location. These data were to help define the plume recirculation heating and region of flow separation for $t > 96$ seconds. Previous flight data at the THETA-B = 270 deg location were very limited. Due to an installation error, two of the gages, BO7R7706 and B07R7707, were installed at the same THETA-B. B07R7706 was located at XB = 1880, and B07R7707 was located at XB = 1870 (Fig. 3c). Consequently, some of the objectives were compromised.

FLIGHT DATA REDUCTION

Overview — In performing the flight data quality assessment, certain adjustments and corrections were required so that the data could be compared to theoretical predictions as well as historic data. The following is an overview of that process.

All flight calorimeter measurements were corrected for the respective zero shifts defined by the gage output at launch. These are tabulated for each gage and flight in Table 2.

Figure 4 defines the way in which the gages were handled. Data from gages on the nose cone were corrected for thermal mismatch (boundary layer temperature jump) and reduced to heat transfer coefficient form. From this; time wise corrected hot wall heating rates, and amplification factors (Hi/Hu) were calculated. Data from the gages aft of the nose cone were simply reduced to heat transfer coefficient form and used to calculate the time wise hot wall heating rates, and corresponding amplification factors. Thermal mismatch corrections were not applied to these data since two of the gages were in a stagnation region (attach ring) and the appropriate boundary layer running length for those on the aft skirt could not be accurately defined.

In reducing the measured heating rates to coefficient form, the gage thermocouple measurements from gages B07R7701 and B07R7702 were used in the following manner: gage temperature from B07R7701 (B07T7603-Fig. 4) was applied to gages BO7R7700,7701,7705,7706,and 7707. Gage temperature from B07R7702 (BO7T7604-Fig. 4) was applied to B07R7702, 7703 and 7704. The rationale was that the temperature rise from B07T7603 was representative of those gages in low heating regions, while the temperature rise from B07T7604 was more closely matched that for gages in shock interference and stagnation regions.

Thermal Mismatch Corrections — Preceding the heat transfer gage is a running length of insulator (MSA-2, etc.) which has a high surface temperature. On encountering the heat gage, which is usually a good conductor, the flow immediately sees a "cool" wall. Consequently, the heating rate, which is proportional to $(T_{recovery} - T_{wall})$, increases substantially over the rate of the insulated wall. In order to correct the gage measurement back to that which the insulated wall would see, thermal mismatch corrections were applied to the gage measured heating rate. The correction equation, after

Westkaemper [4], is of the form:

$$h/hiso = F(L/W) + H'(L/W)\left[\frac{TW2 - TW1}{TW2 - TR}\right]$$

where $F(L/W) = 5/4\left[\frac{2}{1+(L/W)}\right]^{\frac{1}{5}}\left[\frac{1-(L/W)^{\frac{8}{5}}}{1-(L/W)}\right]$

and: $H'(L/W) = 5/4\left[\frac{2}{1+(L/W)}\right]^{\frac{1}{5}}\left[\frac{\left(L/W^{\frac{1}{5}}\right)}{1-(L/W)}\right]\left[(W/L)^{\frac{9}{10}} - 1\right]^{\frac{8}{5}} - F(L/W)$

Definition of terms in the equation and values of these terms for each gage location is given in Fig. 5.

The calculation scheme used to perform the corrections to the flight data is shown in Fig. 6. The correction methodology was programmed into the EXITS heat conduction code [5]. Given the flight measured heating rates and wall temperature, an EXITS one-dimensional model was used to calculate the MSA surface temperature and perform the iterative correction procedure. The resultant output was corrected hot wall and cold wall heating rates, heat transfer coefficient, correction factor magnitude, MSA temperature and interference heating factor (HI/HU). The specific flight trajectory, body geometry and heating technique were supplied to LANMIN [6] which then calculated the local undisturbed heat transfer coefficient and local recovery enthalpy used by EXITS. Corrections were generated for gages B07R7700, B07R7701 and B07R7702 for each of the three redesigned DFI instrumented flights (STS-26R, -27R, and -29R). Results of these calculations are presented in tabular form in Appendix I.

Flight Data Reduction for Gages Aft of the Forward Frustum — Data from gages on the attach ring (B07R7703, 7704) and on the aft skirt (B07R7705-7707) were reduced to heat transfer coefficient and amplification factor form by the procedure shown in Table 3. Undisturbed heating was generated by LANMIN [6] using Spalding-Chi skin friction correlations and a von Kármán Reynolds Analogy. (This is described in greater detail in the following section SRB HEATING PREDICTION METHODOLOGY.) The calculated heat transfer coefficients were hot wall values referenced to the heat gage measured temperatures on the forward frustum. Results of these calculations are presented in tabular form in APPENDIX II for the three DFI instrumented Redesigned flights (STS-26R, -27R, and -29R).

SRB HEATING PREDICTION METHODOLOGY

Heating predictions at each gage location were made by calculating the local clean skin value and then amplifying this with interference factors based on wind tunnel and flight data. A list of the current gage locations with corresponding interference factor body points is given in Table 4.

The undisturbed methodology is summarized in Table 5. The tangent cone technique was used to generate the local pressures. These were calculated based on the SRB geometry alone and did not consider the External Tank 40-deg. conical shock. Spalding-Chi skin friction calculations with a von Kármán Reynolds analogy were used to calculate the local undisturbed heat transfer coefficients. These were hot wall values referenced to the forward frustum heat gage thermocouple measurements.

Local interference factors were based on wind tunnel data from IH-97,72, and 85 [7–9] primarily, and flight test data from STS 1-3, 5 and 6. These data are published in amplification factor form in Ref. [10]. Hi/Hu factors used for this analysis are presented in Table 6.

The calculation scheme used to perform the individual flight predictions is outlined in Fig. 5. MINSRB [6], a REMTECH version of the MINIVER heating code, was used to calculate the undisturbed heating along the flight trajectory. This was done over a range of effective angles of attack. INTERP defined the undisturbed heating at the exact body point (gage) location. These results along with the interference heating data base were fed into RESADM which performed the main interference heating calculations. The interference heating factors (Hi/Hu) are in tabular form as a function of α(−5, 0, 5 deg) β (−9, −5, −3, 0, 3, 5, 9 deg) and Mach Number (M = 3,4). At each time point in the trajectory, a fine matrix of (α , β) is formed and the appropriate value of Hi/Hu is calculated corresponding to the specific trajectory (α , β). The undisturbed heating (qu) is calculated as a function of α effective, where α effective is:

$$\alpha\, eff = -\alpha \cos \theta_B + \beta \sin \theta_B$$

Interference heating (q_i) at each time point was then calculated for each (α , β) by:

$$q_i = [qu \times Hi/Hu]$$

and the maximum value of q_i over the (α , β) matrix was then used. The variation of interference heating factor with Mach number is assumed linear in the log-log plane.

RESULTS AND ANALYSES

Nose Cone and Forward Frustum Gages (B07R7700–7702) — Comparisons from the nose cone and forward frustum gage measurements are made with historic data from STS 1-3, 5, and 6. These comparisons are presented in Fig. 8 in the form of Stanton Number versus Reynolds Number. The Stanton and Reynolds Numbers are based on freestream properties. The data from all three gages on STS-27R and STS-29R compare reasonably with the historic flight data. However, the data from gages

7700 and 7701 on STS-26R exhibit an unusual trend with Reynolds Number. At the present, this trend is not understood. Consequently, these data should not be used for design environment assessment until the physics of these results is understood. Concerning the comparisons of Fig. 8, two of the current measurements (B07R7701 and B07R7702) were located in the same axial location as their historic counterpart (B07R7660 and B07R7657). B07R7700 on the current DFI flights did not have an historic flight counterpart, consequently, comparisons with 7700 measurements were made with the closest historic flight gage. In this case it was B07R7660 which was located on the same circumferential ray, but 44 inches aft of B07R7700.

Trajectory heating rate versus time for each gage and flight is plotted in Figs. 9-11. Each plot consists of the uncorrected heating rate, the heating rate with thermal mismatch corrections, and the flight prediction. The thermal mismatch correction lowers the current data from 40 to 80 percent, in general. Of surprise was the discrepancy between the thermal mismatch corrected data and the flight prediction, since the prediction is based on the most up to date data base. This data base is composed of wind tunnel data from IH-97 [7], as well as corrected flight test data from the historic flights, STS 1-3, 5, 6. The discrepancy is due mainly to the tunnel to flight scaling factor used to adjust the wind tunnel level to full scale flight. A cursory analysis of this discrepancy showed that the scaling factors derived from the current data were lower than those calculated for flights STS 1-3, 5, and 6. The analysis of this discrepancy will be addressed in the design environment evaluation since the objective of the current task is to comment on the quality of ascent measurements.

Attach Ring and Aft Skirt Gages (B07R7703–7707) — Results of the Attach Ring and Aft Skirt measurements are presented in Figs. 12-13 and 14-16 respectively. Again the flight measurements are compared with predictions based on wind tunnel and flight test results. For the Attach Ring instrumentation there were no historic flight test data with which to compare. Similarly, on the Aft Skirt for gages B07R7706-7707, very limited flight test data were available. Predictions, for these cases, were based on the nearest body point for which flight test data were available and/or amplification factors based on the pressure interaction theory [10]. Of these measurements, B07R7703 on the Attach Ring (Fig. 12c) and B07R7707 on the Aft Skirt (Fig. 16c) on STS-29R appear to be questionable. Both are low in magnitude compared to the prediction and a consistency check within the data set. Confirmation of this is presented in Fig. 17. Here a comparison between B07R7706 and 7707 is shown for the three flights. These gages are located at the same circumferential angle (THETA-B = 270 deg), and are spaced approximately 10 inches apart; 7707 being the leading gage. Both gages agree very well and track the prediction within the gage accuracy for STS-26R and -27R. However, on STS-29R, B07R7707 is low. The remainder of the measurements are judged as acceptable, and are recommended for use in the design environment determination process.

Part of the objective of instrumenting the aft skirt at the THETA-B = 180 and 270 deg positions (Fig. 3c) was to gather data on flow separation and help define plume recirculation heating in this region of the SRB. Previous data from the historic flights (STS 1-3, 5, 6) are very limited in this respect. Analysis of the data from the three aft skirt

gages on the current flights showed that plume recirculation heating was extremely low level (~ 0.5 BTU/ft^2-sec) to nonexistant over the circumferential range 180 > THETA-B > 270 deg. Confirmation of this conclusion is presented in Figs. 18-21. Plume recirculation heating manifests itself as an abrupt increase in heating rate beginning around an altitude of 84,000 feet (t ~ 94-100 seconds). This is due to the hot gas plume flow reversal onto the SRB aft motor case. A good example of this is shown in Fig. 18. These data were obtained on STS-5 and corresponds to a gage (B07R7674) on the aft face of the kick ring on the left hand booster. Note the increase in heating at t = 96 seconds. In like manner, an example of an aft skirt gage which did not experience plume recirculation heating is B07R8665 on the right hand SRB shown in Fig. 19. This gage was located outboard at the THETA-B = 34 deg position, Fig. 20. Contrasting these results to the current aft skirt data presented in Figs. 14-16, the only measurement exhibiting any resemblance to plume recirculation heating effects is B07R7705 on STS-27R. B07R7705 is located at the THETA-B = 180 deg position. The magnitude is estimated to be approximately 0.5 BTU/ft^2-sec. This was observed on earlier flights at this circumferential position, as shown in Fig. 21. These data are from gage B07R8443 located at the THETA-B = 180 deg location on the right hand booster, (see Fig. 20). The data were obtained on STS-2. All the other data from the current flights show no signs of plume recirculation.

Calorimeter Wall Temperature Analysis — As previously mentioned, the current flights were the first to have thermocouples installed on several of the heat transfer gages. This measurement (T_{wall}) was required to experimentally define the flight local heat transfer coefficient:

$$Hc = \frac{\dot{q}_{flight}}{HR - C_p T_{wall}}$$

It was also used to correct the flight measurements for boundary layer temperature discontinuity (thermal mismatch). On the first six DFI instrumented flights, the heat gage surface temperature was calculated using a thermal model of the gage and installation. In comparing the measured heat gage temperature rise on the current flights with that calculated on STS 1-6, it was observed that the calculated temperature rise was much greater than the actual measured values. An example of this is shown in Fig. 22. In this plot the gage surface temperature history from STS-3, 5 and 6 is compared to that measured on STS-26R, 27R, and 29R. The data in Fig. 22a correspond to gage B07R7760 (XB = 285) on STS-3,5,6 and B07R7701 (XB = 287) on STS-26R, 27R, and 29R. These data represent a low to moderate heating level. The data in Fig. 22b correspond to gage B07R7657 (XB = 373) for STS-3,5,6 and B07R7702 (XB = 385 on STS-26R, 27R, and 29R). These results represent a high heating area such as downstream of a reflected shock or a stagnation region. All gages were located on the THETA-B = 90 deg circumferential ray. The math model predicted a wall temperature rise of 60 to 90°F at the low to moderate heating location, and 100 to 210°F at the high heating location. Corresponding measured flight values on the current flights are 18 to 28°F at the low to moderate heating location, and 26 to 80°F at the high heating location.

The impact of this difference on flight calculated heat transfer coefficients and the thermal mismatch correction was investigated. Error incurred in the heat transfer coef-

ficient calculation by using an elevated gage wall temperature is presented in Fig. 23. These results were generated using actual flight heating measurements on STS-27R, corresponding recovery enthalpies, and a wall temperature rise from STS-3 and 5 added to the STS-27R flight measured wall temperatures. The impact is seen to be significant at all three gage locations; 7701, 7702, and 7703. Thermal mismatch corrections on STS-27R were recalculated for gages B07R7700 and 7702. These calculations were based on the math model wall temperature rise from STS-3 and 5, rather than the flight measured value. The difference in corrected heating rate (Fig. 24) is seen to be insignificant even at the high heating condition. The clear message is that corresponding heat transfer gage wall temperature measurements need to be made on each flight, at least, areas of similar heating; i.e., low , moderate, and high. In addition, it is clear that while the thermal mismatch correction is not super sensitive to gage wall temperature, the correction should be made; contrast the difference between the corrected and uncorrected heating level in Fig. 24.

SUMMARY AND CONCLUSIONS

In this task, the external heating measurements on the redesigned Solid Rocket Boosters were examined from an ascent heating point of view. The purpose of this effort was to confirm the validity of each measurement, and determine if they were qualified to be used in generating design environments. Since many were obtained at locations where previous flight data did not exist, if acceptable, they would then be used in assessing the current IVBC-3 design environments. The data in question consisted of measurements obtained on STS-26R, -27R, and -29R. These data were corrected for zero shifts and boundary layer temperature jump. The corrected data were compared with predictions based on an extensive wind tunnel and flight test data base.

Of the eight external heat transfer measurements, the following were judged as unacceptable until further investigation could be performed:

a.) Nose cone and forward frustum measurements from gages B07R7700 and 7701 on STS-26R,
b.) Attach Ring measurements from B07R7703 and Aft Skirt measurements from B07R7707 on STS-29R.

The remainder of the heat transfer data from the three flights are judged acceptable and are recommended for use in the design environment determination process.

In addition, the need for making a corresponding heat transfer gage wall temperature measurements on each flight was clearly demonstrated. Errors of 10 to 20 percent in the calculated heat transfer coefficient are easily attainable by using conduction thermal model results. This requires, as a minimum, thermocouples on gages in areas that experience large differences in heating ($\approx$2 BTU/ft^2-sec.).

Last, the ascent heating measurements confirmed the plume recirculation heating to be low level ($\approx$0.5 BTU/ft^2-sec) to nonexistent on aft skirt over the circumferential range 180 < THETA-B < 270 deg.

REFERENCES

[1] Crain, W.K., "Raw Flight Data Report — STS26R," REMTECH RTN 213–01, Dec. 1988.

[2] Frost, Cynthia and Crain, W.K., "Raw Flight Data Report-STS 27R," REMTECH RTN 213–02, Oct. 1989.

[3] Frost, Cynthia and Crain, W.K., "Raw Flight Data Report-STS 29R," REMTECH RTN 213–03, Sept. 1989.

[4] Westkeamper, J.C., "On the Error in Plug-Type Calorimeters Caused by Surface Temperature Mismatch," Journal of Aerospace Sciences, Nov. 1961, pp. 907–908.

[5] Pond, J.E., and Schmitz, C.P., "MINIVER Upgrade for the AVID System," NASA CR 172214, Volume III: "EXITS User's and Input Guide," August 1983.

[6] Engel, Carl D., and Praharaj, Sarat C., "MINIVER Upgrade for the AVID System, Volume 1, LANMIN Users Manual," NASA CR 172212, August 1983.

[7] Crain, William K., and Nutt, Kenneth W., "NASA/Rockwell International IH-97 Space Shuttle Hearing Test," AEDC-TSR-82–V37, Dec. 1982.

[8] Lemoine, P.L., and Marroquin, J., "Results of Heat Transfer Tests of a 0.0175 Scale Shuttle Integrated Vehicle Model 60–OTS in the AEDC-VKF Tunnel A (IH-72)," NASA-CR-160, 843, August 1981.

[9] Foust, J.W., "Test Results from the NASA/Rockwell International Space Shuttle Integrated Vehicle Test Using A 0.0175 — Scale Model (60–OTS) Conducted in the AEDC-VKF Tunnel A (IH-85)," NASA-CR-151, 800, April 1980.

[10]Crain, W.K., Frost, C.L., and Engel, C.D., "Final Report SRB Ascent Aerodynamic Heating Design Criteria Reduction Study," Volume I, II, REMTECH RTR 090–01, Jan. 18, 1989.

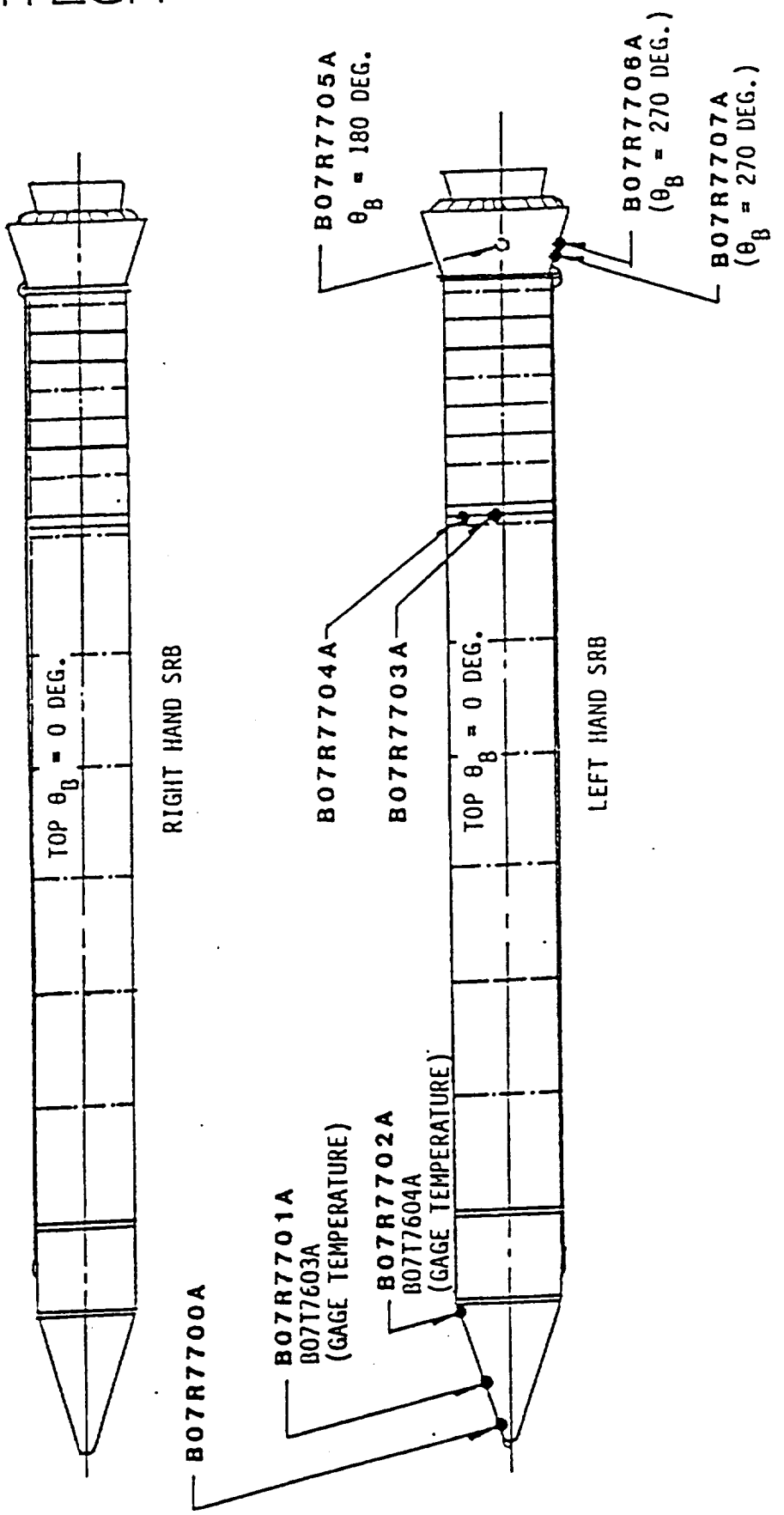

a) External Instrumentation

Figure 1: SRB DFI Instrumentation

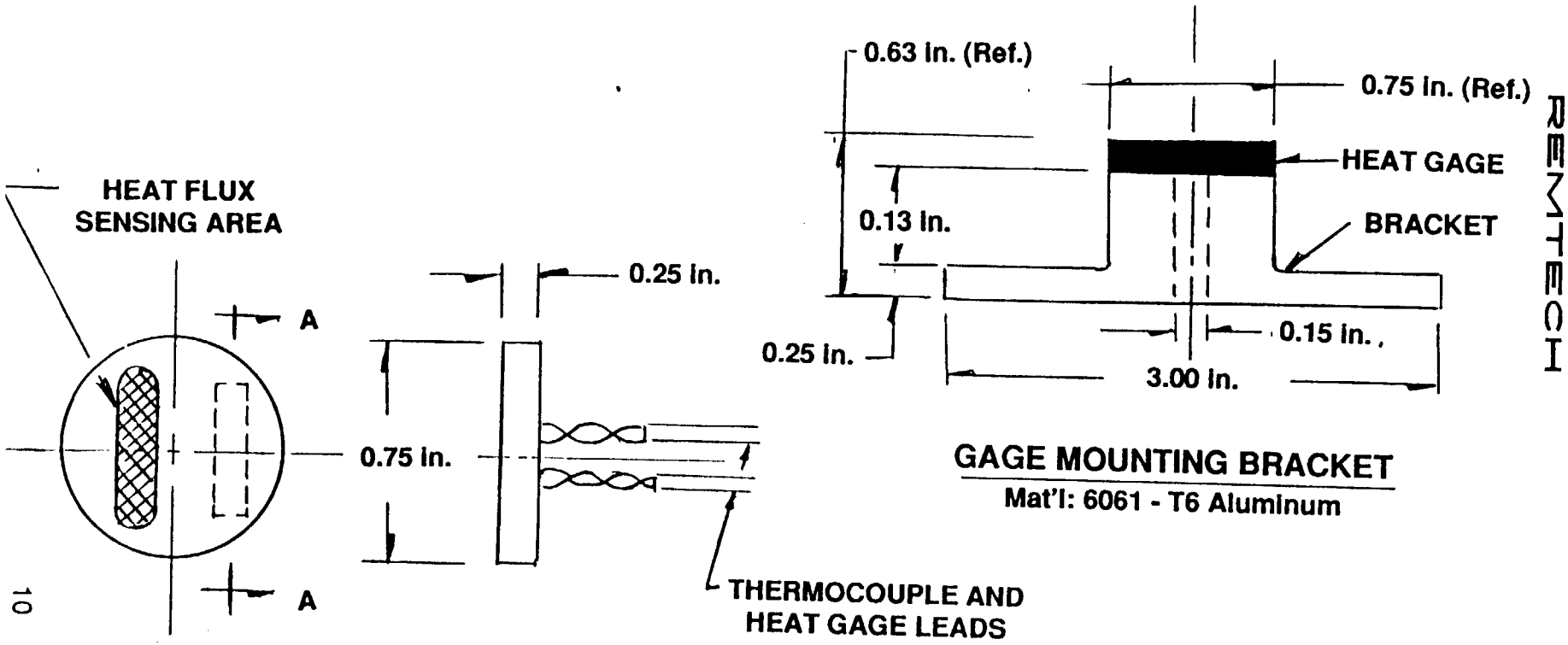

NOTE: Gage B07R7700 Did NOT Have
An Associated Thermocouple

(a) Medtherm Schmidt-Boelter Gage (B07R7700–7702)

Figure 2: Flight External Calorimeter (STS-26R, 27R, and 29R)

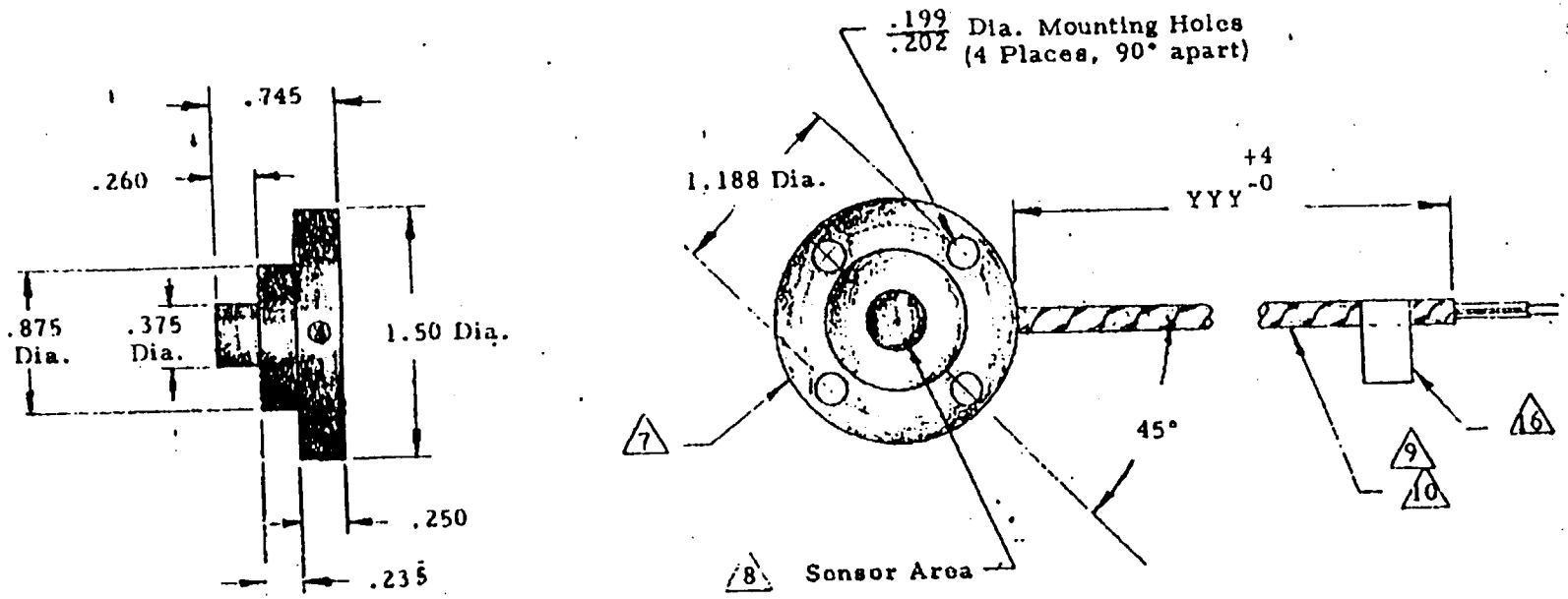

NOTES:

1. Model number designated as follows:
   ZZ - Full scale heat flux in Btu/ft^2-sec.
   YYY - Flexible lead length in inches.
   ( ) - Model Dash No. - See Table, Note 17 for applicability.
2. Full scale output: 15 ± 1.5 mV., except 15 +1.5,-4 for 5 Btu/ft^2-sec. full scale heat flux.
3. Linearity: Better than 3% of full scale output.
4. Time constant: Per Table, Note 17.
5. Repeatability: Better than ±0.5% of full scale output.
6. Output impedance: < 100 ohms.
7. Body material: Oxygen free copper, 16 finish or better.

REVISIONS			ALL DIMENSIONS IN INCHES WITH FOLLOWING TOLERANCES UNLESS OTHERWISE NOTED:			Hy-Cal Engineering	DATE 4-24-78	MATERIAL Pg. 1 of 4
NO.	DATE	BY	DECIMALS	FRACTIONS	ANGLES	SANTA FE SPRINGS CALIFORNIA	SCALE Full	Noted
1			.X ±.050	±	±	ASYMPTOTIC® UNCOOLED CALORIMETER	DRAWN V.A.	DRAWING NO.
2			.XX ±.030		1/2	MODEL C-1202-E-( )-ZZ-YYY	APPD	A-14055
3			.XXX ±.010					
4								
5								

(b) HYCAL Calorimeter (B07R7703–7707)

Figure 2: Flight External Calorimeter (STS-26R, 27R, and 29R)

NOSE CONE/FRUSTUM CALORIMETERS

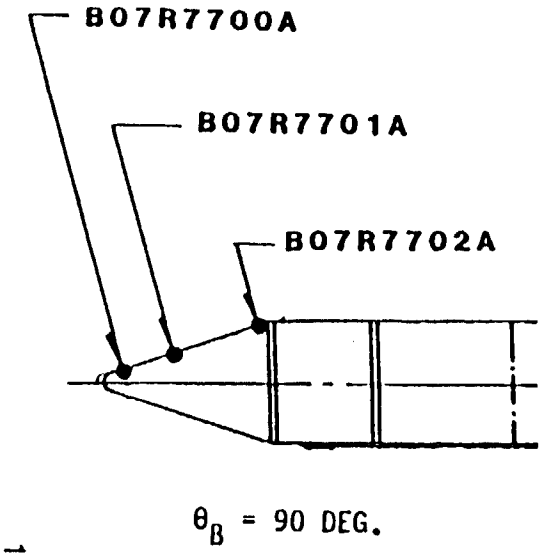

- RESOLVE 90 DEG. RAY HEATING DISCREPANCY
- RESOLVE HIGH HEATING FROM SRB/ET SHOCK IMPINGEMENT ON 90 DEG. RAY

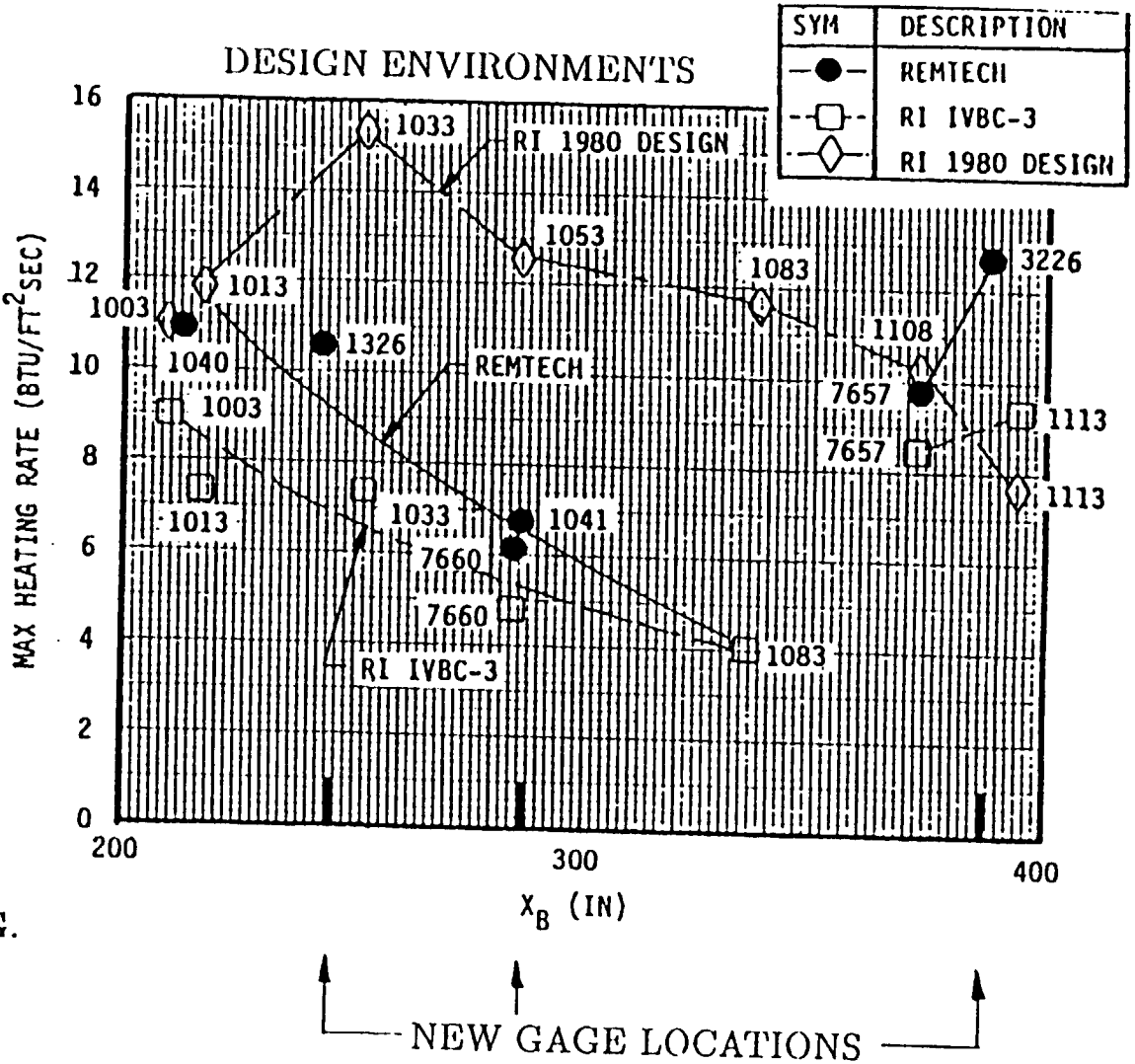

(a) Nose Cone/Frustum Calorimeters

Figure 3: Instrumentation Location and Objective

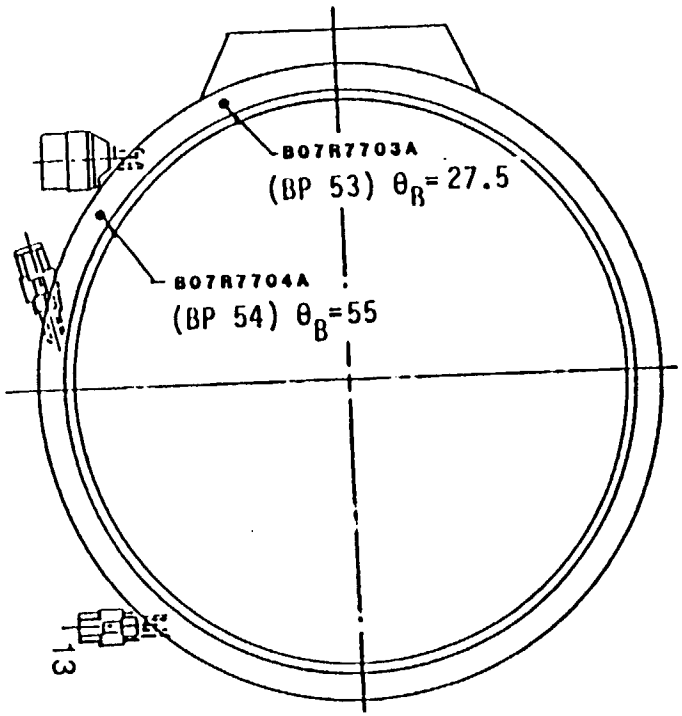

- NO PREVIOUS FLIGHT DATA
- DEFINE HIGH HEATING REGION ON ATTACH RING

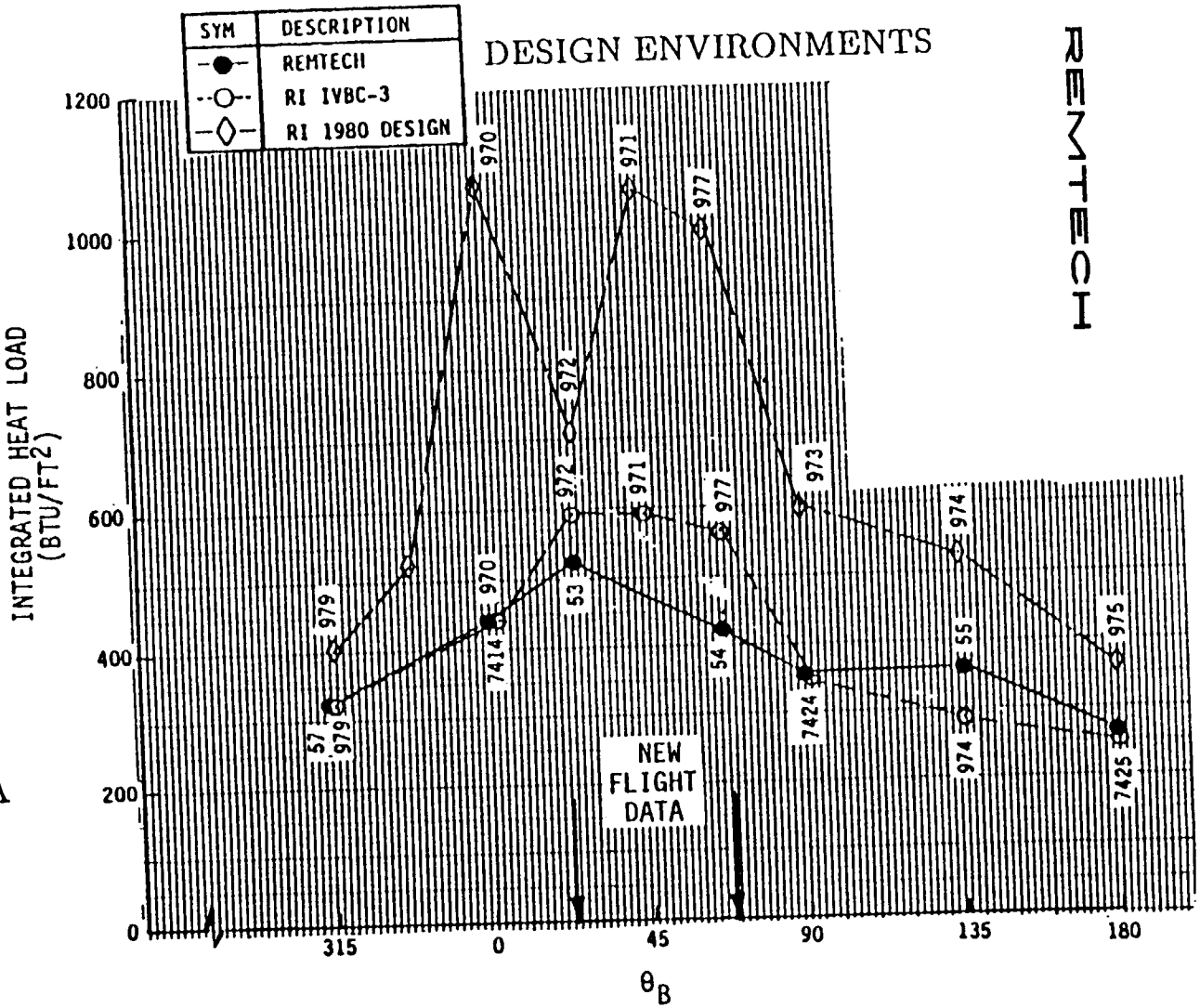

(b) Attach Ring

Figure 3: Instrumentation Location and Objective

REMTECH

RTN 213-14

C-2

(c) Aft Skirt

Figure 3: Instrumentation Location and Objective

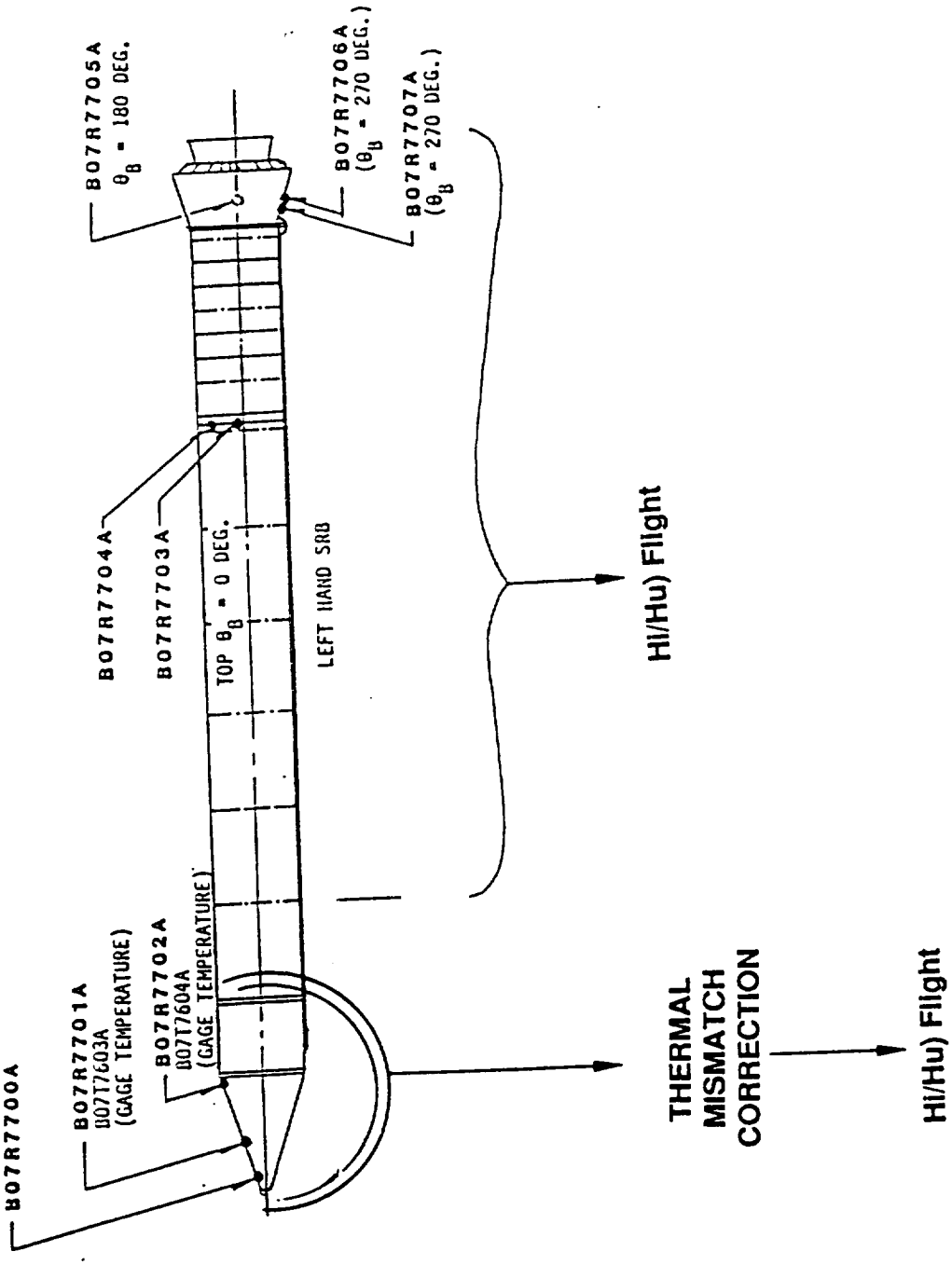

Figure 4: Flight Data Reduction Philosophy

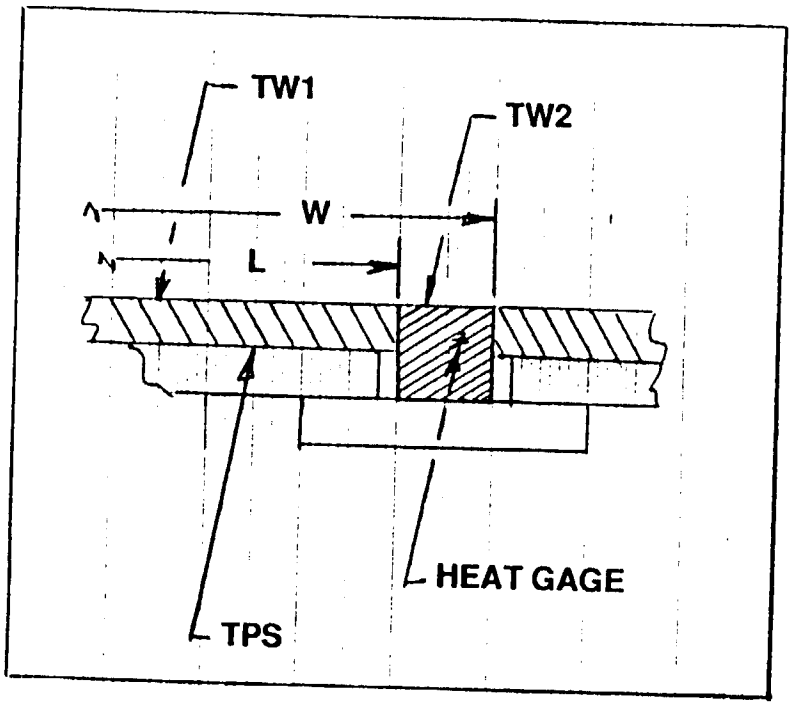

$$\frac{H}{H_{iso}} = F\left(\frac{L}{W}\right) + H'\left(\frac{L}{W}\right)\left[\frac{Tw2 - Tw1}{Tw2 - TR}\right]$$

NOTE:

1) L and W measured from origin of Turbulent Boundary Layer. For this specific case, it was taken as

$$X_B = 200\ in.$$

2) T_R =Local recovery temperature, ^{o}R

GAGE	X_B (in)	RUNNING LENGTH (in)	$\frac{L}{W}$	$F\left(\frac{L}{W}\right)$	$H'\left(\frac{L}{W}\right)$
7700	243	52.25	0.99052	1.0019	0.91049
7701	287	98.52	0.99495	1.0010	1.0488
7702	385	201.56	0.99750	1.0005	1.2150

Figure 5: Thermal Mismatch Correction Definitions and Constants

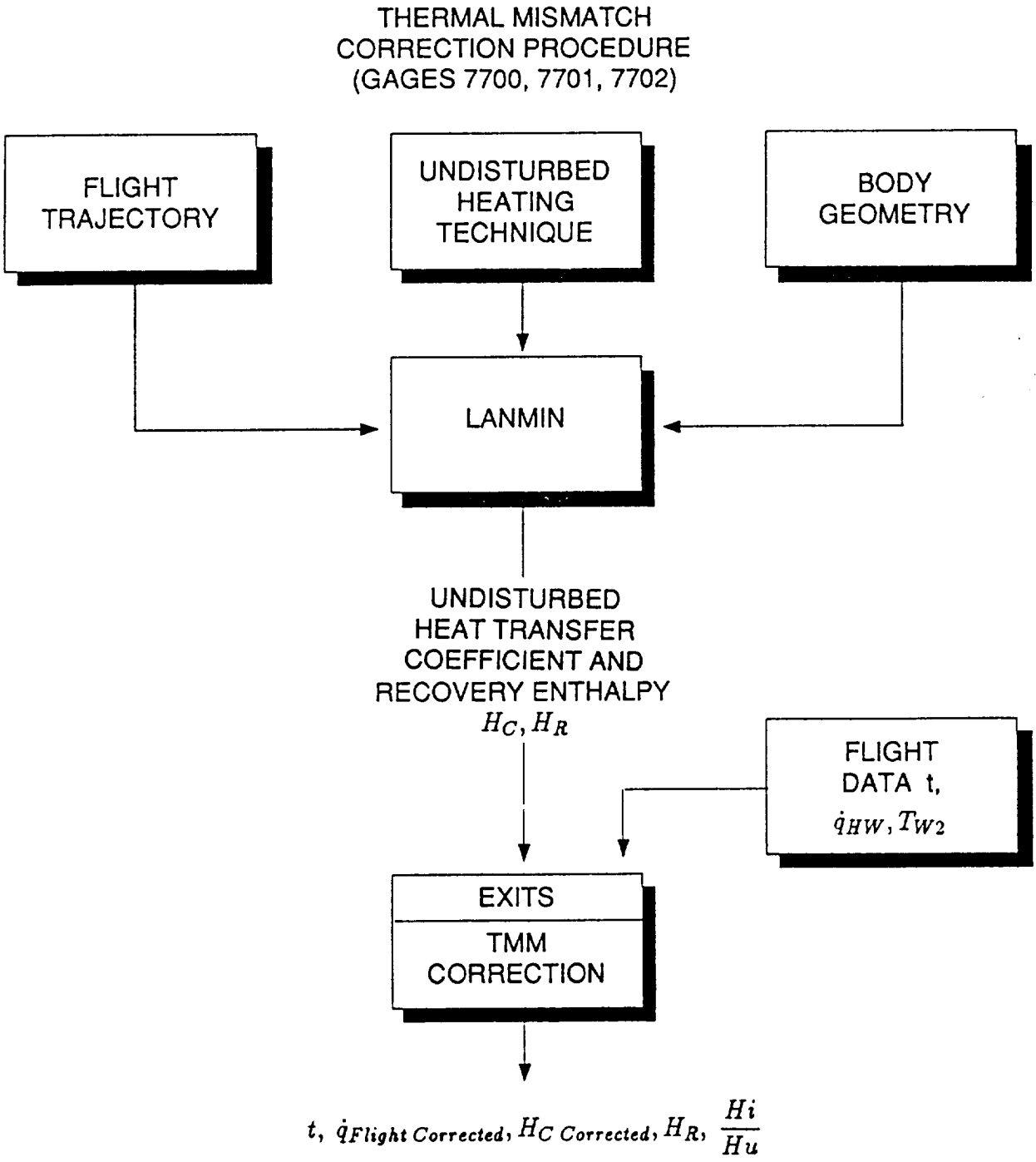

Figure 6: Thermal Mismatch Correction Scheme

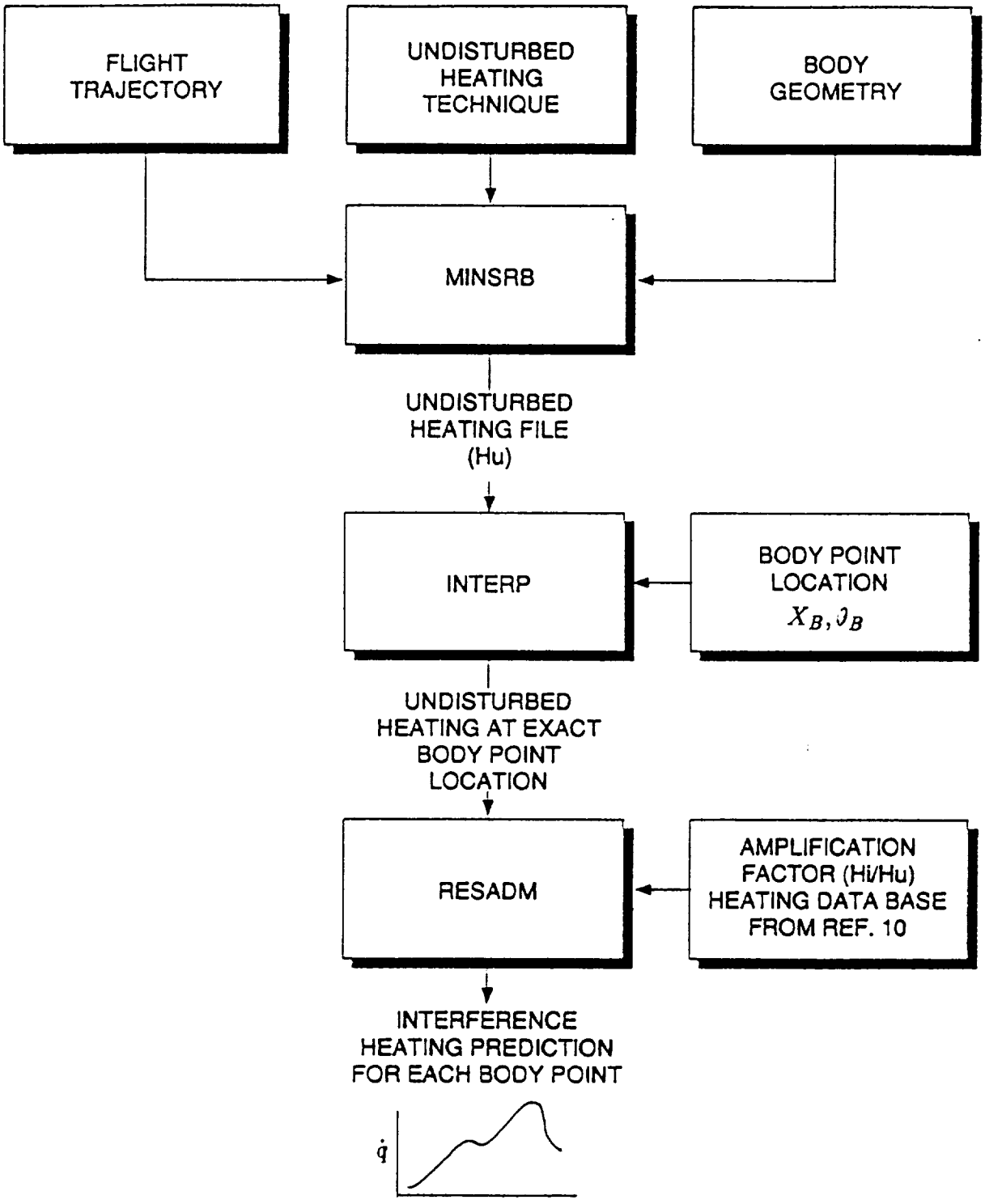

Figure 7: Ascent Heating Prediction Methodology

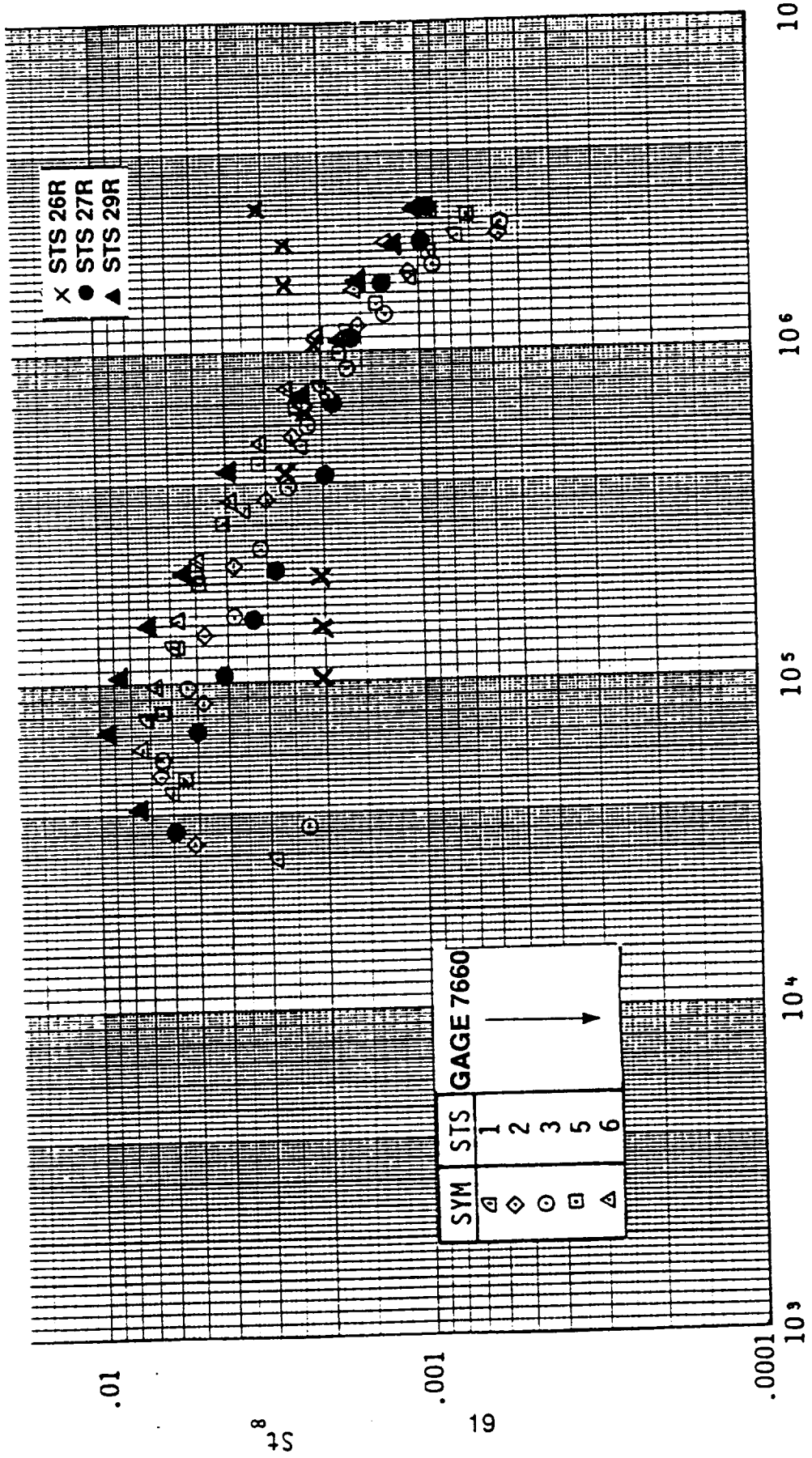

(a) Gage B07R7700

Figure 8: Comparison of Current Flight Data with Historic (STS 1–3, 5, 6) Flight Heating Data

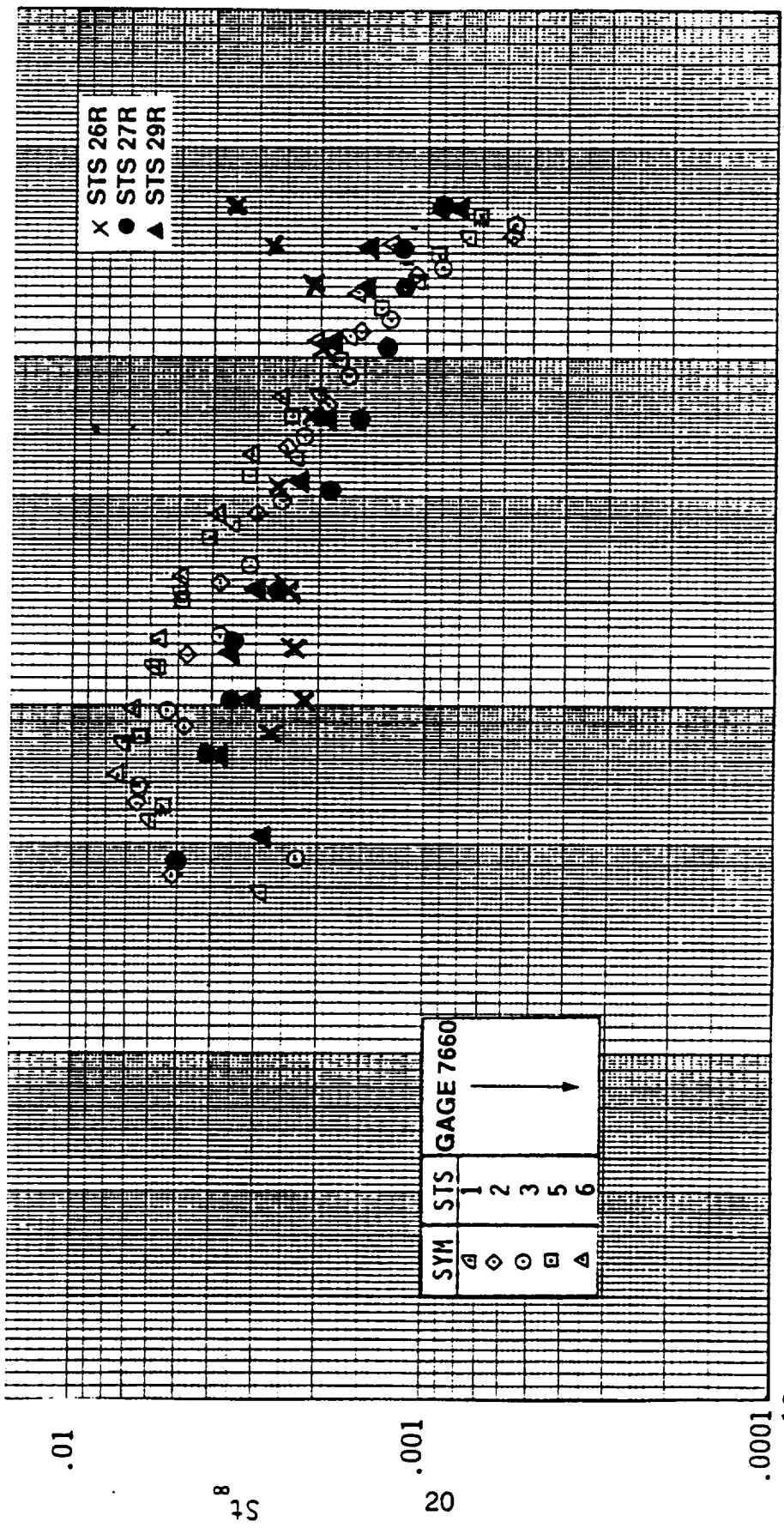

(b) Gage B07R7701

Figure 8: Comparison of Current Flight Data with Historic (STS 1–3, 5, 6) Flight Heating Data

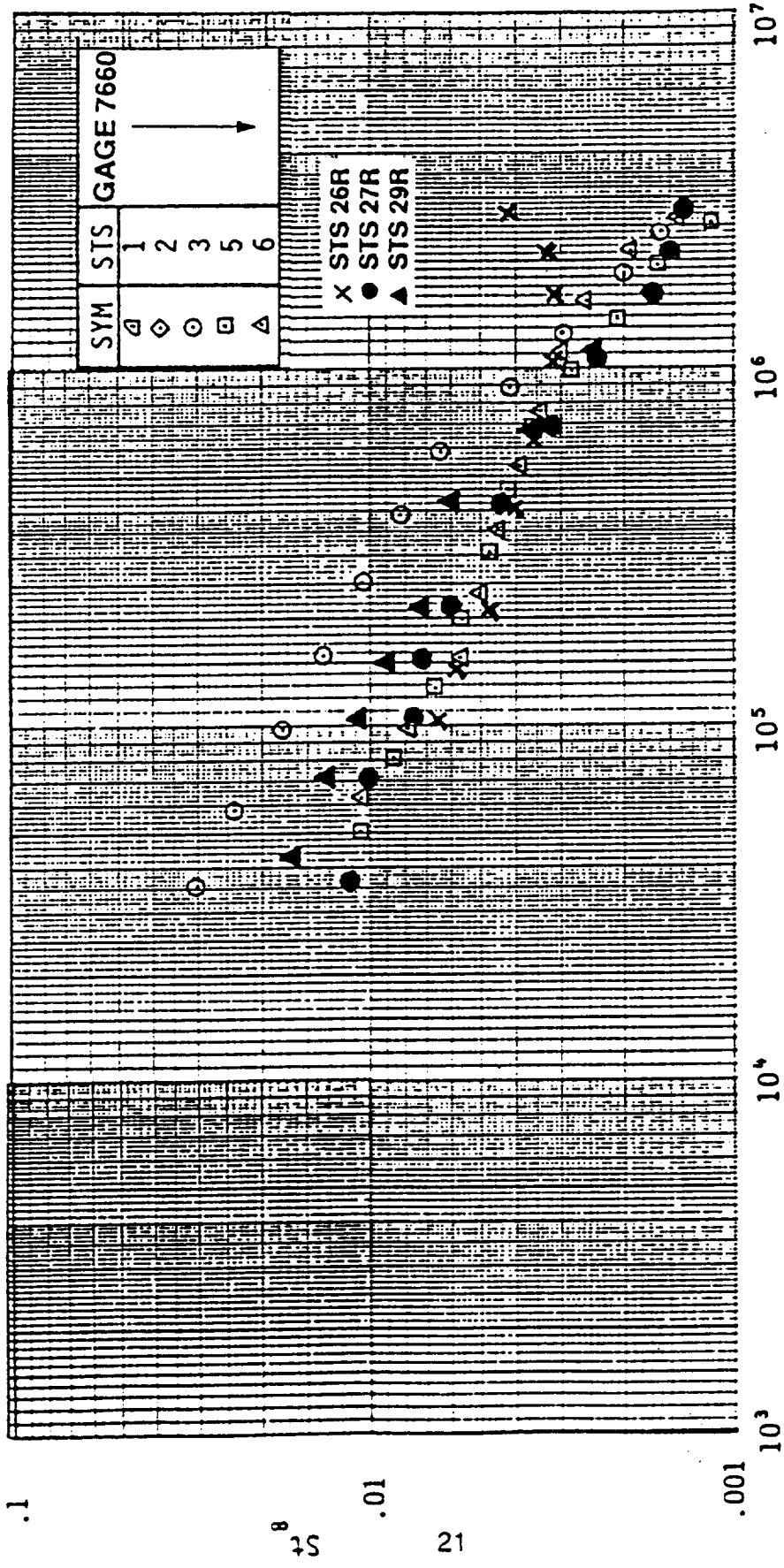

(c) Gage B07R7702

Figure 8: Comparison of Current Flight Data with Historic (STS 1–3, 5, 6) Flight Heating Data

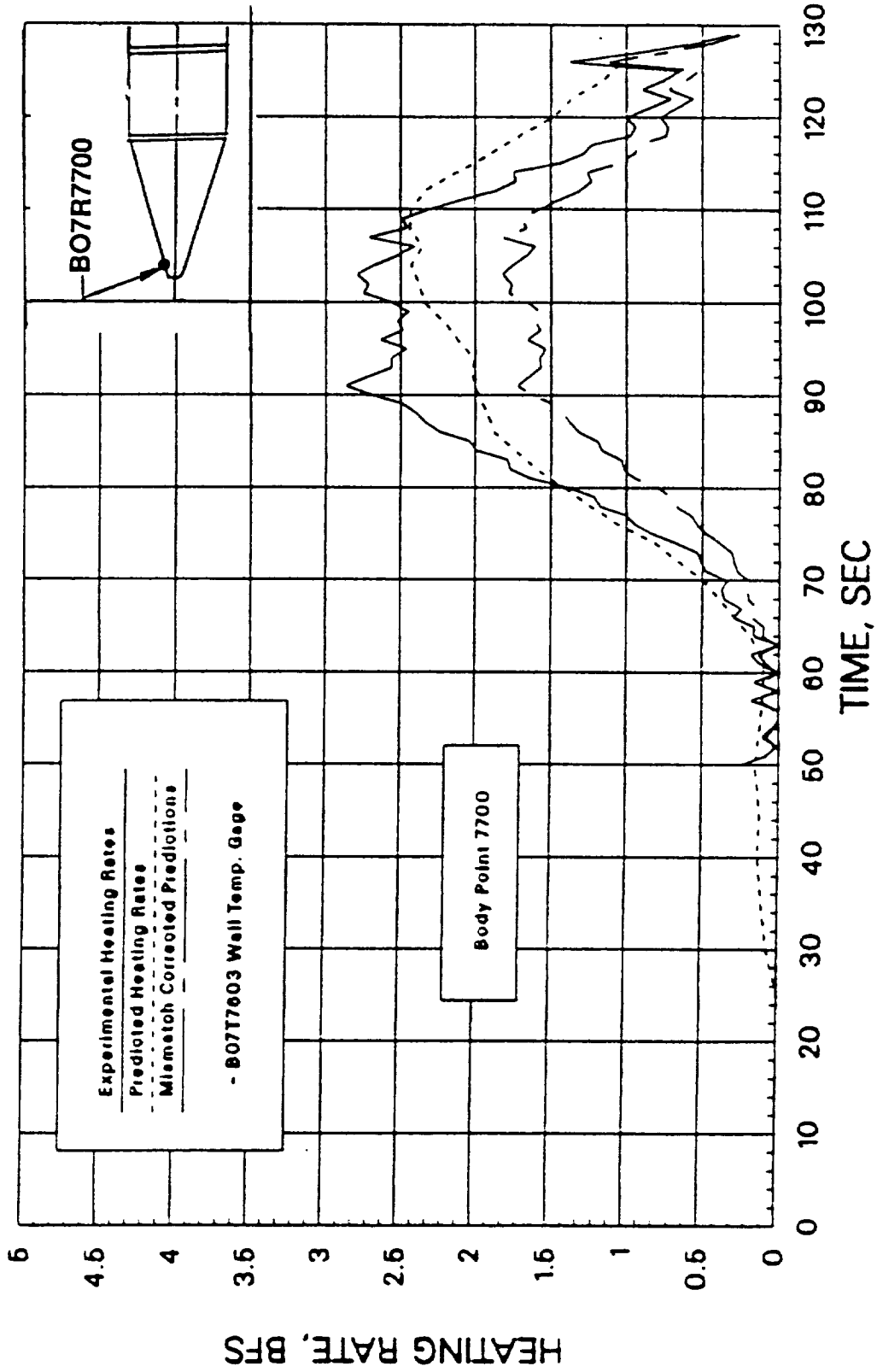

(a) STS-26R

Figure 9: Ascent Flight Heating — B07R7700

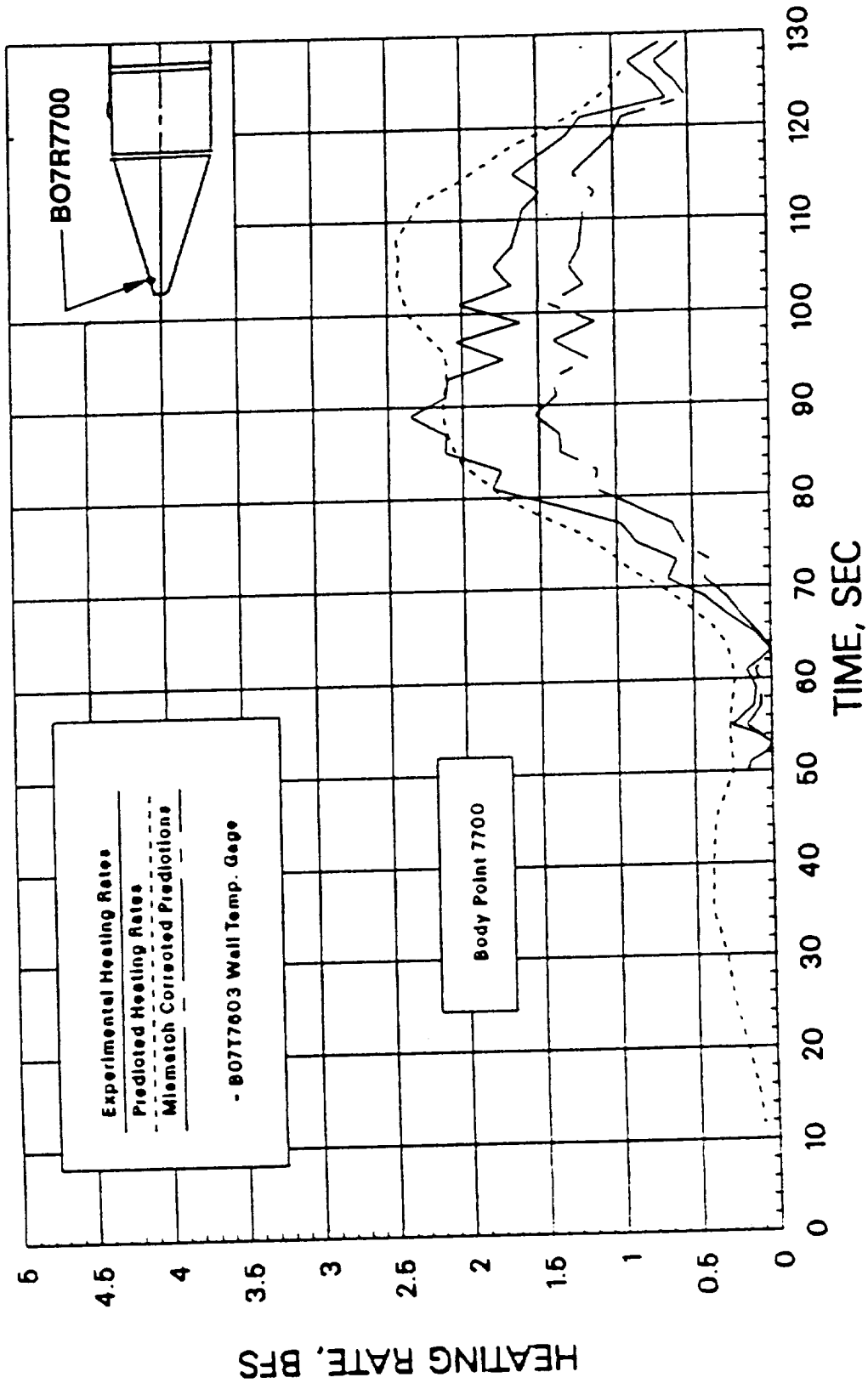

(b) STS-27R

Figure 9: Ascent Flight Heating — B07R7700

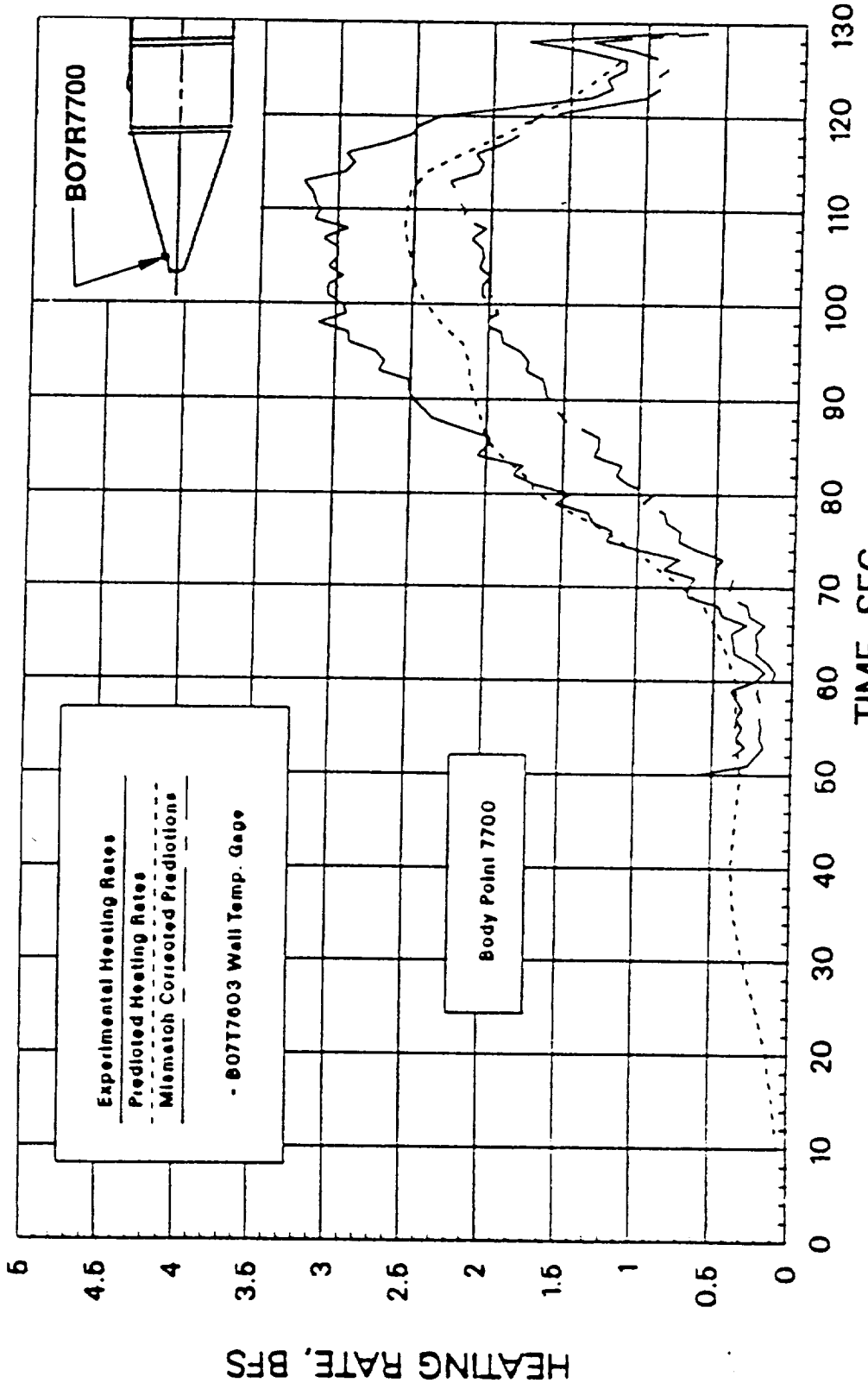

(c) STS-29R

Figure 9: Ascent Flight Heating — B07R7700

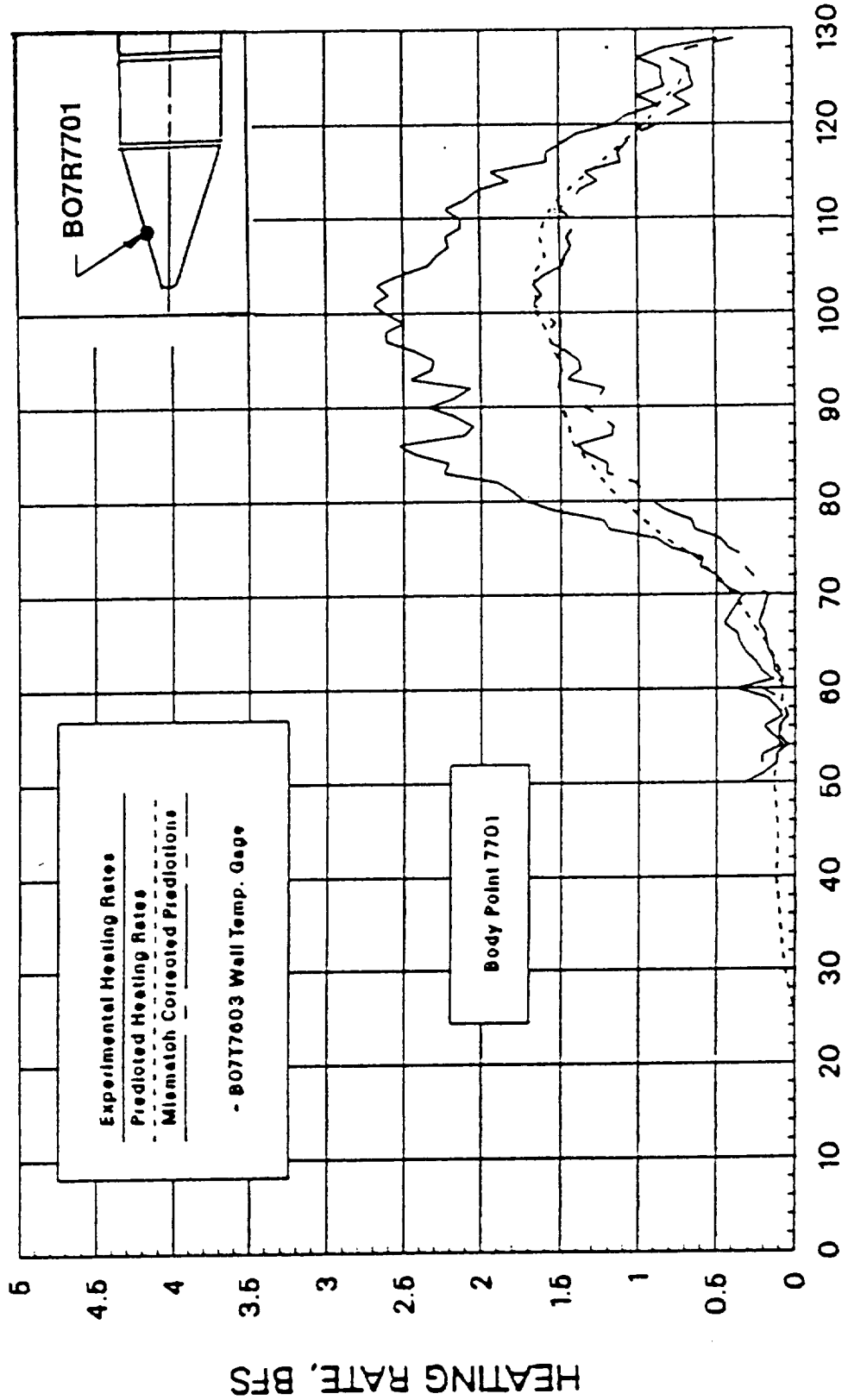

(a) STS-26R

Figure 10: Ascent Flight Heating — B07R7701

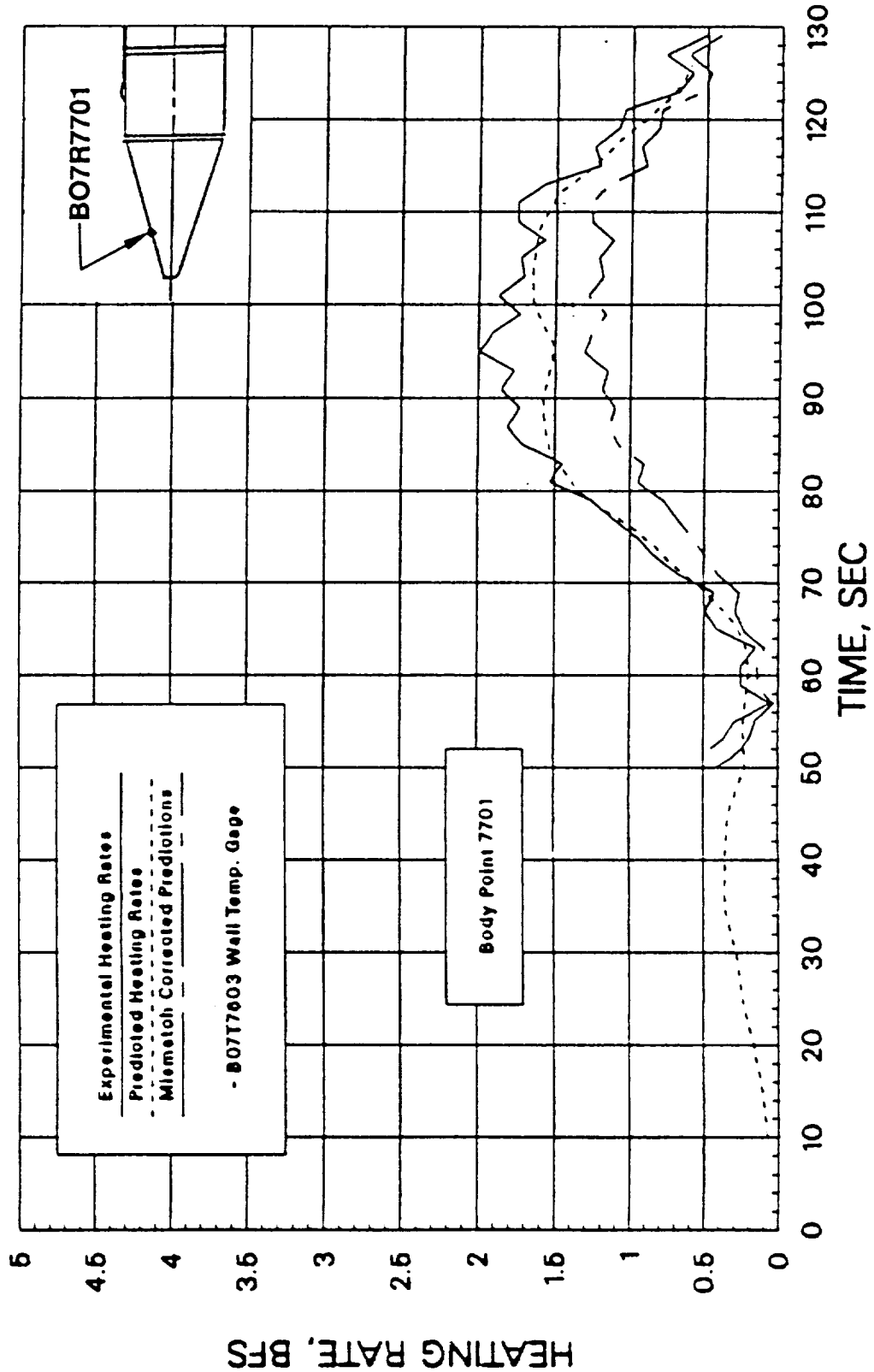

(b) STS-27R

Figure 10: Ascent Flight Heating — B07R7701

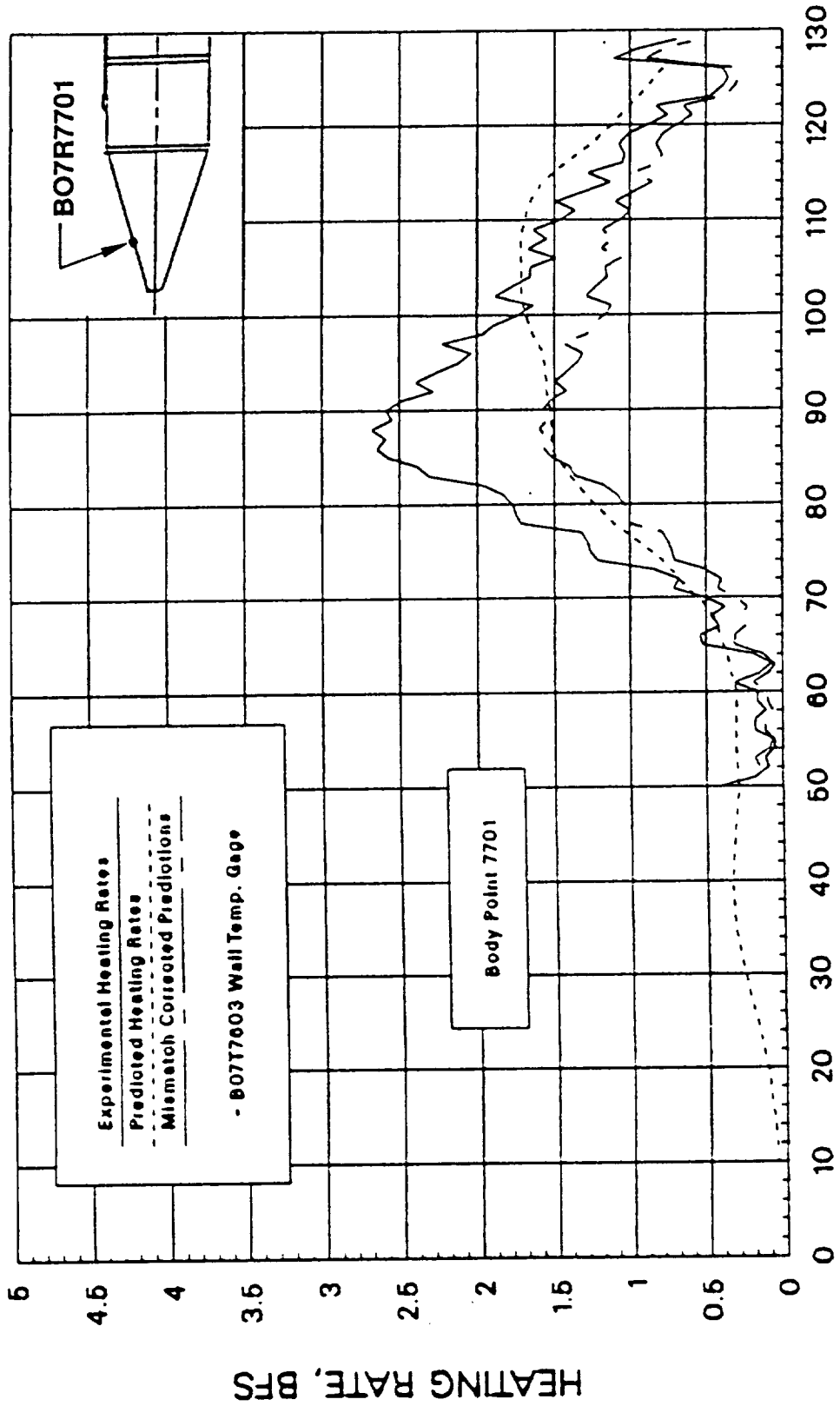

(c) STS-29R

Figure 10: Ascent Flight Heating — B07R7701

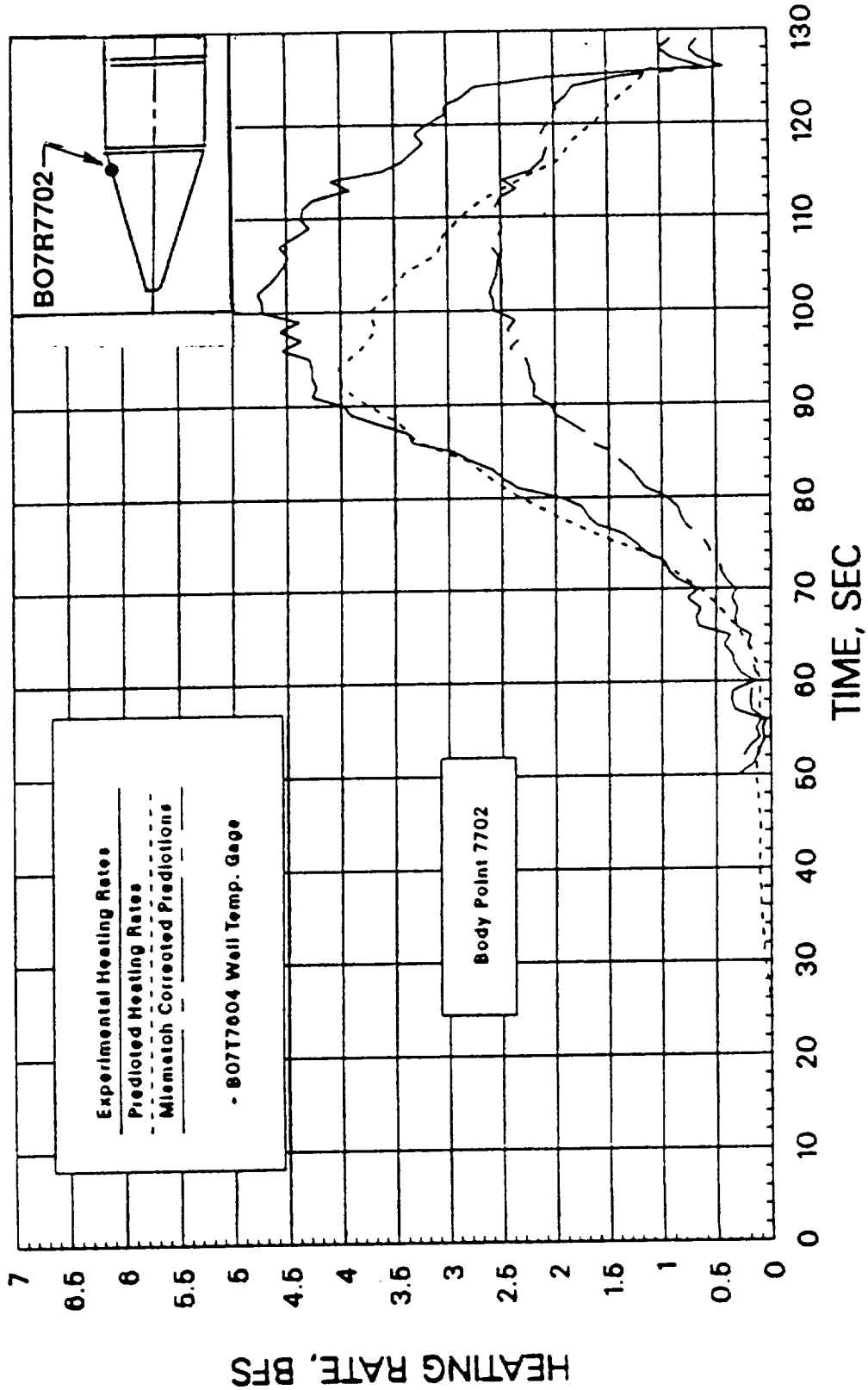

(a) STS-26R

Figure 11: Ascent Flight Heating — B07R7702

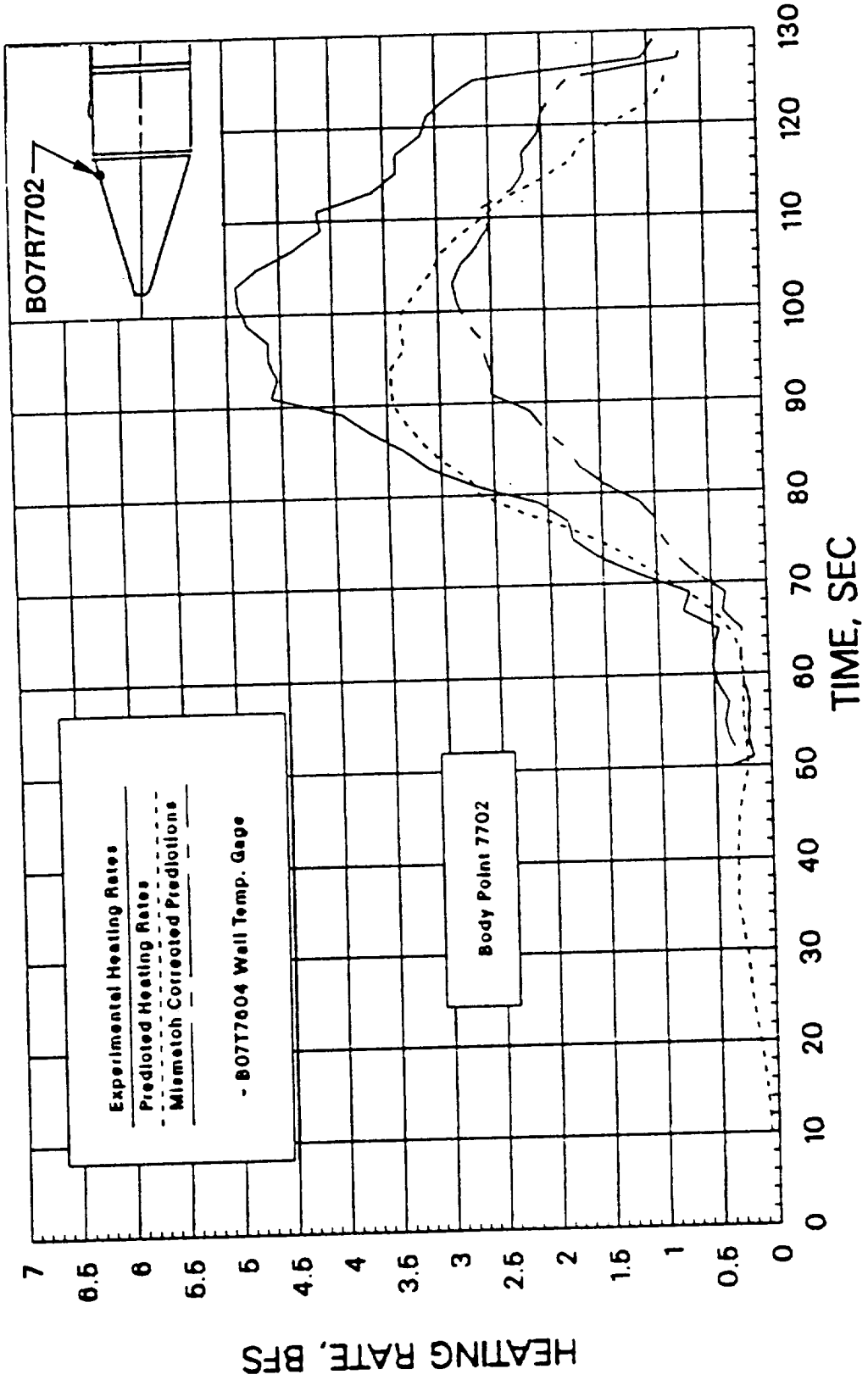

(b) STS-27R

Figure 11: Ascent Flight Heating — B07R7702

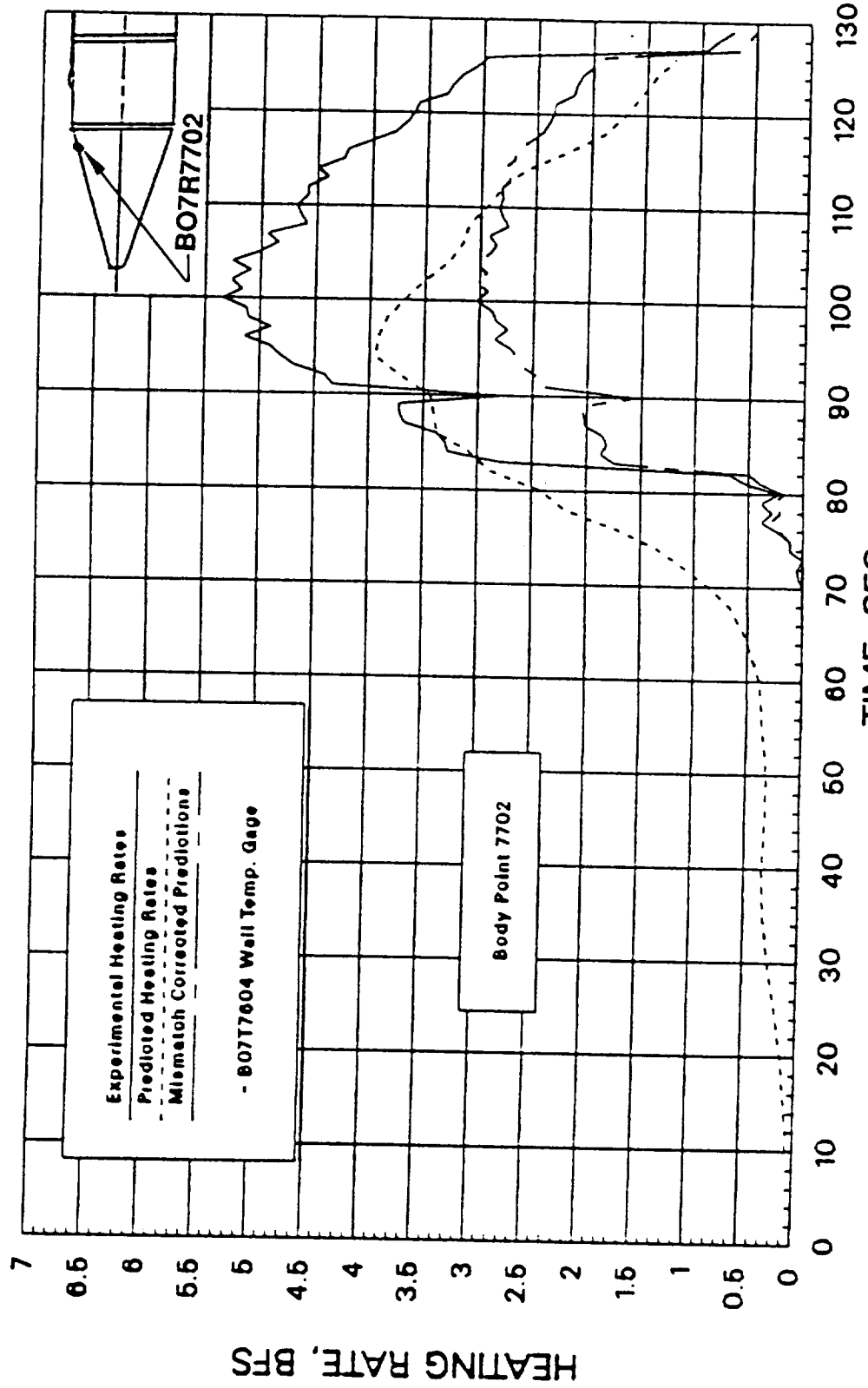

(c) STS-29R

Figure 11: Ascent Flight Heating — B07R7702

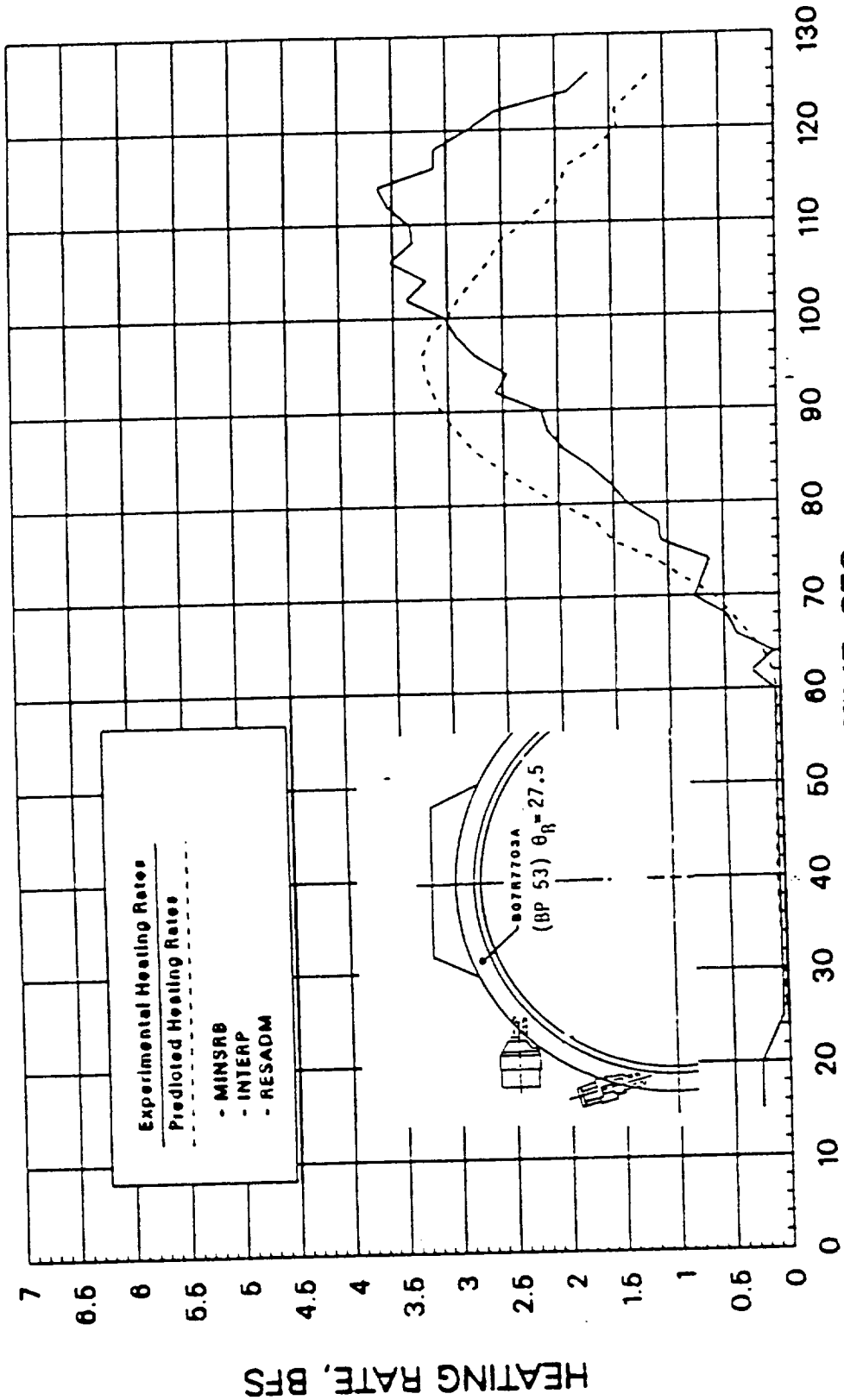

(a) STS-26R

Figure 12: Attach Ring Heating — B07R7703

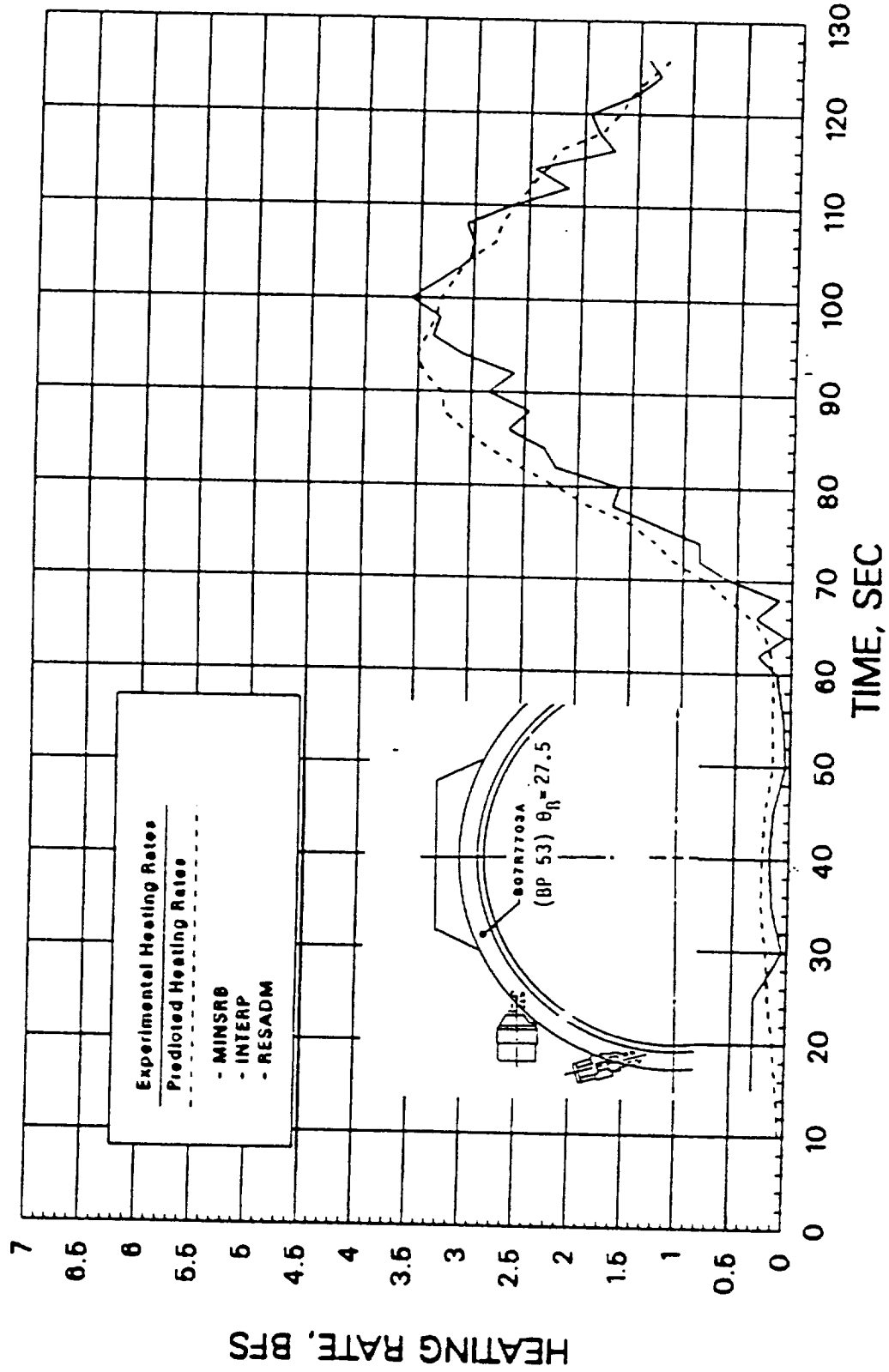

(b) STS-27R

Figure 12: Attach Ring Heating — B07R7703

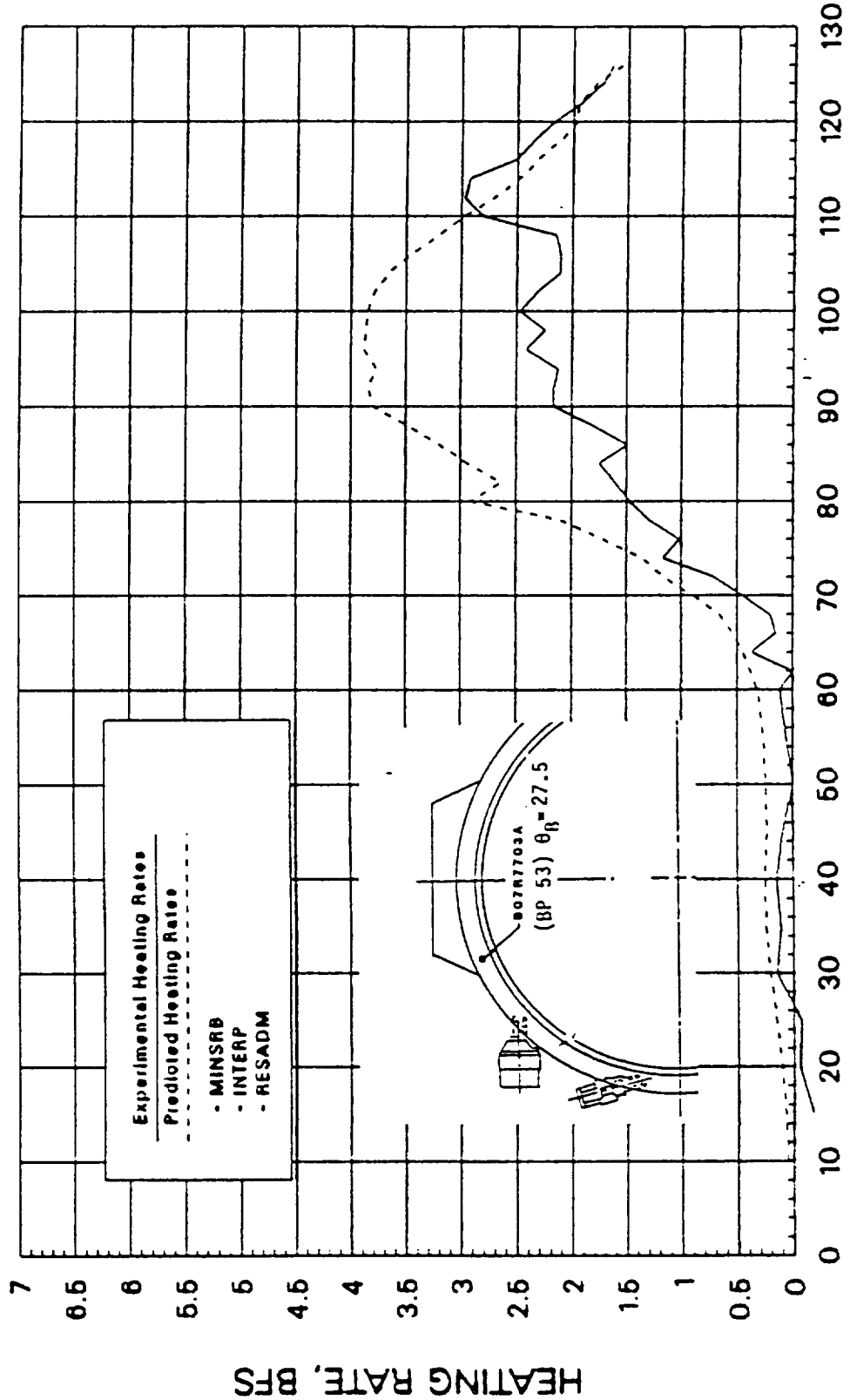

(c) STS-29R

Figure 12: Attach Ring Heating — B07R7703

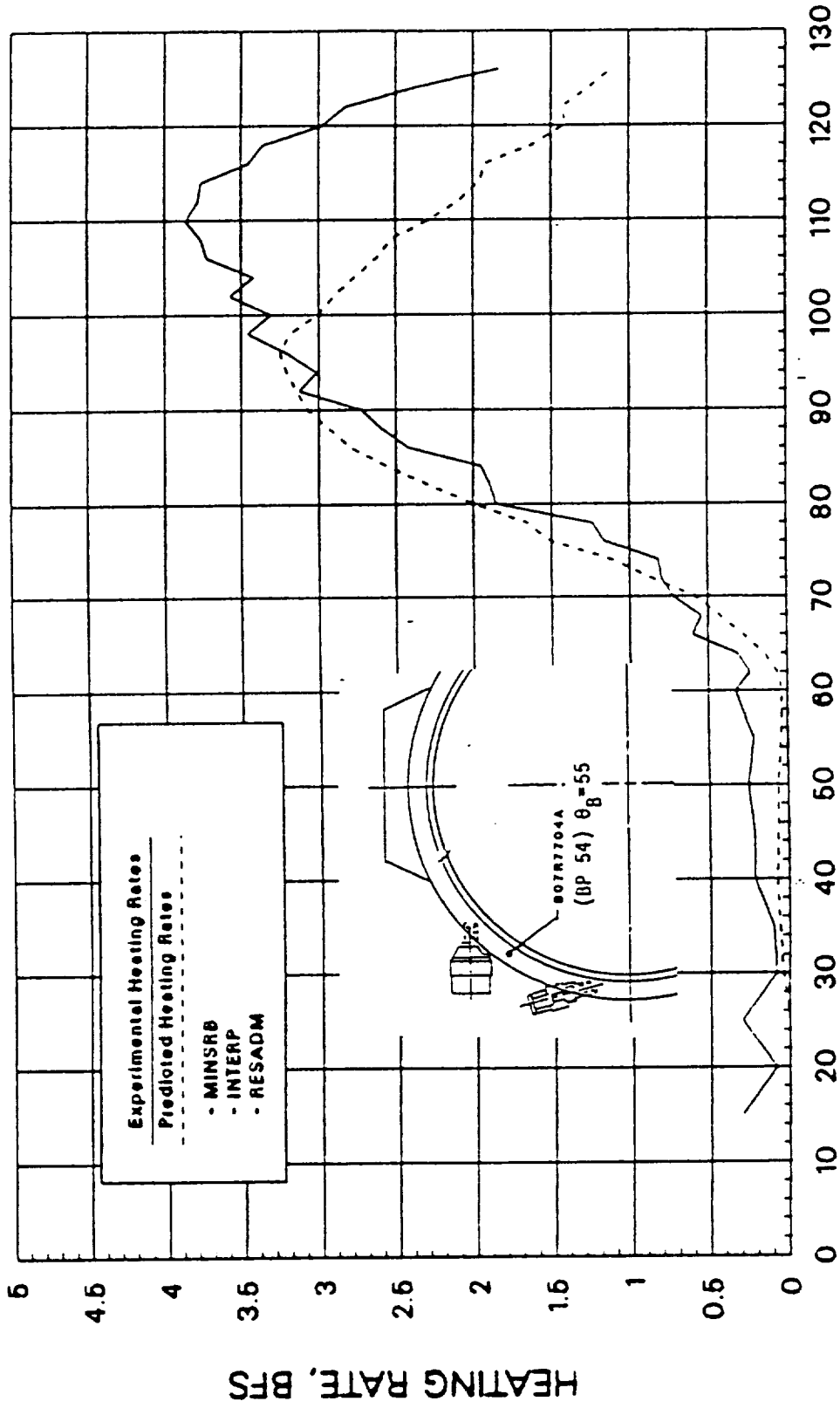

(a) STS-26R

Figure 13: Attach Ring Heating — B07R7704

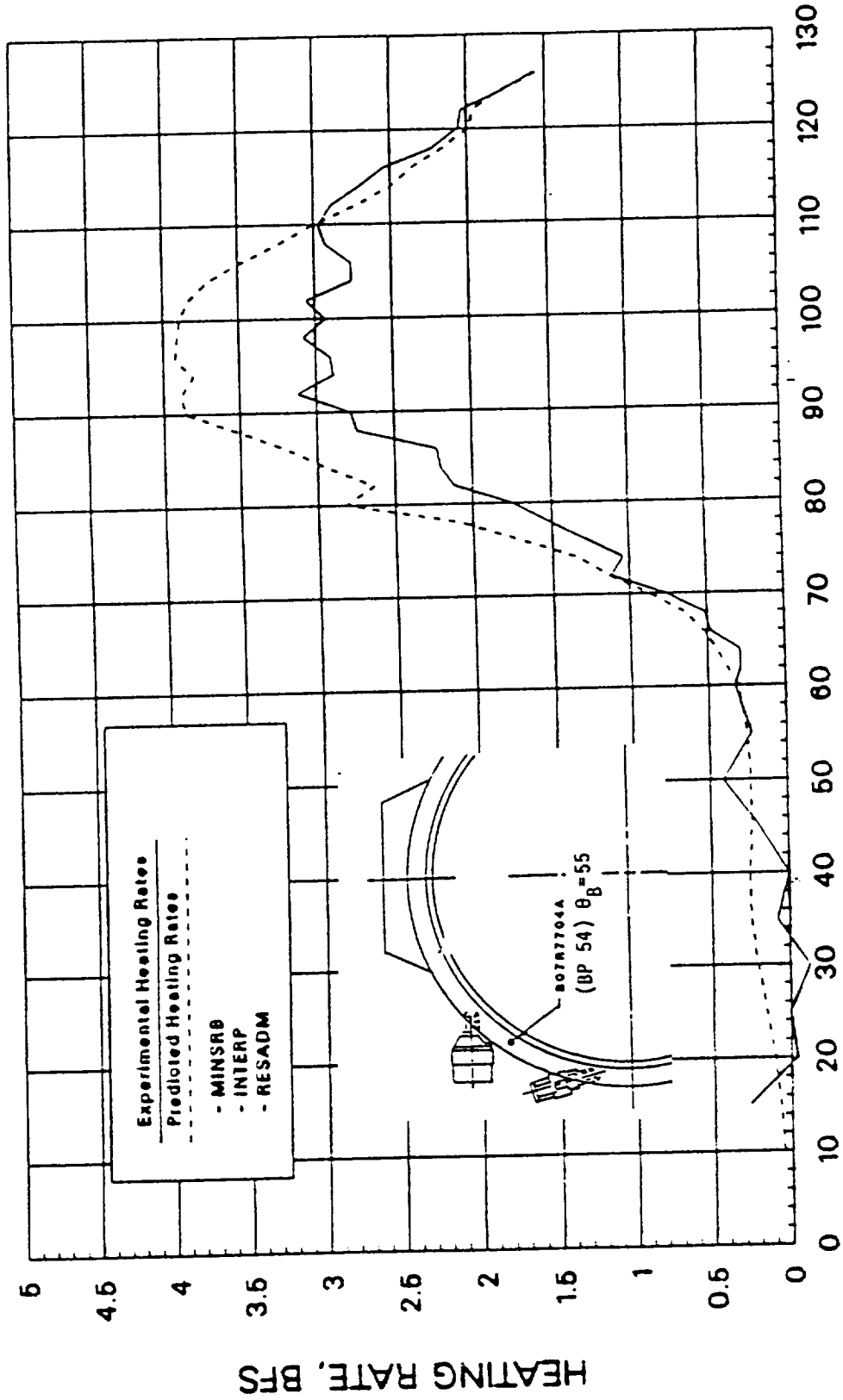

(b) STS-29R

Figure 13: Attach Ring Heating — B07R7704

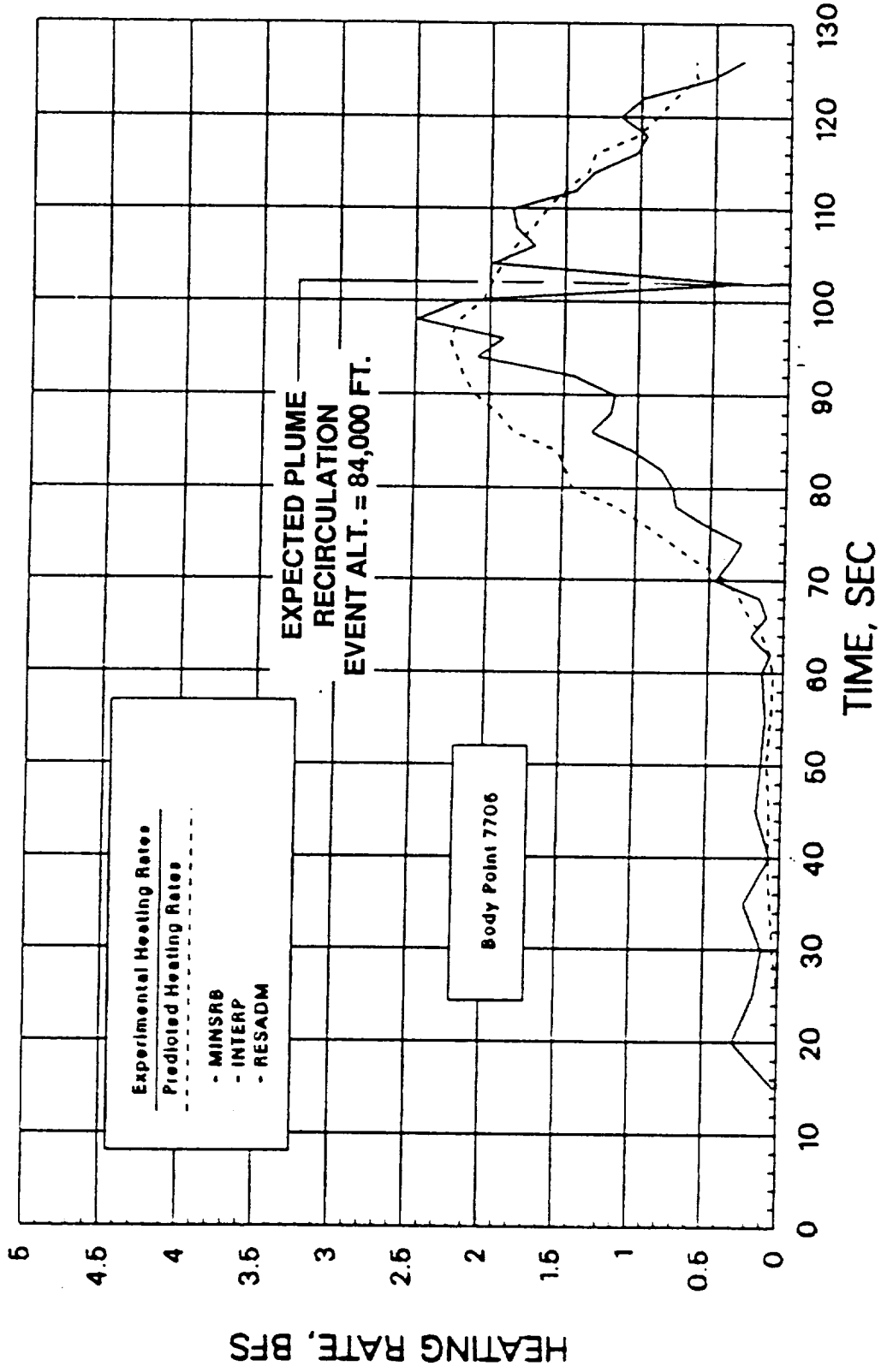

(a) B07R7705 $X_B = 1880, \theta_B = 180deg$

Figure 14: Aft Skirt Heating (STS-26R)

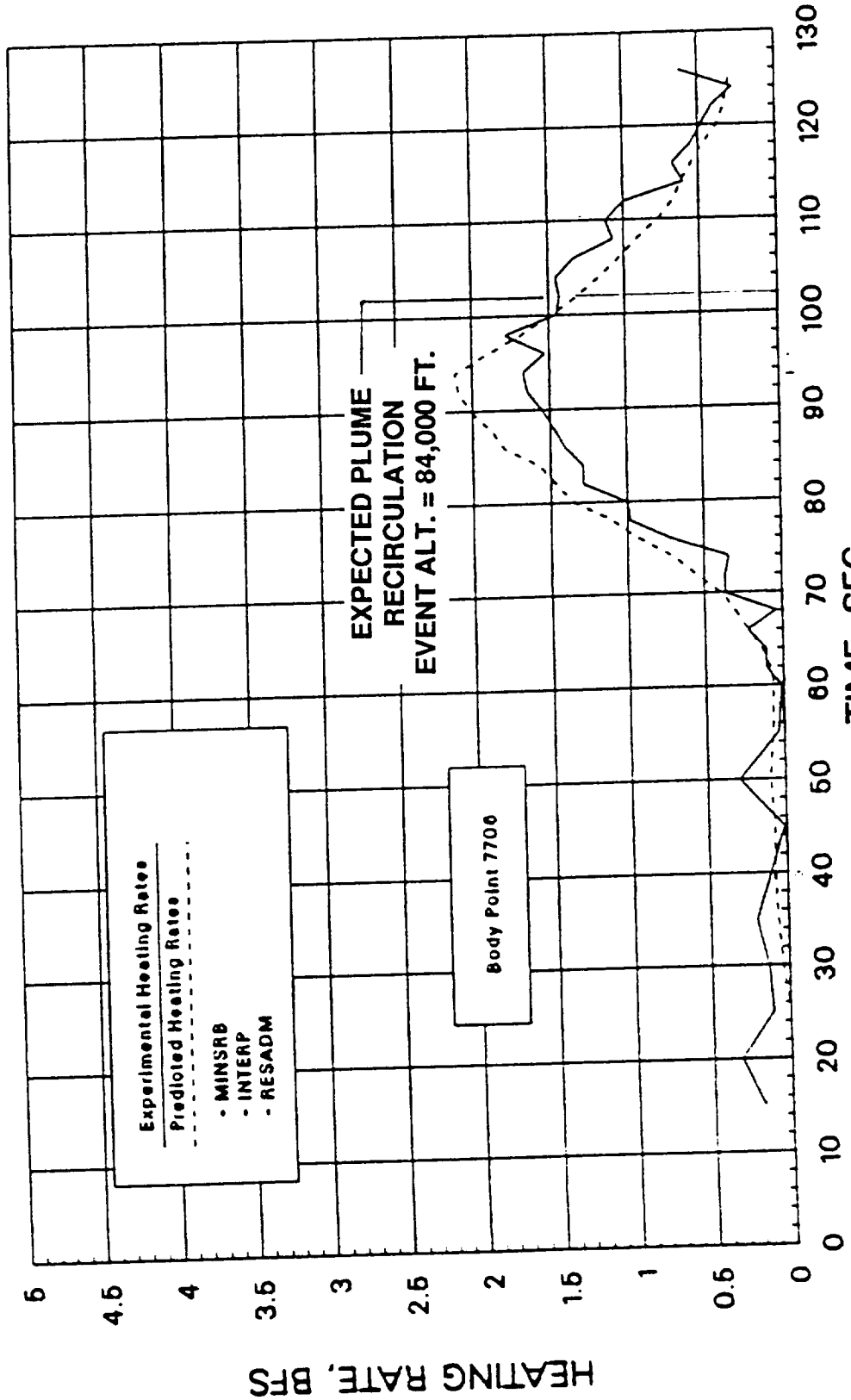

(b) B07R7706 $X_B = 1880, \theta_B = 270deg$

Figure 14: Aft Skirt Heating (STS-26R)

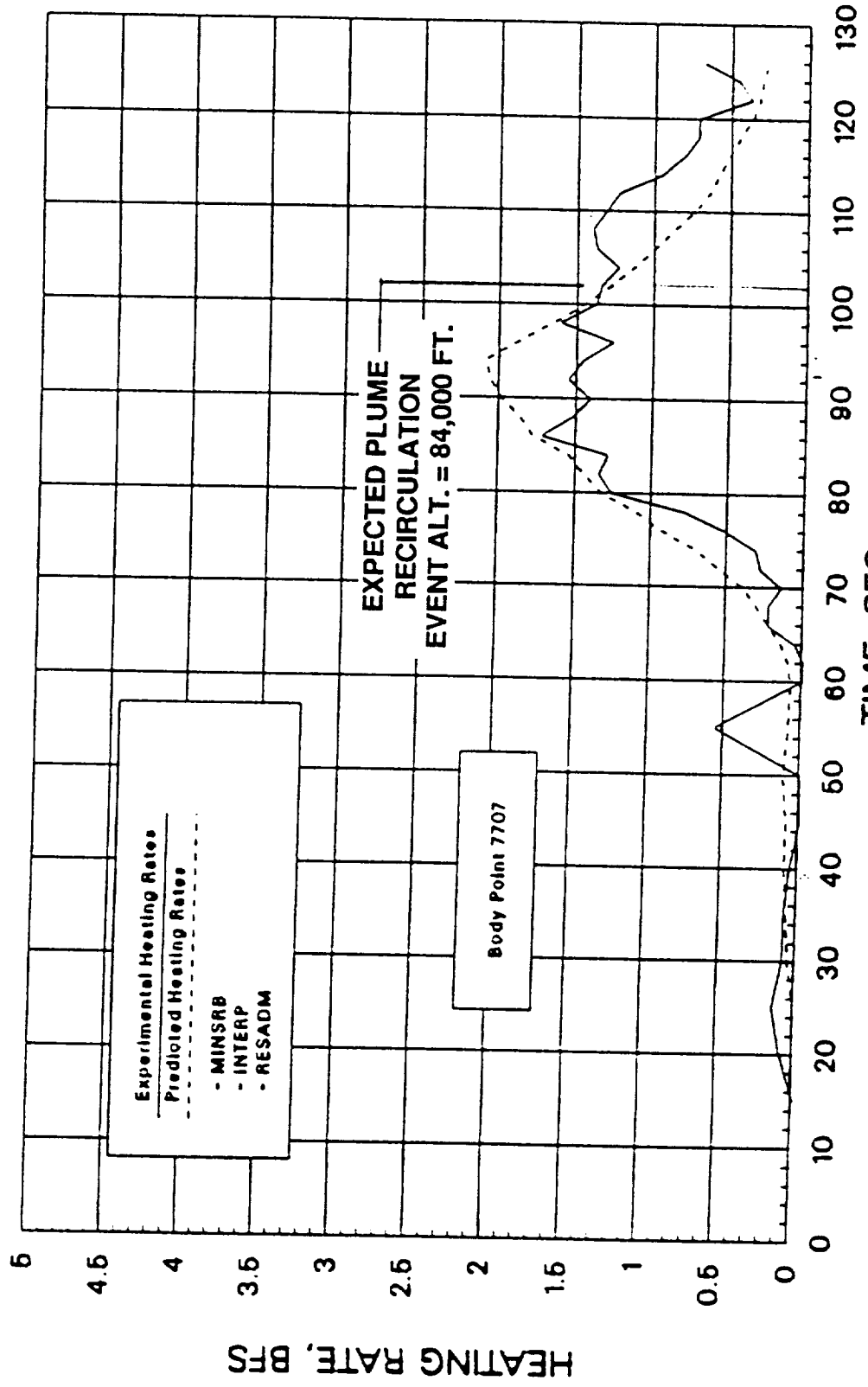

(c) B07R7707 $X_B = 1870, \theta_B = 270deg$

Figure 14: Aft Skirt Heating (STS-26R)

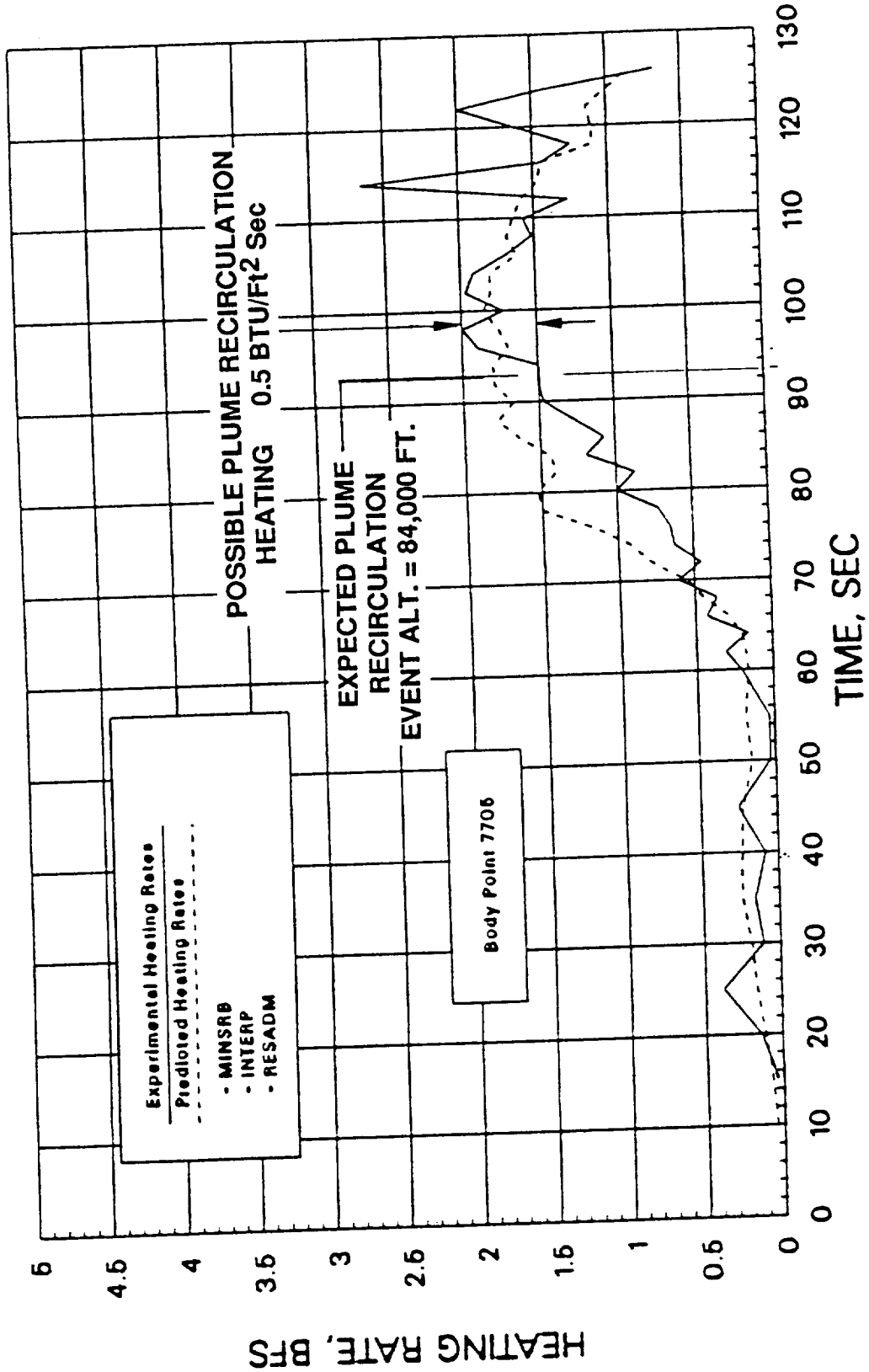

(a) B07R7705 $X_B = 1880, \theta_B = 180deg$

Figure 15: Aft Skirt Heating (STS-27R)

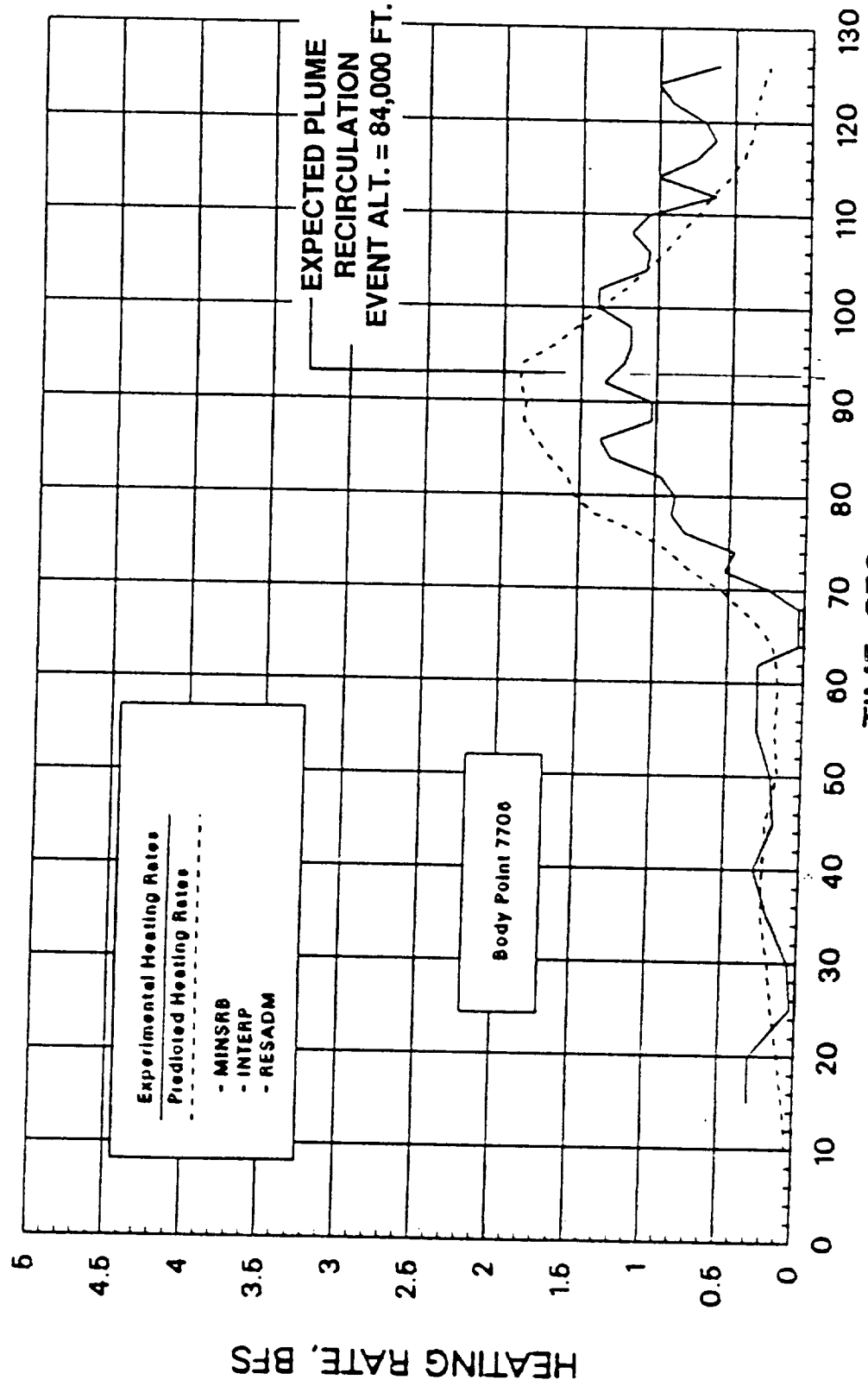

(b) B07R7706 $X_B = 1880, \theta_B = 270deg$

Figure 15: Aft Skirt Heating (STS-27R)

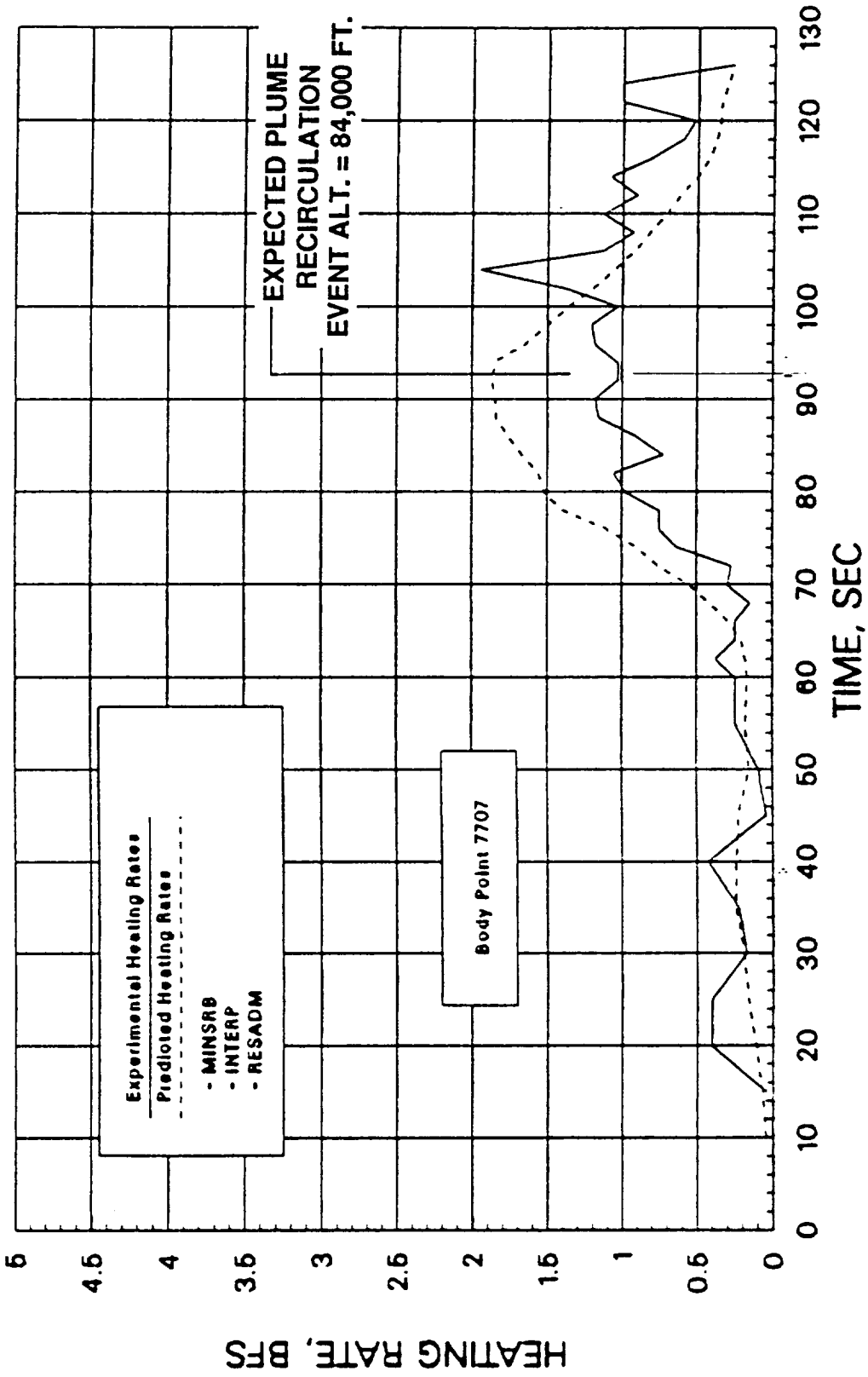

(c) B07R7707 $X_B = 1870, \theta_B = 270deg$

Figure 15: Aft Skirt Heating (STS-27R)

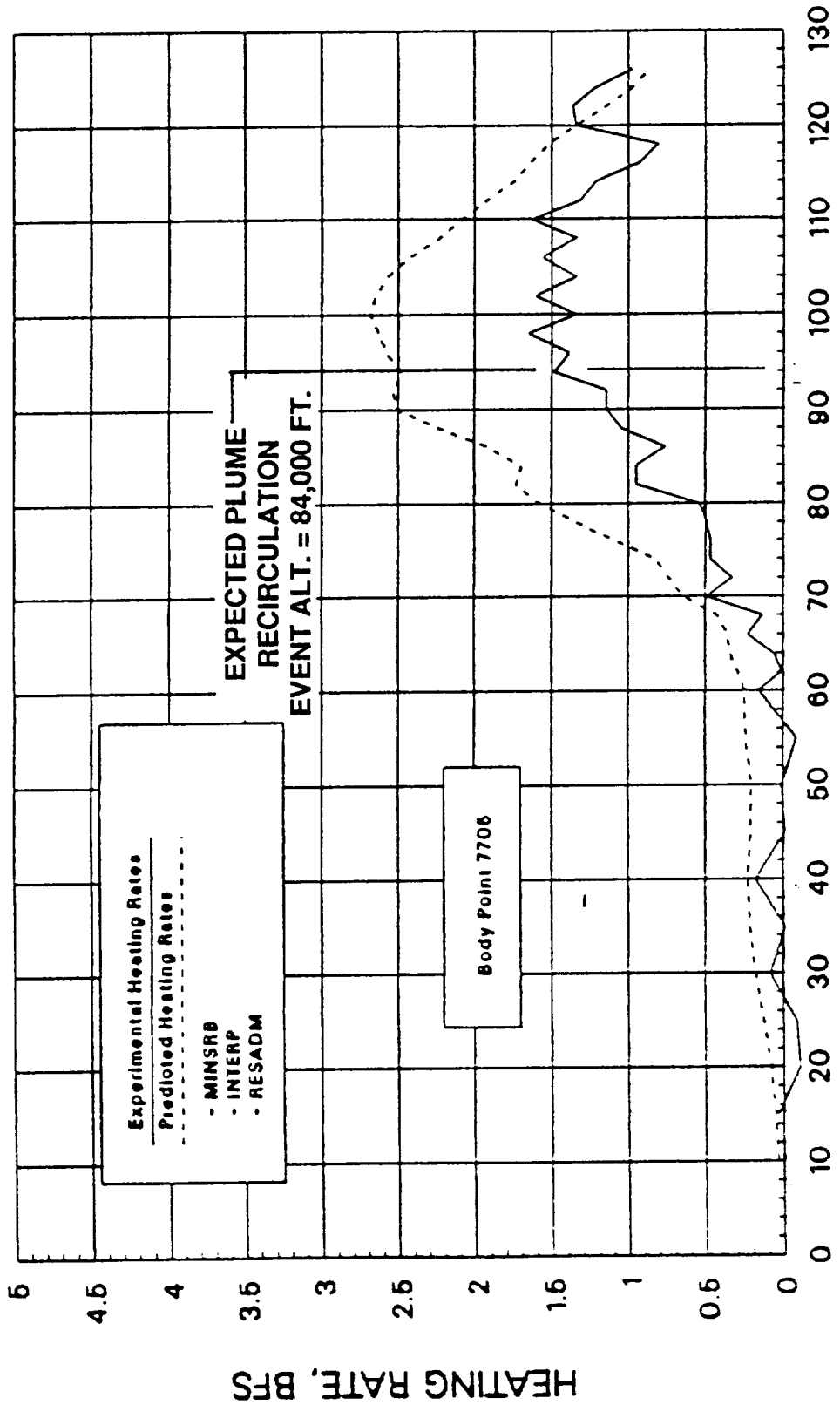

(a) B07R7705 $X_B = 1880, \theta_B = 180deg$

Figure 16: Aft Skirt Heating (STS-29R)

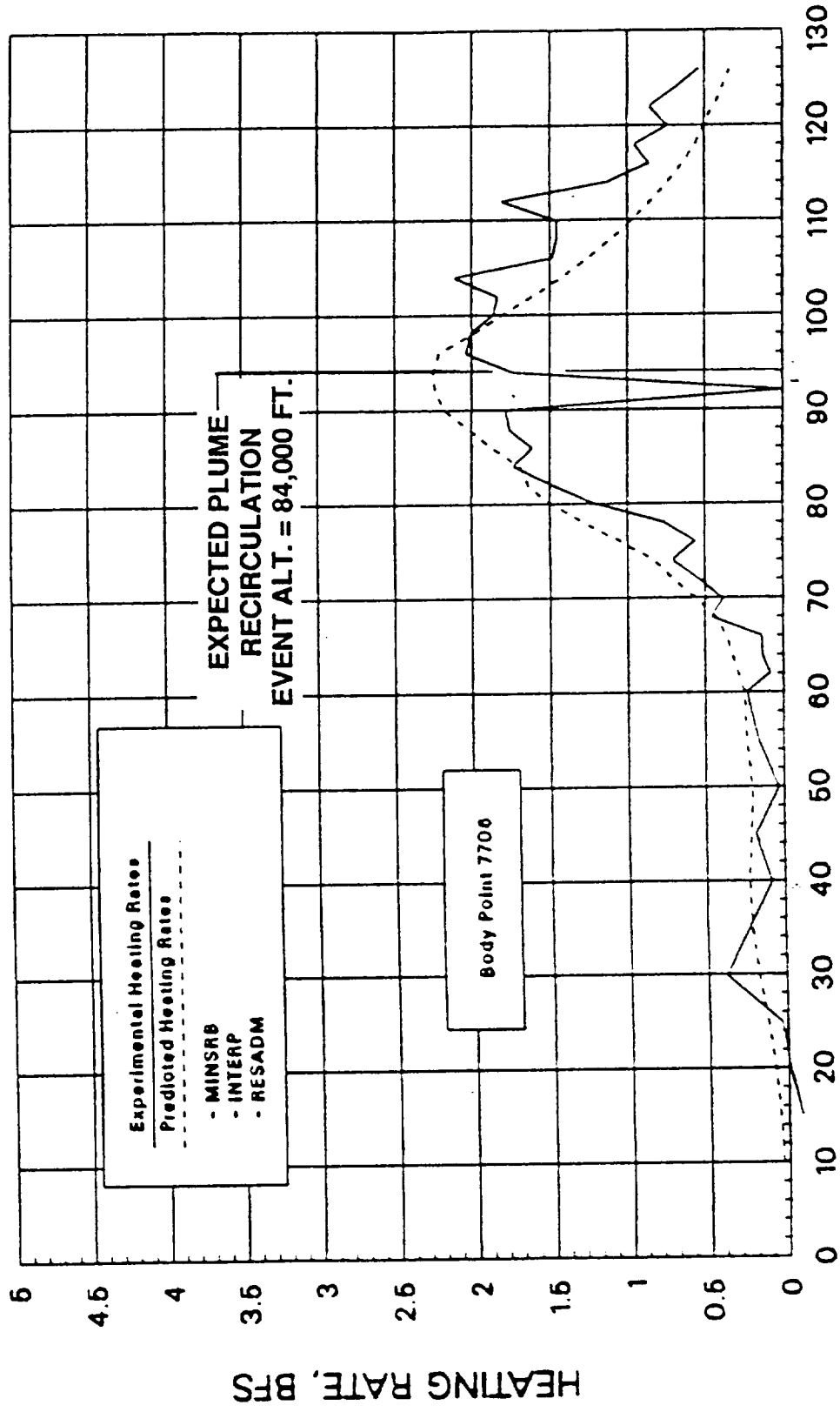

(b) B07R7706 $X_B = 1880, \theta_B = 270deg$

Figure 16: Aft Skirt Heating (STS-29R)

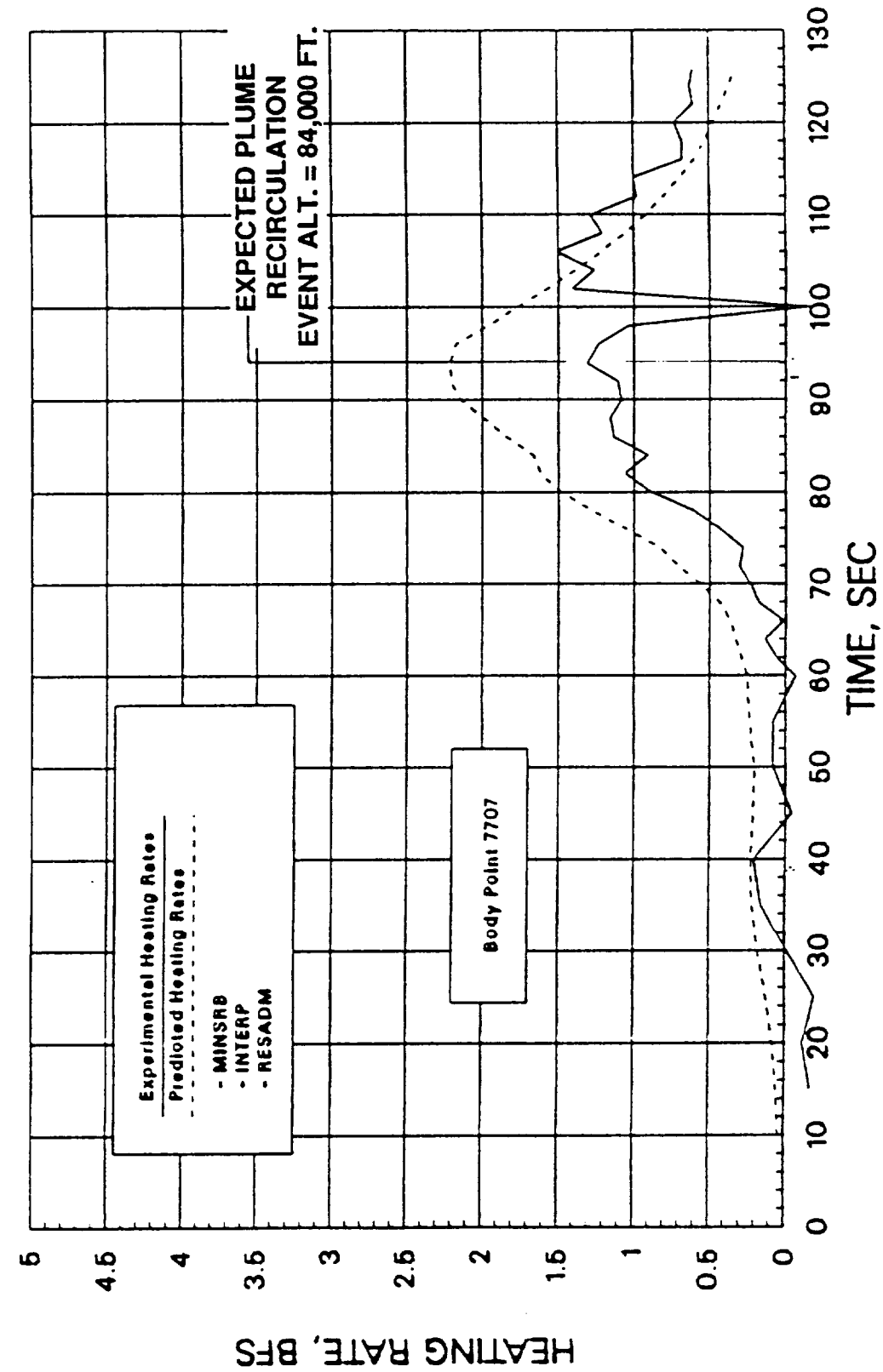

(c) B07R7707 $X_B = 1870, \theta_B = 270deg$

Figure 16: Aft Skirt Heating (STS-29R)

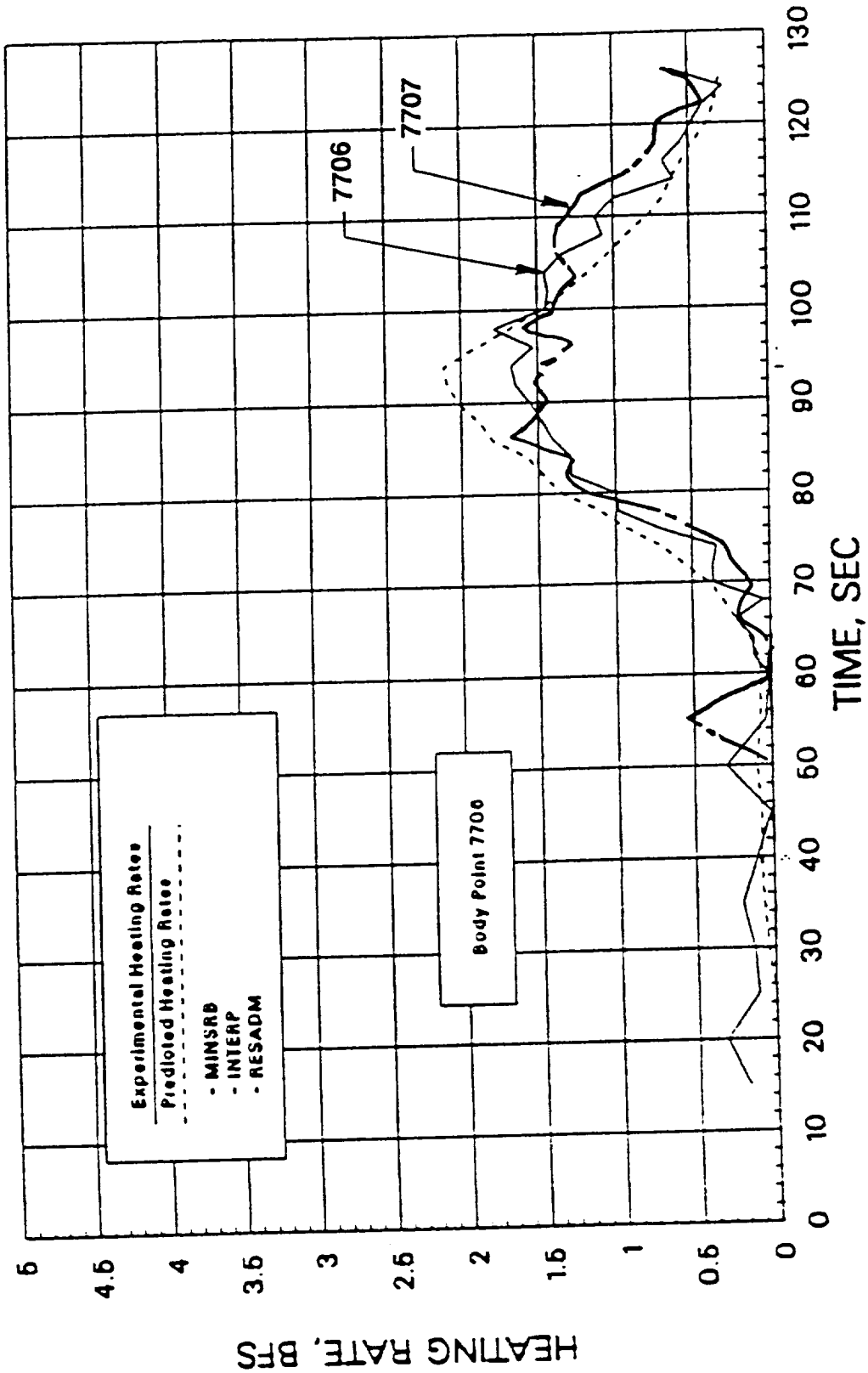

(a) STS-26R

Figure 17: Aft Skirt Comparative Heating Rate History For B07R7706 and 7707 ($\theta_B = 270deg$)

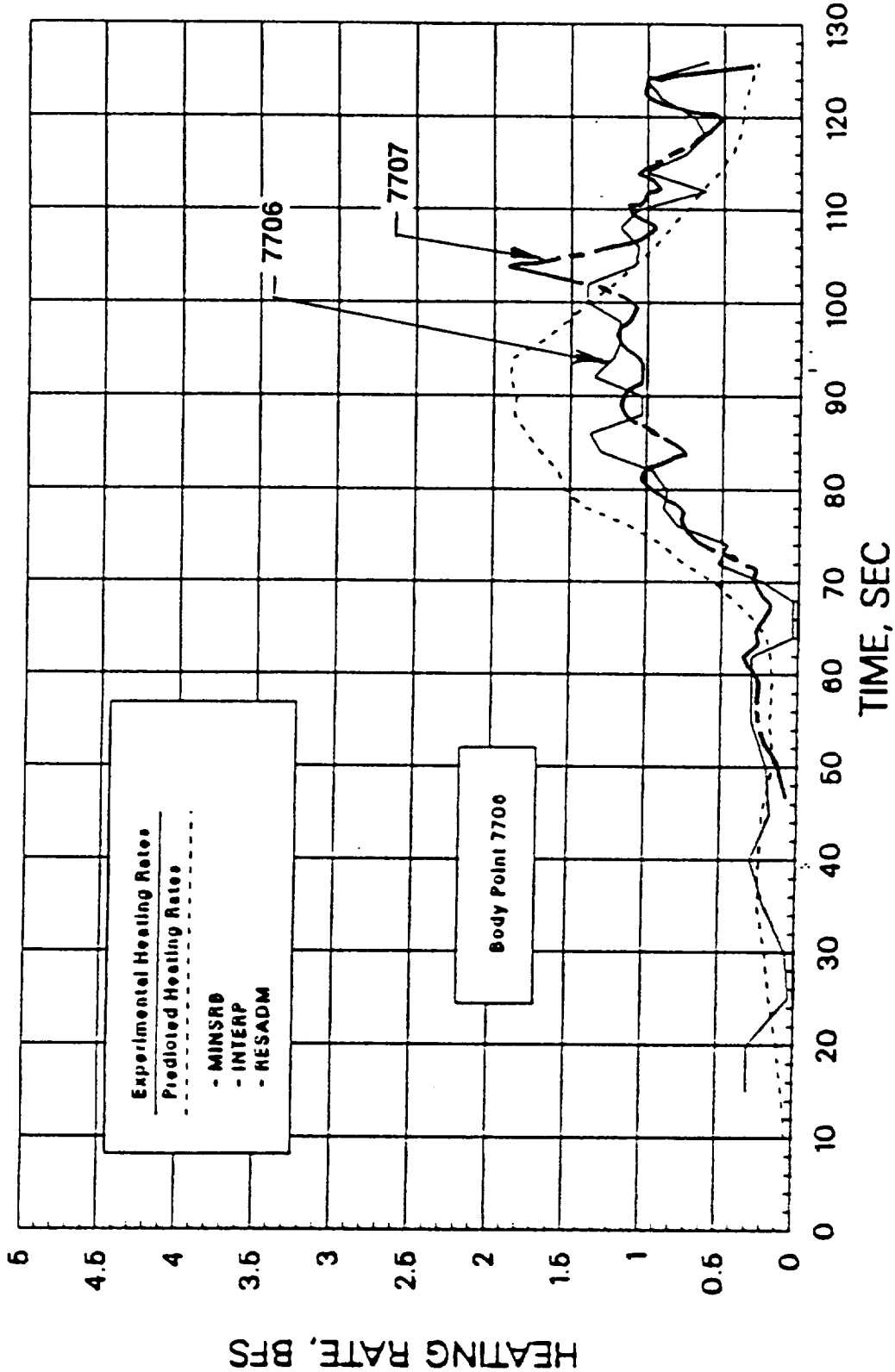

(b) STS-27R

Figure 17: Aft Skirt Comparative Heating Rate History For B07R7706 and 7707 ($\theta_B = 270deg$)

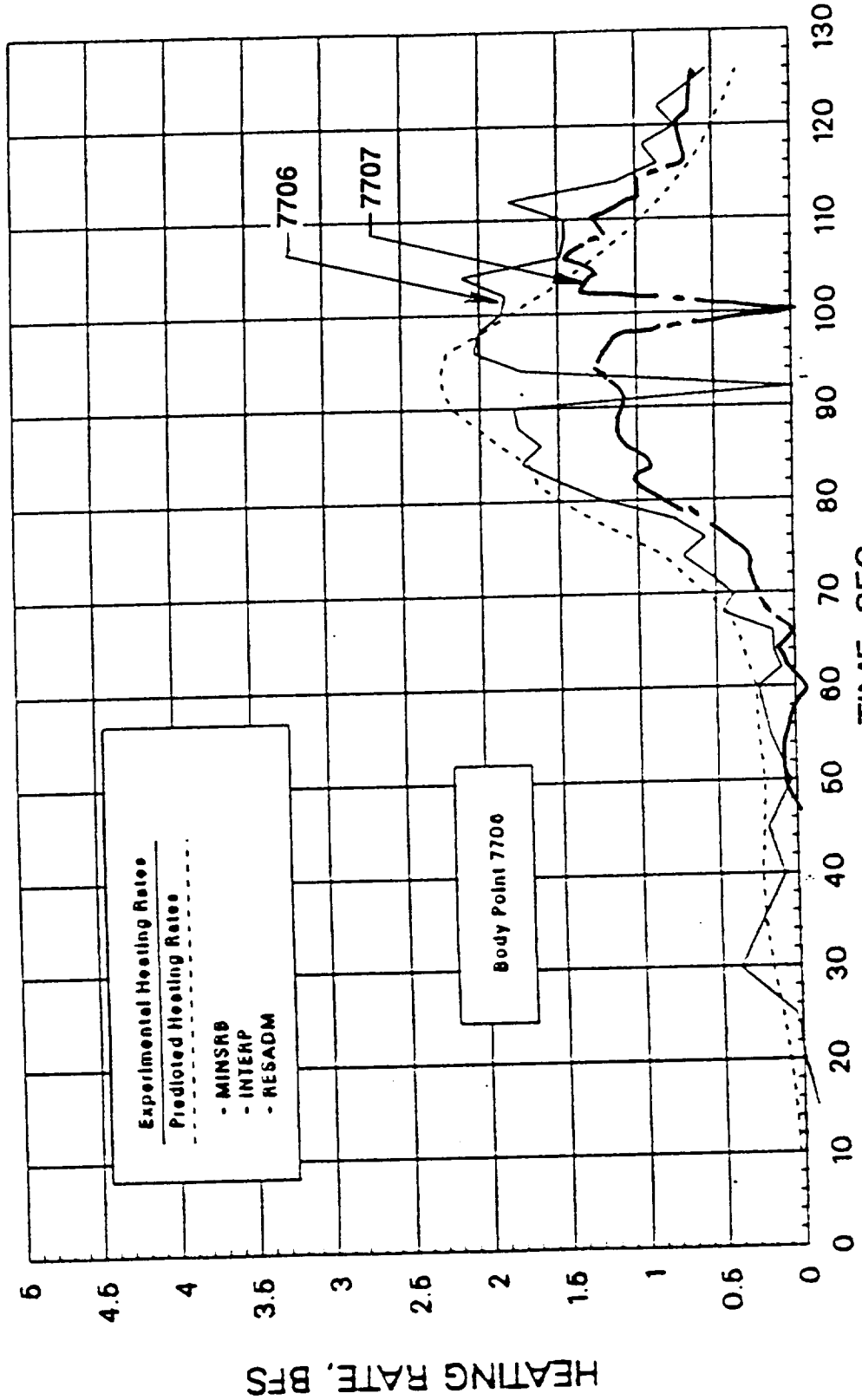

(c) STS-29R

Figure 17: Aft Skirt Comparative Heating Rate History For B07R7706 and 7707 ($\theta_B = 270deg$)

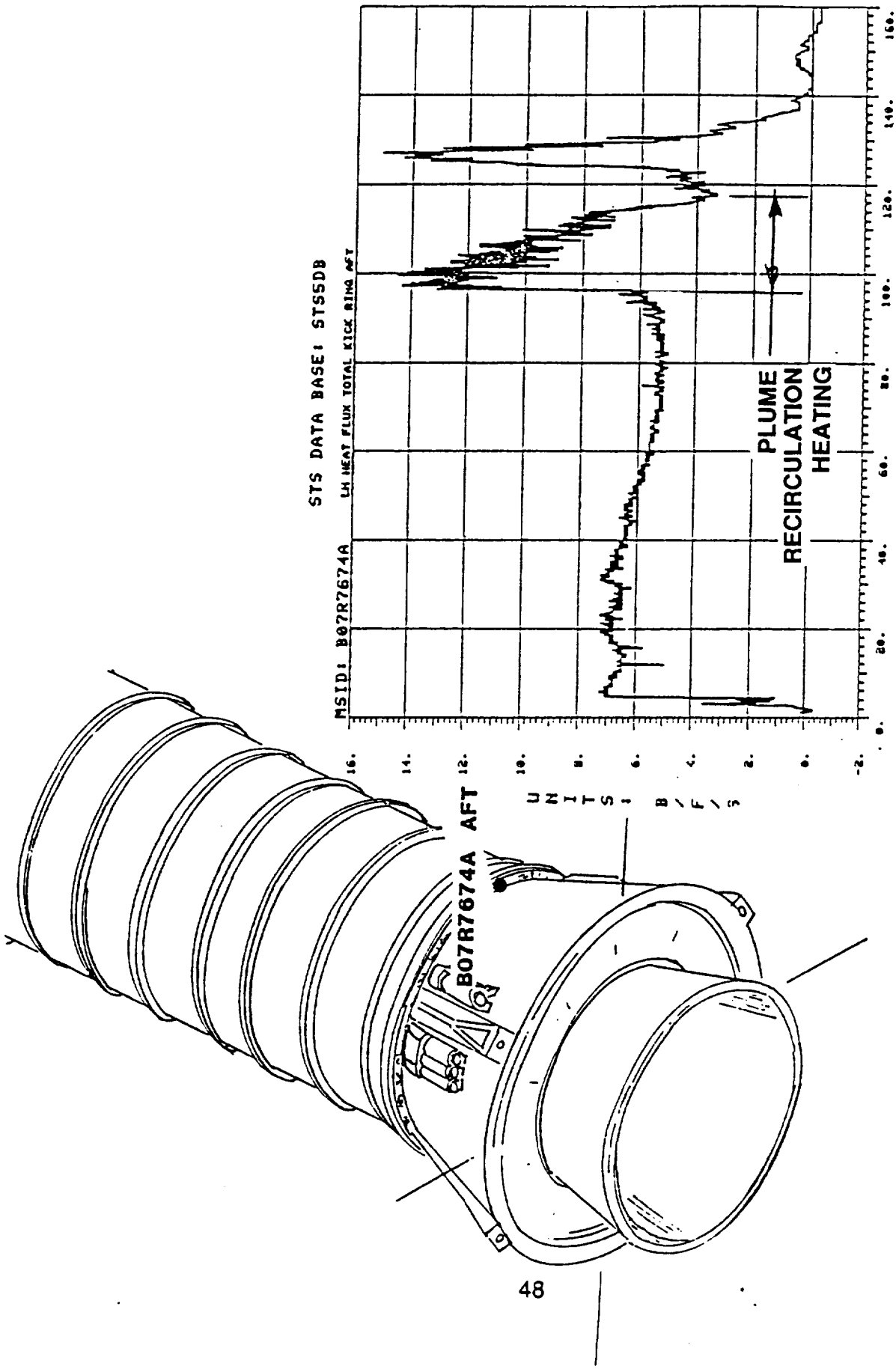

Figure 18: Example of Aft Skirt Gage With Plume Recirculation

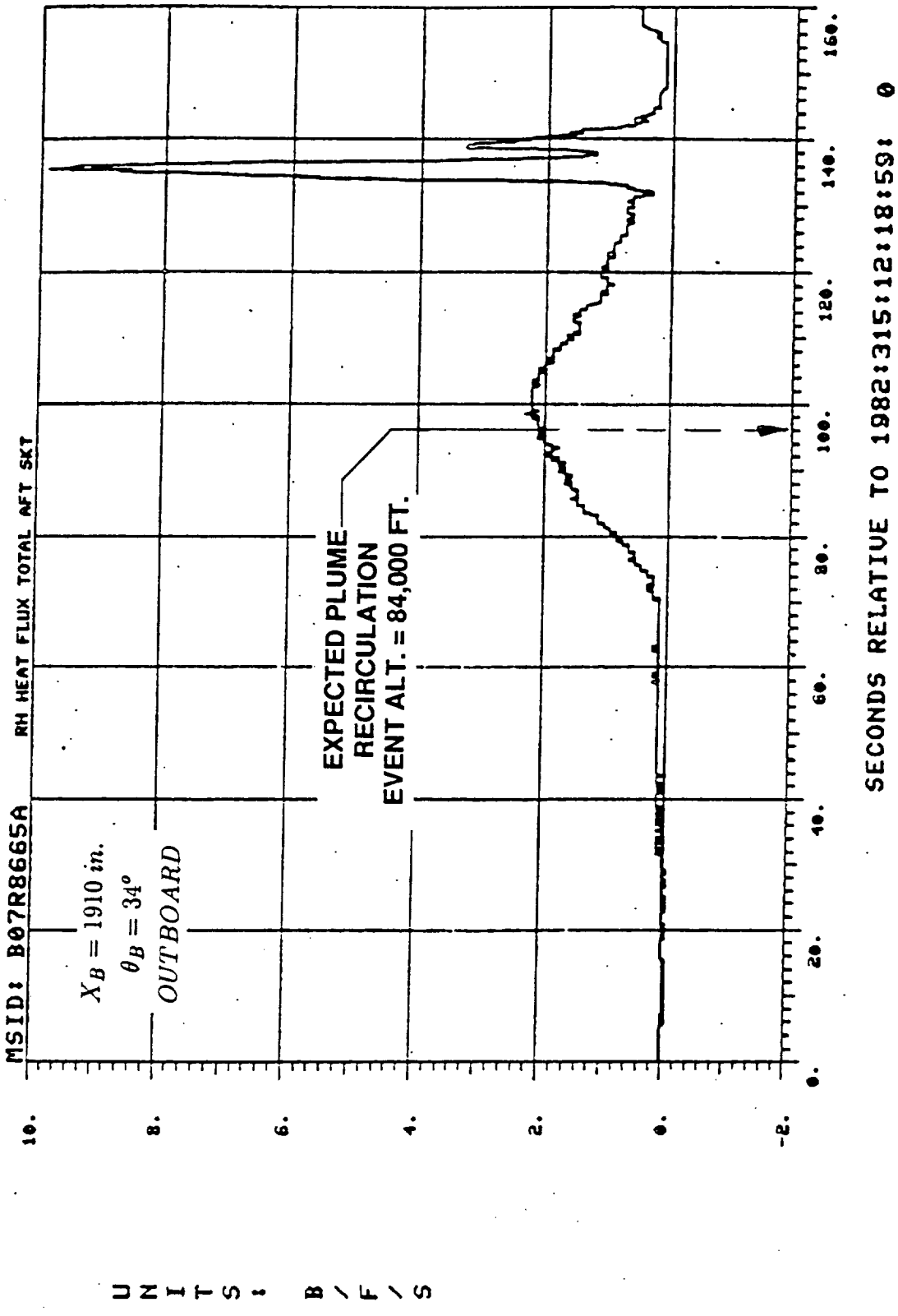

Figure 19: Example of Aft Skirt Gage With No Plume Recirculation (STS-5)

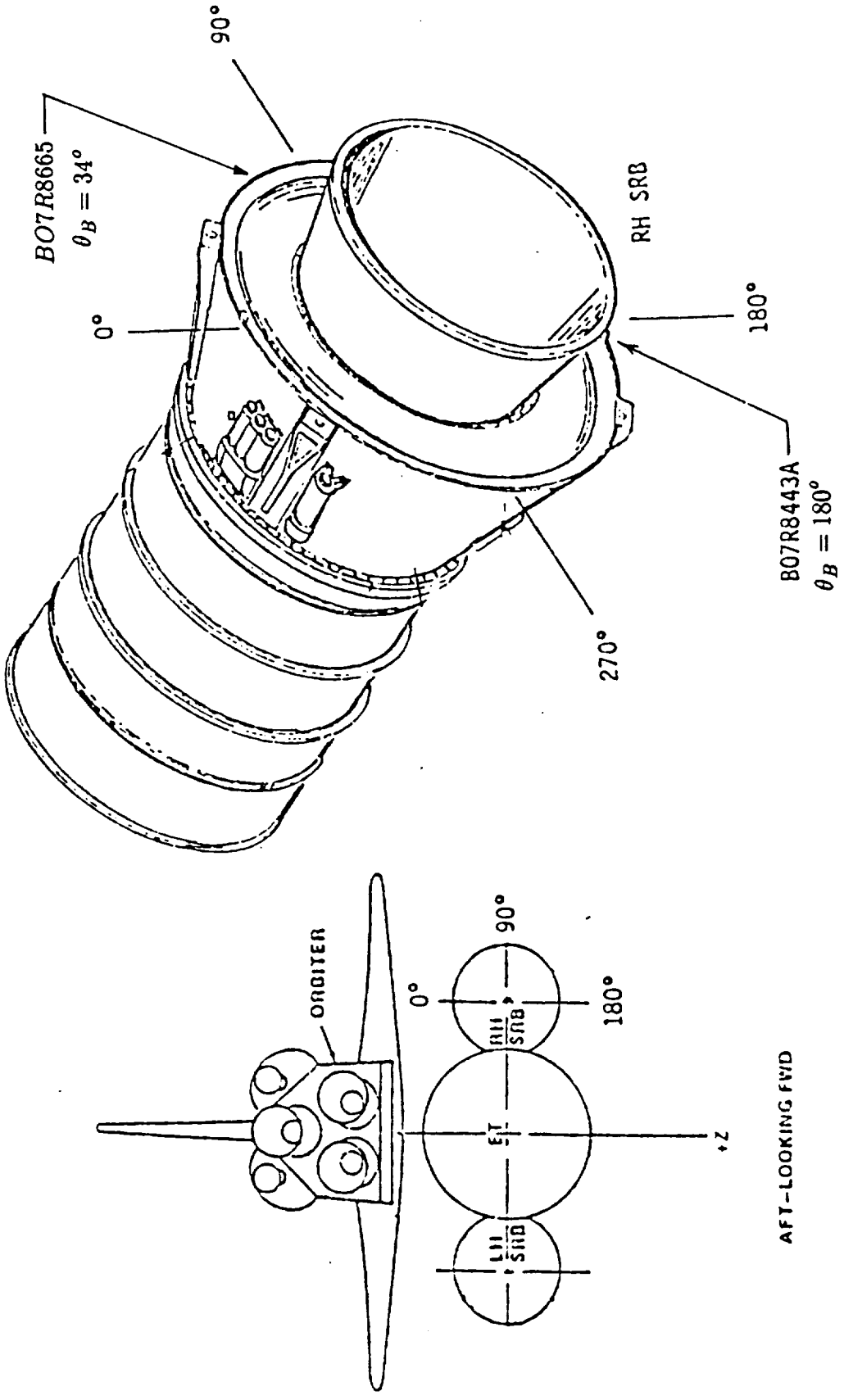

Figure 20: Right Hand SRB Heat Gage Location (STS-5)

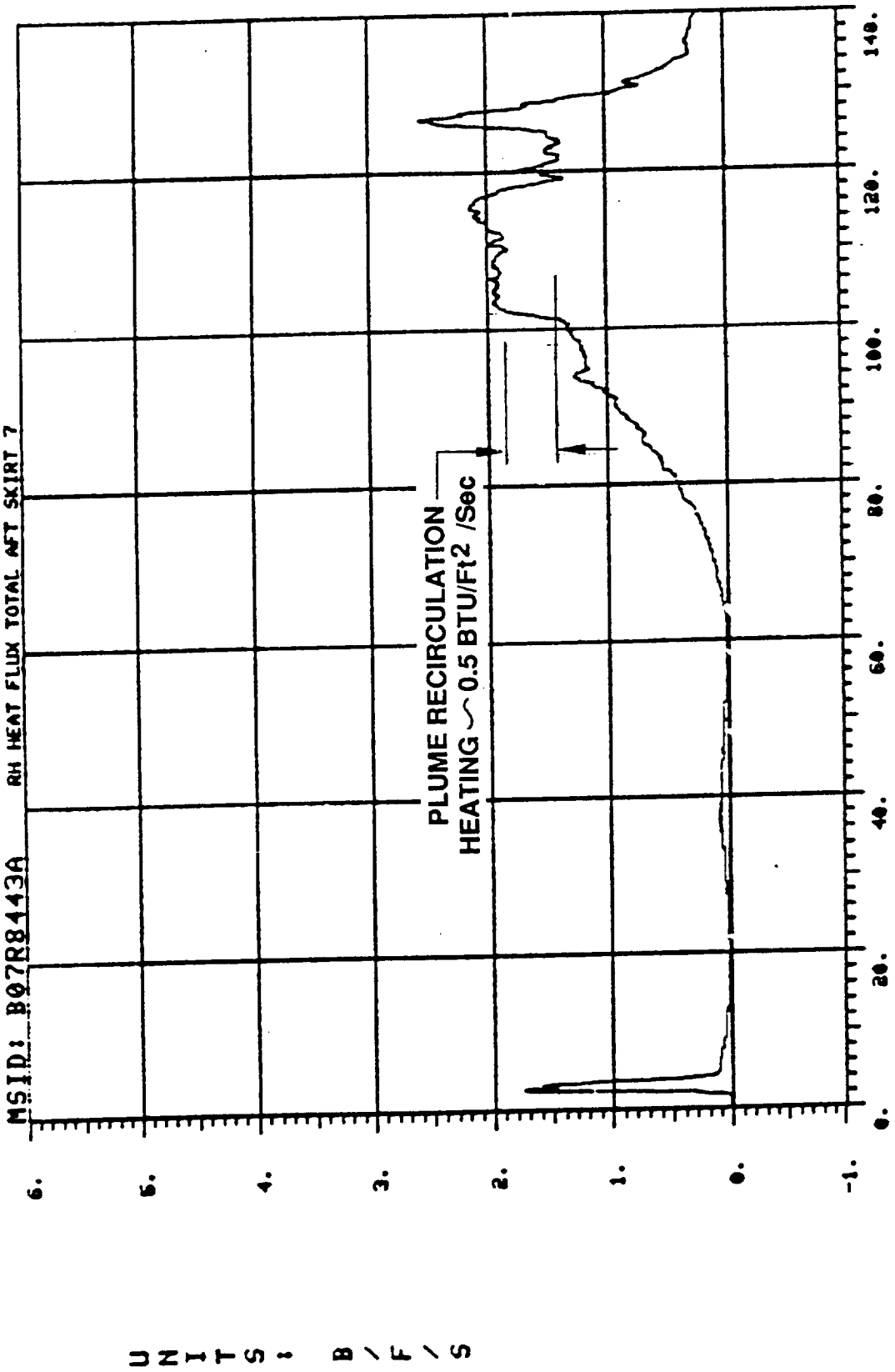

Figure 21: Plume Recirculation Heating at $\theta_B = 180deg$ (STS-2)

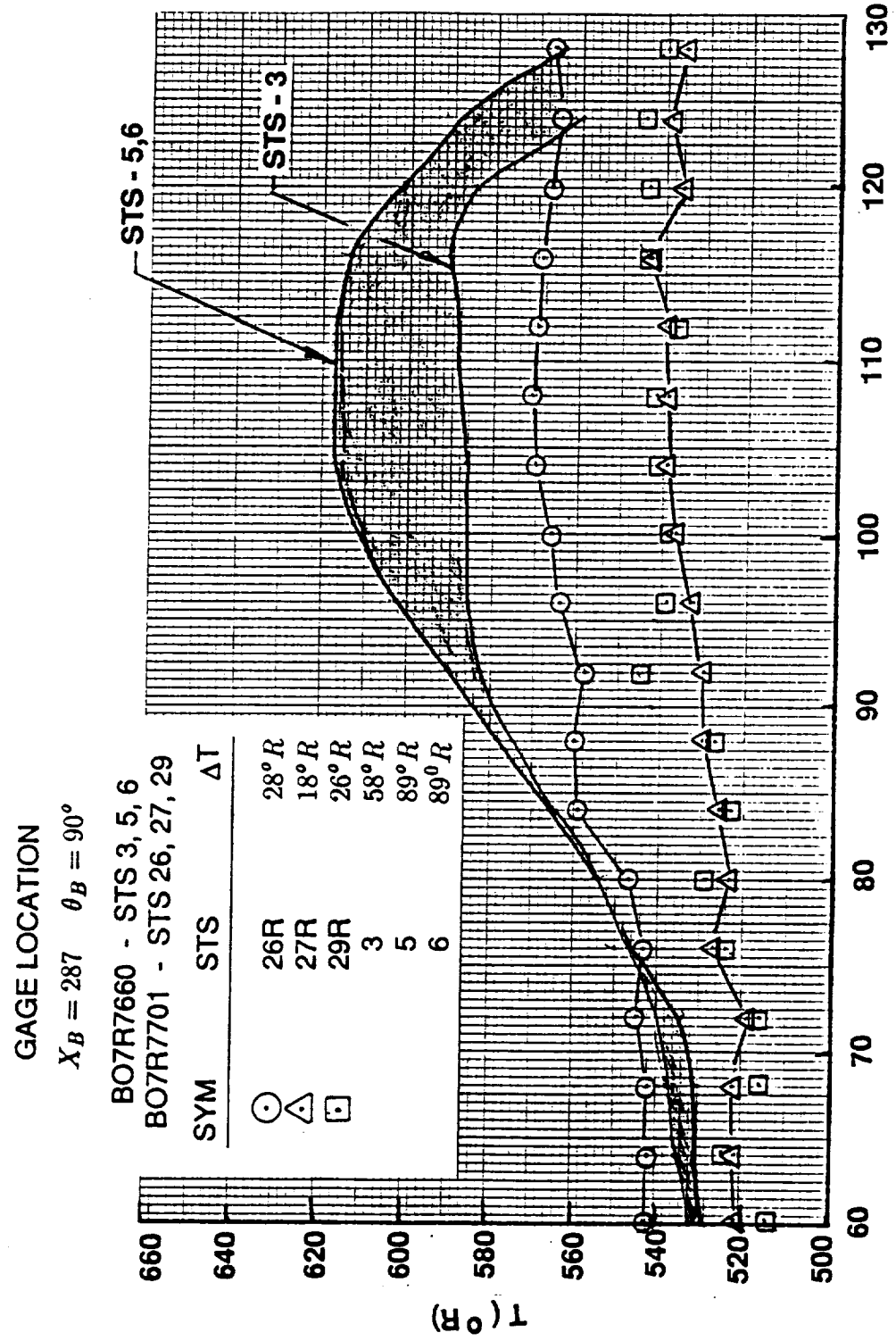

(a) Low to Moderate Heating

Figure 22: Heat Gage Wall Temperature Rise Comparison

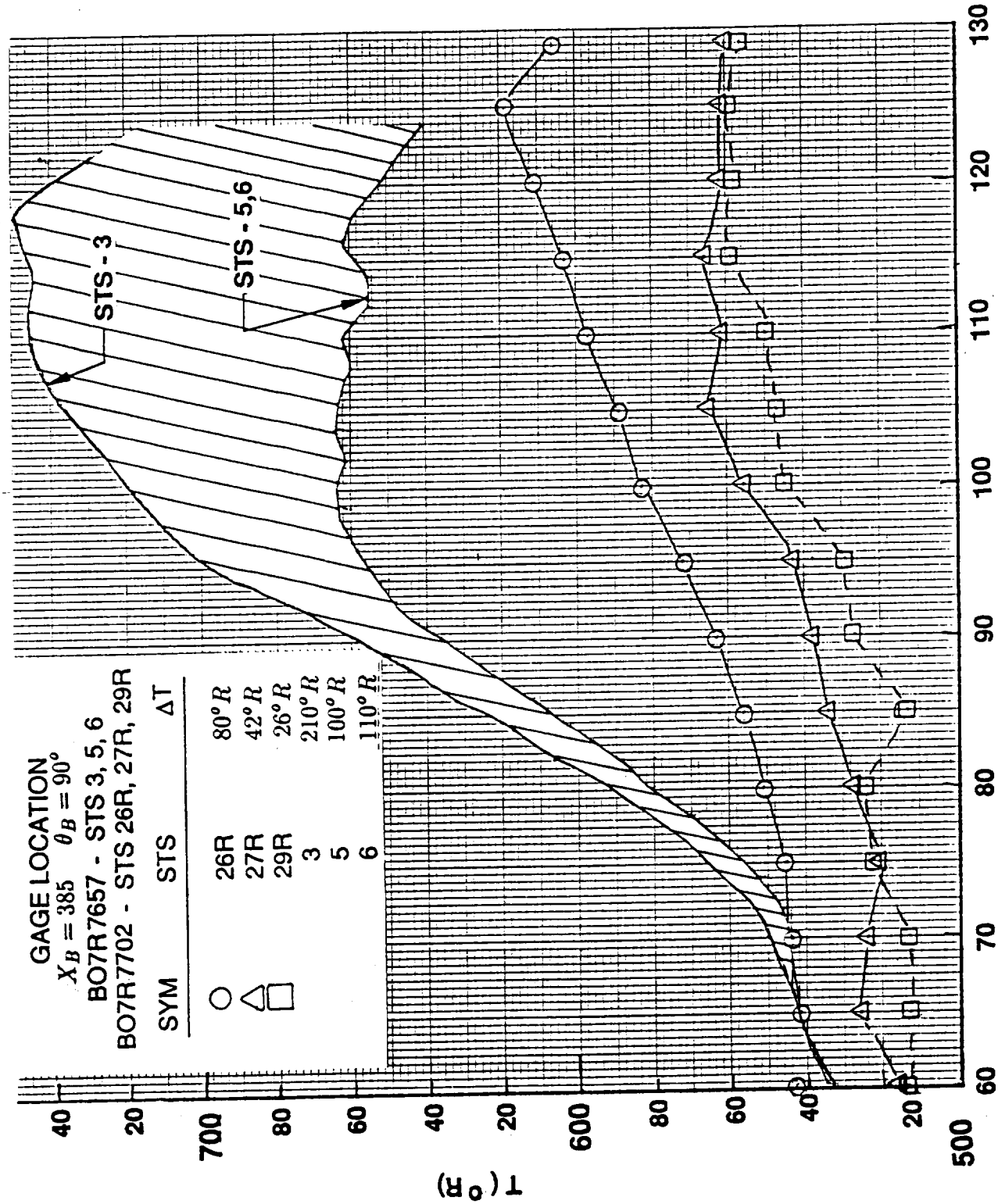

(b) High Heating — Shock Interference or Stagnation Regions

Figure 22: Heat Gage Wall Temperature Rise Comparison

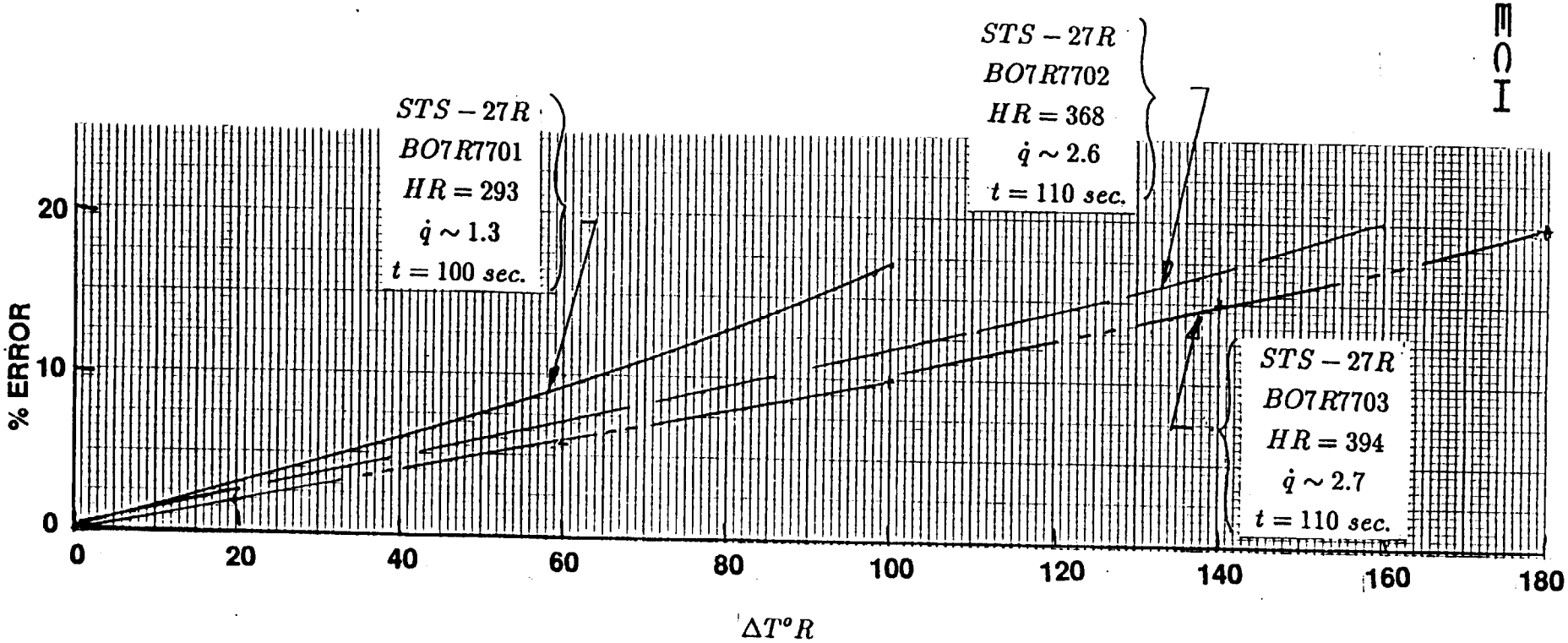

Figure 23: Impact on Typical Flight Heat Transfer Coefficients Due to Erroneous Wall Temperature

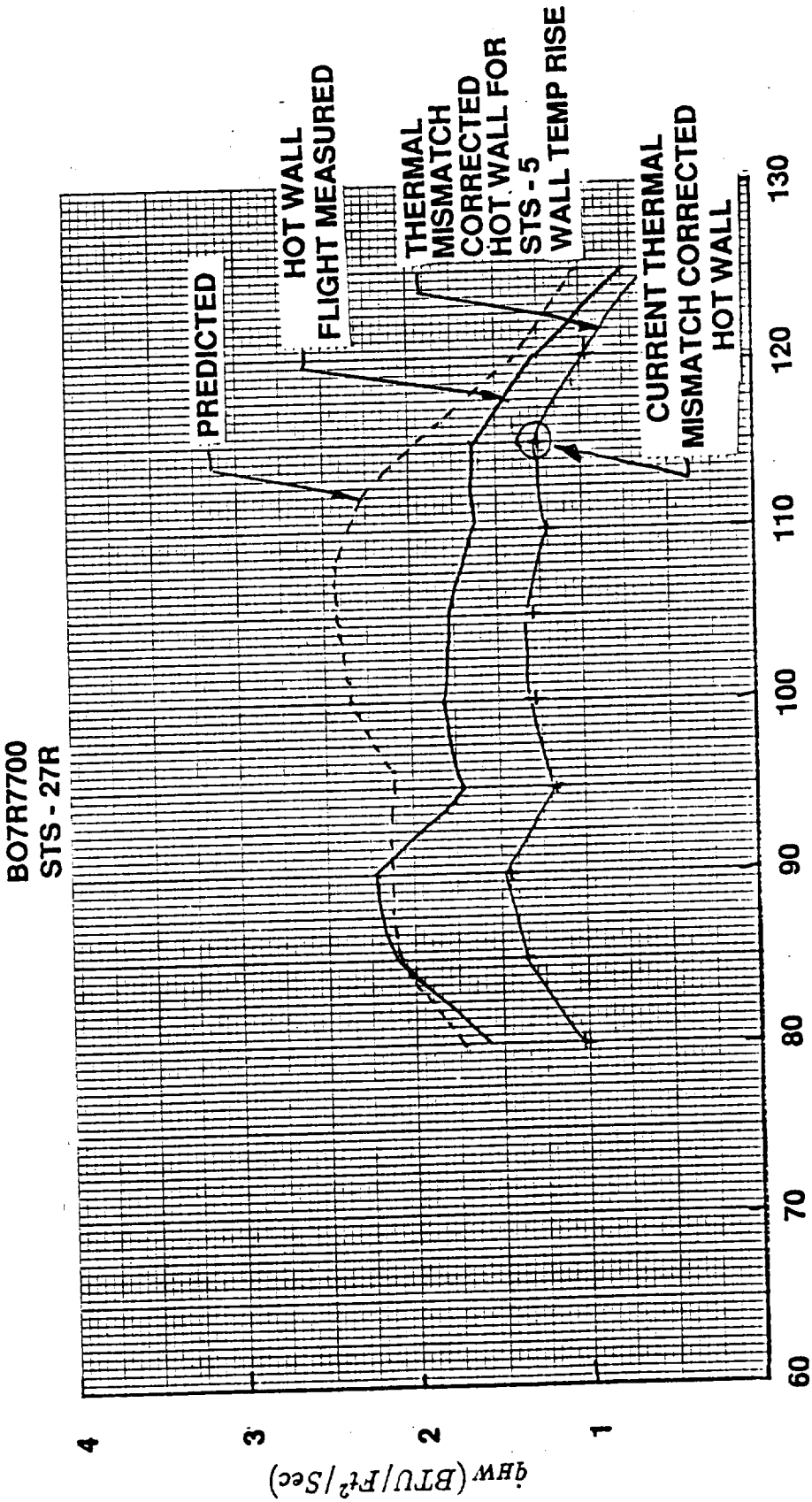

(a) Low to Moderate Heating Level (B07R7700 — STS 27R)

Figure 24: Effect of Math Model Elevated Wall Temperature on the Thermal Mismatch Corrected Flight Heating Rates

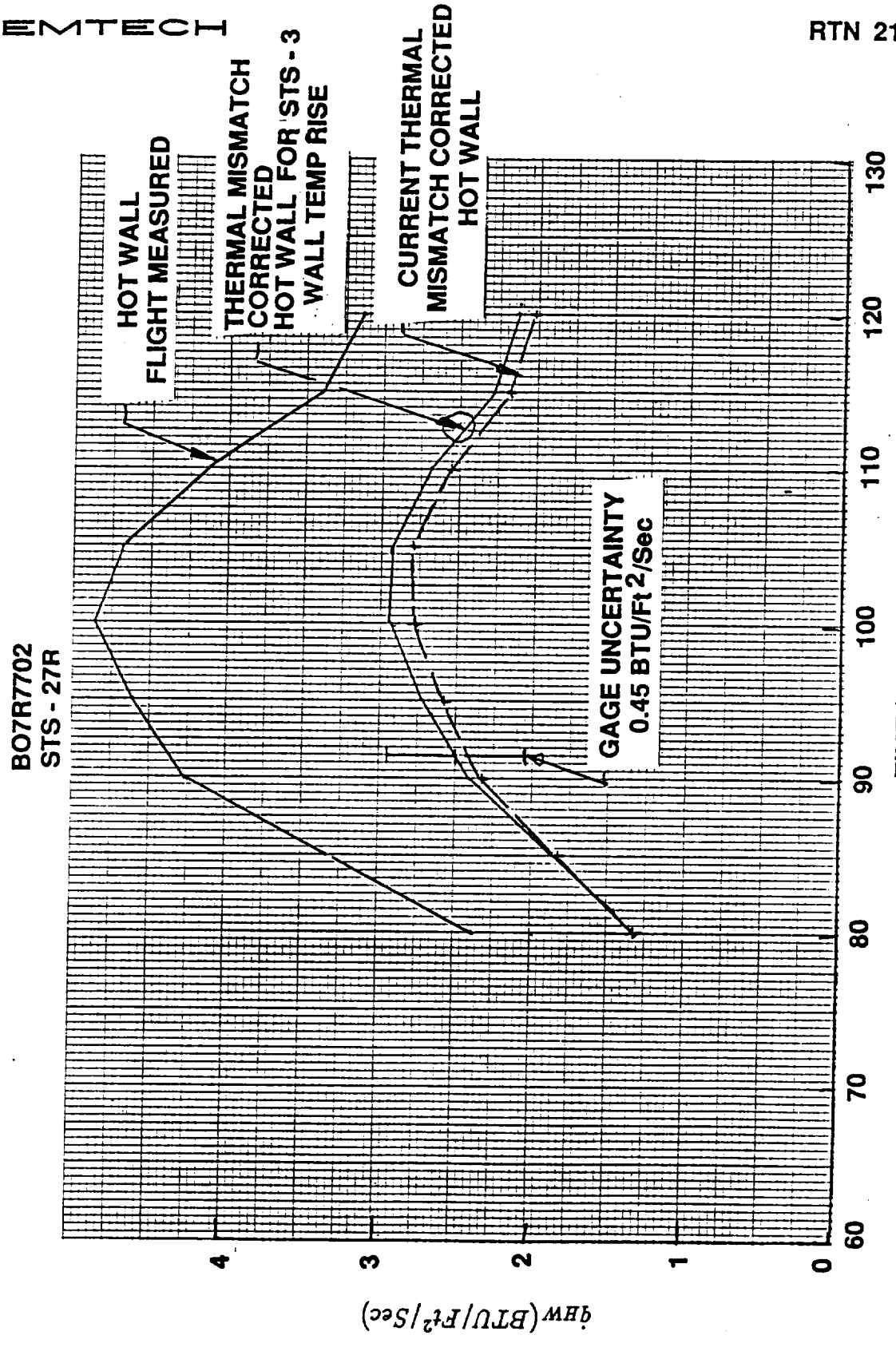

(b) High Heating Level (B07R7702 — STS 27R)

Figure 24: Effect of Math Model Elevated Wall Temperature on the Thermal Mismatch Corrected Flight Heating Rates

Table 1: Left Hand SRB External Instrumentation Location

TYPE	ID B07-	X_B (IN)	θ_B (DEG)	LOCATION
Calorimeter	R7700	243	90	Nose Cone
Calorimeter	R7701	287	90	Nose Cone
Calorimeter	R7702	385	90	Nose Cone
Calorimeter	R7703	1500	27.5	Attach Ring
Calorimeter	R7704	1500	55	Attach Ring
Calorimeter	R7705	1880	180	Aft Skirt
Calorimeter	R7706	1880	270	Aft Skirt
Calorimeter	R7707	1870	270	Aft Skirt
Thermocouple	T7603	287	90	Heat Gage B07R7701
Thermocouple	T7604	385	90	Heat Gage B07R7702

Table 2: Heat Transfer Gage Zero Shift

GAGE (B07R-1)	FLIGHT NO.		
	STS-26R	STS-27R	STS-29R
7700	-0.25	0.00	+0.40
7701	-0.15	-0.30	+0.20
7702	-0.03	-0.30	0.00
7703	-0.25	-0.30	0.00
7704	-0.30	Bad Gage	0.00
7705	-0.30	-0.35	+0.20
7706	-0.25	-0.30	0.00
7707	-0.55	-0.40	+0.15

*Note: Application of the correction was to add back in the (–) shift and subtract the (+) shift

Table 3: External DFI Heating Data Reduction
Procedure for Gages Aft of Nose Cone (7703–7707)

1. $\dot{q}_{FLT}$ Corrected for Zero Shift
2. Calculate Heat Transfer Coefficient

$$H_{C_{HW}} = \frac{\dot{q}_{FLT}}{HR - 0.24\,TW2}, \frac{lb_M}{FT^2\,sec.}$$

3. Calculate Flight Cold Wall (0°F) Heating Rate

$$H_{C_{CW}} = H_{C_{HW}}$$
$$\dot{q}_{FLT_{CW}} = (H_{C_{CW}})(HR - 110.4),\ BTU/FT^2\,sec$$

4. Calculate Amplification Factor (Hi/Hu)

$$Hi/Hu)_{FLT} = \frac{H_{C_{CW}}}{Hu}$$

WHERE

Hu = Local Undisturbed Heating Calculated by LANMIN, lbm/FT^2 sec.

HR = Recovery Enthalpy, BTU/lbm

- For Aft SKirt Gages HR is Calculated by LANMIN for the Specific Flight - STS 26R, 27R, 29R, etc.
- For Gages on Attach Ring HR Based on Freestream Total Temperature,

HR = $0.24T_o$, BTU/lbm

T_o = $T_\infty\,(1 + 0.2M_\infty^2)$, °R

T_∞ = $\left[\frac{V_\infty}{49.002\,M_\infty}\right]^2$, °R

TW2 = Heat Transfer Gage Temperature Measurement, °R

- For Gages 7703 and 7704, B07T7604 (See Fig. 1) was Used
- For Gages 7705-7707, B07T7603 (Fig. 1) was used

Table 4: SRB External DFI Heat Gage Location and Corresponding Hi/Hu Data Base Body Point Location

GAGE	X_B (IN)	θ_B (DEG)	Hi/Hu B.P.	X_B (IN)	θ_B (DEG)
7700	243	90.0	1326	243	90
7701	287	90.0	7660	284.6	90
7702	385	90.0	3226	388	90
7703	1500	27.5	7414	1504	0.0
7704	1500	55.0	7414	1504	0.0
7705	1880	180.0	1280	1873.5	198.0
7706	1880	270.0	8435	1910	275.0
7707	1870	270.0	8435	1910	275.0

Table 5: SRB Undisturbed Heating Methodology

BODY ITEMS	18° FORE-CONE	BARREL	18.67° AFT SKIRT
Shock	Cone	Cone	Cone (Body Angle = 18°) Cone (Body Angle = 18.67°)
Pressure	Tangent-Cone (Body Angle = 18 deg)	Tangent-Cone (Body Angle = 0°)	Tangent Cone (Body Angle = 0°) Tangent Cone (Body Angle = 18.67°)
Heat Transfer	Spalding-Chi	← Same	← Same
Divergence Factor	3: Laminar 2: Turbulent	1: Laminar 1: Turbulent	3: Laminar 2: Turbulent
Reynolds Analogy	Von Karman	← Same	← Same
Running Length	Measured from the Nose	← Same	← Same
Roughness	None	← Same	← Same

Table 6: Interference Factor (Hi/Hu) Data Used for Ascent Predictions At Gage Locations 7700–7707

BODY PT NO7700 X_B = 243.0, θ_B = 90.0			
ALPHA	BETA	MULT3 = 1.00 M = 3.0	MULT4 = 1.65 M = 4.0
-5.0	-9.0	1.85	2.65
-5.0	-5.0	1.60	1.95
-5.0	-3.0	1.44	1.50
-5.0	0.0	1.25	1.40
-5.0	3.0	1.05	1.00
-5.0	5.0	0.95	0.95
-5.0	9.0	0.67	0.65
0.0	-9.0	1.85	2.50
0.0	-5.0	1.58	2.10
0.0	-3.0	1.37	1.60
0.0	0.0	1.15	1.35
0.0	3.0	0.95	1.02
0.0	5.0	0.85	0.85
0.0	9.0	0.60	0.70
5.0	-9.0	2.04	2.75
5.0	-5.0	1.68	2.10
5.0	-3.0	1.44	1.70
5.0	0.0	1.20	1.35
5.0	3.0	1.00	1.10
5.0	5.0	0.90	0.90
5.0	9.0	0.65	0.70

Table 6: Interference Factor (Hi/Hu) Data Used for Ascent Predictions At Gage Locations 7700–7707 (Continued)

BODY PT NO7701 X_B = 287.0, θ_B = 90.0			
ALPHA	BETA	MULT3 = 1.00 M = 3.0	MULT4 = 1.63 M = 4.0
-5.0	-9.0	1.20	2.40
-5.0	-5.0	1.05	1.49
-5.0	-3.0	1.00	1.04
-5.0	0.0	0.94	0.97
-5.0	3.0	0.78	0.92
-5.0	5.0	0.69	0.75
-5.0	9.0	0.48	0.40
0.0	-9.0	1.15	1.30
0.0	-5.0	1.10	1.17
0.0	-3.0	1.01	1.10
0.0	0.0	0.95	0.96
0.0	3.0	0.73	0.75
0.0	5.0	0.60	0.64
0.0	9.0	0.50	0.35
5.0	-9.0	1.17	1.26
5.0	-5.0	1.12	1.14
5.0	-3.0	1.03	1.10
5.0	0.0	0.95	0.99
5.0	3.0	0.78	0.76
5.0	5.0	0.70	0.66
5.0	9.0	0.58	0.40

Table 6: Interference Factor (Hi/Hu) Data Used for Ascent Predictions At Gage Locations 7700–7707 (Continued)

BODY PT NO7702 X_B = 385.0, θ_B = 90.0			
ALPHA	BETA	MULT3 = 1.10 M = 3.0	MULT4 = 1.68 M = 4.0
-5.0	-9.0	2.63	3.23
-5.0	-5.0	2.55	2.93
-5.0	-3.0	2.33	2.21
-5.0	0.0	2.26	1.84
-5.0	3.0	2.05	1.62
-5.0	5.0	1.79	1.35
-5.0	9.0	1.56	1.14
0.0	-9.0	2.30	3.45
0.0	-5.0	2.24	3.12
0.0	-3.0	2.16	2.06
0.0	0.0	2.70	1.69
0.0	3.0	1.58	0.97
0.0	5.0	1.19	0.53
0.0	9.0	0.80	0.10
5.0	-9.0	2.20	2.07
5.0	-5.0	2.15	1.91
5.0	-3.0	2.09	1.75
5.0	0.0	2.05	1.63
5.0	3.0	1.64	1.17
5.0	5.0	1.25	0.74
5.0	9.0	0.85	0.30

Table 6: Interference Factor (Hi/Hu) Data Used for Ascent Predictions At Gage Locations 7700–7707 (Continued)

BODY PT NO7703 X_B = 1500.0, θ_B = 27.5			
ALPHA	BETA	MULT3 = 1.69 M = 3.0	MULT4 = 1.69 M = 4.0
-5.0	-9.0	2.18	3.04
-5.0	-5.0	3.70	4.19
-5.0	-3.0	4.40	6.36
-5.0	0.0	4.90	7.65
-5.0	3.0	4.72	7.70
-5.0	5.0	4.68	7.60
-5.0	9.0	4.08	5.68
0.0	-9.0	3.12	3.74
0.0	-5.0	3.20	3.79
0.0	-3.0	3.30	4.10
0.0	0.0	3.47	4.60
0.0	3.0	4.30	5.75
0.0	5.0	4.82	6.40
0.0	9.0	6.10	8.60
5.0	-9.0	2.28	3.10
5.0	-5.0	2.74	3.20
5.0	-3.0	3.12	3.75
5.0	0.0	3.72	4.64
5.0	3.0	4.40	6.65
5.0	5.0	4.68	7.20
5.0	9.0	5.60	10.10

Table 6: Interference Factor (Hi/Hu) Data Used for Ascent Predictions At Gage Locations 7700–7707 (Continued)

BODY PT NO7704 X_B = 1501.0, θ_B = 55.0			
ALPHA	BETA	MULT3 = 1.69 M = 3.0	MULT4 = 1.69 M = 4.0
-5.0	-9.0	2.18	3.04
-5.0	-5.0	3.70	4.19
-5.0	-3.0	4.40	6.36
-5.0	0.0	4.90	7.65
-5.0	3.0	4.72	7.70
-5.0	5.0	4.68	7.60
-5.0	9.0	4.08	5.68
0.0	-9.0	3.12	3.74
0.0	-5.0	3.20	3.79
0.0	-3.0	3.30	4.10
0.0	0.0	3.47	4.60
0.0	3.0	4.30	5.75
0.0	5.0	4.82	6.40
0.0	9.0	6.10	8.60
5.0	-9.0	2.28	3.10
5.0	-5.0	2.74	3.20
5.0	-3.0	3.12	3.75
5.0	0.0	3.72	4.64
5.0	3.0	4.40	6.65
5.0	5.0	4.68	7.20
5.0	9.0	5.60	10.10

Table 6: Interference Factor (Hi/Hu) Data Used for Ascent Predictions At Gage Locations 7700–7707 (Continued)

BODY PT NO7705 X_B = 1880.0, θ_B = 180.0			
ALPHA	BETA	MULT3 = 4.70 M = 3.0	MULT4 = 4.70 M = 4.0
-5.0	-9.0	0.20	0.25
-5.0	-5.0	0.20	0.25
-5.0	-3.0	0.28	0.70
-5.0	0.0	0.40	0.35
-5.0	3.0	0.88	0.50
-5.0	5.0	1.20	1.00
-5.0	9.0	1.85	0.50
0.0	-9.0	0.26	0.25
0.0	-5.0	0.35	0.35
0.0	-3.0	0.39	0.60
0.0	0.0	0.45	0.45
0.0	3.0	0.57	0.65
0.0	5.0	0.65	0.60
0.0	9.0	0.81	0.35
5.0	-9.0	0.32	0.42
5.0	-5.0	0.25	0.40
5.0	-3.0	0.21	0.45
5.0	0.0	0.15	0.25
5.0	3.0	0.35	0.60
5.0	5.0	0.50	0.50
5.0	9.0	0.75	0.25

Table 6: Interference Factor (Hi/Hu) Data Used for Ascent Predictions At Gage Locations 7700–7707 (Continued)

BODY PT NO7706 X_B = 1881.0, θ_B = 270.0			
ALPHA	BETA	MULT3 = 2.57 M = 3.0	MULT4 = 2.57 M = 4.0
-5.0	-9.0	0.36	0.14
-5.0	-5.0	0.45	0.18
-5.0	-3.0	0.47	0.19
-5.0	0.0	0.77	0.31
-5.0	3.0	0.82	0.33
-5.0	5.0	0.83	0.34
-5.0	9.0	0.87	0.35
0.0	-9.0	0.36	0.14
0.0	-5.0	0.45	0.18
0.0	-3.0	0.47	0.19
0.0	0.0	0.77	0.31
0.0	3.0	0.82	0.33
0.0	5.0	0.83	0.34
0.0	9.0	0.87	0.35
5.0	-9.0	0.36	0.14
5.0	-5.0	0.45	0.18
5.0	-3.0	0.48	0.19
5.0	0.0	0.56	0.23
5.0	3.0	0.42	0.17
5.0	5.0	0.34	0.14
5.0	9.0	0.15	0.06

Table 6: Interference Factor (Hi/Hu) Data Used for Ascent Predictions At Gage Locations 7700–7707 (Concluded)

BODY PT NO7707 X_B = 1870.0, θ_B = 270.0			
ALPHA	BETA	MULT3 = 2.57 M = 3.0	MULT4 = 2.57 M = 4.0
-5.0	-9.0	0.36	0.14
-5.0	-5.0	0.45	0.18
-5.0	-3.0	0.47	0.19
-5.0	0.0	0.77	0.31
-5.0	3.0	0.82	0.33
-5.0	5.0	0.83	0.34
-5.0	9.0	0.87	0.35
0.0	-9.0	0.36	0.14
0.0	-5.0	0.45	0.18
0.0	-3.0	0.47	0.19
0.0	0.0	0.77	0.31
0.0	3.0	0.82	0.33
0.0	5.0	0.83	0.34
0.0	9.0	0.87	0.35
5.0	-9.0	0.36	0.14
5.0	-5.0	0.45	0.18
5.0	-3.0	0.48	0.19
5.0	0.0	0.56	0.23
5.0	3.0	0.42	0.17
5.0	5.0	0.34	0.14
5.0	9.0	0.15	0.06

APPENDIX I

THERMAL MISMATCH CORRECTIONS FOR NOSE CONE/FRUSTUM GAGES B07R7700, B07R7701 AND B07R7702 FOR STS-26R, STS-27R AND STS-29R

STS 26 7700 MISMATCH CORRECTION

TIME	Qhw	CORRECTED Qhw	CORRECTED Qcw	CORRECTED Hcw	Ctm	Hr	Tr	Tw2	Tw1	Hr/Hc
50.0	0.1445	0.2370	4.1563	0.1915	0.6014	132.1	550.42	545.26	543.00	3.30
51.0	0.1252	0.0800	0.9362	0.0432	1.5642	132.1	550.33	542.61	547.40	0.75
52.0	0.0092	0.0071	0.1139	0.0053	1.2885	132.1	550.25	544.60	546.39	0.09
53.0	0.1059	0.0815	2.0477	0.0940	1.3016	132.0	550.17	546.58	547.77	1.67
54.0	0.0479	0.0293	0.2442	0.0113	1.6346	132.0	550.08	539.29	546.81	0.20
55.0	0.0000	0.0000	0.0000	0.0000	-4.2827	132.0	550.00	549.23	544.76	0.00
56.0	0.0092	0.0096	0.1197	0.0055	0.9624	132.1	550.50	543.27	542.97	0.10
57.0	0.1832	0.1262	1.4851	0.0680	1.4528	132.2	551.00	543.27	547.11	1.23
58.0	0.0000	0.0000	0.0000	0.0000	1.4556	132.4	551.50	541.28	546.39	0.00
59.0	0.1639	0.1047	0.6269	0.0284	1.5586	132.5	552.00	536.64	546.06	0.51
60.0	0.0000	0.0000	0.0000	0.0000	1.2521	132.6	552.50	543.27	545.83	0.00
61.0	0.1252	0.0810	0.4851	0.0220	1.5402	132.5	552.00	536.64	545.75	0.40
62.0	0.1832	0.1313	2.8274	0.1288	1.3976	132.4	551.50	547.25	549.11	2.37
63.0	0.0000	0.0000	0.0000	0.0000	1.6081	132.2	551.00	541.28	547.77	0.00
64.0	0.1639	0.1064	1.2202	0.0562	1.5410	132.1	550.50	542.61	547.30	1.05
65.0	0.1639	0.0979	1.0932	0.0506	1.6742	132.0	550.00	541.94	547.91	0.96
66.0	0.2992	0.1722	2.3854	0.1107	1.7375	131.9	549.75	543.27	548.52	2.12
67.0	0.2412	0.1371	1.7810	0.0829	1.7593	131.9	549.50	542.61	548.36	1.61
68.0	0.3572	0.1998	2.6855	0.1254	1.7880	131.8	549.25	542.61	548.36	2.47
69.0	0.3765	0.2078	2.2070	0.1033	1.8118	131.8	549.00	540.62	548.09	2.07
70.0	0.3378	0.1889	3.0597	0.1436	1.7882	131.7	548.75	543.27	548.01	2.92
71.0	0.4731	0.2712	3.2784	0.1493	1.7448	132.4	551.50	543.93	550.12	3.07
72.0	0.5118	0.2941	3.3281	0.1471	1.7405	133.0	554.25	545.92	552.69	3.07
73.0	0.5311	0.3047	2.5175	0.1081	1.7433	133.7	557.00	545.26	554.84	2.29
74.0	0.6664	0.3780	2.2000	0.0919	1.7630	134.3	559.75	542.61	556.97	1.97
75.0	0.8210	0.4645	2.7614	0.1123	1.7678	135.0	562.50	545.26	559.80	2.44
76.0	0.9370	0.5334	2.2747	0.0878	1.7567	136.3	567.92	542.61	563.64	1.95
77.0	0.9950	0.5706	2.3035	0.0847	1.7440	137.6	573.33	545.26	568.20	1.93
78.0	1.1690	0.6651	2.2262	0.0781	1.7576	138.9	578.75	543.27	572.79	1.82
79.0	1.2080	0.6883	2.0898	0.0701	1.7551	140.2	584.17	543.27	577.19	1.67
80.0	1.3820	0.7882	2.4127	0.0776	1.7535	141.5	589.58	547.25	582.28	1.90
81.0	1.6330	0.9379	2.4394	0.0728	1.7413	143.9	599.58	545.92	589.61	1.82
82.0	1.7680	1.0194	2.5835	0.0720	1.7345	146.3	609.58	550.56	598.17	1.83
83.0	1.7870	1.0362	2.4449	0.0634	1.7247	148.9	620.62	552.55	606.73	1.66
84.0	2.0000	1.1640	2.7567	0.0669	1.7183	151.6	631.67	559.18	616.37	1.80
85.0	2.0390	1.1878	2.3431	0.0520	1.7073	155.4	647.71	552.55	626.47	1.45
86.0	2.2320	1.3100	2.4589	0.0503	1.6945	159.3	663.75	555.20	638.00	1.45
87.0	2.3290	1.3703	2.3868	0.0451	1.6913	163.3	680.42	553.87	649.96	1.36
88.0	2.3870	1.4157	2.4575	0.0432	1.6779	167.3	697.08	560.50	662.19	1.37
89.0	2.4830	1.4843	2.4332	0.0393	1.6653	172.2	717.71	560.50	675.37	1.28
90.0	2.6960	1.6185	2.5814	0.0386	1.6582	177.2	738.33	563.82	689.98	1.30
91.0	2.8700	1.7194	2.5730	0.0359	1.6624	182.1	758.96	559.18	704.52	1.26
92.0	2.7150	1.6371	2.3666	0.0309	1.6526	187.1	779.58	558.51	716.95	1.14
93.0	2.5610	1.5650	2.2506	0.0275	1.6310	192.2	800.83	563.82	728.07	1.06
94.0	2.5610	1.5734	2.1615	0.0249	1.6227	197.3	822.08	558.51	738.78	1.01
95.0	2.4640	1.5350	2.0841	0.0225	1.6007	203.1	846.46	561.83	749.62	0.95
96.0	2.6380	1.6555	2.2153	0.0225	1.5889	209.0	870.83	563.82	762.39	1.00
97.0	2.4830	1.5655	2.0596	0.0198	1.5821	214.2	892.71	563.82	774.08	0.93
98.0	2.5220	1.5995	2.0729	0.0190	1.5729	219.5	914.58	563.82	784.53	0.94
99.0	2.4450	1.5655	2.0049	0.0174	1.5582	225.6	939.79	565.14	794.83	0.90
100.0	2.5610	1.6505	2.0879	0.0172	1.5481	231.6	965.00	565.80	806.13	0.95

TIME	Qinc	------- CORRECTED ------- Qcm	Hcm	Cinc	Hr	Tr	Tw2	Tw1	Hr/Hc
101.0	2.7540	1.7803	2.2309	0.0175	1.5434	237.7	990.42	567.13	819.74	1.01
102.0	2.7150	1.7588	2.1691	0.0163	1.5404	243.8	1015.83	565.14	832.63	0.99
103.0	2.7930	1.8182	2.2358	0.0160	1.5329	249.8	1040.62	568.45	844.82	1.03
104.0	2.6770	1.7520	2.1400	0.0147	1.5250	255.7	1065.42	569.78	855.60	1.00
105.0	2.5220	1.6598	1.9864	0.0131	1.5168	262.0	1091.46	563.82	863.32	0.93
106.0	2.4060	1.6034	1.9271	0.0122	1.4981	268.2	1117.50	570.44	869.70	0.91
107.0	2.7150	1.8189	2.1710	0.0132	1.4900	274.9	1145.21	571.11	880.07	1.04
108.0	2.4640	1.6601	1.9666	0.0115	1.4820	281.5	1172.92	571.11	889.69	0.96
109.0	2.4830	1.6904	2.0043	0.0112	1.4667	288.8	1203.12	576.41	897.65	1.01
110.0	2.3090	1.5794	1.8352	0.0099	1.4600	296.0	1233.33	567.79	904.03	0.95
111.0	2.0970	1.4520	1.6836	0.0087	1.4425	303.1	1263.12	570.44	907.06	0.89
112.0	1.8650	1.3079	1.5079	0.0075	1.4245	310.3	1292.92	570.44	907.24	0.81
113.0	1.7290	1.2281	1.4029	0.0068	1.4066	318.0	1325.00	567.79	905.91	0.77
114.0	1.7490	1.2582	1.4348	0.0067	1.3888	325.7	1357.08	570.44	906.39	0.82
115.0	1.4400	1.0464	1.1856	0.0053	1.3751	332.2	1384.17	568.45	904.49	0.70
116.0	1.2650	0.9467	1.0693	0.0047	1.3565	338.7	1411.25	569.12	898.88	0.65
117.0	1.2270	0.9179	1.0317	0.0043	1.3360	347.8	1449.17	569.12	893.84	0.64
118.0	0.9757	0.7428	0.8341	0.0034	1.3130	356.9	1487.08	572.43	886.89	0.54
119.0	0.9370	0.7230	0.8084	0.0032	1.2955	364.4	1518.12	571.77	878.89	0.54
120.0	0.9950	0.7738	0.8577	0.0033	1.2853	371.8	1549.17	566.47	874.35	0.60
121.0	0.8404	0.6614	0.7345	0.0027	1.2702	378.5	1576.88	571.11	869.59	0.53
122.0	0.7051	0.5613	0.6217	0.0023	1.2558	385.1	1604.58	571.11	861.46	0.48
123.0	0.8984	0.7191	0.7916	0.0028	1.2488	391.2	1630.00	567.13	857.61	0.63
124.0	0.7437	0.5988	0.6570	0.0023	1.2416	397.3	1655.42	565.80	854.91	0.54
125.0	0.6471	0.5269	0.5806	0.0020	1.2278	402.1	1675.42	572.43	848.37	0.50
126.0	1.3820	1.1188	1.2257	0.0041	1.2347	406.9	1695.42	567.79	850.42	1.10
127.0	0.9177	0.7399	0.8111	0.0027	1.2399	408.9	1703.75	569.12	868.03	0.79
128.0	0.5504	0.4467	0.4885	0.0016	1.2320	410.9	1712.08	567.13	858.84	0.52
129.0	0.3185	0.2614	0.2855	0.0010	1.2184	410.4	1710.00	565.80	840.25	0.33

STS 26 7701 MISMATCH CORRECTION

TIME	Qinc	Qinc	CORRECTED Qcc	Hcc	Ctm	Hi	Tr	Tw2	Tw1	Hi/Ho
50.0	0.2342	0.3221	5.6482	0.2603	0.7173	132.1	550.42	545.26	543.87	4.93
51.0	0.3706	0.1995	2.3329	0.1076	1.8584	132.1	550.33	542.61	548.93	2.05
52.0	0.2147	0.1199	1.9160	0.0885	1.7903	132.1	550.25	544.60	548.86	1.70
53.0	0.2147	0.1228	3.0877	0.1427	1.7494	132.0	550.17	546.58	549.14	2.77
54.0	0.0783	0.0428	0.3574	0.0165	1.8237	132.0	550.08	539.29	547.77	0.32
55.0	0.1367	0.1041	12.1681	0.5633	1.3180	132.0	550.00	549.23	549.46	11.12
56.0	0.1952	0.1074	1.3439	0.0619	1.8183	132.1	550.50	543.27	548.91	1.22
57.0	0.0783	0.0466	0.5490	0.0251	1.6700	132.2	551.00	543.27	548.21	0.50
58.0	0.1172	0.0698	0.6253	0.0285	1.6687	132.4	551.50	541.28	547.80	0.57
59.0	0.1757	0.0990	0.5931	0.0269	1.7667	132.5	552.00	536.64	547.87	0.53
60.0	0.3706	0.2098	2.1025	0.0947	1.7670	132.6	552.50	543.27	550.02	1.89
61.0	0.1367	0.0727	0.4355	0.0197	1.8764	132.5	552.00	536.64	549.48	0.40
62.0	0.2147	0.1316	2.8328	0.1290	1.6339	132.4	551.50	547.25	549.82	2.61
63.0	0.2537	0.1342	1.2562	0.0575	1.8908	132.2	551.00	541.20	549.54	1.18
64.0	0.3121	0.1660	1.9037	0.0876	1.8806	132.1	550.50	542.61	549.23	1.81
65.0	0.3511	0.1833	2.0471	0.0948	1.9153	132.0	550.00	541.94	548.97	1.97
66.0	0.3706	0.1942	2.6099	0.1249	1.9085	131.9	549.75	543.27	548.88	2.63
67.0	0.4486	0.2315	3.0076	0.1400	1.9377	131.9	549.50	542.61	548.77	2.99
68.0	0.4096	0.2118	2.8462	0.1329	1.9345	131.8	549.25	542.61	548.53	2.88
69.0	0.3706	0.1913	2.0321	0.0951	1.9370	131.8	549.00	540.62	548.11	2.10
70.0	0.3316	0.1743	2.8231	0.1325	1.9026	131.7	548.75	543.27	547.99	2.97
71.0	0.4486	0.2437	2.9460	0.1342	1.8412	132.4	551.50	543.93	550.00	3.04
72.0	0.4876	0.2659	3.0084	0.1330	1.8345	133.0	554.25	545.92	552.55	3.05
73.0	0.6045	0.3247	2.6826	0.1152	1.8623	133.7	557.00	545.26	554.91	2.68
74.0	0.5850	0.3141	1.8280	0.0764	1.8626	134.3	559.75	542.61	556.71	1.80
75.0	0.7799	0.4183	2.4869	0.1011	1.8648	135.0	562.50	545.26	559.48	2.42
76.0	0.8774	0.4733	2.0184	0.0779	1.8539	136.3	567.92	542.61	563.21	1.91
77.0	1.1890	0.6377	2.5744	0.0946	1.8648	137.6	573.33	545.26	568.41	2.37
78.0	1.2280	0.6547	2.1911	0.0769	1.8759	138.9	578.75	543.27	572.90	1.97
79.0	1.5400	0.8164	2.4786	0.0832	1.8865	140.2	584.17	543.27	577.84	2.19
80.0	1.7160	0.9077	2.7784	0.0893	1.8907	141.5	589.58	547.25	583.20	2.41
81.0	1.7930	0.9618	2.5018	0.0747	1.8643	143.9	599.58	545.92	590.14	2.05
82.0	1.8910	1.0228	2.5920	0.0722	1.8491	146.3	609.58	550.56	598.34	2.02
83.0	2.2420	1.2104	2.8560	0.0741	1.8524	148.9	620.62	552.55	607.88	2.13
84.0	2.2030	1.1970	2.8347	0.0688	1.8406	151.6	631.67	559.18	617.28	2.04
85.0	2.4170	1.3217	2.6071	0.0579	1.8289	155.4	647.71	552.55	627.75	1.78
86.0	2.5340	1.3964	2.6210	0.0536	1.8148	159.3	663.75	555.20	639.53	1.71
87.0	2.1050	1.1702	2.0382	0.0385	1.7894	163.3	680.42	553.87	649.12	1.28
88.0	2.0470	1.1619	2.0169	0.0354	1.7523	167.3	697.08	560.50	658.47	1.24
89.0	2.1640	1.2434	2.0383	0.0330	1.7313	172.2	717.71	560.50	670.12	1.19
90.0	2.3390	1.3523	2.1568	0.0323	1.7207	177.2	738.33	563.82	683.74	1.20
91.0	2.1640	1.2568	1.8808	0.0262	1.7146	182.1	758.96	559.18	695.30	1.02
92.0	2.0660	1.2150	1.7563	0.0229	1.6941	187.1	779.58	558.51	704.81	0.93
93.0	2.4560	1.4539	2.0907	0.0256	1.6821	192.2	800.83	563.82	717.95	1.09
94.0	2.3200	1.3726	1.8855	0.0217	1.6843	197.3	822.08	558.51	730.47	0.97
95.0	2.3000	1.3793	1.8727	0.0202	1.6619	203.1	846.46	561.83	741.45	0.94
96.0	2.4170	1.4605	1.9544	0.0198	1.6493	209.0	870.83	563.82	753.09	0.97
97.0	2.6120	1.5775	2.0755	0.0200	1.6502	214.2	892.71	563.82	767.72	1.03
98.0	2.6120	1.5797	2.0472	0.0188	1.6484	219.5	914.58	563.82	780.66	1.02
99.0	2.4950	1.5228	1.9501	0.0169	1.6338	225.6	939.79	565.14	791.55	0.97
100.0	2.6120	1.6050	2.0304	0.0168	1.6228	231.6	965.00	565.80	802.85	1.02

TIME	Qtw	------- CORRECTED ------- Qtw	Htw	Clm	Hr	Tr	Tw2	Tw1	Hr/Hc
101.0	2.6900	2.0813	0.0163	1.6151	237.7	990.42	567.13	815.36	1.05
102.0	2.5930	1.9839	0.0149	1.6079	243.8	1015.83	565.14	826.37	1.00
103.0	2.6710	2.0519	0.0147	1.5967	249.8	1040.62	568.45	837.00	1.05
104.0	2.5340	1.9471	0.0134	1.5861	255.7	1065.42	569.78	846.73	1.01
105.0	2.3390	1.7737	0.0117	1.5750	262.0	1091.46	563.82	853.09	0.92
106.0	2.2810	1.7622	0.0112	1.5527	268.2	1117.50	570.44	858.71	0.93
107.0	2.2030	1.7083	0.0104	1.5364	274.9	1145.21	571.11	864.70	0.91
108.0	2.2220	1.7251	0.0101	1.5232	281.5	1172.92	571.11	871.32	0.94
109.0	2.1250	1.6718	0.0094	1.5047	288.8	1203.12	576.41	877.99	0.93
110.0	2.1250	1.6451	0.0089	1.4986	296.0	1233.33	567.79	884.16	0.94
111.0	2.2220	1.7300	0.0090	1.4868	303.1	1263.12	570.44	891.97	1.01
112.0	2.0860	1.6260	0.0081	1.4769	310.3	1292.92	570.44	898.97	0.97
113.0	2.0080	1.5634	0.0075	1.4653	318.0	1325.00	567.79	903.70	0.96
114.0	1.8130	1.4268	0.0066	1.4474	325.7	1357.08	570.44	906.02	0.90
115.0	1.9300	1.5184	0.0068	1.4383	332.2	1384.17	568.45	909.37	0.99
116.0	1.5790	1.2511	0.0055	1.4243	338.7	1411.25	569.12	909.79	0.85
117.0	1.5790	1.2628	0.0053	1.4041	347.8	1449.17	569.12	908.21	0.87
118.0	1.4820	1.2009	0.0049	1.3846	356.9	1487.08	572.43	907.83	0.86
119.0	1.3840	1.1279	0.0044	1.3710	364.4	1518.12	571.77	906.53	0.84
120.0	1.1500	0.9382	0.0036	1.3577	371.8	1549.17	566.47	901.62	0.72
121.0	1.0530	0.8740	0.0033	1.3372	378.5	1576.88	571.11	894.45	0.71
122.0	0.8579	0.7201	0.0026	1.3189	385.1	1604.58	571.11	885.37	0.62
123.0	0.9943	0.8365	0.0030	1.3078	391.2	1630.00	567.13	879.08	0.74
124.0	0.8189	0.6915	0.0024	1.2962	397.3	1655.42	565.80	873.56	0.64
125.0	0.8384	0.6544	0.0025	1.2807	402.1	1675.42	572.43	867.60	0.69
126.0	0.8384	0.6571	0.0024	1.2753	406.9	1695.42	567.79	863.80	0.72
127.0	0.9943	0.7808	0.0029	1.2729	408.9	1703.75	569.12	864.31	0.93
128.0	0.8384	0.6589	0.0024	1.2719	410.9	1712.08	567.13	863.91	0.86
129.0	0.4681	0.3705	0.4048	1.2631	410.4	1710.00	565.80	852.84	0.53

STS 26 7702 MISMATCH CORRECTION

TIME	Qlw	CORRECTED Qlw	CORRECTED Qcw	CORRECTED Hcw	Ctm	Hi	Ti	Tw2	Tw1	Hi/Hc
50.0	0.2719	0.2988	3.7805	0.1742	0.9174	132.1	550.42	543.27	542.78	3.66
51.0	0.3310	0.1731	3.5438	0.1635	1.9139	132.1	550.33	545.92	549.24	3.46
52.0	0.2522	0.1279	1.6543	0.0764	1.9714	132.1	550.25	543.27	548.85	1.63
53.0	0.1932	0.0968	0.7160	0.0331	1.9854	132.0	550.17	537.97	547.86	0.71
54.0	0.0948	0.0556	0.7345	0.0340	1.7066	132.0	550.08	543.27	547.23	0.74
55.0	0.1341	0.0759	0.9243	0.0428	1.7672	132.0	550.00	542.61	547.28	0.94
56.0	0.0751	0.0430	0.4224	0.0194	1.7365	132.1	550.50	541.28	546.87	0.43
57.0	0.3310	0.1745	1.5299	0.0700	1.8972	132.2	551.00	540.62	548.28	1.54
58.0	0.3506	0.1793	1.8457	0.0840	1.9555	132.4	551.50	542.61	549.60	1.85
59.0	0.3506	0.1791	2.2264	0.1008	1.9583	132.5	552.00	544.60	550.44	2.22
60.0	0.1341	0.0710	0.7118	0.0321	1.8881	132.6	552.50	543.27	550.02	0.71
61.0	0.2719	0.1379	1.0535	0.0477	1.9722	132.5	552.00	539.96	549.59	1.06
62.0	0.3310	0.1651	1.3885	0.0632	2.0050	132.4	551.50	540.62	549.62	1.42
63.0	0.3506	0.1722	1.5098	0.0691	2.0359	132.2	551.00	540.62	549.47	1.57
64.0	0.4294	0.2086	2.2056	0.1015	2.0585	132.1	550.50	541.94	549.40	2.32
65.0	0.3703	0.1793	2.0017	0.0927	2.0658	132.0	550.00	541.94	549.01	2.13
66.0	0.6656	0.3145	2.6987	0.1253	2.1164	131.9	549.75	539.29	548.90	2.93
67.0	0.6852	0.3250	8.1258	0.3783	2.1087	131.9	549.50	545.92	549.19	8.97
68.0	0.6459	0.3036	4.0837	0.1906	2.1262	131.8	549.25	542.61	548.76	4.59
69.0	0.7640	0.3582	4.9885	0.2335	2.1334	131.8	549.00	542.61	548.57	5.71
70.0	0.6656	0.3135	5.7728	0.2710	2.1233	131.7	548.75	543.93	548.39	6.73
71.0	0.8427	0.4056	3.6312	0.1654	2.0783	132.4	551.50	541.28	550.35	4.16
72.0	0.9411	0.4556	5.1548	0.2279	2.0666	133.0	554.25	545.92	553.23	5.81
73.0	0.9805	0.4740	3.9164	0.1682	2.0691	133.7	557.00	545.26	555.59	4.34
74.0	1.1580	0.5580	3.8410	0.1604	2.0759	134.3	559.75	545.26	558.09	4.20
75.0	1.2360	0.5950	3.4069	0.1385	2.0778	135.0	562.50	544.60	560.48	3.68
76.0	1.3540	0.6644	3.4692	0.1339	2.0386	136.3	567.92	547.25	564.92	3.64
77.0	1.5910	0.7765	3.3739	0.1240	2.0493	137.6	573.33	547.25	569.78	3.45
78.0	1.6890	0.8238	2.9799	0.1046	2.0504	138.9	578.75	545.92	574.30	2.98
79.0	1.7480	0.8570	2.9893	0.1003	2.0400	140.2	584.17	548.57	579.04	2.93
80.0	1.9450	0.9520	3.1611	0.1016	2.0434	141.5	589.58	550.56	584.07	3.05
81.0	2.3390	1.1542	3.1580	0.0943	2.0269	143.9	599.58	548.57	591.68	2.88
82.0	2.4760	1.2250	3.0703	0.0855	2.0214	146.3	609.58	549.90	600.07	2.66
83.0	2.5750	1.2836	3.0584	0.0793	2.0062	148.9	620.62	553.21	609.04	2.54
84.0	2.7910	1.3926	3.1263	0.0759	2.0044	151.6	631.67	555.20	618.41	2.50
85.0	2.9490	1.4908	3.0468	0.0676	1.9783	155.4	647.71	555.86	629.81	2.31
86.0	3.3420	1.6891	3.1899	0.0652	1.9787	159.3	663.75	555.86	642.77	2.31
87.0	3.3820	1.7179	3.0894	0.0584	1.9688	163.3	680.42	557.85	655.58	2.16
88.0	3.6570	1.8579	3.1044	0.0546	1.9685	167.3	697.08	555.20	668.30	2.12
89.0	3.9130	2.0096	3.3224	0.0537	1.9473	172.2	717.71	561.83	683.37	2.15
90.0	3.9720	2.0474	3.2529	0.0487	1.9401	177.2	738.33	563.15	698.70	2.01
91.0	4.2670	2.2041	3.3768	0.0471	1.9360	182.1	758.96	563.82	714.15	2.04
92.0	4.2280	2.1932	3.2584	0.0435	1.9279	187.1	779.58	564.48	728.75	1.93
93.0	4.2670	2.2308	3.2719	0.0400	1.9129	192.2	800.83	568.45	743.04	1.90
94.0	4.2670	2.2434	3.2195	0.0370	1.9021	197.3	822.08	569.78	757.11	1.84
95.0	4.2870	2.2766	3.2107	0.0346	1.8831	203.1	846.46	572.43	771.61	1.80
96.0	4.5430	2.4223	3.3350	0.0338	1.8755	209.0	870.83	572.43	787.46	1.85
97.0	4.3660	2.3244	3.1404	0.0302	1.8688	214.2	892.71	572.43	801.44	1.74
98.0	4.5630	2.4447	3.2992	0.0302	1.8568	219.5	914.58	577.73	815.28	1.83
99.0	4.3860	2.3663	3.1073	0.0270	1.8449	225.6	939.79	574.42	828.50	1.73
100.0	4.7200	2.5681	3.3953	0.0280	1.8289	231.6	965.00	583.04	843.61	1.90

TIME	Qhw	CORRECTED Qcw	Hcw	Ctm	Ht	Tr	Tw2	Tw1	Ht/Hc
101.0	4.7200	3.3539	0.0269	1.8256	227.7	990.42	583.04	859.29	1.88
102.0	4.7600	3.3517	0.0251	1.8158	243.8	1015.83	583.04	873.65	1.89
103.0	4.6610	3.3116	0.0238	1.8018	249.8	1040.62	589.00	887.04	1.88
104.0	4.5820	3.2275	0.0222	1.7919	255.7	1065.42	587.68	899.07	1.86
105.0	4.5230	3.1860	0.0210	1.7773	262.0	1091.46	589.00	910.46	1.85
106.0	4.4640	3.1589	0.0200	1.7639	268.2	1117.50	590.33	921.77	1.85
107.0	4.5630	3.2231	0.0196	1.7503	274.9	1145.21	592.98	933.98	1.92
108.0	4.4250	3.1182	0.0182	1.7386	281.5	1172.92	592.98	945.50	1.89
109.0	4.2870	2.4874	0.0172	1.7179	288.8	1203.12	598.94	955.92	1.90
110.0	4.3660	3.0594	0.0167	1.7061	296.0	1233.33	597.62	967.06	1.98
111.0	4.3460	3.1031	0.0160	1.6953	303.1	1263.12	597.62	978.47	2.01
112.0	4.2480	2.5557	0.0152	1.6813	310.3	1292.92	600.93	988.93	2.03
113.0	3.9130	3.0324	0.0136	1.6606	318.0	1325.00	605.57	996.70	1.94
114.0	4.0900	2.8257	0.0137	1.6402	325.7	1357.08	602.92	1005.27	2.08
115.0	3.6180	2.9438	0.0118	1.6347	332.2	1384.17	602.92	1011.06	1.91
116.0	3.4210	2.6120	0.0109	1.6156	338.7	1411.25	604.24	1013.11	1.89
117.0	3.3230	2.4906	0.0103	1.5907	347.8	1449.17	606.23	1016.05	1.90
118.0	3.2240	2.4463	0.0097	1.5704	356.9	1487.08	606.90	1020.14	1.91
119.0	3.3030	2.3909	0.0097	1.5575	364.4	1518.12	608.88	1026.12	2.05
120.0	3.1850	2.4630	0.0091	1.5455	371.8	1549.17	610.87	1032.17	2.07
121.0	3.0270	2.3877	0.0085	1.5336	378.5	1576.88	612.20	1035.89	2.08
122.0	3.0270	2.2812	0.0083	1.5262	385.1	1604.58	606.90	1039.01	2.18
123.0	2.8500	2.2716	0.0077	1.5141	391.2	1630.00	608.88	1040.97	2.15
124.0	2.7320	1.8794	0.0073	1.4978	397.3	1655.42	615.51	1041.60	2.17
125.0	2.0630	2.0936	0.0054	1.4846	402.1	1675.42	608.88	1034.30	1.71
126.0	0.5868	1.5818	0.0015	1.4454	406.9	1695.42	604.24	1004.24	0.52
127.0	0.8821	0.4595	0.0024	1.4020	408.9	1703.75	608.88	971.14	0.88
128.0	1.0000	0.6289	0.0027	1.3784	410.9	1712.08	609.55	952.89	1.10
129.0	0.8821	0.7144	0.0024	1.3661	410.4	1710.00	606.23	938.85	1.07
		0.8235							
		0.7309							

SIS 27 7700 MISMATCH CORRECTION

TIME	Qhw	CORRECTED Qhw	CORRECTED Qcw	CORRECTED Hcw	Ctm	Hr	Tr	Tw2	Tw1	H1/Ho
50.0	0.1560	0.1613	0.5810	0.0285	0.9683	130.8	545.00	521.40	520.58	0.53
51.0	0.1750	0.1390	0.6623	0.0327	1.2514	130.7	544.42	526.70	531.59	0.62
52.0	0.0440	0.0328	0.1601	0.0080	1.3375	130.5	543.83	526.70	533.05	0.15
53.0	0.0000	0.0000	0.0000	0.0000	1.1728	130.4	543.25	526.70	529.84	0.00
54.0	0.0815	0.0643	0.2662	0.0134	1.2655	130.2	542.67	522.72	528.54	0.26
55.0	0.2500	0.1623	0.5709	0.0290	1.5324	130.1	542.08	518.75	532.40	0.57
56.0	0.1840	0.1125	0.3595	0.0183	1.6307	130.0	541.67	516.10	533.81	0.37
57.0	0.1180	0.0717	0.2093	0.0107	1.6444	129.9	541.25	513.44	533.12	0.22
58.0	0.1090	0.0690	0.2416	0.0125	1.5766	129.8	540.83	517.75	532.37	0.25
59.0	0.1000	0.0663	0.2903	0.0150	1.5051	129.7	540.42	522.06	532.24	0.31
60.0	0.1280	0.0822	0.3474	0.0181	1.5524	129.6	540.00	521.07	532.56	0.38
61.0	0.1560	0.1003	0.3741	0.0190	1.5499	130.1	542.08	520.07	533.36	0.40
62.0	0.0720	0.0488	0.1860	0.0092	1.4716	130.6	544.17	522.06	533.51	0.20
63.0	0.0000	0.0000	0.0000	0.0000	1.3116	131.1	546.25	524.05	531.65	0.00
64.0	0.0440	0.0337	0.1092	0.0051	1.3045	131.6	548.33	521.07	530.19	0.11
65.0	0.1000	0.0726	0.2031	0.0094	1.3741	132.1	550.42	518.08	531.36	0.21
66.0	0.1840	0.1333	0.3422	0.0146	1.3760	133.8	557.33	519.41	535.07	0.34
67.0	0.2680	0.1881	0.4507	0.0180	1.4197	135.4	564.25	520.74	540.80	0.42
68.0	0.3435	0.2345	0.5381	0.0202	1.4592	137.1	571.17	522.72	547.15	0.48
69.0	0.4190	0.2796	0.6185	0.0218	1.4927	138.7	578.08	524.71	553.59	0.53
70.0	0.5415	0.3481	0.6877	0.0229	1.5495	140.4	585.00	521.73	559.92	0.56
71.0	0.6640	0.4233	0.7427	0.0227	1.5629	143.2	596.58	518.75	566.87	0.57
72.0	0.6355	0.4073	0.6775	0.0191	1.5552	146.0	608.17	519.08	573.40	0.49
73.0	0.6070	0.3932	0.6260	0.0163	1.5396	148.7	619.75	519.41	578.88	0.43
74.0	0.7395	0.4837	0.7772	0.0189	1.5239	151.5	631.33	524.71	586.06	0.51
75.0	0.8720	0.5683	0.9206	0.0210	1.5291	154.3	642.92	530.01	595.62	0.58
76.0	0.9195	0.6001	0.8944	0.0184	1.5274	159.1	662.75	526.70	605.51	0.53
77.0	0.9670	0.6326	0.8844	0.0166	1.5245	163.8	682.58	523.39	615.10	0.50
78.0	1.1670	0.7625	1.0287	0.0177	1.5260	168.6	702.42	522.72	626.53	0.55
79.0	1.3670	0.8868	1.1617	0.0185	1.5370	173.3	722.25	522.06	640.13	0.60
80.0	1.5870	1.0215	1.3136	0.0194	1.5490	178.1	742.08	522.72	654.98	0.66
81.0	1.8080	1.1548	1.4612	0.0201	1.5609	182.9	762.29	523.39	670.57	0.71
82.0	1.7800	1.1351	1.4164	0.0183	1.5639	187.8	782.50	524.05	684.13	0.67
83.0	1.7510	1.1236	1.3829	0.0167	1.5546	193.2	805.00	524.71	695.45	0.64
84.0	1.9340	1.2451	1.5179	0.0172	1.5494	198.6	827.50	526.04	707.93	0.69
85.0	2.1170	1.3610	1.6459	0.0176	1.5516	203.8	849.17	527.36	722.30	0.74
86.0	2.1170	1.3616	1.6333	0.0166	1.5512	209.0	870.83	528.36	735.68	0.73
87.0	2.1170	1.3668	1.6272	0.0156	1.5454	214.4	893.33	529.35	747.40	0.72
88.0	2.2340	1.4464	1.7104	0.0156	1.5411	219.8	915.83	530.35	759.43	0.76
89.0	2.3500	1.5219	1.7896	0.0156	1.5408	224.9	936.88	531.34	772.21	0.80
90.0	2.2340	1.4500	1.6886	0.0141	1.5377	229.9	957.92	530.35	782.83	0.77
91.0	2.1170	1.3856	1.5976	0.0127	1.5251	235.9	982.71	529.35	790.83	0.73
92.0	2.1080	1.3917	1.5958	0.0121	1.5121	241.8	1007.50	530.01	798.56	0.73
93.0	2.0980	1.3948	1.5915	0.0116	1.5017	247.6	1031.67	530.68	806.76	0.73
94.0	1.9140	1.2837	1.4593	0.0102	1.4888	253.4	1055.83	531.67	813.07	0.68
95.0	1.7310	1.1732	1.3295	0.0090	1.4736	258.8	1078.12	532.67	816.38	0.63
96.0	1.8850	1.2866	1.4513	0.0094	1.4631	264.1	1100.42	532.67	821.45	0.70
97.0	2.0400	1.3999	1.5704	0.0098	1.4552	271.0	1129.17	532.67	830.90	0.77
98.0	1.8280	1.2637	1.4128	0.0084	1.4448	277.9	1157.92	533.66	838.65	0.70
99.0	1.6160	1.1313	1.2603	0.0072	1.4269	285.5	1189.58	534.65	841.74	0.63
100.0	1.8190	1.2863	1.4324	0.0078	1.4125	293.1	1221.25	537.64	847.35	0.73

TIME	Qhw	CORRECTED Qhw	CORRECTED Qcw	CORRECTED Hcw	Clm	Hr	Tr	Tw2	Tw1	Hr/Hc
[illegible]	2.0210	1.4334	1.5963	0.0084	1.4082	300.0	1250.21	540.67	858.78	0.83
[illegible]	1.8470	1.3140	1.4568	0.0074	1.4042	307.0	1279.17	540.29	868.27	0.78
103.0	1.6740	1.2011	1.3256	0.0065	1.3925	314.7	1311.25	539.96	872.45	0.72
104.0	1.7320	1.2522	1.3757	0.0065	1.3819	322.4	1343.33	539.29	876.50	0.76
105.0	1.7890	1.2990	1.4215	0.0065	1.3760	329.3	1372.08	538.63	882.83	0.82
106.0	1.7320	1.2636	1.3794	0.0061	1.3695	336.2	1400.83	538.96	888.76	0.83
107.0	1.6740	1.2306	1.3393	0.0057	1.3593	344.7	1436.25	539.29	893.23	0.82
108.0	1.6550	1.2252	1.3289	0.0055	1.3498	353.2	1471.67	538.96	897.32	0.83
109.0	1.6350	1.2168	1.3161	0.0053	1.3427	360.5	1502.29	538.63	901.36	0.84
110.0	1.6160	1.2092	1.3053	0.0051	1.3355	367.9	1532.92	538.96	905.20	0.86
111.0	1.5970	1.2015	1.2944	0.0049	1.3283	375.4	1564.17	539.29	908.87	0.88
112.0	1.5390	1.1644	1.2522	0.0046	1.3209	382.9	1595.42	539.62	911.69	0.88
113.0	1.4820	1.1250	1.2088	0.0044	1.3166	387.1	1612.92	539.96	913.07	0.89
114.0	1.5680	1.1938	1.2836	0.0046	1.3127	391.3	1630.42	541.94	915.76	1.00
115.0	1.6540	1.2618	1.3573	0.0047	1.3100	396.6	1652.50	543.93	921.36	1.09
116.0	1.5680	1.1980	1.2858	0.0044	1.3081	401.9	1674.58	542.94	925.86	1.00
117.0	1.4820	1.1327	1.2142	0.0041	1.3077	403.5	1681.25	541.94	926.93	1.10
118.0	1.3960	1.0676	1.1397	0.0039	1.3069	405.1	1687.92	537.64	925.35	1.12
119.0	1.3100	1.0038	1.0672	0.0036	1.3044	406.9	1695.42	533.33	921.84	1.11
120.0	1.2620	0.9718	1.0348	0.0035	1.2981	408.7	1702.92	535.65	917.77	1.14
121.0	1.2140	0.9402	1.0024	0.0033	1.2907	411.8	1715.62	537.97	913.94	1.14
122.0	0.9295	0.7252	0.7727	0.0025	1.2813	414.8	1728.33	537.97	905.70	0.92
123.0	0.6450	0.5084	0.5416	0.0018	1.2684	415.8	1732.50	537.97	890.16	0.68
124.0	0.6920	0.5511	0.5876	0.0019	1.2554	416.8	1736.67	539.29	875.22	0.79
125.0	0.7390	0.5928	0.6325	0.0021	1.2463	418.3	1742.92	540.62	865.89	0.91
126.0	0.8150	0.6557	0.6983	0.0023	1.2426	419.8	1749.17	538.63	861.18	1.07
127.0	0.8910	0.7165	0.7618	0.0025	1.2432	419.5	1747.92	536.64	860.24	1.25
128.0	0.7870	0.6333	0.6731	0.0022	1.2423	419.2	1746.67	535.98	858.16	1.19
129.0	0.6830	0.5525	0.5865	0.0019	1.2360	422.0	1750.13	535.32	852.29	1.11

TIME	Qtm	CORRECTED Qtm	CORRECTED Qcw	CORRECTED Hcw	Ctm	Hr	Tr	Tw2	Tw1	H1/Ho
50.0	0.4325	0.4179	1.5036	0.0737	1.0320	130.8	545.00	521.40	522.12	1.51
51.0	0.5320	0.3115	1.4840	0.0732	1.7086	130.7	544.42	526.70	538.67	1.52
52.0	0.4525	0.2471	1.2091	0.0601	1.8313	130.5	543.83	526.70	540.28	1.26
53.0	0.3730	0.2036	1.0241	0.0513	1.8322	130.4	543.25	526.70	539.83	1.09
54.0	0.3330	0.1791	0.7424	0.0374	1.8505	130.2	542.67	522.72	538.90	0.80
55.0	0.2930	0.1574	0.5536	0.0281	1.8557	130.1	542.08	518.75	537.79	0.61
56.0	0.1730	0.0943	0.3012	0.0154	1.8313	130.0	541.67	516.10	536.36	0.34
57.0	0.0530	0.0296	0.0866	0.0044	1.7877	129.9	541.25	513.44	534.33	0.10
58.0	0.1530	0.0894	0.3130	0.0161	1.7063	129.8	540.83	517.75	533.29	0.36
59.0	0.2530	0.1477	0.6469	0.0335	1.7135	129.7	540.42	522.06	534.55	0.76
60.0	0.2530	0.1403	0.5931	0.0309	1.7943	129.6	540.00	521.07	535.41	0.71
61.0	0.2530	0.1432	0.5340	0.0271	1.7587	130.1	542.08	520.07	535.99	0.64
62.0	0.2030	0.1192	0.4537	0.0225	1.6963	130.6	544.17	522.06	536.74	0.53
63.0	0.1530	0.0938	0.3646	0.0176	1.6242	131.1	546.25	524.05	537.26	0.43
64.0	0.2830	0.1672	0.5418	0.0256	1.6836	131.6	548.33	521.07	538.84	0.63
65.0	0.4130	0.2342	0.6548	0.0302	1.7547	132.1	550.42	518.08	541.35	0.75
66.0	0.4530	0.2642	0.6782	0.0290	1.7049	133.8	557.33	519.41	544.90	0.74
67.0	0.4930	0.2903	0.6955	0.0278	1.6890	135.4	564.25	520.74	549.32	0.72
68.0	0.4630	0.2765	0.6344	0.0238	1.6665	137.1	571.17	522.72	553.51	0.62
69.0	0.4330	0.2632	0.5824	0.0205	1.6378	138.7	578.08	524.71	557.17	0.55
70.0	0.5525	0.3315	0.6550	0.0218	1.6590	140.4	585.00	521.73	561.49	0.59
71.0	0.6720	0.4040	0.7089	0.0216	1.6562	143.2	596.58	518.75	567.45	0.60
72.0	0.7520	0.4530	0.7533	0.0212	1.6530	146.0	608.17	519.08	574.55	0.60
73.0	0.8320	0.5005	0.7969	0.0208	1.6553	148.7	619.75	519.41	582.10	0.61
74.0	0.8920	0.5403	0.8682	0.0211	1.6438	151.5	631.33	524.71	590.16	0.63
75.0	0.9520	0.5788	0.9377	0.0214	1.6376	154.3	642.92	530.01	598.65	0.66
76.0	1.0320	0.6321	0.9420	0.0194	1.6262	159.1	662.75	526.70	607.93	0.62
77.0	1.1110	0.6823	0.9540	0.0179	1.6224	163.8	682.58	523.39	617.86	0.59
78.0	1.1810	0.7285	0.9828	0.0169	1.6156	168.6	702.42	522.72	628.19	0.58
79.0	1.2510	0.7737	1.0136	0.0161	1.6115	173.3	722.25	522.06	638.79	0.58
80.0	1.3910	0.8610	1.1072	0.0164	1.6102	178.1	742.08	522.72	650.34	0.61
81.0	1.5310	0.9462	1.1972	0.0165	1.6128	182.9	762.29	523.39	662.98	0.64
82.0	1.4910	0.9235	1.1524	0.0149	1.6098	187.8	782.50	524.05	674.32	0.60
83.0	1.4510	0.9069	1.1163	0.0135	1.5956	193.2	805.00	524.71	683.90	0.57
84.0	1.5800	0.9935	1.2111	0.0137	1.5860	198.6	827.50	526.04	694.48	0.61
85.0	1.7100	1.0760	1.3012	0.0139	1.5849	203.8	849.17	527.36	706.82	0.65
86.0	1.7600	1.1081	1.3293	0.0135	1.5841	209.0	870.83	528.36	719.10	0.66
87.0	1.8100	1.1424	1.3601	0.0131	1.5803	214.4	893.33	529.35	730.76	0.67
88.0	1.7700	1.1223	1.3271	0.0121	1.5735	219.8	915.83	530.35	741.14	0.65
89.0	1.7300	1.1029	1.2969	0.0113	1.5652	224.9	936.88	531.34	-749.90	0.64
90.0	1.7900	1.1451	1.3335	0.0112	1.5599	229.9	957.92	530.35	758.59	0.67
91.0	1.8500	1.1892	1.3711	0.0108	1.5525	235.9	982.71	529.35	768.17	0.69
92.0	1.8100	1.1706	1.3423	0.0102	1.5432	241.8	1007.50	530.01	777.31	0.68
93.0	1.7700	1.1526	1.3152	0.0096	1.5329	247.6	1031.67	530.68	785.25	0.67
94.0	1.8800	1.2303	1.3985	0.0098	1.5252	253.4	1055.83	531.67	794.17	0.72
95.0	1.9900	1.3039	1.4776	0.0100	1.5234	258.8	1078.12	532.67	804.88	0.77
96.0	1.9500	1.2799	1.4438	0.0094	1.5209	264.1	1100.42	532.67	814.64	0.77
97.0	1.9100	1.2628	1.4167	0.0088	1.5100	271.0	1129.17	532.67	822.74	0.77
98.0	1.8200	1.2141	1.3573	0.0081	1.4969	277.9	1157.92	533.66	829.40	0.75
99.0	1.7300	1.1670	1.3000	0.0074	1.4804	285.5	1189.58	534.65	834.65	0.72
100.0	1.8000	1.2265	1.3658	0.0075	1.4656	293.1	1221.25	537.64	841.11	0.77

TIME	Qhw	------- CORRECTED ------- Qcw	Hcw	Clm	Hr	Tr	Tw2	Tw1	Hr/Hc
101.0	1.8700	1.2417	0.0075	1.4570	300.0	1250.00	540.62	849.84	0.82
102.0	1.7900	1.2326	0.0070	1.4503	307.0	1278.17	540.29	857.56	0.81
103.0	1.7100	1.1868	0.0064	1.4397	314.2	1311.25	539.96	862.94	0.79
104.0	1.7200	1.3098	0.0064	1.4288	322.4	1343.33	539.29	868.05	0.82
105.0	1.7300	1.3210	0.0062	1.4217	329.3	1372.08	538.63	873.77	0.85
106.0	1.6500	1.3302	0.0061	1.4131	336.2	1400.83	538.96	878.41	0.85
107.0	1.5710	1.2734	0.0056	1.4000	344.7	1436.25	539.29	881.38	0.83
108.0	1.6610	1.2202	0.0052	1.3901	353.2	1471.67	538.96	885.87	0.90
109.0	1.7500	1.2948	0.0053	1.3859	360.5	1502.29	538.63	893.22	0.97
110.0	1.7500	1.3644	0.0055	1.3819	367.9	1532.92	538.96	900.90	1.00
111.0	1.7500	1.3657	0.0053	1.3770	375.4	1564.17	539.29	907.73	1.04
112.0	1.6610	1.3079	0.0052	1.3704	382.9	1595.42	539.62	912.53	1.02
113.0	1.5710	1.3024	0.0048	1.3661	387.1	1612.92	539.96	914.50	1.01
114.0	1.3910	1.2347	0.0045	1.3573	391.3	1630.42	541.94	912.79	0.95
115.0	1.2110	1.1012	0.0039	1.3438	396.6	1652.50	543.93	907.27	0.87
116.0	1.2310	0.9689	0.0034	1.3330	401.9	1674.58	542.94	902.27	0.93
117.0	1.2510	0.9906	0.0034	1.3296	403.5	1681.25	541.94	899.95	1.02
118.0	1.1710	1.0080	0.0034	1.3279	405.1	1687.92	537.64	897.31	1.04
119.0	1.0910	0.9408	0.0032	1.3245	406.9	1695.42	537.33	892.86	1.02
120.0	1.0710	0.8753	0.0030	1.3169	408.7	1702.92	535.65	888.36	1.06
121.0	1.0510	0.8656	0.0029	1.3089	411.8	1715.62	537.97	884.83	1.09
122.0	0.8715	0.8557	0.0028	1.3003	414.8	1728.33	537.97	878.78	0.95
123.0	0.6920	0.7139	0.0023	1.2898	415.8	1732.50	537.97	868.04	0.81
124.0	0.6420	0.5714	0.0019	1.2775	416.8	1736.67	539.29	856.15	0.81
125.0	0.5920	0.5357	0.0017	1.2658	418.3	1742.92	540.62	845.34	0.80
126.0	0.6820	0.4989	0.0016	1.2595	419.8	1749.17	538.63	838.16	1.00
127.0	0.7720	0.5413	0.0019	1.2592	419.5	1747.92	536.64	836.05	1.20
128.0	0.6420	0.6129	0.0021	1.2571	419.2	1746.67	535.98	832.72	1.07
129.0	0.5120	0.5106	0.0018	1.2481	422.0	1758.13	535.32	824.61	0.93
		0.4101	0.0014						

SIS 27 7702 MISMATCH CORRECTION

TIME	Qtm	Qtm	Qcm	Hcm	Ctm	Hr	Tr	Tw2	Tw1	H1/Hu
		CORRECTED								
50.0	0.3865	0.3563	1.2148	0.0595	1.0764	130.8	545.00	520.07	521.64	1.35
51.0	0.2670	0.1586	0.5354	0.0264	1.6836	130.7	544.42	519.41	533.48	0.61
52.0	0.3170	0.1820	0.8268	0.0411	1.7422	130.5	543.83	525.36	536.65	0.96
53.0	0.3670	0.2027	1.4168	0.0709	1.8114	130.4	543.25	531.34	539.29	1.67
54.0	0.3865	0.1946	0.8489	0.0428	1.9865	130.2	542.67	523.72	539.10	1.02
55.0	0.4060	0.1996	0.6306	0.0320	2.0256	130.1	542.08	516.10	538.03	0.77
56.0	0.3865	0.1922	0.6388	0.0326	2.0014	130.0	541.67	517.09	537.35	0.79
57.0	0.3670	0.1833	0.6428	0.0330	1.9924	129.9	541.25	518.08	537.01	0.81
58.0	0.4165	0.2073	0.7260	0.0374	2.0089	129.8	540.83	517.75	536.92	0.94
59.0	0.4660	0.2294	0.8023	0.0416	2.0313	129.7	540.42	517.42	536.94	1.05
60.0	0.4860	0.2359	0.8007	0.0417	2.0505	129.6	540.00	516.43	536.81	1.07
61.0	0.5060	0.2526	0.7781	0.0395	2.0028	130.1	542.08	515.43	537.43	1.03
62.0	0.4960	0.2515	0.7818	0.0387	1.9721	130.6	544.17	517.09	538.75	1.02
63.0	0.4860	0.2490	0.7811	0.0377	1.9516	131.1	546.25	518.75	540.29	1.01
64.0	0.4660	0.2429	0.8269	0.0390	1.9188	131.6	548.33	522.39	542.01	1.06
65.0	0.4460	0.2361	0.8757	0.0404	1.8893	132.1	550.42	526.04	543.88	1.12
66.0	0.6050	0.3244	0.9212	0.0394	1.8654	133.8	557.33	523.06	547.47	1.11
67.0	0.7640	0.4046	0.9547	0.0382	1.8885	135.4	564.25	520.07	552.38	1.09
68.0	0.7340	0.3911	0.8510	0.0319	1.8766	137.1	571.17	520.07	556.94	0.93
69.0	0.7040	0.3794	0.7723	0.0273	1.8556	138.7	578.08	520.07	560.92	0.80
70.0	0.9325	0.5037	1.0274	0.0342	1.8515	140.4	585.00	523.72	566.67	1.03
71.0	1.1610	0.6302	1.2434	0.0379	1.8425	143.2	596.58	527.36	575.36	1.17
72.0	1.3490	0.7197	1.2578	0.0354	1.8745	146.0	608.17	523.39	584.41	1.12
73.0	1.5380	0.8132	1.2946	0.0338	1.8914	148.7	619.75	519.41	593.03	1.09
74.0	1.6570	0.8759	1.3447	0.0327	1.8919	151.5	631.33	519.74	601.66	1.09
75.0	1.7760	0.9383	1.3971	0.0318	1.8929	154.3	642.92	520.07	610.35	1.09
76.0	1.7960	0.9689	1.3800	0.0284	1.8537	159.1	662.75	520.40	620.42	1.00
77.0	1.8160	0.9917	1.3639	0.0255	1.8313	163.8	682.58	520.74	631.47	0.94
78.0	1.9450	1.0657	1.4431	0.0248	1.8151	168.6	702.42	523.39	643.50	0.95
79.0	2.0740	1.1414	1.5255	0.0242	1.8074	173.3	722.25	526.04	656.43	0.96
80.0	2.3820	1.3074	1.7175	0.0254	1.8120	178.1	742.08	527.36	670.87	1.05
81.0	2.6890	1.4683	1.9000	0.0262	1.8214	182.9	762.29	528.69	686.62	1.13
82.0	2.8970	1.5792	2.0466	0.0264	1.8246	187.8	782.50	533.66	702.54	1.19
83.0	3.1060	1.6960	2.1966	0.0265	1.8216	193.2	805.00	538.63	718.75	1.25
84.0	3.2250	1.7579	2.2186	0.0252	1.8254	198.6	827.50	536.31	734.14	1.24
85.0	3.3440	1.8226	2.2505	0.0241	1.8261	203.8	849.17	533.99	748.29	1.25
86.0	3.5030	1.9141	2.3484	0.0238	1.8217	209.0	870.83	535.90	762.44	1.29
87.0	3.6620	2.0058	2.4459	0.0235	1.8175	214.4	893.33	537.97	777.06	1.33
88.0	3.7910	2.0782	2.5004	0.0229	1.8163	219.8	915.83	536.97	791.50	1.36
89.0	3.9200	2.1492	2.5565	0.0223	1.8163	224.9	936.88	535.98	805.32	1.41
90.0	4.2570	2.3341	2.7718	0.0232	1.8160	229.9	957.92	538.63	820.23	1.56
91.0	4.5950	2.5215	2.9857	0.0238	1.8144	235.9	982.71	541.28	837.16	1.67
92.0	4.5650	2.5117	2.9686	0.0226	1.8100	241.8	1007.50	544.26	853.09	1.67
93.0	4.5350	2.5069	2.9585	0.0216	1.8019	247.6	1031.67	547.25	866.96	1.68
94.0	4.5750	2.5376	2.9613	0.0207	1.7961	253.4	1055.83	545.26	879.81	1.70
95.0	4.6150	2.5660	2.9655	0.0200	1.7920	258.8	1078.12	543.27	891.91	1.74
96.0	4.6150	2.5804	2.9910	0.0195	1.7822	264.1	1100.42	547.91	903.59	1.79
97.0	4.6150	2.6049	3.0231	0.0188	1.7655	271.0	1129.17	552.55	915.83	1.83
98.0	4.7140	2.6771	3.0932	0.0185	1.7548	277.9	1157.92	553.87	929.12	1.90
99.0	4.8130	2.7512	3.1641	0.0181	1.7435	285.5	1189.58	555.20	943.42	1.97
100.0	4.8520	2.7891	3.1909	0.0175	1.7340	293.1	1221.25	555.86	957.82	2.01

TIME	Qhw	------- CORRECTED ------- Qcw	Hcw	Clm	Hr	Tr	Tw2	Tw1	Hr/Hc
101.0	4.8920	2.8238	0.0170	1.7260	300.0	1250.21	556.53	971.55	2.07
102.0	4.9020	2.8435	0.0164	1.7188	307.0	1279.17	557.52	984.47	2.13
103.0	4.9120	2.8678	0.0159	1.7078	314.7	1311.25	558.51	996.99	2.18
104.0	4.8030	2.8263	0.0151	1.6946	322.4	1343.33	561.83	1008.60	2.21
105.0	4.6940	2.7816	0.0144	1.6829	329.3	1372.08	565.14	1018.71	2.25
106.0	4.5250	2.7002	0.0135	1.6716	336.2	1400.83	564.81	1026.90	2.27
107.0	4.3560	2.6272	0.0126	1.6540	344.7	1436.25	564.48	1033.76	2.24
108.0	4.2270	2.5752	0.0118	1.6377	353.2	1471.67	563.48	1040.15	2.22
109.0	4.0980	2.5166	0.0112	1.6249	360.5	1502.29	562.49	1045.85	2.23
110.0	4.1180	2.5473	0.0109	1.6132	367.9	1532.92	562.16	1052.08	2.32
111.0	4.1380	2.5756	0.0107	1.6033	375.4	1564.17	561.83	1059.50	2.41
112.0	3.8700	2.4299	0.0098	1.5896	382.9	1595.42	564.81	1064.95	2.36
113.0	3.6020	2.2762	0.0091	1.5797	387.1	1612.92	567.79	1066.43	2.32
114.0	3.4930	2.2204	0.0087	1.5705	391.3	1630.42	566.80	1066.21	2.38
115.0	3.3840	2.1667	0.0083	1.5593	396.6	1652.50	565.80	1066.03	2.40
116.0	3.3840	2.1801	0.0082	1.5497	401.9	1674.58	564.81	1066.94	2.51
117.0	3.3840	2.1813	0.0081	1.5489	403.5	1681.25	563.82	1068.67	2.71
118.0	3.2650	2.1093	0.0078	1.5455	405.1	1687.92	565.14	1069.25	2.86
119.0	3.1460	2.0398	0.0075	1.5400	406.9	1695.42	566.47	1068.23	2.92
120.0	3.1160	2.0236	0.0074	1.5376	408.7	1702.92	562.16	1066.89	3.06
121.0	3.0860	2.0098	0.0072	1.5333	411.8	1715.62	557.85	1066.01	3.14
122.0	2.9870	1.9571	0.0070	1.5242	414.8	1728.33	561.83	1065.06	3.20
123.0	2.8880	1.8997	0.0068	1.5182	415.8	1732.50	565.80	1063.41	3.31
124.0	2.7590	1.8195	0.0065	1.5145	416.8	1736.67	563.82	1060.43	3.37
125.0	2.6300	1.7413	0.0061	1.5085	418.3	1742.92	561.83	1056.15	3.44
126.0	1.8450	1.2348	0.0043	1.4929	419.8	1749.17	561.16	1043.12	2.62
127.0	1.0610	0.7229	0.0025	1.4670	419.5	1747.92	560.50	1016.85	1.64
128.0	1.0020	0.6960	0.0024	1.4390	419.2	1746.67	560.50	989.08	1.69
129.0	0.9420	0.6665	0.0023	1.4127	422.0	1758.13	560.50	967.28	1.75

STS 29 7700 MISMATCH CORRECTION

TIME	Qlm	CORRECTED Qlm	CORRECTED Qcw	CORRECTED Hcw	Ctm	Hr	Tr	Tw2	Tw1	Hi/Ho
50.0	0.4707	0.5988	3.2464	0.1561	0.7807	131.2	546.67	530.68	526.83	2.85
51.0	0.4707	0.2764	0.7923	0.0379	1.6954	131.3	547.17	516.76	539.98	0.69
52.0	0.3714	0.2235	0.9059	0.0431	1.6522	131.4	547.67	526.04	541.53	0.79
53.0	0.2919	0.1743	0.6552	0.0310	1.6679	131.6	548.17	524.71	541.93	0.57
54.0	0.3515	0.2075	0.6915	0.0325	1.6873	131.7	548.67	522.06	542.14	0.61
55.0	0.3118	0.1933	0.9669	0.0452	1.6131	131.8	549.17	531.34	543.34	0.85
56.0	0.3515	0.2069	0.8386	0.0391	1.6913	131.9	549.42	527.36	544.11	0.74
57.0	0.3118	0.1815	0.6040	0.0281	1.7125	131.9	549.67	522.72	543.81	0.54
58.0	0.3515	0.2059	0.6979	0.0323	1.7010	132.0	549.92	523.39	543.81	0.62
59.0	0.3913	0.2231	0.5477	0.0253	1.7501	132.0	550.17	513.44	543.69	0.49
60.0	0.2324	0.1349	0.3358	0.0155	1.7206	132.1	550.42	514.11	542.84	0.30
61.0	0.1728	0.1060	0.2974	0.0134	1.6263	132.6	552.33	519.41	542.06	0.27
62.0	0.2522	0.1582	0.4632	0.0205	1.5889	133.0	554.25	522.06	542.88	0.41
63.0	0.3714	0.2317	0.7560	0.0328	1.5949	133.5	556.17	526.70	545.95	0.67
64.0	0.3714	0.2243	0.6465	0.0275	1.6495	133.9	558.08	524.05	548.33	0.56
65.0	0.3913	0.2349	0.6300	0.0263	1.6603	134.4	560.00	522.72	549.76	0.55
66.0	0.2919	0.1784	0.4005	0.0159	1.6322	135.5	564.75	518.08	550.49	0.34
67.0	0.4509	0.2775	0.5762	0.0219	1.6194	136.7	569.50	516.76	552.64	0.47
68.0	0.4707	0.2891	0.5680	0.0207	1.6233	137.8	574.25	516.10	555.91	0.45
69.0	0.6694	0.4149	0.9441	0.0331	1.6052	139.0	579.00	526.70	561.46	0.74
70.0	0.6694	0.4054	0.8496	0.0286	1.6450	140.1	583.75	524.71	566.53	0.65
71.0	0.6296	0.3863	0.6961	0.0217	1.6247	142.4	593.50	519.41	570.24	0.50
72.0	0.8280	0.5085	0.8358	0.0243	1.6227	144.8	603.25	516.10	575.70	0.58
73.0	0.7289	0.4558	0.7725	0.0210	1.5940	147.1	613.00	522.72	581.62	0.51
74.0	0.9870	0.6156	1.0359	0.0265	1.5970	149.5	622.75	526.04	589.45	0.66
75.0	1.2060	0.7379	1.1737	0.0284	1.6280	151.8	632.50	524.05	598.85	0.73
76.0	1.1660	0.7225	1.0984	0.0242	1.6083	155.8	649.08	524.71	607.80	0.64
77.0	1.3050	0.8210	1.2888	0.0261	1.5833	159.8	665.67	534.65	618.58	0.72
78.0	1.3250	0.8272	1.1869	0.0223	1.5967	163.7	682.25	527.36	628.87	0.64
79.0	1.5430	0.9666	1.3783	0.0240	1.5907	167.7	698.83	531.34	640.01	0.71
80.0	1.4440	0.9052	1.2425	0.0203	1.5907	171.7	715.42	529.35	650.06	0.62
81.0	1.6820	1.0636	1.4543	0.0220	1.5763	176.5	735.42	533.99	661.48	0.70
82.0	1.8210	1.1494	1.5334	0.0216	1.5795	181.3	755.42	533.99	674.91	0.72
83.0	1.7620	1.1118	1.4168	0.0187	1.5806	186.2	776.04	528.03	686.19	0.65
84.0	2.0600	1.2974	1.5944	0.0197	1.5835	191.2	796.67	522.72	698.28	0.72
85.0	2.0000	1.2688	1.5657	0.0182	1.5723	196.5	818.75	528.03	710.78	0.69
86.0	1.9800	1.2667	1.5608	0.0172	1.5593	201.8	840.83	533.33	722.22	0.68
87.0	2.1790	1.3959	1.7066	0.0177	1.5572	207.1	862.71	533.33	734.90	0.73
88.0	2.3580	1.5036	1.7838	0.0175	1.5645	212.3	884.58	526.70	748.58	0.76
89.0	2.4170	1.5507	1.8532	0.0172	1.5550	218.2	909.17	533.33	762.43	0.78
90.0	2.4770	1.6007	1.9453	0.0174	1.5438	224.1	933.75	543.93	776.76	0.81
91.0	2.5170	1.6245	1.9325	0.0162	1.5460	229.8	957.50	539.29	790.08	0.81
92.0	2.5170	1.6345	1.9541	0.0156	1.5367	235.5	981.25	545.26	802.26	0.82
93.0	2.7150	1.7560	2.0351	0.0156	1.5429	241.1	1004.38	534.65	814.73	0.87
94.0	2.6760	1.7352	1.9953	0.0146	1.5392	246.6	1027.50	533.99	826.26	0.87
95.0	2.7350	1.7887	2.0719	0.0145	1.5261	253.1	1054.58	541.28	837.89	0.90
96.0	2.9140	1.9091	2.1909	0.0147	1.5234	259.6	1081.67	539.96	851.37	0.96
97.0	2.9140	1.9146	2.1807	0.0140	1.5192	266.4	1109.79	539.29	864.60	0.96
98.0	3.1130	2.0463	2.2996	0.0141	1.5184	273.1	1137.92	534.65	878.16	1.02
99.0	2.9340	1.9439	2.1984	0.0129	1.5068	280.2	1167.71	541.94	890.25	0.99
100.0	2.9540	1.9653	2.1977	0.0124	1.5006	287.4	1197.50	537.97	900.59	1.00

TIME	Qin	------- CORRECTED ------- Qcw	Hcw	Clm	Hr	Tr	T-2	T-1	Hi/Hc
101.0	3.0530	2.3097	0.0125	1.4890	294.5	1227.08	547.25	912.36	1.06
102.0	3.0530	2.0483	0.0119	1.4882	301.6	1256.67	539.29	929.95	1.07
103.0	2.9540	1.9979	0.0112	1.4764	308.9	1287.08	545.92	933.69	1.07
104.0	3.0530	2.0712	0.0111	1.4719	316.2	1317.50	541.28	943.60	1.12
105.0	2.9930	2.0431	0.0106	1.4629	323.5	1347.92	545.26	953.35	1.14
106.0	2.9930	2.0531	0.0103	1.4559	330.8	1378.33	545.26	962.38	1.18
107.0	3.0930	2.1241	0.0101	1.4542	338.4	1409.79	535.98	971.91	1.24
108.0	2.9340	2.0301	0.0094	1.4435	345.9	1441.25	541.94	980.03	1.24
109.0	3.1520	2.1870	0.0097	1.4395	353.8	1473.96	534.30	989.40	1.36
110.0	3.1130	2.1689	0.0093	1.4336	361.6	1506.67	538.63	999.66	1.40
111.0	3.1520	2.2081	0.0092	1.4258	369.5	1539.38	543.93	1009.47	1.48
112.0	3.1720	2.2253	0.0090	1.4238	377.3	1572.08	537.30	1018.97	1.54
113.0	3.2320	2.2755	0.0089	1.4188	384.3	1601.25	540.62	1028.43	1.64
114.0	2.9540	2.0910	0.0080	1.4113	391.3	1630.42	543.27	1034.35	1.58
115.0	2.8940	2.0557	0.0077	1.4064	396.6	1652.71	540.62	1037.03	1.61
116.0	2.9540	2.1078	0.0078	1.4001	402.0	1675.00	543.93	1040.95	1.73
117.0	2.7150	1.9433	0.0070	1.3959	406.5	1693.75	541.94	1042.79	1.77
118.0	2.5370	1.8284	0.0065	1.3865	411.0	1712.50	545.92	1041.07	1.90
119.0	2.4770	1.7912	0.0064	1.3818	413.0	1721.04	545.92	1038.71	1.85
120.0	2.3380	1.6960	0.0060	1.3775	415.1	1729.58	543.93	1035.50	1.74
121.0	1.8210	1.3322	0.0047	1.3661	417.1	1738.12	546.58	1025.75	1.45
122.0	1.3650	1.0083	0.0035	1.3532	419.2	1746.67	539.29	1007.60	1.17
123.0	1.2260	0.9168	0.0031	1.3367	420.9	1753.54	538.63	987.89	1.13
124.0	1.2650	0.9575	0.0033	1.3206	422.5	1760.42	545.26	973.16	1.27
125.0	1.1460	0.8731	0.0030	1.3120	424.0	1766.67	541.28	961.19	1.23
126.0	1.1460	0.8800	0.0030	1.3018	425.5	1772.92	543.27	950.80	1.32
127.0	1.4240	1.0924	0.0036	1.3029	427.5	1781.25	532.00	947.66	1.70
128.0	1.7820	1.3677	0.0046	1.3021	429.5	1789.58	540.62	955.08	2.26
129.0	0.8080	0.6222	0.0021	1.2983	431.5	1797.71	533.99	948.04	1.08

STS 29 7701 MISMATCH CORRECTION

TIME	Qhw	CORRECTED Qhw	CORRECTED Qcw	CORRECTED Hcw	Ctm	Hr	Ti	Tw2	Tw1	H1/H0
50.0	0.2775	0.4241	2.2990	0.1105	0.6474	131.2	546.67	530.60	525.31	2.22
51.0	0.2964	0.1758	0.5040	0.0241	1.6778	131.3	547.17	516.76	536.41	0.49
52.0	0.1451	0.0929	0.3767	0.0179	1.5549	131.4	547.67	526.04	537.48	0.36
53.0	0.1830	0.1140	0.4286	0.0203	1.5976	131.6	548.17	524.71	538.07	0.41
54.0	0.0884	0.0549	0.1830	0.0086	1.6072	131.7	548.67	522.06	537.46	0.18
55.0	0.0695	0.0526	0.2630	0.0123	1.3179	131.8	549.17	531.34	536.74	0.25
56.0	0.1830	0.1191	0.4828	0.0225	1.5281	131.9	549.42	527.36	538.47	0.47
57.0	0.1830	0.1103	0.3671	0.0171	1.6529	131.9	549.67	522.72	539.50	0.36
58.0	0.1073	0.0662	0.2242	0.0104	1.6184	132.0	549.92	523.39	539.03	0.22
59.0	0.1640	0.0956	0.2348	0.0108	1.7114	132.0	550.17	513.44	538.35	0.23
60.0	0.1640	0.0966	0.2406	0.0111	1.6937	132.1	550.42	514.11	538.13	0.24
61.0	0.3153	0.1890	0.5300	0.0239	1.6602	132.6	552.33	519.41	540.13	0.52
62.0	0.1451	0.0888	0.2601	0.0115	1.6295	133.0	554.25	522.06	541.38	0.25
63.0	0.0695	0.0465	0.1517	0.0066	1.4926	133.5	556.17	526.70	540.54	0.15
64.0	0.1830	0.1190	0.3430	0.0146	1.5321	133.9	558.08	524.05	541.32	0.33
65.0	0.5234	0.3119	0.8367	0.0349	1.6780	134.4	560.00	522.72	546.82	0.80
66.0	0.5423	0.3089	0.6934	0.0276	1.7470	135.5	564.75	518.08	551.32	0.64
67.0	0.4099	0.2363	0.4907	0.0187	1.7286	136.7	569.50	516.76	553.40	0.44
68.0	0.4666	0.2720	0.5343	0.0195	1.7095	137.8	574.25	516.10	555.44	0.47
69.0	0.3721	0.2276	0.5179	0.0181	1.6285	139.0	579.00	526.70	558.04	0.44
70.0	0.5045	0.3033	0.6357	0.0214	1.6563	140.1	583.75	524.71	561.66	0.53
71.0	0.7125	0.4220	0.7603	0.0237	1.6807	142.4	593.50	519.41	567.50	0.61
72.0	0.6747	0.3989	0.6558	0.0191	1.6850	144.8	603.25	516.10	573.02	0.50
73.0	0.8450	0.5055	0.8566	0.0233	1.6640	147.1	613.00	522.72	578.88	0.63
74.0	1.2040	0.7054	1.1870	0.0304	1.6973	149.5	622.75	526.04	590.34	0.84
75.0	1.2610	0.7251	1.1533	0.0279	1.7309	151.8	632.50	524.05	599.63	0.79
76.0	1.2800	0.7476	1.1366	0.0250	1.7044	155.8	649.08	524.71	608.24	0.73
77.0	1.3180	0.7853	1.2327	0.0250	1.6704	159.8	665.67	534.65	618.40	0.76
78.0	1.7150	1.0034	1.4398	0.0270	1.7010	163.7	682.25	527.36	630.89	0.85
79.0	1.7530	1.0261	1.4632	0.0255	1.7008	167.7	698.83	531.34	643.26	0.83
80.0	1.7720	1.0369	1.4234	0.0232	1.7020	171.7	715.42	529.35	653.90	0.79
81.0	1.8280	1.0829	1.4807	0.0224	1.6813	176.5	735.42	533.99	664.84	0.79
82.0	1.9610	1.1647	1.5539	0.0219	1.6772	181.3	755.42	533.99	676.96	0.80
83.0	2.3010	1.3573	1.7296	0.0228	1.6887	186.2	776.04	528.03	690.88	0.87
84.0	2.3770	1.3970	1.7169	0.0212	1.6955	191.2	796.67	522.72	704.38	0.85
85.0	2.5660	1.5160	1.8707	0.0217	1.6865	196.5	818.75	528.03	718.33	0.91
86.0	2.6420	1.5665	1.9400	0.0212	1.6806	201.8	840.83	533.33	732.89	0.93
87.0	2.5850	1.5374	1.8796	0.0194	1.6760	207.1	862.71	533.33	745.64	0.89
88.0	2.6790	1.5941	1.8912	0.0186	1.6755	212.3	884.58	526.70	757.19	0.89
89.0	2.5470	1.5345	1.8339	0.0170	1.6551	218.2	909.17	533.33	768.07	0.85
90.0	2.5850	1.5772	1.9168	0.0169	1.6342	224.1	933.75	543.93	779.67	0.88
91.0	2.4900	1.5241	1.8131	0.0152	1.6295	229.8	957.50	539.29	790.30	0.84
92.0	2.2820	1.4153	1.6921	0.0135	1.6086	235.5	981.25	545.26	798.26	0.79
93.0	2.3960	1.4883	1.7249	0.0132	1.6062	241.1	1004.38	534.65	806.15	0.81
94.0	2.2630	1.4167	1.6292	0.0120	1.5940	246.6	1027.50	533.99	813.50	0.78
95.0	2.1120	1.3439	1.5567	0.0109	1.5686	253.1	1054.58	541.28	819.55	0.75
96.0	2.0360	1.3094	1.5027	0.0101	1.5521	259.6	1081.67	539.96	825.12	0.73
97.0	2.2250	1.4414	1.6418	0.0105	1.5407	266.4	1109.79	539.29	833.40	0.80
98.0	1.9610	1.2708	1.4371	0.0088	1.5310	273.1	1137.92	534.65	840.08	0.71
99.0	1.8850	1.2491	1.4126	0.0083	1.5068	280.2	1167.71	541.94	844.34	0.70
100.0	1.7340	1.1605	1.2977	0.0073	1.4922	287.4	1197.50	537.97	847.40	0.65

TIME	Qin	CORRECTED Qcw	CORRECTED Hcw	C1m	Hr	Tr	T+2	T+1	Hi/Hc
101.0	1.6390	1.1161	0.0068	1.4666	294.5	1227.00	547.25	849.71	0.64
102.0	1.8850	1.2840	0.0075	1.4629	301.6	1256.67	539.29	855.93	0.74
103.0	1.7720	1.2212	0.0069	1.4492	308.4	1287.08	545.92	863.35	0.71
104.0	1.6500	1.1494	0.0062	1.4409	316.2	1317.50	541.28	867.60	0.69
105.0	1.6500	1.1614	0.0060	1.4260	323.5	1347.92	545.26	871.28	0.72
106.0	1.4880	1.0521	0.0053	1.4136	330.8	1378.33	545.26	873.28	0.67
107.0	1.6770	1.1887	0.0057	1.4093	338.4	1409.79	535.98	877.02	0.77
108.0	1.5450	1.1057	0.0051	1.3960	345.9	1441.25	541.94	881.48	0.75
109.0	1.6390	1.1776	0.0052	1.3905	353.8	1473.96	537.30	886.08	0.82
110.0	1.4690	1.0638	0.0046	1.3798	361.6	1506.67	538.63	889.21	0.76
111.0	1.3560	0.9937	0.0042	1.3637	369.5	1539.38	543.93	889.08	0.74
112.0	1.4880	1.0944	0.0044	1.3586	377.3	1572.08	537.30	891.13	0.84
113.0	1.2990	0.9632	0.0038	1.3477	384.3	1601.25	540.62	892.28	0.77
114.0	1.1290	0.8463	0.0032	1.3333	391.3	1630.42	543.27	888.71	0.71
115.0	1.2800	0.9639	0.0036	1.3271	396.6	1652.71	540.62	887.47	0.84
116.0	1.0530	0.7994	0.0029	1.3166	402.0	1675.00	543.93	885.35	0.73
117.0	1.0340	0.7899	0.0029	1.3085	406.5	1693.75	541.94	880.71	0.80
118.0	1.0720	0.8249	0.0029	1.2989	411.0	1712.50	545.92	878.44	0.96
119.0	1.0150	0.7833	0.0028	1.2952	413.0	1721.04	545.92	876.69	0.90
120.0	0.8830	0.6841	0.0024	1.2902	415.1	1729.58	543.93	872.01	0.78
121.0	0.7503	0.5863	0.0021	1.2793	417.1	1738.12	546.58	863.92	0.71
122.0	0.8260	0.6469	0.0022	1.2763	419.2	1746.67	539.29	857.40	0.84
123.0	0.4666	0.3687	0.0013	1.2654	420.9	1753.54	538.63	846.04	0.51
124.0	0.3910	0.3139	0.0011	1.2453	422.5	1760.42	545.26	829.41	0.47
125.0	0.3532	0.2863	0.0010	1.2337	424.0	1766.67	541.28	814.29	0.45
126.0	0.3910	0.3052	0.0010	1.2211	425.5	1772.92	543.27	802.54	0.54
127.0	1.1100	0.3418	0.0011	1.2346	427.5	1781.25	532.00	811.44	1.57
128.0	0.9580	0.8987	0.0030	1.2409	429.5	1789.58	540.62	827.48	1.43
129.0	0.6936	0.9505	0.0026	1.2454	431.5	1797.71	533.99	829.69	1.08
		0.8215	0.0018						
		0.7717							
		0.5568							
		0.5894							

STS 29 7702 MISMATCH CORRECTION

TIME	------- CORRECTED ------- Qlw	Qcw	Ctm	Hi	Ti	Tw2	Tw1	Hi/Ho
50.0	0.0000	0.0000	1.1499	131.2	546.67	518.00	521.61	0.00
51.0	0.0000	0.0000	0.9907	131.3	547.17	520.74	520.54	0.00
52.0	0.0000	0.0000	1.1377	131.4	547.67	516.10	519.68	0.00
53.0	0.0000	0.0000	0.7440	131.6	548.17	524.05	518.97	0.00
54.0	0.0000	0.0000	0.7589	131.7	548.67	523.39	518.37	0.00
55.0	0.0000	0.0000	1.1301	131.8	549.17	514.11	517.86	0.00
56.0	0.0000	0.0000	0.7586	131.9	549.42	522.72	517.42	0.00
57.0	0.0000	0.0000	0.7430	131.9	549.67	522.72	517.02	0.00
58.0	0.0000	0.0000	1.0867	132.0	549.92	514.11	516.67	0.00
59.0	0.0000	0.0000	0.9602	132.0	550.17	517.42	516.35	0.00
60.0	0.0000	0.0000	1.0651	132.1	550.42	514.11	516.05	0.00
61.0	0.0000	0.0000	1.0329	132.6	552.33	514.77	515.79	0.00
62.0	0.0000	0.0000	1.0434	133.0	554.25	514.11	515.54	0.00
63.0	0.0000	0.0000	0.8805	133.5	556.17	518.75	515.32	0.00
64.0	0.0000	0.0000	1.1695	133.9	558.08	508.14	515.11	0.00
65.0	0.0000	0.0000	1.0549	134.4	560.00	512.78	514.91	0.00
66.0	0.0000	0.0000	0.9991	135.5	564.75	514.77	514.73	0.00
67.0	0.0000	0.0000	0.9954	136.7	569.50	514.77	514.57	0.00
68.0	0.0000	0.0000	0.8040	137.8	574.25	522.72	514.41	0.00
69.0	0.0000	0.0000	0.8951	139.0	579.00	519.41	514.26	0.00
70.0	0.0000	0.0000	1.0231	140.1	583.75	512.78	514.13	0.00
71.0	0.0000	0.0000	1.0585	142.4	593.50	510.79	514.77	0.06
72.0	0.0000	0.0021	1.0078	144.6	603.25	510.79	518.99	0.07
73.0	0.0432	0.0026	1.0328	147.1	613.00	516.76	519.36	0.00
74.0	0.0630	0.0000	1.0456	149.5	622.75	519.41	523.29	0.14
75.0	0.0000	0.0047	1.0997	151.8	632.50	522.72	531.72	0.13
76.0	0.1225	0.0042	1.2178	155.8	649.08	518.08	541.57	0.20
77.0	0.1225	0.0063	1.2643	159.8	665.67	525.38	555.90	0.30
78.0	0.2414	0.0089	1.3534	163.7	682.25	517.42	565.36	0.18
79.0	0.3802	0.0052	1.3376	167.7	698.83	524.71	573.09	0.25
80.0	0.2810	0.0068	1.3398	171.7	715.42	524.05	577.58	0.14
81.0	0.3802	0.0036	1.3638	176.5	735.42	522.06	585.95	0.29
82.0	0.2216	0.0074	1.4030	181.3	755.42	525.38	601.67	0.36
83.0	0.5189	0.0087	1.6076	186.2	776.04	523.39	649.74	1.22
84.0	0.6775	0.0286	1.7501	191.2	796.67	527.36	693.61	1.29
85.0	2.7880	0.0289	1.8109	196.5	818.75	513.44	717.22	1.15
86.0	3.2740	0.0247	1.8073	201.8	840.83	523.39	734.32	1.19
87.0	3.2940	0.0244	1.8087	207.1	862.71	532.00	752.11	1.30
88.0	3.3730	0.0254	1.8206	212.3	884.58	525.38	767.97	1.25
89.0	3.6710	0.0236	1.8122	218.2	909.17	525.38	781.94	1.24
90.0	3.7150	0.0222	1.7826	224.1	933.75	-527.36	789.11	0.93
91.0	3.7300	0.0159	1.7827	229.8	957.50	530.01	805.39	1.44
92.0	2.7790	0.0235	1.7827	235.5	981.25	532.00	827.10	1.47
93.0	4.3250	0.0226	1.7981	241.1	1004.38	532.00	845.32	1.56
94.0	4.4040	0.0227	1.8059	246.6	1027.50	531.34	861.76	1.62
95.0	4.6770	0.0222	1.8091	253.1	1054.58	529.35	877.06	1.65
96.0	4.8000	0.0215	1.8044	259.6	1081.67	537.30	893.53	1.76
97.0	4.9000	0.0218	1.7951	266.4	1109.79	541.28	908.38	1.70
98.0	5.1370	0.0201	1.7846	273.1	1137.92	533.99	922.19	1.76
99.0	4.9000	0.0197	1.7810	280.2	1167.71	539.29	936.61	1.80
100.0	5.1030	0.0191	1.7682	287.4	1197.50	545.26	952.43	1.92
	5.1180	0.0193	1.7585					
	5.3360							

TIME	Qhw	CORRECTED Qcw	CORRECTED Hcw	Clm	Hi	Ti	Tw2	Tw1	Hi/Hc
101.0	5.1570	2.9242	3.2302	0.0175	1.7580	294.5	1227.08	532.67	965.88	1.84
102.0	5.2560	3.0146	3.3981	0.0178	1.7378	301.6	1256.67	549.90	979.10	1.98
103.0	5.0880	2.9312	3.2710	0.0165	1.7306	308.9	1287.08	545.92	991.59	1.94
104.0	5.2560	3.0377	3.3444	0.0163	1.7251	316.2	1317.50	538.63	1003.47	2.04
105.0	4.9990	2.9172	3.2351	0.0152	1.7088	323.5	1347.92	547.25	1014.37	2.02
106.0	4.8400	2.8526	3.1774	0.0144	1.6922	330.6	1378.33	553.87	1023.55	2.05
107.0	4.9390	2.9242	3.2199	0.0141	1.6846	338.4	1409.79	547.25	1033.26	2.15
108.0	4.5820	2.7440	3.0434	0.0129	1.6658	345.9	1441.25	556.53	1041.31	2.11
109.0	4.6420	2.8044	3.1061	0.0128	1.6513	353.8	1473.96	558.51	1049.22	2.23
110.0	4.6810	2.8378	3.1045	0.0124	1.6457	361.6	1506.67	549.90	1058.33	2.31
111.0	4.5820	2.8010	3.0699	0.0119	1.6322	369.5	1539.38	554.54	1066.95	2.37
112.0	4.5820	2.8165	3.0702	0.0115	1.6233	377.3	1572.08	551.89	1075.26	2.47
113.0	4.3990	2.7337	2.9844	0.0109	1.6092	384.3	1601.25	555.86	1080.00	2.50
114.0	4.4830	2.8108	3.0502	0.0109	1.5949	391.3	1630.42	551.89	1080.00	2.67
115.0	4.2650	2.7016	2.9467	0.0103	1.5787	396.6	1652.71	559.18	1080.00	2.69
116.0	4.2260	2.6960	2.9339	0.0101	1.5675	402.0	1675.00	558.51	1080.00	2.80
117.0	4.0080	2.5698	2.7863	0.0094	1.5597	406.5	1693.75	555.86	1080.00	2.98
118.0	3.7890	2.4503	2.6702	0.0089	1.5464	411.0	1712.50	563.15	1080.00	3.26
119.0	3.6900	2.3979	2.6250	0.0087	1.5389	413.0	1721.04	569.12	1080.00	3.18
120.0	3.6310	2.3556	2.5523	0.0084	1.5414	415.1	1729.58	557.85	1080.00	3.07
121.0	3.5910	2.3379	2.5374	0.0083	1.5360	417.1	1738.12	560.50	1080.00	3.25
122.0	3.3340	2.1739	2.3528	0.0076	1.5337	419.2	1746.67	557.85	1080.00	3.22
123.0	3.2790	2.1471	2.3345	0.0075	1.5271	420.9	1753.54	563.82	1080.00	3.41
124.0	3.1950	2.0968	2.2800	0.0073	1.5237	422.5	1760.42	564.48	1080.00	3.57
125.0	3.0560	2.0062	2.1733	0.0069	1.5222	424.0	1766.67	560.50	1078.86	3.62
126.0	2.9570	1.9372	2.0728	0.0066	1.5245	425.5	1772.92	545.92	1075.58	3.70
127.0	0.9550	0.6417	0.6938	0.0022	1.4876	427.5	1781.25	559.18	1048.59	1.30
128.0	0.8509	0.5082	0.6356	0.0020	1.4460	429.5	1789.58	559.18	1010.84	1.25
129.0	0.7171	0.5068	0.5459	0.0017	1.4145	431.5	1797.71	555.86	979.55	1.14

APPENDIX II

FLIGHT HEATING DATA FOR B07R7703–B07R7707 FOR STS-26R, STS-27R AND STS-29R

FLIGHT STS-26

GAGE NO. 7703		BIAS 0.25	XB LOCATION 109.700		
TIME	QDOT FLT	HC	HREC	HUND	HIHU
10.0	0.2500E+00	0.8405E-03			
15.0	0.2500E+00	0.8405E-03			
20.0	0.2500E+00	0.8405E-03			
25.0	0.2500E+00	0.8405E-03			
30.0	0.5000E-01	0.4673E-01	130.91		
35.0	0.5000E-01	0.3049E-01	131.48		
40.0	0.5000E-01	0.2392E-01	131.93		
45.0	0.5000E-01	0.2632E-01	131.74		
50.0	0.5000E-01	0.2941E-01	131.54		
55.0	0.5000E-01	0.4545E-01	130.94		
60.0	0.5000E-01	0.6098E-01	130.66		
62.0	0.2500E+00	0.1799E+00	131.23		
64.0	0.5000E-01	0.1818E-01	132.59		
66.0	0.3920E+00	0.7967E-01	134.76	0.3121E+00	0.26
68.0	0.4780E+00	0.6719E-01	137.29	0.5439E-01	1.24
70.0	0.7720E+00	0.8010E-01	140.15	0.3465E-01	2.31
72.0	0.7030E+00	0.5053E-01	144.76	0.2569E-01	1.97
74.0	0.6330E+00	0.3375E-01	149.94	0.2089E-01	1.62
76.0	0.1069E+01	0.4091E-01	157.65	0.1749E-01	2.34
78.0	0.1086E+01	0.3231E-01	165.47	0.1449E-01	2.23
80.0	0.1367E+01	0.3191E-01	175.03	0.1235E-01	2.58
82.0	0.1509E+01	0.2889E-01	184.76	0.1064E-01	2.72
84.0	0.1704E+01	0.2749E-01	194.84	0.9238E-02	2.98
86.0	0.1954E+01	0.2667E-01	206.47	0.8046E-02	3.31
88.0	0.2098E+01	0.2520E-01	216.78	0.6990E-02	3.61
90.0	0.2152E+01	0.2267E-01	228.82	0.6085E-02	3.72
92.0	0.2568E+01	0.2408E-01	240.87	0.5283E-02	4.56
94.0	0.2459E+01	0.2084E-01	252.56	0.4573E-02	4.56
96.0	0.2750E+01	0.2117E-01	264.81	0.3960E-02	5.34
98.0	0.2915E+01	0.2043E-01	277.88	0.3408E-02	6.00
100.0	0.3025E+01	0.1930E-01	292.31	0.2941E-02	6.56
102.0	0.3376E+01	0.1980E-01	306.43	0.2526E-02	7.84
104.0	0.3191E+01	0.1721E-01	321.64	0.2168E-02	7.94
106.0	0.3524E+01	0.1781E-01	334.43	0.1856E-02	9.60
108.0	0.3320E+01	0.1538E-01	352.46	0.1599E-02	9.62
110.0	0.3339E+01	0.1448E-01	367.22	0.1363E-02	10.62
112.0	0.3543E+01	0.1453E-01	380.45	0.1167E-02	12.45
114.0	0.3636E+01	0.1422E-01	392.33	0.9992E-03	14.23
116.0	0.3117E+01	0.1176E-01	401.64	0.8698E-03	13.52
118.0	0.3117E+01	0.1157E-01	405.92	0.7432E-03	15.57
120.0	0.2805E+01	0.1044E-01	405.25	0.6421E-03	16.26
122.0	0.2550E+01	0.9208E-02	413.48	0.5678E-03	16.22
124.0	0.1882E+01	0.6746E-02	415.52	0.4921E-03	13.71
126.0	0.1686E+01	0.5904E-02	422.11	0.4266E-03	13.84

FLIGHT STS-26

GAGE NO. 7704		BIAS 0.30		XB LOCATION	109.800
TIME	QDOT FLT	HC	HREC	HUND	HIHU
10.0	0.8100E-01	0.2771E-03			
15.0	0.3000E+00	0.1026E-02			
20.0	0.8100E-01	0.2771E-03			
25.0	0.3000E+00	0.1026E-02			
30.0	0.8100E-01	0.7570E-01	130.91		
35.0	0.1000E+00	0.6135E-01	131.47		
40.0	0.2160E+00	0.1038E+00	131.92		
45.0	0.2160E+00	0.1143E+00	131.73		
50.0	0.2540E+00	0.1568E+00	131.46		
55.0	0.2160E+00	0.2160E+00	130.84		
60.0	0.3310E+00	0.4413E+00	130.59		
62.0	0.2350E+00	0.1808E+00	131.14		
64.0	0.3120E+00	0.1177E+00	132.49		
66.0	0.6010E+00	0.1247E+00	134.66	0.4175E+00	0.30
68.0	0.5430E+00	0.7720E-01	137.21	0.5445E-01	1.42
70.0	0.7170E+00	0.7470E-01	140.11	0.3446E-01	2.17
72.0	0.7940E+00	0.5720E-01	144.73	0.2553E-01	2.24
74.0	0.8130E+00	0.4337E-01	149.93	0.2081E-01	2.08
76.0	0.1160E+01	0.4443E-01	157.63	0.1740E-01	2.55
78.0	0.1238E+01	0.3684E-01	165.46	0.1446E-01	2.55
80.0	0.1855E+01	0.4329E-01	175.04	0.1238E-01	3.50
82.0	0.1893E+01	0.3624E-01	184.77	0.1065E-01	3.40
84.0	0.1951E+01	0.3148E-01	194.84	0.9240E-02	3.41
86.0	0.2414E+01	0.3295E-01	206.47	0.8048E-02	4.09
88.0	0.2587E+01	0.3108E-01	216.78	0.6991E-02	4.45
90.0	0.2722E+01	0.2867E-01	228.82	0.6087E-02	4.71
92.0	0.3127E+01	0.2931E-01	240.88	0.5285E-02	5.55
94.0	0.3012E+01	0.2552E-01	252.57	0.4574E-02	5.58
96.0	0.3204E+01	0.2465E-01	264.84	0.3974E-02	6.20
98.0	0.3455E+01	0.2421E-01	277.92	0.3425E-02	7.07
100.0	0.3301E+01	0.2106E-01	292.31	0.2942E-02	7.16
102.0	0.3571E+01	0.2094E-01	306.43	0.2527E-02	8.29
104.0	0.3417E+01	0.1843E-01	321.65	0.2170E-02	8.49
106.0	0.3725E+01	0.1882E-01	334.46	0.1861E-02	10.11
108.0	0.3764E+01	0.1743E-01	352.46	0.1599E-02	10.90
110.0	0.3860E+01	0.1673E-01	367.23	0.1363E-02	12.28
112.0	0.3783E+01	0.1551E-01	380.45	0.1168E-02	13.28
114.0	0.3764E+01	0.1472E-01	392.35	0.1001E-02	14.70
116.0	0.3455E+01	0.1303E-01	401.69	0.8743E-03	14.90
118.0	0.3359E+01	0.1247E-01	405.89	0.7404E-03	16.84
120.0	0.2973E+01	0.1107E-01	405.12	0.6337E-03	17.47
122.0	0.2819E+01	0.1019E-01	413.27	0.5564E-03	18.31
124.0	0.2375E+01	0.8518E-02	415.38	0.4850E-03	17.56
126.0	0.1835E+01	0.6427E-02	422.06	0.4245E-03	15.14

FLIGHT STS-26

GAGE NO.	7705	BIAS 0.30	XB LOCATION		141.200
TIME	QDOT FLT	HC	HREC	HUND	HIHU
10.0	0.1800E-01	0.6045E-04			
15.0	0.1800E-01	0.6045E-04			
20.0	0.3000E+00	0.1007E-02			
25.0	0.1650E+00		129.82		
30.0	0.1160E+00	0.9748E-01	131.03		
35.0	0.2390E+00	0.1320E+00	131.65		
40.0	0.6700E-01	0.2900E-01	132.15		
45.0	0.1650E+00	0.7569E-01	132.02		
50.0	0.1400E+00	0.5072E-01	132.60		
55.0	0.1160E+00	0.5743E-01	131.86		
60.0	0.1400E+00	0.7650E-01	131.67		
62.0	0.9100E-01	0.3808E-01	132.23		
64.0	0.2140E+00	0.5646E-01	133.63		
66.0	0.1160E+00	0.1914E-01	135.90	0.1101E+00	0.17
68.0	0.1650E+00	0.1892E-01	138.56	0.5252E-01	0.36
70.0	0.4600E+00	0.3928E-01	141.55	0.3813E-01	1.03
72.0	0.3620E+00	0.2205E-01	146.26	0.3046E-01	0.72
74.0	0.2880E+00	0.1324E-01	151.59	0.2606E-01	0.51
76.0	0.5340E+00	0.1801E-01	159.49	0.2297E-01	0.78
78.0	0.7320E+00	0.1986E-01	167.45	0.2052E-01	0.97
80.0	0.7570E+00	0.1651E-01	177.19	0.1846E-01	0.89
82.0	0.8320E+00	0.1511E-01	187.17	0.1668E-01	0.91
84.0	0.1030E+01	0.1594E-01	197.46	0.1507E-01	1.06
86.0	0.1305E+01	0.1727E-01	209.19	0.1363E-01	1.27
88.0	0.1180E+01	0.1384E-01	219.63	0.1223E-01	1.13
90.0	0.1155E+01	0.1195E-01	231.75	0.1095E-01	1.09
92.0	0.1430E+01	0.1323E-01	243.97	0.9846E-02	1.34
94.0	0.2084E+01	0.1748E-01	255.86	0.8787E-02	1.99
96.0	0.1908E+01	0.1457E-01	268.28	0.7827E-02	1.86
98.0	0.2490E+01	0.1736E-01	281.59	0.6937E-02	2.50
100.0	0.2186E+01	0.1389E-01	296.24	0.6149E-02	2.26
102.0	0.3000E+00	0.1755E-02	310.60	0.5396E-02	0.33
104.0	0.1983E+01	0.1068E-01	326.02	0.4739E-02	2.25
106.0	0.1706E+01	0.8622E-02	338.99	0.4119E-02	2.09
108.0	0.1832E+01	0.8508E-02	357.22	0.3638E-02	2.34
110.0	0.1857E+01	0.8089E-02	372.21	0.3178E-02	2.55
112.0	0.1430E+01	0.5903E-02	385.62	0.2763E-02	2.14
114.0	0.1305E+01	0.5148E-02	397.66	0.2376E-02	2.17
116.0	0.1030E+01	0.3930E-02	406.97	0.2056E-02	1.91
118.0	0.9560E+00	0.3598E-02	411.33	0.1761E-02	2.04
120.0	0.1130E+01	0.4277E-02	410.58	0.1503E-02	2.85
122.0	0.9810E+00	0.3603E-02	418.70	0.1308E-02	2.75
124.0	0.5340E+00	0.1946E-02	420.75	0.1128E-02	1.73
126.0	0.3120E+00	0.1110E-02	427.48	0.9883E-03	1.12

FLIGHT STS-26

GAGE NO. 7706		BIAS 0.25	XB LOCATION 141.300		
TIME	QDOT FLT	HC	HREC	HUND	HIHU
10.0	0.1560E+00	0.5241E-03			
15.0	0.1800E+00	0.6048E-03			
20.0	0.3190E+00	0.1072E-02			
25.0	0.1100E+00	-.5503E+01	129.82		
30.0	0.1330E+00	0.1118E+00	131.03		
35.0	0.2030E+00	0.1122E+00	131.65		
40.0	0.1100E+00	0.4762E-01	132.15		
45.0	0.1700E-01	0.7798E-02	132.02		
50.0	0.2960E+00	0.1069E+00	132.61		
55.0	0.4000E-01	0.1980E-01	131.86		
60.0	0.1700E-01	0.9239E-02	131.68		
62.0	0.1100E+00	0.4564E-01	132.25		
64.0	0.1100E+00	0.2895E-01	133.64		
66.0	0.2260E+00	0.3723E-01	135.91	0.1093E+00	0.34
68.0	0.4000E-01	0.4577E-02	138.58	0.5238E-01	0.09
70.0	0.3660E+00	0.3123E-01	141.56	0.3804E-01	0.82
72.0	0.3660E+00	0.2226E-01	146.28	0.3037E-01	0.73
74.0	0.3430E+00	0.1576E-01	151.61	0.2597E-01	0.61
76.0	0.7180E+00	0.2423E-01	159.47	0.2304E-01	1.05
78.0	0.9770E+00	0.2652E-01	167.43	0.2062E-01	1.29
80.0	0.1001E+01	0.2186E-01	177.13	0.1861E-01	1.17
82.0	0.1286E+01	0.2341E-01	187.03	0.1678E-01	1.40
84.0	0.1286E+01	0.1997E-01	197.25	0.1514E-01	1.32
86.0	0.1405E+01	0.1862E-01	209.04	0.1373E-01	1.36
88.0	0.1476E+01	0.1734E-01	219.48	0.1232E-01	1.41
90.0	0.1548E+01	0.1604E-01	231.64	0.1104E-01	1.45
92.0	0.1644E+01	0.1522E-01	243.86	0.9950E-02	1.53
94.0	0.1668E+01	0.1400E-01	255.74	0.8886E-02	1.58
96.0	0.1524E+01	0.1165E-01	268.16	0.7925E-02	1.47
98.0	0.1787E+01	0.1247E-01	281.44	0.7022E-02	1.78
100.0	0.1452E+01	0.9237E-02	296.07	0.6233E-02	1.48
102.0	0.1429E+01	0.8368E-02	310.40	0.5479E-02	1.53
104.0	0.1452E+01	0.7831E-02	325.79	0.4846E-02	1.62
106.0	0.1333E+01	0.6747E-02	338.71	0.4234E-02	1.59
108.0	0.1072E+01	0.4985E-02	356.91	0.3761E-02	1.33
110.0	0.1120E+01	0.4884E-02	371.95	0.3293E-02	1.48
112.0	0.1001E+01	0.4138E-02	385.32	0.2875E-02	1.44
114.0	0.6000E+00	0.2371E-02	397.22	0.2481E-02	0.96
116.0	0.6710E+00	0.2565E-02	406.54	0.2143E-02	1.20
118.0	0.5540E+00	0.2088E-02	410.93	0.1830E-02	1.14
120.0	0.4830E+00	0.1829E-02	410.44	0.1552E-02	1.18
122.0	0.4130E+00	0.1518E-02	418.54	0.1350E-02	1.12
124.0	0.2730E+00	0.9963E-03	420.42	0.1165E-02	0.86
126.0	0.6240E+00	0.2223E-02	427.16	0.1019E-02	2.18

FLIGHT STS-26

GAGE NO. 7707 BIAS 0.55 XB LOCATION 140.400

TIME	QDOT FLT	HC	HREC	HUND	HIHU
10.0					
15.0					
20.0					
25.0					
30.0					
35.0					
40.0					
45.0					
50.0					
55.0					
60.0					
62.0					
64.0					
66.0	0.2210E+00	0.3653E-01	135.89	0.1106E+00	0.33
68.0	0.2210E+00	0.2534E-01	138.56	0.5266E-01	0.48
70.0	0.1350E+00	0.1153E-01	141.55	0.3822E-01	0.30
72.0	0.2790E+00	0.1700E-01	146.25	0.3052E-01	0.56
74.0	0.3080E+00	0.1417E-01	151.58	0.2613E-01	0.54
76.0	0.5090E+00	0.1716E-01	159.50	0.2295E-01	0.75
78.0	0.7680E+00	0.2083E-01	167.47	0.2051E-01	1.02
80.0	0.1257E+01	0.2741E-01	177.21	0.1839E-01	1.49
82.0	0.1343E+01	0.2440E-01	187.14	0.1652E-01	1.48
84.0	0.1286E+01	0.1993E-01	197.37	0.1491E-01	1.34
86.0	0.1717E+01	0.2272E-01	209.16	0.1352E-01	1.68
88.0	0.1516E+01	0.1778E-01	219.60	0.1213E-01	1.47
90.0	0.1401E+01	0.1450E-01	231.75	0.1088E-01	1.33
92.0	0.1545E+01	0.1429E-01	243.99	0.9789E-02	1.46
94.0	0.1458E+01	0.1222E-01	255.88	0.8731E-02	1.40
96.0	0.1257E+01	0.9599E-02	268.32	0.7776E-02	1.23
98.0	0.1602E+01	0.1116E-01	281.61	0.6885E-02	1.62
100.0	0.1372E+01	0.8717E-02	296.27	0.6098E-02	1.43
102.0	0.1343E+01	0.7854E-02	310.63	0.5347E-02	1.47
104.0	0.1228E+01	0.6612E-02	326.11	0.4687E-02	1.41
106.0	0.1372E+01	0.6930E-02	339.11	0.4063E-02	1.71
108.0	0.1401E+01	0.6501E-02	357.38	0.3581E-02	1.82
110.0	0.1315E+01	0.5722E-02	372.44	0.3133E-02	1.83
112.0	0.1228E+01	0.5064E-02	385.90	0.2719E-02	1.86
114.0	0.9410E+00	0.3708E-02	397.89	0.2327E-02	1.59
116.0	0.7970E+00	0.3039E-02	407.18	0.2016E-02	1.51
118.0	0.7100E+00	0.2670E-02	411.52	0.1729E-02	1.54
120.0	0.7100E+00	0.2684E-02	410.89	0.1486E-02	1.81
122.0	0.3650E+00	0.1339E-02	418.99	0.1294E-02	1.03
124.0	0.4520E+00	0.1647E-02	420.92	0.1111E-02	1.48
126.0	0.6820E+00	0.2425E-02	427.63	0.9742E-03	2.49

FLIGHT STS-27

GAGE NO. 7703 BIAS 0.30 XB LOCATION 109.700

TIME	QDOT FLT	HC	HREC	HUND	HIHU
10.0	0.3000E+00	0.9231E-01	128.05	0.6003E-01	1.54
15.0	0.3000E+00	0.8929E-01	128.16	0.7936E-01	1.13
20.0	0.3000E+00	0.7500E-01	128.80	0.7353E-01	1.02
25.0	0.3000E+00	0.6024E-01	129.78	0.6564E-01	0.92
30.0	0.4700E-01	0.8530E-02	130.31	0.6344E-01	0.13
35.0	0.1520E+00	0.2269E-01	131.50	0.5799E-01	0.39
40.0	0.1740E+00	0.2597E-01	131.50	0.5633E-01	0.46
45.0	0.1520E+00	0.2346E-01	131.28	0.5478E-01	0.43
50.0	0.4700E-01	0.1022E-01	129.40	0.6706E-01	0.15
55.0	0.6800E-01	0.1667E-01	128.88	0.7165E-01	0.23
60.0	0.1310E+00	0.3475E-01	128.57	0.7259E-01	0.48
62.0	0.3000E+00	0.7317E-01	128.90	0.6037E-01	1.21
64.0	0.4700E-01	0.9438E-02	129.78	0.4579E-01	0.21
66.0	0.3220E+00	0.4587E-01	131.82	0.3417E-01	1.34
68.0	0.1100E+00	0,1066E-01	135.12	0.2773E-01	0.38
70.0	0.5540E+00	0.3896E-01	139.02	0.2354E-01	1.66
72.0	0.8500E+00	0.4343E-01	144.37	0.1998E-01	2.17
74.0	0.8500E+00	0.3455E-01	149.40	0.1718E-01	2.01
76.0	0.1273E+01	0.4050E-01	156.38	0.1492E-01	2.71
78.0	0.1675E+01	0.4083E-01	166.28	0.1312E-01	3.11
80.0	0.1612E+01	0.3192E-01	176.05	0.1153E-01	2.77
82.0	0.2204E+01	0.3693E-01	185.53	0.1012E-01	3.65
84.0	0.2310E+01	0.3299E-01	196.17	0.8907E-02	3.70
86.0	0.2648E+01	0.3315E-01	206.34	0.7808E-02	4.25
88.0	0.2458E+01	0.2723E-01	217.02	0.6833E-02	3.99
90.0	0.2839E+01	0.2839E-01	227.05	0.5959E-02	4.76
92.0	0.2606E+01	0.2340E-01	238.71	0.5200E-02	4.50
94.0	0.3071E+01	0.2508E-01	250.12	0.4521E-02	5.55
96.0	0.3367E+01	0.2538E-01	260.63	0.3918E-02	6.48
98.0	0.3304E+01	0.2262E-01	274.32	0.3396E-02	6.66
100.0	0.3579E+01	0.2227E-01	289.30	0.2947E-02	7.56
102.0	0.3304E+01	0.1898E-01	302.93	0.2545E-02	7.46
104.0	0.3050E+01	0.1614E-01	318.15	0.2188E-02	7.38
106.0	0.3008E+01	0.1487E-01	331.83	0.1881E-02	7.90
108.0	0.3071E+01	0.1404E-01	348.52	0.1622E-02	8.66
110.0	0.2669E+01	0.1146E-01	362.91	0.1394E-02	8.22
112.0	0.2141E+01	0.8648E-02	377.66	0.1204E-02	7.18
114.0	0.2458E+01	0.9614E-02	385.74	0.1034E-02	9.30
116.0	0.1718E+01	0.6465E-02	395.80	0.8946E-03	7.23
118.0	0.1866E+01	0.6930E-02	399.33	0.7734E-03	8.96
120.0	0.1950E+01	0.7154E-02	402.64	0.6701E-03	10.68
122.0	0.1527E+01	0.5489E-02	408.26	0.5873E-03	9.35
124.0	0.1295E+01	0.4623E-02	410.18	0.5137E-03	9.00
126.0	0.1422E+01	0.5021E-02	413.27	0.4456E-03	11.27

FLIGHT STS-27

GAGE NO. 7705 BIAS 0.35 XB LOCATION 141.200

TIME	QDOT FLT	HC	HREC	HUND	HIHU
10.0	0.3500E+00	0.1074E+00	128.06	0.5499E-01	1.95
15.0	0.3700E-01	0.1095E-01	128.18	0.7226E-01	0.15
20.0	0.1350E+00	0.3333E-01	128.85	0.6714E-01	0.50
25.0	0.3790E+00	0.7490E-01	129.86	0.6083E-01	1.23
30.0	0.1100E+00	0.1957E-01	130.42	0.5909E-01	0.33
35.0	0.1590E+00	0.2314E-01	131.67	0.5448E-01	0.42
40.0	0.8600E-01	0.1245E-01	131.71	0.5324E-01	0.23
45.0	0.2570E+00	0.3807E-01	131.55	0.5205E-01	0.73
50.0	0.3700E-01	0.7806E-02	129.54	0.6535E-01	0.12
55.0	0.3700E-01	0.7283E-02	129.88	0.5960E-01	0.12
60.0	0.2080E+00	0.4370E-01	129.56	0.5918E-01	0.74
62.0	0.3060E+00	0.5965E-01	129.93	0.5333E-01	1.12
64.0	0.1590E+00	0.2628E-01	130.85	0.4542E-01	0.58
66.0	0.4280E+00	0.5245E-01	132.96	0.3770E-01	1.39
68.0	0.3550E+00	0.3079E-01	136.33	0.3268E-01	0.94
70.0	0.6000E+00	0.3846E-01	140.40	0.2944E-01	1.31
72.0	0.4530E+00	0.2212E-01	145.88	0.2696E-01	0.82
74.0	0.6250E+00	0.2493E-01	151.07	0.2461E-01	1.01
76.0	0.6490E+00	0.2051E-01	158.25	0.2233E-01	0.92
78.0	0.7230E+00	0.1760E-01	168.29	0.2053E-01	0.86
80.0	0.9950E+00	0.1971E-01	178.28	0.1872E-01	1.05
82.0	0.8720E+00	0.1462E-01	188.05	0.1699E-01	0.86
84.0	0.1194E+01	0.1707E-01	198.93	0.1539E-01	1.11
86.0	0.1070E+01	0.1344E-01	209.24	0.1387E-01	0.97
88.0	0.1269E+01	0.1412E-01	220.06	0.1249E-01	1.13
90.0	0.1468E+01	0.1476E-01	230.24	0.1118E-01	1.32
92.0	0.1493E+01	0.1350E-01	242.02	0.9960E-02	1.36
94.0	0.1493E+01	0.1227E-01	253.65	0.8909E-02	1.38
96.0	0.1895E+01	0.1438E-01	264.40	0.7924E-02	1.81
98.0	0.1996E+01	0.1376E-01	278.30	0.7057E-02	1.95
100.0	0.1719E+01	0.1076E-01	293.50	0.6271E-02	1.72
102.0	0.1971E+01	0.1139E-01	307.39	0.5526E-02	2.06
104.0	0.1920E+01	0.1022E-01	322.87	0.4856E-02	2.10
106.0	0.1694E+01	0.8421E-02	336.77	0.4254E-02	1.98
108.0	0.1518E+01	0.6980E-02	353.68	0.3752E-02	1.86
110.0	0.1569E+01	0.6777E-02	368.32	0.3284E-02	2.06
112.0	0.1269E+01	0.5147E-02	383.34	0.2876E-02	1.79
114.0	0.2656E+01	0.1042E-01	391.78	0.2473E-02	4.21
116.0	0.1443E+01	0.5439E-02	402.09	0.2147E-02	2.53
118.0	0.1244E+01	0.4627E-02	405.68	0.1853E-02	2.50
120.0	0.1618E+01	0.5949E-02	408.78	0.1593E-02	3.73
122.0	0.1996E+01	0.7198E-02	414.09	0.1377E-02	5.23
124.0	0.1418E+01	0.5079E-02	416.00	0.1195E-02	4.25
126.0	0.6740E+00	0.2386E-02	419.23	0.1043E-02	2.29

FLIGHT STS-27

GAGE NO. 7706 BIAS 0.30 XB LOCATION 141.300

TIME	QDOT FLT	HC	HREC	HUND	HIHU
10.0	0.3000E+00	0.9202E-01	128.06	0.5499E-01	1.67
15.0	0.3000E+00	0.8876E-01	128.18	0.7225E-01	1.23
20.0	0.3000E+00	0.7407E-01	128.85	0.6712E-01	1.10
25.0	0.3500E-01	0.6917E-02	129.86	0.6084E-01	0.11
30.0	0.5900E-01	0.1050E-01	130.42	0.5909E-01	0.18
35.0	0.2000E+00	0.2911E-01	131.67	0.5447E-01	0.53
40.0	0.3000E+00	0.4342E-01	131.71	0.5324E-01	0.82
45.0	0.1760E+00	0.2607E-01	131.55	0.5205E-01	0.50
50.0	0.2000E+00	0.4202E-01	129.56	0.6523E-01	0.64
55.0	0.3000E+00	0.5906E-01	129.88	0.5954E-01	0.99
60.0	0.3000E+00	0.6289E-01	129.57	0.5893E-01	1.07
62.0	0.3000E+00	0.5837E-01	129.94	0.5311E-01	1.10
64.0	0.3500E-01	0.5766E-02	130.87	0.4533E-01	0.13
66.0	0.3500E-01	0.4284E-02	132.97	0.3766E-01	0.11
68.0	0.3500E-01	0.3033E-02	136.34	0.3262E-01	0.09
70.0	0.2230E+00	0.1428E-01	140.42	0.2940E-01	0.49
72.0	0.5310E+00	0.2590E-01	145.90	0.2688E-01	0.96
74.0	0.4600E+00	0.1833E-01	151.09	0.2455E-01	0.75
76.0	0.7930E+00	0.2507E-01	158.23	0.2239E-01	1.12
78.0	0.8880E+00	0.2163E-01	168.26	0.2061E-01	1.05
80.0	0.8640E+00	0.1715E-01	178.19	0.1879E-01	0.91
82.0	0.9600E+00	0.1616E-01	187.80	0.1697E-01	0.95
84.0	0.1297E+01	0.1864E-01	198.60	0.1537E-01	1.21
86.0	0.1369E+01	0.1726E-01	208.91	0.1384E-01	1.25
88.0	0.1032E+01	0.1153E-01	219.73	0.1245E-01	0.93
90.0	0.1032E+01	0.1042E-01	229.80	0.1102E-01	0.95
92.0	0.1345E+01	0.1220E-01	241.67	0.9967E-02	1.22
94.0	0.1224E+01	0.1009E-01	253.25	0.8907E-02	1.13
96.0	0.1176E+01	0.8954E-02	263.94	0.7904E-02	1.13
98.0	0.1176E+01	0.8131E-02	277.84	0.7046E-02	1.15
100.0	0.1393E+01	0.8748E-02	293.03	0.6285E-02	1.39
102.0	0.1393E+01	0.8077E-02	306.86	0.5543E-02	1.46
104.0	0.1080E+01	0.5767E-02	322.26	0.4904E-02	1.18
106.0	0.1056E+01	0.5267E-02	336.09	0.4315E-02	1.22
108.0	0.1176E+01	0.5425E-02	352.96	0.3828E-02	1.42
110.0	0.1056E+01	0.4577E-02	367.50	0.3361E-02	1.36
112.0	0.6260E+00	0.2549E-02	382.38	0.2961E-02	0.86
114.0	0.1008E+01	0.3972E-02	390.59	0.2546E-02	1.56
116.0	0.7450E+00	0.2822E-02	400.80	0.2210E-02	1.28
118.0	0.6260E+00	0.2339E-02	404.40	0.1897E-02	1.23
120.0	0.6970E+00	0.2572E-02	407.77	0.1632E-02	1.58
122.0	0.9120E+00	0.3297E-02	413.38	0.1416E-02	2.33
124.0	0.1008E+01	0.3619E-02	415.33	0.1225E-02	2.95
126.0	0.6020E+00	0.2137E-02	418.55	0.1066E-02	2.00

FLIGHT STS-27

GAGE NO. 7707 BIAS 0.40 XB LOCATION 140.400

TIME	QDOT FLT	HC	HREC	HUND	HIHU
10.0	0.4000E+00	0.1227E+00	128.06	0.5504E-01	2.23
15.0	0.4500E-01	0.1331E-01	128.18	0.7231E-01	0.18
20.0	0.4000E+00	0.9877E-01	128.85	0.6719E-01	1.47
25.0	0.4000E+00	0.7905E-01	129.86	0.6087E-01	1.30
30.0	0.1700E+00	0.3025E-01	130.42	0.5913E-01	0.51
35.0	0.2200E+00	0.3202E-01	131.67	0.5452E-01	0.59
40.0	0.4210E+00	0.6093E-01	131.71	0.5327E-01	1.14
45.0	0.4500E-01	0.6667E-02	131.55	0.5210E-01	0.13
50.0	0.9500E-01	0.1996E-01	129.56	0.6521E-01	0.31
55.0	0.2450E+00	0.4823E-01	129.88	0.5966E-01	0.81
60.0	0.2450E+00	0.5147E-01	129.56	0.5934E-01	0.87
62.0	0.3710E+00	0.7232E-01	129.93	0.5348E-01	1.35
64.0	0.2450E+00	0.4043E-01	130.86	0.4554E-01	0.89
66.0	0.2450E+00	0.3002E-01	132.96	0.3778E-01	0.79
68.0	0.1450E+00	0.1259E-01	136.32	0.3274E-01	0.38
70.0	0.2960E+00	0.1897E-01	140.40	0.2951E-01	0.64
72.0	0.2700E+00	0.1318E-01	145.88	0.2701E-01	0.49
74.0	0.6230E+00	0.2486E-01	151.06	0.2469E-01	1.01
76.0	0.7490E+00	0.2367E-01	158.25	0.2231E-01	1.06
78.0	0.7490E+00	0.1822E-01	168.30	0.2050E-01	0.89
80.0	0.9770E+00	0.1936E-01	178.27	0.1858E-01	1.04
82.0	0.1053E+01	0.1769E-01	187.93	0.1669E-01	1.06
84.0	0.7230E+00	0.1037E-01	198.72	0.1513E-01	0.69
86.0	0.9010E+00	0.1134E-01	209.03	0.1363E-01	0.83
88.0	0.1155E+01	0.1288E-01	219.85	0.1227E-01	1.05
90.0	0.1180E+01	0.1190E-01	230.00	0.1097E-01	1.08
92.0	0.1028E+01	0.9312E-02	241.79	0.9810E-02	0.95
94.0	0.1028E+01	0.8469E-02	253.39	0.8757E-02	0.97
96.0	0.1180E+01	0.8975E-02	264.08	0.7768E-02	1.16
98.0	0.1206E+01	0.8329E-02	277.99	0.6915E-02	1.20
100.0	0.1028E+01	0.6449E-02	293.21	0.6155E-02	1.05
102.0	0.1384E+01	0.8015E-02	307.07	0.5418E-02	1.48
104.0	0.1949E+01	0.1039E-01	322.56	0.4751E-02	2.19
106.0	0.1129E+01	0.5621E-02	336.47	0.4146E-02	1.36
108.0	0.9260E+00	0.4263E-02	353.42	0.3650E-02	1.17
110.0	0.1129E+01	0.4883E-02	368.02	0.3186E-02	1.53
112.0	0.9010E+00	0.3659E-02	383.01	0.2786E-02	1.31
114.0	0.1078E+01	0.4237E-02	391.23	0.2389E-02	1.77
116.0	0.7990E+00	0.3019E-02	401.43	0.2080E-02	1.45
118.0	0.5970E+00	0.2226E-02	404.98	0.1792E-02	1.24
120.0	0.5220E+00	0.1923E-02	408.31	0.1548E-02	1.24
122.0	0.1002E+01	0.3616E-02	413.91	0.1346E-02	2.69
124.0	0.1002E+01	0.3591E-02	415.82	0.1168E-02	3.07
126.0	0.2700E+00	0.9567E-03	419.02	0.1020E-02	0.94

FLIGHT STS-29

GAGE NO. 7703		BIAS 0.00		XB LOCATION 109.700	
TIME	QDOT FLT	HC	HREC	HUND	HIHU
10.0					
15.0					
20.0					
25.0					
30.0	0.1500E+00	0.2930E-01	130.40	0.2632E+00	0.11
35.0	0.1140E+00	0.1900E-01	131.28	0.1483E+00	0.13
40.0	0.1500E+00	0.2373E-01	131.60	0.1287E+00	0.18
45.0	0.9500E-01	0.1570E-01	131.33	0.1365E+00	0.12
50.0	0.0000E+00	0.0000E+00	131.04	0.1509E+00	0.00
55.0	0.5900E-01	0.1075E-01	130.77	0.1657E+00	0.06
60.0	0.1140E+00	0.1983E-01	131.03	0.1279E+00	0.16
62.0	0.4000E-02	0.6051E-03	131.89	0.8685E-01	0.01
64.0	0.3700E+00	0.4927E-01	132.79	0.6670E-01	0.74
66.0	0.1500E+00	0.1712E-01	134.04	0.5209E-01	0.33
68.0	0.2050E+00	0.1964E-01	135.72	0.4185E-01	0.47
70.0	0.4440E+00	0.3289E-01	138.78	0.3350E-01	0.98
72.0	0.7020E+00	0.4023E-01	142.73	0.2757E-01	1.46
74.0	0.1167E+01	0.5410E-01	146.85	0.2319E-01	2.33
76.0	0.1018E+01	0.3649E-01	153.38	0.1984E-01	1.84
78.0	0.1279E+01	0.3613E-01	161.28	0.1707E-01	2.12
80.0	0.1466E+01	0.3362E-01	169.89	0.1538E-01	2.19
82.0	0.1597E+01	0.3052E-01	179.02	0.1272E-01	2.40
84.0	0.1748E+01	0.2833E-01	188.79	0.1099E-01	2.58
86.0	0.1485E+01	0.2071E-01	199.21	0.9546E-02	2.17
88.0	0.1804E+01	0.2211E-01	209.49	0.8289E-02	2.67
90.0	0.2164E+01	0.2333E-01	221.05	0.7234E-02	3.23
92.0	0.2164E+01	0.2087E-01	232.38	0.6281E-02	3.32
94.0	0.2126E+01	0.1860E-01	243.41	0.5427E-02	3.43
96.0	0.2411E+01	0.1904E-01	256.15	0.4715E-02	4.04
98.0	0.2240E+01	0.1606E-01	269.41	0.4096E-02	3.92
100.0	0.2469E+01	0.1612E-01	283.53	0.3559E-02	4.53
102.0	0.2316E+01	0.1385E-01	297.58	0.3076E-02	4.50
104.0	0.2107E+01	0.1161E-01	311.87	0.2644E-02	4.39
106.0	0.2107E+01	0.1075E-01	326.34	0.2274E-02	4.73
108.0	0.2145E+01	0.1017E-01	341.27	0.1948E-02	5.22
110.0	0.2794E+01	0.1234E-01	356.81	0.1667E-02	7.40
112.0	0.2967E+01	0.1226E-01	372.34	0.1424E-02	8.61
114.0	0.2929E+01	0.1145E-01	386.22	0.1216E-02	9.41
116.0	0.2507E+01	0.9417E-02	396.53	0.1043E-02	9.03
118.0	0.2354E+01	0.8603E-02	403.94	0.9022E-03	9.54
120.0	0.2164E+01	0.7754E-02	409.40	0.7947E-03	9.76
122.0	0.1918E+01	0.6767E-02	413.77	0.7051E-03	9.60
124.0	0.1729E+01	0.6029E-02	417.10	0.6184E-03	9.75
126.0	0.1635E+01	0.5643E-02	420.08	0.5361E-03	10.53

FLIGHT STS-29

GAGE NO. 7704		BIAS 0.00		XB LOCATION	109.800
TIME	QDOT FLT	HC	HREC	HUND	HIHU
10.0					
15.0					
20.0					
25.0					
30.0					
35.0	0.8300E-01	0.1386E-01	131.27	0.1488E+00	0.09
40.0	0.0000E+00	0.0000E+00	131.59	0.1289E+00	0.00
45.0	0.1870E+00	0.3096E-01	131.32	0.1369E+00	0.23
50.0	0.4150E+00	0.7293E-01	130.97	0.1565E+00	0.47
55.0	0.2280E+00	0.4230E-01	130.67	0.1758E+00	0.24
60.0	0.3320E+00	0.5866E-01	130.94	0.1333E+00	0.44
62.0	0.2910E+00	0.4463E-01	131.80	0.8824E-01	0.51
64.0	0.2910E+00	0.3917E-01	132.71	0.6692E-01	0.59
66.0	0.4780E+00	0.5526E-01	133.93	0.5179E-01	1.07
68.0	0.5190E+00	0.5024E-01	135.61	0.4134E-01	1.22
70.0	0.7480E+00	0.5574E-01	138.70	0.3307E-01	1.69
72.0	0.1122E+01	0.6463E-01	142.64	0.2712E-01	2.38
74.0	0.1039E+01	0.4826E-01	146.81	0.2299E-01	2.10
76.0	0.1288E+01	0.4622E-01	153.35	0.1971E-01	2.34
78.0	0.1517E+01	0.4288E-01	161.26	0.1699E-01	2.52
80.0	0.1746E+01	0.4015E-01	169.77	0.1501E-01	2.68
82.0	0.2120E+01	0.4051E-01	179.03	0.1275E-01	3.18
84.0	0.2203E+01	0.3571E-01	188.79	0.1099E-01	3.25
86.0	0.2224E+01	0.3101E-01	199.21	0.9548E-02	3.25
88.0	0.2744E+01	0.3361E-01	209.54	0.8350E-02	4.03
90.0	0.2785E+01	0.3000E-01	221.14	0.7321E-02	4.10
92.0	0.3118E+01	0.3006E-01	232.44	0.6338E-02	4.74
94.0	0.2889E+01	0.2526E-01	243.47	0.5470E-02	4.62
96.0	0.2910E+01	0.2297E-01	256.22	0.4758E-02	4.83
98.0	0.3076E+01	0.2204E-01	269.48	0.4134E-02	5.33
100.0	0.2931E+01	0.1912E-01	283.61	0.3592E-02	5.32
102.0	0.3055E+01	0.1826E-01	297.66	0.3106E-02	5.88
104.0	0.2764E+01	0.1522E-01	311.97	0.2674E-02	5.69
106.0	0.2764E+01	0.1409E-01	326.44	0.2298E-02	6.13
108.0	0.2931E+01	0.1389E-01	341.35	0.1966E-02	7.06
110.0	0.2972E+01	0.1312E-01	356.88	0.1682E-02	7.80
112.0	0.2889E+01	0.1193E-01	372.41	0.1437E-02	8.30
114.0	0.2702E+01	0.1056E-01	386.30	0.1227E-02	8.60
116.0	0.2536E+01	0.9521E-02	396.68	0.1059E-02	8.99
118.0	0.2224E+01	0.8123E-02	404.12	0.9185E-03	8.84
120.0	0.2058E+01	0.7371E-02	409.52	0.8042E-03	9.17
122.0	0.2037E+01	0.7185E-02	413.81	0.7077E-03	10.15
124.0	0.1767E+01	0.6162E-02	417.09	0.6176E-03	9.98
126.0	0.1559E+01	0.5380E-02	420.09	0.5363E-03	10.03

FLIGHT STS-29

GAGE NO.	7705	BIAS -.20		XB LOCATION	141.200
TIME	QDOT FLT	HC	HREC	HUND	HIHU
10.0					
15.0					
20.0					
25.0					
30.0					
35.0					
40.0					
45.0					
50.0					
55.0					
60.0	0.1560E+00	0.2102E-01	131.98	0.8819E-01	0.24
62.0	0.1300E-01	0.1564E-02	132.87	0.7121E-01	0.02
64.0	0.6100E-01	0.6587E-02	133.82	0.6029E-01	0.11
66.0	0.2270E+00	0.2142E-01	135.16	0.5110E-01	0.42
68.0	0.1320E+00	0.1071E-01	136.88	0.4393E-01	0.24
70.0	0.4900E+00	0.3174E-01	140.00	0.3756E-01	0.84
72.0	0.3230E+00	0.1654E-01	144.09	0.3296E-01	0.50
74.0	0.4660E+00	0.1955E-01	148.40	0.2940E-01	0.66
76.0	0.4660E+00	0.1527E-01	155.08	0.2627E-01	0.58
78.0	0.4900E+00	0.1269E-01	163.18	0.2344E-01	0.54
80.0	0.5380E+00	0.1142E-01	171.69	0.2106E-01	0.54
82.0	0.9470E+00	0.1669E-01	181.29	0.1897E-01	0.88
84.0	0.9470E+00	0.1431E-01	191.32	0.1710E-01	0.84
86.0	0.7540E+00	0.9899E-02	201.89	0.1538E-01	0.64
88.0	0.1044E+01	0.1214E-01	212.28	0.1380E-01	0.88
90.0	0.1141E+01	0.1176E-01	223.95	0.1243E-01	0.95
92.0	0.1141E+01	0.1057E-01	235.37	0.1109E-01	0.95
94.0	0.1482E+01	0.1250E-01	246.59	0.9914E-02	1.26
96.0	0.1384E+01	0.1057E-01	259.52	0.8882E-02	1.19
98.0	0.1653E+01	0.1150E-01	272.94	0.7937E-02	1.45
100.0	0.1335E+01	0.8481E-02	287.20	0.7048E-02	1.20
102.0	0.1604E+01	0.9378E-02	301.42	0.6245E-02	1.50
104.0	0.1335E+01	0.7217E-02	315.94	0.5490E-02	1.31
106.0	0.1555E+01	0.7811E-02	330.63	0.4837E-02	1.61
108.0	0.1335E+01	0.6248E-02	345.80	0.4249E-02	1.47
110.0	0.1628E+01	0.7114E-02	361.55	0.3724E-02	1.91
112.0	0.1311E+01	0.5372E-02	377.33	0.3268E-02	1.64
114.0	0.1214E+01	0.4713E-02	391.45	0.2844E-02	1.66
116.0	0.9230E+00	0.3446E-02	402.02	0.2455E-02	1.40
118.0	0.8030E+00	0.2917E-02	409.46	0.2114E-02	1.38
120.0	0.1335E+01	0.4759E-02	414.71	0.1823E-02	2.61
122.0	0.1360E+01	0.4777E-02	418.84	0.1570E-02	3.04
124.0	0.1214E+01	0.4216E-02	422.10	0.1358E-02	3.10
126.0	0.9720E+00	0.3340E-02	425.20	0.1180E-02	2.83

FLIGHT STS-29

GAGE NO. 7706		BIAS 0.00		XB LOCATION	141.300
TIME	QDOT FLT	HC	HREC	HUND	HIHU
10.0					
15.0					
20.0					
25.0	0.3700E-01	0.7724E-02	129.35		
30.0	0.3830E+00	0.6448E-01	130.50	0.1959E+00	0.33
35.0	0.2340E+00	0.3406E-01	131.43	0.1184E+00	0.29
40.0	0.8600E-01	0.1188E-01	131.80	0.1038E+00	0.11
45.0	0.1850E+00	0.2635E-01	131.58	0.1076E+00	0.24
50.0	0.3700E-01	0.5598E-02	131.17	0.1266E+00	0.04
55.0	0.1600E+00	0.2238E-01	131.71	0.1008E+00	0.22
60.0	0.2340E+00	0.3149E-01	131.99	0.8789E-01	0.36
62.0	0.8600E-01	0.1034E-01	132.88	0.7097E-01	0.15
64.0	0.1360E+00	0.1467E-01	133.83	0.6002E-01	0.24
66.0	0.1360E+00	0.1281E-01	135.18	0.5103E-01	0.25
68.0	0.4570E+00	0.3703E-01	136.90	0.4383E-01	0.84
70.0	0.3830E+00	0.2479E-01	140.01	0.3748E-01	0.66
72.0	0.5320E+00	0.2721E-01	144.11	0.3288E-01	0.83
74.0	0.7060E+00	0.2959E-01	148.42	0.2933E-01	1.01
76.0	0.5560E+00	0.1821E-01	155.10	0.2617E-01	0.70
78.0	0.7550E+00	0.1956E-01	163.16	0.2352E-01	0.83
80.0	0.1205E+01	0.2558E-01	171.66	0.2117E-01	1.21
82.0	0.1482E+01	0.2617E-01	181.19	0.1906E-01	1.37
84.0	0.1734E+01	0.2629E-01	191.11	0.1715E-01	1.53
86.0	0.1608E+01	0.2117E-01	201.69	0.1546E-01	1.37
88.0	0.1759E+01	0.2050E-01	212.10	0.1389E-01	1.48
90.0	0.1784E+01	0.1841E-01	223.79	0.1251E-01	1.47
92.0	0.0000E+00	0.0000E+00	235.23	0.1118E-01	0.00
94.0	0.1734E+01	0.1465E-01	246.44	0.1001E-01	1.46
96.0	0.2038E+01	0.1559E-01	259.36	0.8978E-02	1.74
98.0	0.2012E+01	0.1401E-01	272.79	0.8038E-02	1.74
100.0	0.1860E+01	0.1183E-01	287.07	0.7152E-02	1.65
102.0	0.1835E+01	0.1074E-01	301.28	0.6348E-02	1.69
104.0	0.2114E+01	0.1144E-01	315.77	0.5591E-02	2.05
106.0	0.1482E+01	0.7452E-02	330.41	0.4955E-02	1.50
108.0	0.1456E+01	0.6823E-02	345.52	0.4375E-02	1.56
110.0	0.1456E+01	0.6371E-02	361.23	0.3854E-02	1.65
112.0	0.1810E+01	0.7428E-02	376.95	0.3395E-02	2.19
114.0	0.1130E+01	0.4395E-02	390.97	0.2968E-02	1.48
116.0	0.8550E+00	0.3199E-02	401.45	0.2562E-02	1.25
118.0	0.9550E+00	0.3476E-02	408.92	0.2202E-02	1.58
120.0	0.7300E+00	0.2606E-02	414.30	0.1897E-02	1.37
122.0	0.8550E+00	0.3007E-02	418.45	0.1630E-02	1.85
124.0	0.6810E+00	0.2368E-02	421.73	0.1407E-02	1.68
126.0	0.5320E+00	0.1830E-02	424.85	0.1220E-02	1.50

FLIGHT STS-29

GAGE NO.	7707	BIAS -.15	XB LOCATION		140.400
TIME	QDOT FLT	HC	HREC	HUND	HIHU
10.0					
15.0					
20.0					
25.0					
30.0					
35.0					
40.0					
45.0					
50.0					
55.0					
60.0					
62.0	0.5600E-01	0.6739E-02	132.87	0.7136E-01	0.09
64.0	0.1310E+00	0.1415E-01	133.82	0.6047E-01	0.23
66.0	0.7000E-02	0.6598E-03	135.17	0.5125E-01	0.01
68.0	0.1800E+00	0.1461E-01	136.88	0.4404E-01	0.33
70.0	0.2300E+00	0.1491E-01	139.99	0.3763E-01	0.40
72.0	0.3050E+00	0.1562E-01	144.09	0.3303E-01	0.47
74.0	0.2800E+00	0.1174E-01	148.40	0.2948E-01	0.40
76.0	0.4290E+00	0.1406E-01	155.07	0.2633E-01	0.53
78.0	0.6040E+00	0.1564E-01	163.19	0.2342E-01	0.67
80.0	0.8790E+00	0.1864E-01	171.71	0.2102E-01	0.89
82.0	0.1055E+01	0.1860E-01	181.28	0.1882E-01	0.99
84.0	0.9040E+00	0.1368E-01	191.24	0.1687E-01	0.81
86.0	0.1131E+01	0.1486E-01	201.81	0.1521E-01	0.98
88.0	0.1156E+01	0.1345E-01	212.23	0.1367E-01	0.98
90.0	0.1081E+01	0.1114E-01	223.93	0.1232E-01	0.90
92.0	0.1106E+01	0.1025E-01	235.35	0.1100E-01	0.93
94.0	0.1308E+01	0.1104E-01	246.57	0.9841E-02	1.12
96.0	0.1232E+01	0.9413E-02	259.51	0.8813E-02	1.07
98.0	0.1030E+01	0.7165E-02	272.96	0.7876E-02	0.91
100.0	-.1500E+00	-.9526E-03	287.26	0.7000E-02	-0.14
102.0	0.1409E+01	0.8234E-02	301.49	0.6199E-02	1.33
104.0	0.1257E+01	0.6792E-02	316.02	0.5444E-02	1.25
106.0	0.1510E+01	0.7580E-02	330.74	0.4783E-02	1.58
108.0	0.1207E+01	0.5645E-02	345.93	0.4190E-02	1.35
110.0	0.1282E+01	0.5598E-02	361.72	0.3664E-02	1.53
112.0	0.9800E+00	0.4013E-02	377.50	0.3209E-02	1.25
114.0	0.1005E+01	0.3899E-02	391.64	0.2784E-02	1.40
116.0	0.6790E+00	0.2534E-02	402.13	0.2398E-02	1.06
118.0	0.6790E+00	0.2465E-02	409.58	0.2068E-02	1.19
120.0	0.7290E+00	0.2597E-02	414.91	0.1789E-02	1.45
122.0	0.6040E+00	0.2120E-02	419.03	0.1542E-02	1.38
124.0	0.6290E+00	0.2183E-02	422.29	0.1335E-02	1.64
126.0	0.6040E+00	0.2074E-02	425.37	0.1162E-02	1.78

Appendix II

Solid Rocket Booster (SRB) Ascent Base Heating Flight Evaluation for Flights STS-26R, STS-27R and STS-29R (RTN 213-12)

REMTECH TECHNICAL NOTE

TITLE: Solid Rocket Booster (SRB) Ascent Base Heating Flight Evaluation for Flights STS-26R, STS-27R, and STS-29R

DATE: February 7, 1991

AUTHOR: Maurice J. Prendergast

CONTRACT NO: NAS8-37891

PREPARED FOR: NASA/George C. Marshall Space Flight Center

INTRODUCTION

Ascent base heating data were measured on flights STS-26R, STS-27R and STS-29R at three locations on the SRB aft skirt. REMTECH, under contract NAS8-37891, has evaluated the data from these flights and compared this data with existing design environments to ascertain if changes to the operational flight environment are indicated. This evaluation is summarized in this technical note. Also included is a review and evaluation of the SSME plume impingement heating environments for 16 seconds following separation.

FLIGHT INSTRUMENTATION

The SRB DFI instrumentation and raw flight data for the above flights are outlined in detail in REMTECH Technical Notes (RTN's) [1,2,3]. Data from three calorimeters, and one thermocouple/gas temperature probe are presented in this technical note. A summary of the flight instrumentation is given in Table 1. Figure 1 shows the location of the calorimeters on the aft skirt.

The STS-29R trajectory, Figure 2, was slightly lower (less altitude at a corresponding time in flight) than either STS-26R or STS-27R; however, the altitude differences are easily within the sensitivity of the base heating parameters. Therefore, little difference was expected in the flight data from the three flights.

SRB FLIGHT EVALUATION

Flight data from calorimeters B07R7705A, B07R7706A, and B07R7707A are displayed versus flight time on Figures 3 through 5 respectively. Each figure contains data from the three instrumented flights. These calorimeters measured total heating rate which may be a combination of radiation plus convective heating. At these three gage locations, plume radiation is very small and can be neglected, so the data shown is assumed to be primarily plume recirculation convection. The gages typically do not reach temperatures in excess of 150° F, therefore the data can be considered as cold wall convective environment. The operational flight convective base heating design environments, which are contained in the IVBC-3 SRB Plume Heating data book [4] and are essentially envelopes of previous flight data, are plotted on Figures 3 through 5 for comparison.

The trends and magnitudes of the measured data are within the design constraints, although B07R7706A data exceeds the operational environment on flight STS-29R (the magnitude of data from each of these calorimeters is significantly higher on flight STS-29R in comparison to flights STS-26R and STS-27R). Figure 6 and Figure 7 represent base gas recovery temperature from the gas temperature probe (B07T7605A) versus time. The gas temperature is within the design environment as seen from Figure 6.

Plume Impingement to SRB Aft Skirt

SSME plume impingement to the spent SRB's following separation is evident in the data displayed in Figures 8 through 10. Figure 8 represents data from the three calorimeters positioned on the aft skirt on flight STS-26R, while data from flights STS-27R and STS-29R are shown on Figures 9 and 10 respectively. The results are well within the operational design environment contained in the IVBC-3 SRB Plume Heating data book [4]. Data from calorimeters B07R7706A and B07R7707A are nearly identical due to their close proximity to each other on the aft skirt. The trend in data from B07R7705A is similar but is attenuated. Again these results appear to be similar to previous flights and approximately as expected.

CONCLUSIONS

Based upon this preliminary evaluation, flights STS-26R, STS-27R, and STS-29R were similar to previous shuttle flights and less than or approximately the same as the operational design environments. Nothing unusual or unexpected

was observed in either the magnitude or trends of the measured data. The gas temperature probe data is not representative of actual flight environments because of poor probe design for this application. These data were, however, similar to previous flight measurements made with similar instruments.

References

[1] Crain W. K., "Raw Flight Data Report - STS-26R," RTN 213-01, December, 1988.

[2] Frost C. L., and W. K. Crain, "Raw Flight Data Report - STS-27R," RTN 213-02, October 2, 1989.

[3] Frost C. L., and W. K. Crain, "Raw Flight Data Report - STS-29R," RTN 213-03, September 27, 1989.

[4] Rockwell International Document STS 84-0259, "IVBC-3 SRB Plume Heating Data Book," Oct. 1984, Change Notice 1.

Table 1: Flight Instruments on the External SRB Aft Skirt

FLIGHT	TYPE	GAGE	X_B (in.)	Θ_B (Deg.)	LOCATION
STS-26R	Calorimeter	B07R7605A	1880	180	Aft Skirt External
STS-27R		B07R7606A	1880	270	
STS-29R		B07R7607A	1870	270	
STS-27R STS-29R	Gas Temp. Probe	B07T7605A	1931	45	Aft Ring External
STS-26R STS-27R STS-29R	Pressure Gages	B47P1300C	485	320	SRM Chamber A

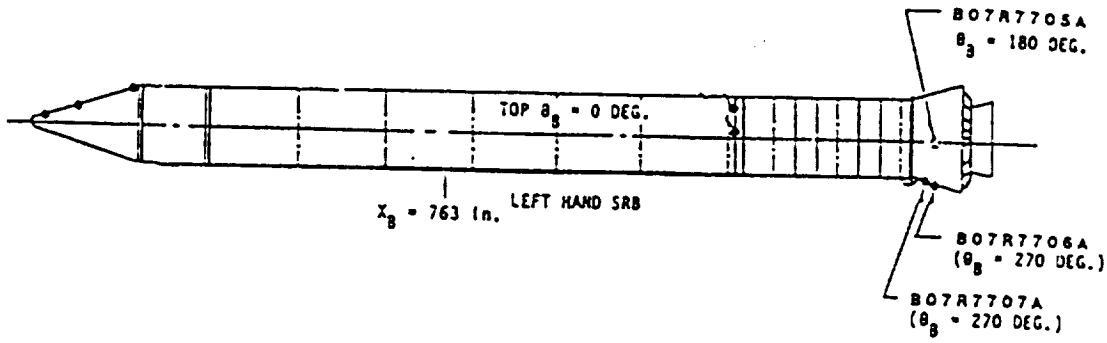

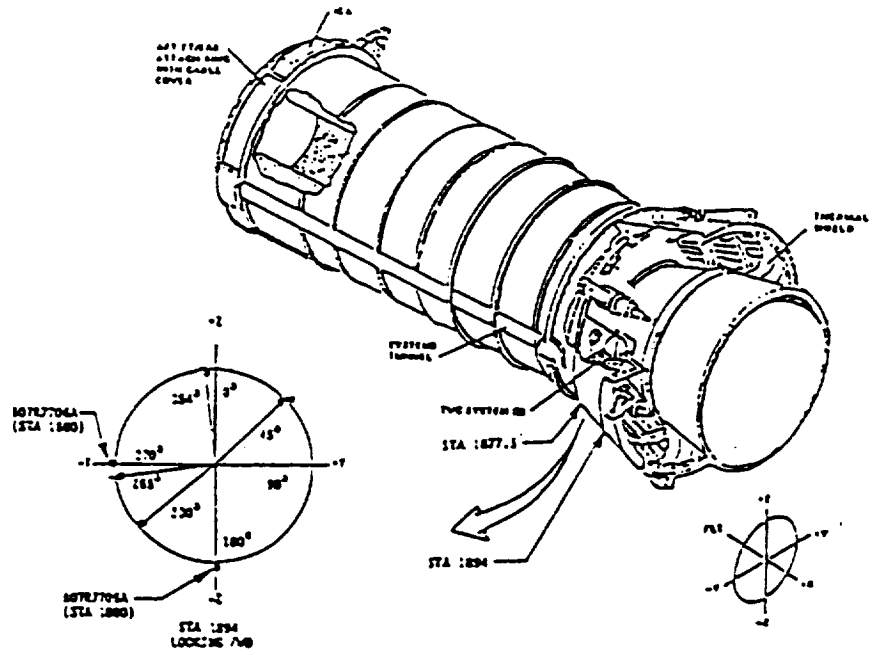

Figure 1: External SRB DFI Instrumentation

C-3

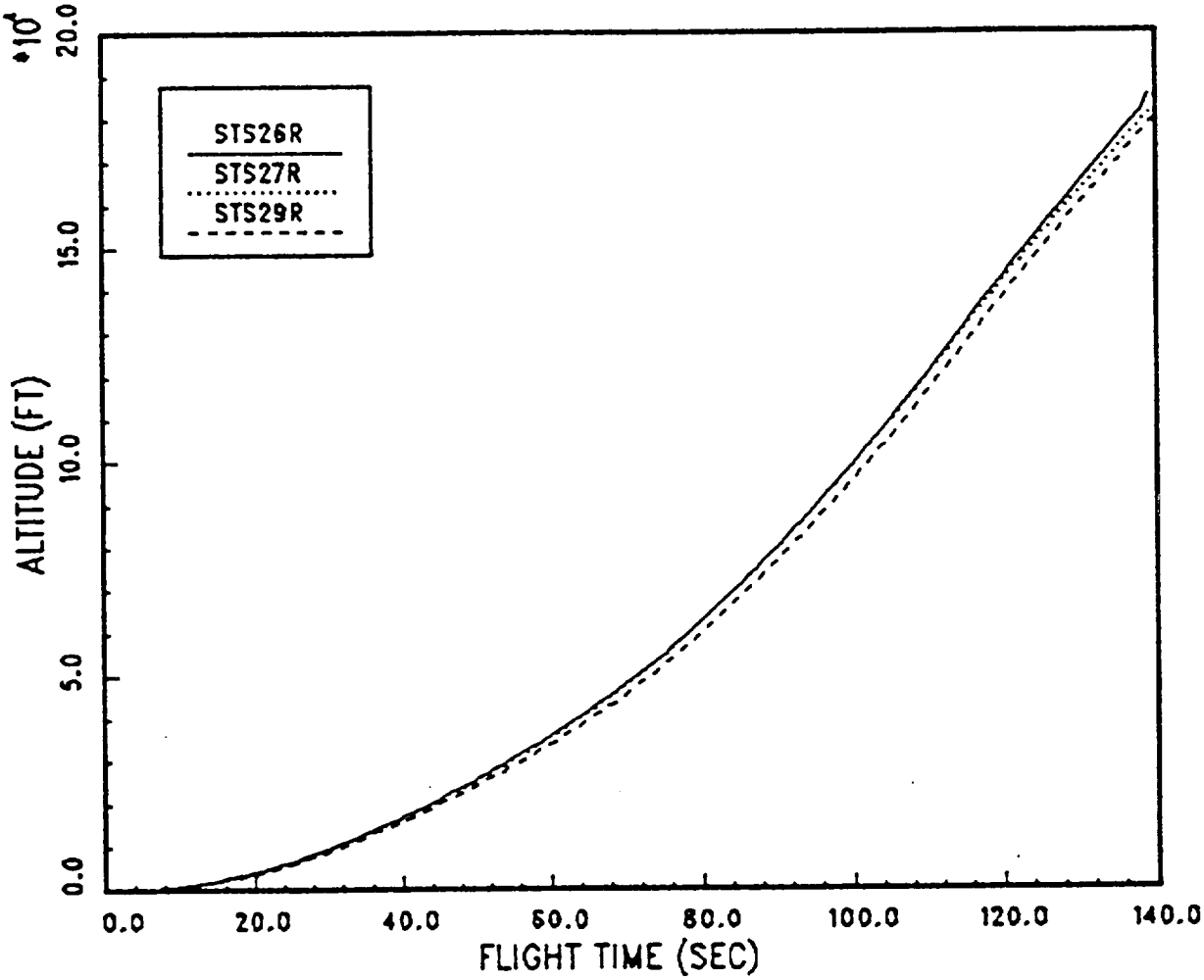

Figure 2: Time - Altitude Comparisons for Instrument Flights

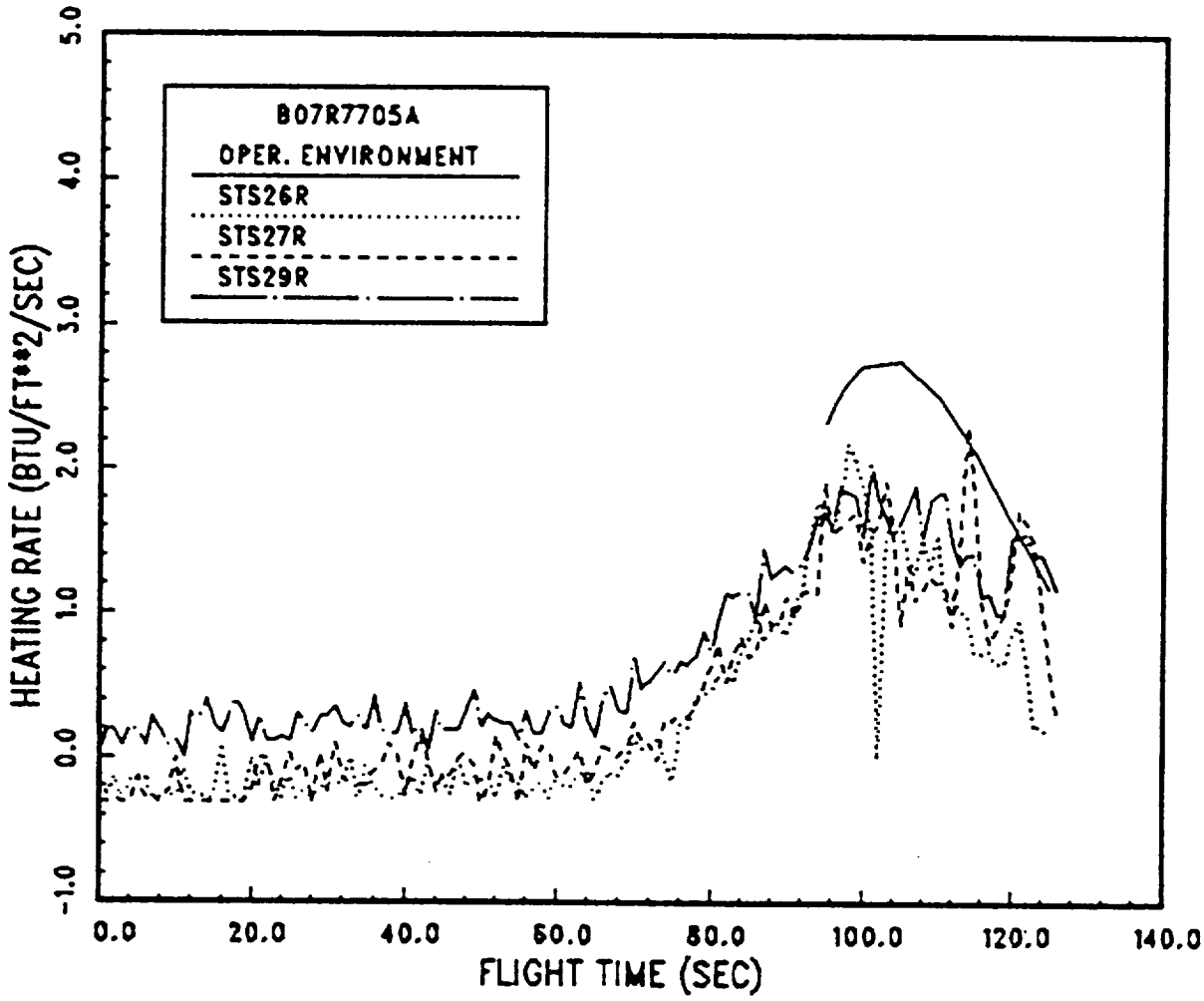

Figure 3: SRB Base Heating Environment - Q_c vs Time - Aft Skirt (B07R7705A)

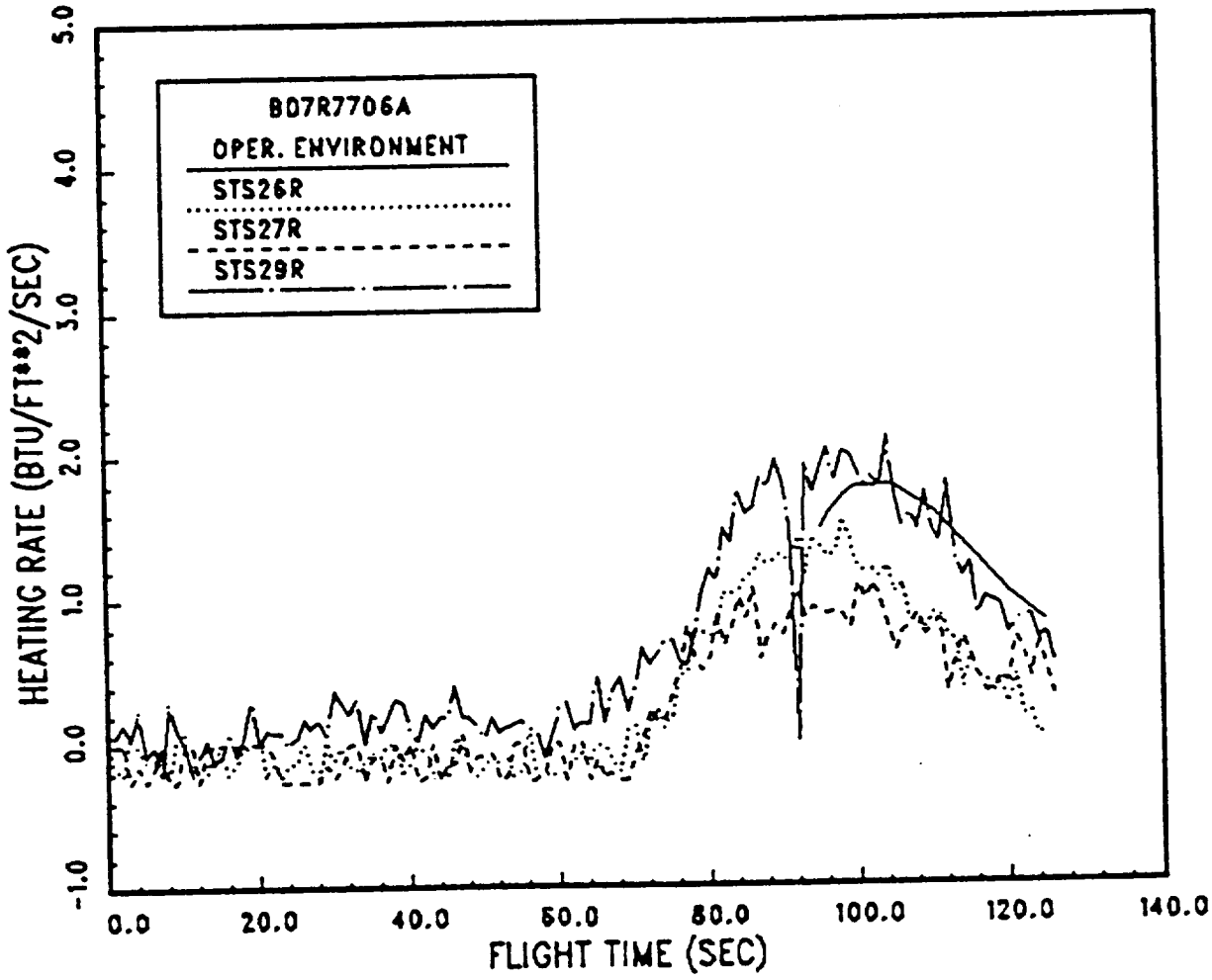

Figure 4: SRB Base Heating Environment - Q_c vs Time - Aft Skirt (B07R7706A)

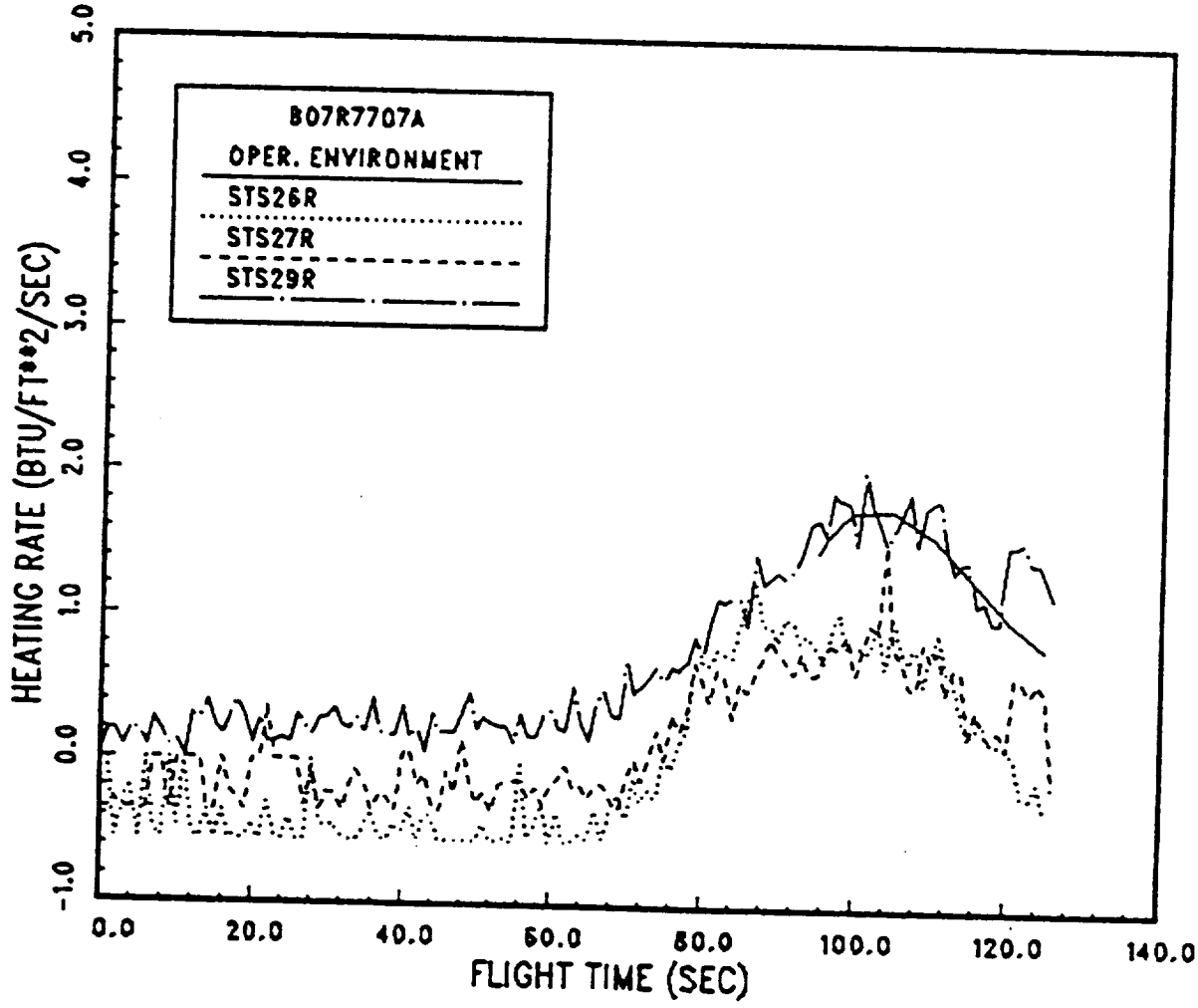

Figure 5: SRB Base Heating Environment - Q_c vs Time - Aft Skirt (B07R7707A)

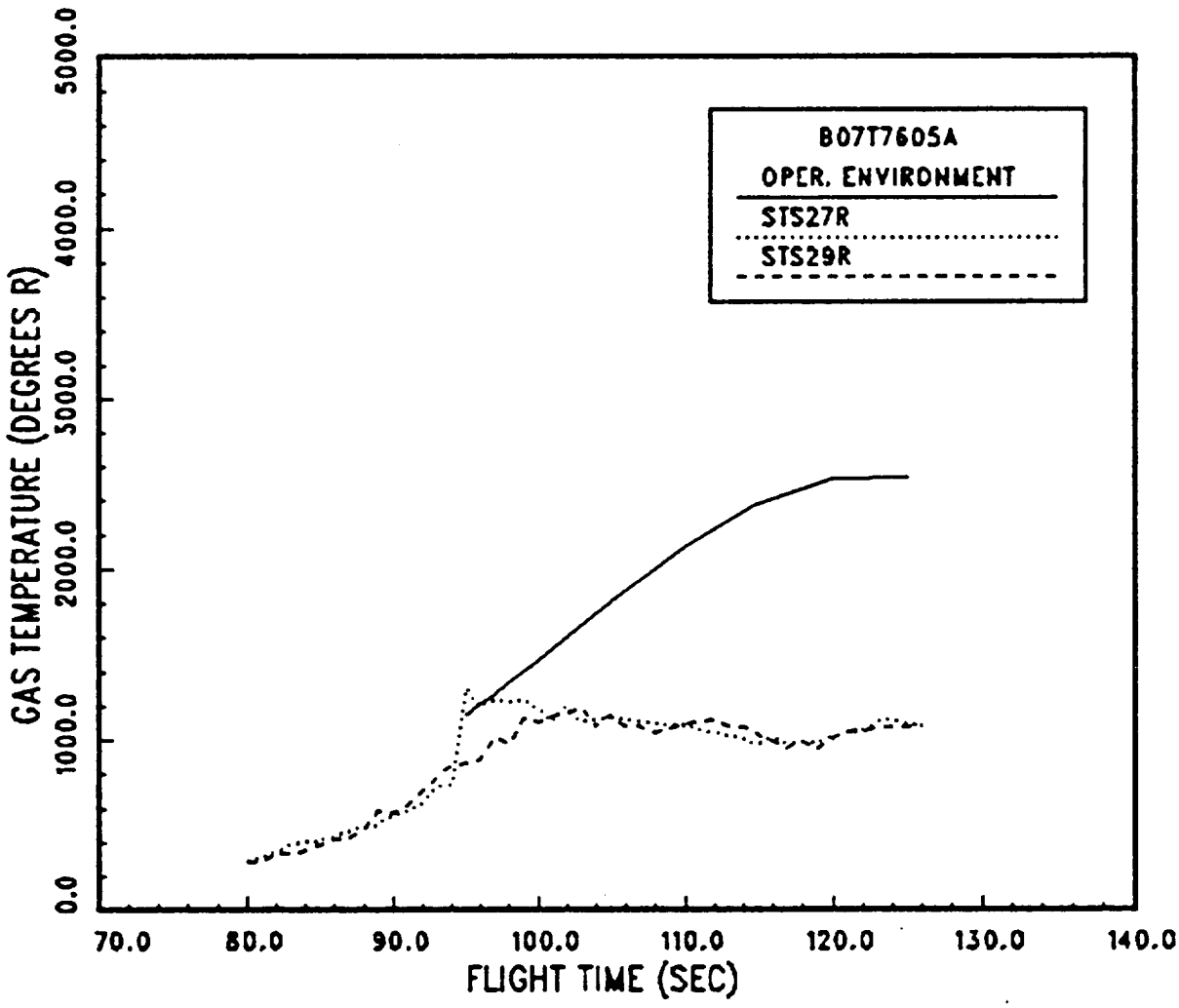

Figure 6: SRB Base Heating Environment - Base Gas Recovery Temperature vs Time - Aft Skirt

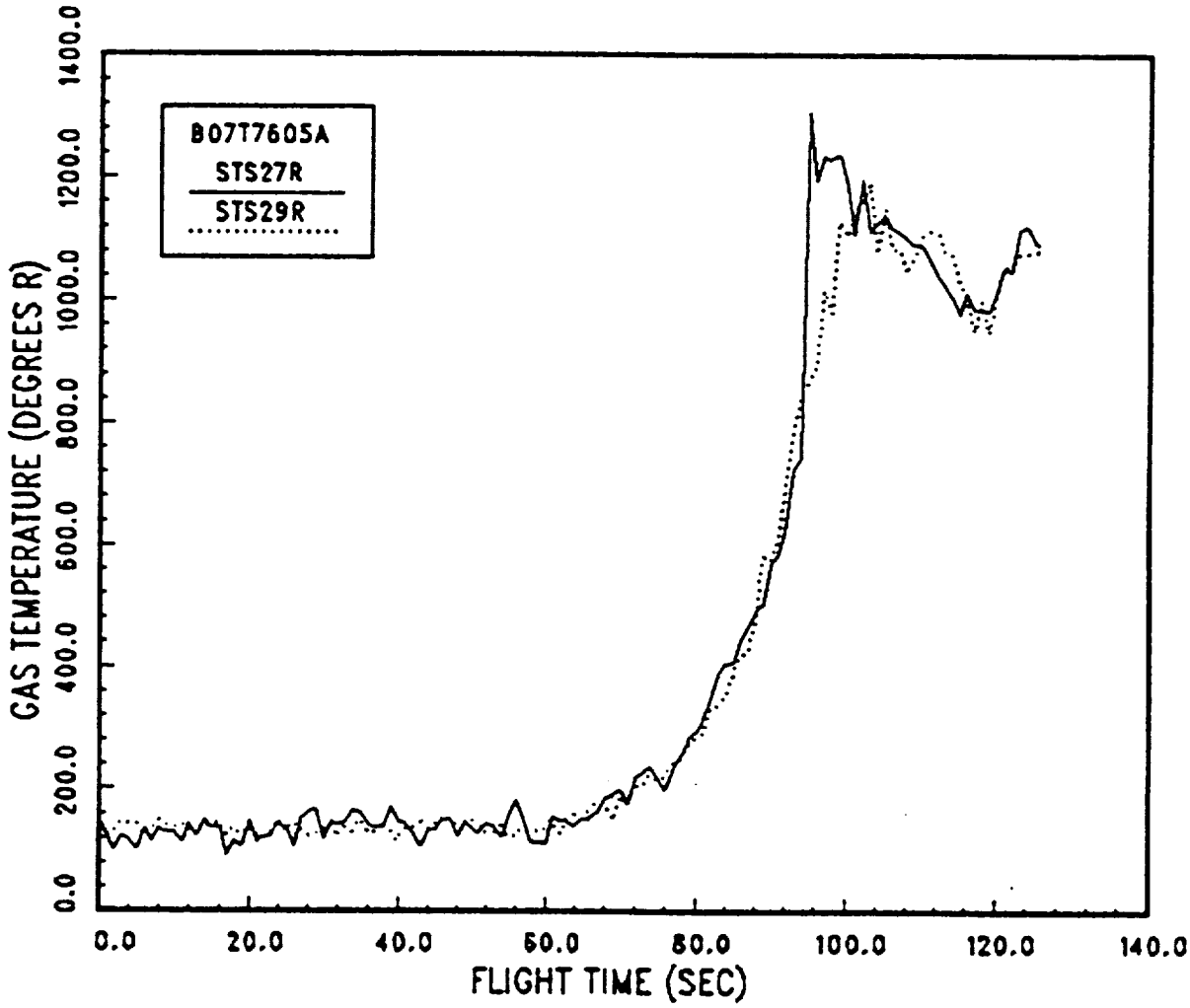

Figure 7: SRB Base Heating Environment - Base Gas Recovery Temperature vs Time - Aft Skirt

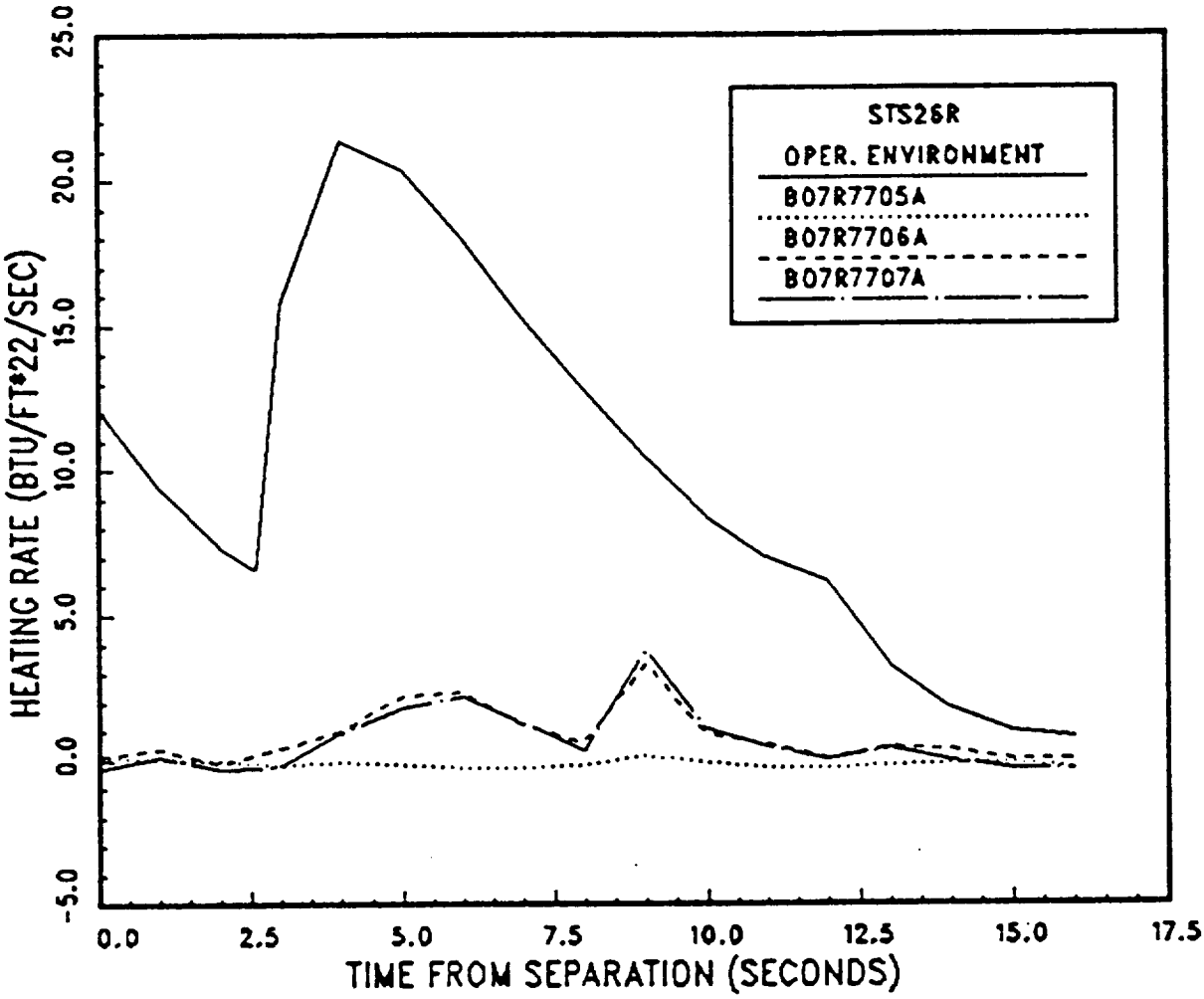

Figure 8: STS-26R Convective Heating Environment to SRB Aft Skirt for 16 Seconds following Separation

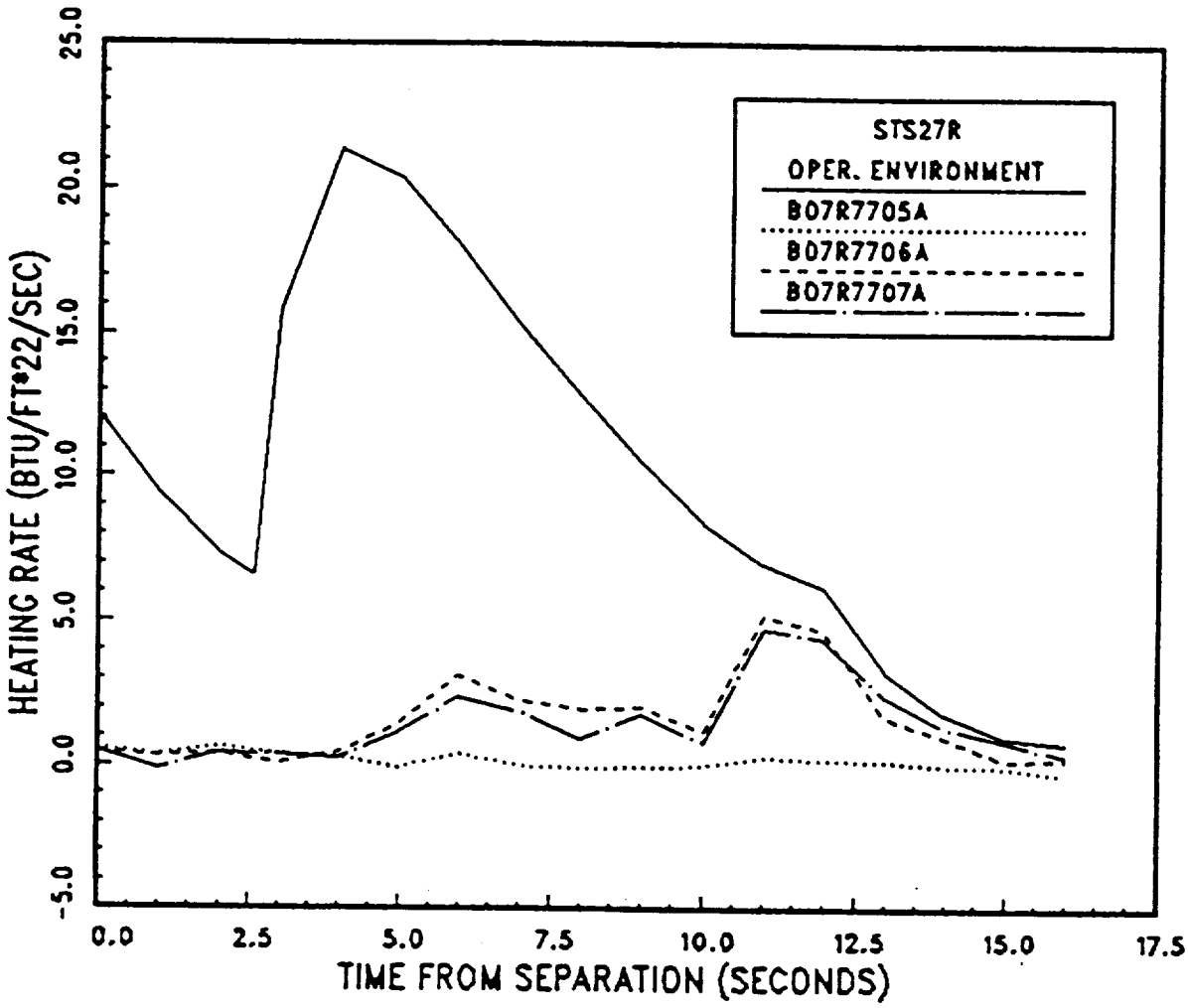

Figure 9: STS-27R Convective Heating Environment to SRB Aft Skirt for 16 Seconds following Separation

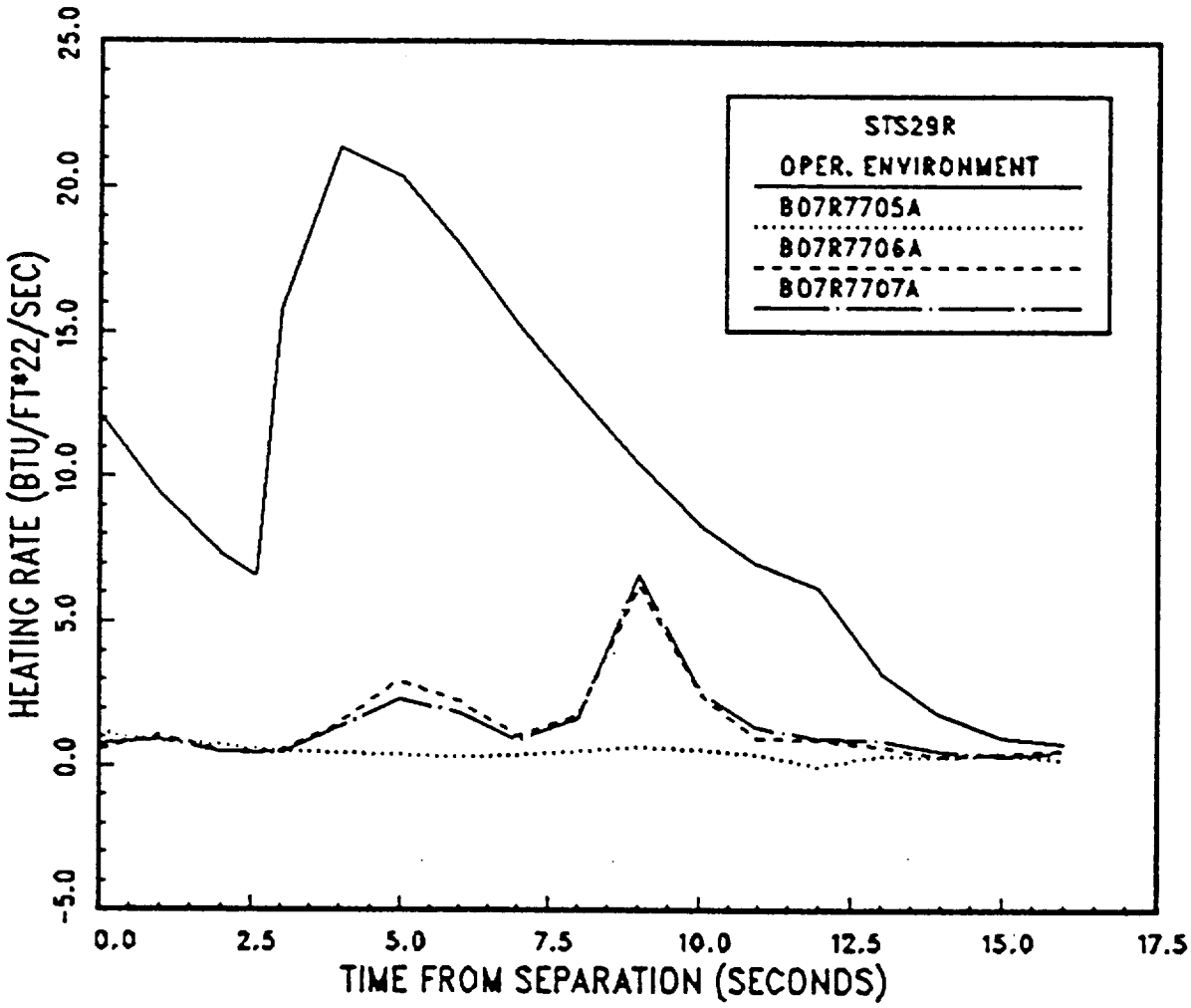

Figure 10: STS-29R Convective Heating Environment to SRB Aft Skirt for 16 Seconds following Separation

Appendix III

Calculations of SRB Pitch and Roll Characteristics During Reentry for Flights STS-27R and 29R (RTN 213-05)

REMTECH TECHNICAL NOTE

SUBJECT: Calculations of SRB Pitch and Roll Characteristics During Reentry for Flights STS-27R and STS-29R

DATE: May 1991

AUTHORS: Robert D. Kirchner and William K. Crain

CONTRACT NO.: NAS8-37891

PREPARED FOR: NASA/George C. Marshall Space Flight Center

INTRODUCTION

The left-hand SRB on Space Transportation System (STS) Flights 27R and 29R was instrumented with 12 static pressure transducers located circumferentially at the 763 inch body station as shown in Fig. 1. Pressure data recorded with this instrumentation were then used to establish the SRB pitch and roll characteristics during reentry with the semi-empirical computer code "BATER" (Booster Aerodynamic Trajectory Evaluation and Reconstruction). This note describes the use of BATER to model SRB pitch and roll maneuvers for these flights, the effect that inaccuracies in radar velocity data and atmospheric pressure profiles have on the results, and comparisons of the results with other STS flights.

BASIC PROCEDURE

The methodology used to establish SRB angles-of-attack and roll during reentry is described in detail by Hair and Engel [1]. It uses flight static pressure measurements to determine the location of the stagnation pressure and the SRB circumferential pressure distribution. The location of maximum calculated pressure is used to establish the SRB roll orientation, and the stagnation pressure coefficient is used to determine the SRB angle-of-attack with respect to the SRB body axis. The angle-of-attack and roll angle are defined from 0 to 180 deg as shown in Fig. 2.

Raw pressure data from flights STS-27R and STS-29R are initially provided for program BATER. After accounting for the zero shifts for each of the pressure transducers, BATER compares the pressure readings around the SRB circumference to establish the location of maximum pressure. This stagnation pressure location is determined by comparing five different curve fits through the circumferential static pressure data that are centered about the peak reading. BATER then selects the curve fit with the minimum standard deviation to find the stagnation pressure coefficient and its location on the SRB circumference.

BATER models the SRB angle-of-attack with a proven parallel shock theory for swept cylinders when the SRB is at high angles-of-attack ($Cp_{stag} > 0.35$). This theory allows the angle-of-attack to be expressed implicitly in terms of the static pressure ratio across the shock and the free-stream Mach number with the relation

$$P3/P1 = \left[\frac{7M^2\sin^2(\alpha) - 1}{6}\right]\left[1 + (0.2)\frac{M^2\sin^2(\alpha) + 5}{7M^2\sin^2(\alpha) - 1}\right]^{3.5}$$

This equation can also be expressed in terms of the function $n = 7M^2\sin^2(\alpha)$ to produce a seventh-order polynomial that can be solved numerically. The real positive roots of this polynomial are determined in program BATER and compared with an approximate solution for $\sin\alpha$ to establish the SRB angle-of-attack.

When the maximum pressure coefficient is less than 0.35, the SRB is assumed to be at an angle-of-attack approaching 180 deg. Here the parallel shock theory can no longer be applied, and an extrapolation of empirical data is used to establish the SRB angle-of-attack from the stagnation pressure coefficient as shown below.

$$\alpha = \sin^{-1}\left([0.53694\,C_p]^{1/2.2}\right)$$

EXPERIMENTAL PROCEDURE AND DATA MANIPULATION

The 12 static pressure transducers were mounted at 30 deg intervals around the SRB circumference to provide static pressure measurements for analysis by BATER. Tare pressure readings were established for each transducer from these data during the period from 150 to 250 sec after liftoff, when the SRB trajectory is near its apogee (Table 1). These tare readings were then subtracted from each transducer measurement over the full range of the flight. While previous flights were instrumented with additional pressure ports to establish the SRB nose-tail orientation with respect to the ground, the current analysis assumed that the SRB would be in a tail-first orientation after 270 sec into the flight.

Values for the SRB free-stream velocity were obtained by differentiating the radar range and altitude data collected during the STS-27R and STS-29R flights. Manipulation of these data resulted in the development of a data file that contained SRB altitudes and velocities at 0.1 sec intervals throughout the flight. The considerable scatter that resulted in the calculation of these SRB velocities was eliminated with the use of either a polynomial or an exponential curve fit in the analysis.

Free-stream pressures, temperatures, and densities used in the analysis were obtained from either balloon measurements collected prior to the shuttle ascent to orbit or from 1963 Patrick atmospheric tables. When ascent trajectory measurements were used, the ambient conditions at altitude were assumed to be the same at corresponding altitudes during the ascent and reentry portions of the flight. The use of this "Best Estimated Trajectory" (BET) data with the SRB radar velocity data and static pressure readings provided BATER with all of the information needed to calculate the SRB angle-of-attack and roll orientation as a function of the SRB altitude and time in flight at 0.1 sec intervals.

RESULTS AND DISCUSSION

BATER calculations of the SRB angle-of-attack and roll orientation resulted in the development of angle-of-attack and roll angle plots for both STS-27R and STS-29R flights as shown in Figs. 3–6. Both test cases were limited to periods between 270 and 328 sec after lift-off because of limitations in the pressure and radar velocity data. Data for flight STS-29R were also limited due to data system malfunction during the time periods from 293.0 to 296.1 sec, 308.1 to 309.5 sec, and 324.2 to 328.0 sec. The results shown in these figures were established using exponential velocity curve fits for the velocity data and the ascent trajectory BET pressure profiles. Figures 7 and 8 present correlations between differentiated radar velocity data and this exponential velocity curve fit. Variations in the velocity curve can be expected to have an effect on the angle-of-attack, as shown in Fig. 9 for flight STS-29R with the 1963 Patrick pressure profile.

Similarly, the effect of ambient pressure on SRB reentry angle-of-attack was also investigated. During the analysis of BATER calculations for flight STS-29R, it was observed that the ambient pressures for flights STS-27R and STS-29R were considerably lower than for the historic flights STS1-6 as well as many of the reference atmospheric models. This difference was as much as −23 percent in the case of flight STS-29R. The BET pressure profiles are believed to be in error. Consequently, a 1963 Patrick atmospheric model was incorporated into BATER to generate data that could be directly compared with the results from flight STS-29R using the actual BET ambient conditions. (The Patrick model is more representative of the ambient conditions for flights STS1-6.) When 1963 Patrick atmospheric data are used, a significant increase results in the calculated angle-of-attack as shown in Fig. 10. These increases in angle-of-attack result from the corresponding decrease in the calculated pressure coefficient.

Since both STS-27R and STS-29R BET ambient conditions appeared low (−23 percent for STS-29R and −8.5 percent for STS-27R) compared to historic data, a method was sought that would allow a more accurate determination of the ambient pressure during reentry than was apparently defined by the BET ascent trajectory. Both the BET and Patrick atmospheric pressure profiles resulted in a predicted angle-of-attack that seemed to dwell at 180 deg for extended periods of time. This suggested that the ambient pressures might be exceeding the surface pressures. In order to study this possibility in more detail, the SRB circumferential pressure distributions were evaluated to establish the times at which the SRB pressure distributions were most uniform, corresponding to a vertical or 180 degree orientation. Since the pressure coefficients would be zero at this orientation, the ambient and surface pressures had to be equal at these times. The average circumferential surface pressure reading was therefore assumed to be closer to the actual ambient pressures and used to develop an empirical pressure profile for use in BATER calculations. Table 2 presents the results of this analysis, with PINF being the averaged circumferential surface pressure. PINF is the BET ambient pressure.

Because of the added possibility of exceeding the maximum allowable pressure coefficient when the SRB is normal to the free stream, a further study was conducted to modify the BET pressure profile to ensure that no stagnation pressure would exceed

the maximum allowable stagnation pressure as defined by normal shock theory. This involved a direct comparison between the measured stagnation pressures and theoretical stagnation pressures behind a normal shock that were based on local BET ambient conditions. Whenever the measured stagnation pressure was found to exceed this theoretical limit, the BET ambient pressure was assumed to be in error and was appropriately modified to restrict the maximum stagnation pressures in the BATER calculations. These efforts to modify the BET pressure profile led directly to the development of empirical ambient pressure profiles for STS-27R and 29R. These are presented in Fig. 11and compared with the BET and Patrick pressure profiles. The change in slope of the calculated pressure profile, shown in Fig. 11(a), resulted from a change in the criteria used to determine the ambient pressure during the reentry. The ambient pressure was established by limiting the maximum possible stagnation pressure at higher altitudes and by limiting the excessive dwell at 180 deg at lower altitudes. Such a modification in the criteria for calculating the pressure was not required for flight STS-29R as there was no need to limit the maximum stagnation pressure during the reentry. When the resulting empirical pressure profiles were incorporated into the BATER calculations, the excessive dwell was eliminated from the angle-of-attack profiles. Figure 12 demonstrates this improvement for flight STS-27R.

The BATER program calculates the SRB reentry angle-of-attack and roll orientation from a body centered reference frame (Fig. 2). Due to the coordinate system chosen for angle-of-attack and roll, SRB pitch past α = 180 deg and continuous roll from 0 to 360 deg are not calculated. Ranges of α are from 0 to 180 deg and ϕ from -180 to +180 deg (Fig. 3). The presentation of the resulting values of vehicle α and ϕ, therefore, indicate a more rapid motion than visual reentry observations convey. An analysis of the flight data suggests that the SRB does pitch beyond its vertical position when its angle-of-attack approaches 180 deg and the SRB experiences a corresponding shift in the location of maximum pressure by approximately 180 deg. Such an interpretation is suggested for flight STS-27R at 289.5 sec [Figs. 3(a) and (b)]. Similar interpretations of the SRB pitch and roll behavior can be made for flight STS-27R at approximately 271.5, 282.5, and 294.5 sec into the flight. An example of this is shown in Fig. 13 in the form of circumferential pressure distribution variation over the time frame 280.7 sec to 290.1 sec. Note the stagnation line location at t = 288.7, 289.5 and 289.9 sec. If one assumes that these periods of rapid shift in the location of maximum pressure result from a pitch beyond α = 180 deg, a more gradual SRB pitch and roll maneuver can be predicted, than shown in Figs. 3 and 4. BATER was modified to assume that a pitch past α = 180 deg would occur whenever the roll orientation shifted from 70 to 290 deg within a 0.5 sec time period. Based on these modifications, reentry orientation calculations for the lefthand SRB in STS-27R were made and are presented in Figs. 14 and 15. As previously stated, the pitch and roll motion is more gentle than that of Fig. 3. This is not to imply that the BATER calculations of Fig. 3 are in error, only that from a visual data presentation standpoint, the modified BATER results tend to line up with visual observations of SRB reentry more than the standard BATER output. Due to the compatibility of the standard BATER results with the STATE reentry heating code used to

calculate SRB reentry heating, STS-27R and -29R reentry orientation calculations were retained in the original format.

The BATER-generated angles-of-attack for STS-27R and 29R were compared with the statistical envelopes for the lofted and non-lofted trajectories taken from Ref. [2]. This comparison is shown in Fig. 16. The statistical trajectories were composed of 200 Monte Carlo simulations, and the comparison shows that the BATER reconstructions for STS-27R and 29R are within the design envelopes. The data presented in these correlations for flight STS-29R were modified to reflect faired angle-of-attack values during those time periods in which zero pressure readings were obtained. Figure 17 also presents a direct comparison of the angle-of-attack histories for flights STS-27R and STS-29R with flights STS-3, STS-5, and STS-6 during similar reentry time periods [3] to further verify the results of the current analysis. Excellent agreement is observed between STS-5, 6, 27R and 29R in period and damping. STS-3 has a much longer period and less damping. This is believed to be attributable to the much higher apogee experienced by STS-3. Consequently, at the same trajectory time, the dynamic pressure is lower. Table 3 presents a brief reentry event time history for these flights and clearly shows that the maximum dynamic pressure and transition to subsonic flight occurs some 12 to 13 seconds later for STS-3.

This analysis of the SRB reentry was particularly successful in demonstrating the effects of variations in the ambient pressure and velocity on the SRB angle-of-attack and suggests that future analyses take these effects into consideration. Appendix A presents the final tabulated results for flights STS-27R and STS-29R from 270 to 328 sec into their flights at 0.1 sec intervals. These results are based on SRB altitudes established from the radar trajectory data and BET ambient pressures that were modified to eliminate both excessive dwell at 180 deg and pressure coefficients that exceeded maximum allowable values. The SRB velocities were obtained from the exponential curve fit through the radar trajectory velocity data, and corresponding values for the Mach number and dynamic pressure are provided.

REFERENCES

[1] Hair, M. Leroy and Engel, Carl D., "Calculating SRB Alpha and Roll from 16 Static Pressures ('BATER')", RTN 039-12, June 15, 1982.

[2] Engel, Carl D., "SRB Reentry Thermal Environment Data Book Vol. 1, Steel Case SRB with Nozzle Extension-On Reentry Thermal Environment," RTR 039-13, Jan. 1986.

[3] Engel, Carl D., "STS-6 SRB Reentry Heating Flight Evaluation," Volume I, RTR 039-12, Oct. 1983.

FIGURES

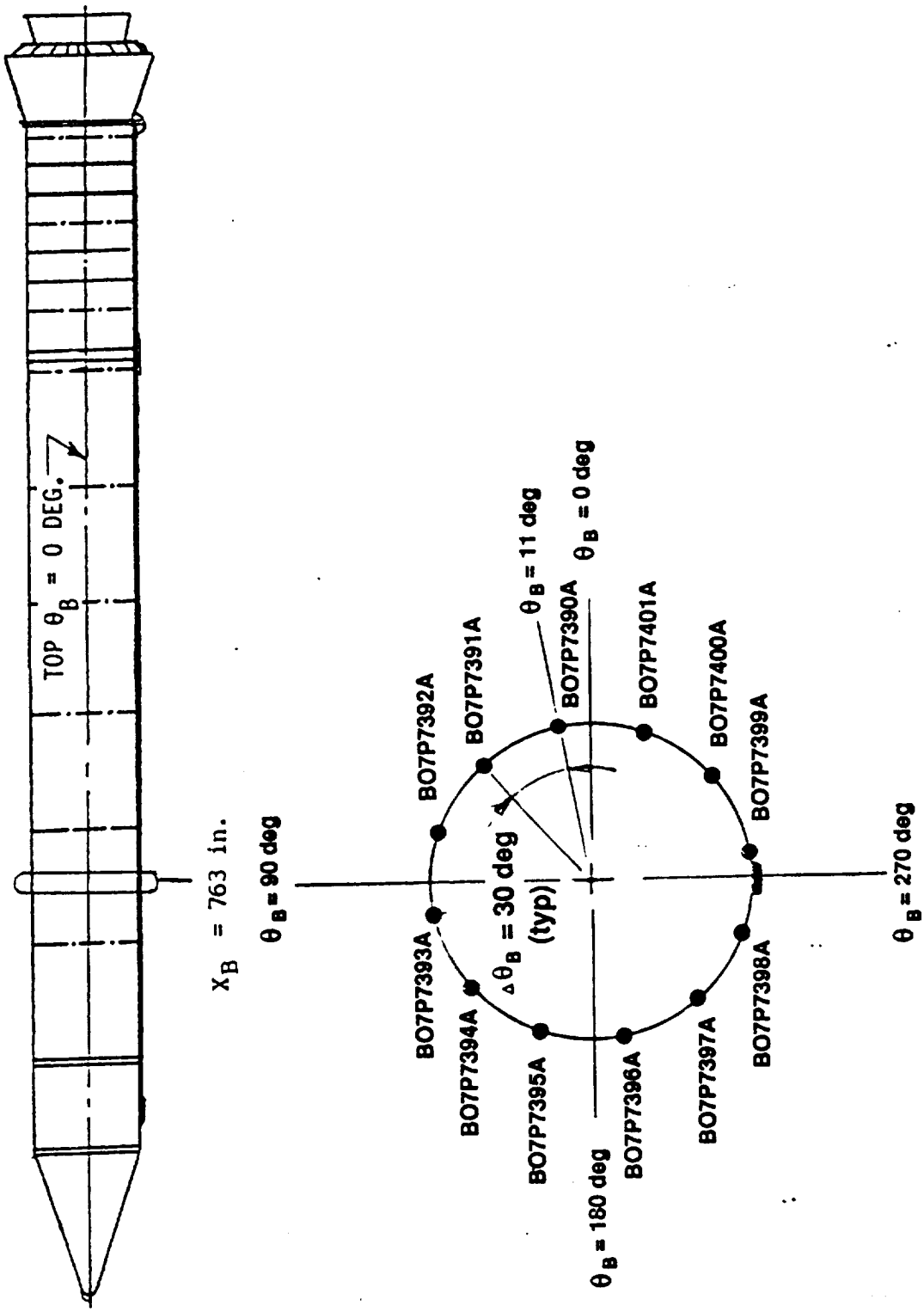

Figure 1: SRB DFI External Pressure Instrumentation (STS-27R, 29R)

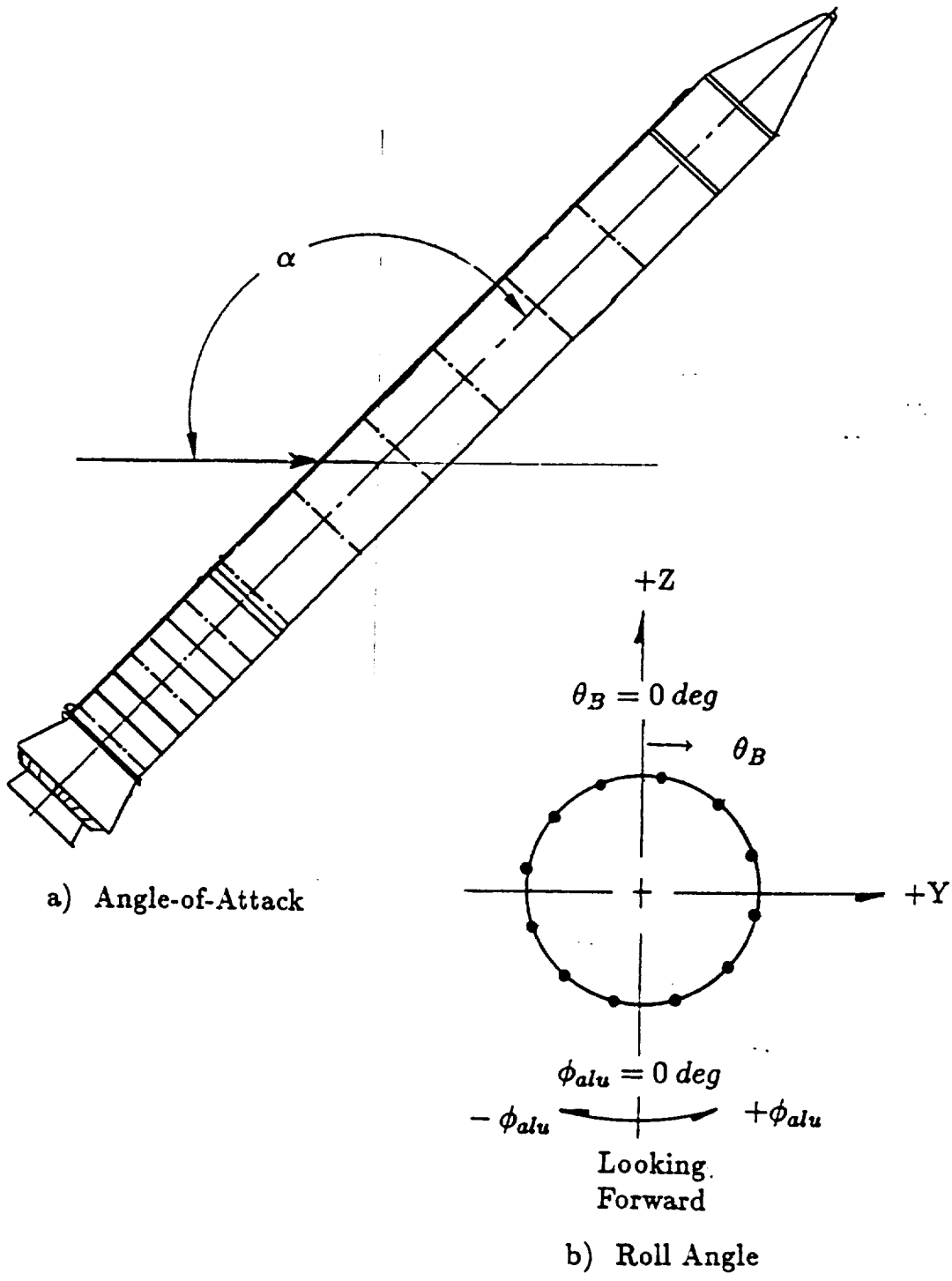

Figure 2: Angle-of-Attack and Roll Definition

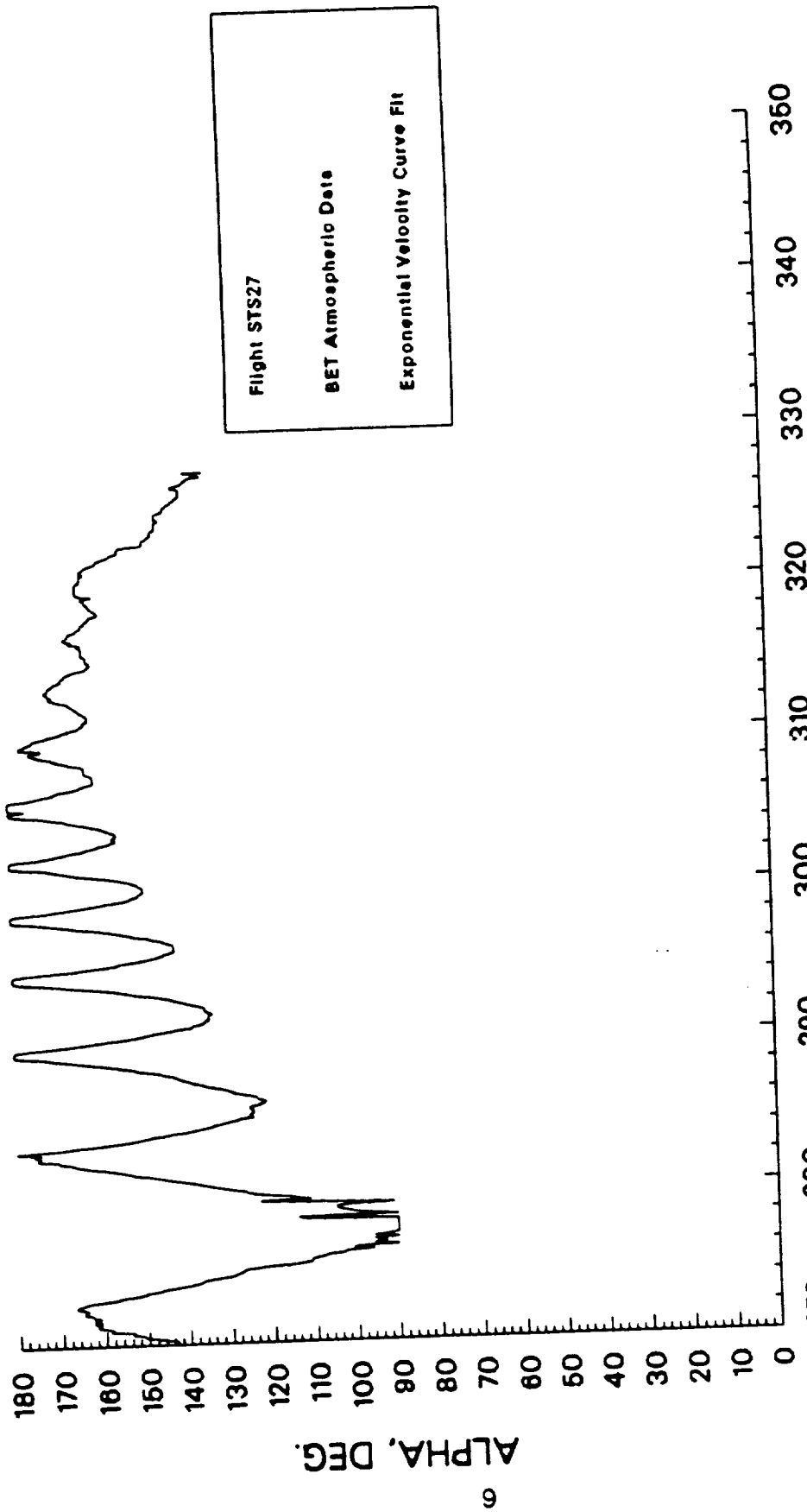

a) L/H SRB Angle of Attack

Figure 3: SRB Reentry Orientation for STS-27R

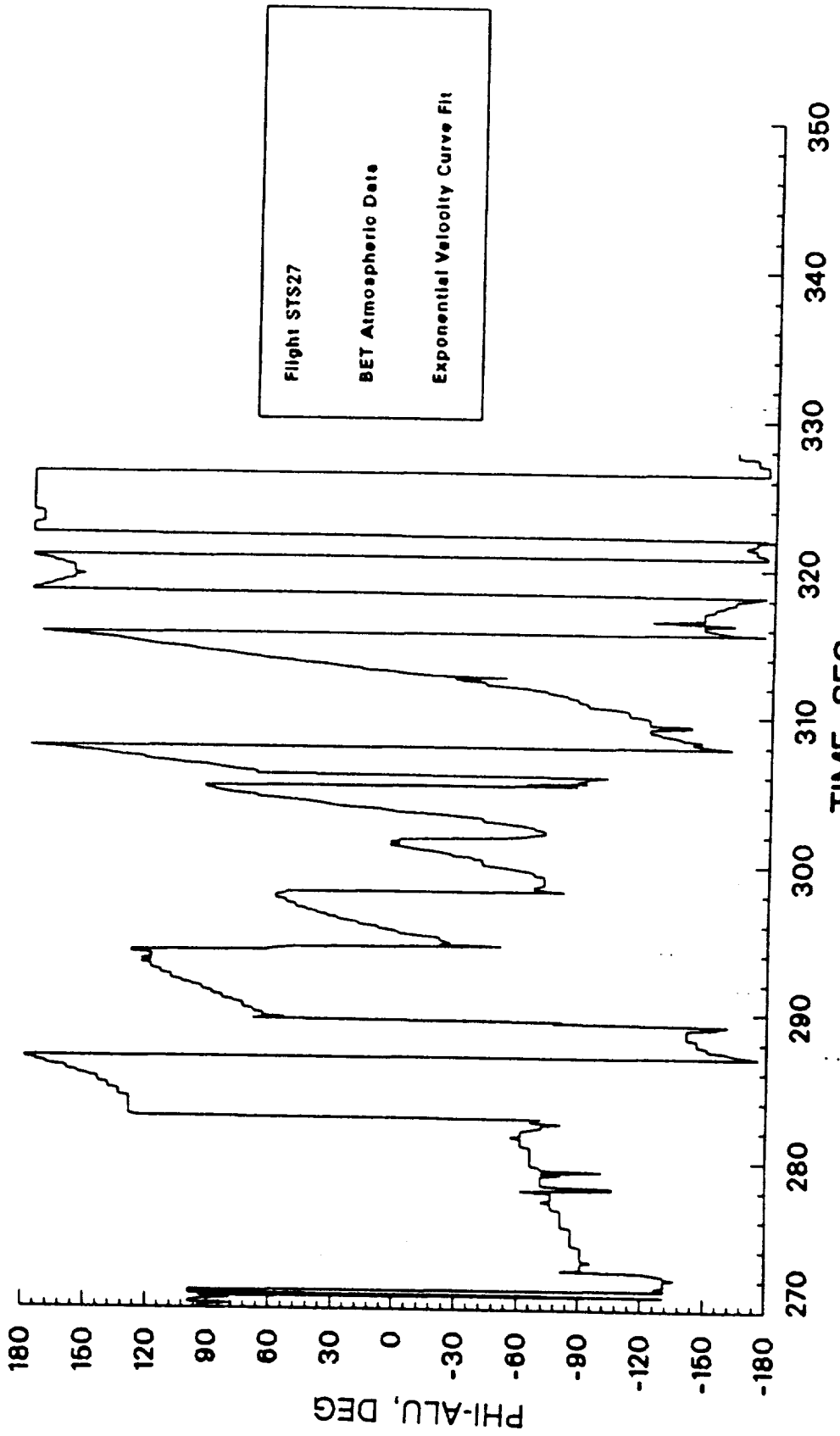

b) L/H SRB Roll Angle

Figure 3: SRB Reentry Orientation for STS-27R (Concluded)

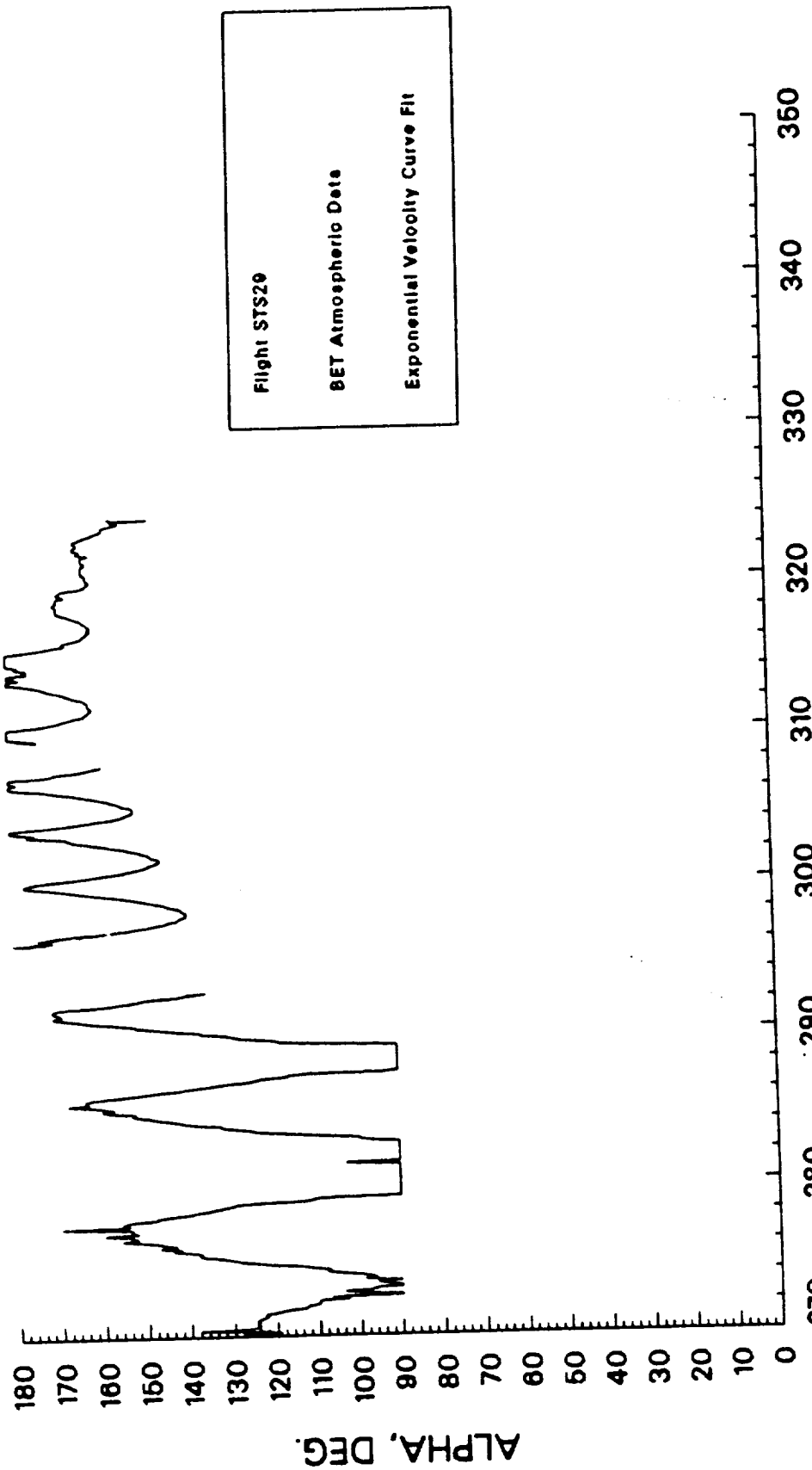

a) L/H SRB Angle of Attack

Figure 4: SRB Reentry Orientation for STS-29R

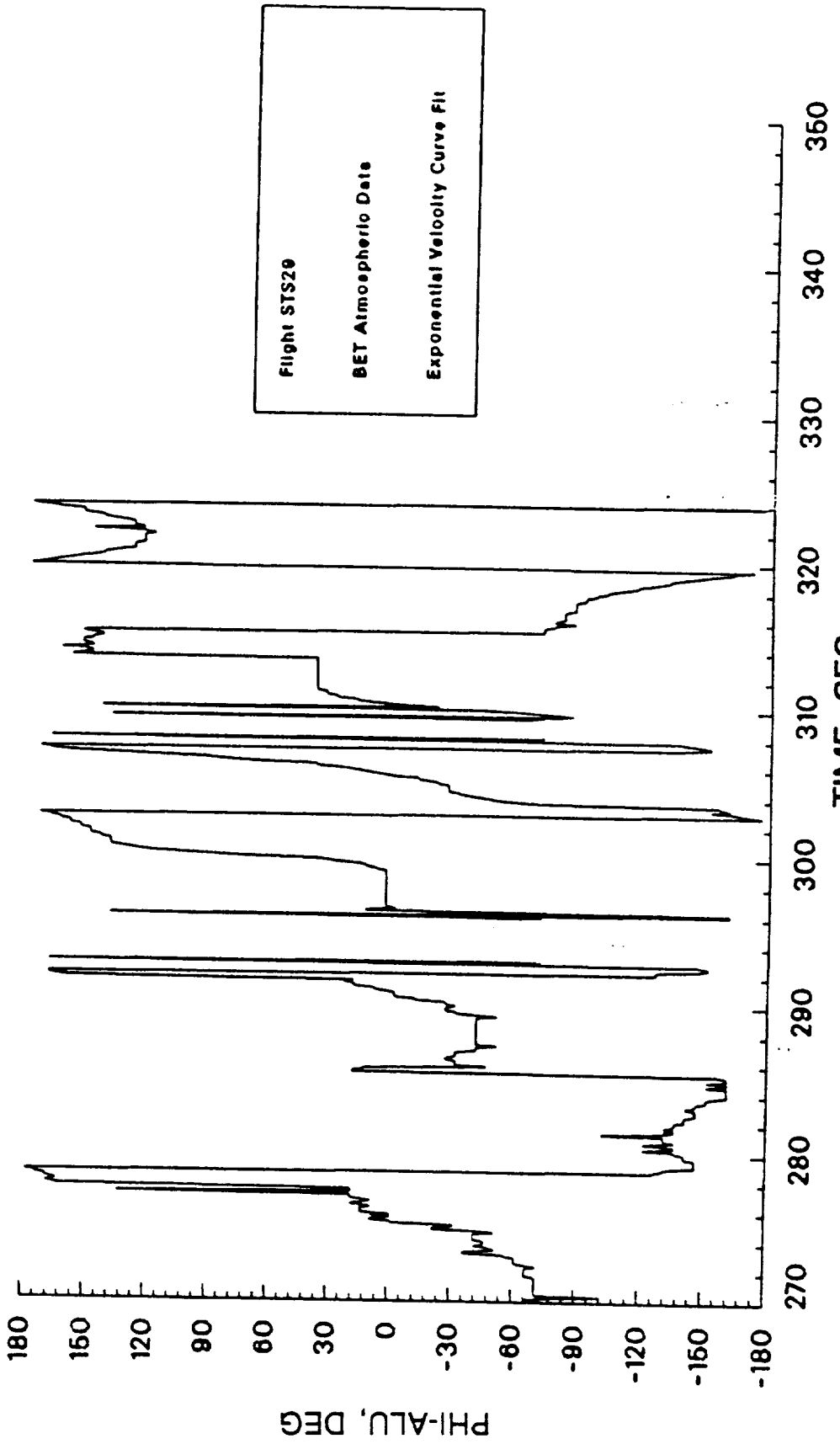

b) L/H SRB Roll Angle

Figure 4: SRB Reentry Orientation for STS-29R (Concluded)

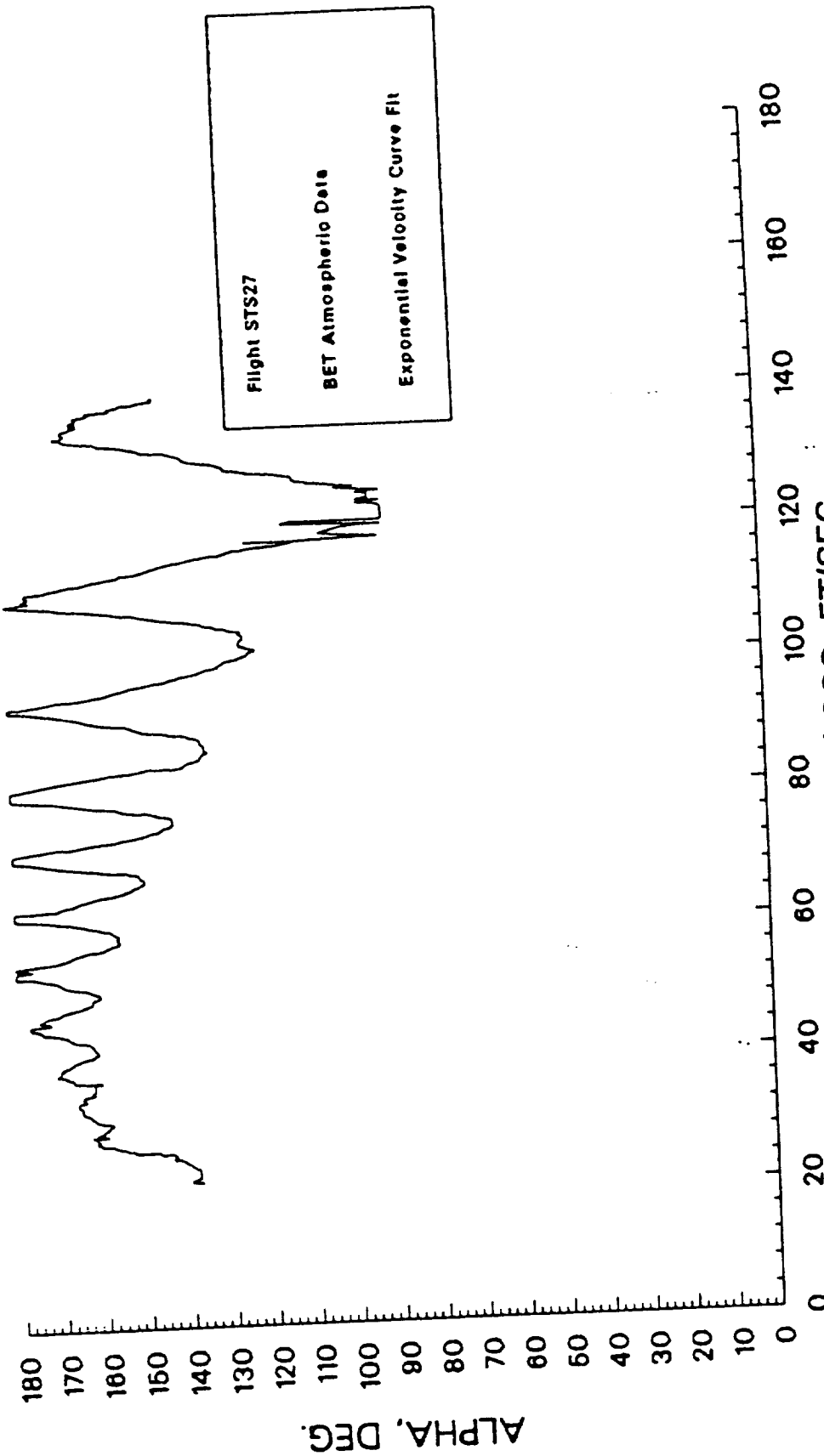

Figure 5: L/H SRB Reentry Angle of Attack with Altitude for STS-27R

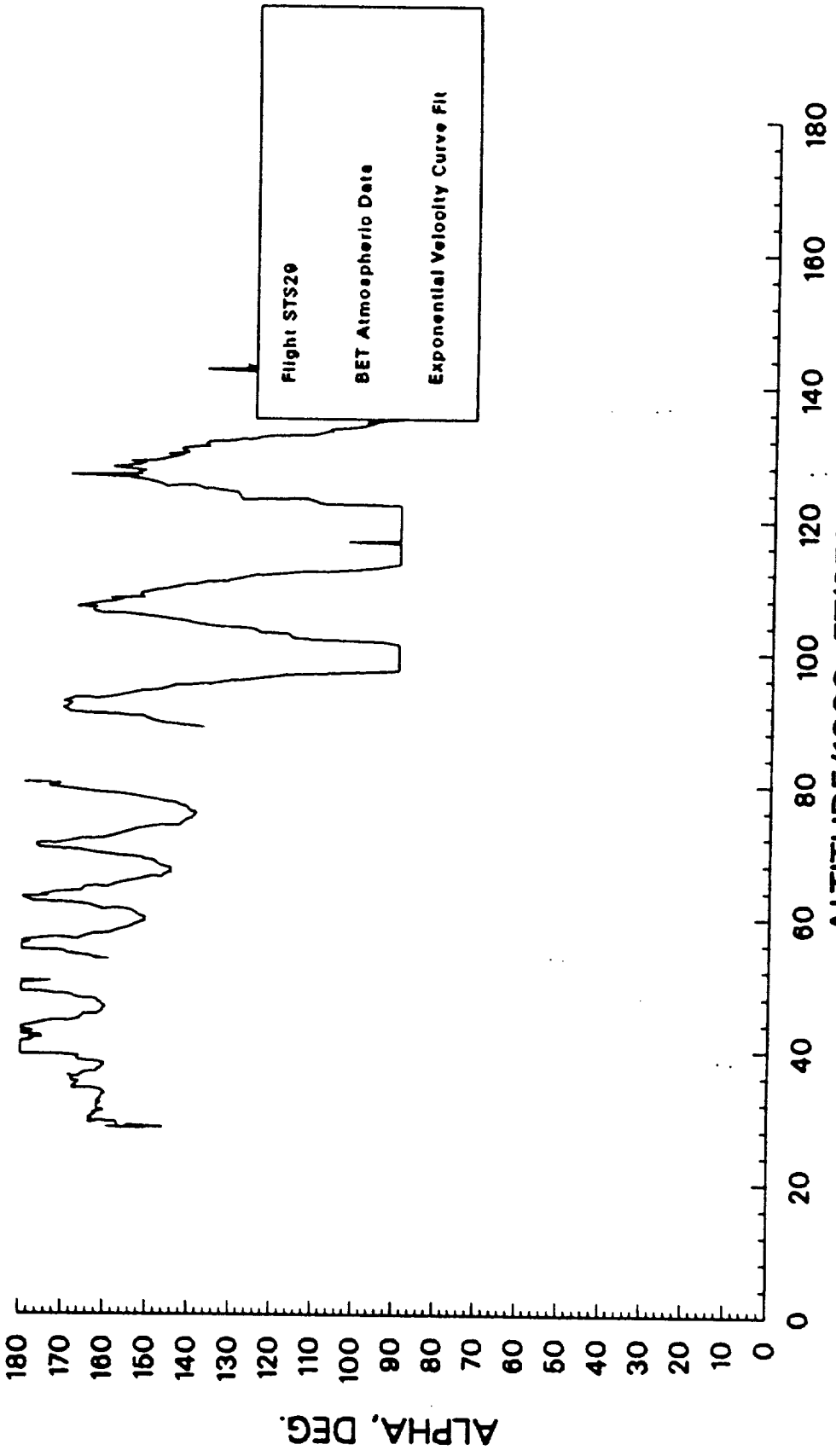

Figure 6: L/H SRB Reentry Angle of Attack with Altitude for STS-29R

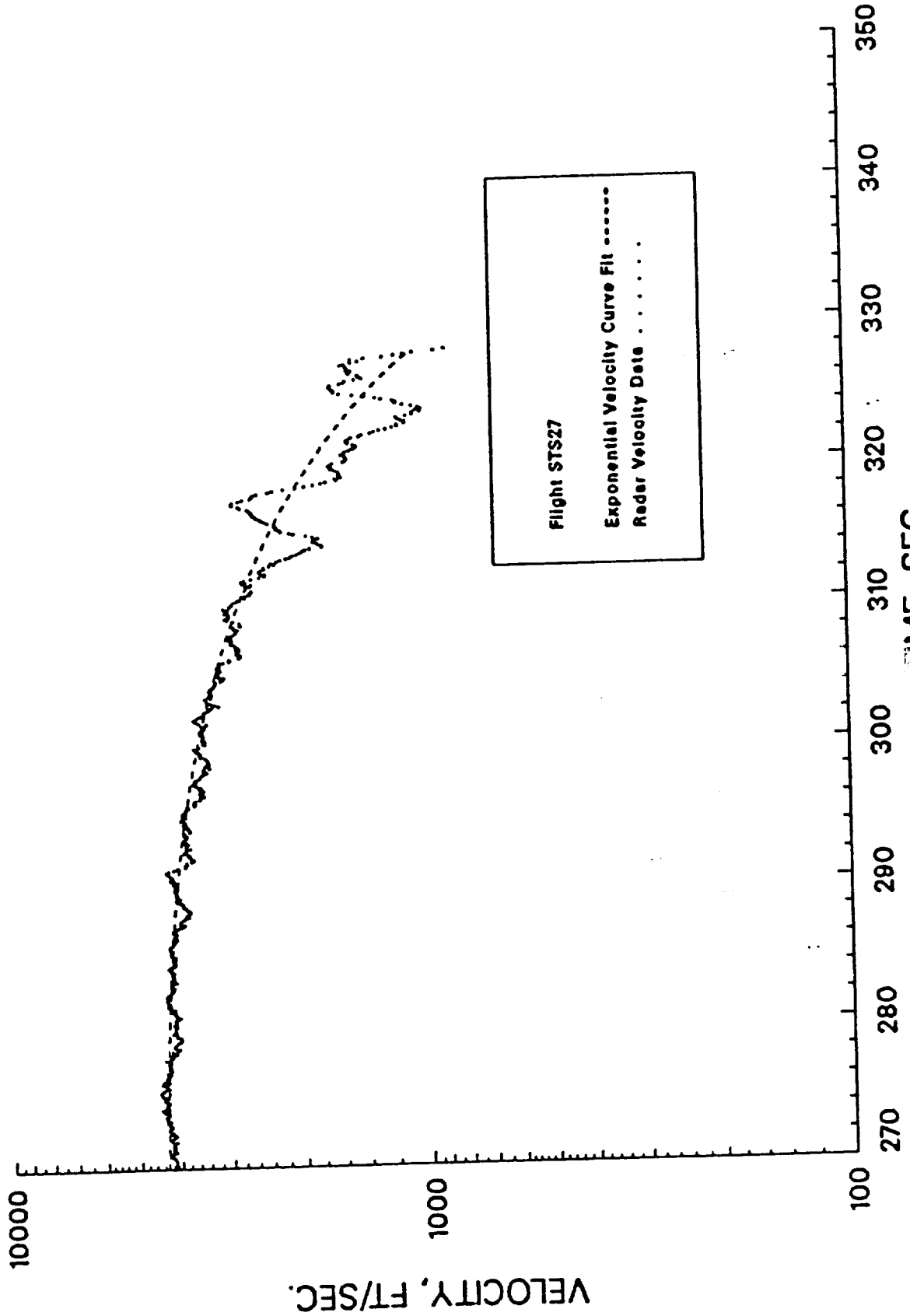

Figure 7: L/H SRB Reentry Radar Velocity for STS-27R

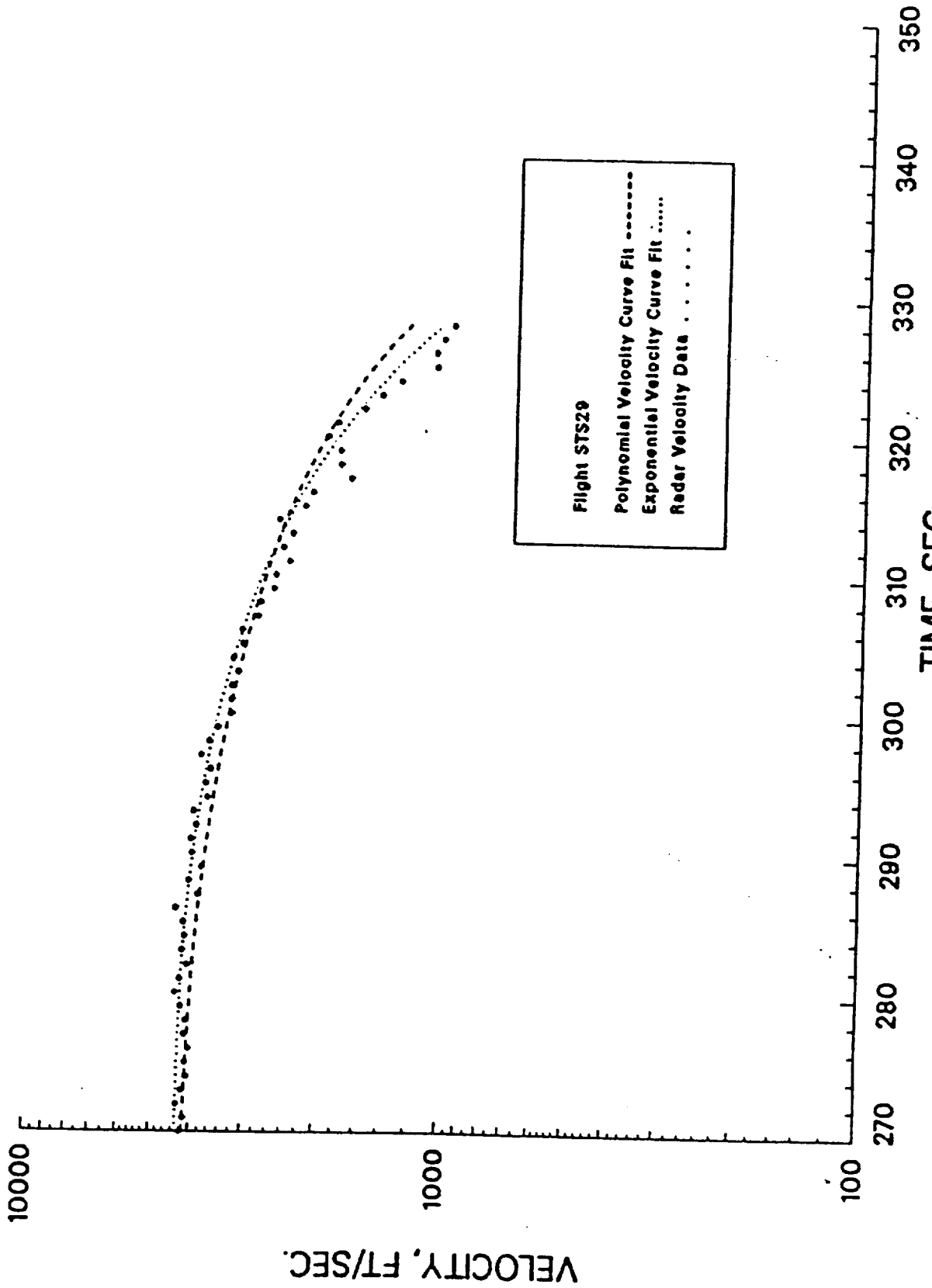

Figure 8: L/H SRB Reentry Radar Velocity for STS-29R

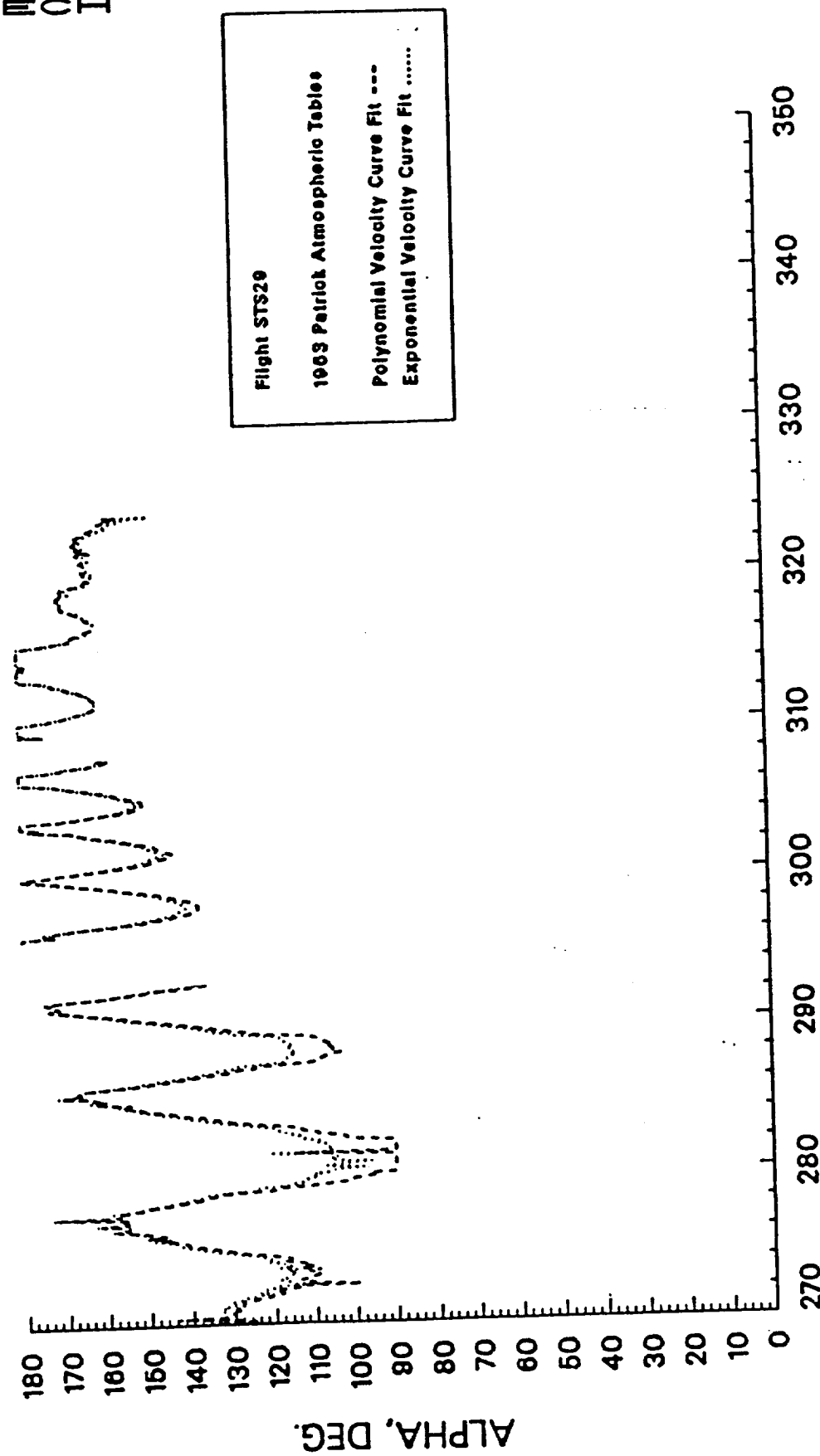

Figure 9: Effect of Velocity Curve Fit on SRB Reentry Angle of Attack

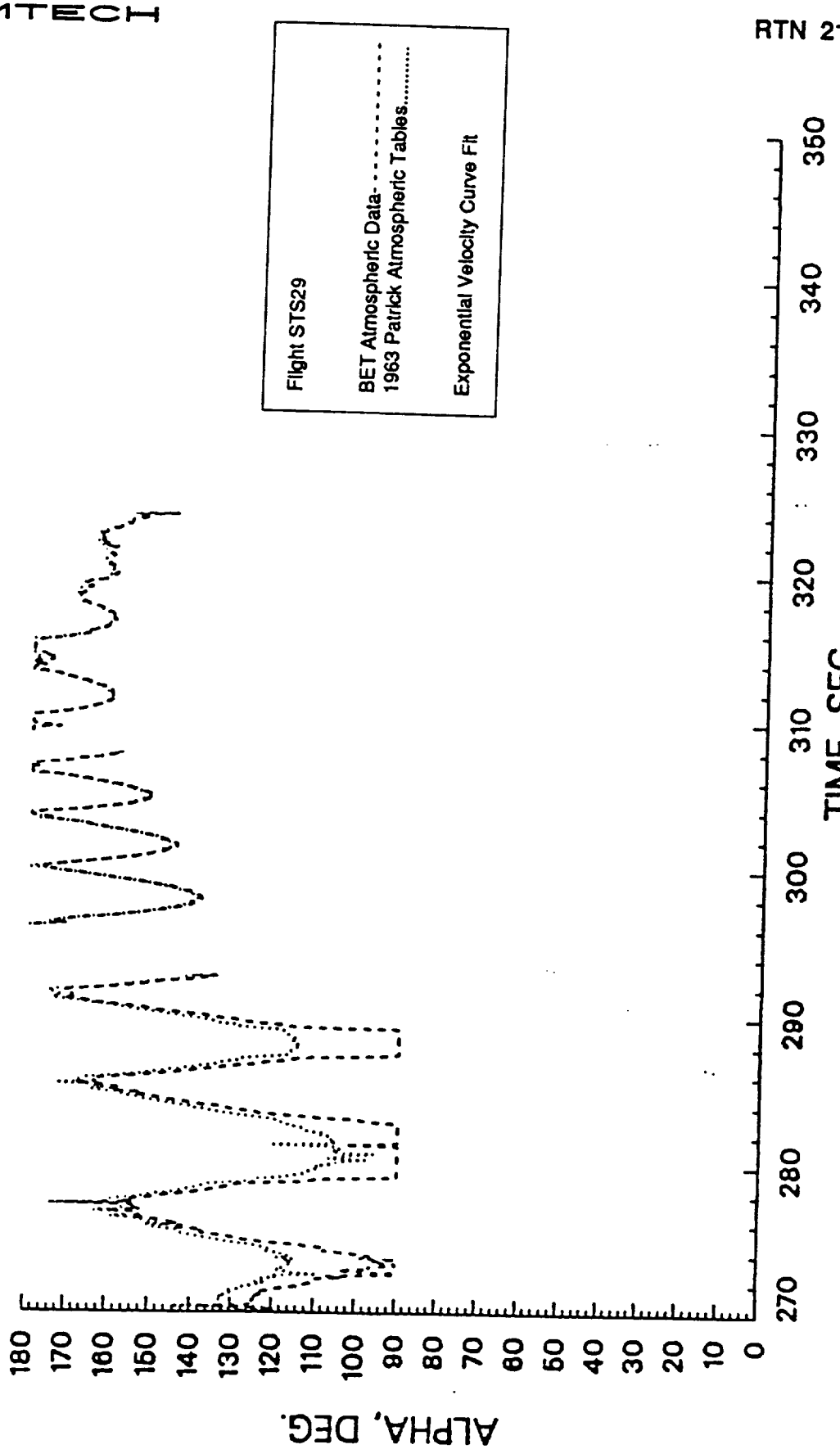

Figure 10: Effect of Ambient Pressure on SRB Reentry Orientation

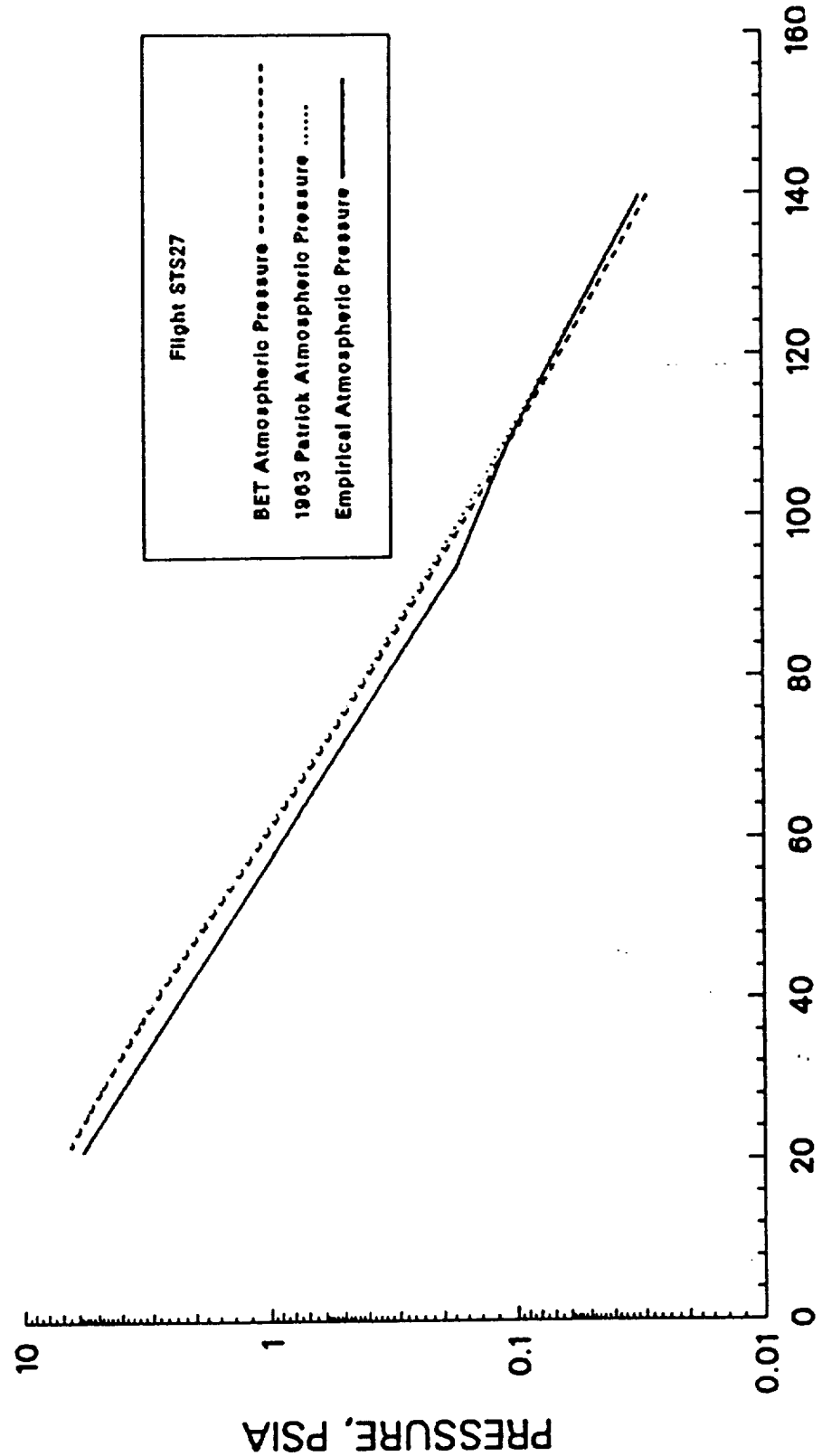

a) STS-27R

Figure 11: SRB Flight Derived Ambient Pressure

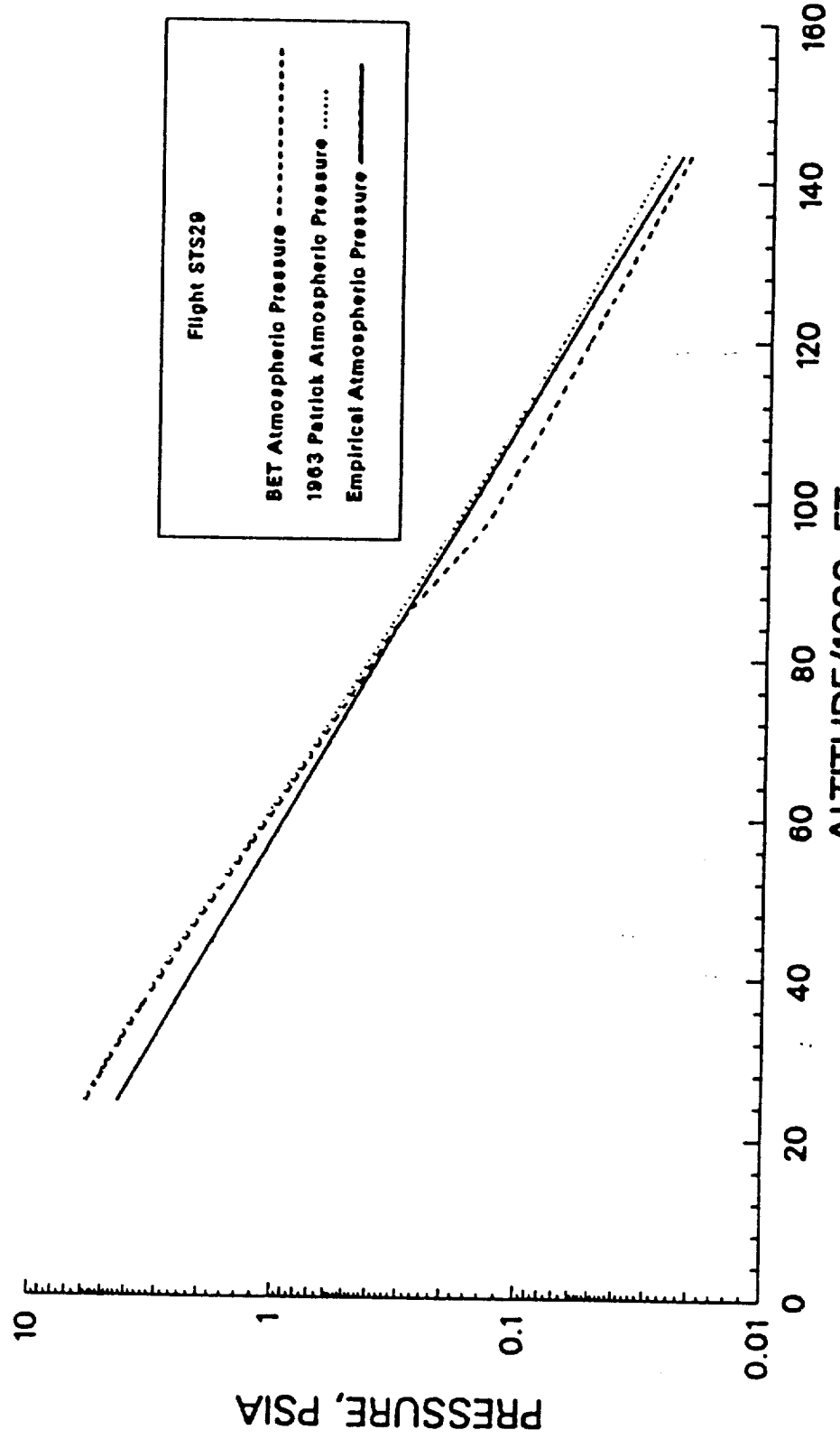

b) STS-29R

Figure 11: SRB Flight Derived Ambient Pressure (Concluded)

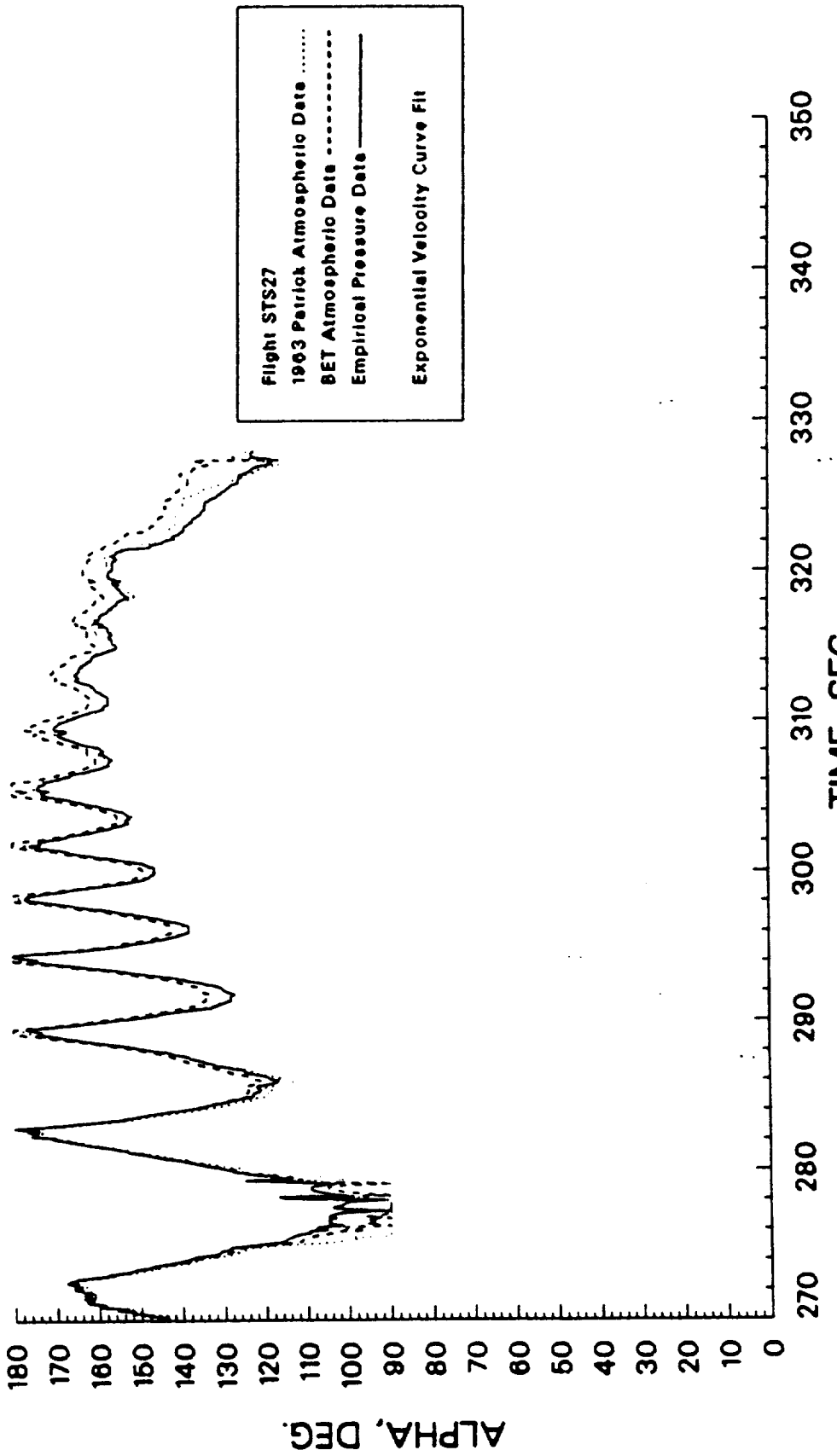

Figure 12: L/H SRB Reentry Angle of Attack Using Flight Derived Ambient Pressure

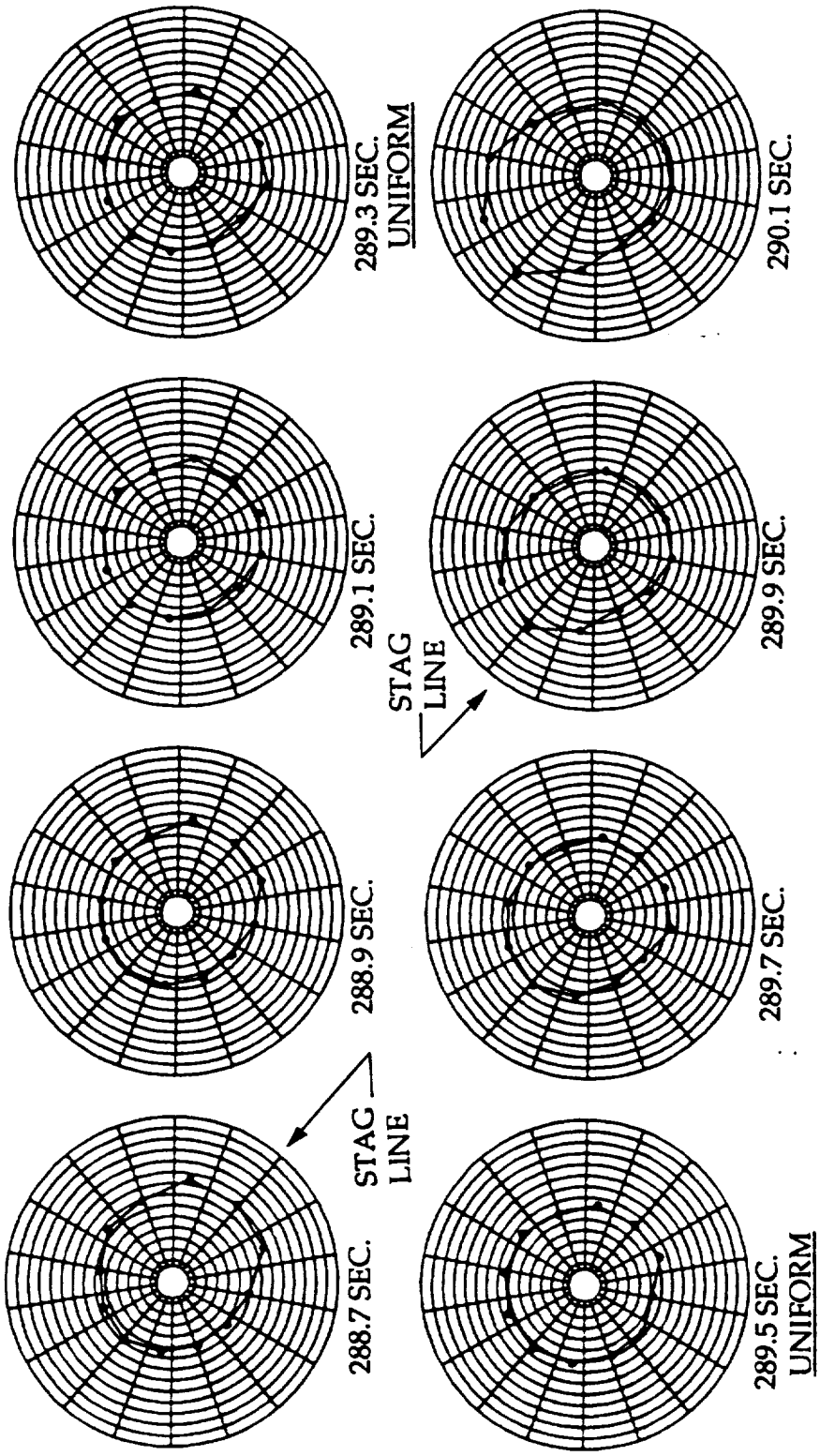

Figure 13: SRB Pressure Distribution Shift for Pitch Past α = 180Deg (STS-27R)

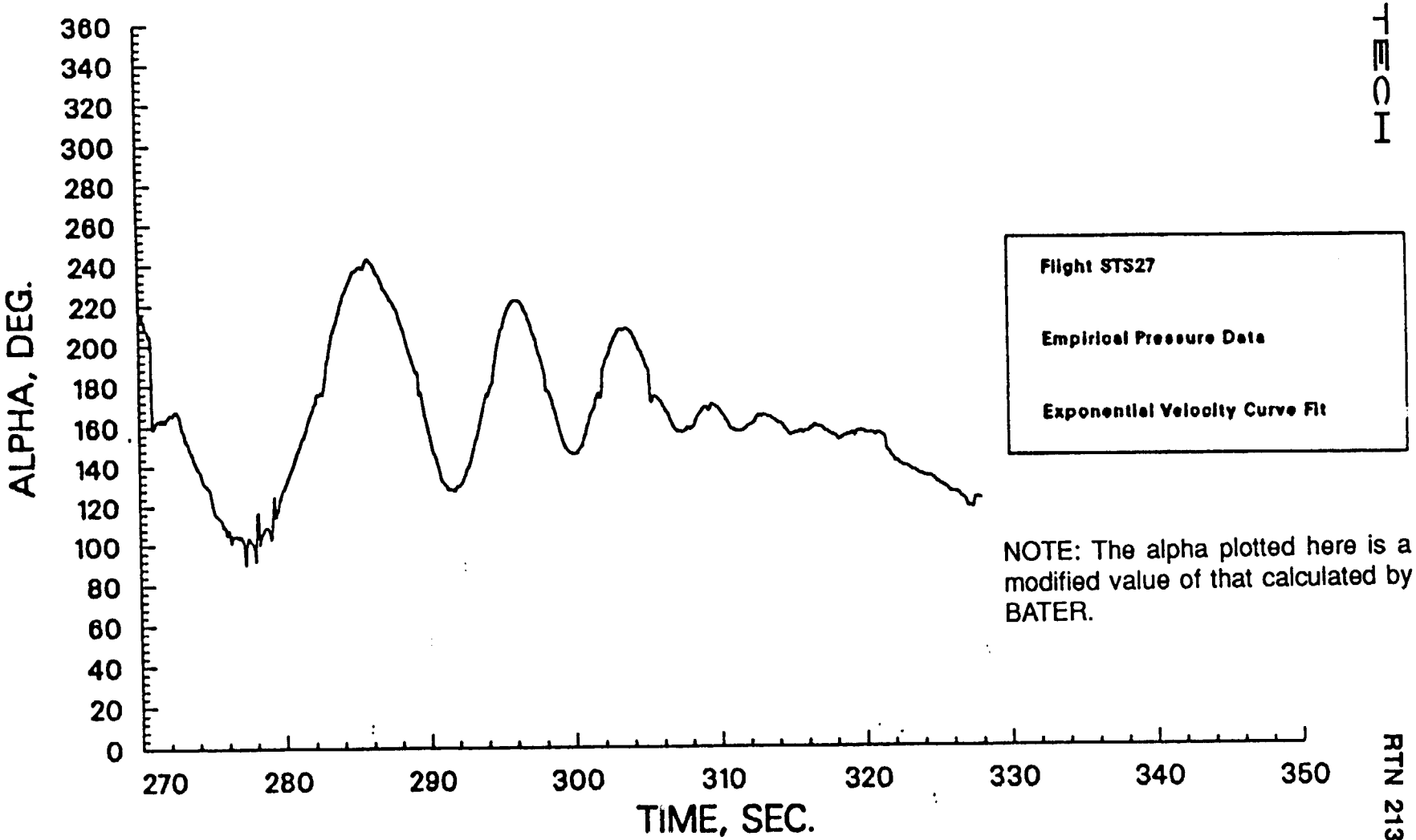

Figure 14: SRB Reentry Angle of Attack History Allowing for Pitch Past180 Deg

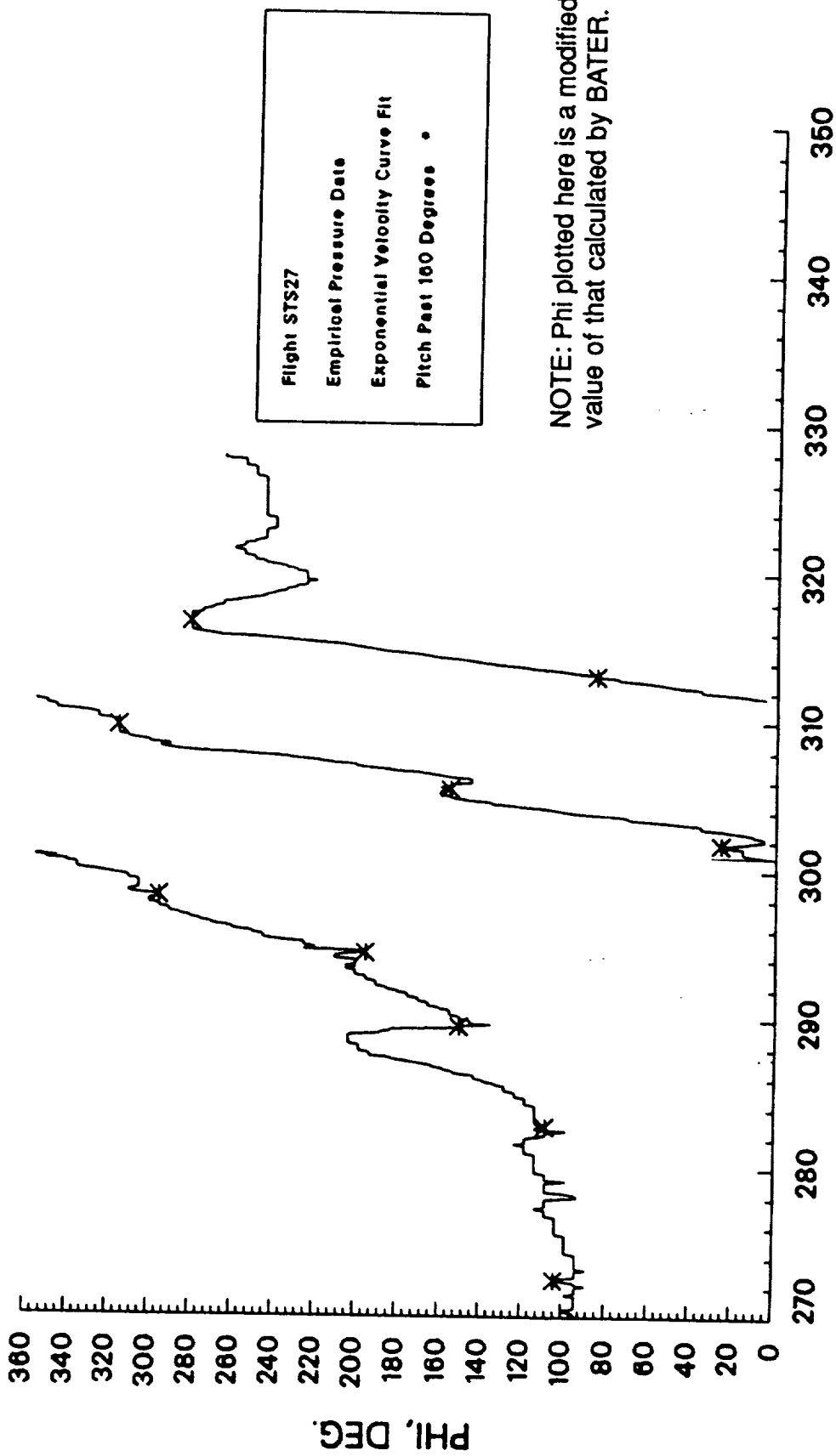

Figure 15: SRB Continuous Roll History

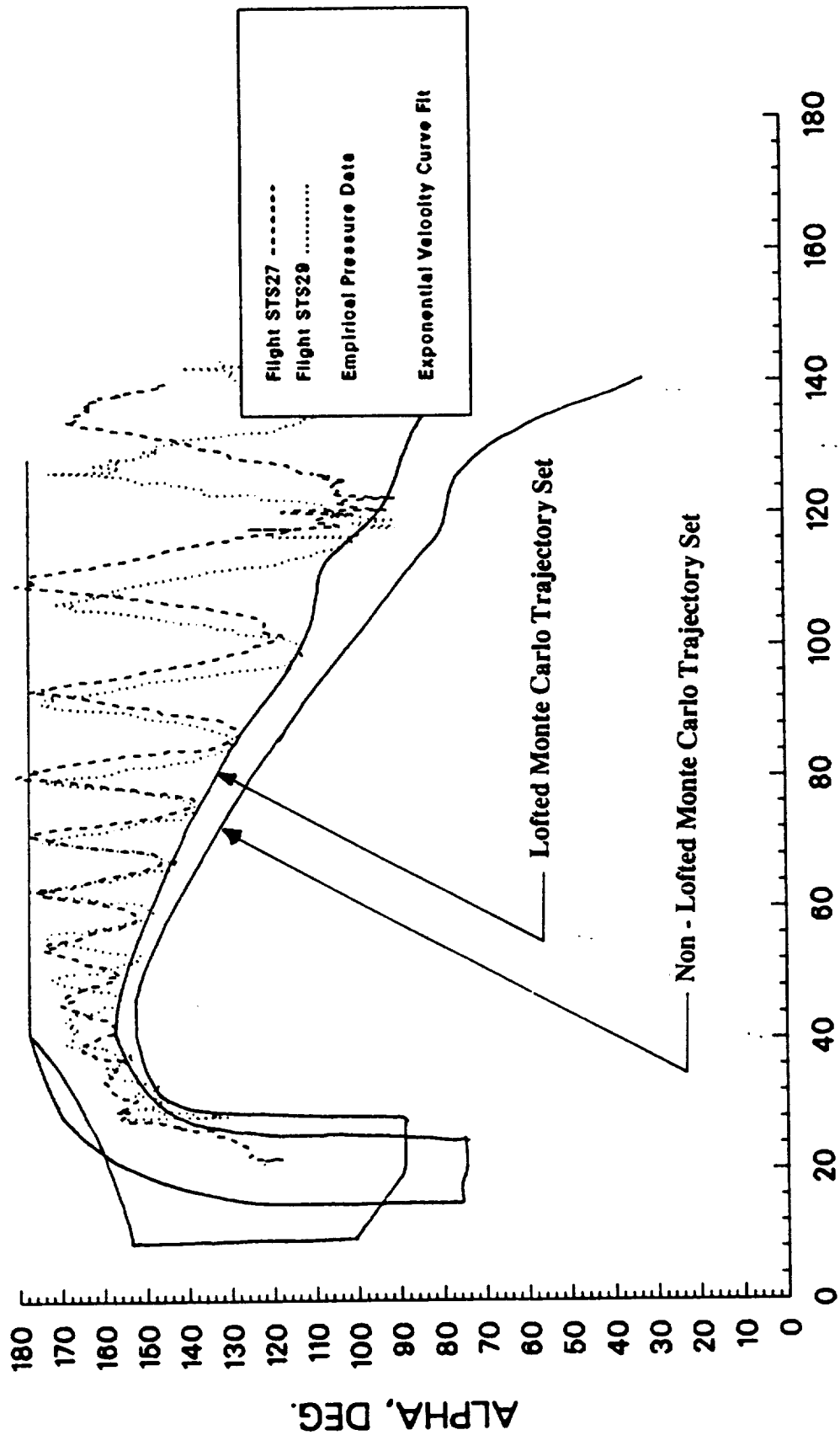

Figure 16: Comparison of STS-27R and 29R Reentry Angle of Attack with the Design Trajectory Set

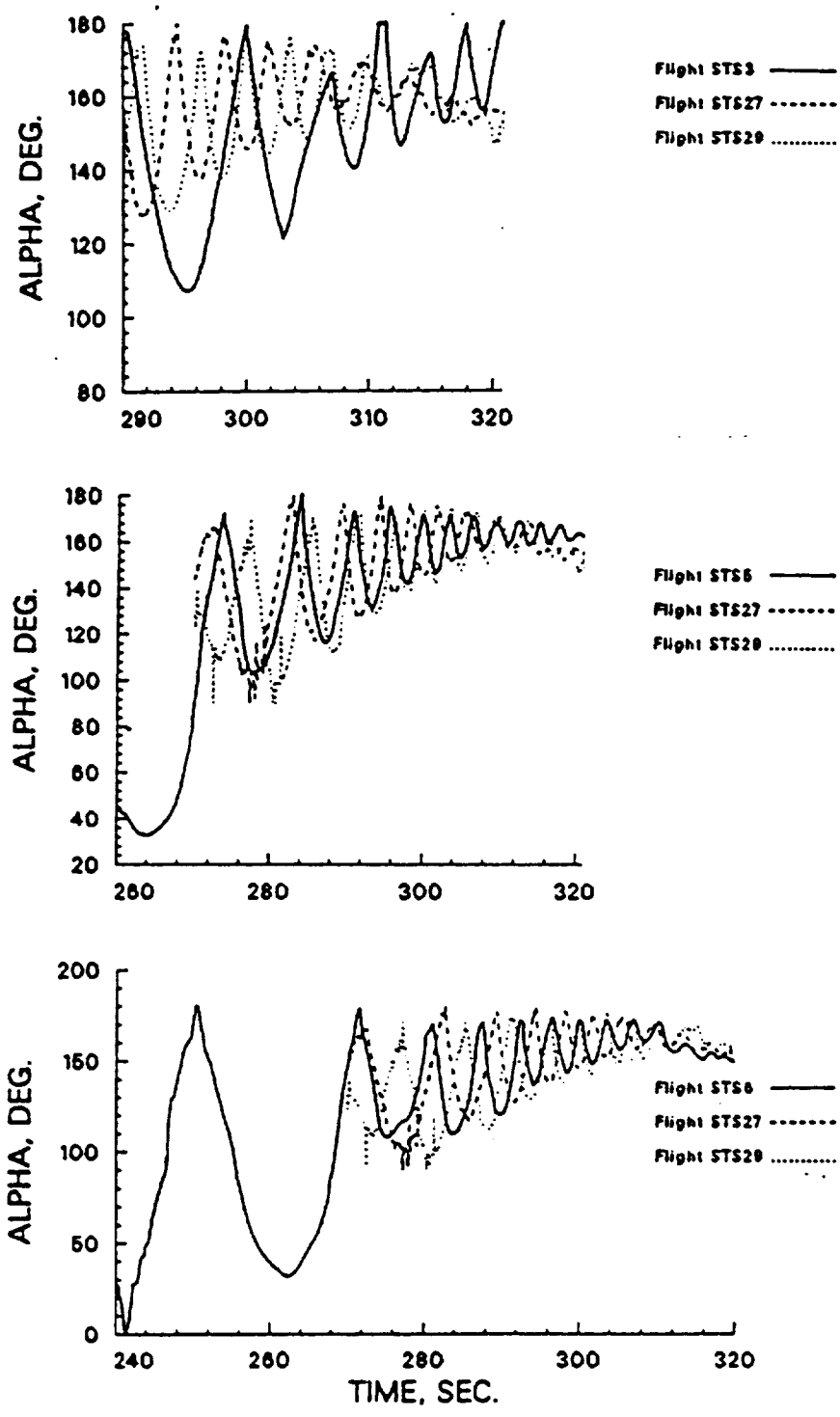

Figure 17: Comparison of STS-27R and 29R Reentry Angle of Attack with Historic Data from STS-3, 5, and 6

TABLES

Table 1: Pressure Transducer Tare Readings in Psia (Gages 1-12 in Sequence)

Flight STS-27R					
.024	.073	.032	−.006	−.005	.095
.072	.059	.720	.084	−.046	.032
Flight STS-29R					
.000	.000	.000	.000	1.600	.013
.080	.080	−.058	.050	.000	.220

Table 2: Atmospheric Pressure Profile Corrections

Time (Sec)	Alt (Ft)	PINF (Psia)	PINF′ (Psia)
Flight STS-27R			
282.300	111000.0	0.096	0.057
289.300	93770.0	0.209	0.137
294.500	80140.0	0.393	0.262
298.300	71390.0	0.597	0.448
301.800	62830.0	0.911	0.696
305.700	53960.0	1.430	1.181
309.500	45940.0	2.145	1.770
313.100	38660.0	3.072	2.407
316.700	33810.0	3.846	3.211
320.400	29000.0	4.758	3.926
Flight STS-29R			
Time (Sec)	Alt (Ft)	PINF (Psia)	PINF′ (Psia)
310.000	49499.9	1.778	1.433
313.900	42303.7	2.544	2.220

Table 3: SRB Reentry Event Time History

	STS-3		STS-27R		STS-29R	
	Time (Sec)	Alt (kft)	Time (Sec)	Alt (kft)	Time (Sec)	Alt (kft)
Apogee	—	247.0	—	226.5	—	226.0
Max Q	324.5	44.6	311.3	41.9	311.8	45.8
M = 1.0	339.8	23.1	327.8	21.2	328.0	24.5

APPENDIX

STS-27R REENTRY TRAJECTORY L/H SRB

SUMMARY FOR FLIGHT STS27.

TIME (SEC)	ALTITUDE (FT)	MINF	VEL (FT/SEC)	PINF (PSIA)	QINF (PSIA)	TINF (DEG R)	ALP (DEG)	PHI-ALU (DEG)
270.0	139900.	4.063	4299.703	0.031	0.356	465.7	144	94
270.1	139800.	4.065	4299.698	0.031	0.358	465.1	146	94
270.2	139500.	4.069	4299.682	0.031	0.363	464.2	145	94
270.3	139300.	4.073	4299.657	0.032	0.366	463.4	147	79
270.4	139000.	4.080	4299.621	0.032	0.372	461.7	149	99
270.5	139000.	4.080	4299.575	0.032	0.372	461.7	152	99
270.6	138700.	4.086	4299.518	0.032	0.378	460.3	152	94
270.7	138400.	4.092	4299.451	0.033	0.383	459.1	156	79
270.8	138200.	4.097	4299.374	0.033	0.387	458.0	154	94
270.9	137900.	4.101	4299.285	0.033	0.393	456.9	160	-131
271.0	137800.	4.103	4299.186	0.034	0.395	456.4	159	99
271.1	137500.	4.111	4299.077	0.034	0.401	454.7	160	99
271.2	137300.	4.114	4298.957	0.034	0.405	454.0	163	99
271.3	137200.	4.116	4298.825	0.034	0.407	453.6	163	-131
271.4	136900.	4.118	4298.683	0.035	0.412	453.1	162	-131
271.5	136600.	4.120	4298.530	0.035	0.418	452.6	164	-126
271.6	136400.	4.122	4298.365	0.035	0.422	452.2	162	-131
271.7	136200.	4.122	4298.190	0.036	0.425	452.0	164	-131
271.8	136000.	4.124	4298.003	0.036	0.429	451.6	162	-131
271.9	135600.	4.126	4297.806	0.037	0.436	451.1	164	-131
272.0	135500.	4.127	4297.596	0.037	0.438	450.8	164	-131
272.1	135300.	4.129	4297.375	0.037	0.442	450.5	166	-136
272.2	135000.	4.130	4297.144	0.038	0.448	450.1	166	-131
272.3	134700.	4.131	4296.900	0.038	0.454	449.8	165	-13
272.4	134300.	4.133	4296.645	0.039	0.461	449.3	166	-12
272.5	134300.	4.133	4296.378	0.039	0.461	449.3	168	-121
272.6	134200.	4.133	4296.100	0.039	0.463	449.2	167	-81
272.7	134100.	4.133	4295.810	0.039	0.465	449.1	166	-91
272.8	133700.	4.135	4295.508	0.040	0.473	448.7	165	-91
272.9	133400.	4.137	4295.194	0.040	0.479	448.3	161	-91
273.0	133300.	4.137	4294.868	0.040	0.481	448.2	158	-91
273.1	132900.	4.139	4294.530	0.041	0.489	447.7	157	-91
273.2	132800.	4.138	4294.180	0.041	0.491	447.7	154	-96
273.3	132600.	4.138	4293.818	0.041	0.495	447.7	152	-91
273.4	132500.	4.138	4293.444	0.041	0.497	447.7	151	-91
273.5	132000.	4.138	4293.057	0.042	0.507	447.6	148	-91
273.6	131700.	4.137	4292.658	0.043	0.513	447.6	147	-91
273.7	131600.	4.137	4292.246	0.043	0.515	447.6	145	-91
273.8	131600.	4.137	4291.822	0.043	0.515	447.6	143	-91
273.9	131200.	4.137	4291.386	0.044	0.523	447.5	141	-91
274.0	130900.	4.136	4290.936	0.044	0.530	447.5	139	-91
274.1	130600.	4.135	4290.474	0.045	0.536	447.6	138	-91
274.2	130100.	4.132	4289.999	0.046	0.546	448.1	137	-91
274.3	129900.	4.132	4289.512	0.046	0.550	448.2	134	-86
274.4	129700.	4.130	4289.011	0.046	0.554	448.4	132	-86
274.5	129600.	4.129	4288.498	0.047	0.556	448.5	131	-86
274.6	129300.	4.127	4287.971	0.047	0.562	448.8	131	-86
274.7	129100.	4.126	4287.431	0.048	0.567	448.9	129	-86
274.8	128700.	4.124	4286.878	0.048	0.575	449.3	129	-86
274.9	128500.	4.122	4286.312	0.049	0.579	449.5	127	-86

SUMMARY FOR FLIGHT STS27.

TIME (SEC)	ALTITUDE (FT)	MINF	VEL (FT/SEC)	PINF (PSIA)	QINF (PSIA)	TINF (DEG R)	ALP (DEG)	PHI-ALU (DEG)
275.0	128100.	4.121	4285.732	0.049	0.588	449.7	123	-86
275.1	127900.	4.120	4285.139	0.050	0.593	449.9	119	-86
275.2	127500.	4.118	4284.532	0.051	0.602	450.1	116	-86
275.3	127500.	4.117	4283.912	0.051	0.602	450.1	115	-86
275.4	127100.	4.115	4283.279	0.052	0.611	450.4	115	-86
275.5	126700.	4.114	4282.631	0.052	0.620	450.6	114	-86
275.6	126600.	4.113	4281.969	0.053	0.622	450.7	113	-81
275.7	126300.	4.112	4281.295	0.053	0.630	450.7	112	-81
275.8	126200.	4.112	4280.605	0.053	0.632	450.6	109	-81
275.9	126100.	4.112	4279.902	0.054	0.635	450.5	110	-81
276.0	125800.	4.113	4279.186	0.054	0.643	450.1	105	-81
276.1	125600.	4.113	4278.455	0.055	0.648	449.9	108	-81
276.2	125500.	4.113	4277.709	0.055	0.651	449.8	107	-81
276.3	125100.	4.114	4276.949	0.056	0.661	449.4	101	-81
276.4	124800.	4.115	4276.175	0.057	0.670	449.0	105	-81
276.5	124600.	4.115	4275.387	0.057	0.675	448.8	104	-81
276.6	124000.	4.118	4274.584	0.058	0.693	448.1	105	-81
276.7	123700.	4.119	4273.766	0.059	0.702	447.6	105	-81
276.8	123600.	4.119	4272.934	0.059	0.704	447.4	103	-76
276.9	123200.	4.122	4272.087	0.060	0.717	446.6	105	-76
277.0	123000.	4.123	4271.226	0.061	0.723	446.2	104	-76
277.1	122800.	4.123	4270.349	0.061	0.729	446.0	102	-76
277.2	122800.	4.122	4269.457	0.061	0.728	446.0	100	-76
277.3	122500.	4.124	4268.551	0.062	0.738	445.5	90	-71
277.4	122200.	4.125	4267.629	0.063	0.747	445.0	101	-76
277.5	121700.	4.132	4266.692	0.064	0.765	443.3	104	-76
277.6	121500.	4.136	4265.740	0.065	0.773	442.3	102	-76
277.7	121400.	4.137	4264.773	0.065	0.776	441.8	101	-76
277.8	121100.	4.142	4263.791	0.066	0.787	440.6	101	-76
277.9	121000.	4.143	4262.792	0.066	0.791	440.1	99	-76
278.0	120600.	4.150	4261.778	0.067	0.807	438.4	92	-61
278.1	120600.	4.149	4260.749	0.067	0.806	438.5	115	-106
278.2	120300.	4.154	4259.704	0.068	0.818	437.3	117	-106
278.3	120000.	4.160	4258.643	0.069	0.830	435.8	100	-81
278.4	119900.	4.160	4257.566	0.069	0.834	435.5	104	-71
278.5	119600.	4.167	4256.473	0.070	0.847	433.8	106	-71
278.6	119300.	4.172	4255.365	0.070	0.859	432.5	108	-71
278.7	119000.	4.178	4254.240	0.071	0.872	431.2	109	-71
278.8	118900.	4.180	4253.100	0.072	0.876	430.5	109	-71
278.9	118700.	4.184	4251.942	0.072	0.885	429.5	109	-71
279.0	118600.	4.184	4250.769	0.073	0.889	429.1	106	-71
279.1	118200.	4.191	4249.580	0.074	0.906	427.5	103	-81
279.2	117800.	4.201	4248.373	0.075	0.925	425.3	113	-71
279.3	117800.	4.199	4247.150	0.075	0.924	425.4	125	-101
279.4	117700.	4.200	4245.911	0.075	0.928	424.9	114	-71
279.5	117400.	4.201	4244.655	0.076	0.940	424.4	116	-71
279.6	117100.	4.204	4243.382	0.077	0.953	423.6	118	-71
279.7	116900.	4.205	4242.092	0.078	0.961	423.2	123	-66
279.8	116600.	4.208	4240.787	0.079	0.974	422.3	125	-66
279.9	116600.	4.207	4239.463	0.079	0.973	422.3	128	-66

SUMMARY FOR FLIGHT STS27.

TIME (SEC)	ALTITUDE (FT)	MINF	VEL (FT/SEC)	PINF (PSIA)	QINF (PSIA)	TINF (DEG R)	ALP (DEG)	PHI-ALU (DEG)
280.0	116500.	4.205	4238.122	0.079	0.977	422.3	128	-66
280.1	115900.	4.211	4236.764	0.081	1.003	420.9	130	-66
280.2	115900.	4.211	4235.390	0.081	1.003	420.7	132	-66
280.3	115700.	4.211	4233.998	0.081	1.011	420.3	134	-66
280.4	115500.	4.210	4232.588	0.082	1.019	420.2	136	-66
280.5	115300.	4.207	4231.161	0.083	1.026	420.5	138	-66
280.6	115100.	4.205	4229.716	0.083	1.033	420.6	139	-66
280.7	115000.	4.203	4228.254	0.084	1.036	420.8	141	-66
280.8	114600.	4.200	4226.775	0.085	1.051	421.2	144	-66
280.9	114200.	4.196	4225.277	0.087	1.066	421.7	146	-66
281.0	113800.	4.192	4223.762	0.088	1.081	422.2	148	-61
281.1	113500.	4.189	4222.228	0.089	1.093	422.5	150	-61
281.2	113400.	4.188	4220.677	0.089	1.097	422.4	152	-61
281.3	113000.	4.187	4219.107	0.091	1.114	422.2	153	-61
281.4	112900.	4.185	4217.520	0.091	1.118	422.2	155	-61
281.5	112700.	4.185	4215.914	0.092	1.127	422.0	157	-61
281.6	112500.	4.184	4214.290	0.093	1.135	421.9	160	-56
281.7	112000.	4.184	4212.647	0.095	1.158	421.6	162	-61
281.8	112000.	4.182	4210.987	0.095	1.157	421.6	164	-61
281.9	111800.	4.181	4209.307	0.095	1.166	421.5	166	-61
282.0	111600.	4.180	4207.609	0.096	1.175	421.4	168	-61
282.1	111400.	4.178	4205.893	0.097	1.183	421.3	171	-66
282.2	111200.	4.178	4204.157	0.098	1.193	421.1	171	-71
282.3	111000.	4.177	4202.403	0.098	1.202	420.8	176	-71
282.4	110600.	4.179	4200.629	0.100	1.222	420.2	175	-71
282.5	110400.	4.178	4198.837	0.101	1.232	420.0	175	-81
282.6	109900.	4.180	4197.026	0.103	1.258	419.2	177	-66
282.7	109800.	4.179	4195.195	0.103	1.262	419.1	175	-66
282.8	109400.	4.180	4193.346	0.105	1.283	418.5	180	-71
282.9	109100.	4.178	4191.477	0.106	1.298	418.5	176	124
283.0	108800.	4.175	4189.588	0.107	1.309	418.7	169	129
283.1	108400.	4.172	4187.680	0.109	1.324	418.9	166	129
283.2	108200.	4.170	4185.753	0.109	1.331	419.0	161	129
283.3	107900.	4.167	4183.807	0.110	1.342	419.2	157	129
283.4	107700.	4.164	4181.840	0.111	1.349	419.3	154	129
283.5	107400.	4.161	4179.853	0.112	1.360	419.5	152	129
283.6	107400.	4.159	4177.847	0.112	1.359	419.5	150	129
283.7	107100.	4.157	4175.820	0.113	1.370	419.6	148	129
283.8	106800.	4.154	4173.775	0.114	1.382	419.7	145	129
283.9	106500.	4.152	4171.708	0.115	1.393	419.7	143	129
284.0	106300.	4.150	4169.622	0.116	1.401	419.8	140	129
284.1	106200.	4.148	4167.515	0.117	1.404	419.8	138	129
284.2	106000.	4.145	4165.388	0.117	1.411	419.8	135	129
284.3	105800.	4.143	4163.241	0.118	1.418	419.9	134	134
284.4	105500.	4.141	4161.073	0.119	1.430	419.9	132	134
284.5	105300.	4.138	4158.885	0.120	1.438	420.0	130	134
284.6	105000.	4.136	4156.676	0.121	1.450	419.9	129	134
284.7	105000.	4.135	4154.446	0.121	1.449	419.7	127	134
284.8	104600.	4.137	4152.196	0.123	1.470	418.8	125	139
284.9	104500.	4.136	4149.925	0.123	1.473	418.7	123	139

SUMMARY FOR FLIGHT STS27.

TIME (SEC)	ALTITUDE (FT)	MINF	VEL (FT/SEC)	PINF (PSIA)	QINF (PSIA)	TINF (DEG R)	ALP (DEG)	PHI-ALU (DEG)
285.0	104400.	4.134	4147.632	0.123	1.477	418.5	123	139
285.1	104100.	4.135	4145.319	0.125	1.492	417.8	123	139
285.2	103900.	4.136	4142.985	0.125	1.502	417.2	122	144
285.3	103700.	4.135	4140.631	0.126	1.511	416.9	121	144
285.4	103300.	4.137	4138.254	0.128	1.531	416.1	121	144
285.5	102900.	4.139	4135.856	0.129	1.553	415.1	122	144
285.6	102400.	4.142	4133.437	0.132	1.579	414.1	122	149
285.7	102000.	4.144	4130.996	0.133	1.601	413.2	120	149
285.8	101800.	4.144	4128.535	0.134	1.612	412.7	118	154
285.9	101800.	4.142	4126.051	0.134	1.610	412.7	117	154
286.0	101600.	4.141	4123.546	0.135	1.619	412.3	117	159
286.1	101200.	4.143	4121.019	0.137	1.642	411.4	119	159
286.2	100900.	4.142	4118.470	0.138	1.657	411.0	119	159
286.3	100700.	4.140	4115.899	0.139	1.666	410.9	120	164
286.4	100200.	4.139	4113.307	0.141	1.691	410.7	122	169
286.5	100100.	4.136	4110.692	0.142	1.695	410.7	124	169
286.6	99770.	4.134	4108.055	0.143	1.711	410.5	125	174
286.7	99370.	4.132	4105.396	0.145	1.731	410.4	125	174
286.8	99050.	4.131	4102.716	0.146	1.747	410.2	127	179
286.9	98910.	4.128	4100.013	0.147	1.753	410.1	129	179
287.0	98430.	4.128	4097.287	0.149	1.780	409.7	132	-176
287.1	98240.	4.125	4094.539	0.150	1.788	409.6	132	-171
287.2	98020.	4.124	4091.768	0.151	1.799	409.4	134	-166
287.3	97970.	4.121	4088.976	0.151	1.800	409.3	135	-161
287.4	97720.	4.119	4086.159	0.153	1.813	409.1	136	-161
287.5	97590.	4.117	4083.321	0.153	1.818	409.0	138	-151
287.6	97430.	4.115	4080.459	0.154	1.826	408.9	138	-151
287.7	97170.	4.113	4077.575	0.155	1.839	408.7	140	-151
287.8	97090.	4.110	4074.668	0.156	1.841	408.6	142	-146
287.9	96940.	4.108	4071.738	0.156	1.849	408.4	143	-146
288.0	96760.	4.108	4068.785	0.157	1.859	407.9	145	-146
288.1	96500.	4.109	4065.808	0.159	1.875	407.1	148	-146
288.2	96290.	4.109	4062.809	0.160	1.888	406.5	150	-146
288.3	95850.	4.113	4059.787	0.162	1.917	405.2	152	-141
288.4	95490.	4.115	4056.740	0.164	1.942	404.1	155	-141
288.5	95280.	4.115	4053.670	0.165	1.955	403.4	157	-141
288.6	94990.	4.116	4050.577	0.166	1.974	402.6	160	-141
288.7	94820.	4.113	4047.460	0.167	1.982	402.7	163	-141
288.8	94810.	4.110	4044.321	0.167	1.979	402.7	165	-141
288.9	94450.	4.105	4041.157	0.169	1.997	403.0	168	-141
289.0	94280.	4.101	4037.969	0.170	2.004	403.1	170	-156
289.1	93940.	4.096	4034.758	0.172	2.021	403.4	172	-156
289.2	93940.	4.093	4031.523	0.172	2.018	403.4	174	-161
289.3	93770.	4.089	4028.265	0.173	2.025	403.5	173	-76
289.4	93600.	4.085	4024.981	0.174	2.038	403.7	175	-81
289.5	93360.	4.081	4021.674	0.176	2.057	403.8	177	69
289.6	93220.	4.077	4018.342	0.178	2.068	403.9	172	54
289.7	92910.	4.072	4014.987	0.180	2.094	404.2	169	64
289.8	92480.	4.067	4011.608	0.184	2.132	404.6	165	64
289.9	92120.	4.061	4008.204	0.187	2.163	405.0	162	64

SUMMARY FOR FLIGHT STS27.

TIME (SEC)	ALTITUDE (FT)	MINF	VEL (FT/SEC)	PINF (PSIA)	QINF (PSIA)	TINF (DEG R)	ALP (DEG)	PHI-ALU (DEG)
290.0	91540.	4.055	4004.775	0.193	2.218	405.6	158	69
290.1	91120.	4.049	4001.323	0.197	2.257	406.0	155	69
290.2	90880.	4.046	3997.845	0.199	2.280	405.9	152	69
290.3	90800.	4.043	3994.345	0.200	2.285	405.8	149	74
290.4	90290.	4.043	3990.818	0.205	2.341	405.2	146	74
290.5	89800.	4.042	3987.267	0.210	2.396	404.7	145	74
290.6	89750.	4.038	3983.691	0.210	2.398	404.6	142	74
290.7	89590.	4.036	3980.090	0.212	2.414	404.4	139	79
290.8	89300.	4.034	3976.466	0.215	2.445	404.1	137	79
290.9	89130.	4.031	3972.816	0.216	2.462	403.9	133	84
291.0	88930.	4.027	3969.140	0.219	2.481	403.9	132	84
291.1	88670.	4.024	3965.440	0.221	2.508	403.8	131	84
291.2	88420.	4.020	3961.715	0.224	2.534	403.8	130	89
291.3	87840.	4.017	3957.965	0.230	2.602	403.6	129	89
291.4	87610.	4.013	3954.190	0.233	2.626	403.6	128	89
291.5	87310.	4.010	3950.390	0.236	2.660	403.5	128	94
291.6	86920.	4.009	3946.563	0.241	2.709	403.0	128	94
291.7	86790.	4.006	3942.712	0.242	2.723	402.7	128	94
291.8	86640.	4.003	3938.836	0.244	2.738	402.5	127	99
291.9	86390.	4.002	3934.935	0.247	2.770	402.0	128	99
292.0	85800.	4.003	3931.006	0.254	2.851	401.0	129	104
292.1	85650.	4.000	3927.053	0.256	2.868	400.7	130	104
292.2	85590.	3.997	3923.075	0.257	2.871	400.6	130	109
292.3	85340.	3.995	3919.072	0.260	2.903	400.2	131	109
292.4	85020.	3.994	3915.042	0.264	2.947	399.6	132	109
292.5	84570.	3.993	3910.986	0.270	3.011	398.8	134	109
292.6	84330.	3.991	3906.904	0.273	3.043	398.4	135	114
292.7	84220.	3.988	3902.797	0.274	3.054	398.2	138	114
292.8	84290.	3.983	3898.665	0.273	3.037	398.3	139	114
292.9	84260.	3.979	3894.506	0.274	3.035	398.3	141	119
293.0	84290.	3.975	3890.321	0.273	3.024	398.3	144	119
293.1	83880.	3.974	3886.110	0.279	3.083	397.6	146	119
293.2	83780.	3.971	3881.873	0.280	3.093	397.4	149	119
293.3	83640.	3.967	3877.611	0.282	3.108	397.2	152	124
293.4	83570.	3.963	3873.322	0.283	3.113	397.1	154	119
293.5	83280.	3.961	3869.007	0.287	3.153	396.7	157	124
293.6	83020.	3.958	3864.665	0.291	3.187	396.5	160	119
293.7	82690.	3.954	3860.297	0.295	3.232	396.3	163	119
293.8	82470.	3.951	3855.904	0.298	3.261	396.1	166	119
293.9	82100.	3.948	3851.484	0.304	3.315	395.8	170	119
294.0	81520.	3.946	3847.037	0.312	3.405	395.3	173	129
294.1	81460.	3.941	3842.563	0.313	3.407	395.3	176	129
294.2	81120.	3.939	3838.064	0.319	3.461	394.7	174	64
294.3	80930.	3.936	3833.540	0.322	3.486	394.5	177	59
294.4	80350.	3.935	3828.986	0.331	3.585	393.6	180	49
294.5	80140.	3.932	3824.408	0.334	3.615	393.3	180	-51
294.6	79940.	3.929	3819.802	0.337	3.644	393.0	172	-21
294.7	79640.	3.926	3815.169	0.342	3.691	392.7	168	-26
294.8	79300.	3.922	3810.512	0.348	3.745	392.5	164	-26
294.9	78990.	3.918	3805.826	0.353	3.793	392.4	160	-21

SUMMARY FOR FLIGHT STS27.

TIME (SEC)	ALTITUDE (FT)	MINF	VEL (FT/SEC)	PINF (PSIA)	QINF (PSIA)	TINF (DEG R)	ALP (DEG)	PHI-ALU (DEG)
295.0	78570.	3.913	3801.113	0.360	3.862	392.3	157	-21
295.1	78500.	3.909	3796.374	0.362	3.867	392.2	153	-21
295.2	78410.	3.904	3791.607	0.363	3.874	392.2	152	-11
295.3	77940.	3.900	3786.816	0.371	3.955	392.0	150	-6
295.4	77710.	3.898	3781.997	0.376	3.994	391.5	147	-1
295.5	77730.	3.892	3777.150	0.375	3.979	391.6	145	-1
295.6	77460.	3.891	3772.277	0.380	4.028	390.9	143	4
295.7	77220.	3.888	3767.376	0.385	4.070	390.3	141	9
295.8	77160.	3.884	3762.451	0.386	4.072	390.2	140	9
295.9	77060.	3.880	3757.497	0.388	4.084	389.9	139	14
296.0	76770.	3.879	3752.515	0.393	4.138	389.2	138	19
296.1	76510.	3.877	3747.507	0.398	4.187	388.5	138	19
296.2	76310.	3.874	3742.472	0.402	4.222	388.0	138	24
296.3	75830.	3.872	3737.411	0.411	4.316	387.4	138	29
296.4	75810.	3.867	3732.322	0.412	4.308	387.4	138	29
296.5	75550.	3.862	3727.205	0.417	4.352	387.3	139	34
296.6	75350.	3.857	3722.062	0.421	4.383	387.2	140	34
296.7	74840.	3.852	3716.891	0.431	4.481	387.1	142	39
296.8	74650.	3.847	3711.694	0.435	4.511	387.0	144	39
296.9	74440.	3.842	3706.469	0.440	4.545	386.9	145	44
297.0	73930.	3.838	3701.217	0.451	4.648	386.6	147	44
297.1	73840.	3.833	3695.938	0.453	4.655	386.6	149	49
297.2	73730.	3.828	3690.631	0.455	4.668	386.5	151	49
297.3	73420.	3.824	3685.299	0.462	4.728	386.2	154	49
297.4	73340.	3.818	3679.938	0.464	4.733	386.2	156	54
297.5	73140.	3.814	3674.549	0.468	4.767	386.0	158	54
297.6	72820.	3.809	3669.133	0.476	4.830	385.8	161	54
297.7	72600.	3.804	3663.690	0.481	4.869	385.6	164	59
297.8	72630.	3.798	3658.222	0.480	4.846	385.7	166	59
297.9	72410.	3.794	3652.724	0.485	4.887	385.4	169	59
298.0	72160.	3.790	3647.199	0.491	4.937	385.0	172	54
298.1	71820.	3.787	3641.647	0.499	5.011	384.4	175	54
298.2	71630.	3.783	3636.068	0.504	5.045	384.1	177	-81
298.3	71390.	3.779	3630.463	0.509	5.094	383.7	177	-71
298.4	71140.	3.775	3624.829	0.516	5.145	383.3	176	-66
298.5	70800.	3.772	3619.167	0.524	5.222	382.7	174	-66
298.6	70690.	3.767	3613.479	0.527	5.235	382.6	172	-71
298.7	70200.	3.763	3607.762	0.540	5.350	382.1	169	-71
298.8	69900.	3.759	3602.021	0.547	5.415	381.8	167	-71
298.9	69600.	3.754	3596.250	0.555	5.481	381.5	164	-71
299.0	69360.	3.749	3590.452	0.562	5.529	381.3	161	-71
299.1	69270.	3.744	3584.626	0.564	5.537	381.2	158	-71
299.2	68970.	3.739	3578.773	0.573	5.604	380.9	155	-71
299.3	68840.	3.734	3572.896	0.576	5.624	380.7	153	-66
299.4	68810.	3.728	3566.988	0.577	5.613	380.7	151	-66
299.5	68620.	3.723	3561.054	0.582	5.649	380.5	149	-66
299.6	68620.	3.716	3555.092	0.582	5.630	380.5	148	-61
299.7	68270.	3.712	3549.103	0.592	5.713	380.1	147	-56
299.8	67830.	3.708	3543.088	0.605	5.822	379.7	147	-51
299.9	67690.	3.702	3537.044	0.609	5.844	379.5	146	-46

SUMMARY FOR FLIGHT STS27.

TIME (SEC)	ALTITUDE (FT)	MINF	VEL (FT/SEC)	PINF (PSIA)	QINF (PSIA)	TINF (DEG R)	ALP (DEG)	PHI-ALU (DEG)
300.0	67600.	3.696	3530.973	0.612	5.851	379.4	146	-41
300.1	67090.	3.695	3524.875	0.627	5.993	378.3	146	-41
300.2	67090.	3.689	3518.749	0.627	5.973	378.3	146	-41
300.3	66940.	3.685	3512.598	0.632	6.001	377.9	146	-41
300.4	66790.	3.680	3506.418	0.636	6.032	377.4	147	-36
300.5	66610.	3.676	3500.211	0.642	6.071	376.9	148	-36
300.6	66190.	3.676	3493.977	0.655	6.194	375.6	149	-26
300.7	65840.	3.675	3487.716	0.666	6.296	374.5	151	-26
300.8	65530.	3.672	3481.429	0.676	6.381	373.7	154	-21
300.9	65220.	3.669	3475.113	0.686	6.466	373.0	156	-16
301.0	64990.	3.665	3468.771	0.694	6.523	372.5	159	-11
301.1	64520.	3.663	3462.400	0.710	6.664	371.6	161	-6
301.2	64090.	3.660	3456.004	0.725	6.795	370.7	164	-1
301.3	63920.	3.654	3449.582	0.731	6.828	370.6	166	4
301.4	63450.	3.648	3443.131	0.747	6.960	370.5	167	-1
301.5	63430.	3.641	3436.653	0.748	6.941	370.5	169	4
301.6	63260.	3.634	3430.148	0.754	6.972	370.5	172	-1
301.7	63230.	3.627	3423.616	0.755	6.955	370.5	174	-1
301.8	62830.	3.620	3417.059	0.770	7.063	370.5	176	-51
301.9	62700.	3.613	3410.474	0.775	7.082	370.4	173	-61
302.0	62220.	3.606	3403.861	0.793	7.218	370.5	174	-66
302.1	62140.	3.598	3397.222	0.796	7.216	370.6	173	-71
302.2	61910.	3.590	3390.556	0.805	7.264	370.8	171	-71
302.3	61740.	3.583	3383.865	0.812	7.293	370.9	168	-71
302.4	61480.	3.575	3377.146	0.822	7.352	371.1	167	-66
302.5	61430.	3.568	3370.399	0.824	7.340	371.1	165	-66
302.6	61200.	3.559	3363.626	0.833	7.388	371.3	162	-61
302.7	60960.	3.551	3356.827	0.843	7.440	371.5	161	-56
302.8	60710.	3.544	3350.003	0.853	7.498	371.6	159	-51
302.9	60570.	3.537	3343.151	0.859	7.520	371.5	157	-41
303.0	60290.	3.531	3336.272	0.870	7.595	371.3	156	-41
303.1	60190.	3.523	3329.366	0.875	7.600	371.3	154	-41
303.2	59610.	3.517	3322.435	0.899	7.790	371.0	153	-31
303.3	59260.	3.511	3315.478	0.915	7.893	370.8	152	-26
303.4	58910.	3.512	3308.494	0.930	8.033	369.0	153	-16
303.5	58850.	3.506	3301.483	0.933	8.031	368.6	153	-1
303.6	58550.	3.507	3294.446	0.947	8.151	366.9	152	4
303.7	58430.	3.503	3287.383	0.952	8.181	366.1	152	9
303.8	58300.	3.500	3280.296	0.958	8.215	365.3	152	19
303.9	58000.	3.500	3273.180	0.972	8.338	363.6	153	29
304.0	57860.	3.496	3266.039	0.979	8.376	362.8	153	34
304.1	57570.	3.496	3258.872	0.993	8.489	361.4	155	39
304.2	57180.	3.490	3251.678	1.011	8.622	361.0	156	44
304.3	57140.	3.482	3244.461	1.013	8.600	361.0	158	54
304.4	57140.	3.474	3237.217	1.013	8.562	361.0	159	59
304.5	56840.	3.468	3229.946	1.028	8.655	360.7	161	69
304.6	56410.	3.462	3222.649	1.050	8.807	360.3	163	69
304.7	56090.	3.456	3215.327	1.066	8.910	360.0	164	79
304.8	55560.	3.447	3207.981	1.094	9.094	360.2	166	84
304.9	55340.	3.438	3200.608	1.105	9.147	360.3	168	89

SUMMARY FOR FLIGHT STS27.

TIME (SEC)	ALTITUDE (FT)	MINF	VEL (FT/SEC)	PINF (PSIA)	QINF (PSIA)	TINF (DEG R)	ALP (DEG)	PHI-ALU (DEG)
305.0	55240.	3.430	3193.209	1.111	9.149	360.3	170	89
305.1	55000.	3.422	3185.785	1.124	9.210	360.4	172	94
305.2	54970.	3.414	3178.336	1.125	9.180	360.4	173	94
305.3	54650.	3.405	3170.863	1.143	9.276	360.5	173	-86
305.4	54400.	3.395	3163.363	1.157	9.329	361.1	171	-61
305.5	54190.	3.384	3155.838	1.168	9.364	361.7	174	-91
305.6	54060.	3.374	3148.288	1.176	9.370	362.0	174	-86
305.7	53960.	3.365	3140.712	1.181	9.362	362.3	174	-91
305.8	53740.	3.354	3133.114	1.194	9.401	362.9	173	-91
305.9	53610.	3.344	3125.489	1.202	9.406	363.2	172	-101
306.0	53320.	3.332	3117.839	1.218	9.471	364.0	172	69
306.1	53270.	3.323	3110.164	1.221	9.442	364.2	171	69
306.2	52980.	3.312	3102.465	1.239	9.510	364.9	169	69
306.3	52730.	3.301	3094.743	1.254	9.564	365.4	168	79
306.4	52470.	3.290	3086.994	1.269	9.621	366.0	166	84
306.5	52110.	3.278	3079.221	1.292	9.719	366.8	166	89
306.6	51720.	3.267	3071.424	1.316	9.832	367.6	164	94
306.7	51500.	3.257	3063.602	1.330	9.881	367.8	162	104
306.8	51290.	3.248	3055.758	1.344	9.925	368.0	161	109
306.9	51260.	3.240	3047.888	1.346	9.888	368.0	159	119
307.0	50930.	3.231	3039.994	1.367	9.990	368.2	158	124
307.1	50500.	3.221	3032.075	1.396	10.138	368.5	157	124
307.2	50310.	3.212	3024.133	1.409	10.175	368.6	157	134
307.3	50240.	3.203	3016.169	1.414	10.155	368.6	157	139
307.4	50230.	3.195	3008.180	1.414	10.109	368.5	157	144
307.5	50190.	3.187	3000.167	1.417	10.075	368.5	156	154
307.6	50150.	3.179	2992.129	1.420	10.043	368.4	157	159
307.7	49810.	3.172	2984.069	1.443	10.165	368.0	157	174
307.8	49820.	3.163	2975.987	1.443	10.106	368.0	158	179
307.9	49700.	3.156	2967.880	1.451	10.114	367.8	159	-161
308.0	49590.	3.147	2959.749	1.459	10.115	367.7	158	-151
308.1	49110.	3.142	2951.596	1.493	10.315	367.0	158	-146
308.2	49070.	3.133	2943.419	1.496	10.278	367.0	159	-141
308.3	48920.	3.126	2935.222	1.507	10.303	366.7	159	-146
308.4	48460.	3.112	2926.999	1.541	10.442	367.9	161	-146
308.5	48400.	3.102	2918.754	1.545	10.407	368.1	163	-136
308.6	48040.	3.089	2910.486	1.572	10.498	369.2	164	-136
308.7	47920.	3.079	2902.195	1.581	10.491	369.5	165	-131
308.8	47500.	3.065	2893.885	1.614	10.610	370.7	166	-126
308.9	47330.	3.055	2885.549	1.627	10.627	371.0	167	-126
309.0	47150.	3.045	2877.191	1.641	10.649	371.3	168	-121
309.1	46750.	3.033	2868.811	1.673	10.776	371.9	169	-121
309.2	46690.	3.025	2860.409	1.678	10.744	371.9	169	-121
309.3	46370.	3.014	2851.987	1.704	10.833	372.4	167	-141
309.4	46180.	3.003	2843.541	1.720	10.859	372.7	167	-141
309.5	45940.	2.997	2835.073	1.740	10.941	372.0	170	-121
309.6	45650.	2.992	2826.583	1.764	11.052	371.2	170	-121
309.7	45430.	2.985	2818.072	1.783	11.121	370.6	170	-121
309.8	45330.	2.977	2809.541	1.792	11.116	370.3	169	-121
309.9	45050.	2.971	2800.987	1.816	11.223	369.5	169	-121

SUMMARY FOR FLIGHT STS27.

TIME (SEC)	ALTITUDE (FT)	MINF	VEL (FT/SEC)	PINF (PSIA)	QINF (PSIA)	TINF (DEG R)	ALP (DEG)	PHI-ALU (DEG)
310.0	44780.	2.963	2792.411	1.840	11.307	369.3	168	-116
310.1	44780.	2.954	2783.815	1.840	11.238	369.3	167	-111
310.2	44590.	2.942	2775.197	1.857	11.253	369.9	166	-111
310.3	44500.	2.932	2766.561	1.865	11.222	370.2	165	-111
310.4	44120.	2.918	2757.901	1.899	11.319	371.5	164	-111
310.5	43690.	2.903	2749.221	1.939	11.440	372.9	163	-106
310.6	43430.	2.892	2740.520	1.964	11.493	373.5	162	-101
310.7	43320.	2.881	2731.798	1.974	11.472	373.8	161	-91
310.8	43280.	2.872	2723.059	1.978	11.417	373.9	159	-91
310.9	43170.	2.861	2714.297	1.989	11.395	374.2	158	-91
311.0	42780.	2.848	2705.514	2.026	11.506	375.2	158	-86
311.1	42410.	2.835	2696.712	2.063	11.609	376.1	158	-86
311.2	42350.	2.826	2687.889	2.069	11.564	376.2	157	-86
311.3	41920.	2.813	2679.049	2.112	11.698	377.2	157	-81
311.4	41770.	2.802	2670.188	2.127	11.695	377.5	157	-81
311.5	41740.	2.793	2661.305	2.131	11.631	377.6	157	-76
311.6	41500.	2.781	2652.404	2.155	11.673	378.1	157	-71
311.7	41390.	2.771	2643.483	2.167	11.650	378.3	157	-71
311.8	41130.	2.760	2634.546	2.194	11.699	378.9	158	-66
311.9	41020.	2.749	2625.587	2.206	11.666	379.4	158	-61
312.0	41020.	2.739	2616.609	2.206	11.586	379.4	159	-51
312.1	40900.	2.728	2607.612	2.219	11.558	379.9	160	-41
312.2	40830.	2.718	2598.596	2.226	11.508	380.2	160	-41
312.3	40770.	2.707	2589.564	2.233	11.453	380.5	160	-41
312.4	40650.	2.696	2580.511	2.246	11.424	381.0	161	-31
312.5	40460.	2.683	2571.439	2.266	11.424	381.8	161	-26
312.6	39760.	2.663	2562.350	2.344	11.633	385.1	163	-51
312.7	39600.	2.650	2553.242	2.362	11.609	386.1	164	-16
312.8	39520.	2.638	2544.119	2.371	11.556	386.6	165	-6
312.9	39430.	2.627	2534.975	2.382	11.508	387.1	164	-1
313.0	39170.	2.612	2525.813	2.412	11.522	388.7	164	4
313.1	38660.	2.593	2516.634	2.472	11.636	391.6	165	19
313.2	38390.	2.579	2507.437	2.504	11.664	392.9	165	19
313.3	38410.	2.570	2498.226	2.502	11.571	392.8	164	29
313.4	38370.	2.560	2488.994	2.507	11.502	393.0	164	34
313.5	38330.	2.550	2479.746	2.512	11.432	393.2	164	39
313.6	38300.	2.540	2470.480	2.515	11.361	393.3	164	49
313.7	38230.	2.529	2461.197	2.524	11.302	393.7	163	54
313.8	37950.	2.515	2451.901	2.558	11.329	395.1	163	64
313.9	37810.	2.504	2442.585	2.575	11.300	395.8	162	69
314.0	37550.	2.490	2433.253	2.608	11.318	397.1	162	74
314.1	37400.	2.478	2423.904	2.627	11.293	397.8	161	79
314.2	37330.	2.467	2414.539	2.636	11.232	398.2	161	84
314.3	37210.	2.456	2405.161	2.651	11.193	398.8	161	94
314.4	37340.	2.448	2395.764	2.635	11.056	398.1	160	99
314.5	37170.	2.436	2386.351	2.656	11.034	399.0	159	104
314.6	37190.	2.427	2376.923	2.654	10.939	398.9	158	109
314.7	37190.	2.417	2367.479	2.654	10.855	398.8	157	119
314.8	37160.	2.407	2358.022	2.658	10.779	399.0	156	124
314.9	37190.	2.398	2348.548	2.654	10.683	398.8	155	129

SUMMARY FOR FLIGHT STS27.

TIME (SEC)	ALTITUDE (FT)	MINF	VEL (FT/SEC)	PINF (PSIA)	QINF (PSIA)	TINF (DEG R)	ALP (DEG)	PHI-ALU (DEG)
315.0	37220.	2.389	2339.059	2.650	10.584	398.7	155	134
315.1	37200.	2.379	2329.554	2.652	10.505	398.8	155	139
315.2	37200.	2.369	2320.034	2.652	10.420	398.8	156	144
315.3	37230.	2.360	2310.503	2.649	10.324	398.6	156	154
315.4	37320.	2.351	2300.955	2.637	10.205	398.2	156	164
315.5	37400.	2.343	2291.391	2.627	10.092	397.8	156	174
315.6	37390.	2.333	2281.814	2.628	10.010	397.9	157	-176
315.7	37270.	2.321	2272.223	2.643	9.968	398.5	157	-161
315.8	37040.	2.308	2262.620	2.673	9.967	399.6	156	-156
315.9	36690.	2.293	2253.001	2.718	10.006	401.4	156	-151
316.0	36400.	2.280	2243.368	2.757	10.030	402.6	157	-146
316.1	35930.	2.265	2233.722	2.820	10.125	404.5	157	-146
316.2	35790.	2.254	2224.062	2.839	10.093	405.0	157	-146
316.3	35530.	2.241	2214.392	2.875	10.107	406.0	157	-161
316.4	35110.	2.227	2204.706	2.934	10.188	407.4	159	-146
316.5	34490.	2.212	2195.006	3.023	10.352	409.5	158	-121
316.6	34270.	2.200	2185.294	3.055	10.353	410.2	160	-146
316.7	33810.	2.187	2175.570	3.124	10.455	411.6	160	-146
316.8	33420.	2.174	2165.836	3.183	10.528	412.8	159	-146
316.9	33060.	2.160	2156.086	3.239	10.578	414.3	159	-146
317.0	32730.	2.146	2146.325	3.291	10.612	415.8	159	-146
317.1	32420.	2.133	2136.551	3.341	10.636	417.3	159	-146
317.2	32340.	2.122	2126.766	3.353	10.572	417.6	158	-151
317.3	31890.	2.107	2116.971	3.427	10.651	419.7	157	-151
317.4	31800.	2.096	2107.163	3.442	10.588	420.1	157	-151
317.5	31490.	2.083	2097.342	3.494	10.613	421.5	157	-156
317.6	31370.	2.072	2087.510	3.514	10.559	422.1	156	-156
317.7	31270.	2.061	2077.667	3.531	10.501	422.5	156	-161
317.8	31190.	2.051	2067.817	3.545	10.434	422.8	155	-161
317.9	31150.	2.040	2057.952	3.552	10.350	423.0	155	-161
318.0	31140.	2.031	2048.077	3.553	10.256	423.0	155	-166
318.1	31140.	2.021	2038.191	3.553	10.155	423.1	154	-171
318.2	31040.	2.010	2028.295	3.571	10.098	423.4	153	-176
318.3	30930.	1.999	2018.391	3.590	10.043	423.8	152	179
318.4	30660.	1.987	2008.475	3.637	10.049	424.9	153	179
318.5	30550.	1.976	1998.548	3.656	9.993	425.3	153	174
318.6	30190.	1.963	1988.612	3.720	10.037	426.6	154	174
318.7	30010.	1.953	1978.667	3.752	10.014	427.0	154	169
318.8	29830.	1.942	1968.715	3.785	9.989	427.5	154	169
318.9	29740.	1.931	1958.750	3.802	9.926	427.7	155	164
319.0	29680.	1.921	1948.776	3.813	9.849	427.9	155	164
319.1	29620.	1.911	1938.794	3.824	9.774	428.0	155	159
319.2	29590.	1.901	1928.802	3.829	9.686	428.1	156	159
319.3	29370.	1.890	1918.806	3.870	9.677	428.6	156	159
319.4	29170.	1.879	1908.797	3.908	9.657	429.1	154	154
319.5	29090.	1.869	1898.780	3.923	9.589	429.3	156	159
319.6	29050.	1.859	1888.756	3.930	9.504	429.4	157	159
319.7	29000.	1.849	1878.723	3.940	9.424	429.5	157	159
319.8	29090.	1.839	1868.685	3.923	9.287	429.3	157	159
319.9	29100.	1.829	1858.637	3.921	9.183	429.3	157	159

SUMMARY FOR FLIGHT STS27.

TIME (SEC)	ALTITUDE (FT)	MINF	VEL (FT/SEC)	PINF (PSIA)	QINF (PSIA)	TINF (DEG R)	ALP (DEG)	PHI-ALU (DEG)
320.0	29160.	1.819	1848.581	3.910	9.060	429.2	157	159
320.1	29210.	1.810	1838.518	3.900	8.942	429.1	156	164
320.2	29250.	1.800	1828.447	3.893	8.829	429.0	156	164
320.3	29240.	1.790	1818.373	3.895	8.737	429.0	156	169
320.4	29000.	1.779	1808.289	3.940	8.730	429.5	156	169
320.5	28940.	1.769	1798.198	3.951	8.654	429.7	156	174
320.6	28720.	1.758	1788.100	3.993	8.639	430.2	156	179
320.7	28660.	1.748	1777.996	4.005	8.564	430.3	156	179
320.8	28580.	1.737	1767.889	4.021	8.496	430.5	155	-176
320.9	28450.	1.727	1757.773	4.046	8.446	430.8	155	-176
321.0	28250.	1.716	1747.651	4.085	8.420	431.3	156	-176
321.1	28040.	1.705	1737.523	4.127	8.394	432.0	156	-171
321.2	28010.	1.694	1727.390	4.133	8.306	432.1	155	-171
321.3	27800.	1.683	1717.255	4.175	8.279	432.8	155	-171
321.4	27650.	1.672	1707.111	4.205	8.232	433.3	154	-171
321.5	27630.	1.662	1696.962	4.209	8.142	433.3	153	-166
321.6	27610.	1.652	1686.809	4.213	8.051	433.4	147	-166
321.7	27510.	1.641	1676.650	4.234	7.985	433.8	147	-171
321.8	27340.	1.631	1666.490	4.268	7.945	434.3	146	-171
321.9	27190.	1.620	1656.323	4.299	7.894	434.9	144	-171
322.0	27070.	1.609	1646.152	4.324	7.834	435.4	144	-176
322.1	26820.	1.597	1635.977	4.377	7.811	436.5	143	-176
322.2	26860.	1.587	1625.797	4.369	7.703	436.3	141	179
322.3	26540.	1.574	1615.617	4.436	7.699	437.8	142	179
322.4	26500.	1.564	1605.431	4.445	7.613	438.0	141	179
322.5	26490.	1.554	1595.241	4.447	7.520	438.0	140	179
322.6	26500.	1.544	1585.048	4.445	7.421	438.0	140	179
322.7	26490.	1.534	1574.853	4.447	7.329	438.0	139	179
322.8	26460.	1.524	1564.657	4.454	7.244	438.1	139	179
322.9	26260.	1.513	1554.456	4.497	7.204	439.0	139	174
323.0	26190.	1.502	1544.252	4.512	7.129	439.3	139	174
323.1	26110.	1.492	1534.046	4.530	7.056	439.7	138	174
323.2	26190.	1.483	1523.837	4.512	6.942	439.3	138	174
323.3	26260.	1.473	1513.630	4.497	6.831	439.0	137	174
323.4	26280.	1.463	1503.418	4.492	6.732	439.0	137	174
323.5	26260.	1.453	1493.205	4.497	6.648	439.0	137	174
323.6	26260.	1.443	1482.990	4.497	6.557	439.0	136	174
323.7	26270.	1.433	1472.773	4.495	6.464	439.0	136	179
323.8	26290.	1.424	1462.559	4.490	6.370	438.9	135	179
323.9	26330.	1.414	1452.341	4.482	6.272	438.7	135	179
324.0	26330.	1.404	1442.122	4.482	6.184	438.7	135	179
324.1	26230.	1.393	1431.903	4.503	6.119	439.2	134	179
324.2	26080.	1.382	1421.683	4.536	6.067	439.8	134	179
324.3	25990.	1.372	1411.466	4.556	6.000	440.3	134	179
324.4	25750.	1.360	1401.246	4.609	5.969	441.3	134	179
324.5	25600.	1.349	1391.026	4.642	5.915	442.0	134	179
324.6	25530.	1.339	1380.807	4.658	5.843	442.4	134	179
324.7	25360.	1.328	1370.588	4.696	5.795	443.1	133	179
324.8	25380.	1.318	1360.373	4.692	5.704	443.1	133	179
324.9	25340.	1.308	1350.155	4.701	5.628	443.2	132	179

SUMMARY FOR FLIGHT STS27.

TIME (SEC)	ALTITUDE (FT)	MINF	VEL (FT/SEC)	PINF (PSIA)	QINF (PSIA)	TINF (DEG R)	ALP (DEG)	PHI-ALU (DEG)
325.0	25200.	1.297	1339.939	4.733	5.572	443.9	131	179
325.1	25100.	1.286	1329.724	4.756	5.509	444.3	131	179
325.2	25020.	1.276	1319.510	4.774	5.442	444.6	130	179
325.3	24770.	1.265	1309.301	4.832	5.409	445.7	130	179
325.4	24590.	1.254	1299.091	4.874	5.362	446.5	129	179
325.5	24410.	1.243	1288.883	4.917	5.315	447.3	129	179
325.6	24140.	1.231	1278.677	4.981	5.283	448.7	128	179
325.7	23920.	1.219	1268.473	5.034	5.240	449.9	128	179
325.8	23890.	1.209	1258.275	5.042	5.162	450.1	127	179
325.9	23570.	1.197	1248.077	5.120	5.138	451.8	126	179
326.0	23170.	1.185	1237.881	5.220	5.134	453.5	126	179
326.1	22910.	1.174	1227.689	5.286	5.101	454.6	126	179
326.2	22690.	1.163	1217.500	5.342	5.060	455.5	126	179
326.3	22430.	1.152	1207.317	5.410	5.026	456.6	125	179
326.4	22050.	1.140	1197.135	5.510	5.016	458.2	126	-176
326.5	21870.	1.130	1186.957	5.558	4.966	458.9	125	-176
326.6	21860.	1.120	1176.782	5.561	4.883	459.0	124	-176
326.7	21780.	1.110	1166.612	5.582	4.814	459.3	123	-176
326.8	21720.	1.100	1156.449	5.598	4.742	459.5	123	-176
326.9	21720.	1.090	1146.288	5.598	4.659	459.5	122	-176
327.0	21730.	1.081	1136.132	5.596	4.575	459.5	121	-176
327.1	21870.	1.072	1125.981	5.558	4.469	458.9	119	-171
327.2	21850.	1.062	1115.834	5.563	4.392	459.0	118	-171
327.3	21780.	1.052	1105.697	5.582	4.325	459.3	119	-171
327.4	21780.	1.042	1095.561	5.582	4.246	459.3	118	-171
327.5	21780.	1.033	1085.432	5.582	4.168	459.3	118	-171
327.6	21620.	1.022	1075.308	5.625	4.116	459.9	122	-161
327.7	21390.	1.012	1065.190	5.688	4.077	460.7	123	-161
327.8	21180.	1.001	1055.082	5.746	4.034	461.5	123	-161
327.9	21120.	0.992	1044.977	5.763	3.967	461.7	123	-161
328.0	21030.	0.982	1034.879	5.788	3.905	462.0	122	-161

STS-29R REENTRY TRAJECTORY L/H SRB

SUMMARY FOR FLIGHT STS29.

TIME (SEC)	ALTITUDE (FT)	MINF	VEL (FT/SEC)	PINF (PSIA)	QINF (PSIA)	TINF (DEG R)	ALP (DEG)	PHI-ALU (DEG)
270.0	143464.	4.008	4299.703	0.024	0.265	478.5	131	-76
270.1	142810.	4.011	4299.698	0.024	0.273	477.9	131	-71
270.2	142421.	4.012	4299.682	0.025	0.278	477.5	123	-66
270.3	142531.	4.012	4299.657	0.025	0.276	477.6	126	-81
270.4	142274.	4.013	4299.621	0.025	0.279	477.4	140	-101
270.5	142023.	4.014	4299.575	0.025	0.283	477.1	130	-71
270.6	141845.	4.015	4299.518	0.025	0.285	476.9	128	-71
270.7	141769.	4.015	4299.451	0.025	0.286	476.8	128	-71
270.8	141566.	4.016	4299.374	0.026	0.289	476.6	129	-71
270.9	141450.	4.016	4299.285	0.026	0.290	476.5	128	-71
271.0	141093.	4.018	4299.186	0.026	0.295	476.1	129	-71
271.1	140918.	4.018	4299.077	0.026	0.297	476.0	128	-71
271.2	140298.	4.021	4298.957	0.027	0.306	475.3	127	-71
271.3	140030.	4.022	4298.825	0.027	0.310	475.0	127	-71
271.4	139937.	4.022	4298.683	0.027	0.311	474.9	127	-71
271.5	139561.	4.024	4298.530	0.028	0.316	474.4	126	-71
271.6	139301.	4.025	4298.365	0.028	0.320	474.1	124	-71
271.7	139442.	4.024	4298.190	0.028	0.318	474.3	122	-71
271.8	139305.	4.025	4298.003	0.028	0.320	474.1	119	-66
271.9	138927.	4.027	4297.806	0.029	0.326	473.7	119	-66
272.0	138785.	4.027	4297.596	0.029	0.328	473.5	117	-66
272.1	138516.	4.028	4297.375	0.029	0.332	473.2	117	-66
272.2	137982.	4.031	4297.144	0.030	0.340	472.6	117	-66
272.3	137676.	4.032	4296.900	0.030	0.345	472.2	117	-66
272.4	137843.	4.031	4296.645	0.030	0.342	472.4	113	-71
272.5	137548.	4.033	4296.378	0.030	0.347	472.0	115	-66
272.6	137174.	4.035	4296.100	0.031	0.353	471.5	90	-61
272.7	136952.	4.036	4295.810	0.031	0.357	471.2	108	-61
272.8	136571.	4.038	4295.508	0.032	0.363	470.6	112	-61
272.9	136520.	4.038	4295.194	0.032	0.364	470.6	114	-61
273.0	136238.	4.039	4294.868	0.032	0.369	470.2	110	-61
273.1	136015.	4.040	4294.530	0.033	0.372	469.9	111	-56
273.2	136105.	4.039	4294.180	0.032	0.371	470.0	109	-56
273.3	135896.	4.040	4293.818	0.033	0.374	469.7	108	-36
273.4	135504.	4.042	4293.444	0.033	0.381	469.2	110	-36
273.5	135042.	4.044	4293.057	0.034	0.389	468.5	111	-51
273.6	134906.	4.045	4292.658	0.034	0.392	468.3	108	-51
273.7	134481.	4.047	4292.246	0.035	0.400	467.8	112	-46
273.8	134602.	4.046	4291.822	0.035	0.397	467.9	111	-41
273.9	134305.	4.047	4291.386	0.035	0.403	467.5	111	-46
274.0	133774.	4.050	4290.936	0.036	0.413	466.8	113	-46
274.1	133556.	4.051	4290.474	0.036	0.417	466.5	115	-46
274.2	133394.	4.051	4289.999	0.037	0.420	466.3	117	-41
274.3	133041.	4.053	4289.512	0.037	0.427	465.8	117	-41
274.4	133090.	4.052	4289.011	0.037	0.426	465.9	117	-41
274.5	132501.	4.055	4288.498	0.038	0.438	465.1	120	-41
274.6	132511.	4.054	4287.971	0.038	0.437	465.1	121	-41
274.7	132454.	4.054	4287.431	0.038	0.438	465.0	126	-51
274.8	132247.	4.055	4286.878	0.038	0.442	464.7	129	-41
274.9	131876.	4.057	4286.312	0.039	0.450	464.2	132	-21

SUMMARY FOR FLIGHT STS29.

TIME (SEC)	ALTITUDE (FT)	MINF	VEL (FT/SEC)	PINF (PSIA)	QINF (PSIA)	TINF (DEG R)	ALP (DEG)	PHI-ALU (DEG)
275.0	131926.	4.056	4285.732	0.039	0.449	464.3	134	-21
275.1	131733.	4.056	4285.139	0.039	0.453	464.0	135	-31
275.2	131627.	4.056	4284.532	0.039	0.455	463.9	137	-31
275.3	131576.	4.056	4283.912	0.040	0.456	463.8	140	-1
275.4	131234.	4.058	4283.279	0.040	0.463	463.3	141	-1
275.5	130825.	4.059	4282.631	0.041	0.472	462.8	141	9
275.6	130850.	4.059	4281.969	0.041	0.471	462.8	143	9
275.7	130534.	4.060	4281.295	0.041	0.478	462.4	147	-1
275.8	129908.	4.063	4280.605	0.043	0.492	461.6	146	9
275.9	129609.	4.064	4279.902	0.043	0.499	461.2	150	-1
276.0	129729.	4.062	4279.186	0.043	0.496	461.4	146	14
276.1	129225.	4.065	4278.455	0.044	0.507	460.7	148	14
276.2	129033.	4.065	4277.709	0.044	0.512	460.4	150	14
276.3	128570.	4.067	4276.949	0.045	0.523	459.8	152	14
276.4	128530.	4.067	4276.175	0.045	0.524	459.8	158	9
276.5	128354.	4.067	4275.387	0.046	0.528	459.5	155	14
276.6	128235.	4.067	4274.584	0.046	0.530	459.3	155	19
276.7	128022.	4.067	4273.766	0.046	0.536	459.1	155	14
276.8	127613.	4.069	4272.934	0.047	0.546	458.5	162	9
276.9	127199.	4.071	4272.087	0.048	0.556	457.9	155	14
277.0	127011.	4.071	4271.226	0.048	0.561	457.7	156	19
277.1	126626.	4.073	4270.349	0.049	0.571	457.1	156	19
277.2	126642.	4.072	4269.457	0.049	0.570	457.2	156	19
277.3	126464.	4.072	4268.551	0.050	0.575	456.9	172	134
277.4	126129.	4.073	4267.629	0.050	0.583	456.4	157	19
277.5	126032.	4.073	4266.692	0.050	0.586	456.3	159	19
277.6	125955.	4.073	4265.740	0.051	0.588	456.2	158	19
277.7	125832.	4.072	4264.773	0.051	0.591	456.0	154	164
277.8	125196.	4.075	4263.791	0.052	0.608	455.1	151	164
277.9	124847.	4.077	4262.792	0.053	0.618	454.6	150	169
278.0	125026.	4.075	4261.778	0.053	0.613	454.9	148	164
278.1	125033.	4.074	4260.749	0.053	0.612	454.9	144	164
278.2	124549.	4.076	4259.704	0.054	0.626	454.2	143	169
278.3	124551.	4.075	4258.643	0.054	0.626	454.2	140	169
278.4	124264.	4.076	4257.566	0.055	0.634	453.8	139	169
278.5	124136.	4.075	4256.473	0.055	0.637	453.6	138	174
278.6	123961.	4.075	4255.365	0.055	0.642	453.3	135	174
278.7	122901.	4.081	4254.240	0.058	0.675	451.8	135	179
278.8	122981.	4.080	4253.100	0.058	0.672	451.9	130	-126
278.9	123005.	4.078	4251.942	0.058	0.671	451.9	123	-126
279.0	122595.	4.080	4250.769	0.059	0.683	451.4	122	-131
279.1	122263.	4.081	4249.580	0.059	0.694	450.9	121	-131
279.2	122089.	4.081	4248.373	0.060	0.699	450.6	114	-146
279.3	121941.	4.081	4247.150	0.060	0.703	450.4	112	-146
279.4	121692.	4.081	4245.911	0.061	0.711	450.1	109	-146
279.5	121450.	4.081	4244.655	0.062	0.719	449.7	107	-146
279.6	121208.	4.082	4243.382	0.062	0.727	449.4	106	-146
279.7	120389.	4.086	4242.092	0.065	0.755	448.2	107	-146
279.8	120454.	4.084	4240.787	0.064	0.752	448.3	105	-141
279.9	120169.	4.085	4239.463	0.065	0.762	447.9	103	-141

SUMMARY FOR FLIGHT STS29.

TIME (SEC)	ALTITUDE (FT)	MINF	VEL (FT/SEC)	PINF (PSIA)	QINF (PSIA)	TINF (DEG R)	ALP (DEG)	PHI-ALU (DEG)
280.0	119539.	4.088	4238.122	0.067	0.784	446.9	105	-141
280.1	119887.	4.084	4236.764	0.066	0.771	447.5	100	-141
280.2	119526.	4.085	4235.390	0.067	0.784	446.9	97	-136
280.3	119339.	4.085	4233.998	0.068	0.790	446.6	96	-136
280.4	119165.	4.085	4232.588	0.068	0.796	446.4	90	-121
280.5	118600.	4.088	4231.161	0.070	0.817	445.5	100	-136
280.6	118324.	4.088	4229.716	0.071	0.827	445.1	99	-136
280.7	118213.	4.087	4228.254	0.071	0.831	444.9	90	-131
280.8	117907.	4.088	4226.775	0.072	0.842	444.5	90	-121
280.9	117915.	4.087	4225.277	0.072	0.841	444.5	99	-136
281.0	117670.	4.087	4223.762	0.073	0.850	444.2	99	-131
281.1	117377.	4.087	4222.228	0.074	0.862	443.8	99	-131
281.2	116983.	4.088	4220.677	0.075	0.877	443.2	99	-131
281.3	116734.	4.088	4219.107	0.076	0.887	442.9	98	-131
281.4	116545.	4.088	4217.520	0.076	0.894	442.6	119	-101
281.5	116371.	4.087	4215.914	0.077	0.900	442.3	101	-131
281.6	116128.	4.087	4214.290	0.078	0.910	442.0	100	-136
281.7	115851.	4.088	4212.647	0.079	0.921	441.6	102	-131
281.8	115858.	4.086	4210.987	0.079	0.920	441.6	100	-136
281.9	115400.	4.088	4209.307	0.080	0.940	440.9	103	-131
282.0	115169.	4.088	4207.609	0.081	0.949	440.6	102	-136
282.1	114780.	4.089	4205.893	0.083	0.966	440.0	105	-136
282.2	114638.	4.088	4204.157	0.083	0.972	439.8	104	-136
282.3	114375.	4.088	4202.403	0.084	0.983	439.4	108	-141
282.4	114025.	4.089	4200.629	0.085	0.998	438.9	109	-141
282.5	113837.	4.088	4198.837	0.086	1.006	438.6	109	-141
282.6	113430.	4.089	4197.026	0.088	1.025	438.1	112	-141
282.7	113259.	4.088	4195.195	0.088	1.032	437.8	114	-146
282.8	113162.	4.087	4193.346	0.089	1.036	437.7	115	-146
282.9	112621.	4.089	4191.477	0.091	1.062	436.9	117	-146
283.0	112437.	4.088	4189.588	0.091	1.070	436.7	118	-146
283.1	112374.	4.087	4187.680	0.092	1.072	436.6	118	-146
283.2	112033.	4.087	4185.753	0.093	1.088	436.1	122	-141
283.3	112033.	4.085	4183.807	0.093	1.087	436.1	125	-146
283.4	111831.	4.085	4181.840	0.094	1.097	435.8	128	-146
283.5	111482.	4.085	4179.853	0.095	1.114	435.4	132	-146
283.6	111524.	4.083	4177.847	0.095	1.111	435.4	133	-151
283.7	110983.	4.084	4175.820	0.097	1.138	434.7	136	-151
283.8	110707.	4.084	4173.775	0.099	1.151	434.4	139	-151
283.9	110553.	4.082	4171.708	0.099	1.159	434.2	139	-156
284.0	110470.	4.081	4169.622	0.100	1.162	434.1	142	-161
284.1	110043.	4.081	4167.515	0.102	1.184	433.5	145	-161
284.2	110008.	4.080	4165.388	0.102	1.185	433.5	146	-161
284.3	109722.	4.079	4163.241	0.103	1.200	433.1	149	-161
284.4	109354.	4.079	4161.073	0.105	1.219	432.7	151	-161
284.5	109259.	4.078	4158.885	0.105	1.223	432.6	153	-161
284.6	108914.	4.077	4156.676	0.107	1.242	432.1	155	-161
284.7	108682.	4.076	4154.446	0.108	1.254	431.9	157	-151
284.8	108039.	4.078	4152.196	0.111	1.290	431.1	155	-161
284.9	108001.	4.076	4149.925	0.111	1.291	431.1	161	-161

SUMMARY FOR FLIGHT STS29.

TIME (SEC)	ALTITUDE (FT)	MINF	VEL (FT/SEC)	PINF (PSIA)	QINF (PSIA)	TINF (DEG R)	ALP (DEG)	PHI-ALU (DEG)
285.0	107895.	4.074	4147.632	0.112	1.296	430.9	163	-151
285.1	107828.	4.072	4145.319	0.112	1.299	430.9	160	-161
285.2	107372.	4.072	4142.985	0.114	1.325	430.3	163	-161
285.3	107221.	4.071	4140.631	0.115	1.333	430.2	165	-161
285.4	106619.	4.072	4138.254	0.118	1.369	429.5	171	-156
285.5	106495.	4.070	4135.856	0.119	1.375	429.4	166	19
285.6	106431.	4.068	4133.437	0.119	1.378	429.3	167	19
285.7	105962.	4.068	4130.996	0.121	1.406	428.8	167	14
285.8	105674.	4.067	4128.535	0.123	1.423	428.5	165	14
285.9	105624.	4.065	4126.051	0.123	1.425	428.4	161	-46
286.0	105423.	4.063	4123.546	0.124	1.437	428.2	157	-31
286.1	105096.	4.063	4121.019	0.126	1.457	427.8	153	-31
286.2	104848.	4.061	4118.470	0.127	1.472	427.6	151	-31
286.3	104564.	4.060	4115.899	0.129	1.489	427.3	147	-31
286.4	104183.	4.060	4113.307	0.131	1.514	426.8	145	-26
286.5	103840.	4.059	4110.692	0.133	1.536	426.5	142	-26
286.6	103635.	4.057	4108.055	0.134	1.549	426.2	140	-31
286.7	103623.	4.055	4105.396	0.134	1.548	426.2	137	-31
286.8	103460.	4.053	4102.716	0.135	1.557	426.0	134	-31
286.9	102805.	4.054	4100.013	0.139	1.603	425.3	133	-31
287.0	102824.	4.051	4097.287	0.139	1.600	425.4	131	-41
287.1	102625.	4.049	4094.539	0.140	1.612	425.1	128	-41
287.2	101963.	4.050	4091.768	0.145	1.660	424.4	127	-41
287.3	101774.	4.048	4088.976	0.146	1.673	424.2	124	-51
287.4	101397.	4.047	4086.159	0.148	1.700	423.8	118	-41
287.5	101035.	4.047	4083.321	0.151	1.726	423.4	115	-41
287.6	100812.	4.045	4080.459	0.152	1.742	423.1	115	-41
287.7	100636.	4.043	4077.575	0.153	1.753	423.0	115	-41
287.8	100631.	4.040	4074.668	0.153	1.751	422.9	114	-41
287.9	100352.	4.039	4071.738	0.155	1.772	422.6	113	-41
288.0	100256.	4.036	4068.785	0.156	1.777	422.5	113	-41
288.1	100241.	4.033	4065.808	0.156	1.776	422.5	112	-41
288.2	99787.	4.033	4062.809	0.159	1.811	422.0	113	-41
288.3	99704.	4.030	4059.787	0.160	1.815	421.9	112	-41
288.4	99294.	4.029	4056.740	0.163	1.847	421.5	112	-41
288.5	98867.	4.028	4053.670	0.166	1.881	421.0	113	-41
288.6	98754.	4.026	4050.577	0.166	1.888	420.9	112	-41
288.7	98315.	4.025	4047.460	0.170	1.924	420.5	113	-41
288.8	98292.	4.022	4044.321	0.170	1.923	420.4	114	-41
288.9	98133.	4.020	4041.157	0.171	1.934	420.3	115	-41
289.0	97680.	4.019	4037.969	0.174	1.972	419.8	115	-41
289.1	97508.	4.016	4034.758	0.176	1.984	419.6	115	-41
289.2	97078.	4.016	4031.523	0.179	2.021	419.1	117	-41
289.3	96603.	4.016	4028.265	0.183	2.064	418.4	123	-51
289.4	96415.	4.014	4024.981	0.184	2.079	418.2	128	-41
289.5	96274.	4.011	4021.674	0.185	2.089	418.0	129	-31
289.6	95934.	4.010	4018.342	0.188	2.119	417.5	132	-31
289.7	95713.	4.008	4014.987	0.190	2.138	417.2	134	-26
289.8	95515.	4.006	4011.608	0.192	2.154	416.9	136	-26
289.9	95517.	4.003	4008.204	0.192	2.150	416.9	138	-26

SUMMARY FOR FLIGHT STS29.

TIME (SEC)	ALTITUDE (FT)	MINF	VEL (FT/SEC)	PINF (PSIA)	QINF (PSIA)	TINF (DEG R)	ALP (DEG)	PHI-ALU (DEG)
290.0	95084.	4.002	4004.775	0.195	2.191	416.3	141	-31
290.1	95133.	3.999	4001.323	0.195	2.182	416.4	143	-26
290.2	94933.	3.997	3997.845	0.197	2.199	416.1	146	-26
290.3	94885.	3.993	3994.345	0.197	2.200	416.0	148	-26
290.4	94185.	3.995	3990.818	0.203	2.271	414.9	152	-11
290.5	93986.	3.993	3987.267	0.205	2.288	414.6	154	-11
290.6	94007.	3.989	3983.691	0.205	2.282	414.7	155	-1
290.7	93451.	3.990	3980.090	0.210	2.338	413.8	158	-1
290.8	93057.	3.989	3976.466	0.214	2.378	413.2	162	-1
290.9	92754.	3.987	3972.816	0.216	2.408	412.7	165	-1
291.0	92902.	3.983	3969.140	0.215	2.387	413.0	167	4
291.1	92901.	3.979	3965.440	0.215	2.382	413.0	170	9
291.2	92303.	3.980	3961.715	0.221	2.446	412.1	173	9
291.3	92195.	3.977	3957.965	0.222	2.454	411.9	171	19
291.4	91959.	3.975	3954.190	0.224	2.477	411.5	171	19
291.5	91509.	3.974	3950.390	0.228	2.526	410.8	172	19
291.6	91402.	3.971	3946.563	0.230	2.534	410.7	173	24
291.7	91500.	3.967	3942.712	0.229	2.517	410.8	174	19
291.8	90790.	3.968	3938.836	0.236	2.598	409.8	170	159
291.9	90543.	3.966	3934.935	0.238	2.624	409.4	165	164
292.0	90404.	3.963	3931.006	0.240	2.636	409.2	160	169
292.1	90158.	3.960	3927.053	0.242	2.661	408.8	157	169
292.2	90171.	3.956	3923.075	0.242	2.654	408.8	154	-126
292.3	89615.	3.956	3919.072	0.248	2.720	408.0	151	-126
292.4	89166.	3.956	3915.042	0.253	2.772	407.3	149	-126
292.5	88813.	3.954	3910.986	0.257	2.813	406.8	144	-146
292.6	88785.	3.950	3906.904	0.257	2.811	406.7	142	-151
292.7	88329.	3.949	3902.797	0.263	2.867	406.1	139	-151
292.8	88012.	3.948	3898.665	0.266	2.904	405.6	137	-146
292.9	87587.	3.946	3894.506	0.271	2.957	404.9	135	169
293.0	87521.	3.943	3890.321	0.272	2.960	404.8	134	-71
293.1	87163.	3.941	3886.110	0.276	3.004	404.3	133	-71
293.2	87036.	3.938	3881.873	0.278	3.016	404.1	132	-71
293.3	86652.	3.936	3877.611	0.283	3.064	403.6	131	-71
293.4	86684.	3.931	3873.322	0.282	3.053	403.6	130	-71
293.5	86551.	3.928	3869.007	0.284	3.065	403.4	130	-71
293.6	86175.	3.926	3864.665	0.289	3.113	402.9	129	-71
293.7	85672.	3.925	3860.297	0.295	3.181	402.1	129	-71
293.8	85771.	3.920	3855.904	0.294	3.159	402.3	129	-71
293.9	85331.	3.919	3851.484	0.299	3.219	401.6	129	-71
294.0	84843.	3.918	3847.037	0.306	3.287	400.8	130	-71
294.1	84307.	3.918	3842.563	0.313	3.364	400.0	130	-71
294.2	84460.	3.912	3838.064	0.311	3.332	400.2	130	-71
294.3	84358.	3.908	3833.540	0.312	3.340	400.1	131	-71
294.4	83809.	3.909	3828.986	0.320	3.422	399.0	132	-71
294.5	83738.	3.905	3824.408	0.321	3.427	398.7	133	-71
294.6	83638.	3.902	3819.802	0.322	3.437	398.4	134	-71
294.7	83545.	3.899	3815.169	0.324	3.445	398.0	135	-71
294.8	83080.	3.903	3810.512	0.330	3.523	396.3	137	-71
294.9	82750.	3.904	3805.826	0.335	3.576	395.1	138	-71

SUMMARY FOR FLIGHT STS29.

TIME (SEC)	ALTITUDE (FT)	MINF	VEL (FT/SEC)	PINF (PSIA)	QINF (PSIA)	TINF (DEG R)	ALP (DEG)	PHI-ALU (DEG)
295.0	82627.	3.902	3801.113	0.337	3.591	394.7	140	-71
295.1	82440.	3.900	3796.374	0.340	3.617	394.0	142	-71
295.2	82248.	3.899	3791.607	0.343	3.645	393.3	144	-71
295.3	81891.	3.898	3786.816	0.348	3.702	392.3	146	-71
295.4	81771.	3.894	3781.997	0.350	3.714	392.1	148	-71
295.5	81768.	3.889	3777.150	0.350	3.705	392.1	150	-71
295.6	81699.	3.885	3772.277	0.351	3.707	392.0	153	-71
295.7	81400.	3.882	3767.376	0.356	3.751	391.6	155	-71
295.8	80712.	3.883	3762.451	0.366	3.866	390.5	158	-71
295.9	80397.	3.880	3757.497	0.372	3.915	390.0	161	-71
296.0	80377.	3.875	3752.515	0.372	3.908	389.9	164	-71
296.1	80140.	3.871	3747.507	0.376	3.940	389.7	168	139
296.2	79971.	3.865	3742.472	0.378	3.958	389.8	171	-161
296.3	79678.	3.859	3737.411	0.383	3.997	389.9	172	-161
296.4	79530.	3.854	3732.322	0.386	4.012	390.0	173	14
296.5	79329.	3.848	3727.205	0.389	4.035	390.0	170	14
296.6	79134.	3.843	3722.062	0.393	4.058	390.1	168	-1
296.7	78760.	3.837	3716.891	0.399	4.112	390.3	163	4
296.8	78595.	3.831	3711.694	0.402	4.129	390.3	158	4
296.9	78421.	3.825	3706.469	0.405	4.149	390.4	155	4
297.0	78115.	3.821	3701.217	0.410	4.195	390.2	152	4
297.1	77847.	3.816	3695.938	0.415	4.234	390.0	150	4
297.2	77559.	3.812	3690.631	0.421	4.277	389.8	147	4
297.3	77327.	3.807	3685.299	0.425	4.310	389.7	145	4
297.4	77135.	3.802	3679.938	0.428	4.335	389.6	143	4
297.5	76813.	3.797	3674.549	0.435	4.386	389.3	141	4
297.6	76473.	3.794	3669.133	0.441	4.444	388.9	140	4
297.7	76298.	3.790	3663.690	0.444	4.470	388.5	139	4
297.8	75771.	3.791	3658.222	0.455	4.576	387.2	139	4
297.9	75738.	3.786	3652.724	0.455	4.569	387.1	138	4
298.0	75652.	3.781	3647.199	0.457	4.575	386.9	138	4
298.1	75447.	3.778	3641.647	0.461	4.608	386.4	138	4
298.2	74840.	3.779	3636.068	0.474	4.736	384.9	138	4
298.3	74859.	3.773	3630.463	0.473	4.717	385.0	139	4
298.4	74627.	3.770	3624.829	0.478	4.757	384.4	140	4
298.5	73668.	3.775	3619.167	0.499	4.974	382.2	141	4
298.6	73686.	3.769	3613.479	0.498	4.954	382.2	143	4
298.7	73679.	3.763	3607.762	0.498	4.940	382.2	144	4
298.8	73730.	3.756	3602.021	0.497	4.912	382.3	145	4
298.9	73627.	3.751	3596.250	0.500	4.921	382.1	147	4
299.0	73392.	3.748	3590.452	0.505	4.963	381.6	150	4
299.1	73142.	3.745	3584.626	0.510	5.009	381.0	152	4
299.2	72606.	3.742	3578.773	0.522	5.121	380.3	154	9
299.3	72191.	3.738	3572.896	0.532	5.203	379.8	157	9
299.4	71720.	3.735	3566.988	0.543	5.301	379.3	160	14
299.5	71602.	3.729	3561.054	0.546	5.313	379.2	163	14
299.6	71592.	3.723	3555.092	0.546	5.298	379.2	165	19
299.7	71221.	3.717	3549.103	0.555	5.369	379.0	168	29
299.8	70908.	3.710	3543.088	0.563	5.421	379.2	171	34
299.9	70957.	3.704	3537.044	0.561	5.392	379.2	173	39

SUMMARY FOR FLIGHT STS29.

TIME (SEC)	ALTITUDE (FT)	MINF	VEL (FT/SEC)	PINF (PSIA)	QINF (PSIA)	TINF (DEG R)	ALP (DEG)	PHI-ALU (DEG)
300.0	70803.	3.697	3530.973	0.565	5.408	379.3	174	74
300.1	70246.	3.689	3524.875	0.579	5.516	379.7	174	89
300.2	70225.	3.682	3518.749	0.580	5.502	379.7	172	104
300.3	70068.	3.675	3512.598	0.584	5.519	379.9	169	119
300.4	69923.	3.668	3506.418	0.587	5.533	380.0	166	124
300.5	69547.	3.661	3500.211	0.597	5.604	380.0	162	129
300.6	69333.	3.657	3493.977	0.603	5.644	379.5	159	134
300.7	69085.	3.653	3487.716	0.609	5.694	378.9	156	139
300.8	69034.	3.647	3481.429	0.611	5.687	378.8	153	139
300.9	68858.	3.643	3475.113	0.615	5.717	378.4	151	139
301.0	68487.	3.640	3468.771	0.626	5.803	377.5	149	139
301.1	68471.	3.634	3462.400	0.626	5.786	377.5	147	139
301.2	67897.	3.634	3456.004	0.642	5.932	376.1	146	144
301.3	67553.	3.630	3449.582	0.652	6.010	375.5	145	144
301.4	67428.	3.624	3443.131	0.655	6.024	375.3	144	149
301.5	67275.	3.619	3436.653	0.660	6.047	375.0	143	149
301.6	67492.	3.610	3430.148	0.653	5.960	375.4	142	149
301.7	66796.	3.609	3423.616	0.674	6.143	374.1	143	149
301.8	66132.	3.608	3417.059	0.693	6.317	373.0	144	154
301.9	65873.	3.601	3410.474	0.701	6.367	372.9	145	154
302.0	65973.	3.594	3403.861	0.698	6.314	372.9	146	154
302.1	66017.	3.587	3397.222	0.697	6.277	373.0	147	159
302.2	66006.	3.580	3390.556	0.697	6.255	373.0	148	159
302.3	65638.	3.574	3383.865	0.709	6.335	372.8	150	159
302.4	65520.	3.567	3377.146	0.712	6.344	372.7	151	164
302.5	65151.	3.561	3370.399	0.724	6.425	372.5	154	164
302.6	64841.	3.555	3363.626	0.734	6.489	372.3	156	169
302.7	64359.	3.549	3356.827	0.749	6.607	372.0	158	169
302.8	64521.	3.541	3350.003	0.744	6.531	372.1	160	174
302.9	64426.	3.534	3343.151	0.747	6.533	372.1	163	-176
303.0	63814.	3.529	3336.272	0.767	6.691	371.6	164	-171
303.1	63809.	3.522	3329.366	0.768	6.665	371.6	166	-166
303.2	63607.	3.515	3322.435	0.774	6.699	371.4	170	-161
303.3	63070.	3.510	3315.478	0.793	6.838	371.0	173	-151
303.4	62983.	3.503	3308.494	0.796	6.836	370.9	171	-161
303.5	62905.	3.496	3301.483	0.799	6.832	370.8	173	-156
303.6	62916.	3.489	3294.446	0.798	6.799	370.8	177	-156
303.7	62758.	3.482	3287.383	0.804	6.821	370.6	175	-71
303.8	62139.	3.478	3280.296	0.826	6.992	369.9	173	-61
303.9	62092.	3.471	3273.180	0.827	6.977	369.8	169	-51
304.0	61905.	3.464	3266.039	0.834	7.007	369.6	165	-46
304.1	61630.	3.458	3258.872	0.844	7.067	369.3	162	-41
304.2	61015.	3.452	3251.678	0.867	7.236	368.9	159	-36
304.3	61156.	3.444	3244.461	0.862	7.159	368.9	156	-31
304.4	61142.	3.437	3237.217	0.863	7.132	368.9	154	-31
304.5	60908.	3.429	3229.946	0.871	7.174	368.9	151	-26
304.6	60481.	3.422	3222.649	0.888	7.279	368.7	150	-26
304.7	60002.	3.415	3215.327	0.907	7.403	368.6	149	-26
304.8	59946.	3.407	3207.981	0.909	7.387	368.5	149	-26
304.9	59783.	3.400	3200.608	0.915	7.408	368.4	148	-26

SUMMARY FOR FLIGHT STS29.

TIME (SEC)	ALTITUDE (FT)	MINF	VEL (FT/SEC)	PINF (PSIA)	QINF (PSIA)	TINF (DEG R)	ALP (DEG)	PHI-ALU (DEG)
305.0	59546.	3.396	3193.209	0.925	7.466	367.7	148	-21
305.1	59388.	3.390	3185.785	0.931	7.493	367.2	148	-21
305.2	58851.	3.390	3178.336	0.954	7.671	365.5	149	-16
305.3	58635.	3.385	3170.863	0.963	7.721	364.8	150	-11
305.4	58330.	3.382	3163.363	0.976	7.809	363.9	152	-11
305.5	58151.	3.375	3155.838	0.983	7.840	363.5	153	-1
305.6	58012.	3.368	3148.288	0.989	7.854	363.3	155	4
305.7	57546.	3.362	3140.712	1.010	7.988	362.9	157	9
305.8	57336.	3.355	3133.114	1.019	8.027	362.6	159	14
305.9	57337.	3.347	3125.489	1.019	7.988	362.6	160	19
306.0	56991.	3.340	3117.839	1.034	8.078	362.3	163	24
306.1	56498.	3.330	3110.164	1.057	8.206	362.6	165	29
306.2	56766.	3.325	3102.465	1.045	8.083	362.0	167	39
306.3	56778.	3.317	3094.743	1.044	8.039	362.0	168	39
306.4	56464.	3.305	3086.994	1.058	8.095	362.7	172	64
306.5	56301.	3.295	3079.221	1.066	8.102	363.1	172	79
306.6	56226.	3.286	3071.424	1.070	8.083	363.3	172	89
306.7	56029.	3.275	3063.602	1.079	8.100	363.8	172	94
306.8	56071.	3.267	3055.758	1.077	8.046	363.7	172	119
306.9	55767.	3.255	3047.888	1.091	8.095	364.5	173	139
307.0	55158.	3.241	3039.994	1.121	8.238	365.9	173	159
307.1	54917.	3.232	3032.075	1.133	8.279	366.0	172	169
307.2	54789.	3.223	3024.133	1.139	8.281	366.1	169	169
307.3	54762.	3.214	3016.169	1.140	8.247	366.1	166	174
307.4	54356.	3.205	3008.180	1.161	8.346	366.3	165	-136
307.5	53995.	3.196	3000.167	1.179	8.429	366.5	161	-151
307.6	53530.	3.187	2992.129	1.203	8.558	366.4	159	-151
307.7	53485.	3.179	2984.069	1.206	8.530	366.4	157	-146
307.8	53374.	3.171	2975.987	1.212	8.527	366.3	156	-141
307.9	53244.	3.162	2967.880	1.219	8.531	366.2	154	-136
308.0	53138.	3.154	2959.749	1.224	8.526	366.1	153	169
308.1	53199.	3.145	2951.596	1.221	8.455	366.2	152	-71
308.2	53144.	3.137	2943.419	1.224	8.430	366.1	152	-71
308.3	53032.	3.128	2935.222	1.230	8.426	366.0	151	-71
308.4	52970.	3.120	2926.999	1.233	8.403	366.0	151	-71
308.5	52127.	3.111	2918.754	1.280	8.670	366.0	152	-71
308.6	52054.	3.101	2910.486	1.284	8.644	366.2	152	-71
308.7	52058.	3.093	2902.195	1.284	8.594	366.2	153	-71
308.8	51896.	3.082	2893.885	1.293	8.596	366.6	153	-71
308.9	51841.	3.073	2885.549	1.296	8.564	366.7	154	-71
309.0	51766.	3.063	2877.191	1.300	8.538	366.9	156	-71
309.1	51081.	3.047	2868.811	1.340	8.706	368.6	157	-71
309.2	51051.	3.038	2860.409	1.341	8.665	368.6	159	-71
309.3	50319.	3.025	2851.987	1.385	8.872	369.6	161	-71
309.4	50348.	3.016	2843.541	1.383	8.809	369.5	163	-71
309.5	50266.	3.007	2835.073	1.388	8.787	369.6	165	139
309.6	50224.	2.998	2826.583	1.391	8.749	369.6	168	-86
309.7	50061.	2.988	2818.072	1.401	8.755	369.8	169	-81
309.8	49872.	2.978	2809.541	1.412	8.770	370.0	170	-71
309.9	49741.	2.969	2800.987	1.420	8.764	370.1	171	-61

SUMMARY FOR FLIGHT STS29.

TIME (SEC)	ALTITUDE (FT)	MINF	VEL (FT/SEC)	PINF (PSIA)	QINF (PSIA)	TINF (DEG R)	ALP (DEG)	PHI-ALU (DEG)
310.0	49500.	2.959	2792.411	1.435	8.797	370.3	172	-41
310.1	49377.	2.949	2783.815	1.443	8.785	370.6	171	144
310.2	49056.	2.937	2775.197	1.464	8.839	371.2	171	-21
310.3	48660.	2.925	2766.561	1.489	8.919	372.0	170	-6
310.4	48573.	2.915	2757.901	1.495	8.893	372.1	170	4
310.5	48584.	2.906	2749.221	1.494	8.834	372.1	168	14
310.6	48278.	2.895	2740.520	1.514	8.882	372.7	167	19
310.7	48298.	2.886	2731.798	1.513	8.819	372.7	165	19
310.8	48114.	2.875	2723.059	1.525	8.827	372.9	164	29
310.9	47703.	2.865	2714.297	1.553	8.925	373.1	162	29
311.0	47563.	2.856	2705.514	1.562	8.920	373.2	161	34
311.1	47587.	2.847	2696.712	1.561	8.853	373.2	159	34
311.2	47465.	2.837	2687.889	1.569	8.841	373.2	158	34
311.3	46974.	2.827	2679.049	1.603	8.968	373.4	157	39
311.4	47036.	2.818	2670.188	1.599	8.886	373.4	157	39
311.5	46639.	2.808	2661.305	1.627	8.977	373.6	156	39
311.6	46463.	2.798	2652.404	1.639	8.985	373.6	156	39
311.7	46324.	2.788	2643.483	1.649	8.977	373.7	156	39
311.8	45810.	2.778	2634.546	1.687	9.115	373.9	156	39
311.9	45716.	2.769	2625.587	1.694	9.089	373.9	156	39
312.0	45701.	2.759	2616.609	1.695	9.033	373.9	156	39
312.1	45538.	2.749	2607.612	1.707	9.034	374.0	157	39
312.2	45479.	2.740	2598.596	1.712	8.992	374.1	157	39
312.3	45239.	2.729	2589.564	1.730	9.015	374.5	157	39
312.4	45216.	2.719	2580.511	1.731	8.960	374.5	159	39
312.5	45254.	2.710	2571.439	1.729	8.884	374.5	160	39
312.6	44578.	2.696	2562.350	1.780	9.059	375.6	161	39
312.7	44447.	2.686	2553.242	1.791	9.041	375.8	162	39
312.8	44198.	2.675	2544.119	1.810	9.064	376.2	163	39
312.9	44272.	2.665	2534.975	1.804	8.974	376.1	164	39
313.0	44288.	2.656	2525.813	1.803	8.903	376.1	165	39
313.1	44293.	2.646	2516.634	1.803	8.837	376.0	165	39
313.2	44157.	2.636	2507.437	1.814	8.819	376.3	166	39
313.3	43793.	2.623	2498.226	1.843	8.876	377.1	167	39
313.4	43312.	2.610	2488.994	1.882	8.973	378.2	169	39
313.5	43001.	2.598	2479.746	1.908	9.012	378.8	169	159
313.6	42991.	2.588	2470.480	1.908	8.948	378.9	168	154
313.7	42615.	2.576	2461.197	1.940	9.012	379.6	167	149
313.8	42599.	2.566	2451.901	1.941	8.949	379.6	168	149
313.9	42304.	2.555	2442.585	1.967	8.984	380.1	167	154
314.0	42196.	2.544	2433.253	1.976	8.953	380.4	168	164
314.1	42013.	2.533	2423.904	1.992	8.947	380.7	166	149
314.2	41889.	2.523	2414.539	2.003	8.921	380.9	167	149
314.3	41646.	2.510	2405.161	2.024	8.929	381.7	166	154
314.4	41647.	2.501	2395.764	2.024	8.859	381.7	167	154
314.5	41384.	2.488	2386.351	2.047	8.869	382.6	167	154
314.6	41222.	2.476	2376.923	2.062	8.848	383.2	167	149
314.7	41115.	2.465	2367.479	2.072	8.809	383.6	167	149
314.8	40547.	2.449	2358.022	2.124	8.913	385.6	167	144
314.9	39836.	2.435	2348.548	2.191	9.091	386.9	168	144

SUMMARY FOR FLIGHT STS29.

TIME (SEC)	ALTITUDE (FT)	MINF	VEL (FT/SEC)	PINF (PSIA)	QINF (PSIA)	TINF (DEG R)	ALP (DEG)	PHI-ALU (DEG)
315.0	39802.	2.425	2339.059	2.194	9.030	387.0	168	149
315.1	39792.	2.415	2329.554	2.195	8.960	387.0	168	154
315.2	39464.	2.403	2320.034	2.227	9.001	387.6	169	149
315.3	39368.	2.393	2310.503	2.236	8.966	387.5	168	-71
315.4	39158.	2.384	2300.955	2.257	8.980	387.3	167	-71
315.5	39182.	2.374	2291.391	2.254	8.895	387.3	166	-71
315.6	39196.	2.364	2281.814	2.253	8.815	387.3	164	-71
315.7	39162.	2.354	2272.223	2.256	8.755	387.3	163	-76
315.8	39156.	2.344	2262.620	2.257	8.684	387.3	162	-76
315.9	38952.	2.335	2253.001	2.277	8.693	387.0	159	-86
316.0	38724.	2.326	2243.368	2.300	8.711	386.8	160	-76
316.1	38295.	2.317	2233.722	2.344	8.811	386.3	159	-76
316.2	38199.	2.307	2224.062	2.354	8.769	386.4	158	-81
316.3	38137.	2.297	2214.392	2.360	8.715	386.5	157	-81
316.4	38080.	2.287	2204.706	2.366	8.660	386.5	156	-81
316.5	38069.	2.277	2195.006	2.367	8.587	386.5	155	-81
316.6	38010.	2.266	2185.294	2.373	8.532	386.6	154	-81
316.7	37981.	2.256	2175.570	2.376	8.467	386.6	154	-81
316.8	37927.	2.246	2165.836	2.382	8.410	386.7	153	-86
316.9	37605.	2.235	2156.086	2.416	8.446	387.0	154	-86
317.0	37572.	2.225	2146.325	2.419	8.381	387.0	153	-86
317.1	37558.	2.215	2136.551	2.420	8.309	387.0	153	-86
317.2	37173.	2.203	2126.766	2.462	8.365	387.4	154	-86
317.3	37135.	2.193	2116.971	2.466	8.298	387.6	154	-86
317.4	36862.	2.180	2107.163	2.495	8.298	388.6	155	-86
317.5	36600.	2.167	2097.342	2.524	8.294	389.6	155	-91
317.6	36602.	2.157	2087.510	2.524	8.216	389.6	156	-91
317.7	36563.	2.146	2077.667	2.528	8.150	389.8	156	-91
317.8	36390.	2.134	2067.817	2.547	8.120	390.4	157	-96
317.9	35866.	2.118	2057.952	2.606	8.184	392.6	158	-96
318.0	35830.	2.107	2048.077	2.610	8.115	392.7	159	-101
318.1	35723.	2.096	2038.191	2.623	8.064	393.2	159	-101
318.2	35974.	2.089	2028.295	2.594	7.922	392.1	159	-106
318.3	35898.	2.078	2018.391	2.603	7.864	392.4	159	-111
318.4	35897.	2.067	2008.475	2.603	7.788	392.4	160	-116
318.5	35877.	2.057	1998.548	2.605	7.716	392.5	160	-116
318.6	36003.	2.048	1988.612	2.591	7.608	392.0	160	-121
318.7	35986.	2.038	1978.667	2.593	7.537	392.0	159	-126
318.8	35815.	2.025	1968.715	2.612	7.502	392.8	159	-131
318.9	35469.	2.011	1958.750	2.652	7.509	394.4	159	-131
319.0	35109.	1.997	1948.776	2.694	7.519	396.0	159	-136
319.1	35068.	1.986	1938.794	2.699	7.453	396.2	158	-141
319.2	34538.	1.970	1928.802	2.762	7.501	398.8	158	-146
319.3	34102.	1.954	1918.806	2.816	7.527	400.9	158	-151
319.4	34030.	1.943	1908.797	2.824	7.466	401.2	158	-161
319.5	34082.	1.934	1898.780	2.818	7.375	401.0	157	-161
319.6	34104.	1.924	1888.756	2.815	7.292	400.9	154	-171
319.7	33961.	1.912	1878.723	2.833	7.248	401.5	153	179
319.8	33942.	1.901	1868.685	2.835	7.175	401.6	152	174
319.9	33659.	1.888	1858.637	2.871	7.160	403.1	152	169

SUMMARY FOR FLIGHT STS29.

TIME (SEC)	ALTITUDE (FT)	MINF	VEL (FT/SEC)	PINF (PSIA)	QINF (PSIA)	TINF (DEG R)	ALP (DEG)	PHI-ALU (DEG)
320.0	33544.	1.876	1848.581	2.885	7.108	403.7	148	164
320.1	33238.	1.862	1838.518	2.924	7.097	405.3	147	159
320.2	32864.	1.848	1828.447	2.972	7.102	407.2	148	154
320.3	32685.	1.836	1818.373	2.996	7.065	408.0	148	149
320.4	32745.	1.826	1808.289	2.988	6.973	407.8	147	144
320.5	32538.	1.814	1798.198	3.015	6.943	408.7	148	144
320.6	32180.	1.800	1788.100	3.063	6.947	410.3	152	139
320.7	32068.	1.789	1777.996	3.078	6.894	410.8	152	134
320.8	31768.	1.776	1767.889	3.118	6.882	412.2	153	129
320.9	31666.	1.764	1757.773	3.132	6.826	412.7	152	129
321.0	31664.	1.754	1747.651	3.132	6.748	412.7	148	129
321.1	31959.	1.747	1737.523	3.092	6.607	411.2	147	129
321.2	31927.	1.737	1727.390	3.097	6.537	411.4	147	124
321.3	31855.	1.726	1717.255	3.106	6.476	411.7	147	124
321.4	31230.	1.709	1707.111	3.192	6.527	414.8	148	124
321.5	31043.	1.697	1696.962	3.219	6.488	415.8	147	124
321.6	30973.	1.686	1686.809	3.229	6.425	416.1	147	124
321.7	30874.	1.675	1676.650	3.243	6.368	416.6	147	124
321.8	30722.	1.663	1666.490	3.264	6.322	417.4	145	119
321.9	30462.	1.651	1656.323	3.302	6.297	418.7	147	124
322.0	30423.	1.640	1646.152	3.307	6.227	418.9	147	124
322.1	30310.	1.629	1635.977	3.324	6.173	419.4	146	149
322.2	29671.	1.613	1625.797	3.418	6.222	422.6	152	124
322.3	29624.	1.602	1615.617	3.425	6.154	422.8	148	129
322.4	29585.	1.592	1605.431	3.431	6.084	423.0	147	129
322.5	29567.	1.581	1595.241	3.433	6.010	423.1	147	129
322.6	29412.	1.570	1585.048	3.457	5.963	423.9	147	129
322.7	28974.	1.556	1574.853	3.524	5.969	426.1	147	134
322.8	28935.	1.545	1564.657	3.530	5.900	426.3	146	139
322.9	29118.	1.537	1554.456	3.501	5.789	425.4	145	144
323.0	29201.	1.527	1544.252	3.489	5.698	425.0	144	144
323.1	29119.	1.517	1534.046	3.501	5.638	425.4	143	149
323.2	29068.	1.506	1523.837	3.509	5.572	425.7	141	154
323.3	29074.	1.496	1513.630	3.508	5.497	425.6	140	154
323.4	29049.	1.486	1503.418	3.512	5.427	425.7	139	154
323.5	28796.	1.474	1493.205	3.551	5.399	426.9	139	164
323.6	28242.	1.460	1482.990	3.638	5.426	429.2	138	169
323.7	28162.	1.449	1472.773	3.651	5.366	429.5	137	174
323.8	28306.	1.440	1462.559	3.628	5.266	428.9	135	179
323.9	28481.	1.431	1452.341	3.600	5.162	428.2	133	-176
324.0	28549.	1.422	1442.122	3.590	5.078	427.9	135	-161
324.1	28309.	1.410	1431.903	3.628	5.047	428.9	130	-161
324.2	27992.	1.398	1421.683	3.678	5.029	430.2	180	-71
324.3	27672.	1.385	1411.466	3.730	5.010	431.7	180	-71
324.4	27662.	1.375	1401.246	3.732	4.939	431.8	180	-71
324.5	27616.	1.365	1391.026	3.739	4.875	432.0	180	-71
324.6	27412.	1.353	1380.807	3.773	4.836	432.9	180	-71
324.7	27371.	1.343	1370.588	3.780	4.771	433.1	180	-71
324.8	27111.	1.331	1360.373	3.823	4.741	434.3	180	-71
324.9	26992.	1.320	1350.155	3.843	4.688	434.9	180	-71

SUMMARY FOR FLIGHT STS29.

TIME (SEC)	ALTITUDE (FT)	MINF	VEL (FT/SEC)	PINF (PSIA)	QINF (PSIA)	TINF (DEG R)	ALP (DEG)	PHI-ALU (DEG)
325.0	26977.	1.310	1339.939	3.845	4.620	435.0	180	-71
325.1	26979.	1.300	1329.724	3.845	4.550	434.9	180	-71
325.2	27004.	1.290	1319.510	3.841	4.476	434.8	180	-71
325.3	26881.	1.279	1309.301	3.862	4.425	435.4	180	-71
325.4	26621.	1.268	1299.091	3.906	4.393	436.7	180	-71
325.5	26536.	1.257	1288.883	3.920	4.337	437.1	180	-71
325.6	26609.	1.248	1278.677	3.908	4.258	436.7	180	-71
325.7	26639.	1.238	1268.473	3.903	4.186	436.6	180	-71
325.8	26671.	1.228	1258.275	3.897	4.115	436.4	180	-71
325.9	26673.	1.218	1248.077	3.897	4.048	436.4	180	-71
326.0	26653.	1.208	1237.881	3.900	3.985	436.5	180	-71
326.1	26444.	1.197	1227.689	3.936	3.946	437.5	180	-71
326.2	26194.	1.185	1217.500	3.979	3.913	438.7	180	-71
326.3	26160.	1.175	1207.317	3.985	3.852	438.9	180	-71
326.4	26238.	1.166	1197.135	3.972	3.778	438.5	180	-71
326.5	26233.	1.156	1186.957	3.973	3.714	438.6	180	-71
326.6	26179.	1.145	1176.782	3.982	3.658	438.8	180	-71
326.7	26028.	1.135	1166.612	4.008	3.612	439.5	180	-71
326.8	26005.	1.125	1156.449	4.012	3.552	439.6	180	-71
326.9	26008.	1.115	1146.288	4.012	3.490	439.6	180	-71
327.0	26107.	1.105	1136.132	3.995	3.417	439.2	180	-71
327.1	26176.	1.096	1125.981	3.982	3.349	438.8	180	-71
327.2	25998.	1.085	1115.834	4.014	3.308	439.7	180	-71
327.3	25462.	1.072	1105.697	4.109	3.306	442.2	180	-71
327.4	24985.	1.060	1095.561	4.196	3.298	444.5	180	-71
327.5	24778.	1.049	1085.432	4.234	3.259	445.5	180	-71
327.6	24221.	1.036	1075.308	4.338	3.258	448.1	180	-71
327.7	24235.	1.026	1065.190	4.336	3.196	448.0	180	-71
327.8	24341.	1.017	1055.082	4.315	3.124	447.5	180	-71
327.9	24440.	1.008	1044.977	4.297	3.055	447.0	180	-71
328.0	24541.	0.999	1034.879	4.278	2.986	446.6	180	-71

Appendix IV

SRB Reentry Flight Heating Analysis of STS-26R, 27R and 29R (RTN 213–15)

REMTECH TECHNICAL NOTE

SUBJECT: SRB Reentry Flight Heating Analysis of STS-26R, 27R, and 29R

DATE: June 1991

AUTHORS: William K. Crain and Robert D. Kirchner

CONTRACT NO.: NAS8–37891

PREPARED FOR: Induced Environments Branch (ED33), George C. Marshall Space Flight Center

INTRODUCTION

Previous DFI flights (STS 1–6) were heavily instrumented to acquire a flight data base. However, several significant holes existed in the instrumentation locations. The instrumentation on STS-26R, 27R and 29R was chosen to cover these areas of significant heating not previously addressed on the former flights. These measurements ranged from internal pressure and gas temperature to heat flux and surface static pressure. The measurements covered both the ascent and reentry phase of flight. (The objectives of each set of instrumentation are shown in Table 1.) Data from the current DFI flights were analyzed from a reentry heating point of view. This analysis covered the external calorimeter and internal aft skirt calorimeter and gas temperature probe measurements. In this analysis the current data were compared with historic measurements from STS 1–6 as well as semi-empirical predictions based on the wind tunnel and flight test data base. The objective was to summarize the reentry heating and verify some of the trends observed in the data. The purpose of this report is to document this analysis.

Reentry trajectory construction using the left hand SRB external circumferential pressure measurements as well as the reentry frustum venting analysis is addressed in Refs. [1,2]. The basic uncorrected raw flight data were compiled and presented in tabular and plotted form in Refs. [3–5].

INSTRUMENTATION AND LOCATION

The left hand SRB was instrumented with external calorimeters and internal aft skirt calorimeters, radiometer, and gas temperature probes The right hand SRB contained internal aft skirt instrumentation only. This consisted of calorimeters, and gas temperature probes which were placed in the same location as those on the left hand SRB. Instrumentation type and location is illustrated in Figs. 1–3 and tabulated in Tables 2 and 3. Instrumentation inside the aft skirts was located, primarily, on and around the TVC (Thrust Vector Control) components. The left hand SRB internal aft skirt (Fig. 2) had three total calorimeters, one radiometer, and eight gas temperature probes. The right

hand SRB had two total calorimeters and six gas temperature probes (Fig. 3). External SRB instrumentation (Fig. 1) consisted of seven total calorimeters.

The calorimeters used on the current DFI flights were a combination of Medtherm Schmidt-Boelter gages and Hy-Cal asymptotic calorimeters. A sketch of these is shown in Fig. 4, along with a sketch of a typical aft skirt gas temperature probe. The Schmidt-Boelter gages were used on the forward frustum. The remainder of external and internal aft skirt heat gages were the Hy-Cal calorimeters. Gage ranges used were 0–15 BTU/ft^2-sec on the forward frustum and attach ring, 0–20 BTU/ft^2-sec on the external aft skirt, and 0–25 BTU/ft^2-sec inside the left and right hand SRB aft skirt. Uncertainty in the gages alone is quoted to be ± 3 percent of full scale.

FLIGHT REENTRY HEATING SUMMARY

A reentry heating summary for the three flights is presented in Figs. 5–12. The summary is are composed of a trajectory characterization, external calorimeter load summary and internal aft skirt load and gas temperature summary. Key events from the three flights (Fig. 5, Table 4) compare fairly well with each other, as well as those from STS 1–6. SRB separation occurred at approximately 150–160 Kft. for STS-27R and 29R. Separation for STS-26R was somewhat earlier (132 Kft.); however, apogee and the beginning of aeroheating occurred at approximately the same altitude as the historic and current data. The nozzle extension was jettisoned at apogee on STS-29R, which led to the thermal curtain opening sooner, i.e., higher than the previous flights. The reentry trajectory is very similar for the three, especially during the thermal curtain opening time and peak aeroheating phase of flight. This can be seen by overlaying the plots of Fig. 6, which is a presentation of reentry velocity and altitude. Also included in the plots is the design envelope. STS-26R and 27R exceeded the design boundary during the latter phase of the aeroheating and subsonic portion of the flight. Heating to the external surface of the SRBs (Fig. 7) was well below the design maximum except for B07R7702 on STS-29R. For this case the integrated load was approximately the 95 percentile design value of 72 BTU/ft^2. A point not clearly understood at this time is that, although the reentry altitude-velocity history for the current DFI flights tends toward the hotter side of the design envelope, the integrated heat loads to the external surface, especially on the aft skirt, are for the most part on the low side of the design range. Potential explanations for this discrepancy is that the data base for the aft skirt is extremely limited, and that the aerodynamics that predict the design envelope are inaccurate. Heat loads from gages on the forward frustum and forward face of the attach ring would be expected to be low, since they experience a leeside heating. However, those on the aft skirt should be a better reentry indicator of the severity of the reentry trajectory.

Internal aft skirt heating was nominal to low for STS-26R and 27R; however, severance of the nozzle extension at apogee on STS-29R, produced the hottest flight to date for the internal aft skirt and its components. This resulted in a design exceedance for the right hand booster. These results are summarized in Fig. 8 which is a presentation of integrated heat load from the right and left hand booster calorimeters. B07R8454 and B07R8456 exceed the steel case nozzle extension off (SCNEOFF) design load by 9 to

25 BTU/ft^2. Loads from 7454 and 7456 on the left hand booster are substantially greater than those on STS-26R and 27R also. This was due to the extended periods of nozzle flame entrainment encountered by the aft skirt during reentry. Peak heating rates in excess of 30 BTU/ft^2-sec and gas temperatures of 2600°F were measured over a significant period of time. These conclusions are illustrated in Figs. 9–12. Figure 9 is a comparison of STS-29R internal aft skirt gas temperature history (nozzle extension-off) to a case with the nozzle extension-on (STS-26R). Typical reentry aerodynamic heating produces internal aft skirt peak gas temperatures of 800–1000°F, with associated heating rates of 10 BTU/ft^2-sec and less (Fig. 10), as illustrated by STS-26R. In the presence of nozzle flame heating, the gas temperature immediately goes to 2000+°F with an associated rise in heating rate, in this case, 30 BTU/ft^2-sec. Peak gas temperature is summarized in Fig. 11 for the three flights. Historic gas temperature measurements from STS 7–14 are included, also. Of the flights compared, nozzle flame heating was measured on STS-8, Fig. 11a. Some brief period of nozzle flame heating was observed on STS-27R on the let hand SRB also, Fig. 11a. This is seen to be only a brief 10 second spike imposed on top of the normal reentry aeroheating, Fig. 12. However, with the nozzle extension off, nozzle flame entrainment is experienced by both boosters, Fig. 11b, for a significantly longer period of time as shown in Figs. 9 and 10.

FLIGHT DATA VERIFICATION

Instrumentation on STS-27R and 29R included a ring of circumferential pressures on the cylindrical portion of the left hand SRB. These were used to infer SRB attitude during reentry [1]. With the attitude known, heating predictions could be calculated and used for confirmation of the flight measurements. STS-26R was not instrumented in this way, consequently flight prediction comparisons could not be made for verification of STS-26R data. This was done through inspection of STS-26R measurement history, as well as comparison with historic integrated heat loads and peak gas temperatures.

External SRB Reentry Heating Measurements — Comparison of the external reentry heating measurements from STS-27R and 29R with predictions from the wind tunnel and flight heating data base are presented in Figs. 13 and 14, respectively. The predictions were based on a wall temperature of 140°F (600°R), which is approximately the same as the flight measured calorimeter reentry temperature of 90–115°F (540–575°R).

The predictions were made using the STATE reentry heating code [6]. This code uses a Beckwith-Gallagher swept cylinder stagnation line heating calculation to nondimensionalize the circumferential clean skin distribution. On determining the orientation both circumferentially and with angle-of-attack of the body point in question, the code interpolates within an extensive wind tunnel flight test data base to determine the local interference factor. This is then used as a multiplier to the clean skin heating ratio ($h_{clean}/h_{Beckwith-Gallagher}$) to calculate the local interference heating. A list of the external calorimeters and their location, along with the corresponding data base body points used to make the heating predictions and their location, is given in Table 5.

Flight measurements from STS-27R and 29R generally agree with the predictions in magnitude and frequency on the nose cone and attach ring. There is, however,

a discrepancy in predicting the peaks on the aft skirt for both flights. As previously mentioned, gages on the attach ring and aft skirt were located at positions where very few previous flight measurements had been made. This is considered to be the major reason for the lack of agreement between flight measurement and prediction on the aft skirt and a clear indication that the interference factor data base in this area should be updated.

The review of the current external heating measurements associated with this analysis indicate that the measurements are valid, and should be used for design impact assessment. Exceptions to this is gage B07R7704 on STS-27R which was bad during the entire flight. Also, on STS-29R, there were two periods of time during reentry when the data recorder malfunctioned. These flight times were t = 292–296 and 325–334 seconds. The instrumentation was functional during this time frame; however, the recorded signal went to zero. Consequently, in the plots presented in this report, flight data for these times are not presented.

Internal Aft Skirt Reentry Heating Measurements — Gas temperature probe data are presented for the three flights in Figs. 15–17. For validation purposes, a semi-empirical prediction of internal aft skirt gas temperature is presented. This prediction is based on a correlation of historical flight gas temperature data from STS 1–6 [7], and was calculated using the STATE reentry heating code [6]. The correlation predicts fairly well the magnitude and trend of the gas temperature on STS-26R. The thermal curtain opening, as observed by the rise characteristics of the gas temperature, appears to be more rapid and occurs at a higher dynamic pressure (i.e., lower altitude) than predicted by the correlation.

Aft skirt gas temperature for STS-27R is characterized by seven second ingestion of flame from the nozzle on the left hand SRB (Fig. 16a). Peak gas temperatures of 2400 to 2800°R were encountered. Once the flame disappears, the measured gas temperature is confirmed very well by the STATE prediction. This is true of the right hand SRB, also. Peak gas temperatures from STS-26R and 27R compare well with historic flight data as previously shown in Fig. 11a. A table listing the gas temperature probes used on the internal aft skirt on the left and right hand boosters for the current DFI flights is presented in Table 6. This listing defines those which are usable measurements and those which are faulty.

Figure 17 is a presentation of the internal aft skirt gas temperatures for STS-29R. The measured data are dominated with significant time periods of nozzle flame heating on both boosters. This resulted in the failure of many of the aft skirt gas temperature probes. This list is summarized in Table 6 along with results from the other two DFI flights. Peak gas temperatures of 2800–3000°R were recorded. With the nozzle extension in place during the major portion of reentry, a shielding of some degree is provided to the internal aft skirt components. The removal of the extension at apogee on STS-29R exposed the internal aft skirt to the nozzle flame environment for an extended period of time. The gas temperature and heating which would have been experienced in STS-29R, had there been no nozzle flame entrainment, is represented by the STATE gas temperature prediction in Fig. 17.

Internal aft skirt heating rate predictions were made on flights STS-27R and 29R to validate the calorimeter measurements. These comparisons are presented in Figs. 18–24. Reentry data base body points used to make the heating rate calculations are listed in Table 7 along with the corresponding calorimeter locations. For the predicted heating rates, the recovery enthalpy was based on the internal aft skirt gas temperature algorithm [7] developed from previous flights (see Figs. 15–17). Use of this value predicts the measured heating rate level for the case of no nozzle flame entrainment. However, in the presence of the nozzle flame, the gage incident heat flux is much higher. Use of the gas temperature probe results to define the recovery enthalpy, yields excellent agreement between the calculated and measured heating rates. The best demonstration of this is shown in Fig. 18, which is a comparison of measured and predicted heating rates for calorimeter B07R7454 located near the left hand booster fuel supply module (FSM) at THETA-B = 265 deg. Figure 18a shows the prediction using the gas temperature algorithm results (Fig. 17). Figure 18b is a comparison of measured and predicted aft skirt heating rates with the recovery enthalpy being based on the flight gas temperature measurement from B07T7601, Fig. 17. These results imply that the data base heat transfer coefficients are constant, and that the increase in heating is caused by flame temperature. Figure 19 is a comparison of the same calorimeter, gas temperature probe and prediction body point heating rate, except these results pertain to STS-27R. On STS-27R there was a flame event between 290 and 297 seconds on the left hand booster (Fig. 16a). This is manifested as a spike in the measured heating rate for B07R7454 over the same time frame (Fig. 19a). Using the STATE gas temperature algorithm, the prediction yields a heating rate of approximately 6 BTU/ft^2-sec, whereas the measured value is 17–18 BTU/ft^2-sec. When the recovery enthalpy is based on the flight measured gas temperature, corresponding heating rates are calculated (Fig. 19b). There is a spike in the prediction around t = 308 sec, which was not present in the flight measurement. This is an indication that the data base needs to be examined in light of the current flight data.

Flight data and predictions for calorimeter B07R7456, located on the left hand SRB fuel isolation valve (FIV) cover, are presented in Figs. 20 and 21. Figure 21 is for STS-29R while Fig. 22 pertains to STS-27R. These comparisons indicate that the calorimeter may have been faulty or obscured by instafoam for STS-29R, but the STS-27R results are valid. Gage measurement on STS-29R neither agree with predictions using the gas temperature algorithm (no nozzle flame — Fig. 20a), or those where the recovery enthalpy is based on the nozzle flame gas temperature measurement (Fig. 20b). Comparisons of raw heating rate from the three flights, Fig. 22, indicates that the incident heat flux seen by B07R7456 on STS-29R in the time frame 290 to 310 seconds, is considerably below even that level expected with no nozzle flame heating. Consequently, it recommended that results from this gage on STS-29R be used guardedly.

In like manner, the response of calorimeter B07R7457, on STS-26R and 27R appears to be delayed, and the output is low. The gage is located on the mid ring facing aft, near the +Z axis (THETA-B = 354 deg). Comparison of data from this gage for these two flights with data from STS-5 (Fig. 23), indicates a "normal" heating level of 4–6 BTU/ft^2-

sec and peaks of 12 BTU/ft^2-sec. In addition, STATE predictions for STS-27R (Fig. 24) show similar type heating levels as the historic data from STS-5. Gage output for the current flights is 2–4 BTU/ft^2-sec. The data from B07R7457 on STS-29R are bad, since there was virtually no output from the gage.

A status of the internal aft skirt calorimeter measurements is given in Table 8.

SUMMARY AND CONCLUSIONS

In this task the SRB DFI calorimeter and gas temperature probe data from STS-26R, 27R, and 29R were analyzed from a reentry heating point of view. These data included external heat transfer gage, internal aft skirt heat transfer gage and gas temperature probe measurements. These were compared with semi-empirical predictions and historic SRB flight data for the purpose of validating some of the trends observed in the data. The major conclusions concerning this analysis, and items which impact the existing data base are as follows:

1. SRB external reentry heating tended toward the low side of design, even though the reentry trajectories were on the "hot" side of the design envelope, i.e., lower and faster. On two of the flights (STS-26R and 27R), the reentry velocity-altitude characteristics exceeded the design boundary during the latter part of the aeroheating and subsonic portion of flight.
2. Internal aft skirt heating was nominal to low for STS-26R and 27R. However, severance of the nozzle extension at apogee on STS-29R, resulted in the hottest flight to date for the internal aft skirt and its components. This was due to nozzle flame entrainment into the aft skirt for extended periods of time. This produced a design exceedance of 9–25 BTU/ft^2 on the right hand SRB and elevated loads on the left hand booster.
3. Predictions of internal aft skirt heating and gas temperature using the STATE code agree very well with flight measurements for the case of no nozzle flame. In the presence of flame entrainment, heating predictions agree with the flight measurements if the recovery enthalpy used in the calculations is based on the flame temperature. This implies that the increase in aft skirt heating is due to the increase in driving potential, as opposed to an increase in heat transfer coefficient.
4. External calculations using STATE predict the magnitude and frequency on the nose cone and attach ring. However, on the aft skirt, the code predicts the general magnitude only. This is due to the lack of flight data in the THETA-B = 180–270 deg locations, and points to the fact that the data base should be updated in light of the current results.
5. Flight measured calorimeter temperatures were in the 540–575°R range. Consequently, design calculations, based on a wall temperature of 600°R, are comparative with flight test data.

REFERENCES

1. Kirchner, Robert D. and Crain, William K., "Calculations of SRB Pitch and Roll Characteristics During Reentry for Flights STS-27R and STS-29R," REMTECH RTN 213–05, May 1991.
2. Crain, William K. "SRB Ascent and Reentry Frustum Venting Analysis and Update (STS-26R, 27R and 29R)," REMTECH RTN 213–16, June 1991.
3. Crain, William K., "Raw Flight Data Report — STS26R," REMTECH RTN 213–01, Dec. 1988.
4. Frost, Cynthia L. and Crain, W. K., "Raw Flight Data Report — STS27R," REMTECH RTN 213–02, Oct. 1989.
5. Frost, Cynthia L. and Crain, W. K., "Raw Flight Data Report — STS29R," REMTECH RTN 213–03, Sep. 1989.
6. Kirchner, Robert D. and Hollman, David, "User's Guide for Program STATE," REMTECH RTN 213–07, Dec. 1990.
7. Engel, Carl D., "STS-7, 8, 9, 11 and 14 SRB Reentry Heating Flight Evaluation," REMTECH RTN 039–14, Oct. 1984.

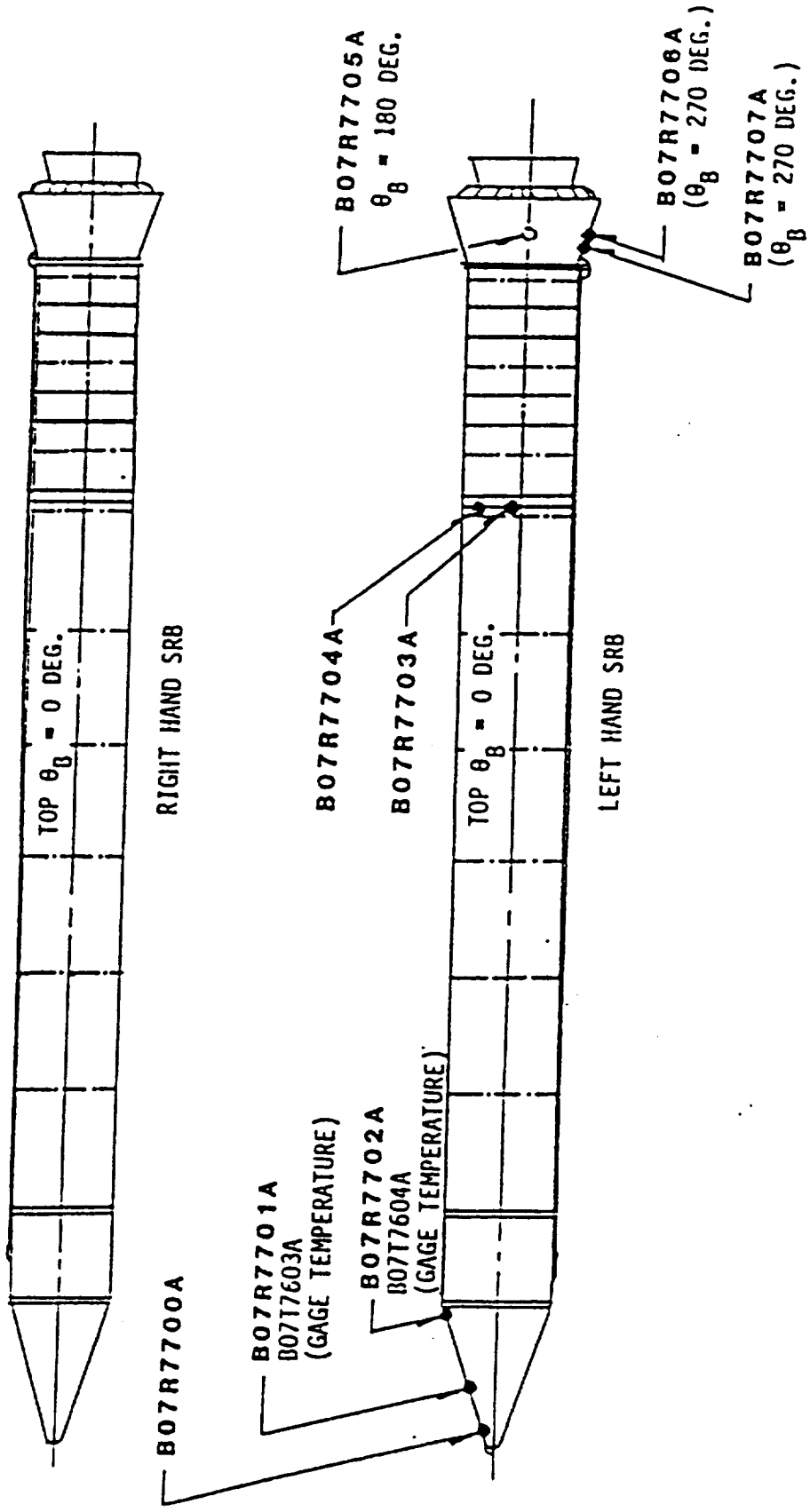

Figure 1: SRB External DFI Instrumentation

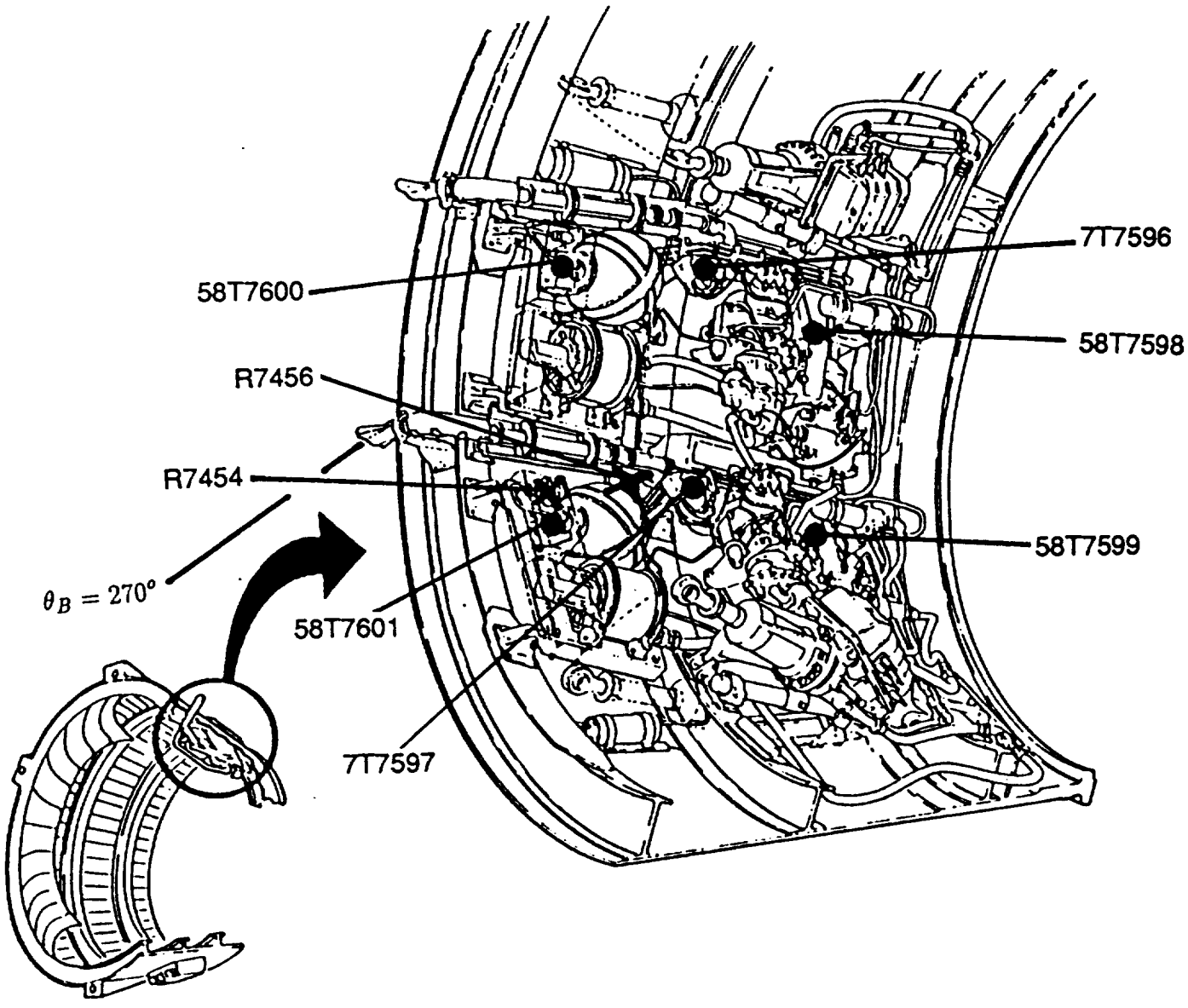

Figure 2: Left Hand SRB Interna

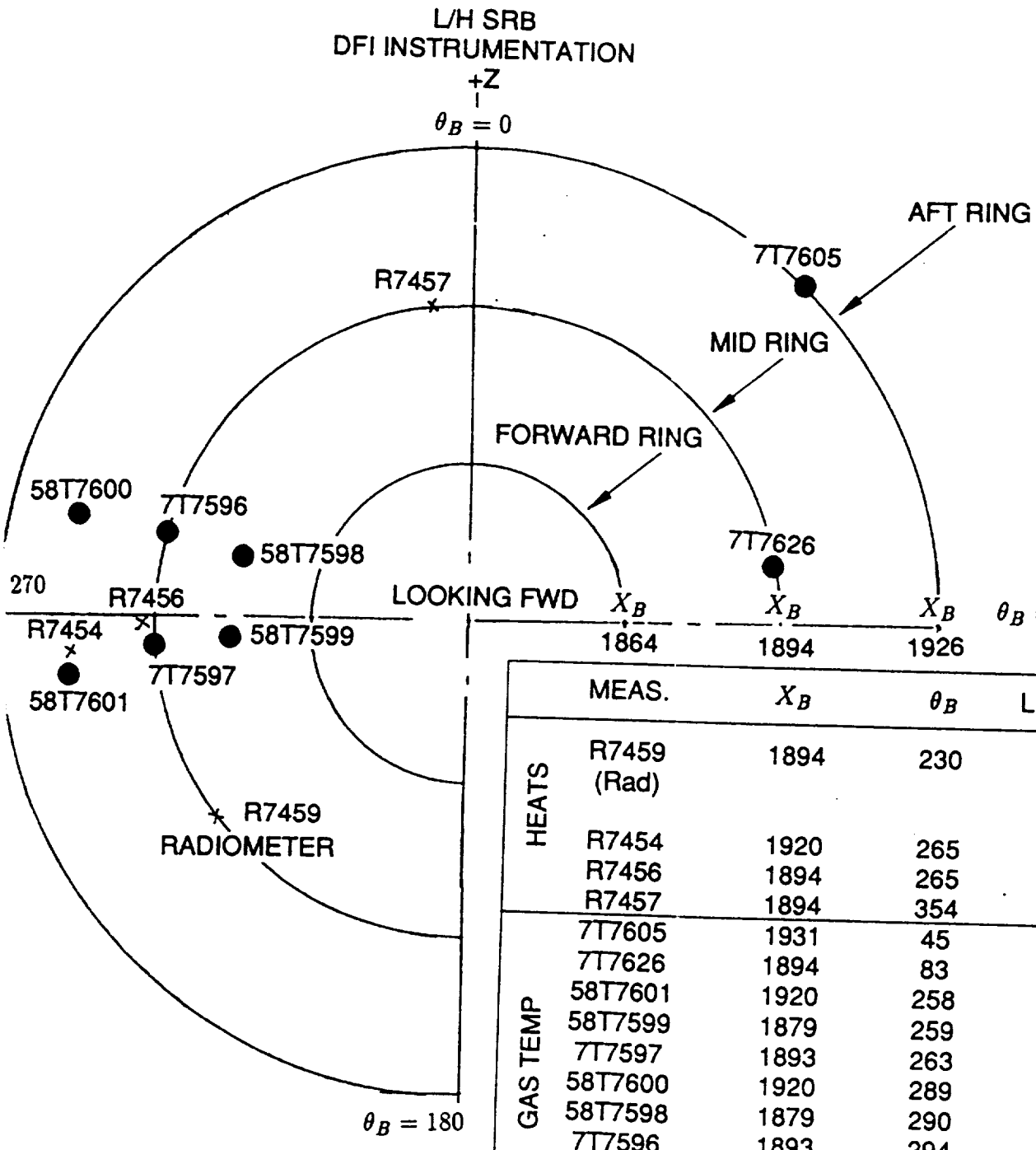

	MEAS.	X_B	θ_B	LOOKING
HEATS	R7459 (Rad)	1894	230	AFT
	R7454	1920	265	INBD
	R7456	1894	265	AFT
	R7457	1894	354	AFT
GAS TEMP	7T7605	1931	45	AFT
	7T7626	1894	83	AFT
	58T7601	1920	258	INBD
	58T7599	1879	259	INBD
	7T7597	1893	263	INBD
	58T7600	1920	289	INBD
	58T7598	1879	290	INBD
	7T7596	1893	294	INBD

Aft Skirt DFI Instrumentation

2

FOLDOUT FRAME

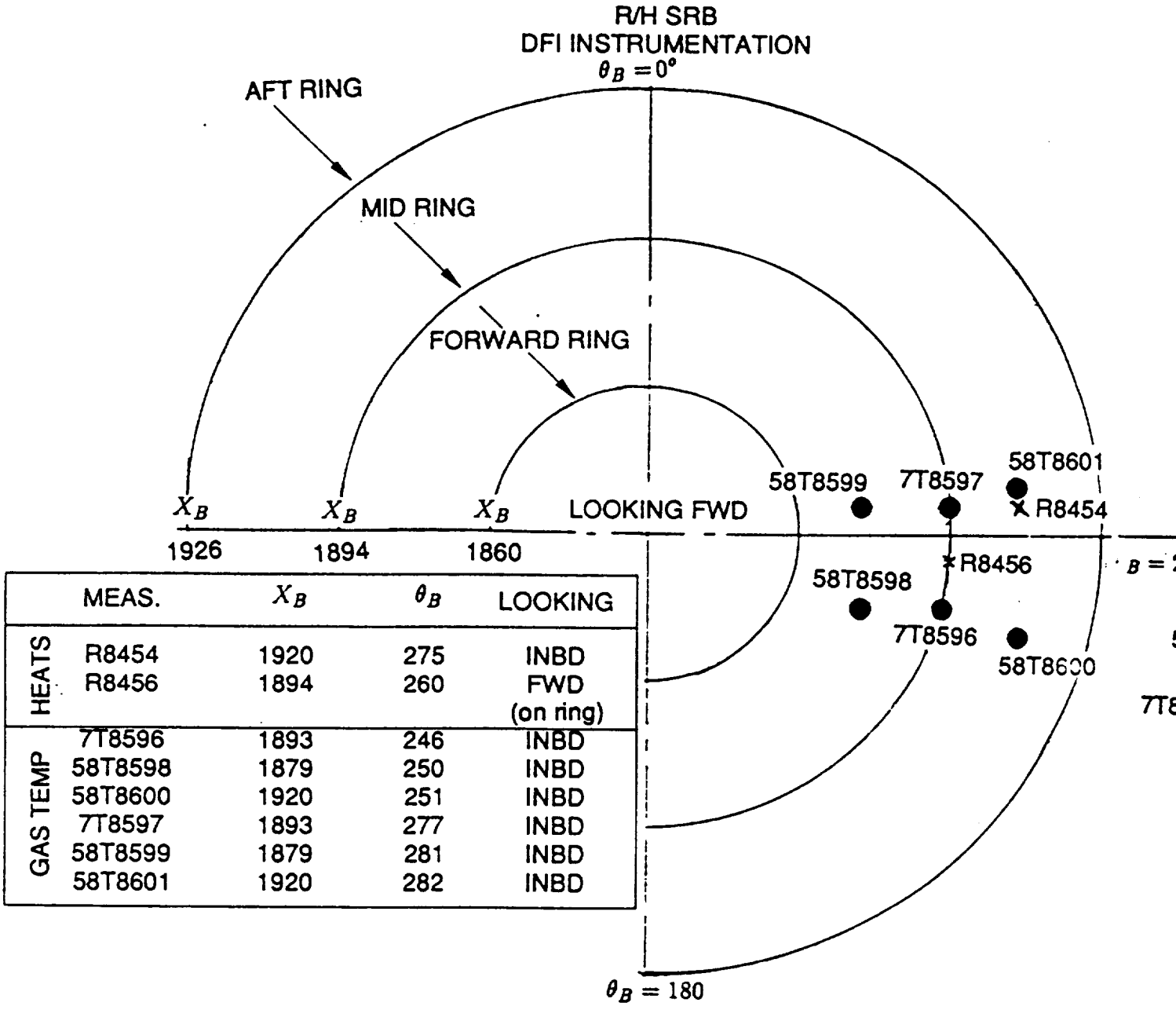

	MEAS.	X_B	θ_B	LOOKING
HEATS	R8454	1920	275	INBD
	R8456	1894	260	FWD (on ring)
GAS TEMP	7T8596	1893	246	INBD
	58T8598	1879	250	INBD
	58T8600	1920	251	INBD
	7T8597	1893	277	INBD
	58T8599	1879	281	INBD
	58T8601	1920	282	INBD

Figure 3: Right Hand SRB Instrumentation

FOLDOUT FRAME

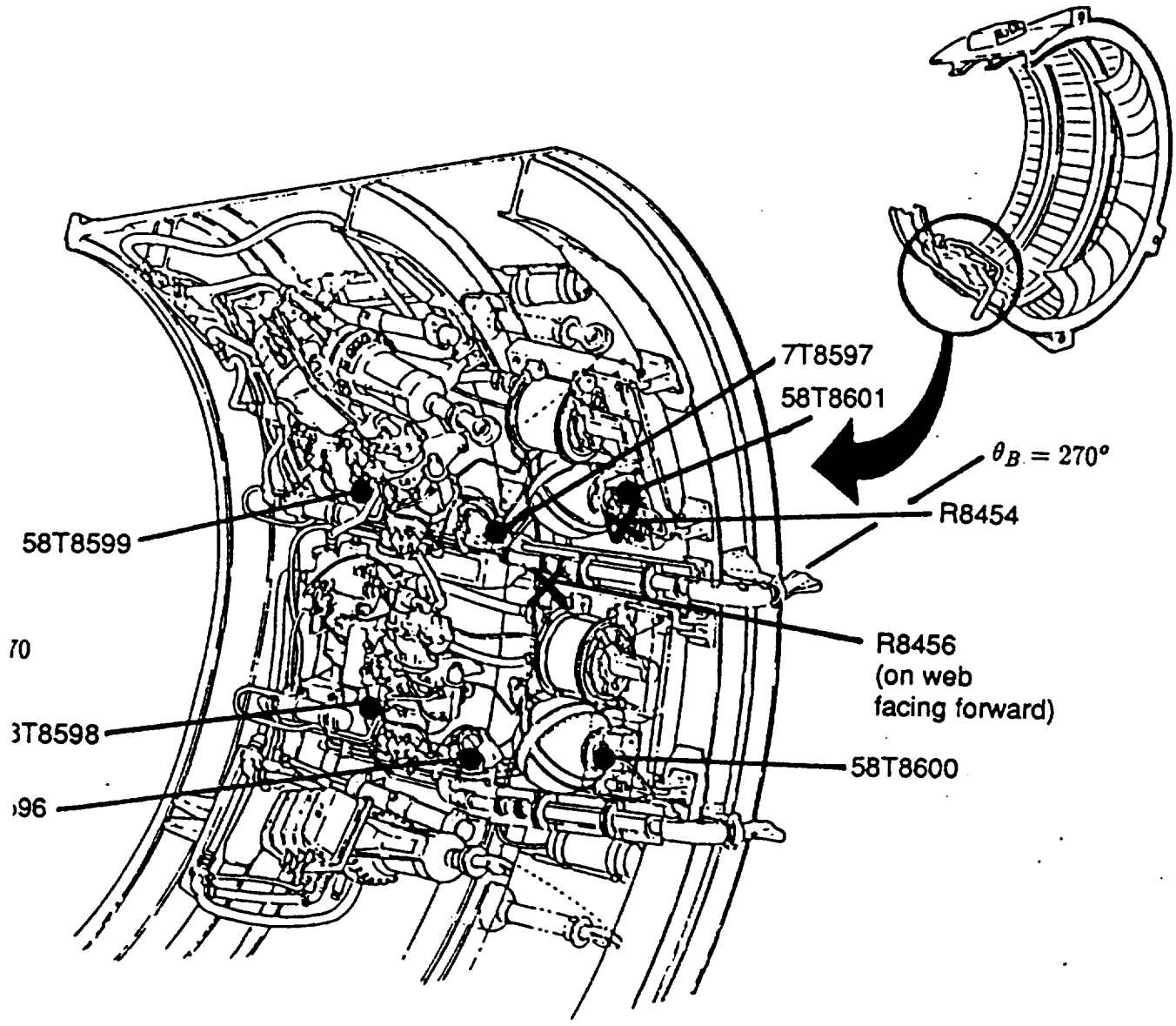

Aft Skirt DFI Instrumentation

FOLDOUT FRAME

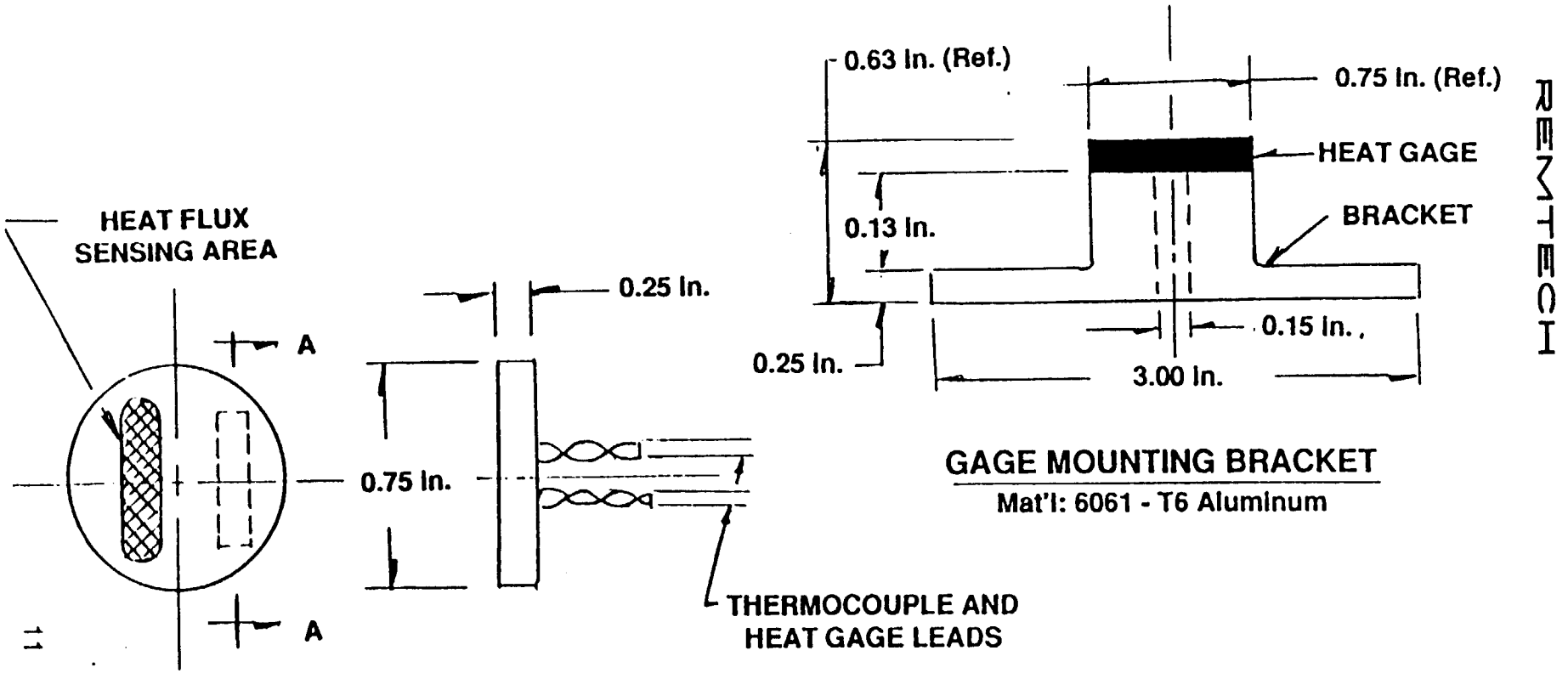

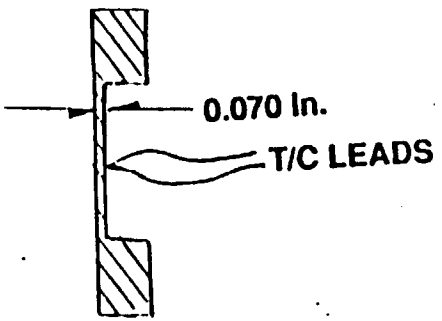

NOTE: Gage B07R7700 Did NOT Have
An Associated Thermocouple

Characterization of Gage
T/C Installation
(Not to scale)

a) Medtherm Schmidt-Boelter Gage (B07R7700 — 7702)

Figure 4: Heat Transfer Gage Details

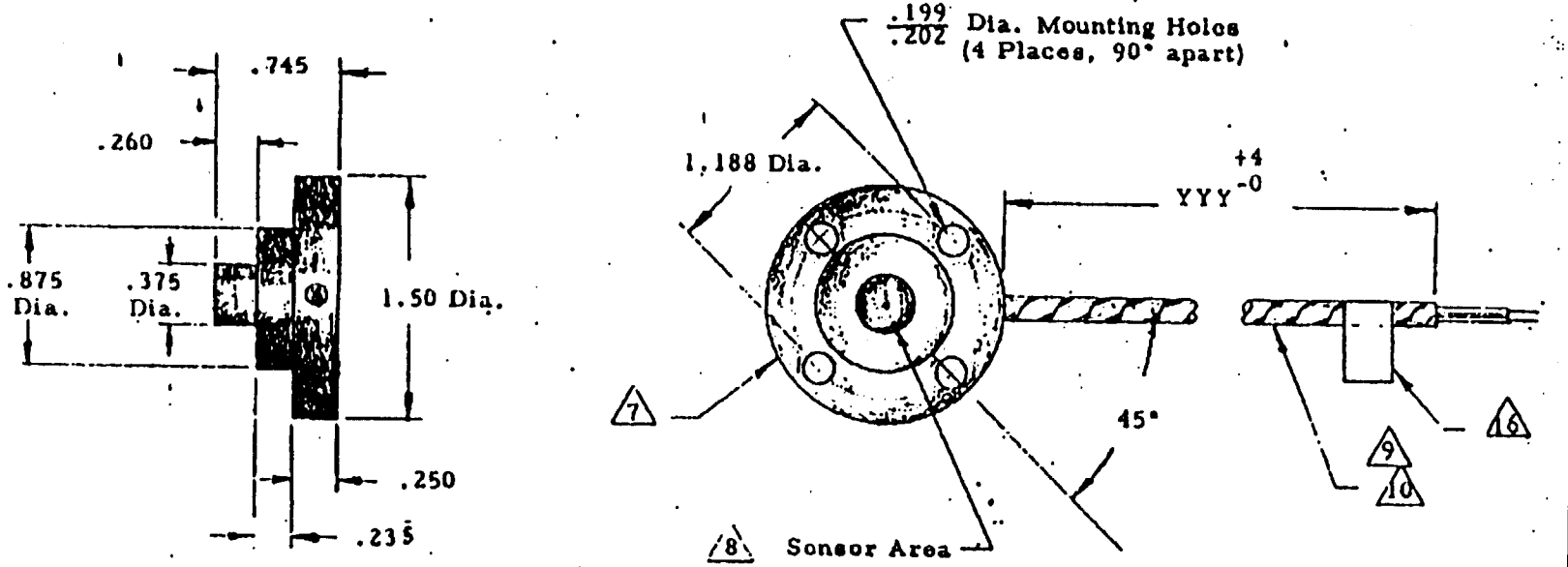

NOTES:

1. Model number designated as follows:
   ZZ - Full scale heat flux in Btu/ft^2-sec.
   YYY - Flexible lead length in inches.
   ( ) - Model Dash No. - See Table, Note 17 for applicability.
2. Full scale output: 15 ± 1.5 mV., except 15 +1.5, -4 for 5 Btu/ft^2-sec. full scale heat flux.
3. Linearity: Better than 3% of full scale output.
4. Time constant: Per Table, Note 17.
5. Repeatability: Better than ±0.5% of full scale output.
6. Output impedance: < 100 ohms.
7. Body material: Oxygen free copper, 16 finish or better.

REVISIONS		
NO.	DATE	BY
1		
2		
3		
4		
5		

ALL DIMENSIONS IN INCHES WITH FOLLOWING TOLERANCES UNLESS OTHERWISE NOTED:
DECIMALS: X ±.050, XX ±.030, XXX ±.010 | FRACTIONS: ± | ANGLES: ± 1/2

Hy-Cal Engineering
SANTA FE SPRINGS CALIFORNIA

ASYMPTOTIC® UNCOOLED CALORIMETER
MODEL C-1202-E-( )-ZZ-YYY

DATE 1-24-78
SCALE Full
DRAWN V.A.
APP'D W.R.C

MATERIAL Pg. 1 of 2 Noted
DRAWING NO. A-14055

b) Hy-Cal Calorimeter (B07R7703 — 7707)

Figure 4: Heat Transfer Gage Details (Continued)

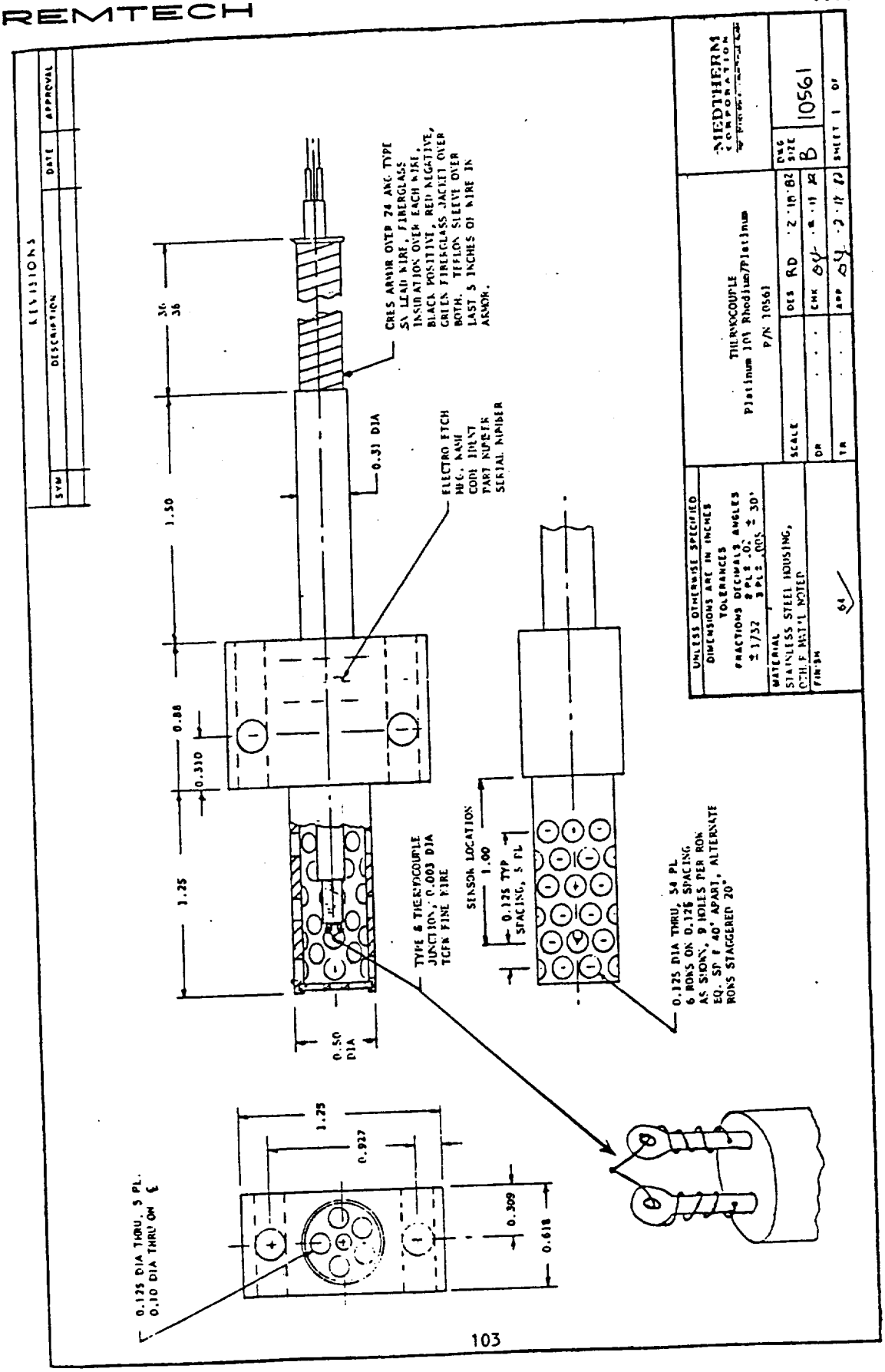

c)Typical Aft Skirt Gas Temperature Probe

Figure 4: Heat Transfer Gage Details (Concluded)

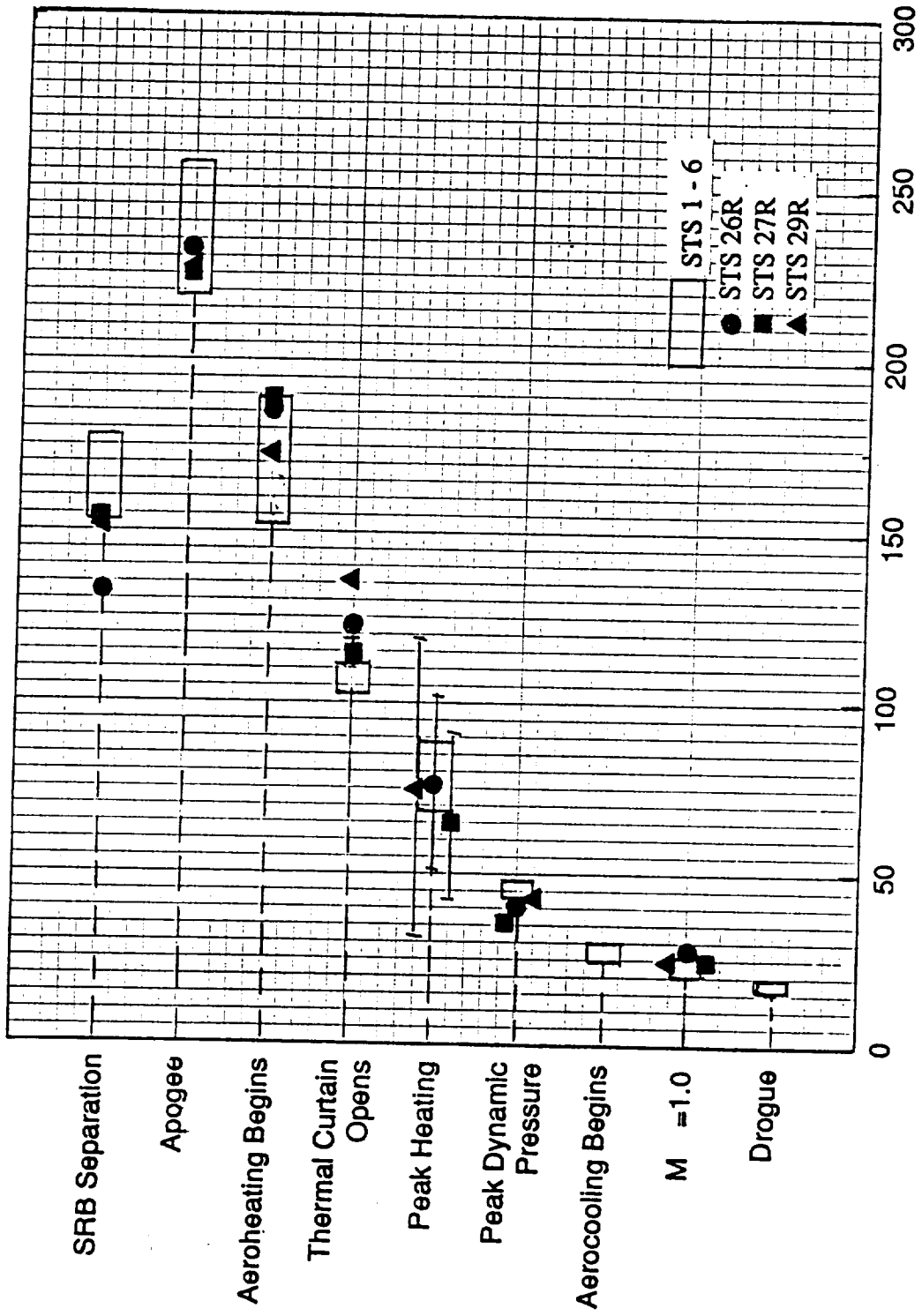

Figure 5: Reentry Event Summary

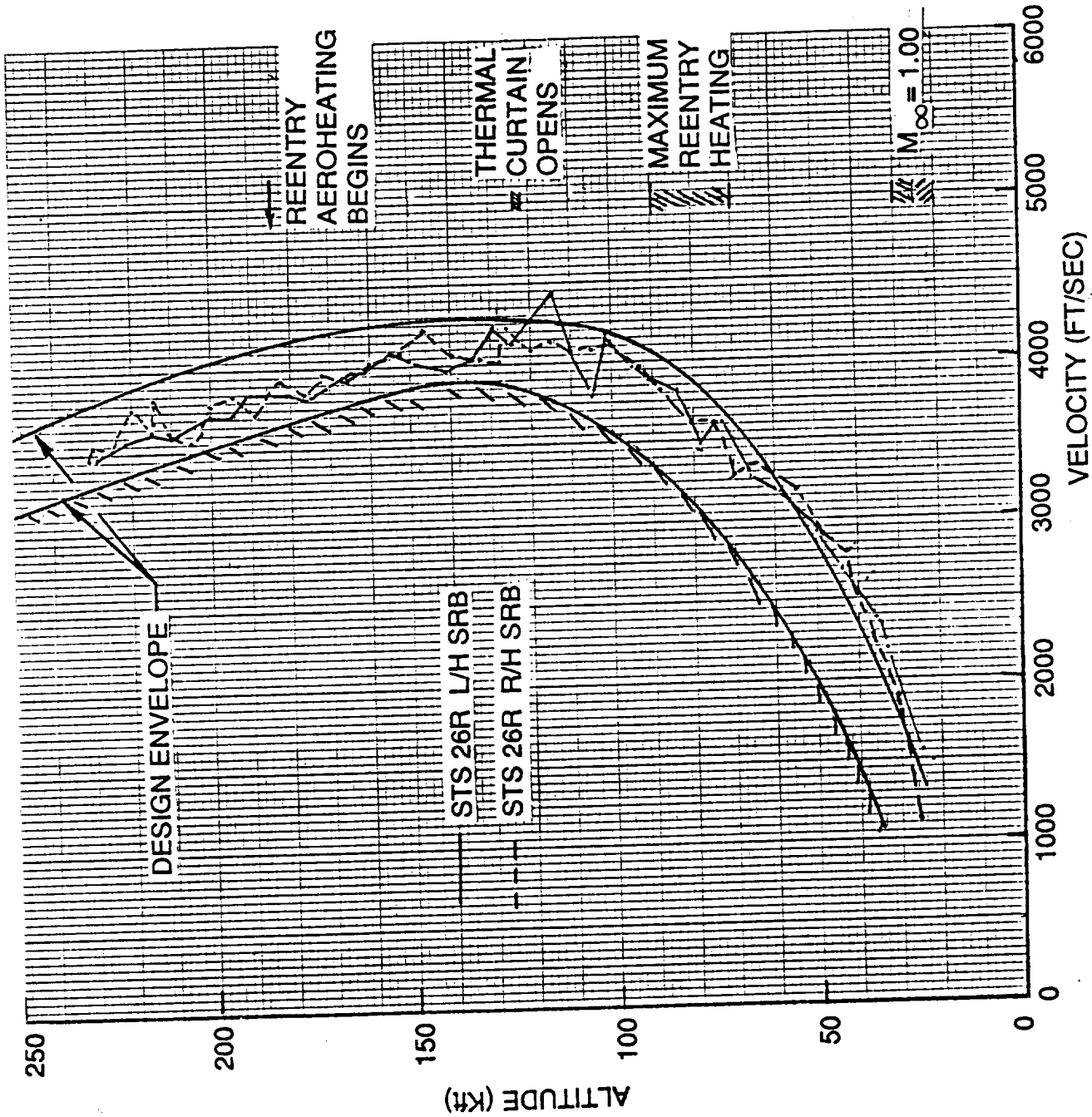

a) STS-26R

Figure 6: Reentry Trajectory Summary

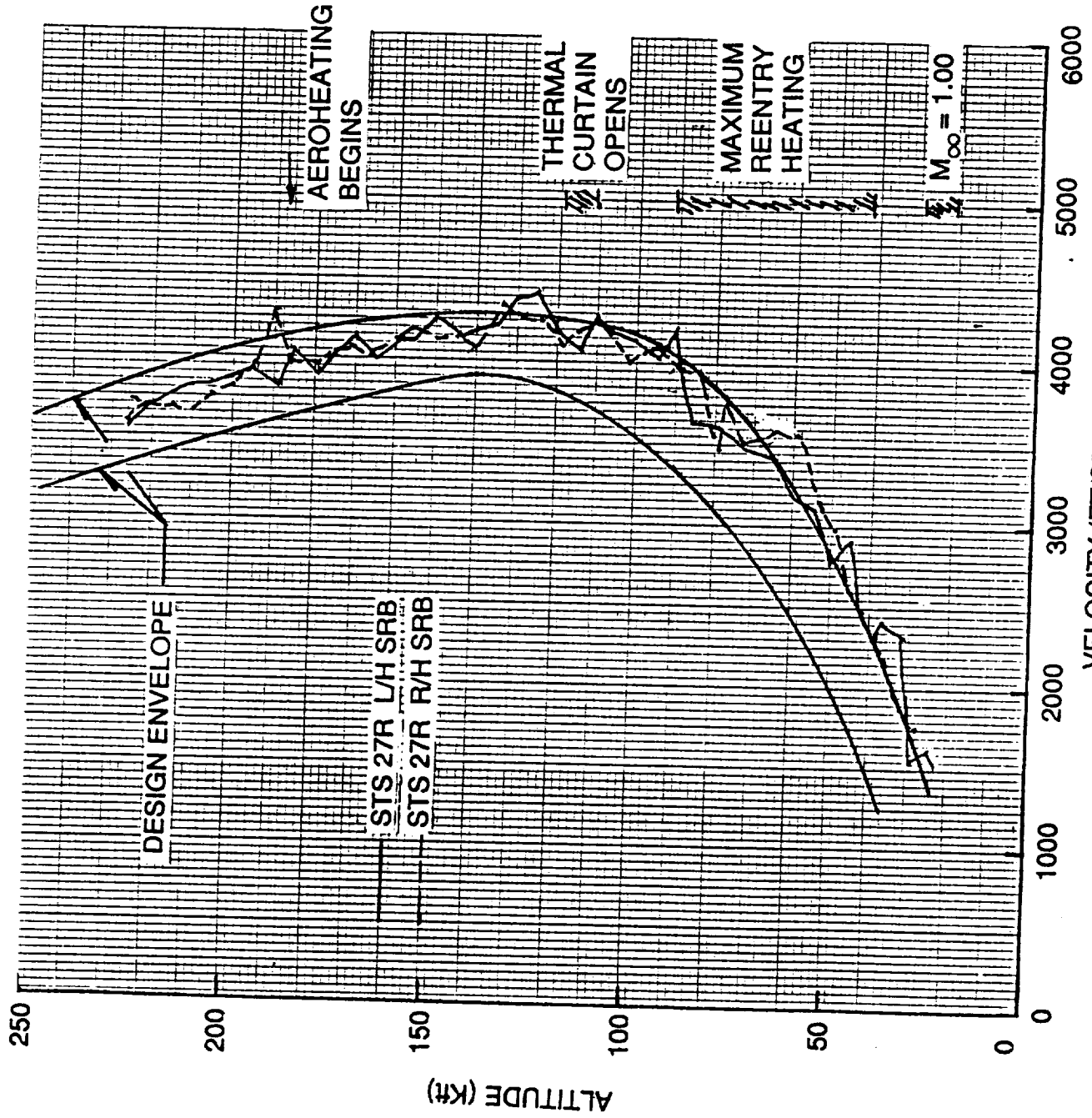

b) STS-27R

Figure 6: Reentry Trajectory Summary (Continued)

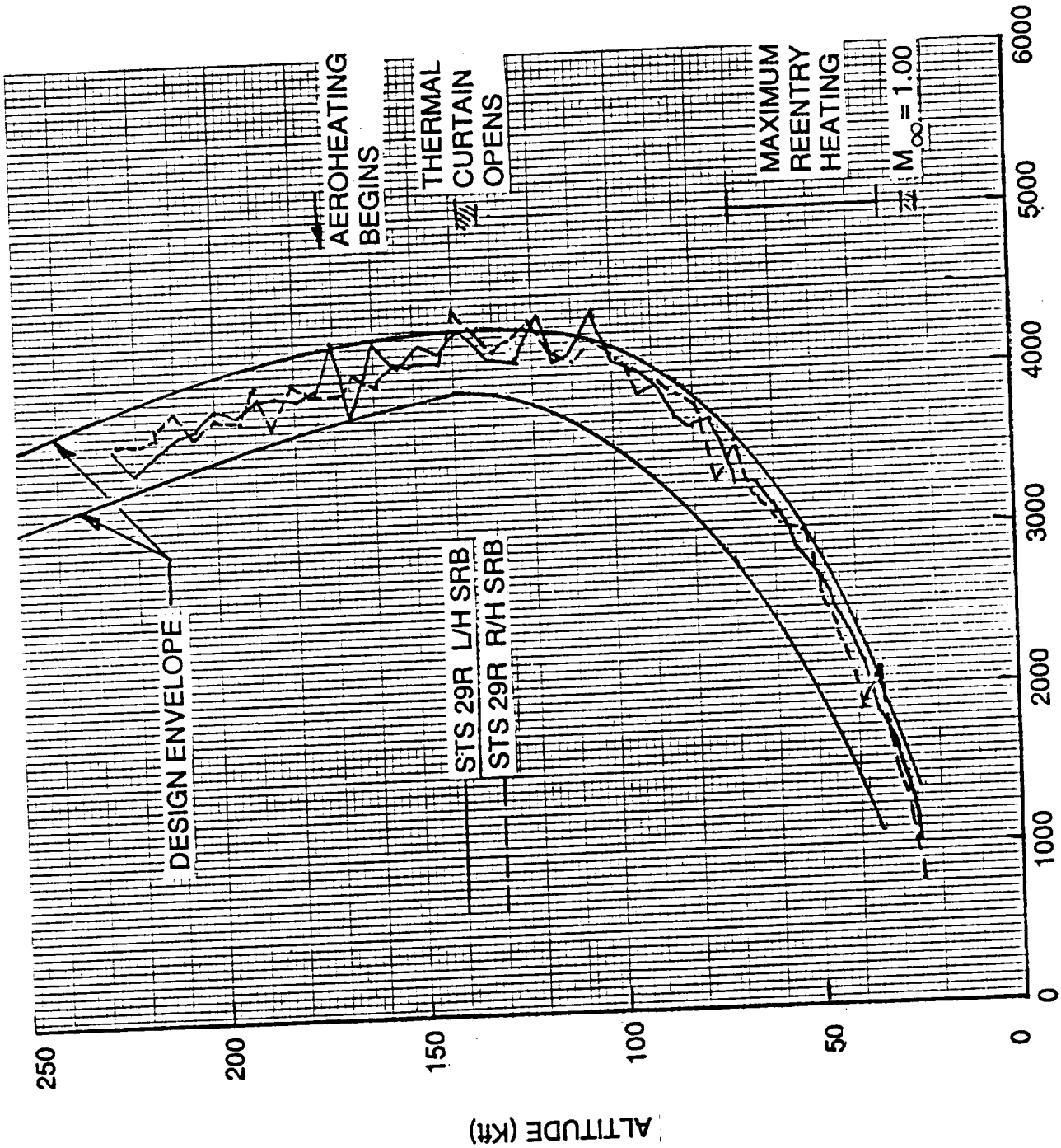

c) STS-29R

Figure 6: Reentry Trajectory Summary (Concluded)

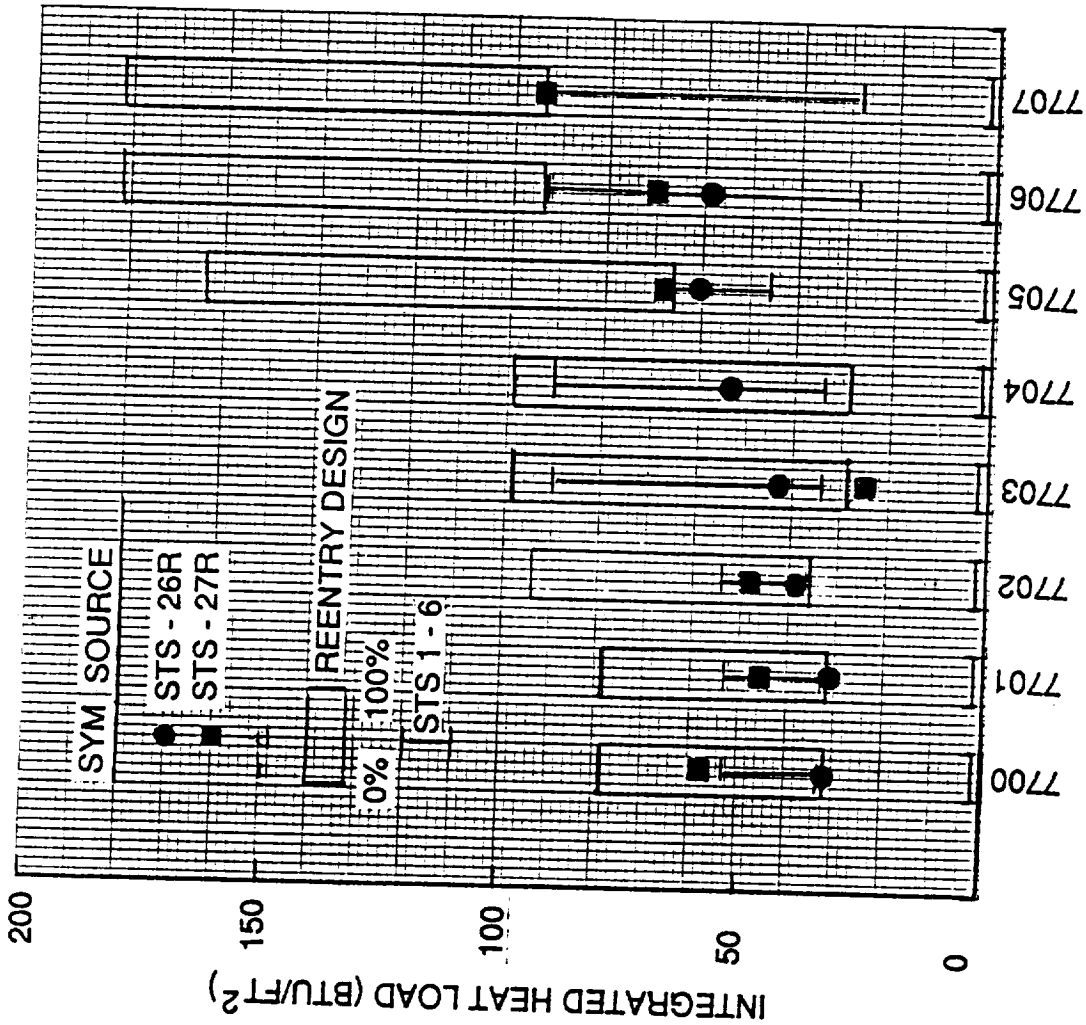

a) Steel Case Nozzle Extension-On

Figure 7: Reentry External Heat Load Summary

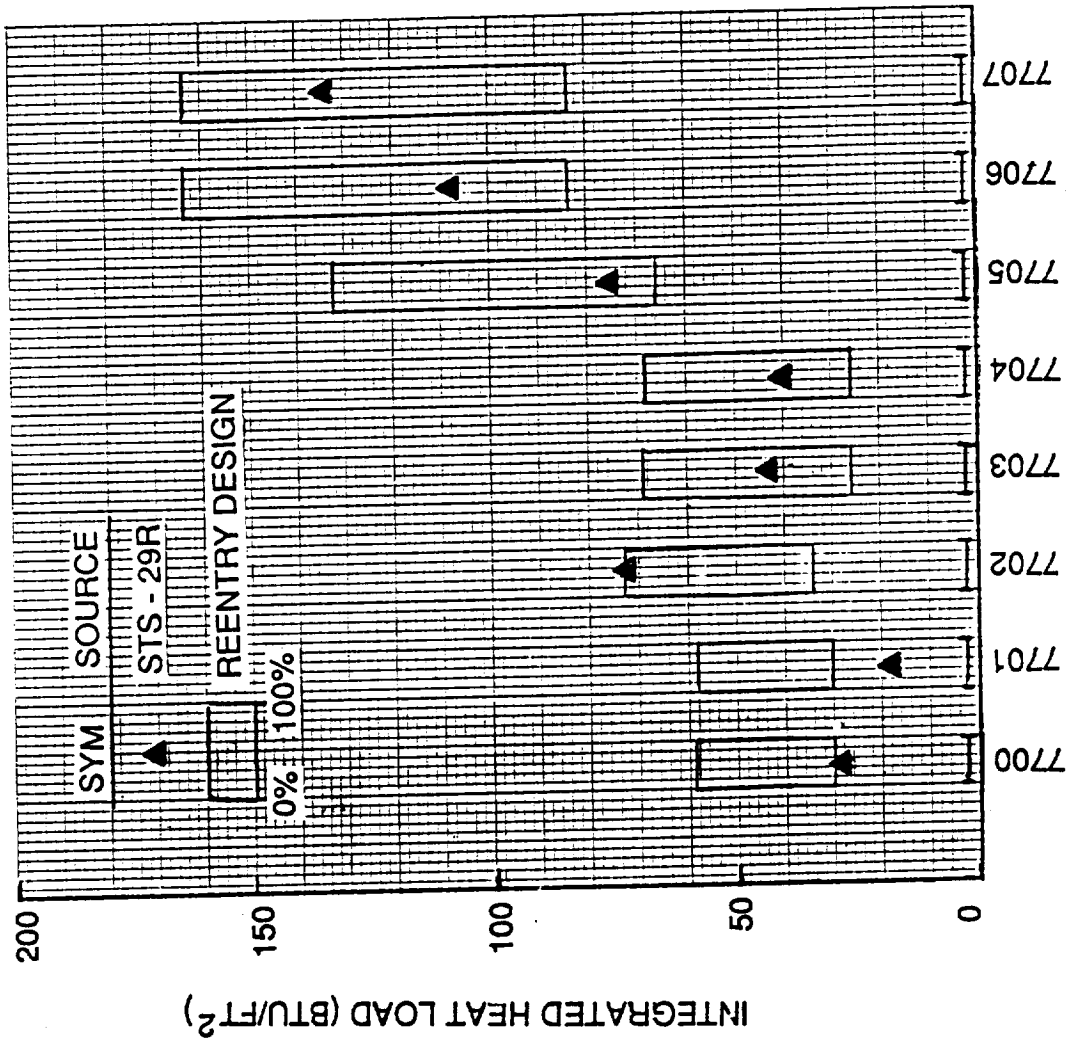

b) Steel Case Nozzle Extension-Off

Figure 7: Reentry External Heat Load Summary (Concluded)

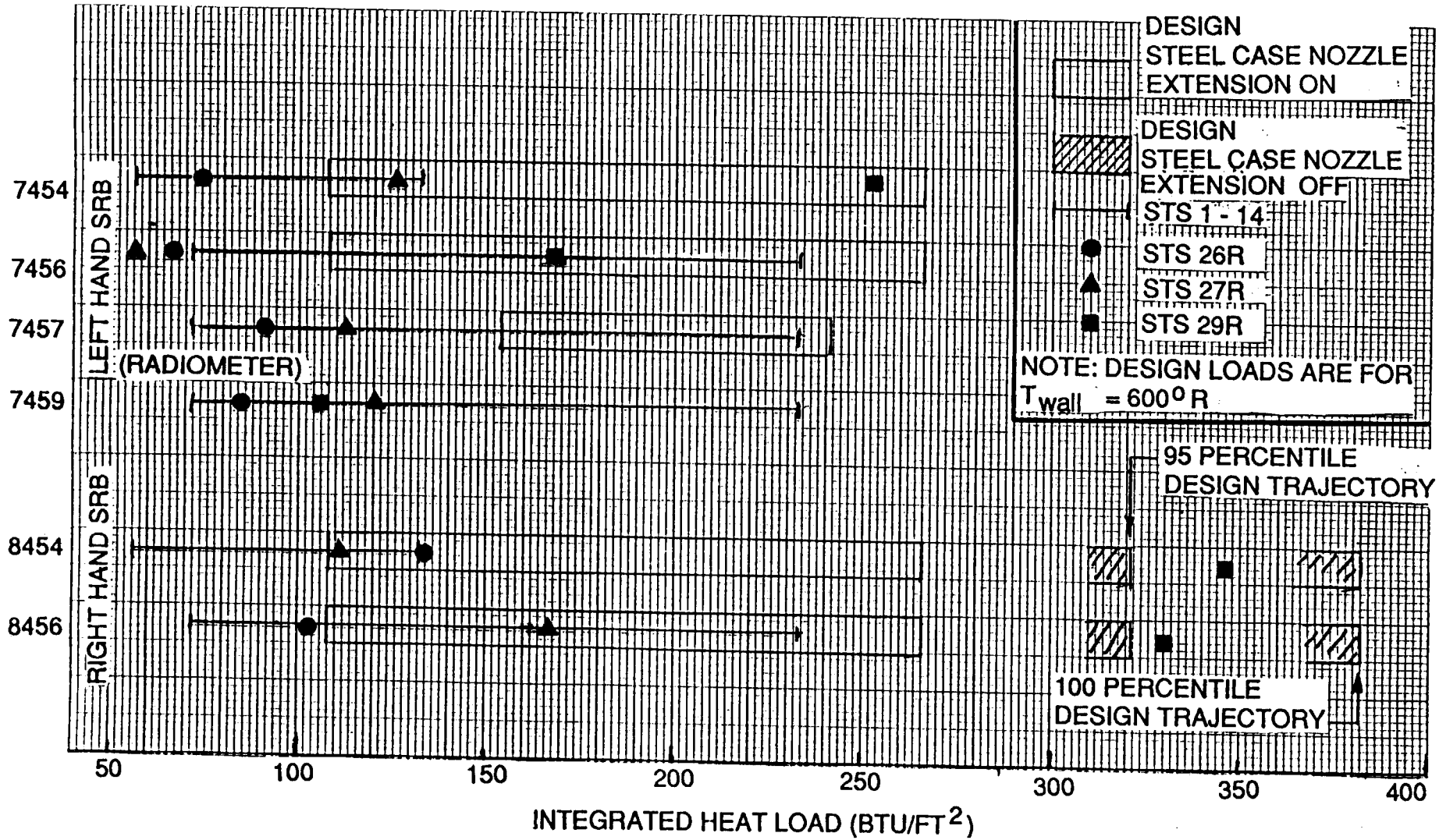

Figure 8: Internal Aft Skirt Heat Load Summary

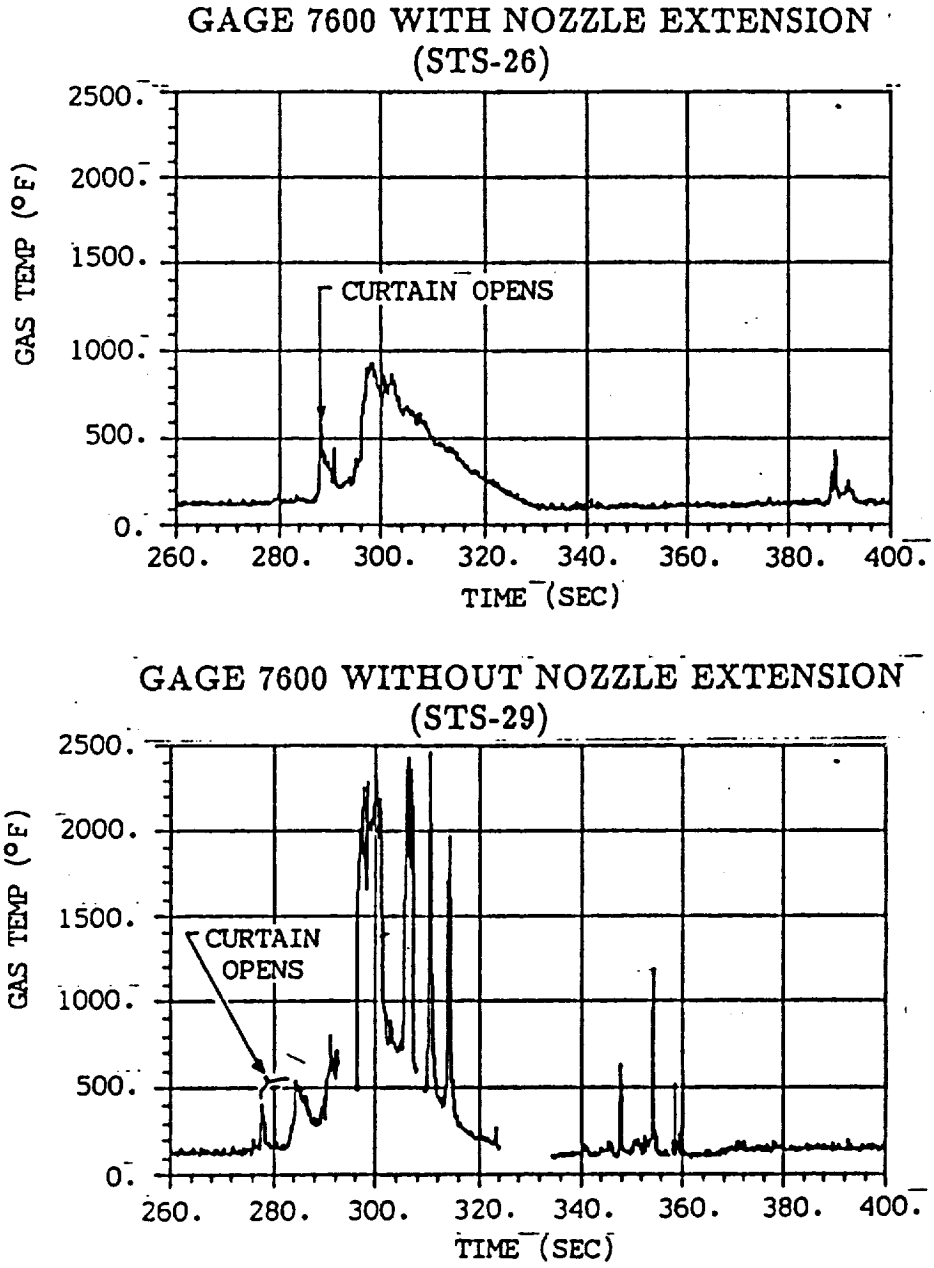

Figure 9: STS-29R Flame Entrainment Contribution to Internal Aft Skirt Reentry Gas Temperature

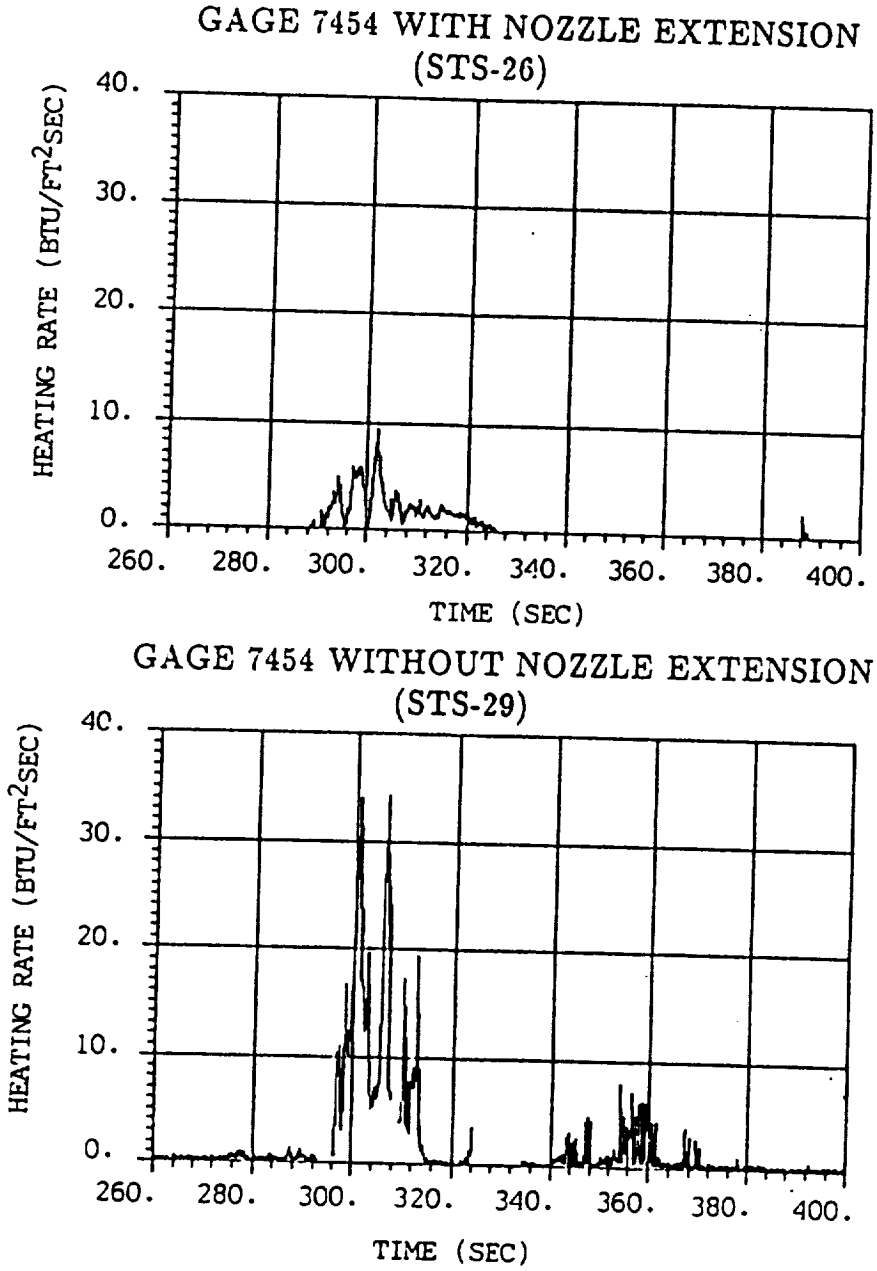

Figure 10: STS-29R Flame Entrainment Contribution to Internal Aft Skirt Reentry Heating Rates

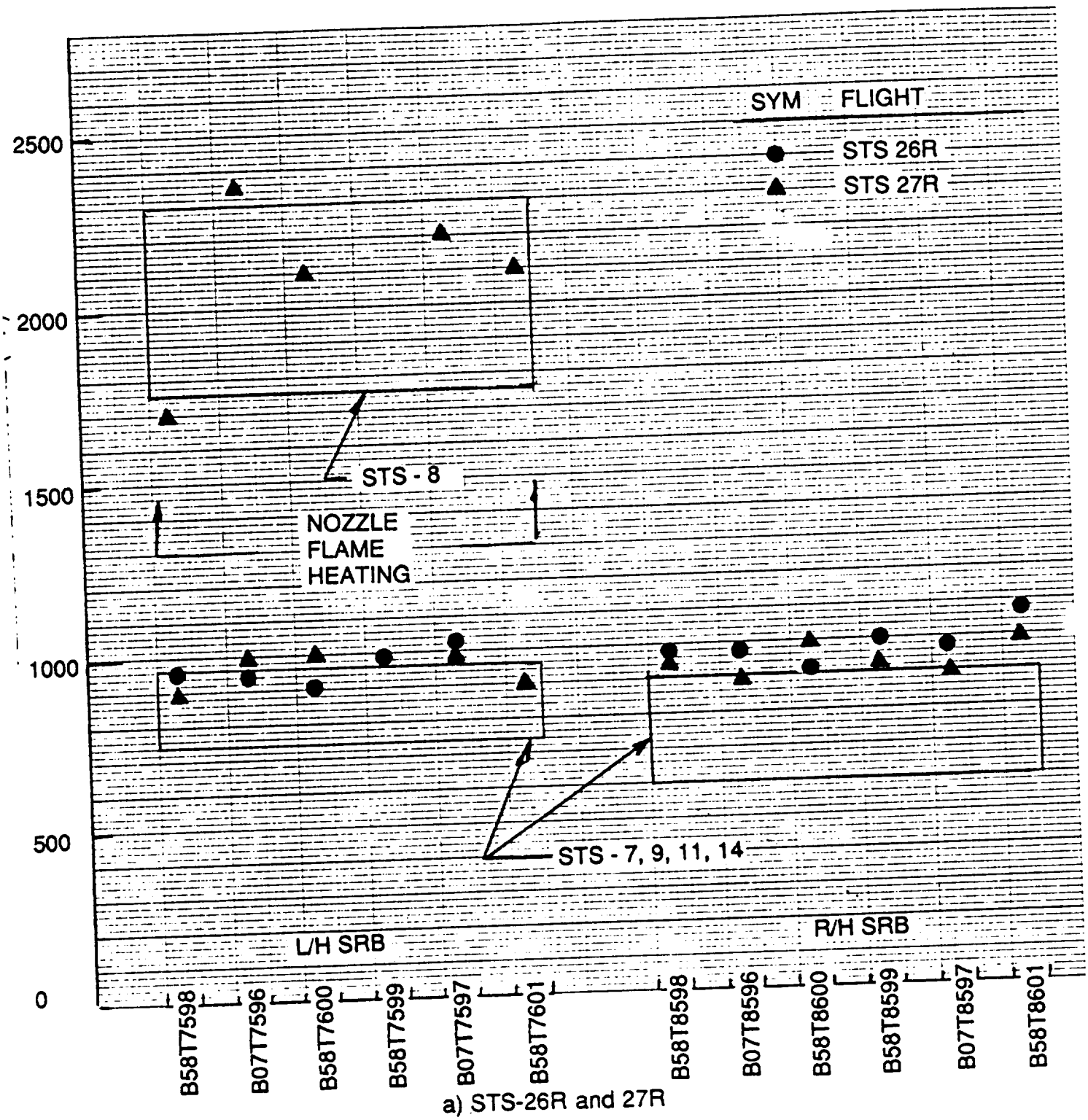

Figure 11: Internal Aft Skirt Gas Temperature Probe Summary

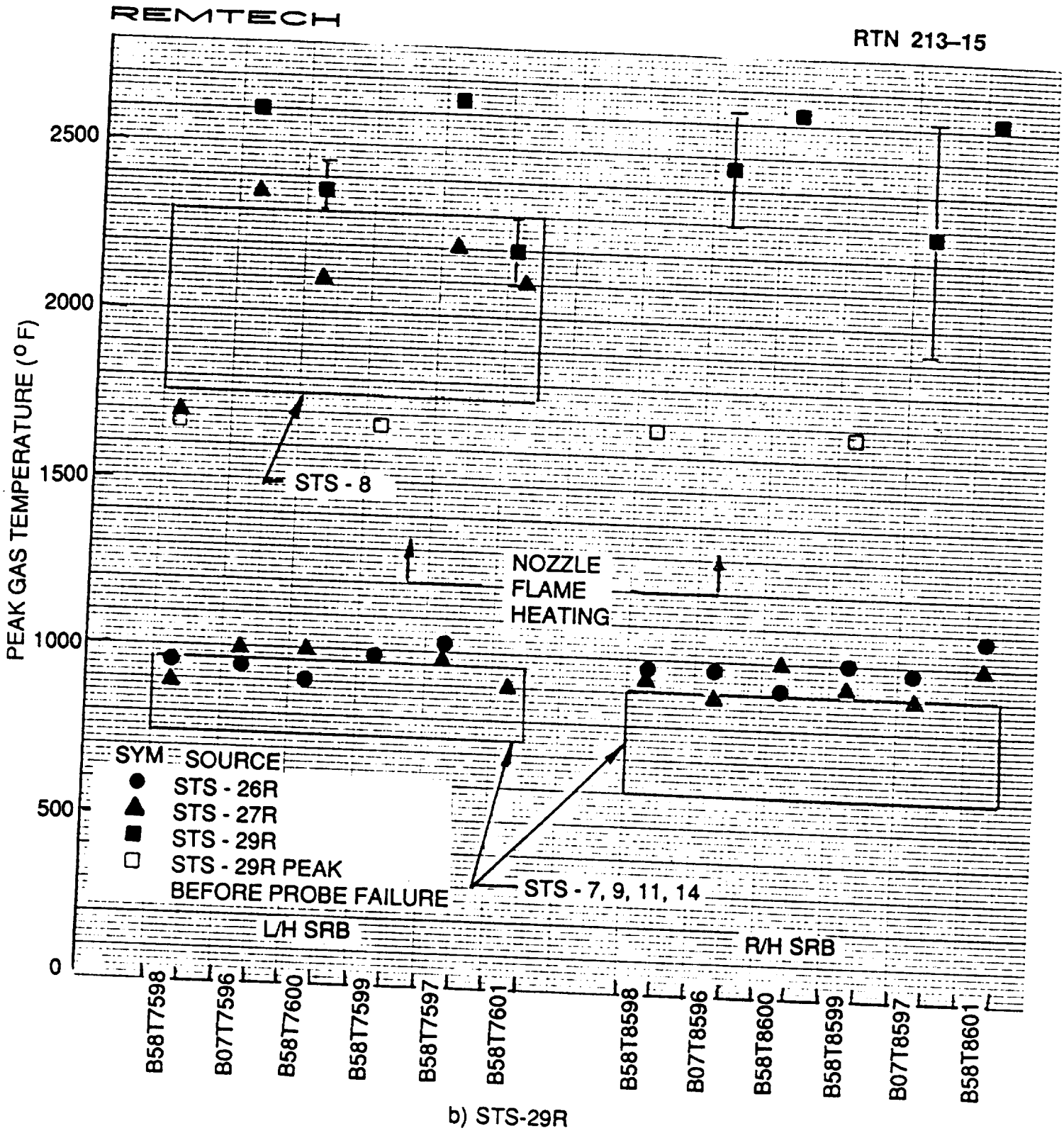

Figure 11: Gas Temperature Probe Summary (Concluded)

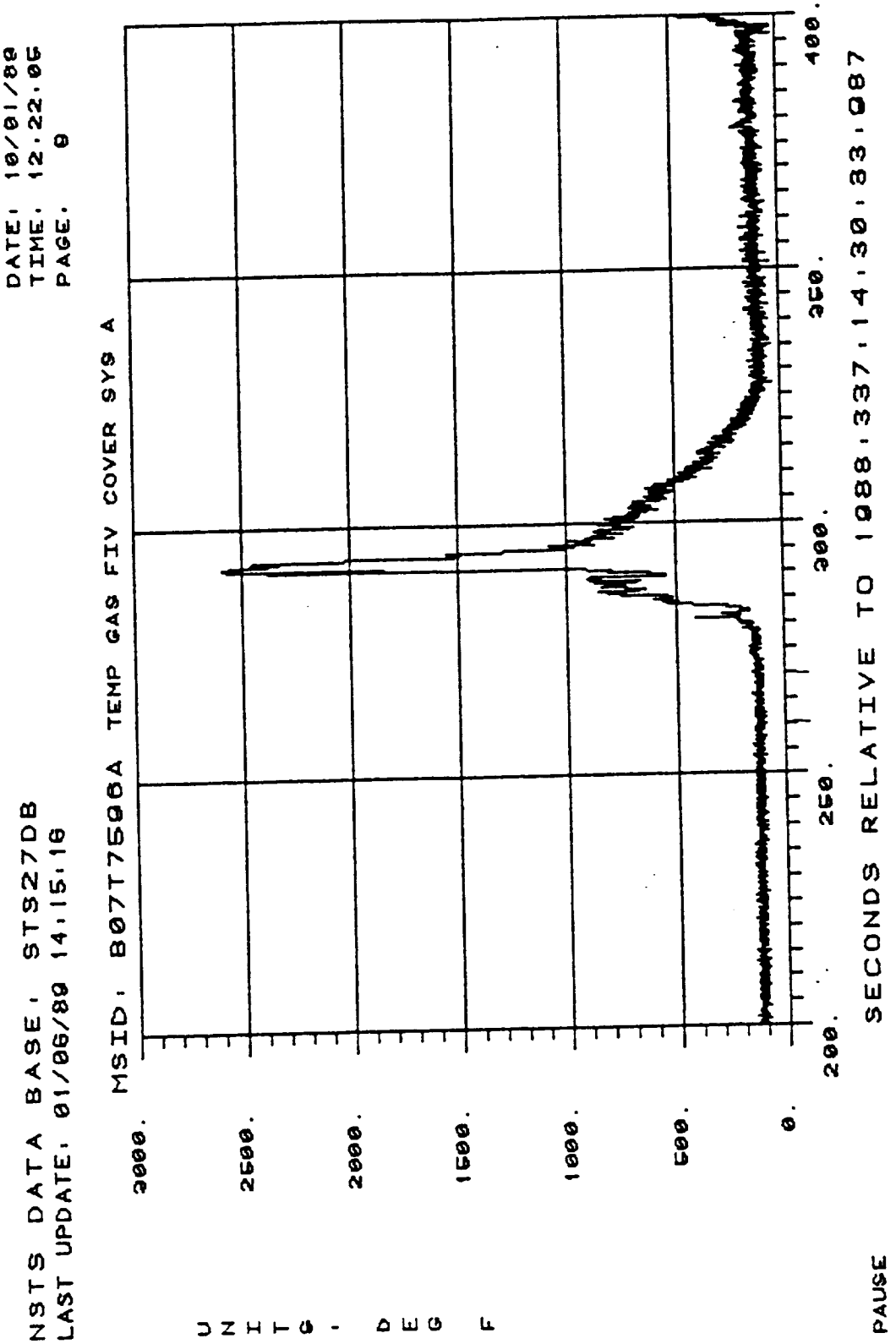

Figure 12: Example of Nozzle Flame Heating on STS-27R (Left Hand SRB)

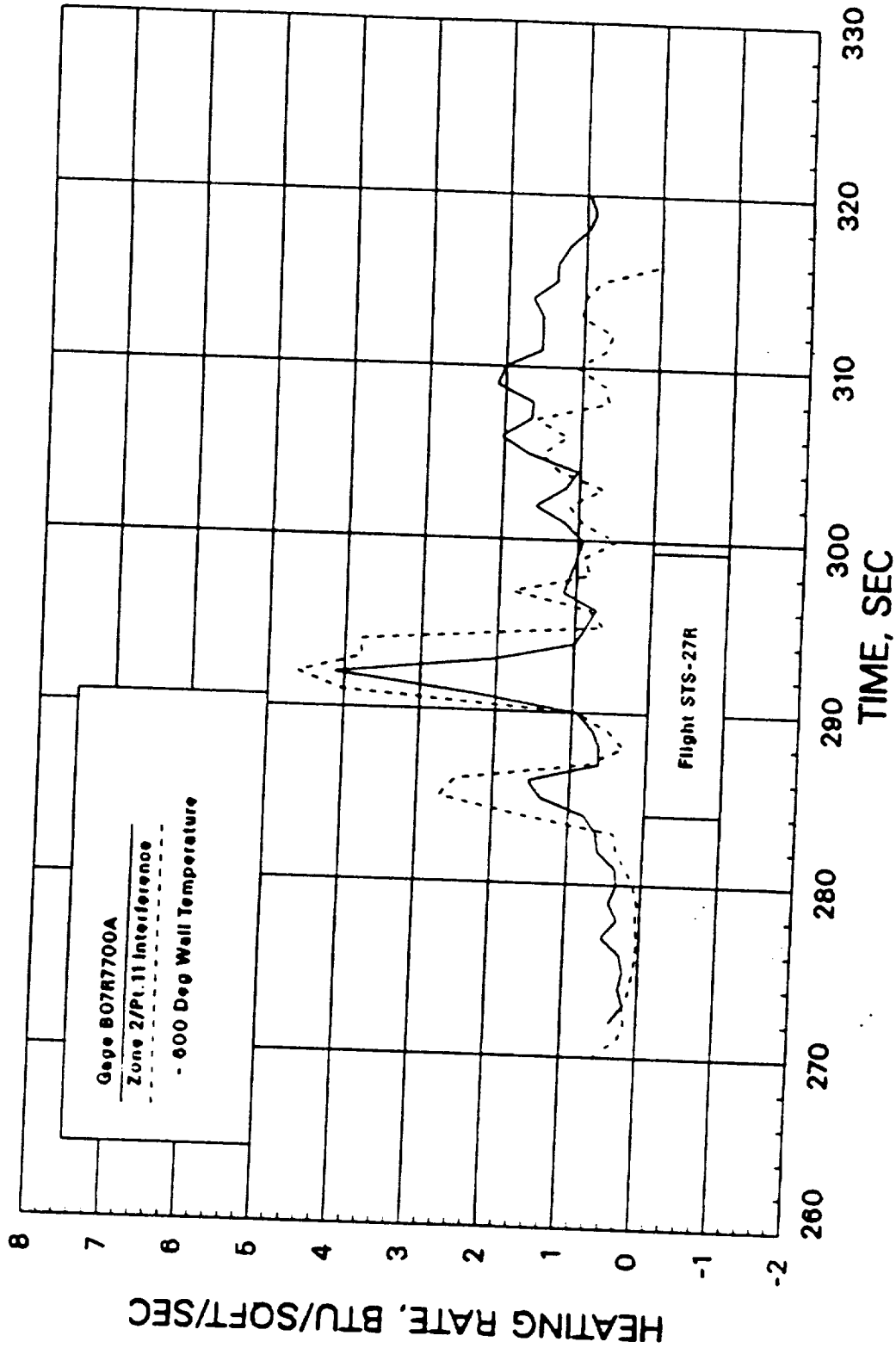

a) B07R7700 — Nose Cone

Figure 13: External Reentry Flight Heating Validation STS-27R

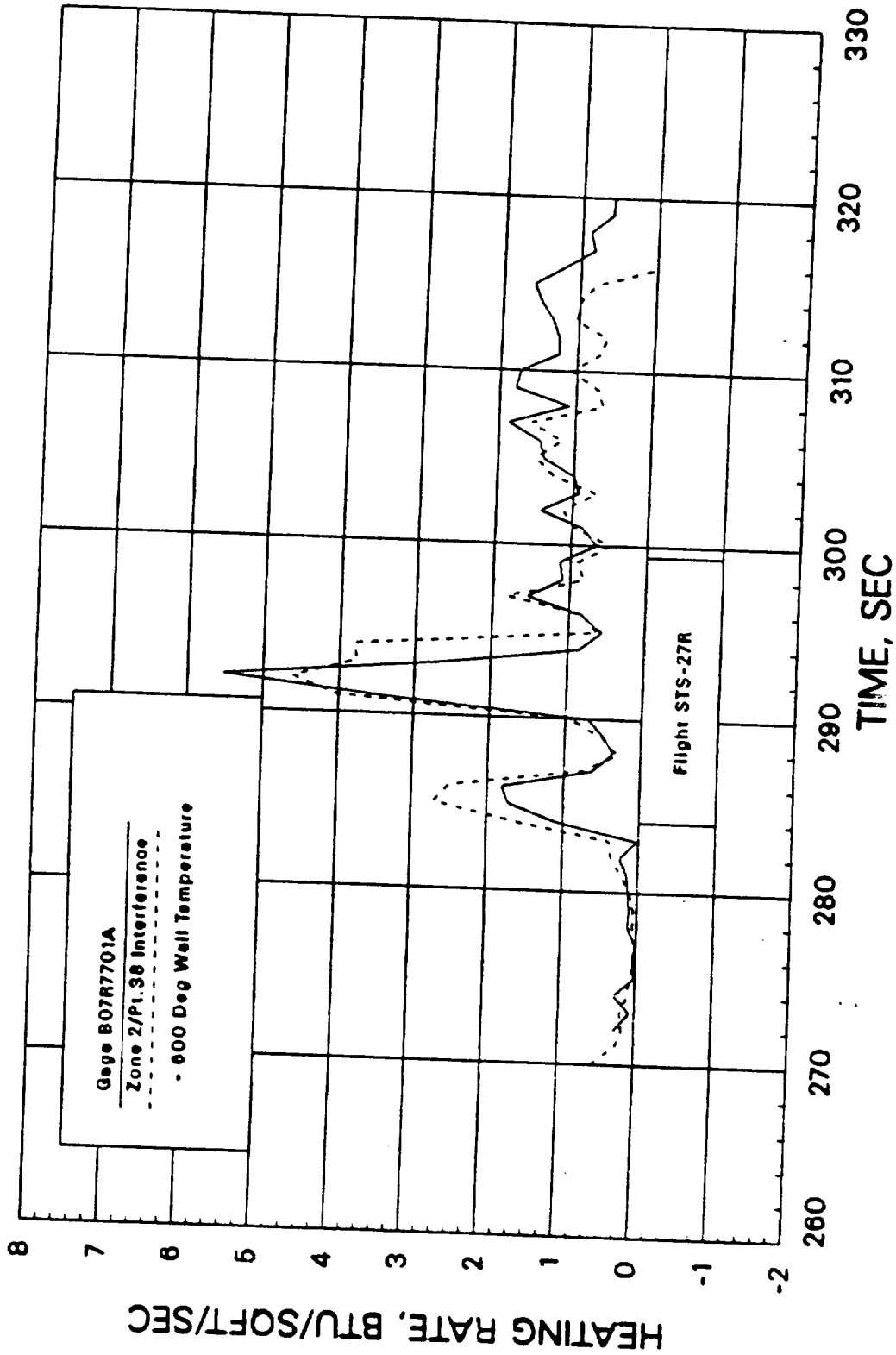

b) B07R7701 — Nose Cone

Figure 13: External Reentry Flight Heating Validation STS-27R (Continued)

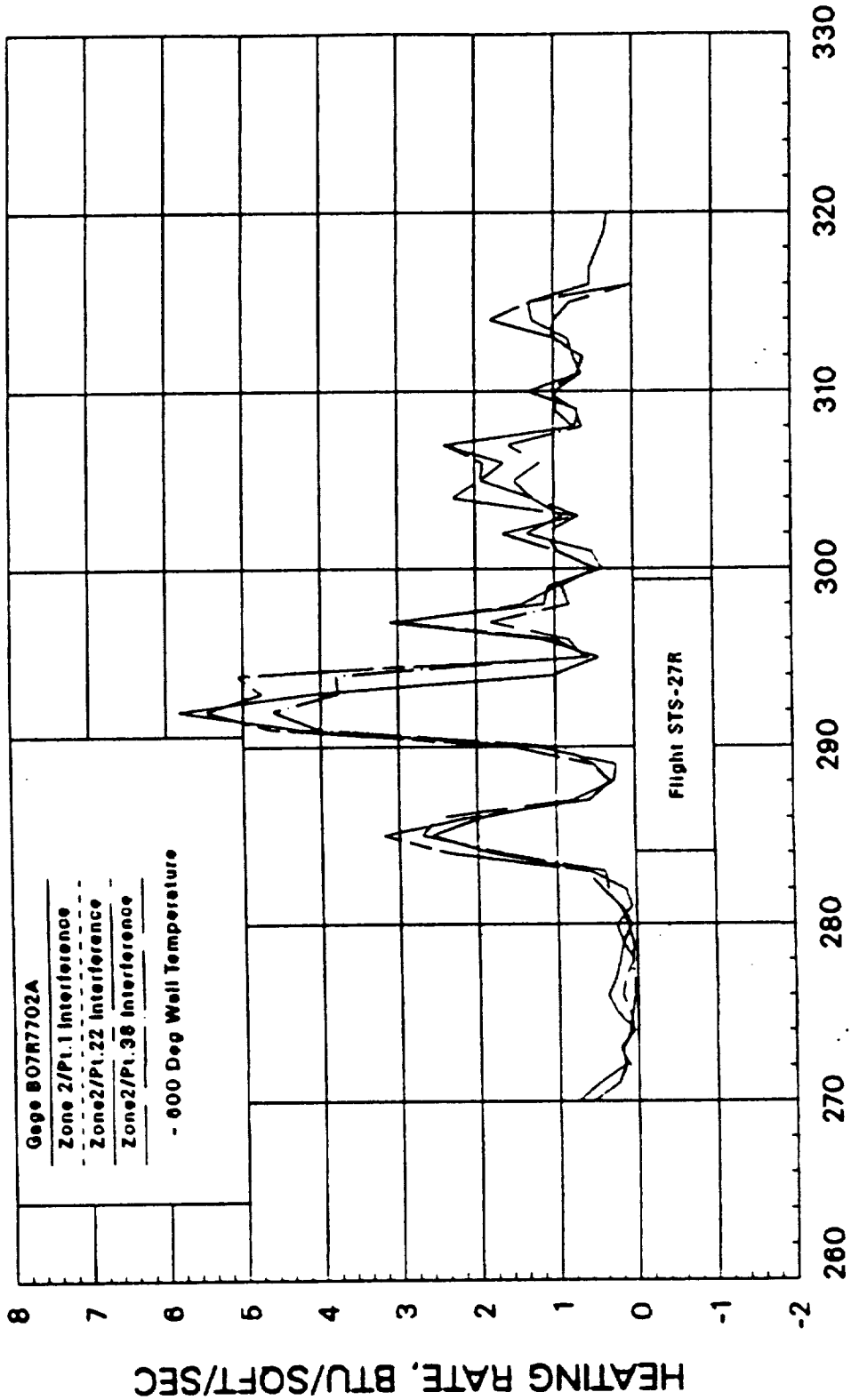

c) B07R7702 — Nose Cone

Figure 13: External Reentry Flight Heating Validation STS-27R (Continued)

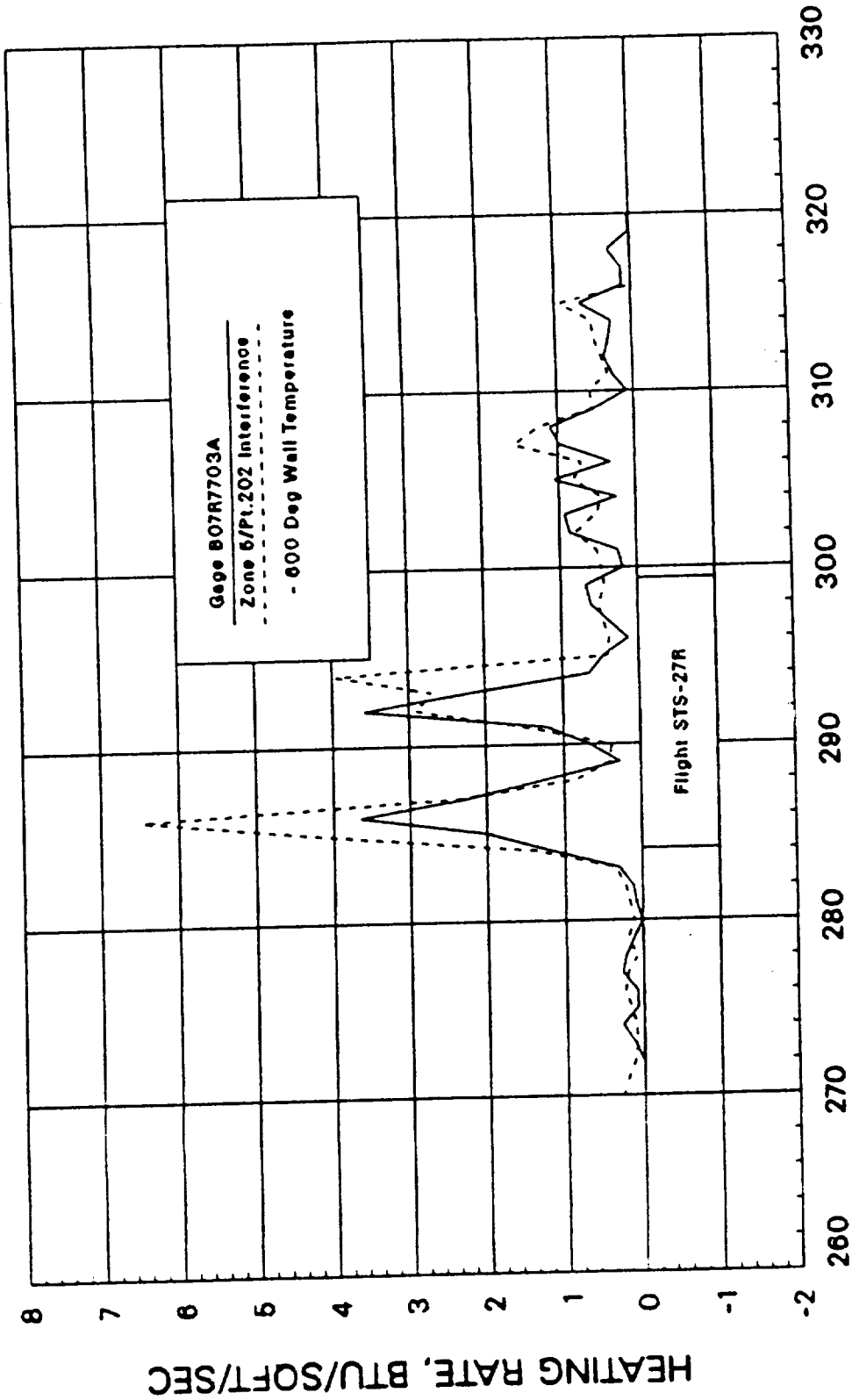

d) B07R7703 — Attach Ring

Figure 13: External Reentry Flight Heating Validation STS-27R (Continued)

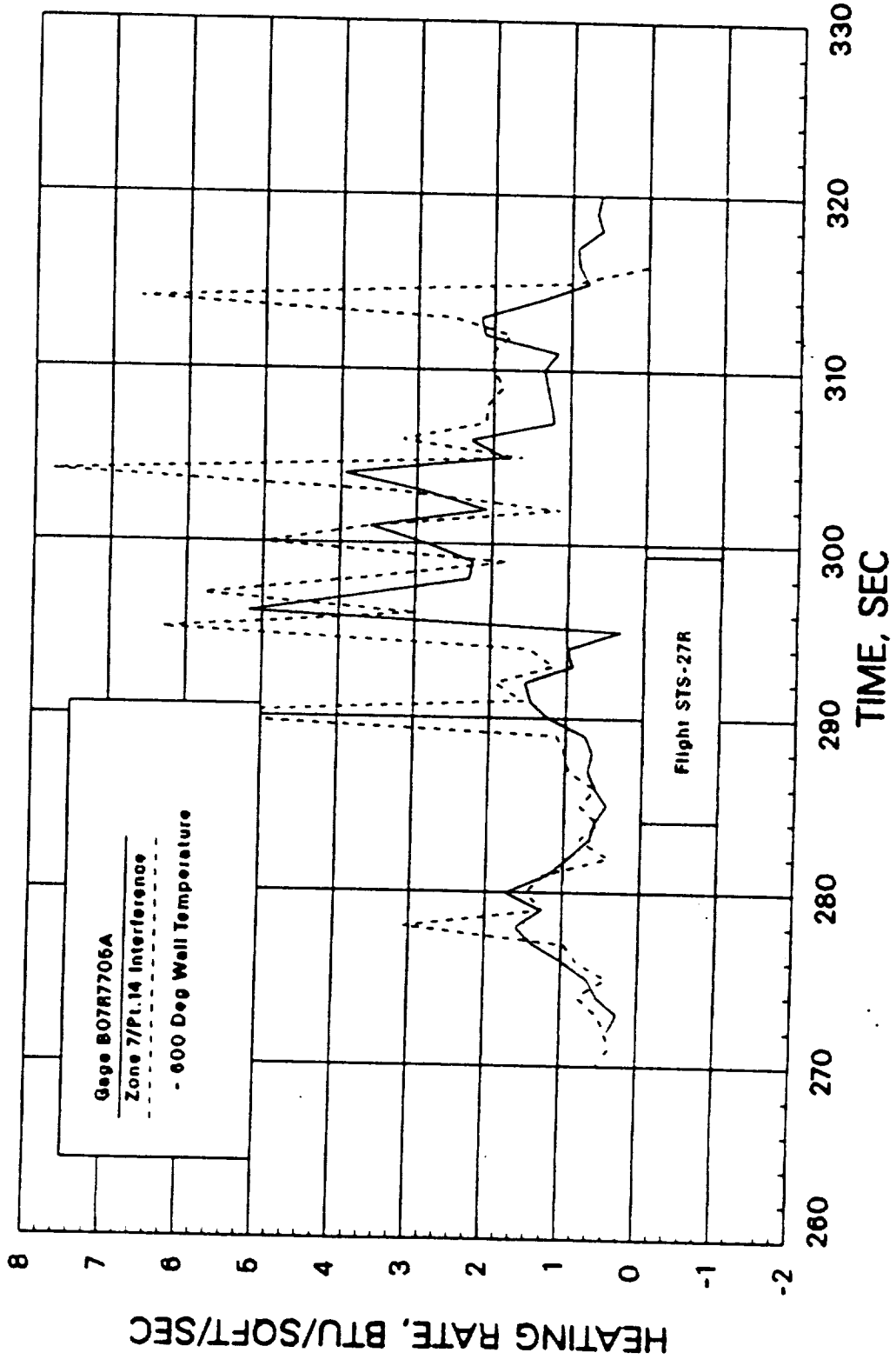

e) B07R7705 — Aft Skirt

Figure 13: External Reentry Flight Heating Validation STS-27R (Continued)

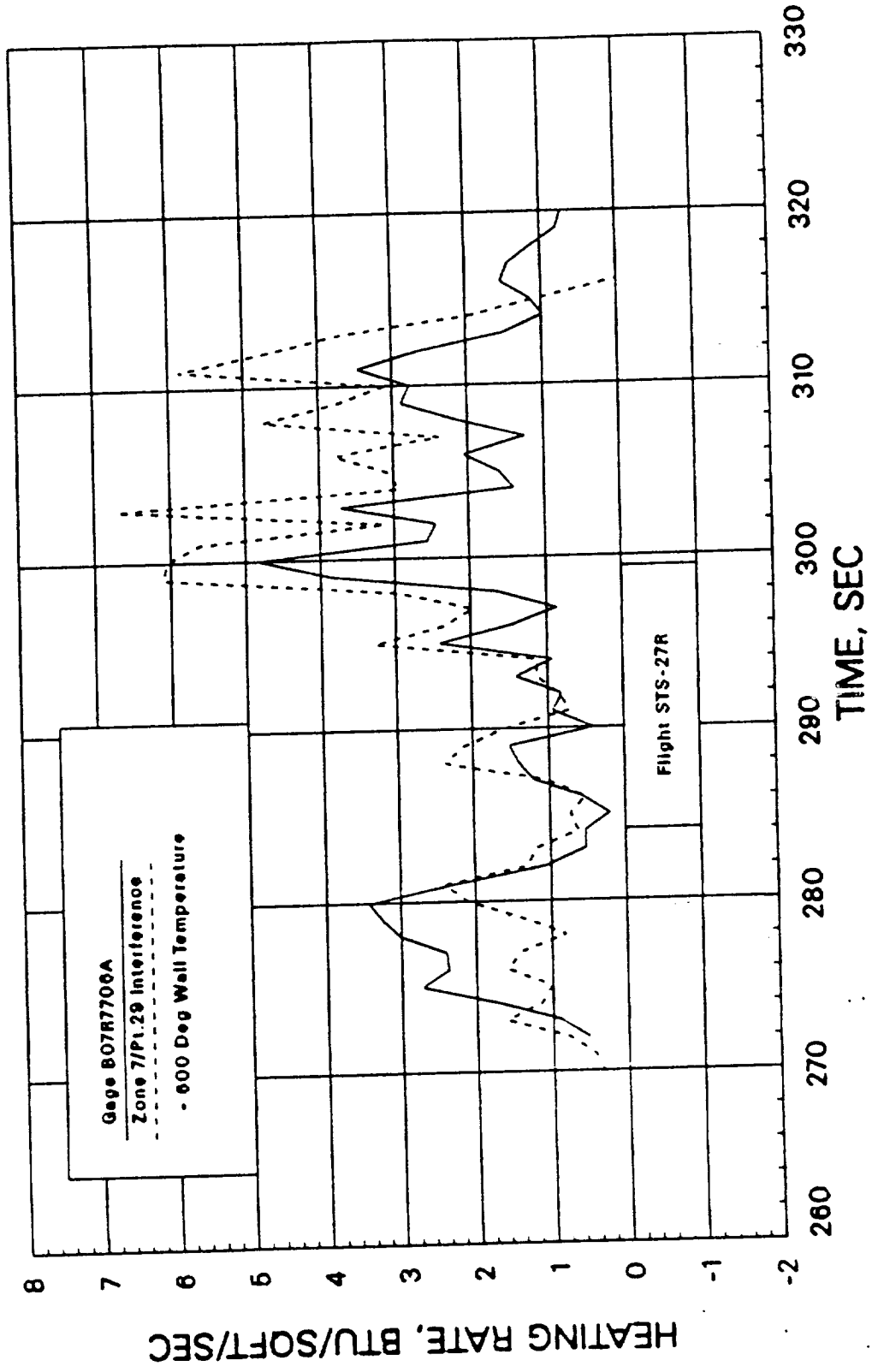

f) B07R7706 — Aft Skirt

Figure 13: External Reentry Flight Heating Validation STS-27R (Continued)

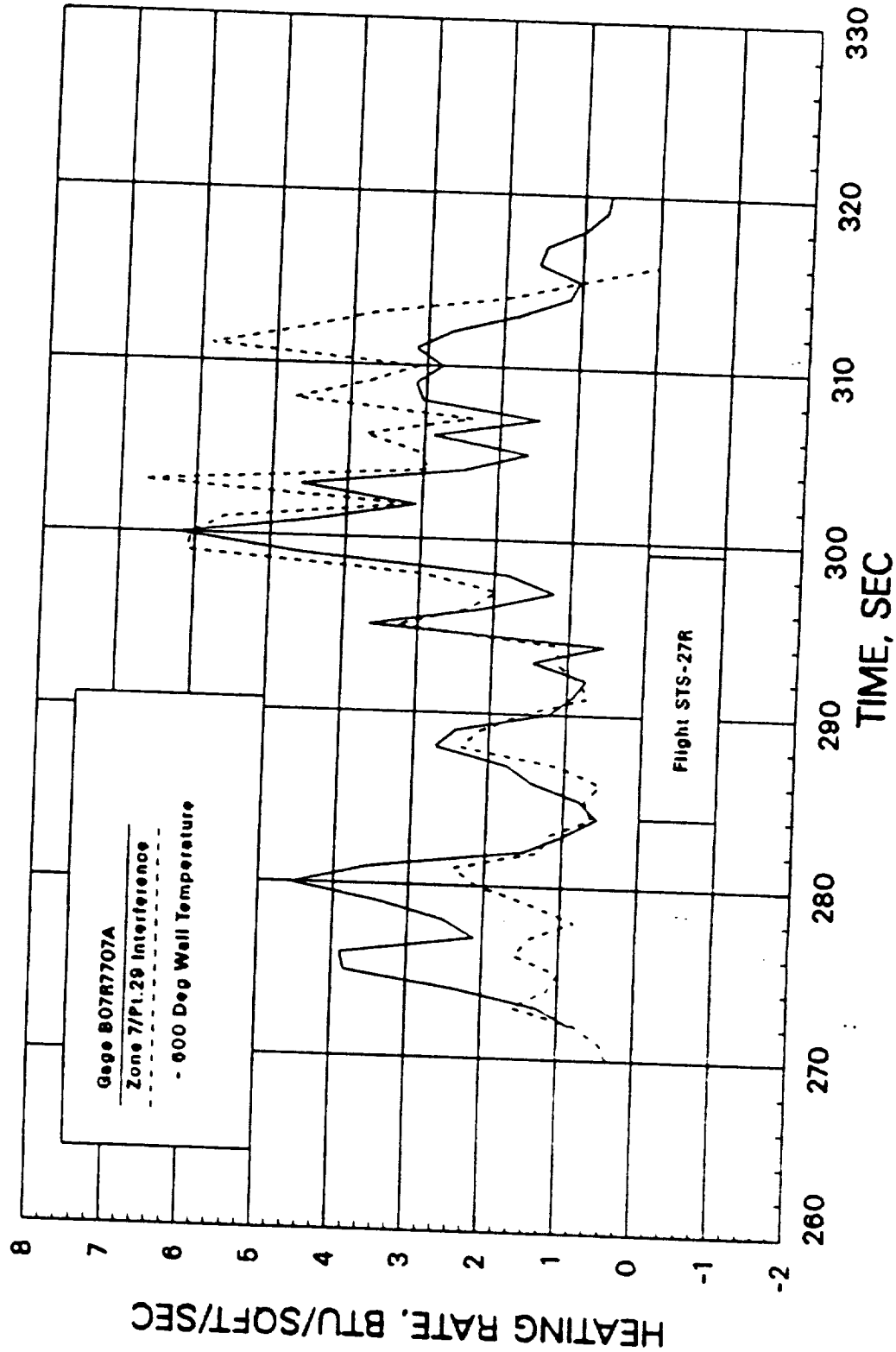

g) B07R7707 — Aft Skirt

Figure 13: External Reentry Flight Heating Validation STS-27R (Concluded)

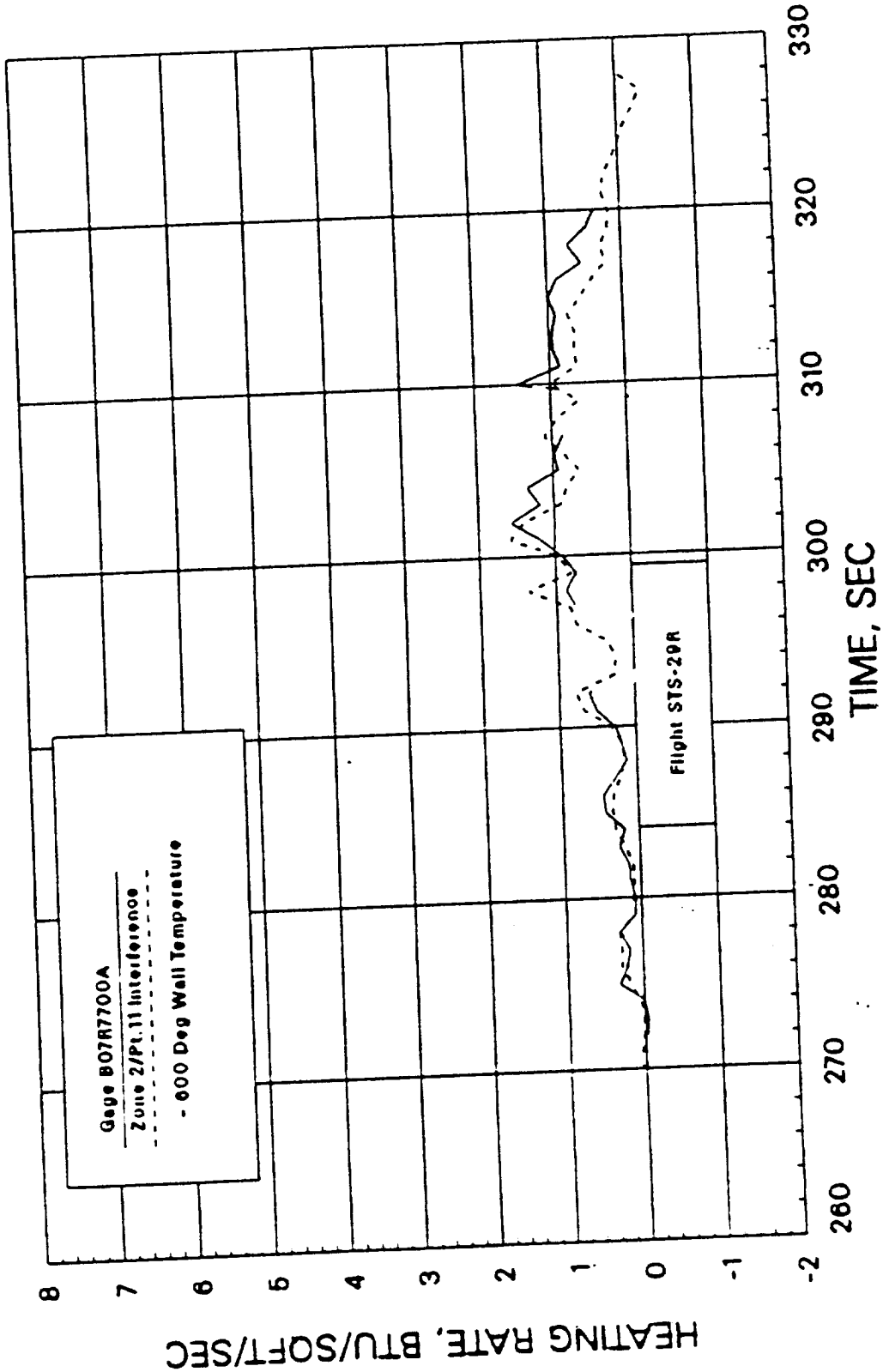

a) B07R7700 — Nose Cone

Figure 14: External Reentry Flight Heating Validation STS-29R

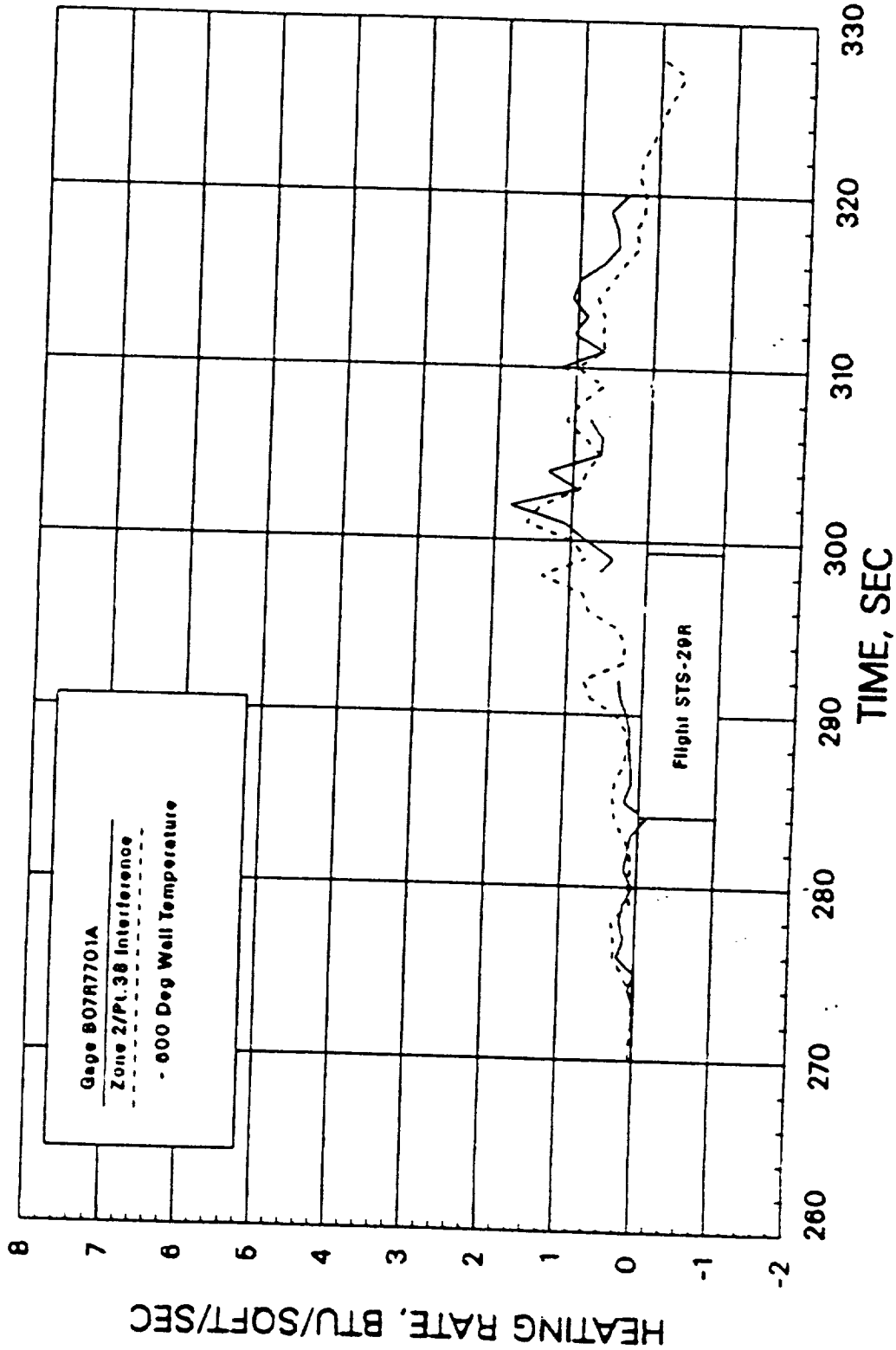

b) B07R7701 — Nose Cone

Figure 14: External Reentry Flight Heating Validation STS-29R (Continued)

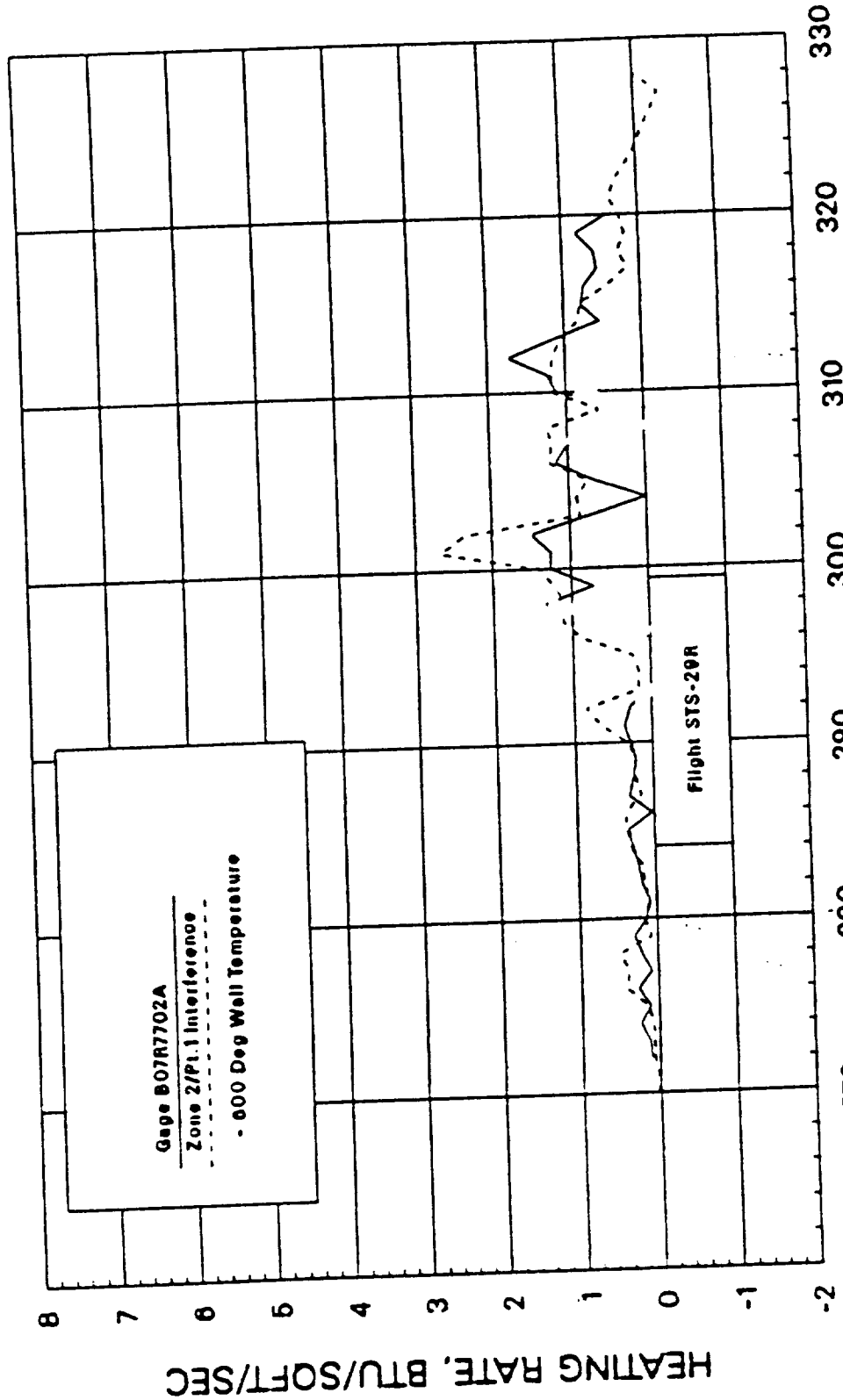

c) B07R7702 — Nose Cone

Figure 14: External Reentry Flight Heating Validation STS-29R (Continued)

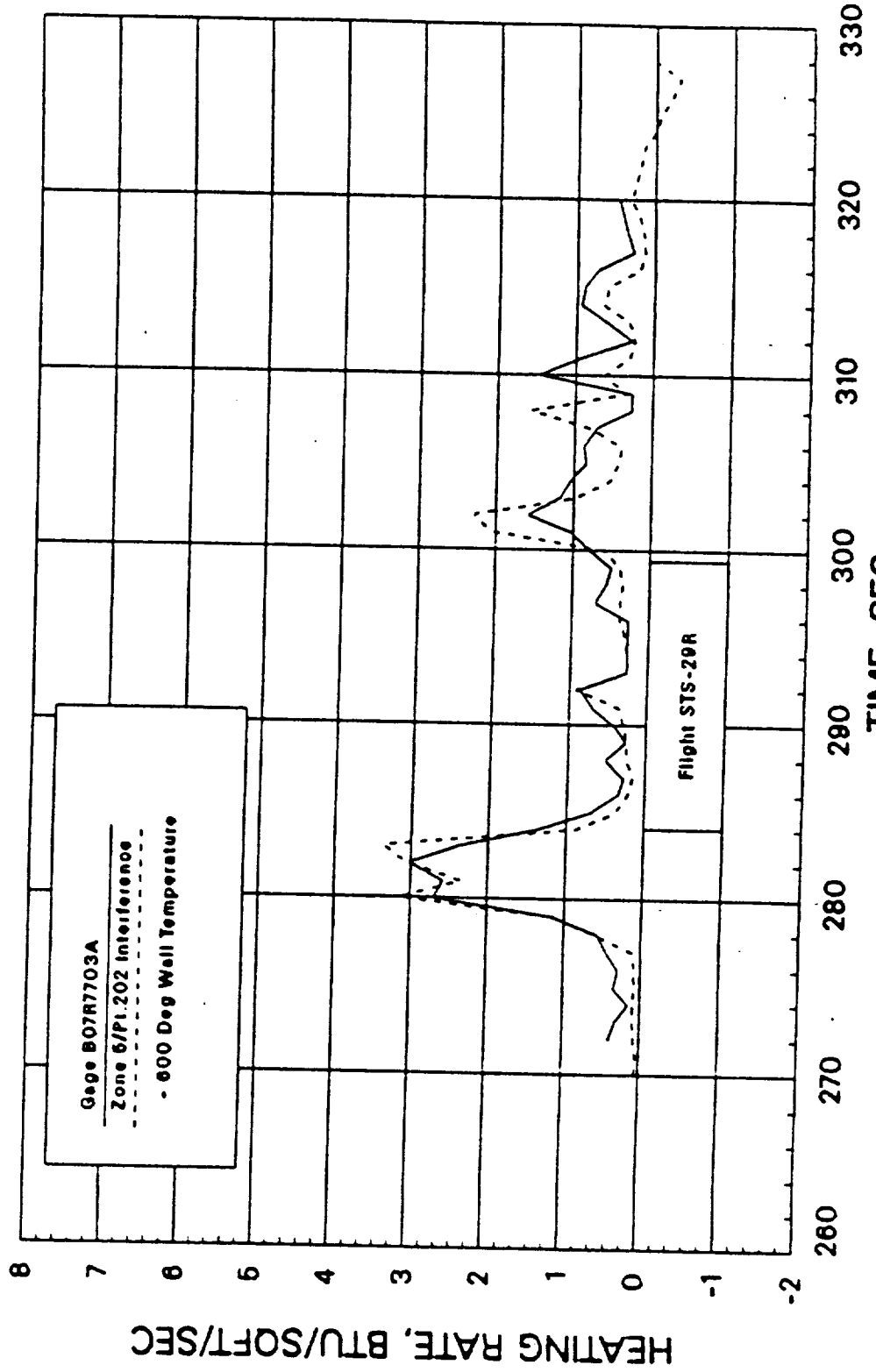

d) B07R7703 — Attach Ring

Figure 14: External Reentry Flight Heating Validation STS-29R (Continued)

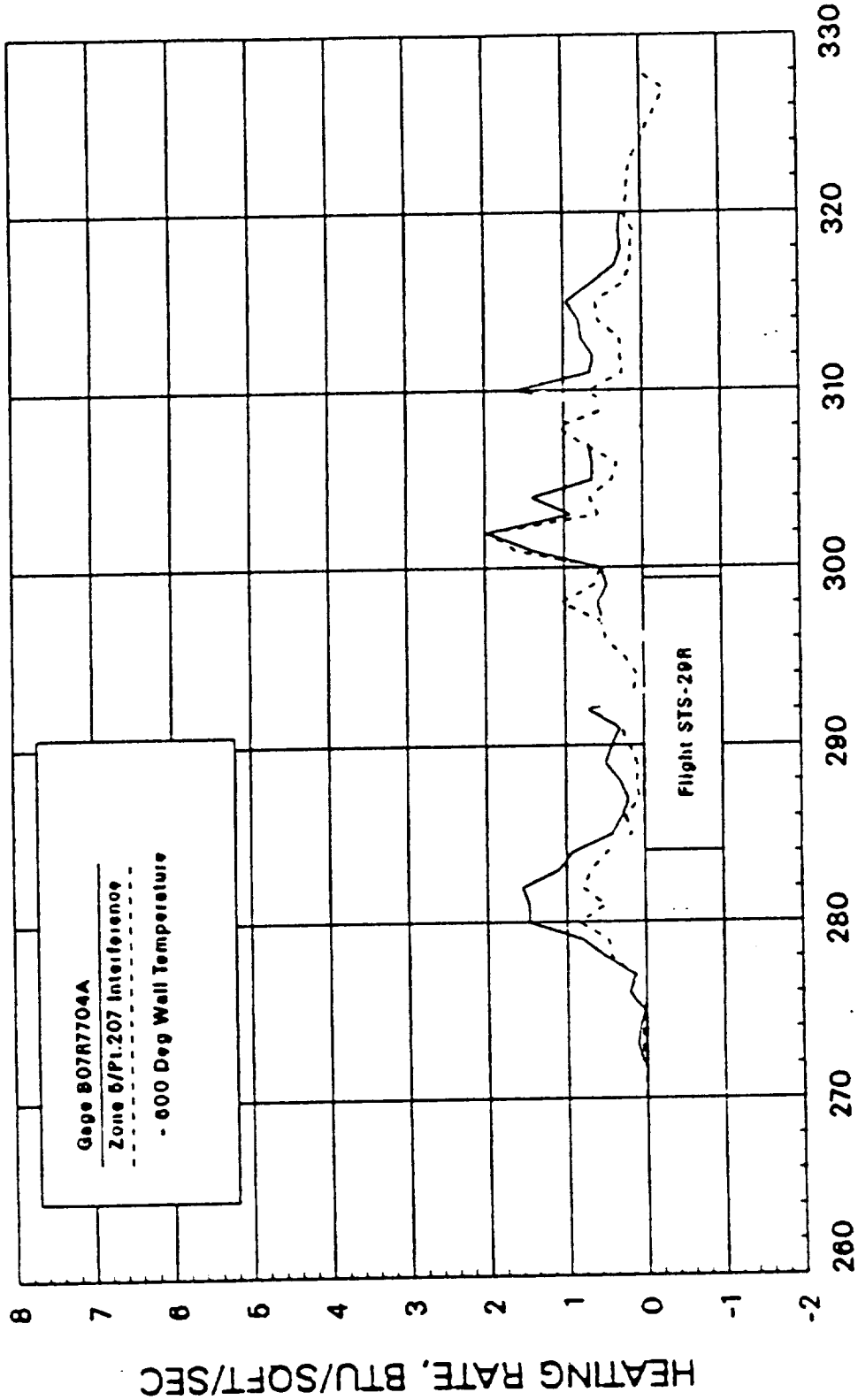

e) B07R7704 — Attach Ring

Figure 14: External Reentry Flight Heating Validation STS-29R (Continued)

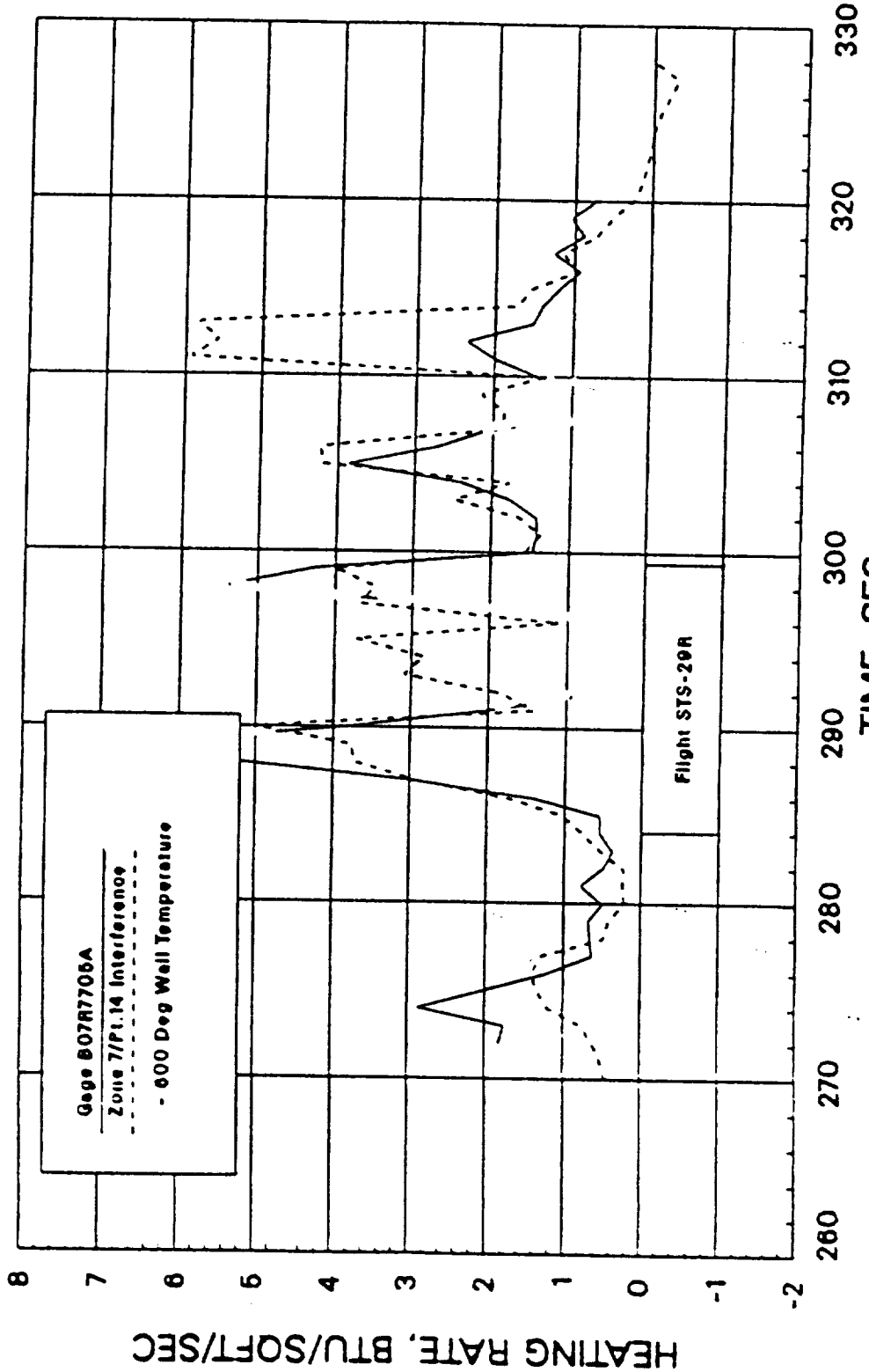

f) B07R7705 — Aft Skirt

Figure 14: External Reentry Flight Heating Validation STS-29R (Continued)

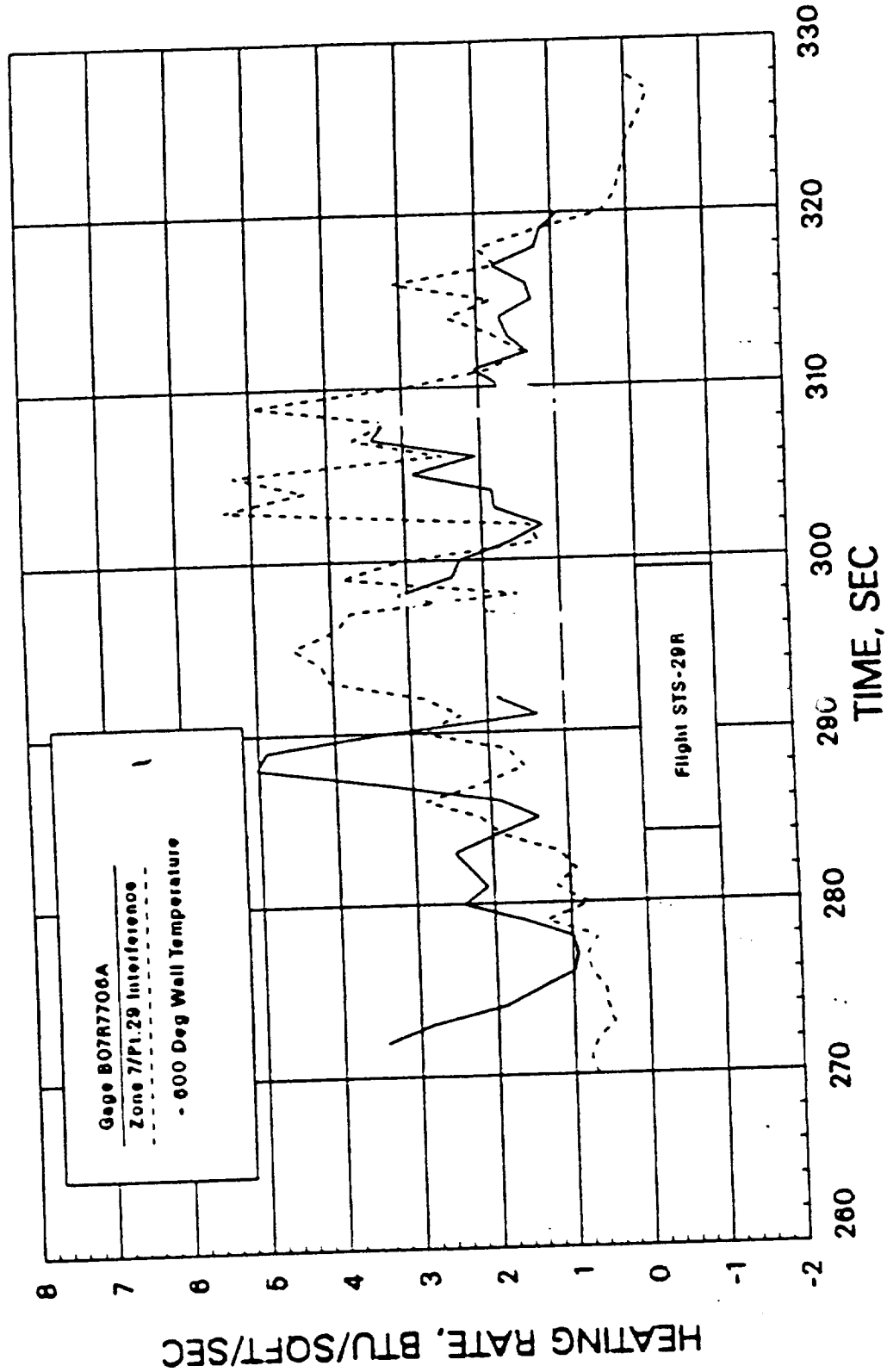

g) B07R7706 — Aft Skirt

Figure 14: External Reentry Flight Heating Validation STS-29R (Continued)

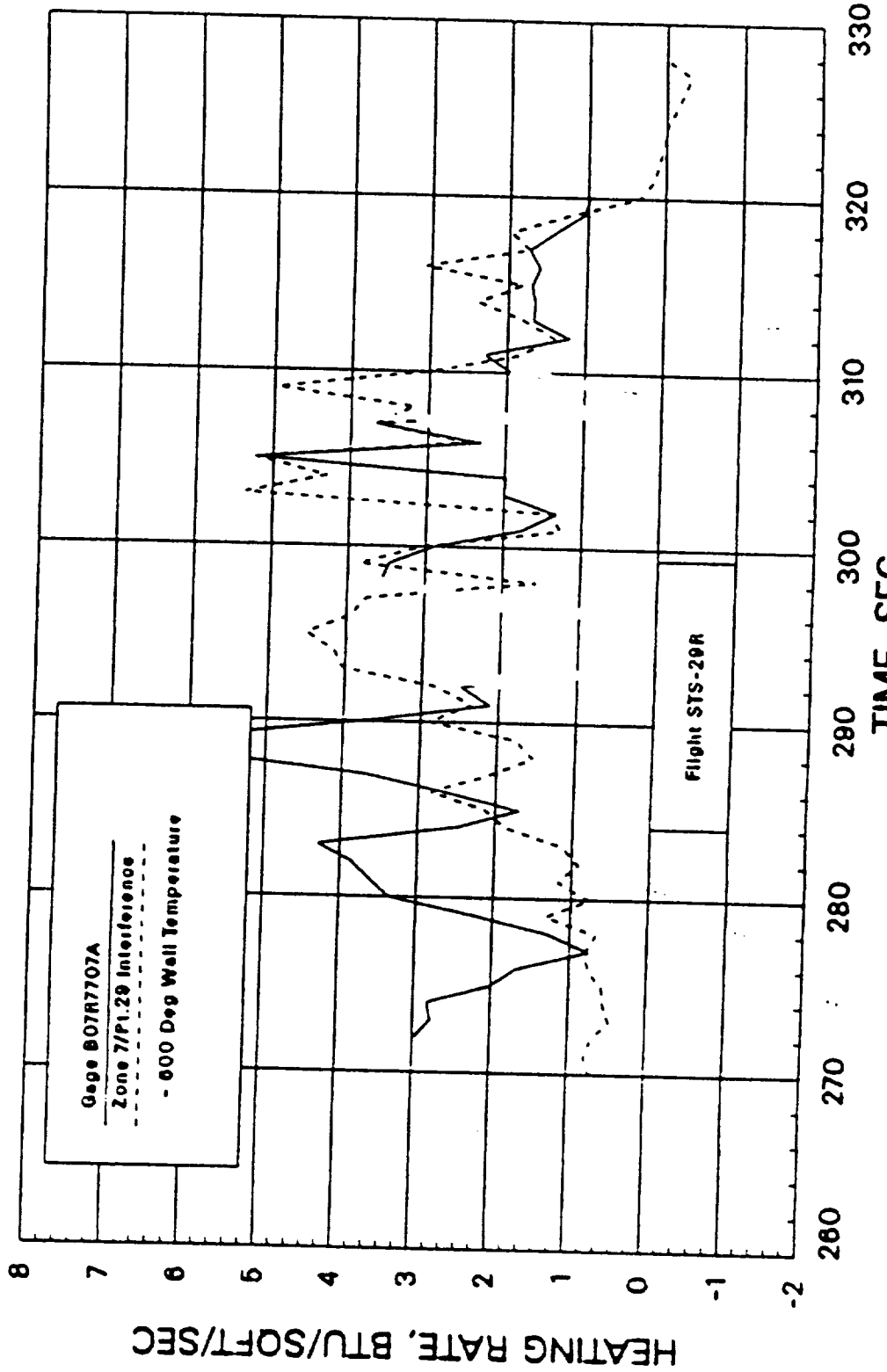

h) B07R7707 — Aft Skirt

Figure 14: External Reentry Flight Heating Validation STS-29R (Concluded)

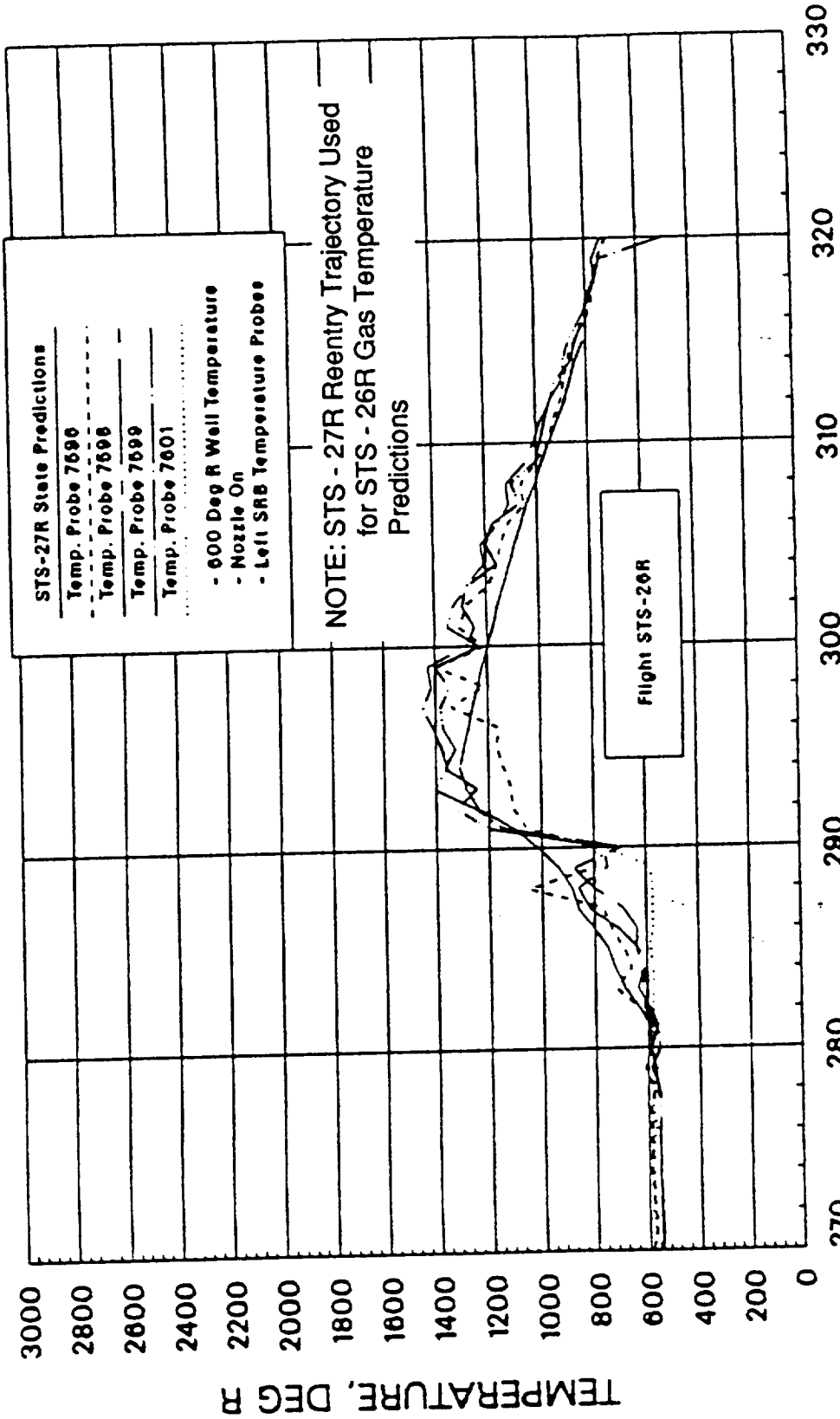

a) Left Hand SRB

Figure 15: SRB Internal Aft Skirt Gas Temperature STS-26R

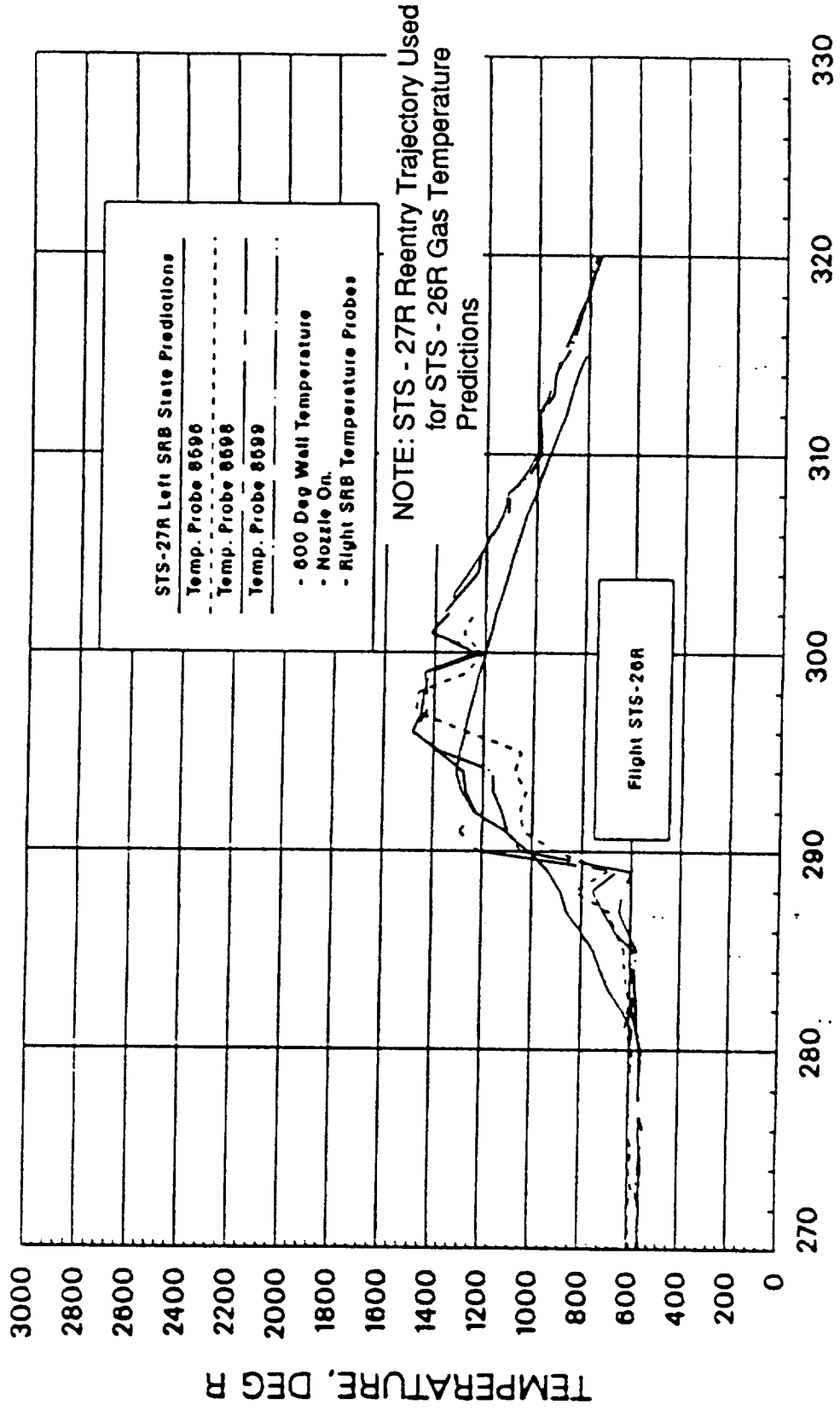

b) Right Hand SRB

Figure 15: SRB Internal Aft Skirt Gas Temperature STS-26R (Concluded)

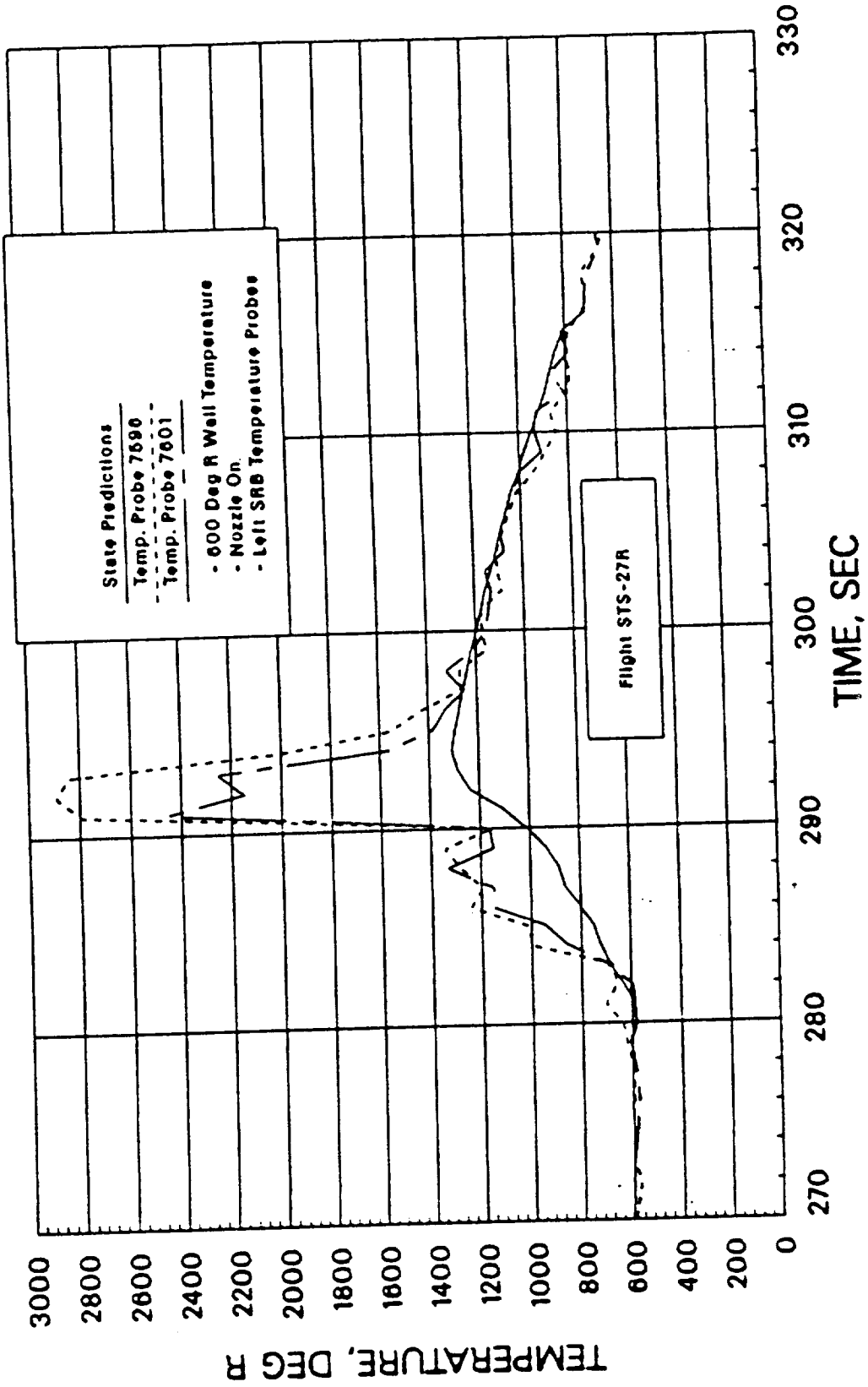

a) Left Hand SRB

Figure 16: SRB Internal Aft Skirt Gas Temperature STS-27R

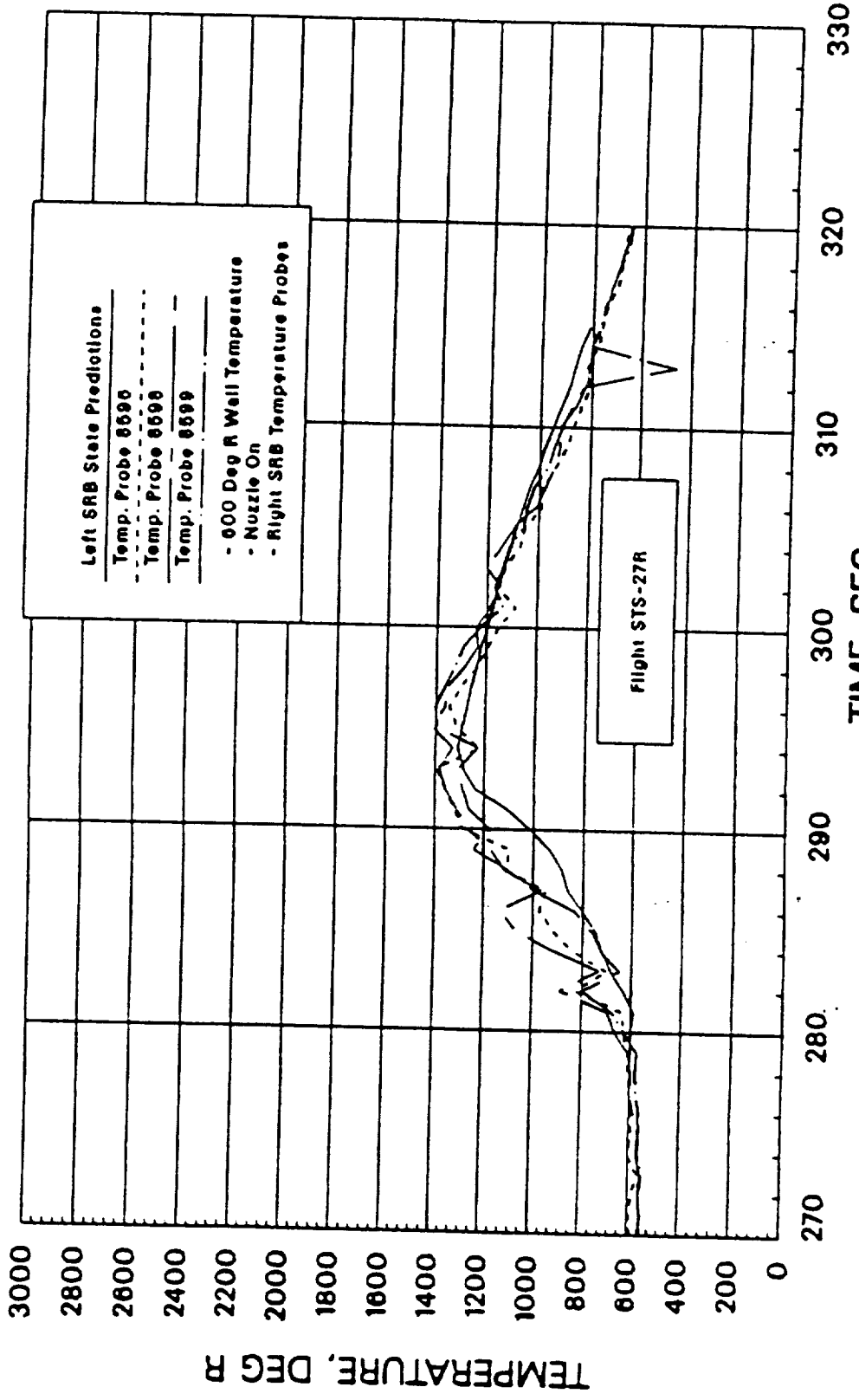

b) Right Hand SRB

Figure 16: SRB Internal Aft Skirt Gas Temperature STS-27R (Concluded)

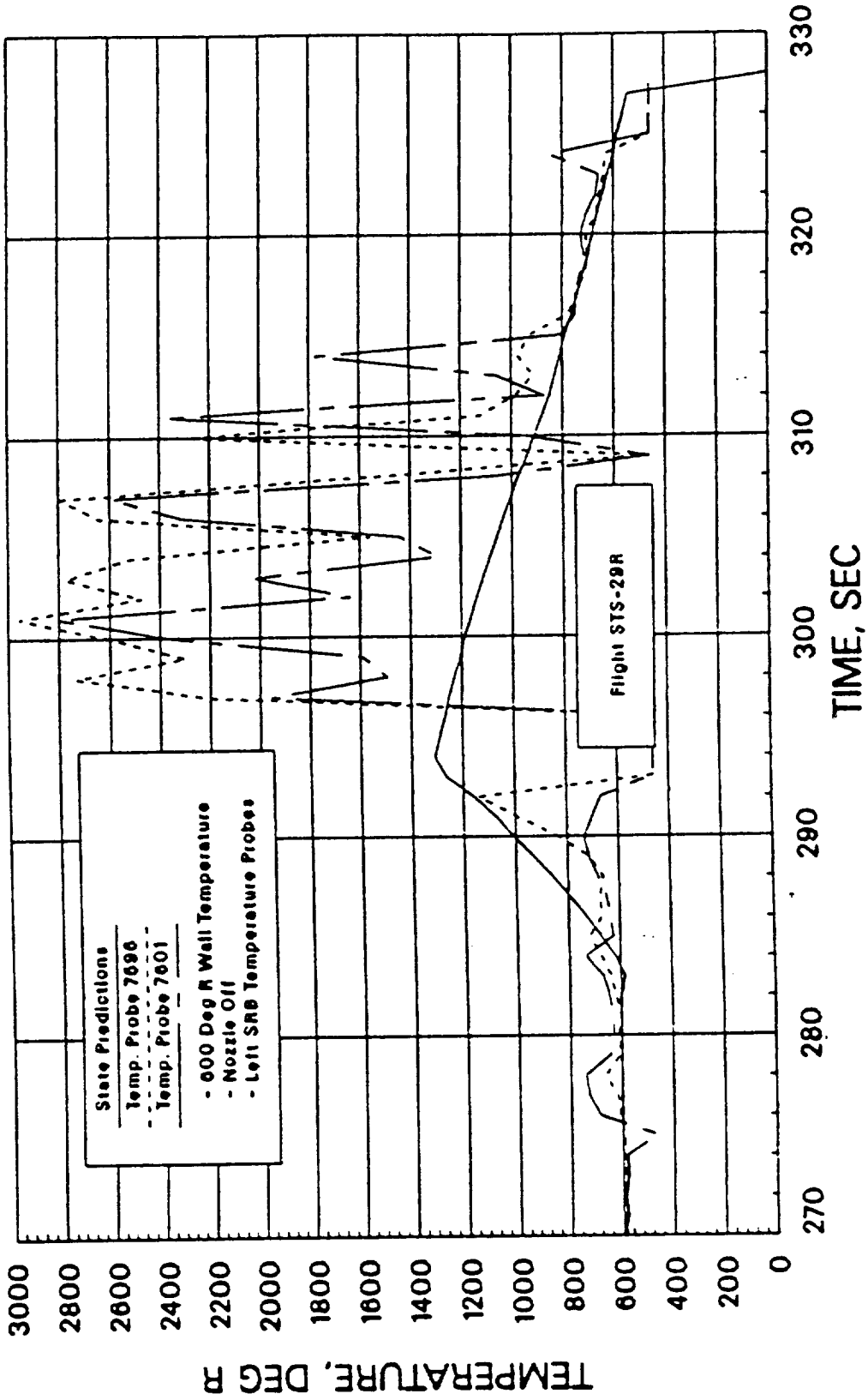

a) Left Hand SRB

Figure 17: SRB Internal Aft Skirt Gas Temperature STS-29R

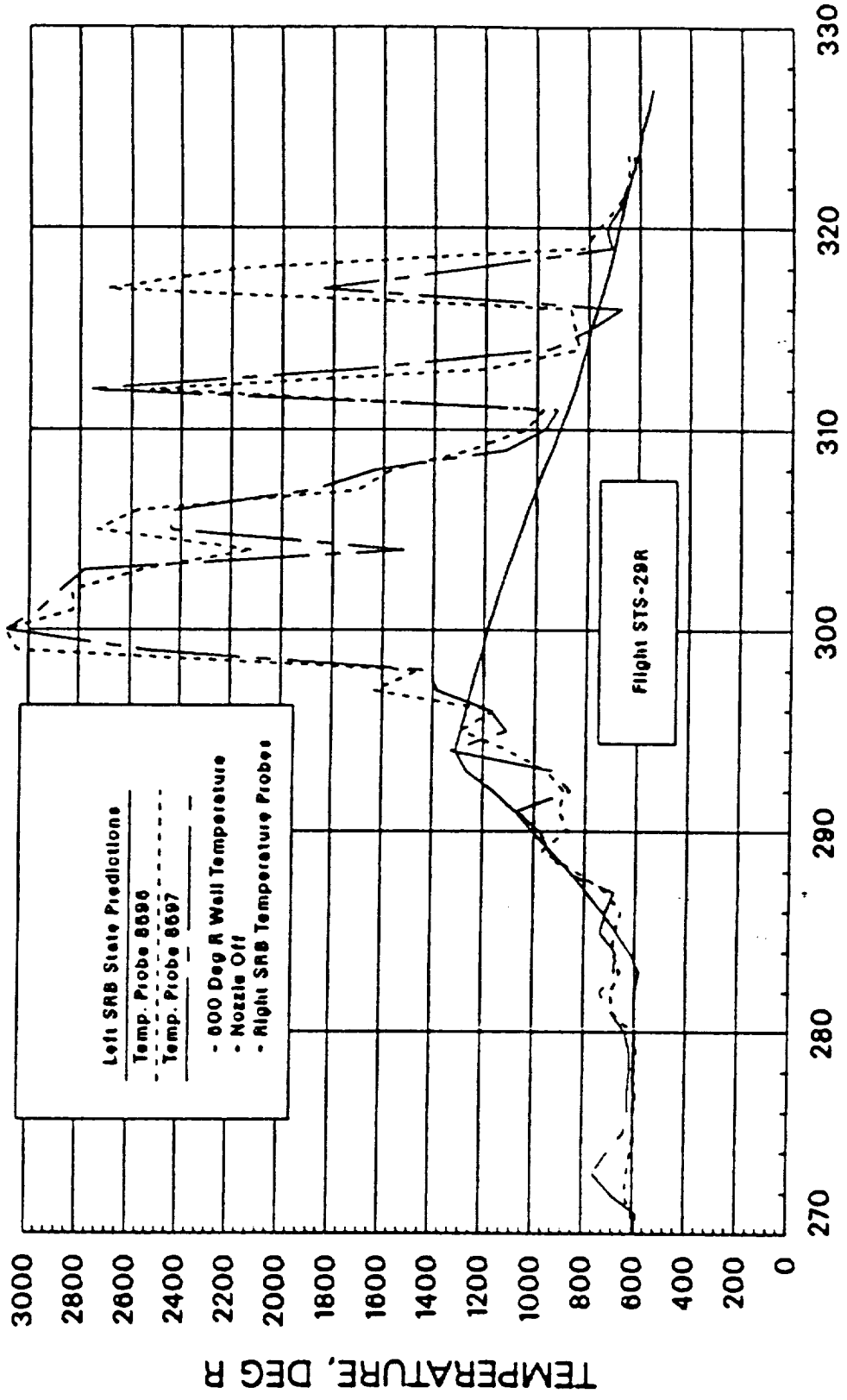

b) Right Hand SRB

Figure 17: SRB Internal Aft Skirt Gas Temperature STS-29R (Concluded)

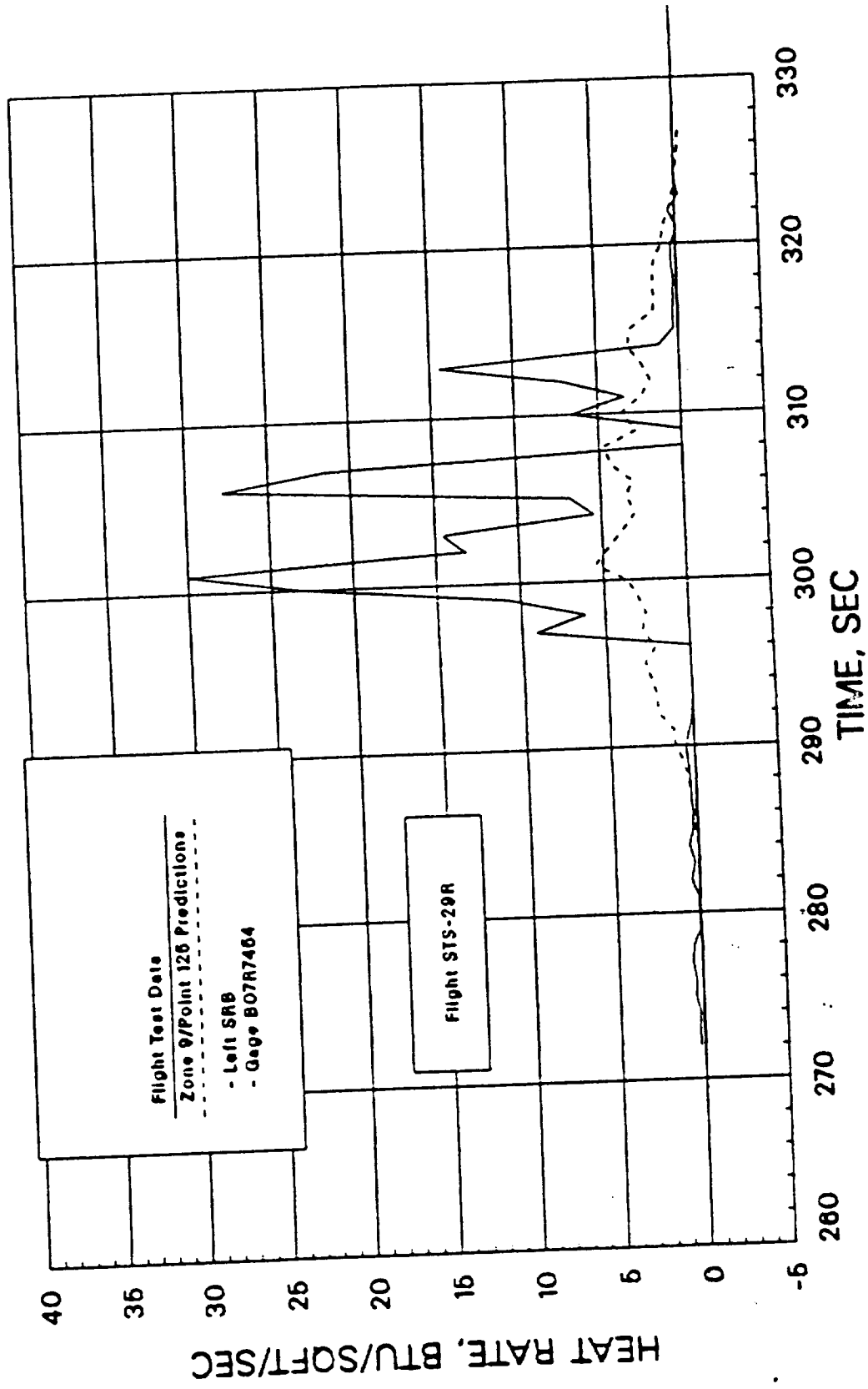

a) Using STATE Gas Temperature Algorithm

Figure 18: Internal Aft Skirt Heating Rate Validation B07R7454 STS-29R

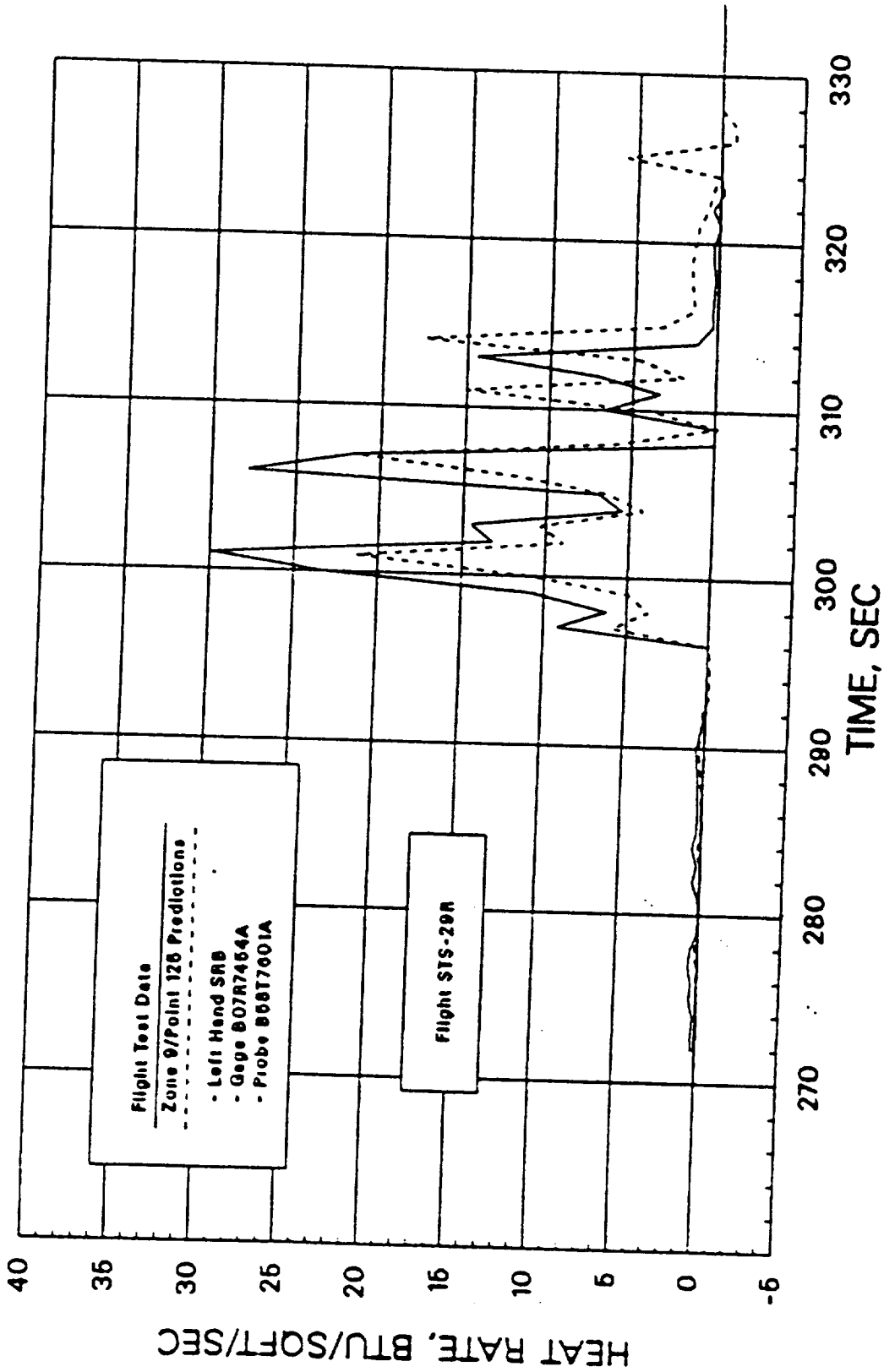

b) Using Flight Gas Temperature Measurement (B07T7601)

Figure 18: Internal Aft Skirt Heating Rate Validation B07R7454 STS-29R (Concluded)

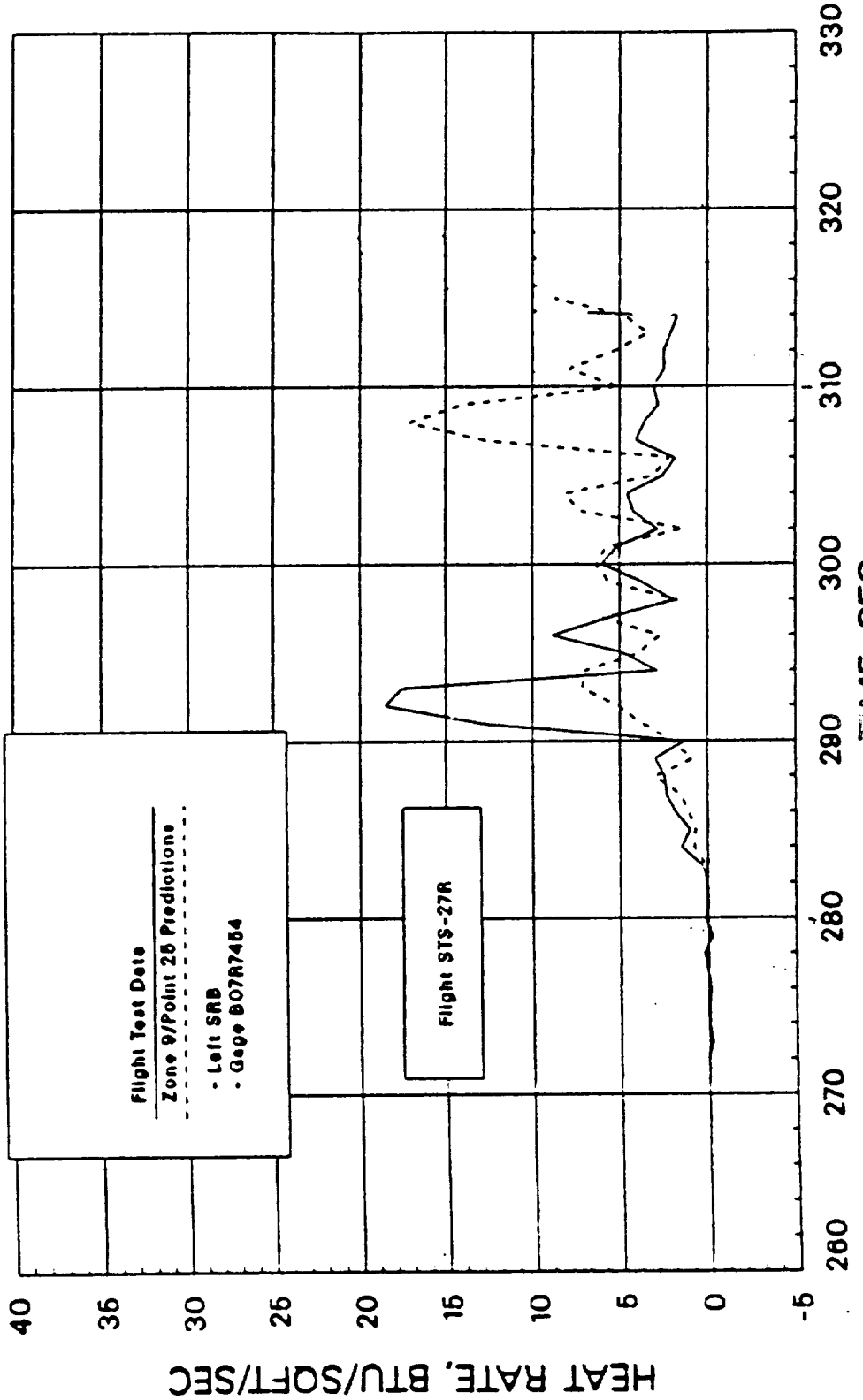

a) Using STATE Gas Temperature Algorithm

Figure 19: Internal Aft Skirt Heating Rate Validation B07R7454 STS-27R

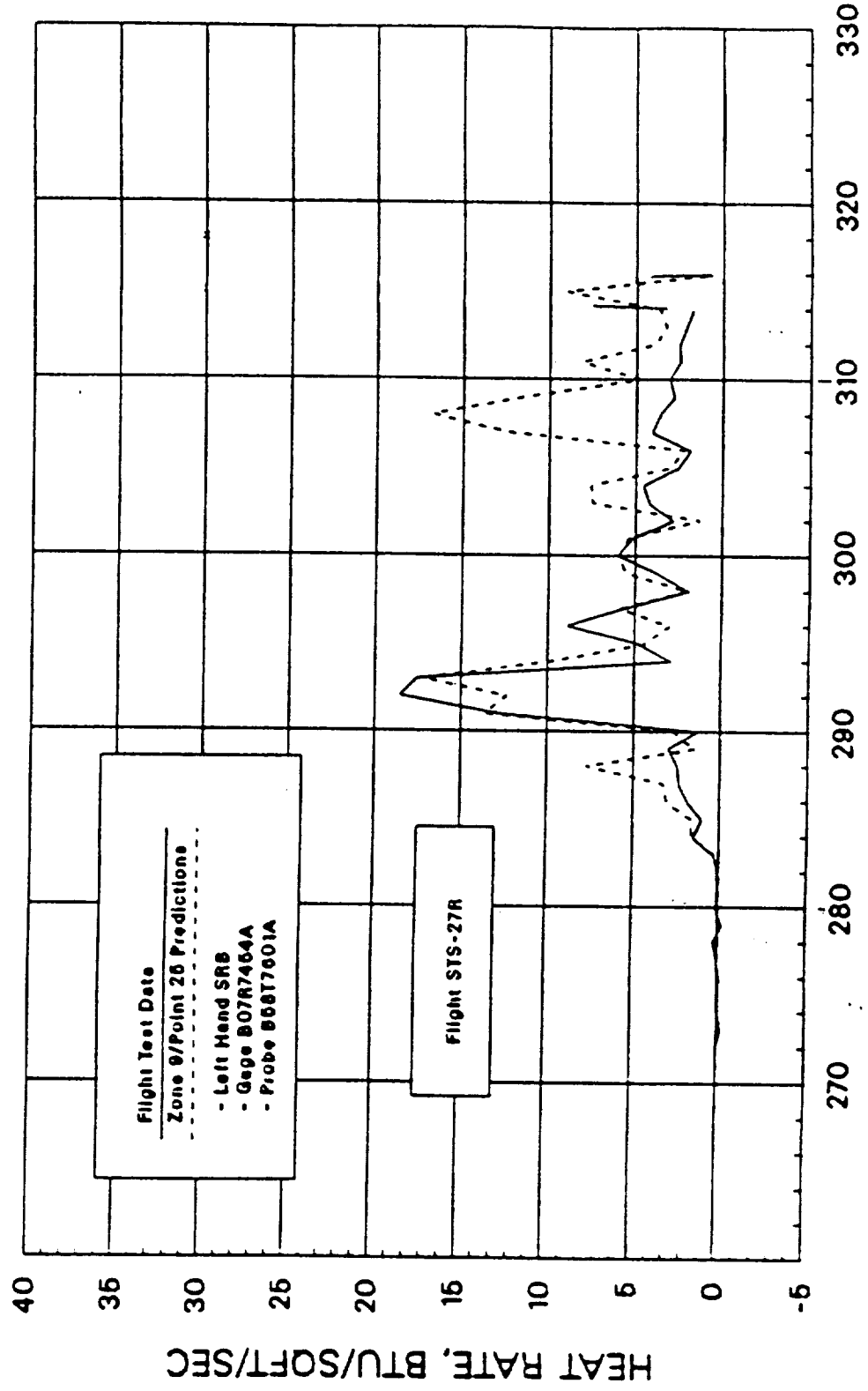

b) Using Flight Gas Temperature Measurement (B07T7601)

Figure 19: Internal Aft Skirt Heating Rate Validation B07R7454 STS-27R (Concluded)

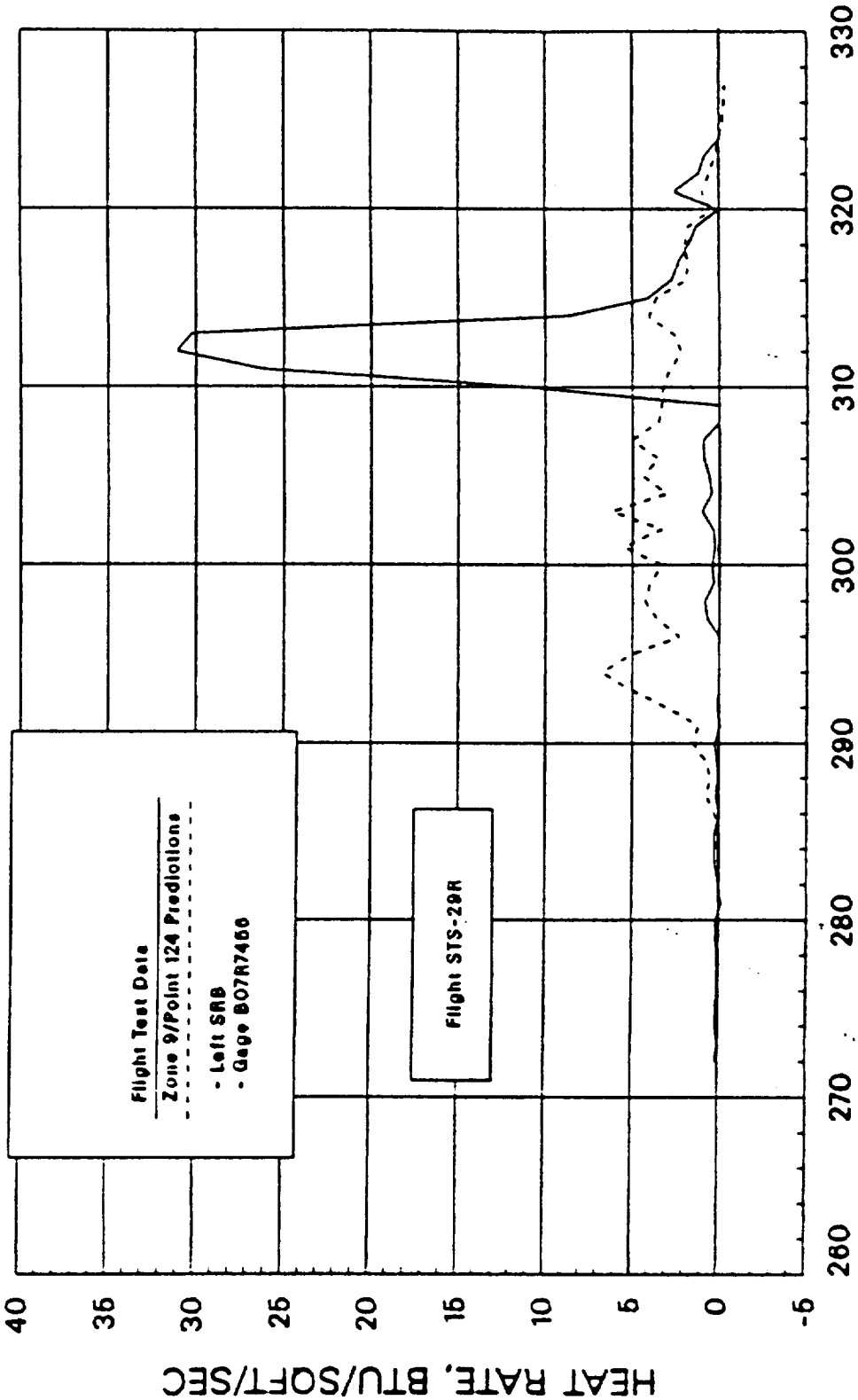

a) Using STATE Gas Temperature Algorithm

Figure 20: Internal Aft Skirt Heating Rate Validation B07R7456 STS-29R

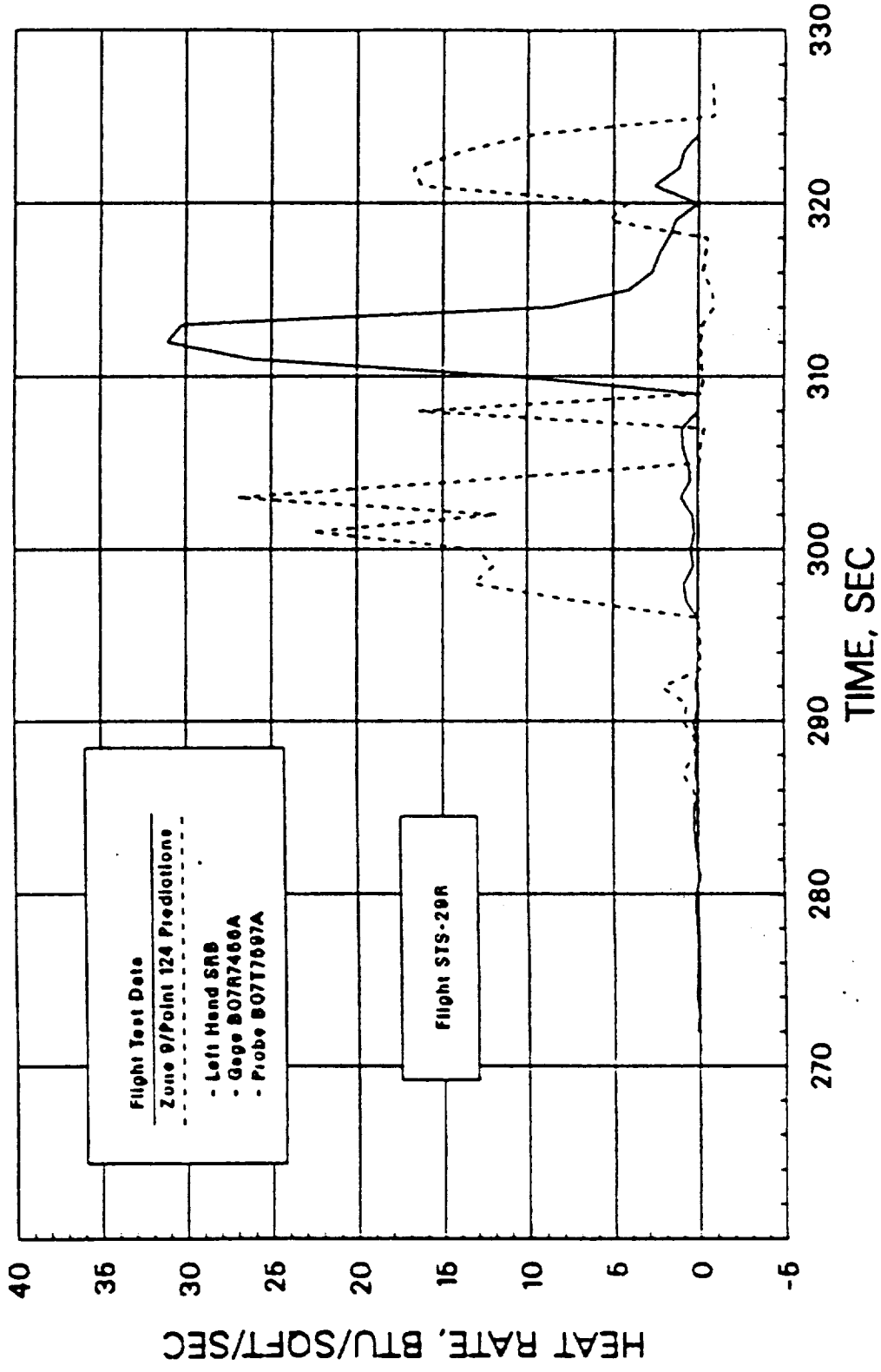

b) Using Flight Gas Temperature Measurement (B07T7597)

Figure 20: Internal Aft Skirt Heating Rate Validation B07R7456 STS-29R (Concluded)

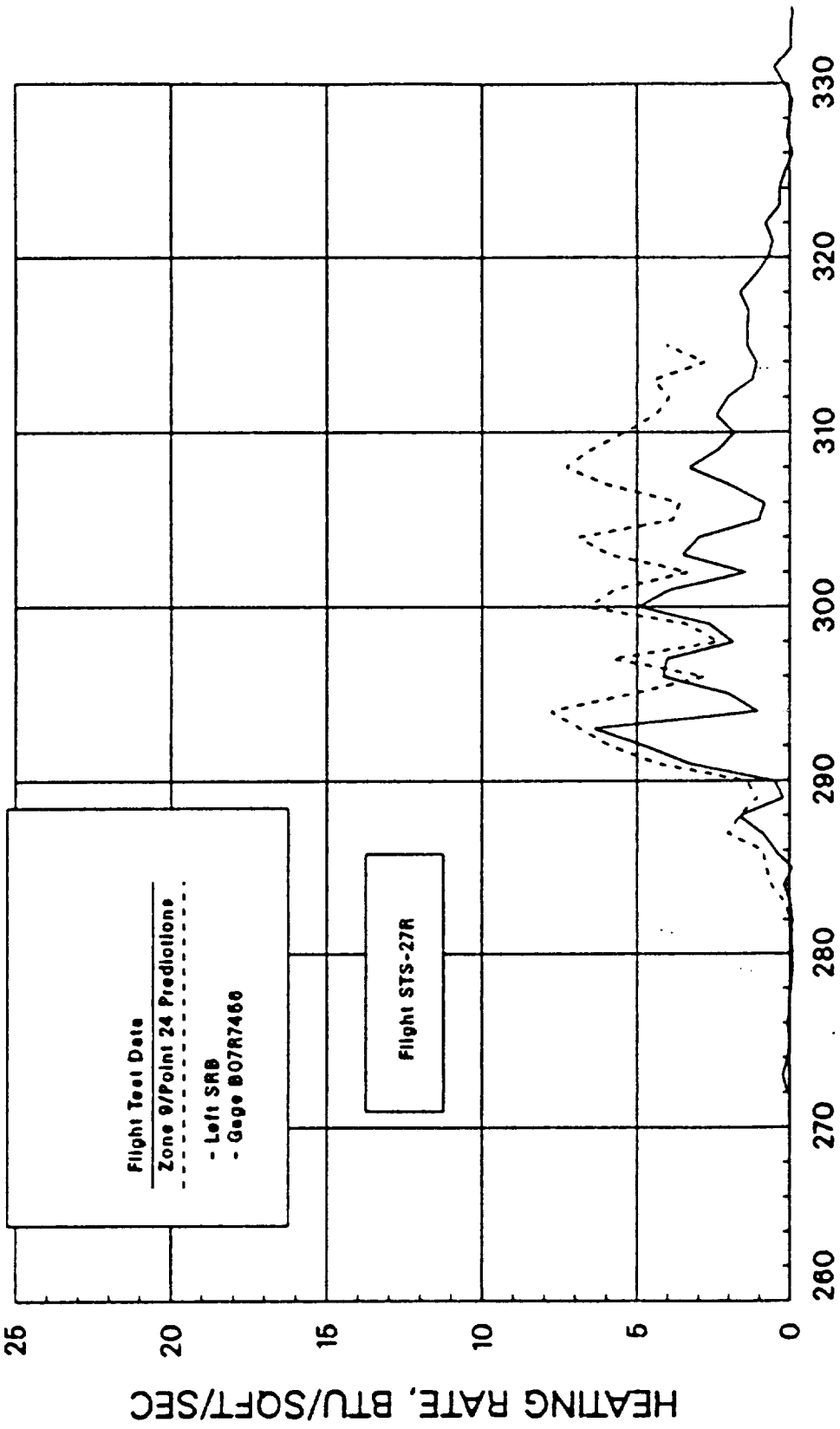

a) Using STATE Gas Temperature Algorithm

Figure 21: Internal Aft Skirt Heating Rate Validation B07R7456 STS-27R

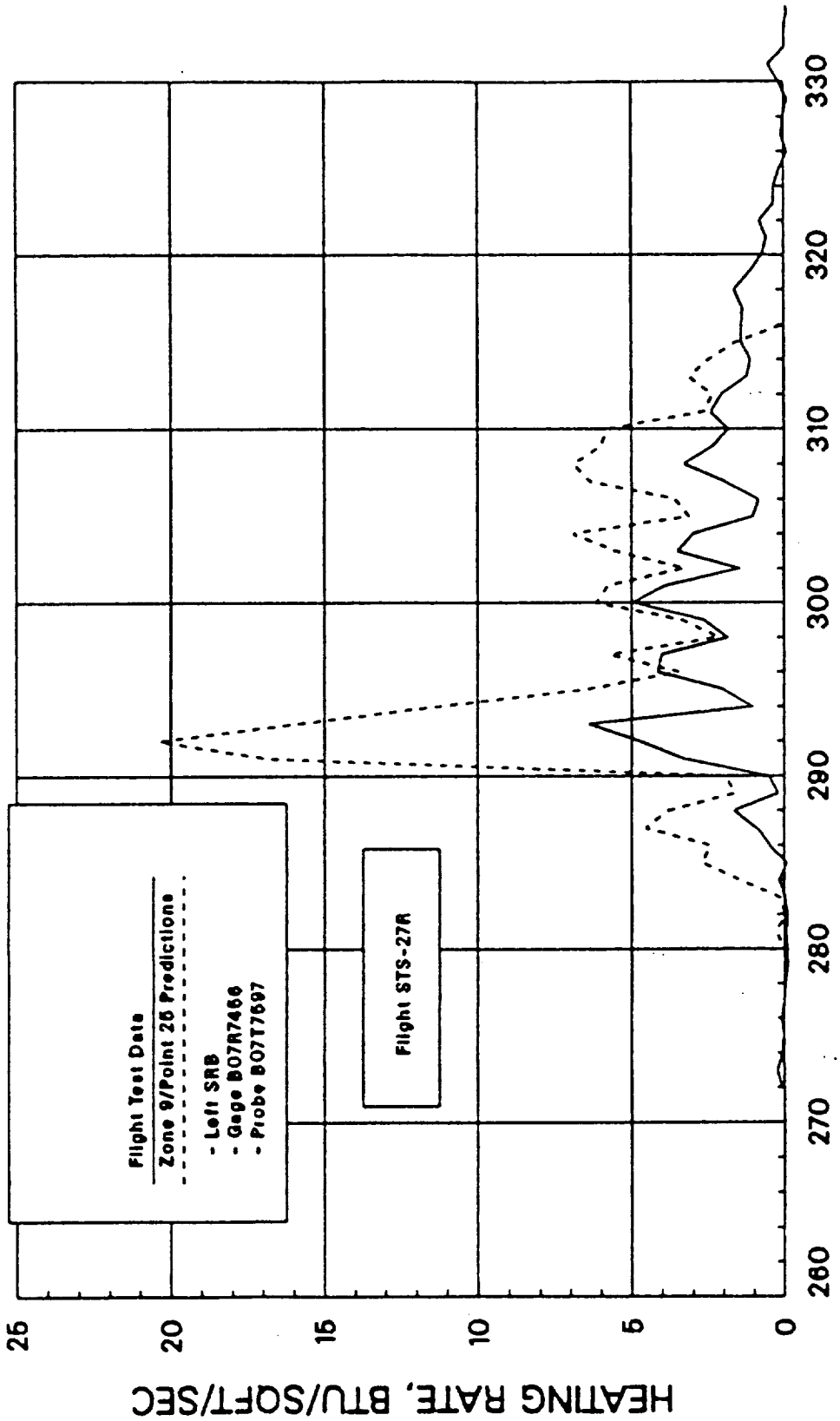

b) Using Flight Gas Temperature Measurement (B07T7597)

Figure 21: Internal Aft Skirt Heating Rate Validation B07R7456 STS-27R (Concluded)

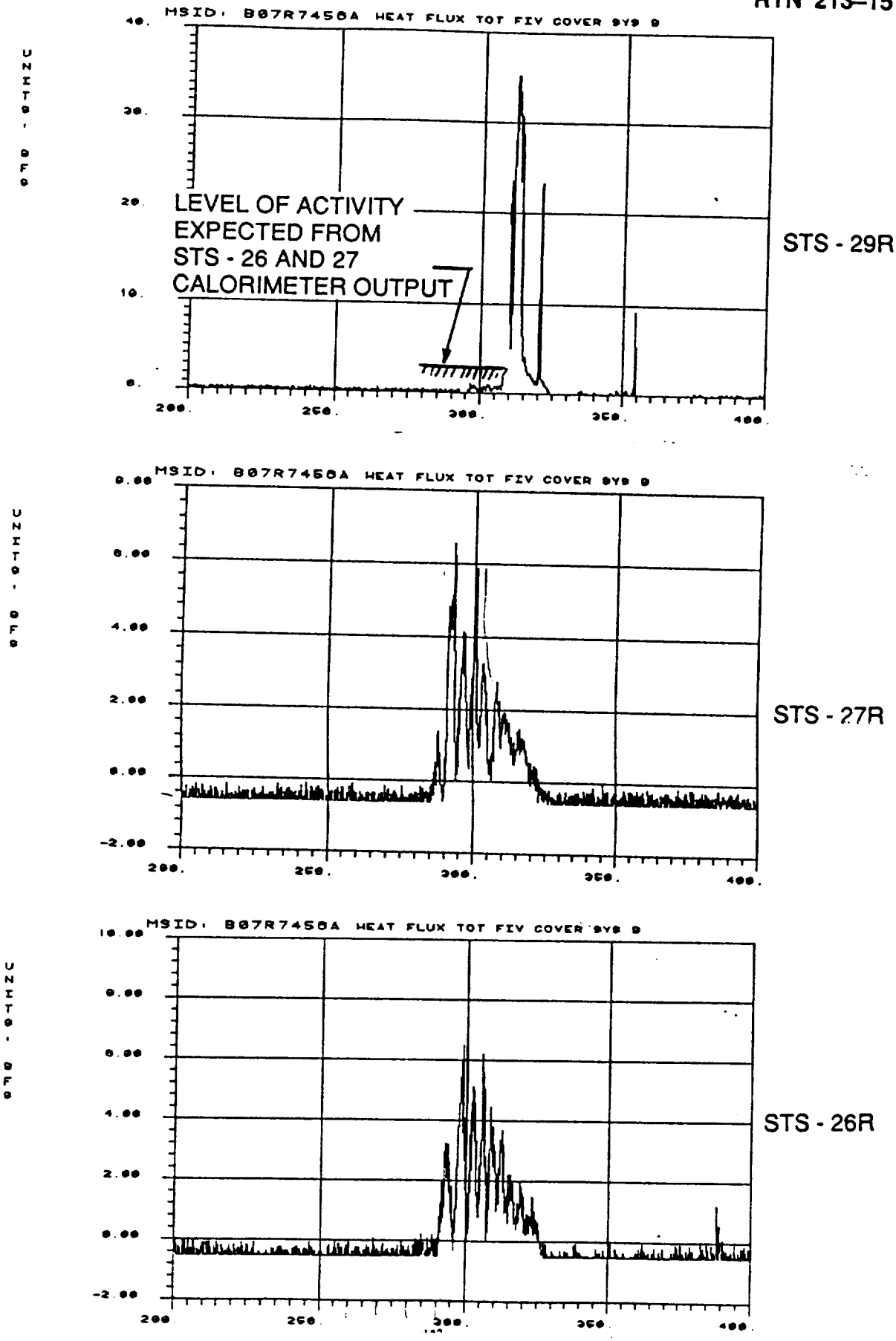

Figure 22: Comparison of Calorimeter Output (B07R7456) on STS-29R with Other Current DFI Flights

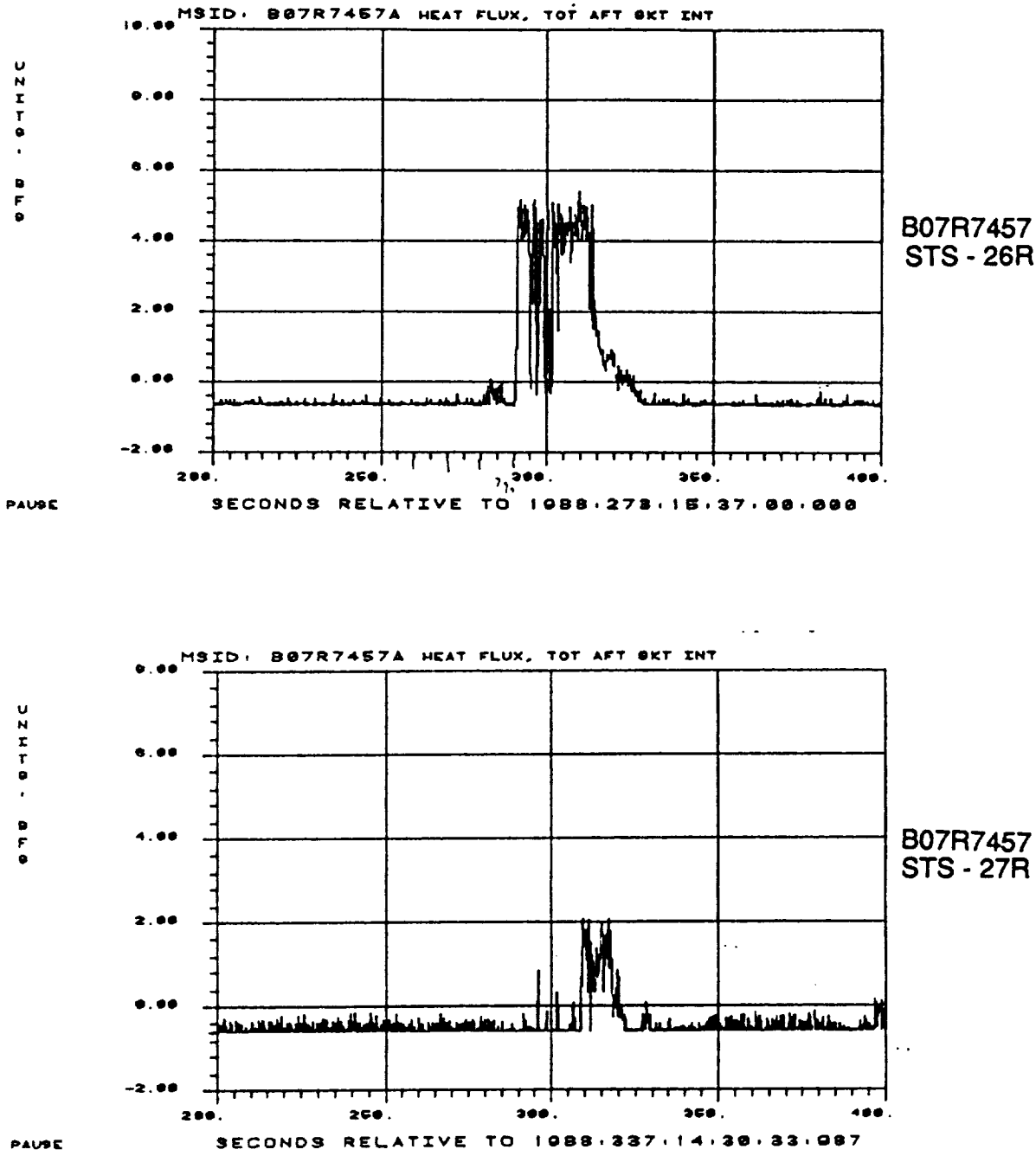

a) Current DFI Measurements

Figure 23: Comparison of Calorimeter B07R7457 Measurement for STS-26R and STS-27R with STS-5 Data

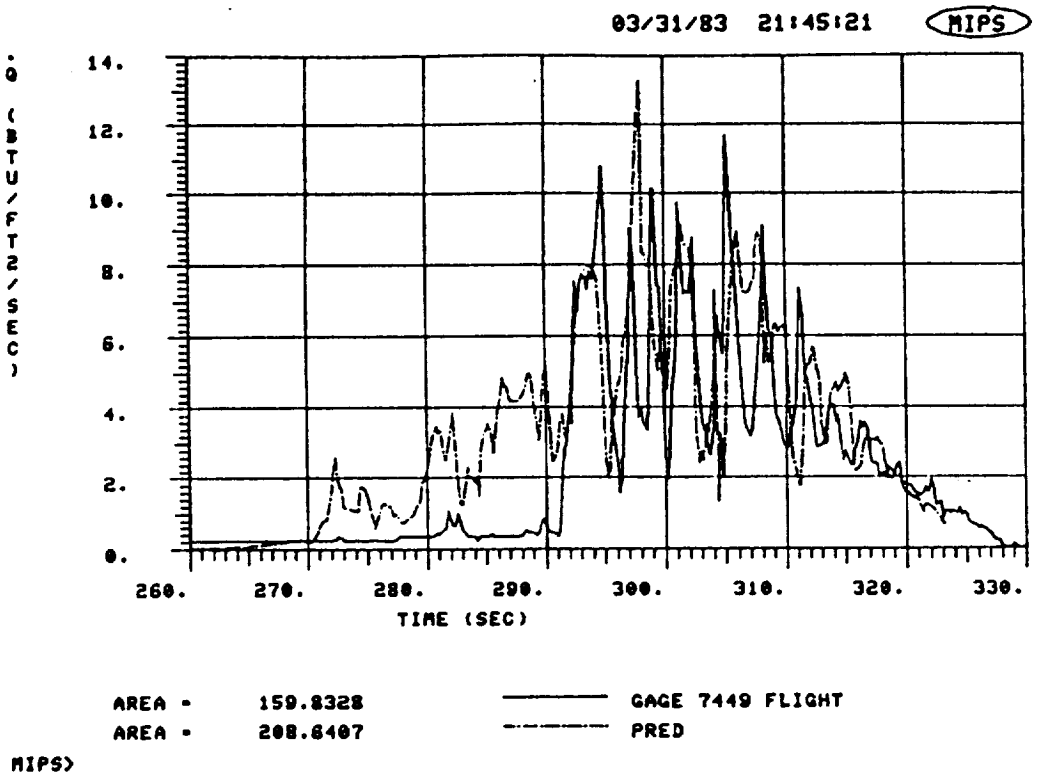

7449

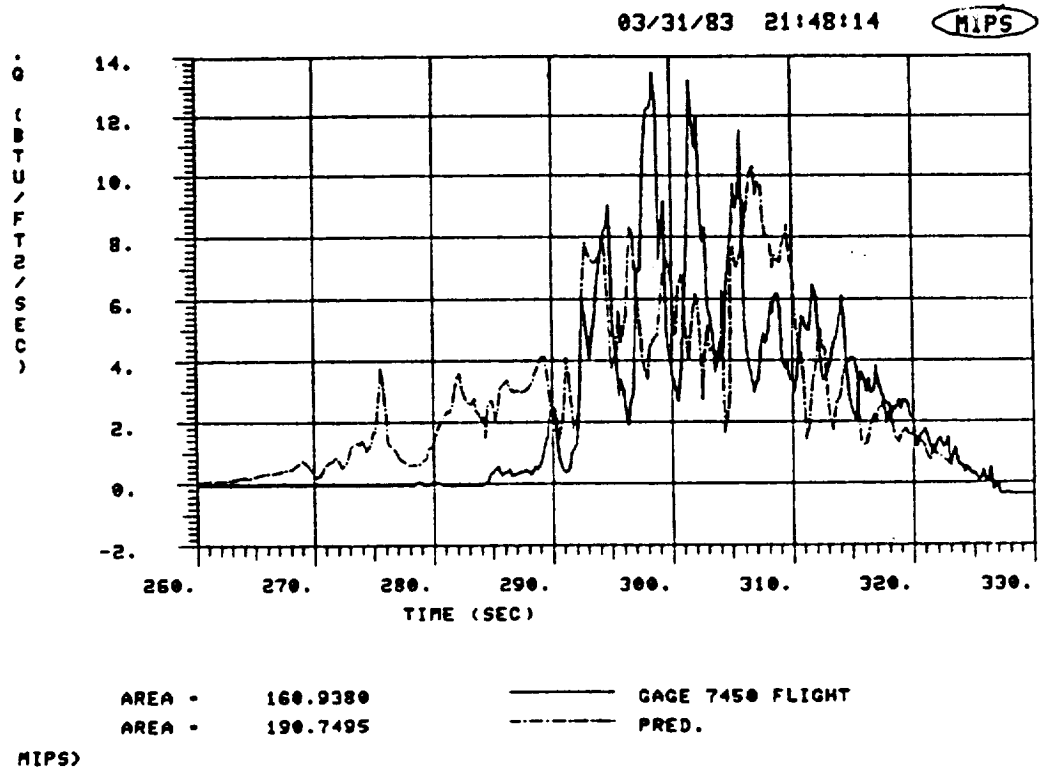

7450

b) STS-5

Figure 23: Comparison of Calorimeter B07R7457 Measurement for STS-26R and STS-27R with STS-5 Data (Concluded)

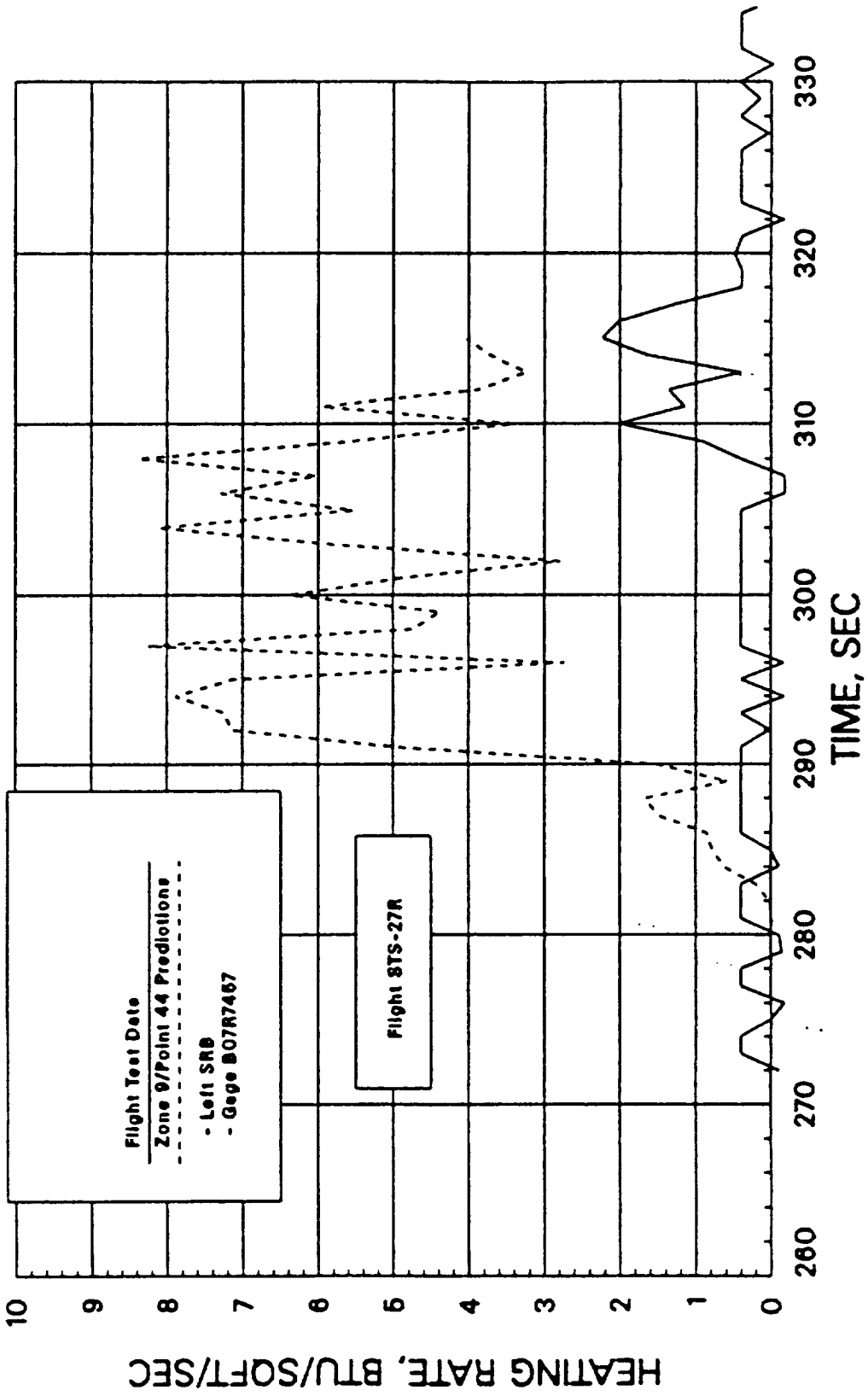

Figure 24: Comparison of Flight Measured Heating Rates from B07R7457 with STATE Prediction — STS-27R

Table 1: DFI Instrumentation Location and Purpose

LOCATION	INTENT
Nosecap/Frustum:	Clarify math model discrepancies and validate design.
Frustum Calorimeter Temperatures:	Verify previous DFI thermal models, improve flight heat transfer coefficient accuracy and improve thermal mismatch corrections.
Frustum Gas Temperature and Pressure:	Determine venting temperatures during reentry for internal environment definition.
Circumferential Pressures:	Determine reentry trajectory roll and angle of attack.
Attach Ring Calorimeters:	Verify math model in peak ascent heating locations.
Aft Skirt Calorimeters:	Obtain clean skin aft skirt data during reentry and improve plume impingement distribution model.
Internal Aft Skirt Calorimeters, Gas Temperature Probes and Radiometer:	Quantify locational effects within aft skirt and expand data base.

Table 2: Left Hand SRB Instrumentation

1. Calorimeters

Gage	X_B (In)	θ_B (Deg)	Location
B07R7700A	243	90	Nose Cone — External
B07R7701A	287	90	Nose Cone — External
B07R7702A	385	90	Nose Cone — External
B07R7703A	1500	27.5	Attach Ring — Forward Face
B07R7704A	1500	55	Attach Ring — Forward Face
B07R7705A	1880	180	Aft Skirt — External
B07R7706A	1880	270	Aft Skirt — External
B07R7707A	1870	270	Aft Skirt — External
B07R7457A	1894	354	Internal Aft Skirt
B07R7456A	1894	265	Internal Aft Skirt
B07R7454A	1920	265	Internal Aft Skirt

2. Radiometers

B07R7459A	1894	230	Internal Aft Skirt

3. Thermocouples/Gas Temperature Probe

Gage	X_B (In)	θ_B (Deg)	Type	Location
B07T7603A	287	90	T/C	Calorimeter Temp. (B07R7701A)
B07T7604A	385	90	T/C	Calorimeter Temp. (B07R7702A)
B07T7602A	215	0	Gas Temp.	Nose Cone — Internal
B07T7595A	300	320	Gas Temp.	Nose Cone — Internal

Table 2: (Continued) Left Hand SRB Instrumentation

Gage	X_B (In)	θ_B (Deg)	Type	Location
B07T7605A	1931	45	Gas Temp.	Aft Ring — External
B07T7626A	1894	83	Gas Temp.	Internal Aft Skirt
B07T7598A	1879	290	Gas Temp.	— TVC Up Frame Sys A
B07T7596A	1893	294	Gas Temp.	— FIV Cover Sys A
B07T7600A	1920	289	Gas Temp.	— FSM Cover Sys A
B07T7599A	1879	259	Gas Temp.	— TVC Up Frame Sys B
B07T7597A	1893	263	Gas Temp.	— FIV Cover Sys B
B07T7601A	1920	258	Gas Temp.	— FSM Cover Sys B

4. Pressure Gages

Gage	X_B (In)	θ_B (Deg)	Location
B07P7357A	295	320	Forward Frustum – Internal (Parachute)
B07P7390A	763	11	Forward SRM Section
B07P7391A	763	41	Forward SRM Section
B07P7392A	763	71	Forward SRM Section
B07P7393A	763	101	Forward SRM Section
B07P7394A	763	131	Forward SRM Section
B07P7395A	763	161	Forward SRM Section
B07P7396A	763	191	Forward SRM Section
B07P7397A	763	221	Forward SRM Section
B07P7398A	763	251	Forward SRM Section
B07P7399A	763	281	Forward SRM Section
B07P7400A	763	311	Forward SRM Section
B07P7401A	763	341	Forward SRM Section

Table 3: Right Hand SRB Instrumentation

1. Calorimeters — Internal Aft Skirt

Gage	X_B (In)	θ_B (Deg)	Location
B07R8456A	1894	83	FIV Cover
B07R8454A	1920	85	FSM Cover

2. Thermocouples/Gas Temperature Probe — Internal Aft Skirt

Gage	X_B (In)	θ_B (Deg)	Type	Location
B07T8596A	1893	114	Gas Temp.	FIV Cover Sys A
B07T8597A	1893	83	Gas Temp.	FIV Cover Sys B
B58T8598A	1879	110	Gas Temp.	TVC Up Frame Sys A
B58T8599A	1879	79	Gas Temp.	TVC Up Frame Sys B
B58T8600A	1920	109	Gas Temp.	FSM Cover Sys A
B58T8601A	1920	78	Gas Temp.	FSM Cover Sys B

Table 4: Redesign DFI Flight Significant Events Summary

Event	STS-26 L	STS-26 R	STS-27 L	STS-27 R	STS-29 L	STS-29 R
1. SRB Separation	131,800 ft 124.9 sec		154,188 125.8 sec		150,900 126 sec	
2. Apogee	232,244 (195 sec)	232,844 (197 sec)	223,603 (193 sec)	226,565 (194 sec)	226,089 (196 sec)	225,924 (197 sec)
3. Aeroheating Begins	185,579 (252 sec)	*	187,570 (245 sec)	*	172,972 (255 sec)	*
4. Thermal Curtain Opens	122,314 (282 sec)	123,578 (282 sec)	111,595 (282 sec)	119,514 (274 sec)	133,774 (274 sec)	137,673 (272 sec)
5. Peak Reentry Heating	88,159 - 51,831 ft (290-310 sec)	103,441 - 54,549 ft (290-310 sec)	91,539 - 67,596 ft (290-310 sec)	89,770 - 42,891 ft (290-310 sec)	119,539 - 49,499 ft (280-310 sec)	70,441 - 32,043 ft. (300-320 sec)
6. Peak Dynamic Pressure	4,414 psf @ t = 317 sec 37,567 ft.	2,207 psf @ t = 315 sec 43,002 ft	2,354 psf @ t = 318 sec 31,143 ft.	2,604 psf @ t = 312 sec 38,363 ft	1,887 psf @ t = 314 sec 42,195 ft.	1,635 psf @ t = 311 sec 45,909 ft.
7. Aerocooling Begins						
8. M = 1.00	29,694 ft @ t = 323 sec	25,669 ft @ t = 327 sec	21,216 ft (327.7 sec)	< 28,384 ft (> 319 sec)	26,107 ft (327 sec)	22,503 ft (332 sec)
9. Drogue Deployment						

* - Cannot tell for R/H SRB since no external instrumentation

Table 5: External DFI Location and Corresponding Prediction Body Points

FLIGHT			CORRESPONDING PREDICTION BODY POINTS			
Gage	X_B	θ_B	Zone	Body Point	X_B	θ_B
7700	243	90.0	2	11	209.2	310.0
7701	287	90.0	2	38	303.5	90.0
*7702	385	90.0	2	38	303.5	90.0
7703	1500	27.5	5	202	1500	0.0
7704	1500	55.0	5	207	1500	90.0
7705	1880	180.0	7	14	1874	180.0
7706	1880	270.0	7	29	1874	270.0
7707	1870	270.0	7	29	1874	270.0

* — Predictions for this location also include:

BP	X_B	θ_B
1	391	120
22	391	0

Table 6: Gas Temperature Probe Data Status Summary

	Good		Bad	
STS-29R				
L/H	B07T7596		B07T7597	t > 300 sec
	B07T7597	to t = 300 sec	B58T7598	
	B07T7605		B58T7599	
	B07T7626			
	B58T7600			
	B58T7601			
R/H	B07T8596			
	B07T8597			
	B58T8598	t < 295 sec	B58T8598	t > 295 sec
	B58T8599	t < 295 sec	B58T8599	t > 295 sec
	B58T8600	t < 305 sec	B58T8600	t > 305 sec
	B58T8601	t < 305 sec	B58T8601	t > 305 sec
STS-27R				
L/H	B07T7596		B07T7626	t > 290 sec
	B07T7597		B58T7598	t > 390 sec
	B07T7605		B58T7599	
	B07T7626	t < 290 sec		
	B58T7598	t < 390 sec		
	B58T7600			
	B58T7601			
STS-26R				
L/H	B07T7596			
	B07T7597			
	B07T7626		B07T7626	t = 290-296 sec
	B58T7598		B58T7601	
	B58T7599			
	B58T7600			
R/H	B07T8596	t < 300 sec	B07T8596	t > 300 sec
	B07T8597			
	B58T8598			
	B58T8599			
	B58T8600			
	B58T8601			

Table 7: Internal Aft Skirt DFI Location and Corresponding Prediction Body Point

←FLIGHT→				←CORRESPONDING PREDICTION BODY POINTS→			
Gage	X_B	θ_B	Direction	Zone	Body Point	X_B	θ_B
A) STS-27R: Steel Case Nozzle On							
7454	1920	265	Inboard	9	25	1894	210
7456	1894	265	Aft	9	24	1894	210
7457	1894	354	Aft	9	44	1894	330
B) STS-29R: Steel Case Nozzle Off							
7454	1920	265	Inboard	9	125	1894	210
7456	1894	265	Aft	9	124	1894	210
7457	1894	354	Aft	9	144	1894	330

Table 8: Internal Aft Skirt Calorimeter Data Status Summary

Good	Bad
STS-26R	
L/H Booster	
B07R7454	
B07R7456	
B07R7459	B07R7457 (Data Questionable)
R/H Booster	
B07R8454 $t < 305$ sec	B07R8454 $t > 305$ sec
B07R8456	
STS-27R	
L/H Booster	
B07R7454 $t < 315$ sec	B07R7454 $t > 315$ sec
B07R7456	
B07R7459	B07R7457 (Data Questionable)
R/H Booster	
B07R8454 $t < 305$ sec	B07R8454 $t > 305$ sec
B07R8456	
STS-29R	
L/H Booster	
B07R7454	B07R7457
B07R7459	B07R7456 (Data Questionable)
	Data recording problems on L/H SRB between t = 292-296 and 325-334 sec caused the calorimeter data to be lost. Tabulated data indicate zeros; however, gages are operational during this time frame.
R/H Booster	
B07R8454	
B07R8456	

Appendix V

SRB Ascent and Reentry Frustum Venting Analysis and Design Update (STS-26R, 27R and 29R) (RTN 213–16)

REMTECH TECHNICAL NOTE

SUBJECT: SRB Ascent and Reentry Frustum Venting Analysis and Update (STS26R, 27R AND 29R)

DATE: June 1991

AUTHOR: William K. Crain

CONTRACT NO.: NAS8-37891

PREPARED FOR: Induced Environments Branch (ED33), George C. Marshall Space Flight Center

INTRODUCTION

Design heating environments to the SRB internal nose cap and frustum compartment, housing the parachutes, were previously calculated using a nonadiabatic venting code. Up to this point there were no supporting flight data against which the math model could be tested. Consequently, the issues of concern, i.e., is the frustum freely vented, and how good is the design math model, could not be determined. However, on STS-26R, 27R, and 29R, internal measurements of gas temperature and pressure were acquired for the first time in Shuttle history. These measurements, when compared with the design calculations (Fig. 1), made it clear that revisions needed to be made in the math model. In this comparison, some of the flight measurements are above the design on ascent (Fig. 1a), and considerably below design on reentry (Fig 1b). Consequently, analysis of the current DFI data was begun. The frustum and nose cap internal flight measurements were used to upgrade the environment math model. These results were then used to predict new ascent and reentry design environments. The purpose of this report is to summarize this work.

NOSE CONE GEOMETRY AND FLIGHT INSTRUMENTATION

The SRB nose cone consists of a nose cap and frustum. The pilot and drogue chutes are housed in the nose cap, with the three main chutes located in the frustum. Internal geometry of the nose cap and frustum are shown in Fig. 2. The volume ratio of the nose cap to frustum without the chutes is 0.10; with the chutes, it is 0.07. The two compartments are separate, but freely vented to each other. Consequently, the venting model was generated for the frustum with the intent that the internal environment for the frustum would be applied to the nose cap components.

Instrumentation location in the cap and frustum is shown in Fig. 3. This consisted of a gas temperature probe located in the nose cap at X_B = 215, θ_B = 0 deg, and at X_B = 300, θ_B = 300 deg in the frustum. In addition, a pressure transducer was located in the frustum at X_B = 295 and θ_B = 320 deg.

FLIGHT MEASUREMENTS AND PREDICTIONS

Ascent Calculations

Frustum and nose cap gas temperature history for the three DFI flights is presented in Fig. 4. The nose cap temperature remains fairly constant, while the frustum gas temperature decreases about 10°F during the first 50 seconds of flight, and then climbs to a value roughly equal to that at lift-off. In upgrading the math model to predict a more accurate design environment set, the current DFI flight measurements were used to adjust the math model constants so that it would calculate the frustum internal gas temperature on STS-26R, 27R and 29R. In this respect, the effective parachute heat transfer area was parametrically varied until the calculated frustum gas temperature matched the flight value. The nose cap was assumed to be freely vented to the frustum, since the volume ratio without chutes is 0.10 and with chutes is 0.07. The heat transfer areas of these two volumes were combined for the calculations. Other constants such as parachute, frustum and nose cap volumes and surface areas, as well as forced and natural convection considerations, are summarized in Table 1. From the flight data and volume considerations, the nose cap temperature was considered to be isothermal, and equal to the nose cap structure temperature at lift-off, (Fig. 5). The INVENT nonadiabatic venting code [1] was used to make the frustum calculations. This code solves the continuity and energy equations between the frustum interior and exterior. Results of these calculations are presented in Figs. 6 and 7 in the form of frustum gas temperature and pressure history for the three DFI flights. Figure 6 is a presentation of predicted and flight measured compartment pressure. Figure 7 presents frustum calculated and flight measured gas temperature. The agreement is fairly good. The high frequency oscillation in the measured gas temperature (Fig. 7) is data system channel noise. As previously stated, given the internal pressure, the effective parachute heat transfer area was varied until the calculated and measured internal gas temperatures matched. This resulted in an effective area of about 80 percent of the parachute nylon surface area.

Reentry Calculations

SRB reentry is characterized by large variations in pitch and roll as shown by the orientation calculations for STS-27R, presented in Fig. 8. Hot boundary layer air adjacent to the MSA-2 nose cone insulation enters the frustum through the three open vent holes in a manner depicted in Fig. 9. The temperature of the air entering the frustum is somewhere between the MSA-2 temperature and an average temperature across the boundary layer. For this particular case, it was assumed to be equal to the MSA-2 surface temperature. This was calculated for each flight using the EXITS conduction code [2] with measured nose cone heating rates from flight calorimeter B07R7701A. Calorimeter measured heating rates were corrected for thermal mismatch by a constant factor (1.5) prior to input to the EXITS code. The initial temperature of the outside layer of TPS, prior to reentry, was assumed to be 470°F based on flight data from STS-3. MSA-2 backside aluminum structure (see Fig. 9) temperature was assumed to be the

same as the frustum compartment gas temperature at lift-off. These were 75, 55, and 55° for STS-26R, 27R, and 29R, respectively. The resulting MSA-2 surface temperature calculations are presented for the three flights in Fig. 10.

Nose cone external static pressures were obtained from wind tunnel data [3] on the SRB. The vehicle was assumed to be trimmed at an angle of attack of 170 deg. Pressure coefficient versus Mach number was converted to static pressure on the vehicle for each flight, using the BET ascent ambient conditions along with the velocity data from the radar reentry measurements. A comparison of nose cone external static pressure and frustum internal measured pressure is presented in Fig. 11. The data are in the form of local-to-free-stream-static-pressure ratio versus Mach number. Examination of these data at several Mach numbers shows that the frustum internal-to-external-pressure ratios are in the range of 0.64-0.78, indicating that the vent hole is unchoked.

Reentry venting methodology is shown in Fig. 12. As with the ascent venting calculations, the INVENT code was used. Inputs to the code were external gas pressure and MSA-2 temperature, vent hole area, internal volume, heat transfer area, and heat transfer mechanism (i.e., natural or forced convection). These values are summarized in Table 2. The code then calculated the internal pressure and gas temperature rise along with the convective heat transfer coefficient. The heat transfer area was composed of exposed metal area and effective parachute area. As stated before, the latter was unknown and was parametrically varied until the calculated frustum gas temperature response agreed with flight. Frustum predicted compartment temperatures using INVENT are presented in Fig. 13 along with the compartment measured temperatures for each flight. Flight data analyses indicated that the theoretical models could not be made to agree with flight data if total temperature was used as input. The use of the MSA surface temperature as the input made reasonable comparisons possible. Agreement with STS-27R flight data leaves something to be desired; however, based on the STS-26R and 29R results, it was felt that the venting model was adequate to extend the calculations to design.

DESIGN ENVIRONMENT CALCULATION

Ascent

Frustum ascent design venting calculations were based on the Light Weight Tank (LWT) design and STS-1 trajectories. These are defined in Figs. 14 and 15. Frustum local external pressure and boundary layer edge temperature (Figs. 16 and 17) were calculated using the LANMIN code [4]. These results were used along with the physical constants derived from the STS-26R-29R predictions (Table 1) as input to the INVENT code. Ascent design venting environments of frustum internal gas temperature and heat transfer coefficient were then calculated. The design gas temperature history for the two trajectories is presented in Fig. 18. The initial design temperature at lift-off was defined as 110°F. Since the LWT trajectory is the most conservative, it was taken as the design case. From the flight data analysis conclusions, it was determined that the nose cap temperature is constant over the ascent phase of flight, and that the temperature is

essentially the same as the inside structure temperature. Consequently, the nose cap design temperature was defined as 110°F over the ascent phase.

Reentry

Frustum and nose cap reentry design gas temperature calculations were made using the methodology outlined in Fig. 12. Reentry trajectories from the statistical design set [5] were identified. These were consistent with the 0, 50, 95, and 100 percentile integrated heat loads. These trajectories were chosen based on the hottest external reentry body point in the vicinity of the vent holes. This was Body Point 2-19, shown in Fig. 19 along with the corresponding ascent body point B. P. 10665. These trajectories were used to define the free-stream conditions and local external heat transfer coefficients, so that the local static pressure and MSA-2 temperature could be calculated. These results are shown in Figs. 20 and 21, respectively. These were then used as input to the INVENT code, along with the reentry venting model derived from the flight calculation phase (Table 2), to calculate the frustum internal design reentry gas temperature and convective heat transfer coefficient. Results of the gas temperature calculations for each of the statistical trajectories are presented in Fig. 22. Peak gas temperatures of 156, 160, 164 and 174°F are seen with the maximum gas temperature being 174°F for the 100 percentile trajectory case. These magnitudes are well below the existing design calculations for reentry (Fig. 1b).

This set was combined with the ascent design calculations to produce a design gas temperature history from lift-off to drogue deployment. These are shown in Fig. 23. In combining the ascent and reentry results, the frustum gas temperature and heat transfer coefficient were held constant at the magnitude attained at SRB separation until surpassed by the reentry values for the four trajectories. Consequently, the design curves are constant between 126 seconds and 280 seconds. This rationale was incorporated to keep the design conservative and above the DFI gas temperature measurements. Since SRB reentry design is usually based on the 95 percentile trajectory, the combined ascent- reentry gas temperature set consistent with this trajectory was compared with the existing ascent-reentry design set, Fig. 24. The calculations based on the current flight data are seen to be approximately 50°R hotter during ascent and a minimum of 90-150°R cooler during reentry. (The existing reentry design is shown as an envelope of the maximum and minimum values. For the original calculations, the Booster was allowed to pitch and roll, thereby giving an oscillating heating history. For the current calculations, it was assumed to be trimmed at $\alpha = 170$ deg.) Another reason for the decrease in reentry heating level is that the initial temperature assumption at the beginning of reentry was taken as the value measured at the end of ascent, instead of the 660°R minimum limit.

In this effort to define a more accurate design venting model, a considerable amount of thought has gone into determining the maximum gas temperature entering the vent holes during reentry. All design calculations up to this point used the free-stream total temperature (T_o). In this analysis, the MSA-2 temperature was used since it was felt that the use of T_o was too high and only a certain percentage of the boundary layer flow actually enters the vent holes. As a check to see what type of differences existed

between the two philosophies, design venting calculations were made using the current upgraded venting model and the 95 percentile trajectory with T_o as the maximum entering gas temperature. These results, in the form of frustum gas temperature and heat transfer coefficient, are compared with the calculations using the MSA-2 temperature in Figs. 25 and 26. By way of illustration, the MSA-2 surface temperature and T_o history are plotted in Fig. 25 also. Although a large difference exists between the MSA-2 temperature and the free-stream total (T_o), the effect on the frustum reentry gas temperature and heat transfer coefficient is small compared with total or surface temperature. However, the internal gas temperature change produced by using total or MSA surface is significant compared with the value of the internal temperature. The large heat transfer surface area of the compartment and parachutes produce the nonadiabatic effect of reducing the gas temperature to near the internal structural temperature. Other compartments usually do not have this large an internal heat transfer area to volume ratio as does the frustum.

SUMMARY AND CONCLUSIONS

For the first time in Shuttle history, DFI pressure and gas temperature measurements were made on STS-26R, 27R, and 29R inside the Booster frustum and nose cap. These measurements made it possible to determine how good the existing design venting environment for these components is. Comparison of the flight measurements with design made it clear that revisions needed to be made in the math model. The flight measurements were above design on ascent and considerably below design on reentry. Nonadiabatic venting calculations were made for the nose cap and frustum using the DFI flight measurements to adjust the math model such that a good match on internal gas temperature was obtained. This math model was then extended to the design trajectory case. A new proposed venting environment was calculated which is some 50°R above the current ascent and a minimum of 90-150°R below the current reentry design gas temperature.

REFERENCES

[1] Engel, Carl D., Frost, Cynthia L., Hulsey, Donald R., Pond, John E., and Praharaj, Sarat C., "Nonadiabatic Compartment Venting Heating," REMTECH RTR 129-1, June 1985.

[2] Pond, John E. and Schmitz, Craig P., "MINIVER II Upgrade for the AVID System, Volume III: EXITS Users and Input Guide," REMTECH RTR 123-03, Feb. 1988.

[3] Braddock, W. F. and Streby, G. D., "An Investigation to Determine the Static Pressure Distribution of the 0.00548 Space Shuttle Solid Rocket Booster (MSFC Model Number 648) During Reentry in the NASA/MSFC 14 Inch Trisonic Wind Tunnel (SA28F)," Northrup Services Report M-9230-75-416, April 1975.

[4] Engel, C. D. and Schmitz, C. P., "MINIVER Upgrade for the AVID System, Volume II: LANMIN Input Guide," REMTECH Technical Report RTR 123-02, Feb. 1988.

[5] Engel, C. D. and Hulsey, Donald R., "The Steel Case SRB Reentry Thermal Environment Data Book," REMTECH Report RTR 039-14, Oct. 1984.

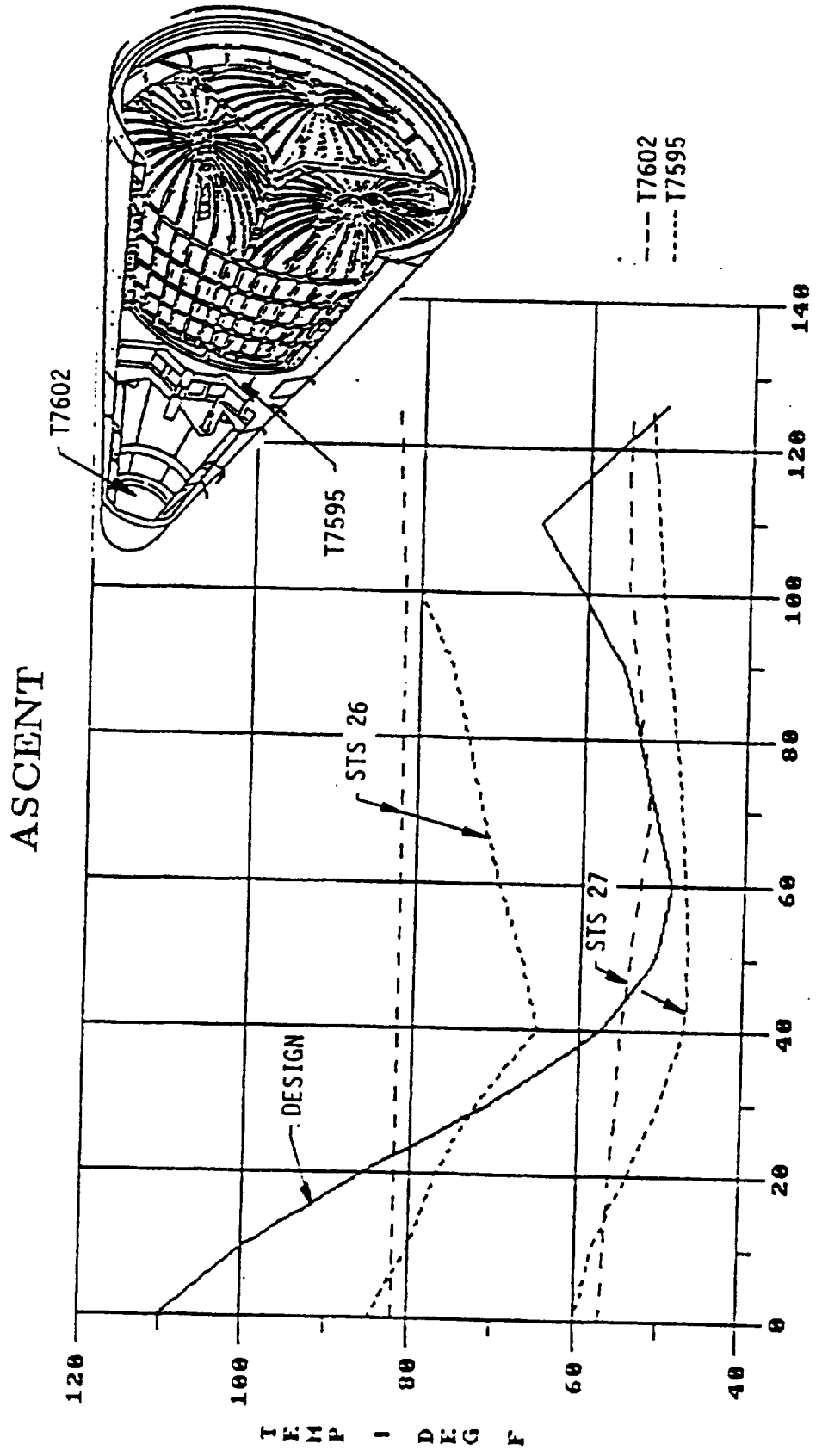

a) Ascent

Figure 1: Frustum Design Gas Temperature Compared with Current DFI Flights

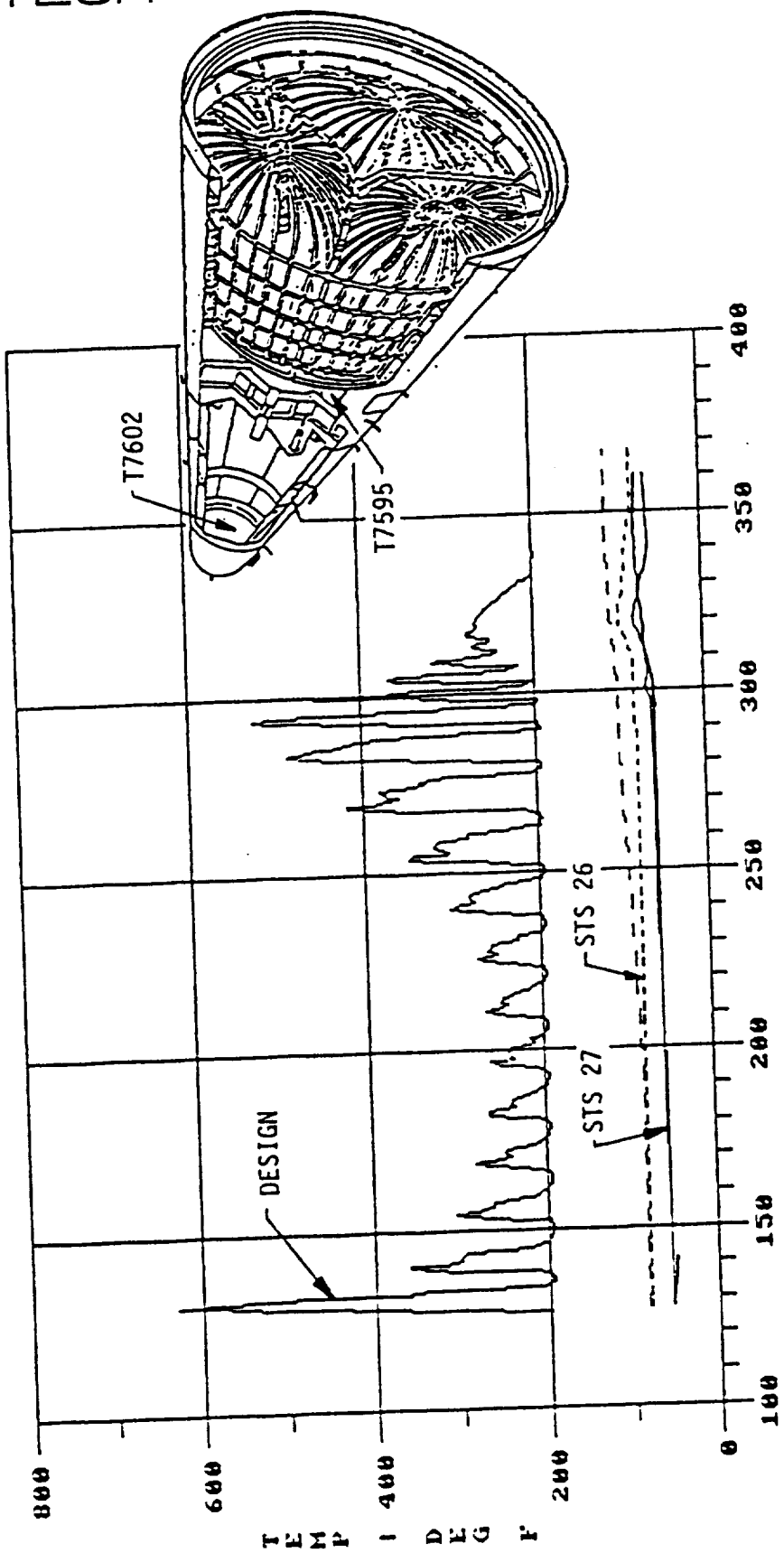

b) Reentry

Figure 1: Frustum Design Gas Temperature Compared with Current DFI Flights (Concluded)

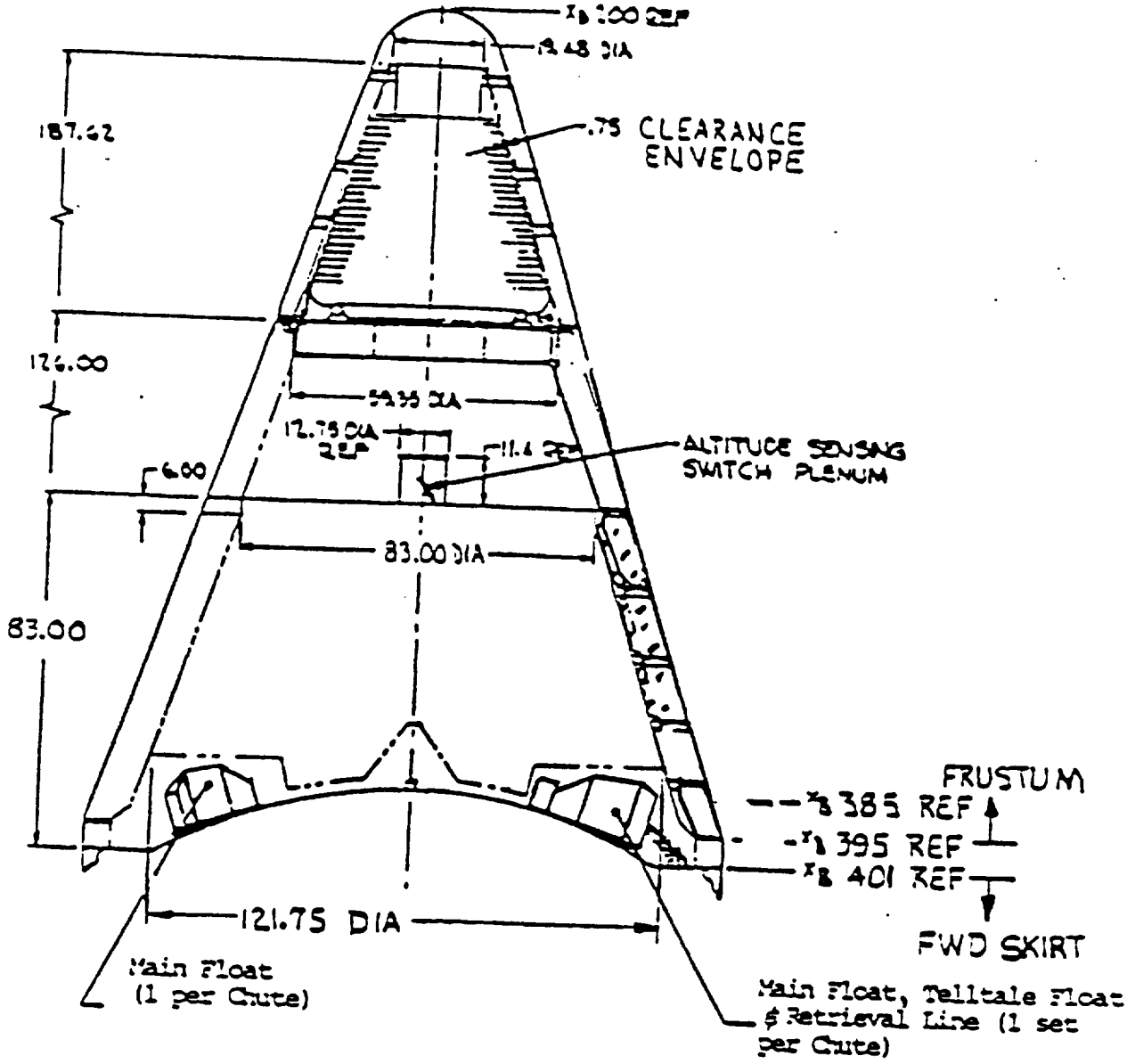

Figure 2: Nose Cone Geometry

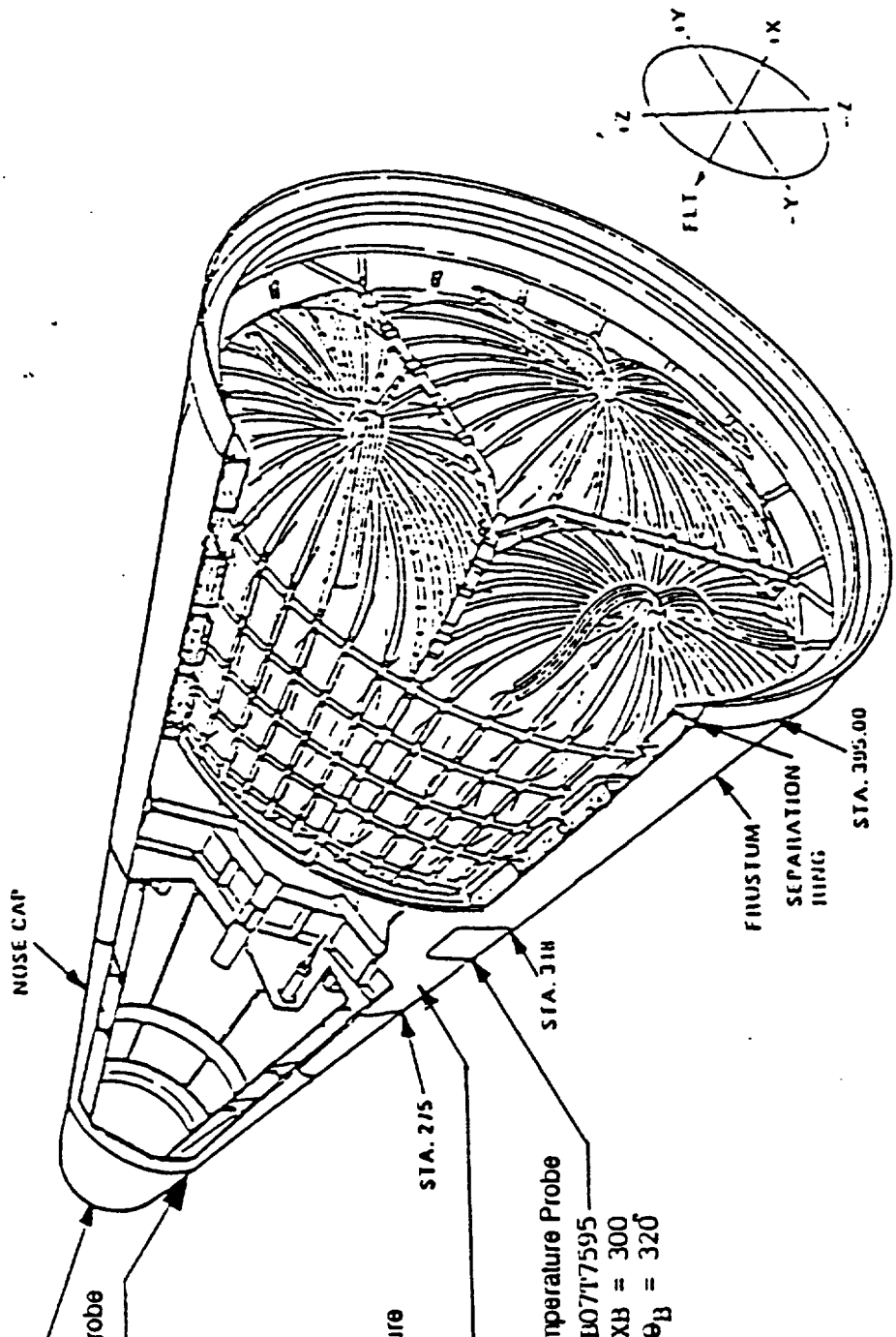

Figure 3: Nose Cone Flight Instrumentation Locations

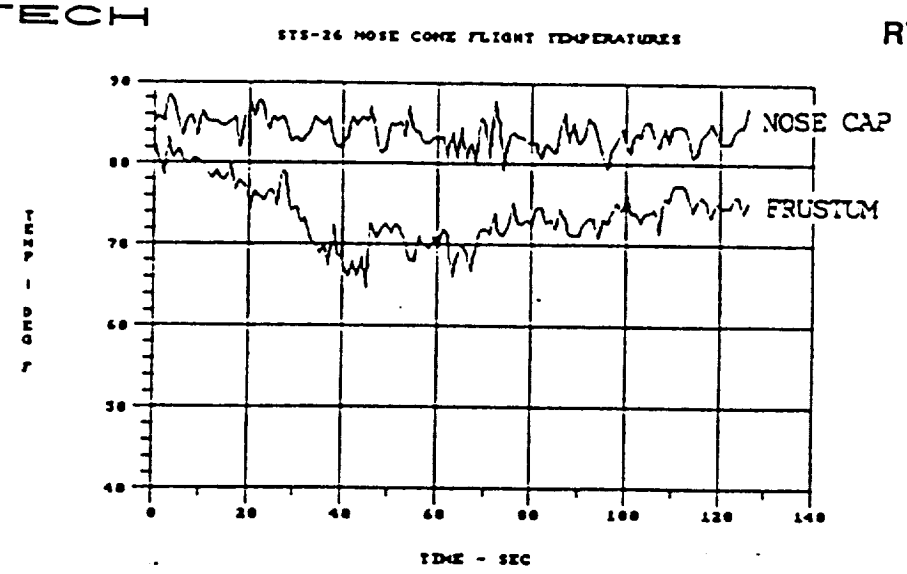

STS26R

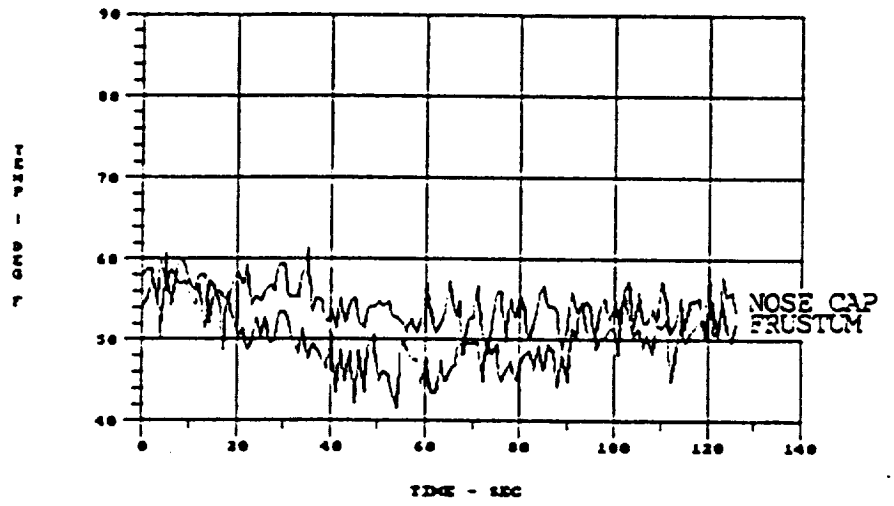

STS27R

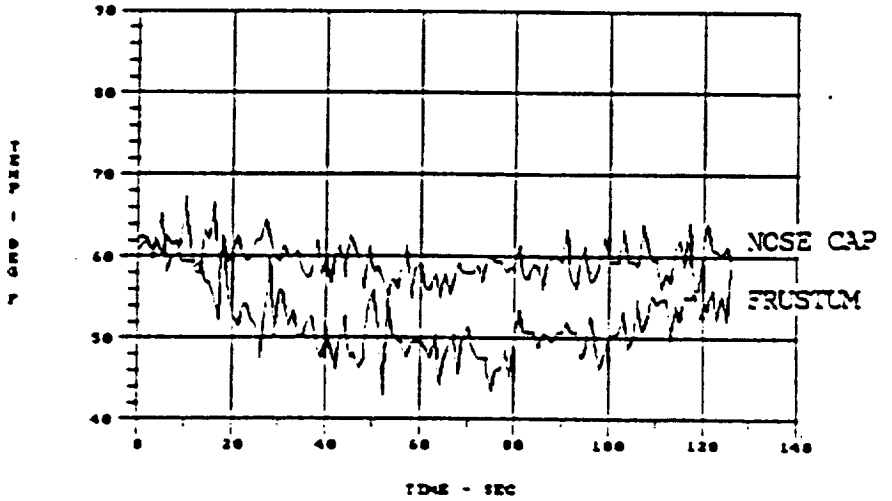

STS29R

(a) Ascent

Figure 4: Gas Temperature Response for STS-26R, 27R and 29R

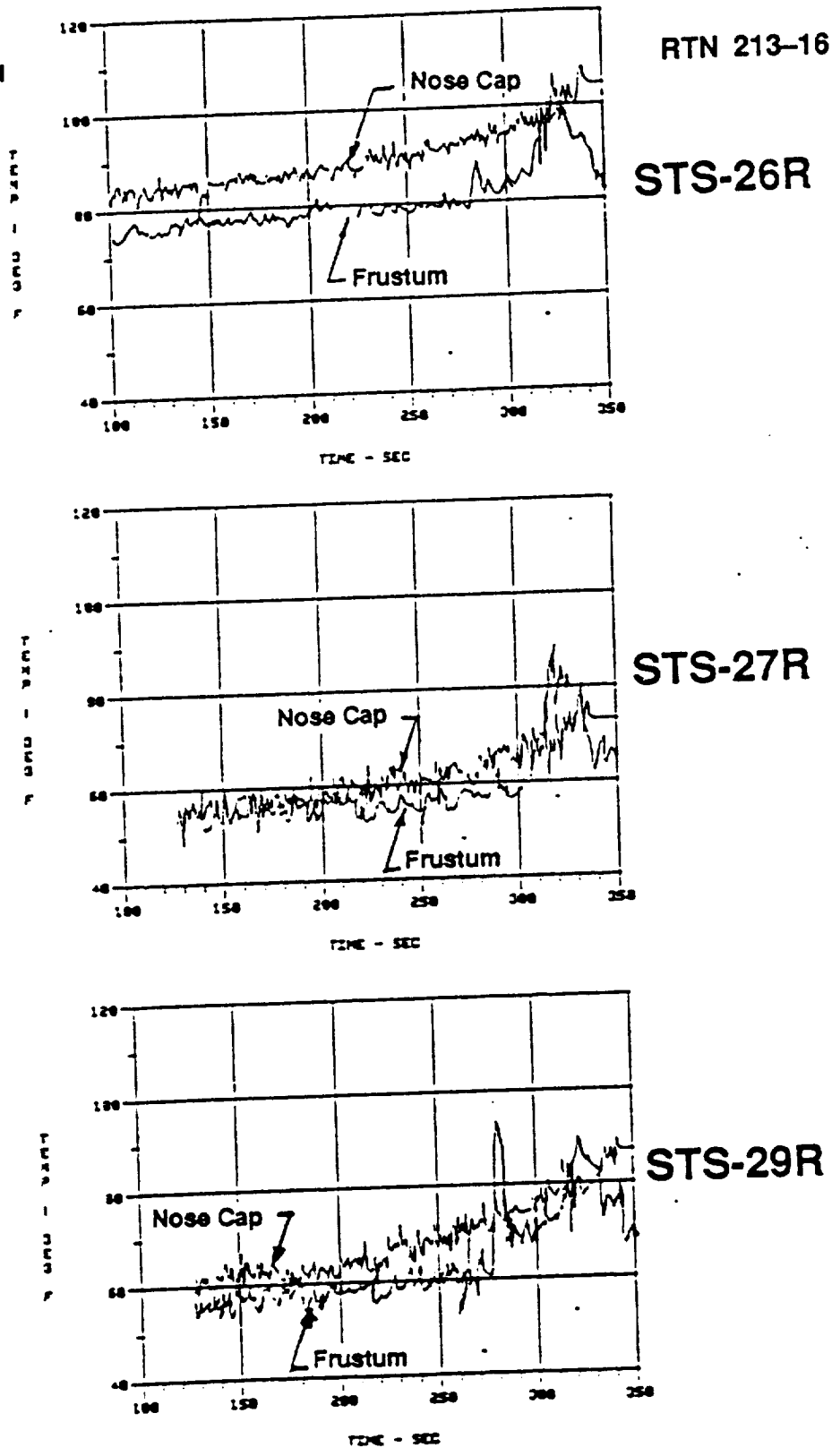

(b) Reentry

Figure 4: Gas Temperature Response for STS-26R, 27R and 29R (Concluded)

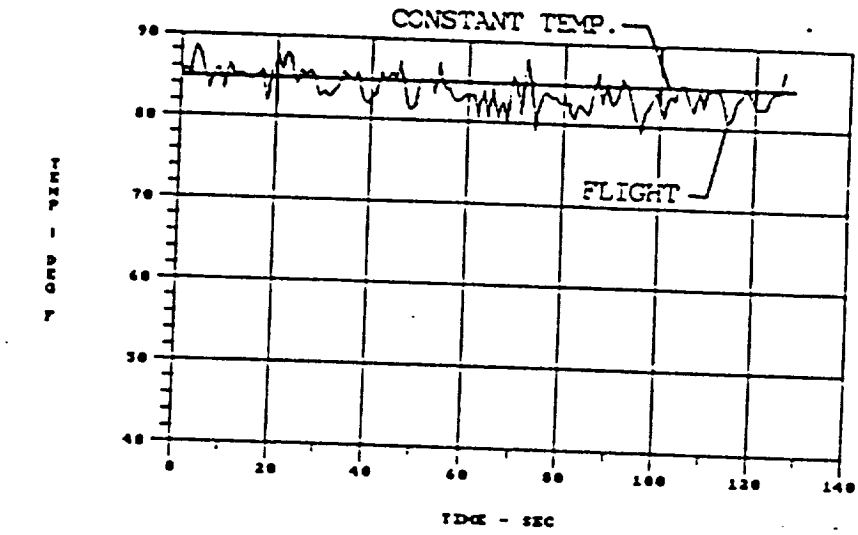

STS26R

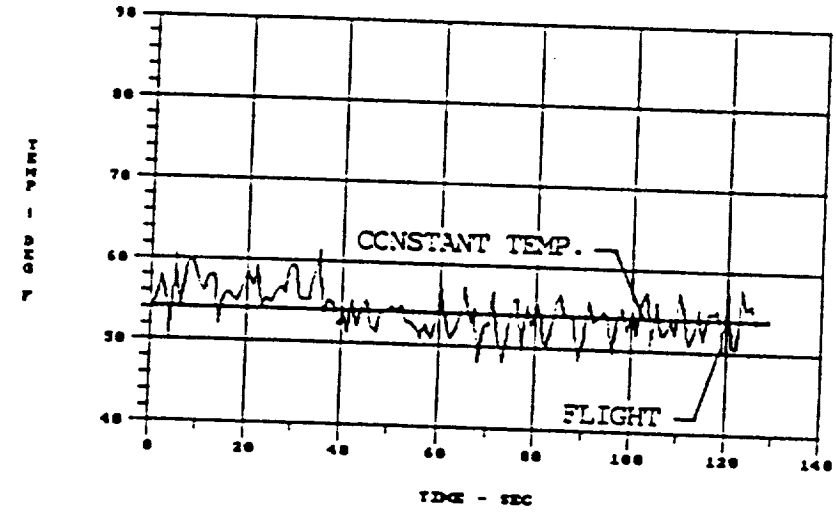

STS27R

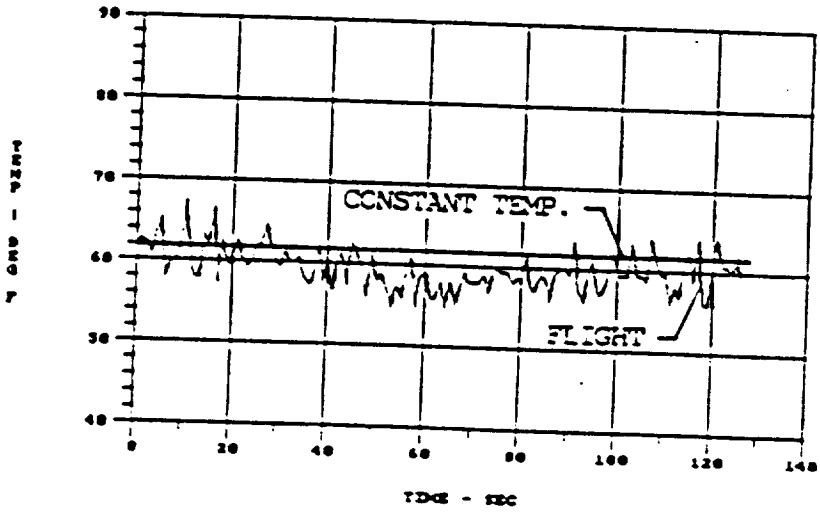

STS29R

Figure 5: Nose Cap Predicted Compartment Temperatures

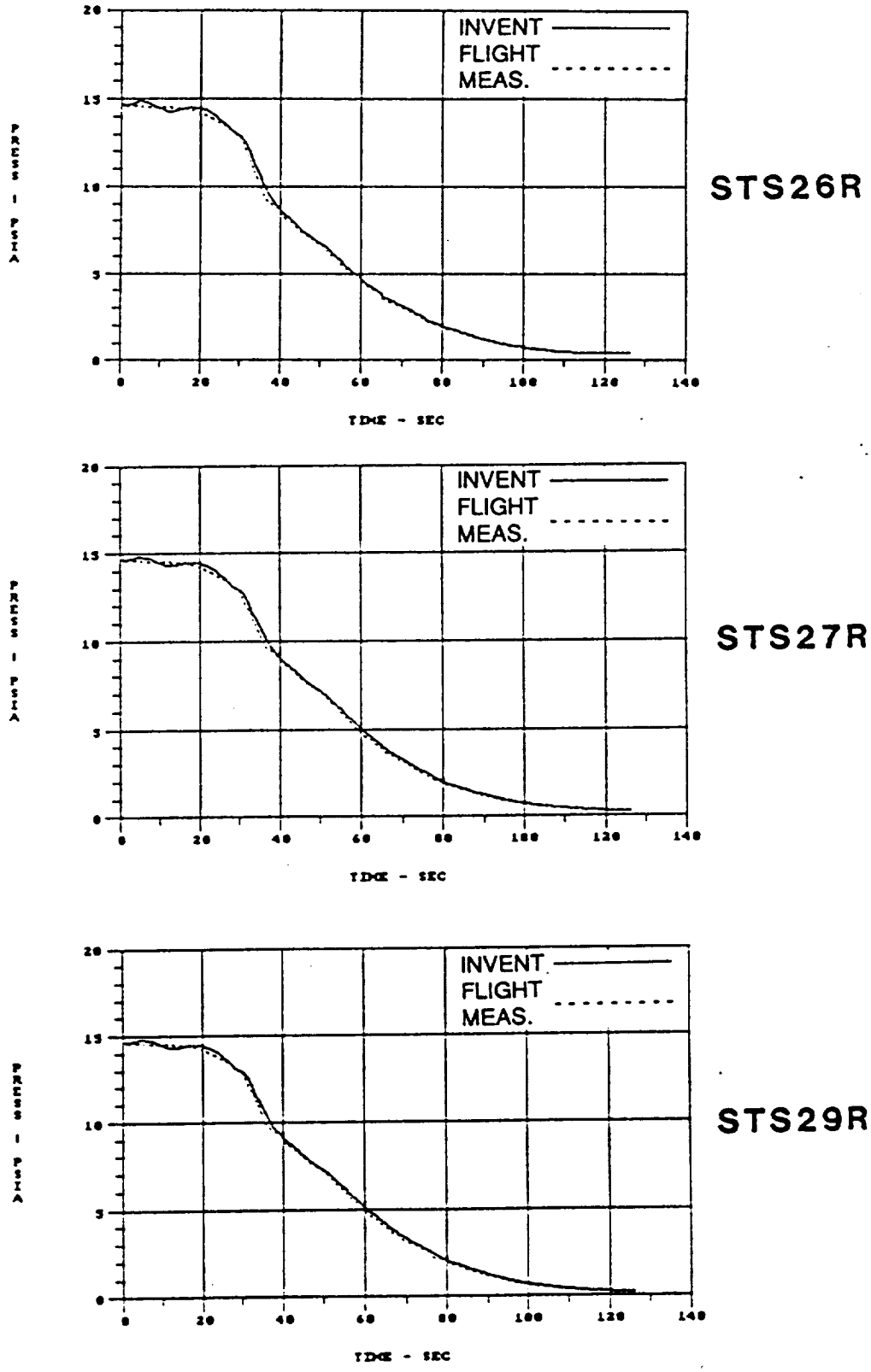

Figure 6: Frustum Predicted Compartment Pressures

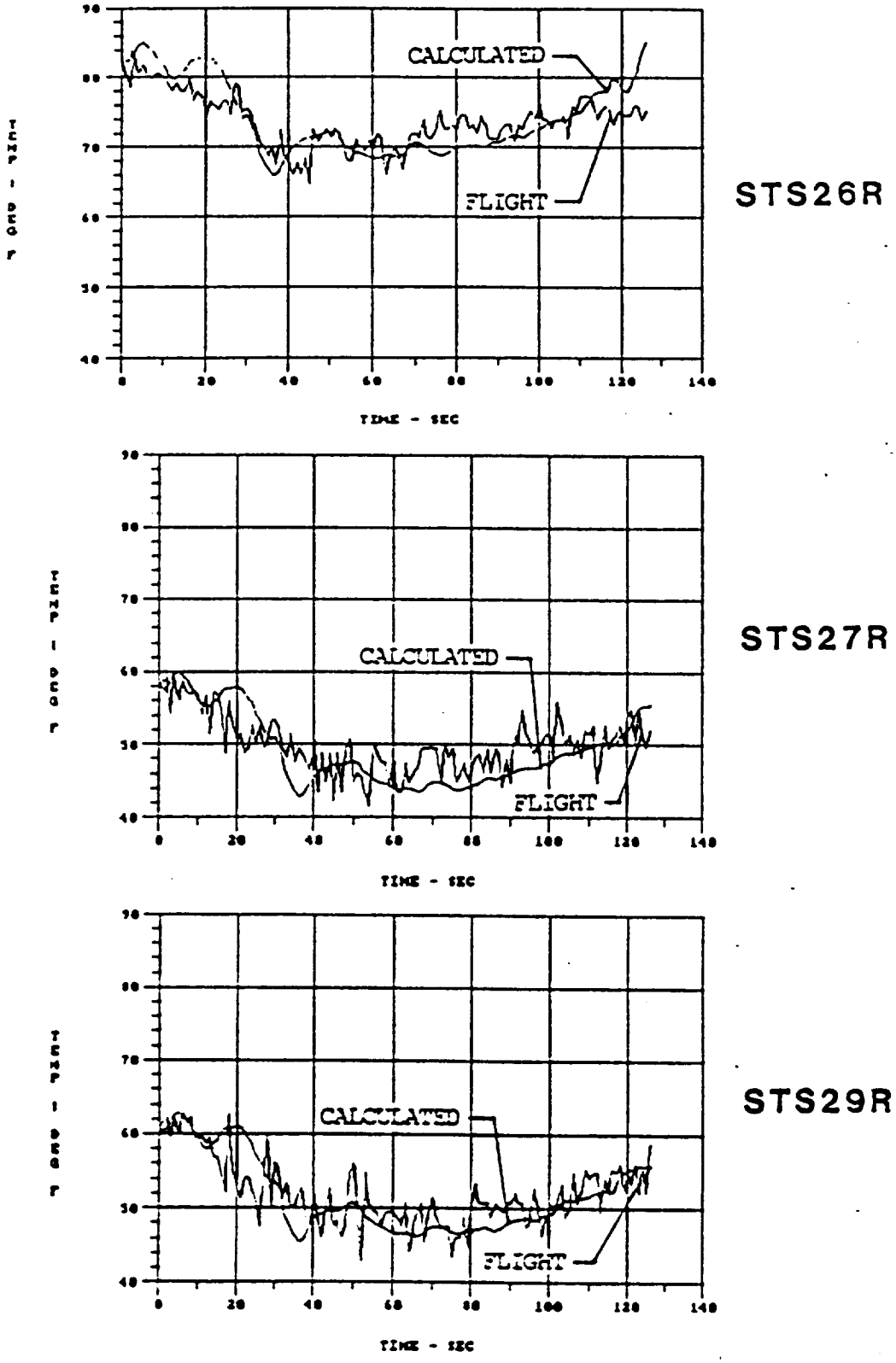

Figure 7: Frustum Predicted Compartment Temperatures

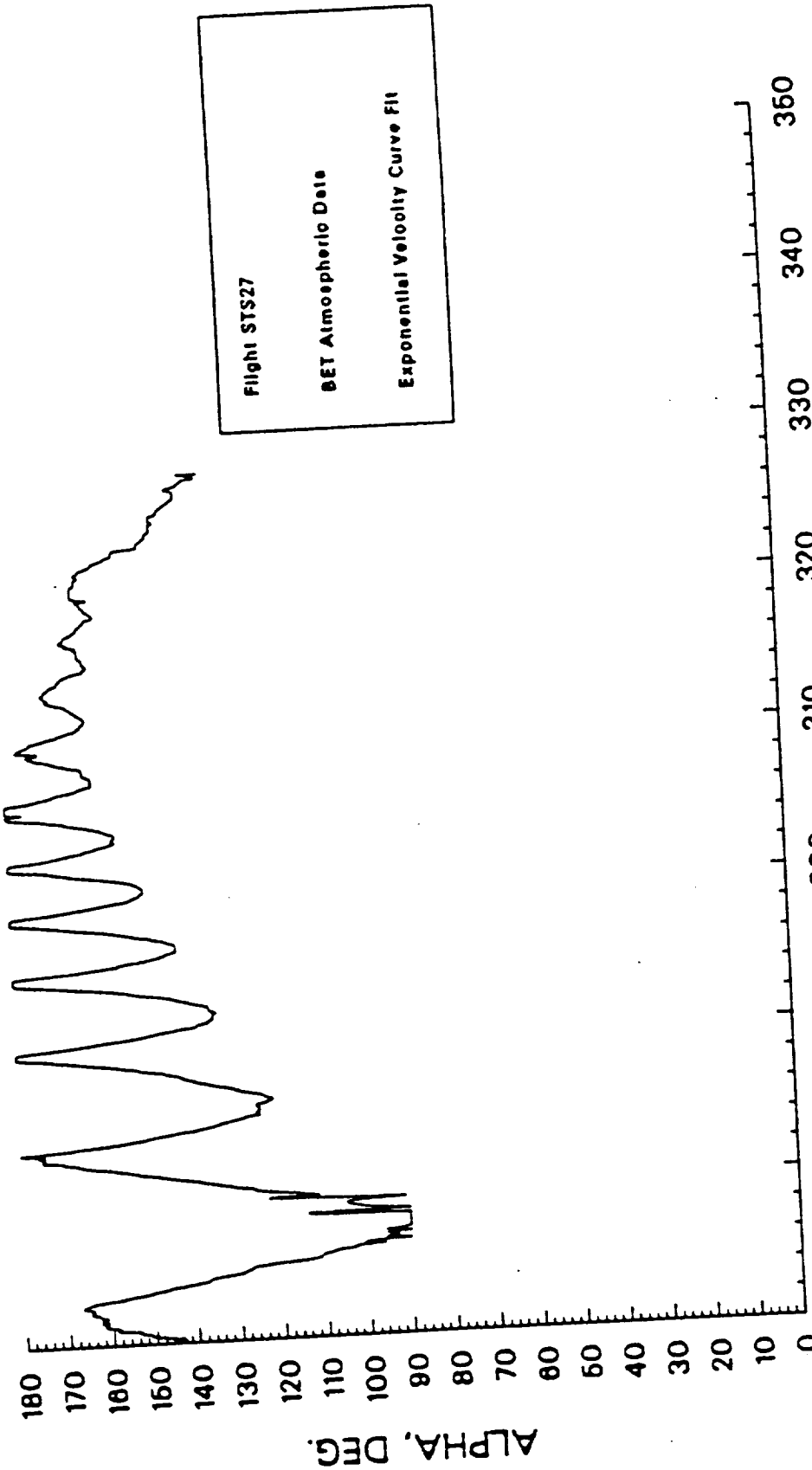

(a) L/H SRB Angle of Attack

Figure 8: SRB Reentry Orientation for STS-27R

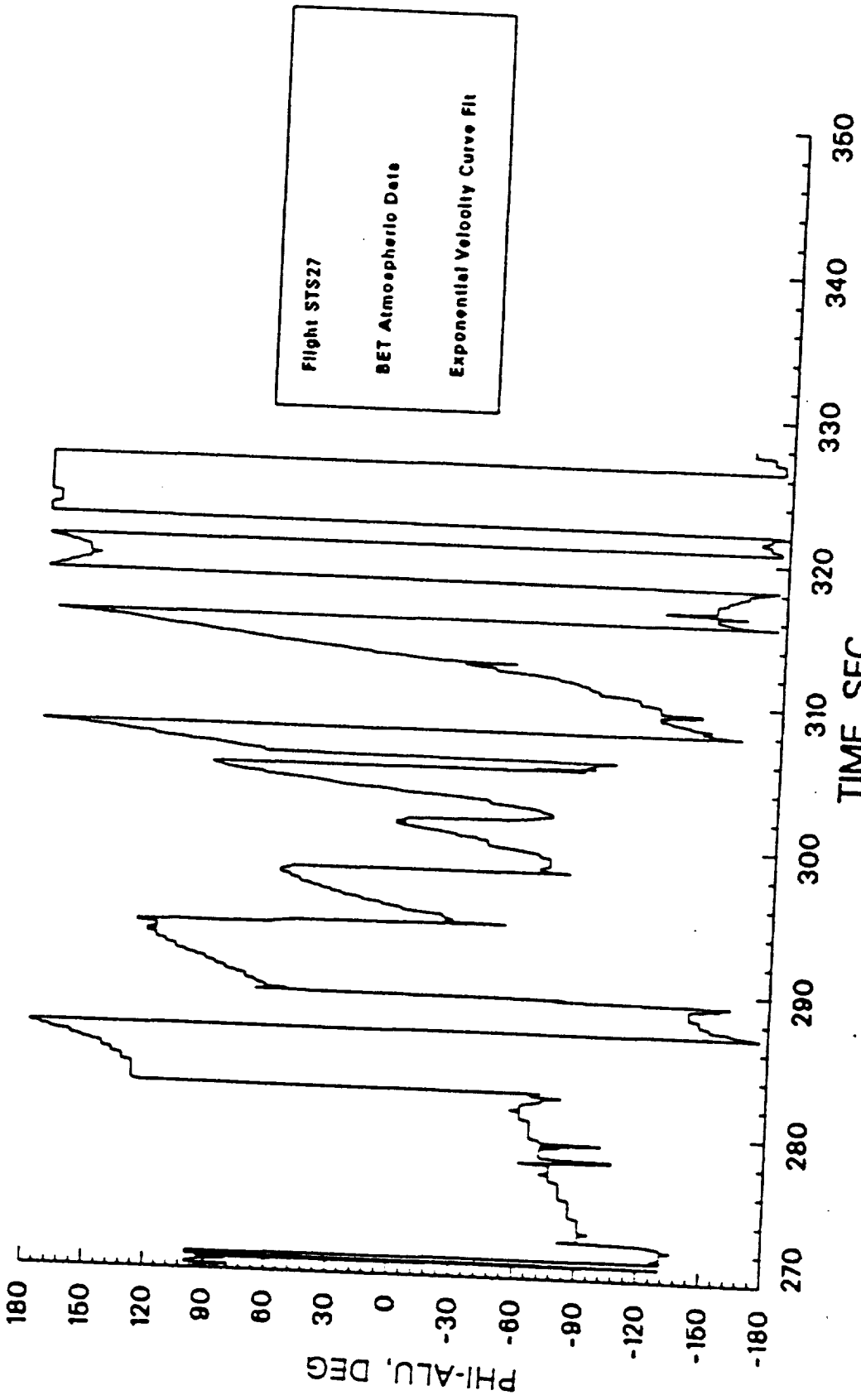

(b) L/H SRB Roll Angle

Figure 8: SRB Reentry Orientation for STS-27R (Concluded)

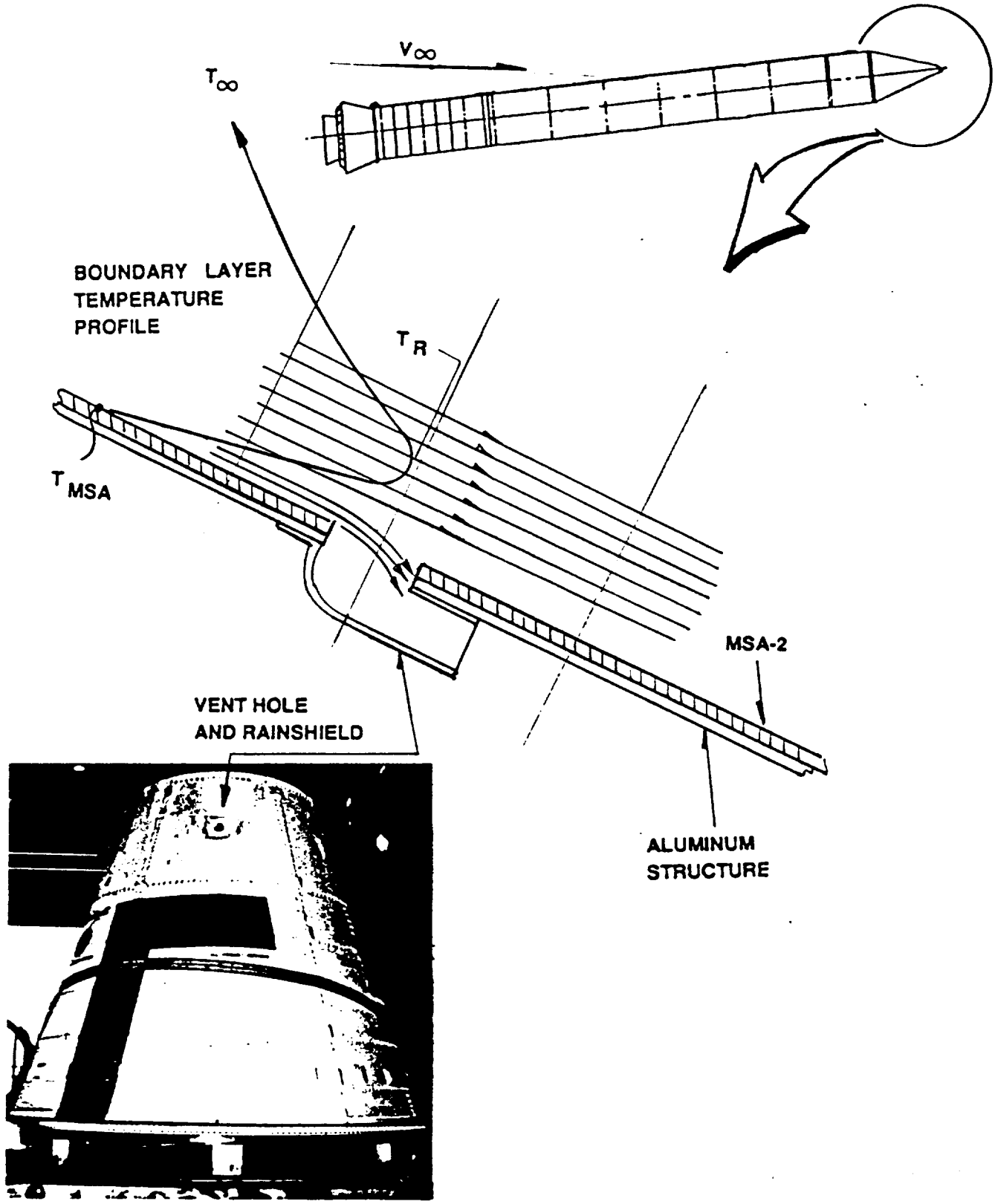

Figure 9: Local Flow Conditions in Vicinity of a Vent Hole

Constants used
In EXITS Program:
$T_{SINK} = -30^{O}$ F
$\alpha = 0.25$
View Factor = 1.00

Structure:
0.13 In MSA-2
0.30 In Aluminum

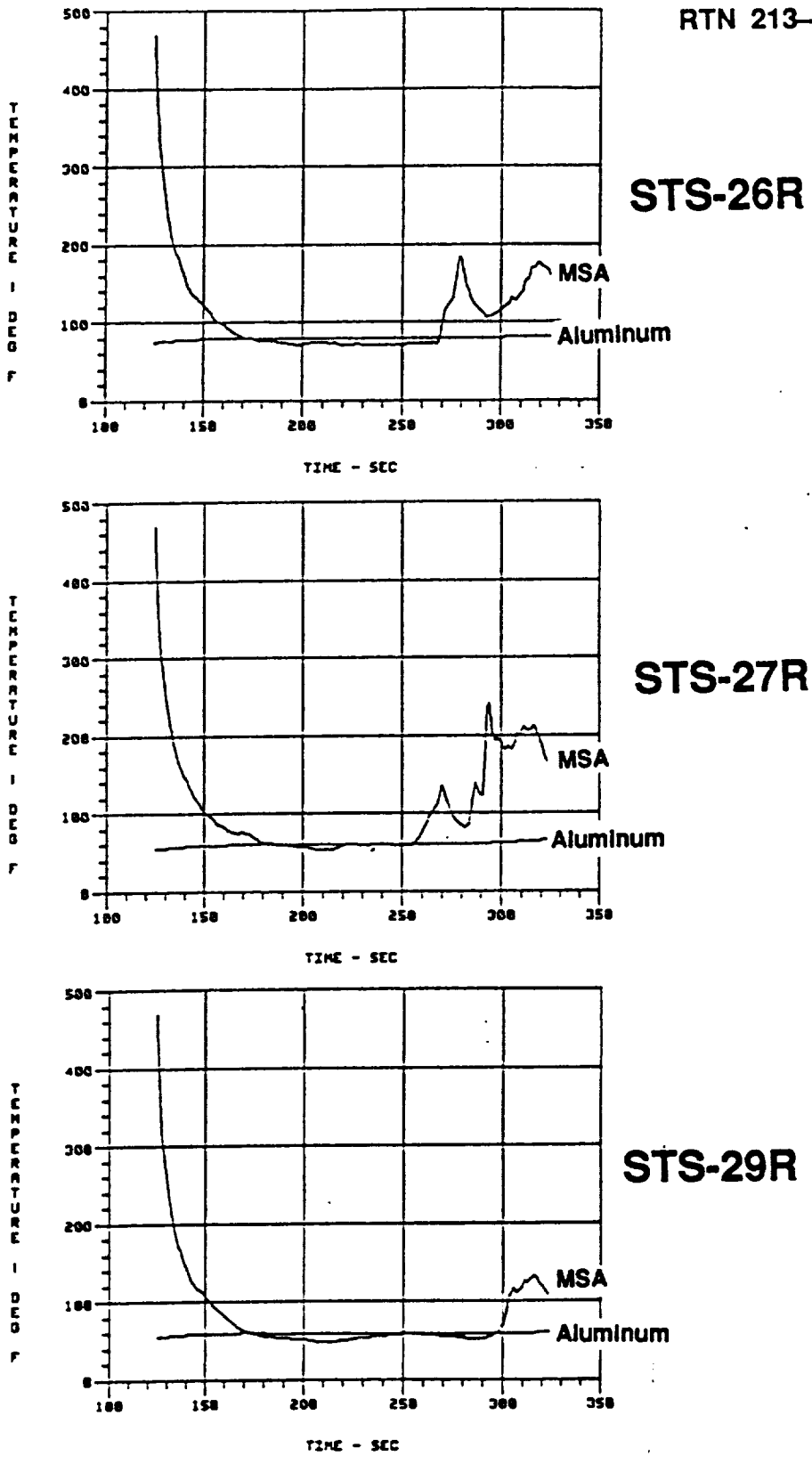

Figure 10: Nose Cone MSA–2 Temperature Predictions for STS-26R, 27R and 29R

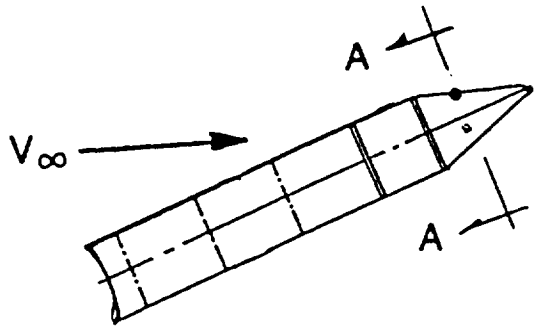

NOTE: 1) Wind Tunnel Data are External Measurements
2) Flight Data are Internal Measurements

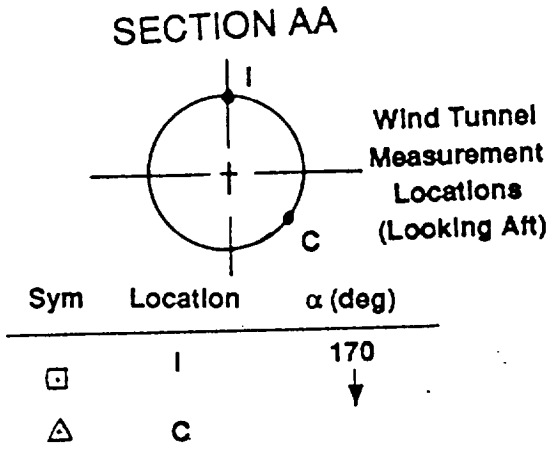

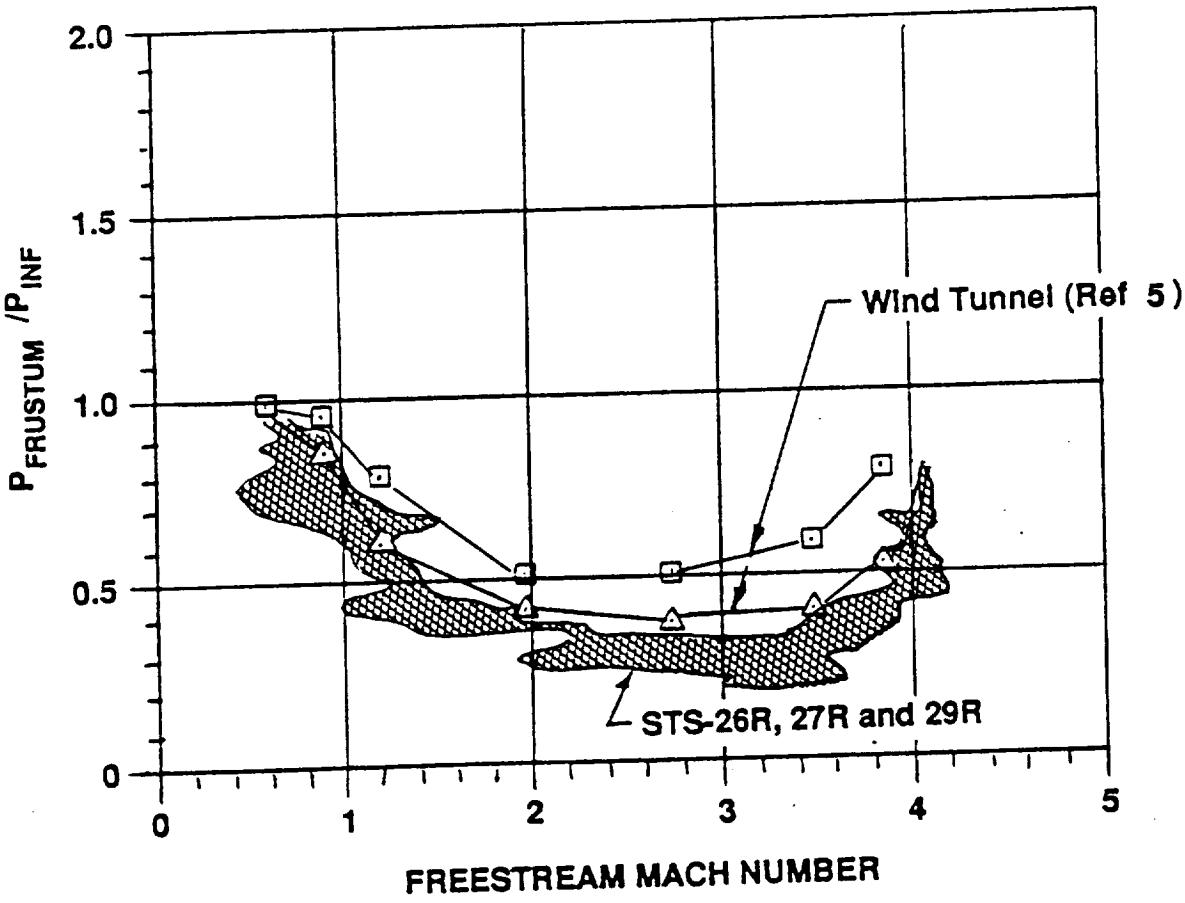

Figure 11: SRB Nose Cone Wind Tunnel and Flight Pressure Ratio Summary

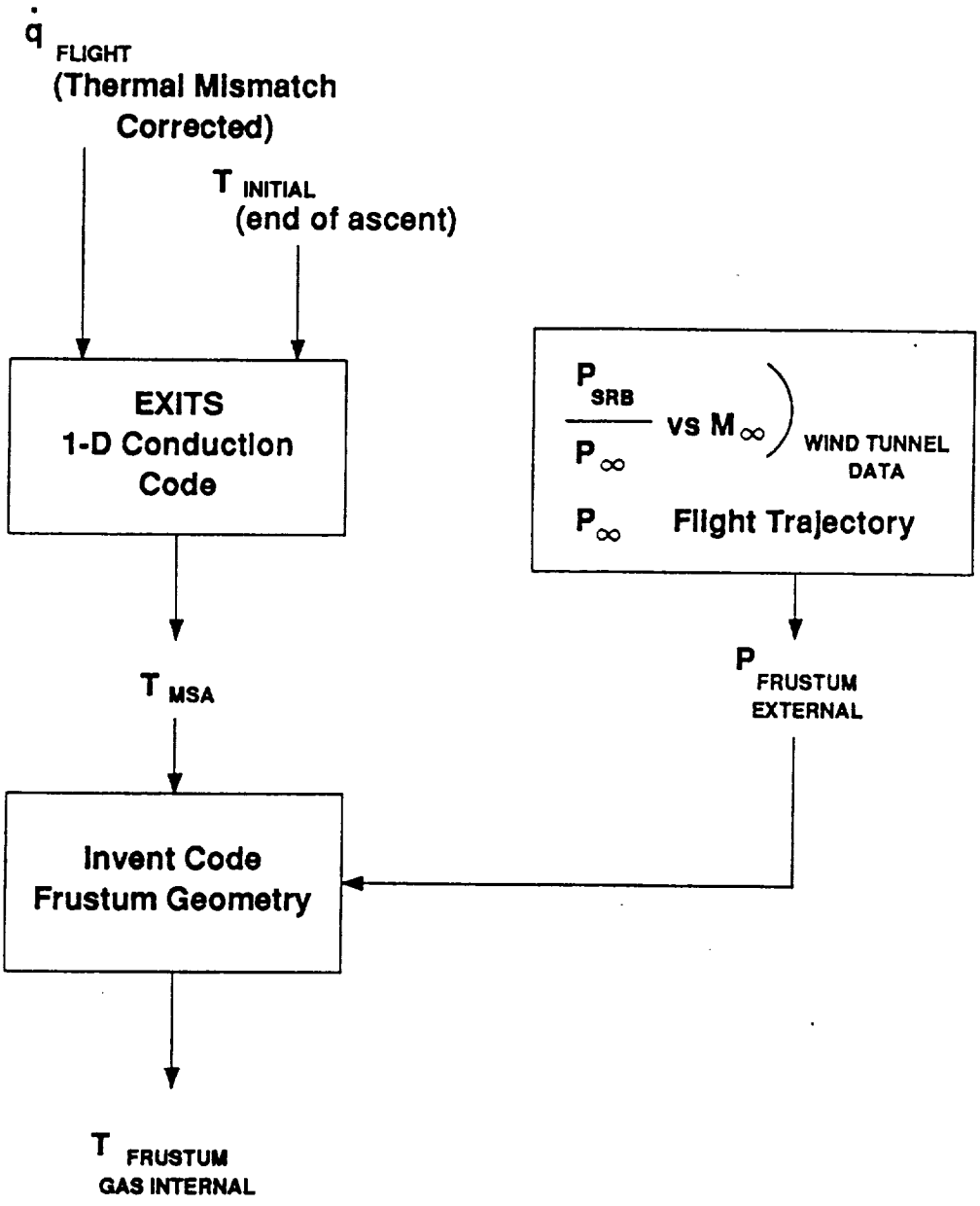

Figure 12: Frustum Internal Gas Temperature Calculation Methodology

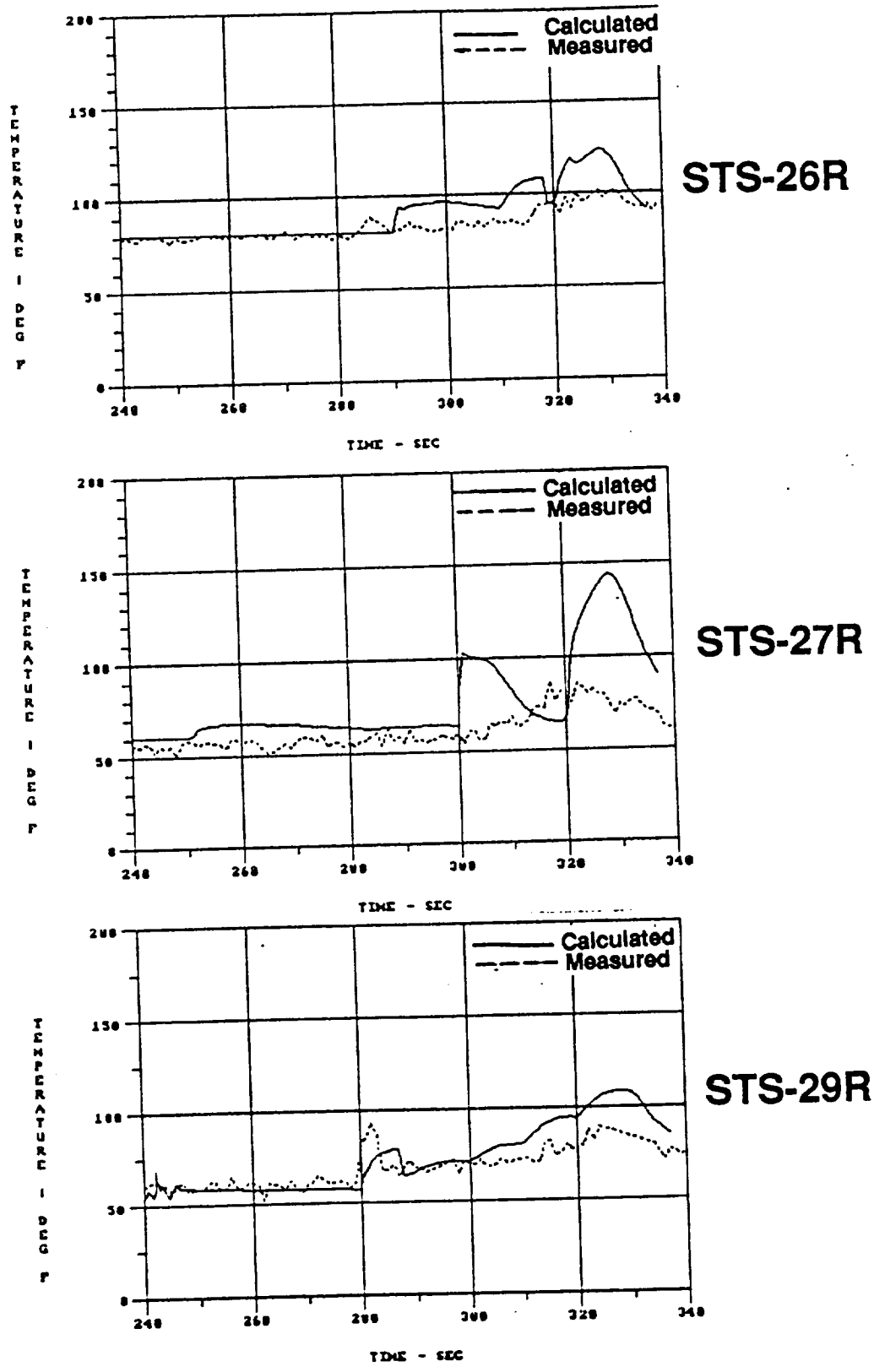

Figure 13: Comparison of Frustum Predicted Internal Gas Temperature with DFI Flight Measurements

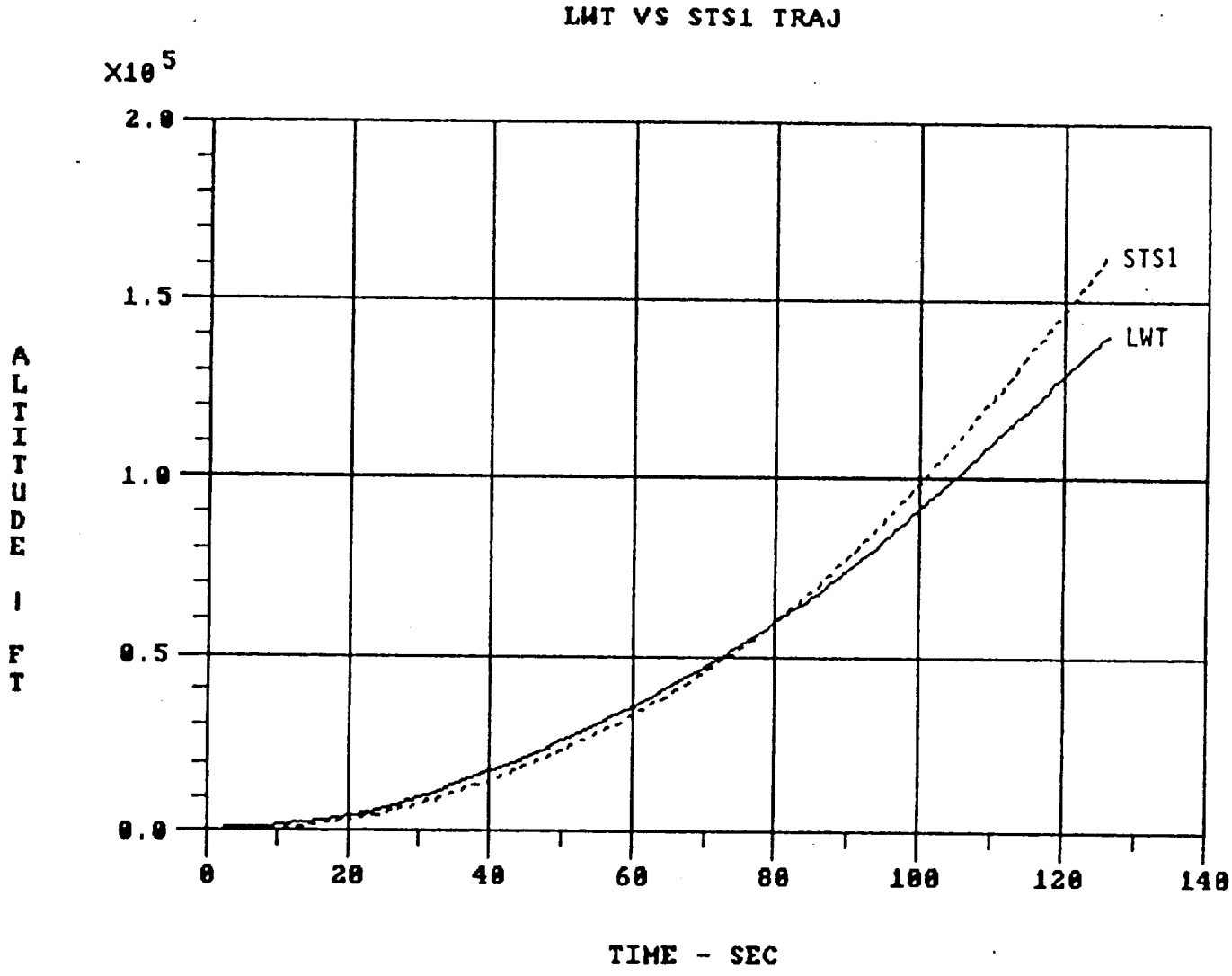

Figure 14: Comparison of LWT and STS-1 Trajectory Altitudes

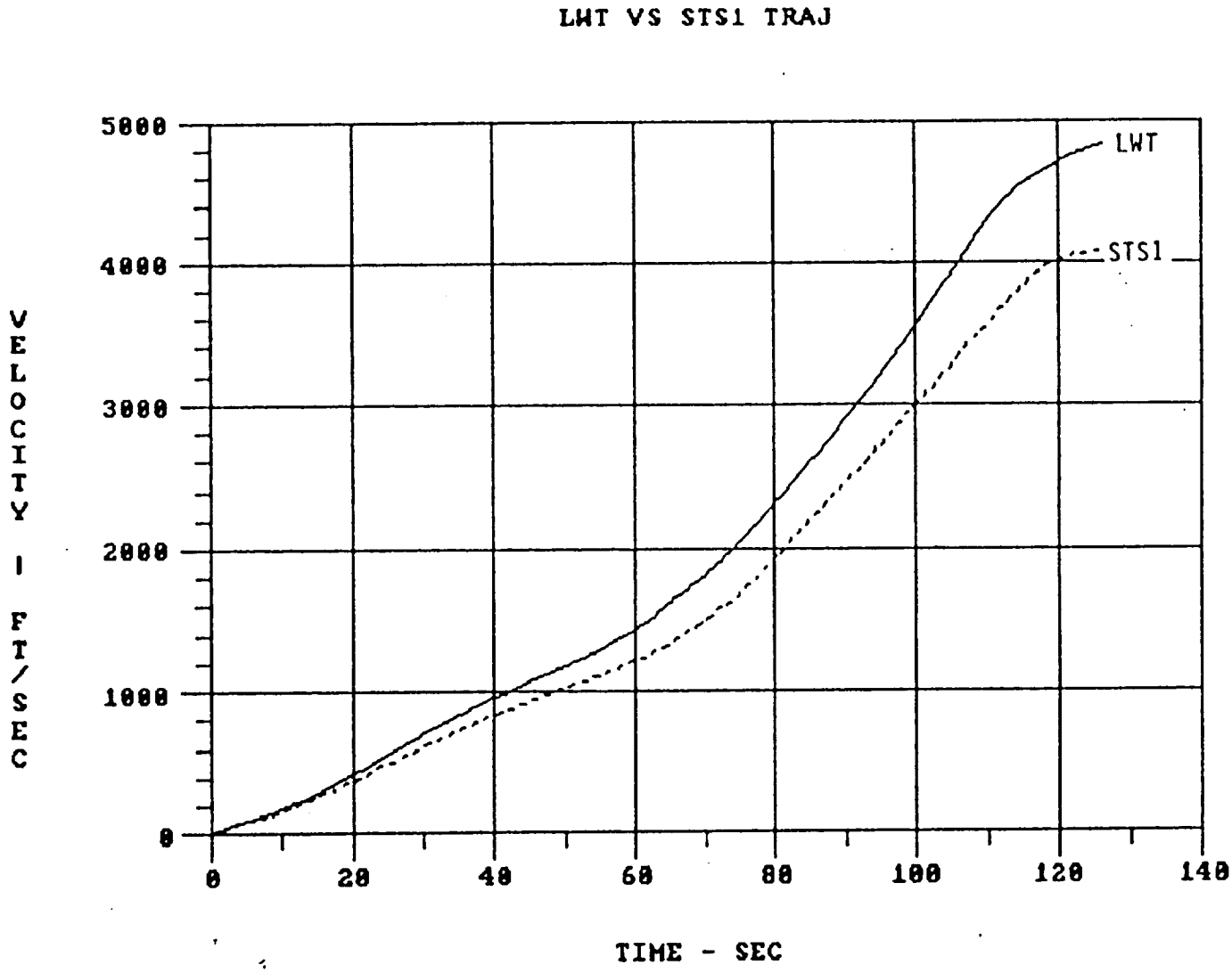

Figure 15: Comparison of LWT and STS-1 Trajectory Velocities

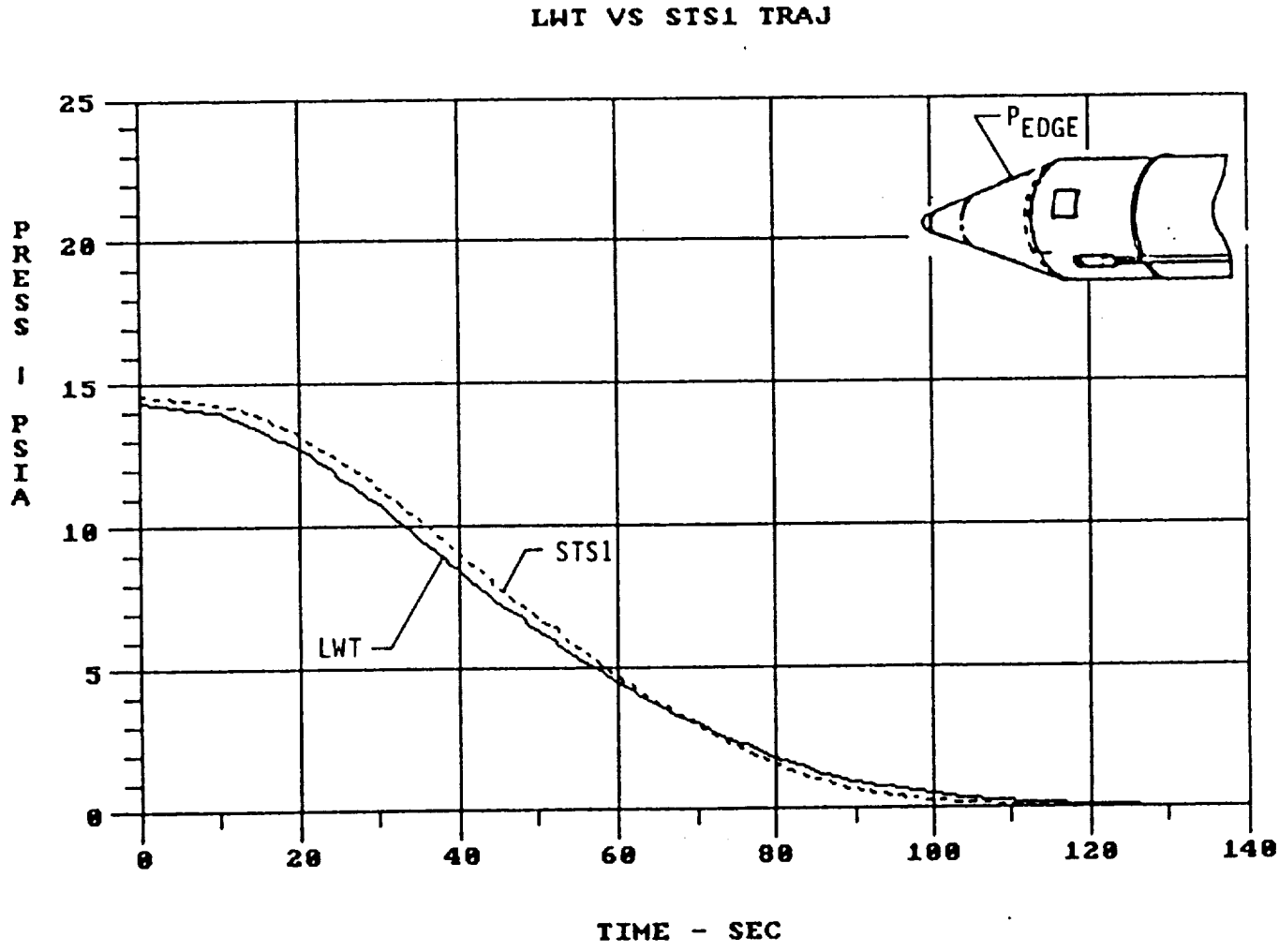

Figure 16: Comparison of LWT and STS-1 Trajectory Pressures (LANMIN Output)

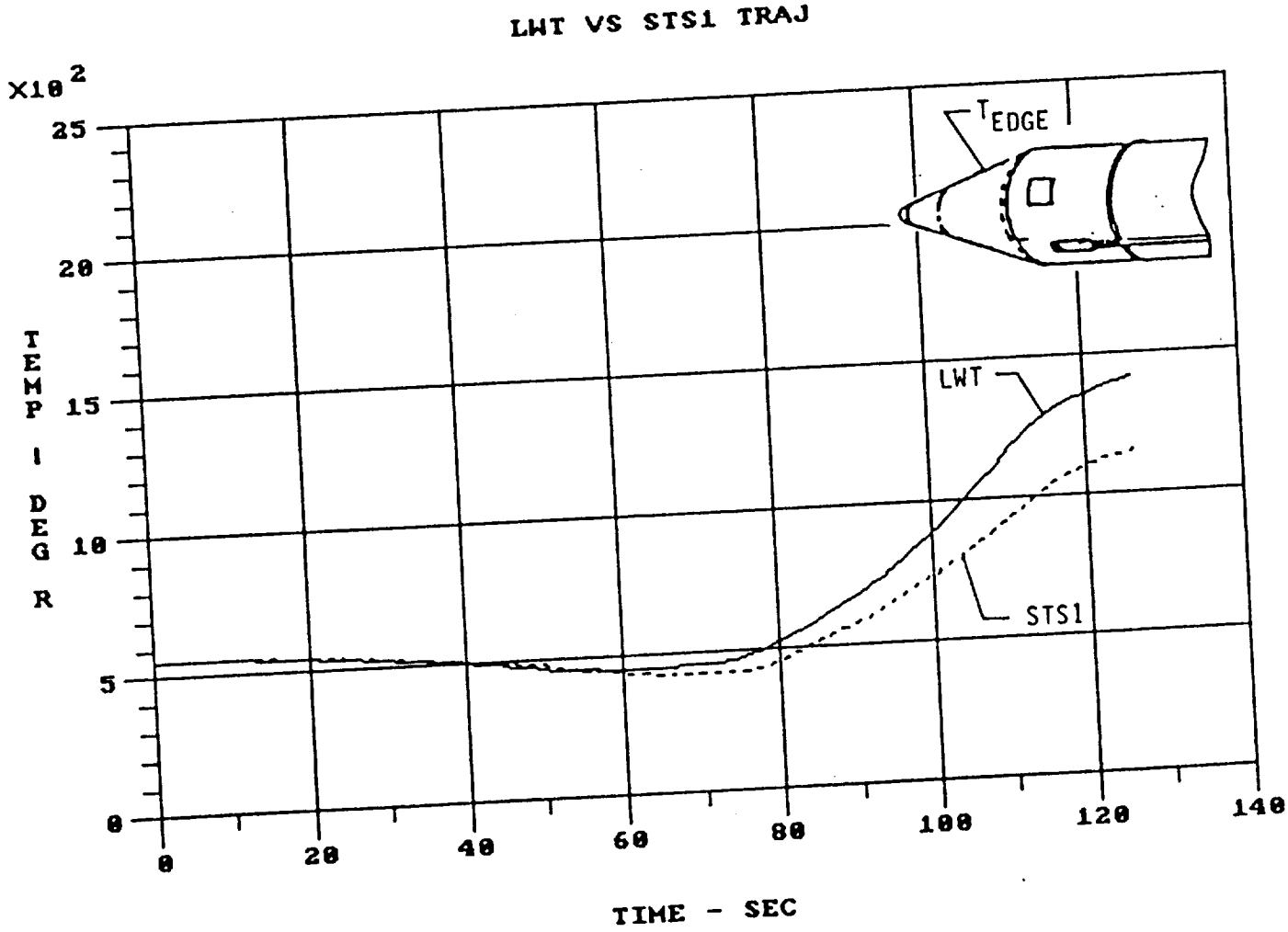

Figure 17: Comparison of LWT and STS-1 Trajectory Temperatures (LANMIN Output)

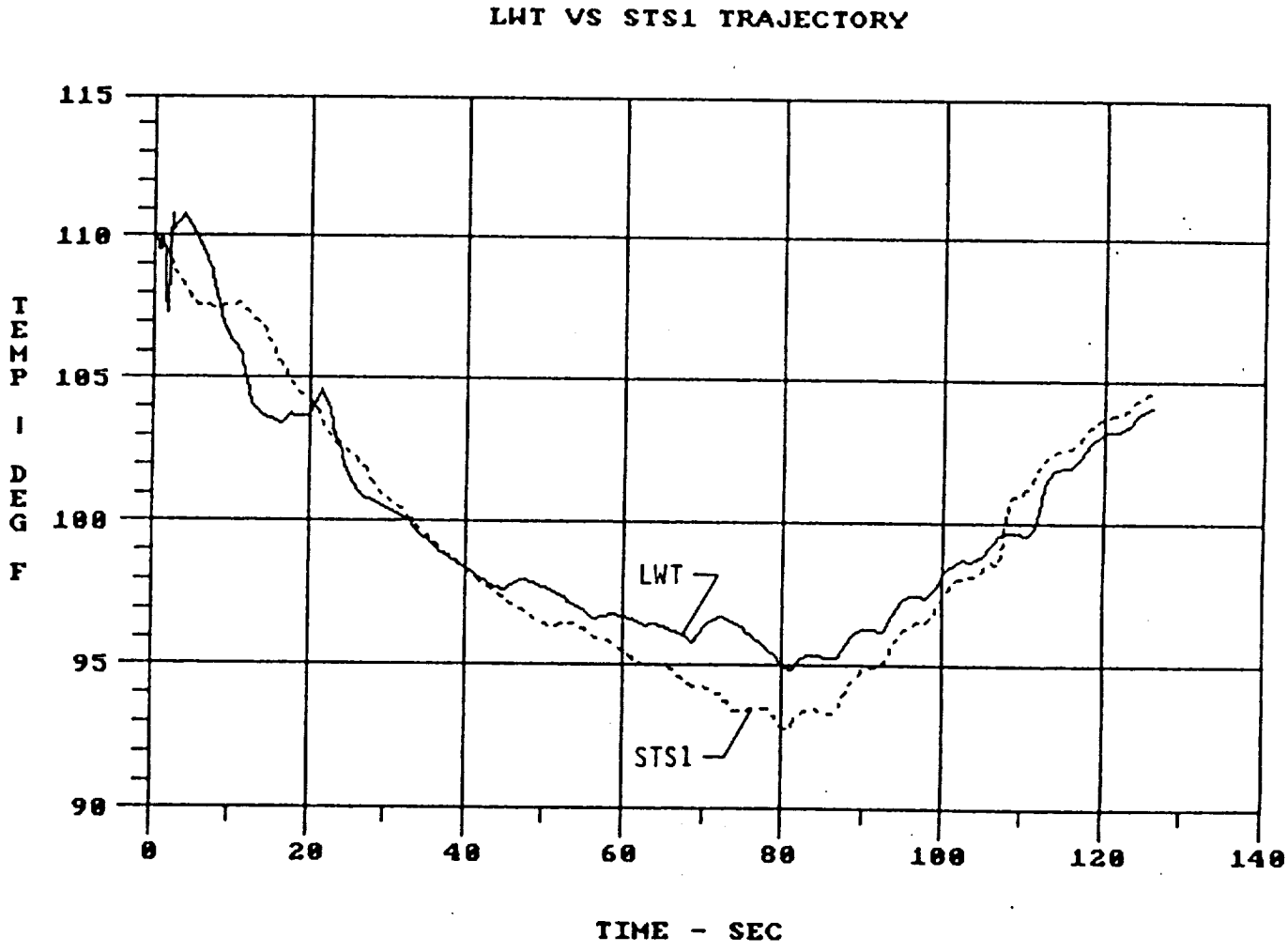

Figure 18: Comparison of LWT and STS-1 Trajectory Frustum Gas Temperatures (INVENT Output)

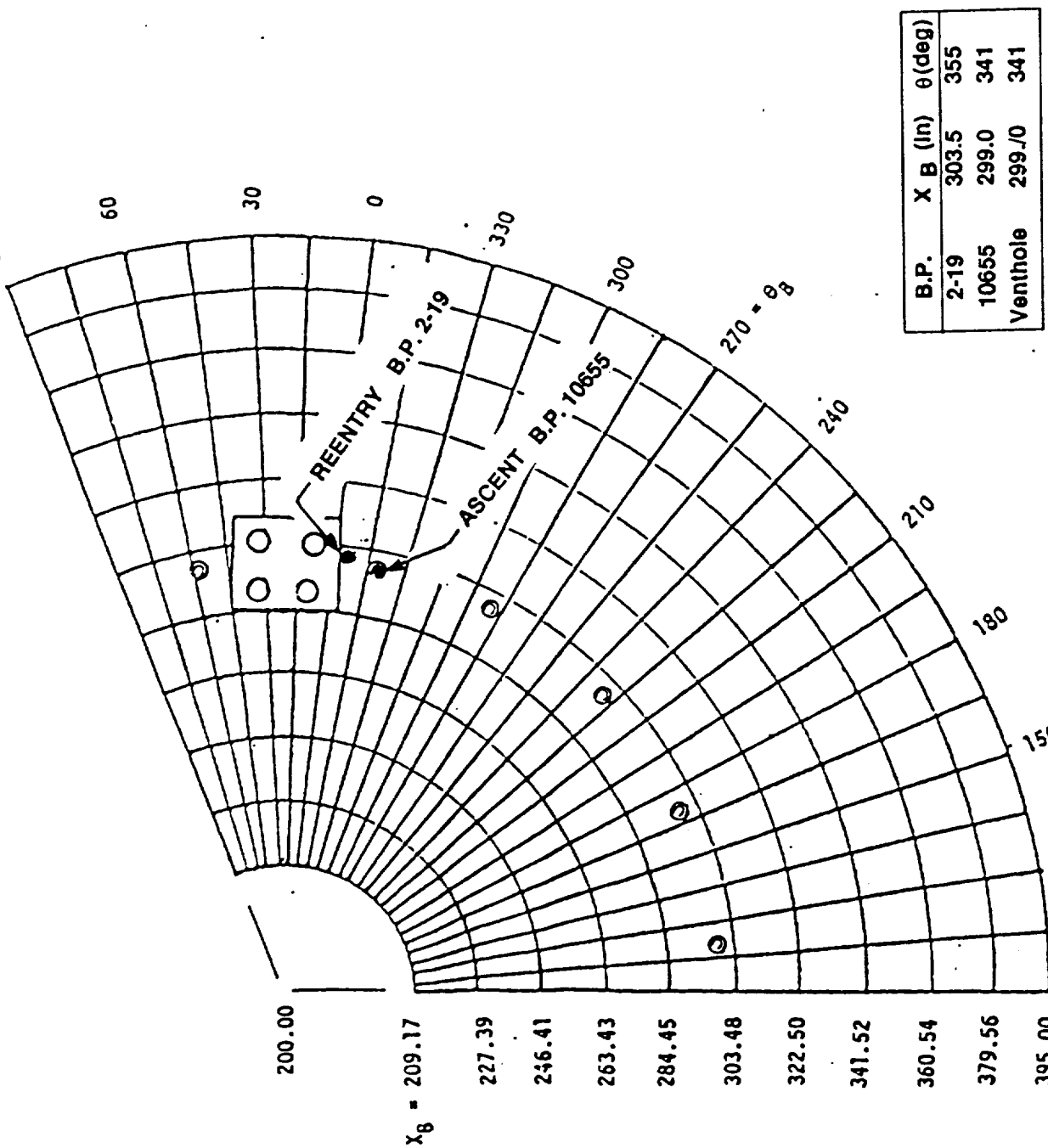

B.P.	X_B (in)	θ(deg)
2-19	303.5	355
10655	299.0	341
Venthole	299./0	341

Figure 19: Body Points Used to Determine Vent Hole External Environment

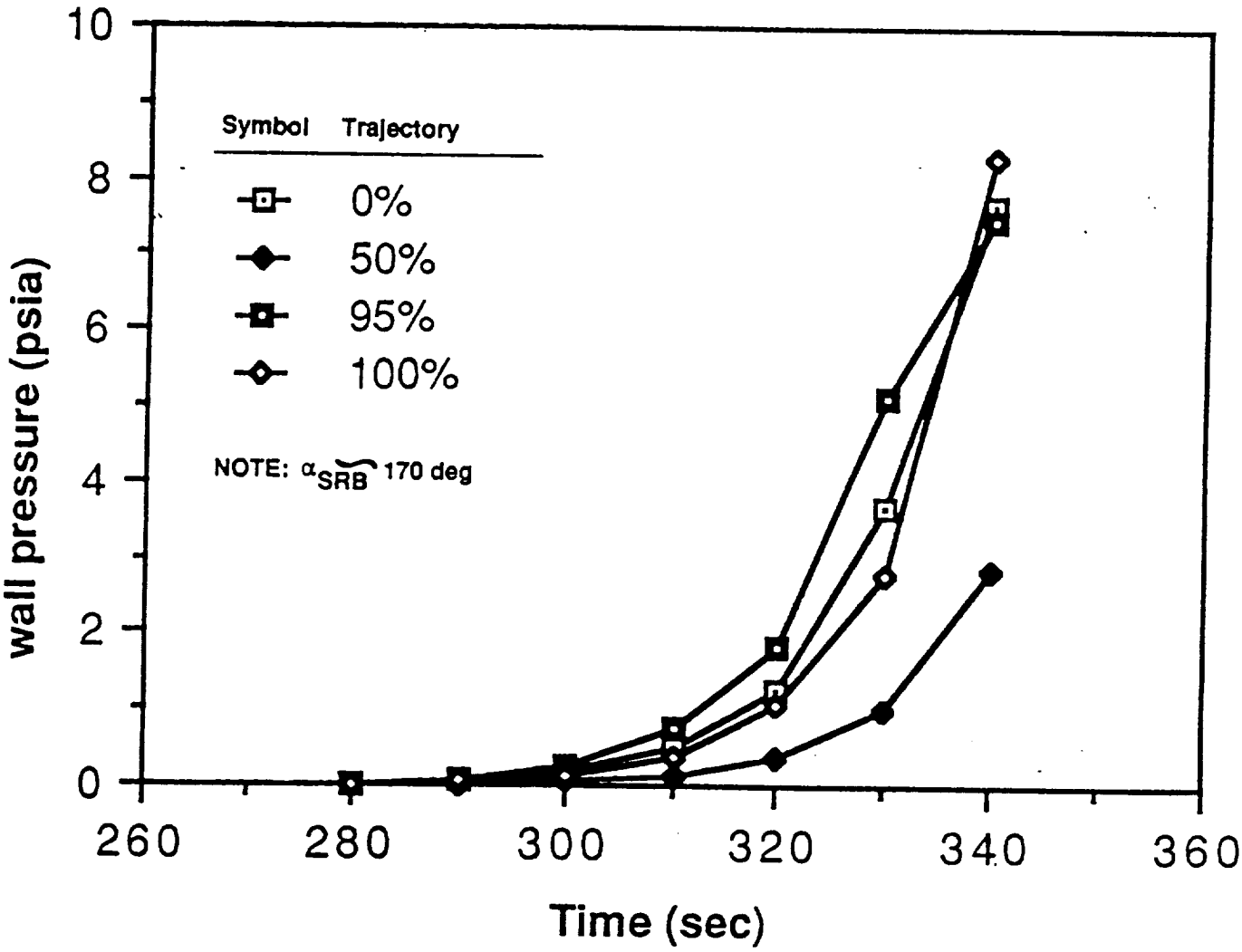

Figure 20: SRB Nose Cone Vent Hole Reentry External Pressure

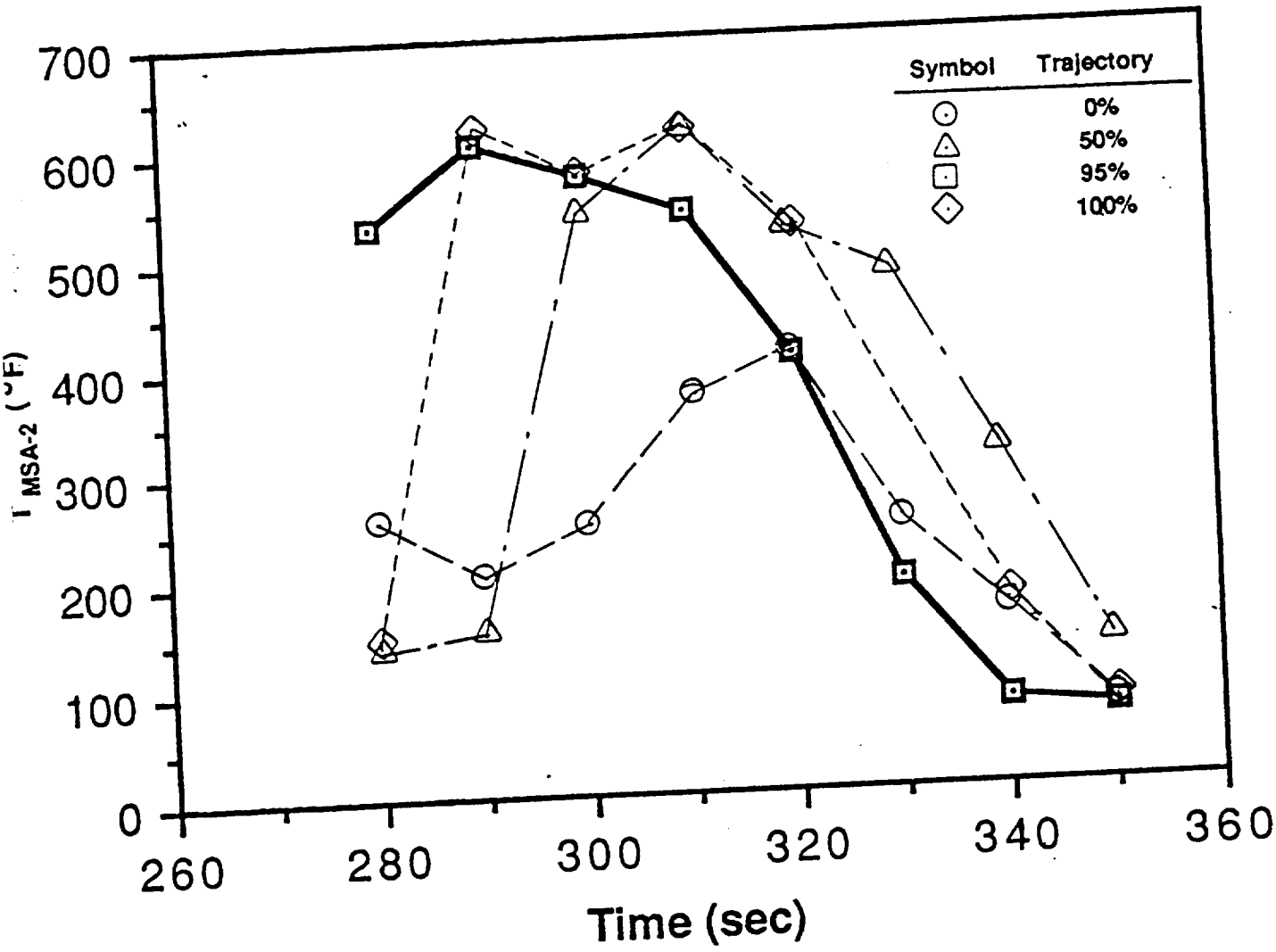

Figure 21: SRB Nose Cone Vent Hole Reentry External Gas Temperature (MSA-2 Surface Temperature)

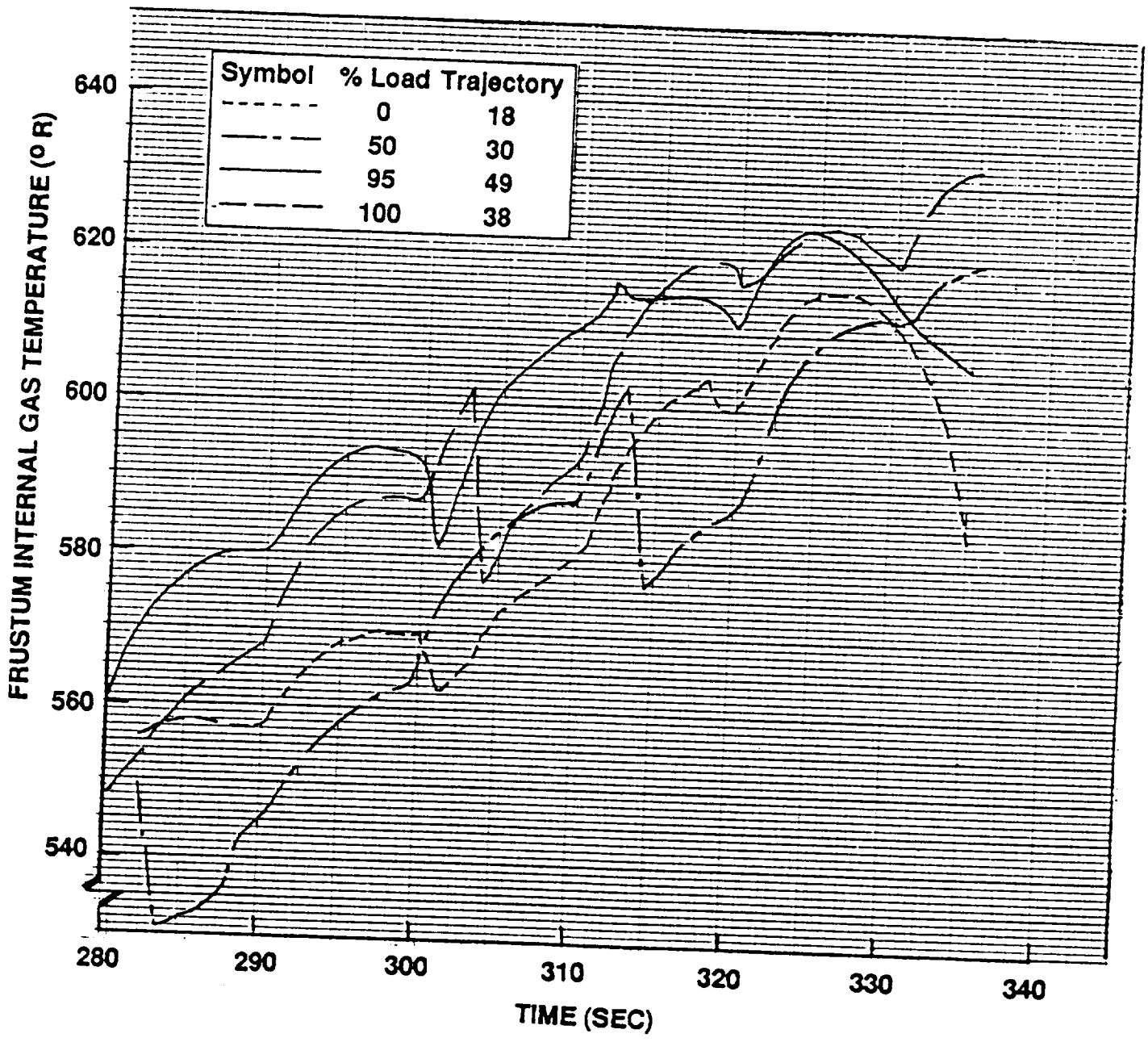

Figure 22: Frustum Design Reentry Internal Gas Temperature Calculations

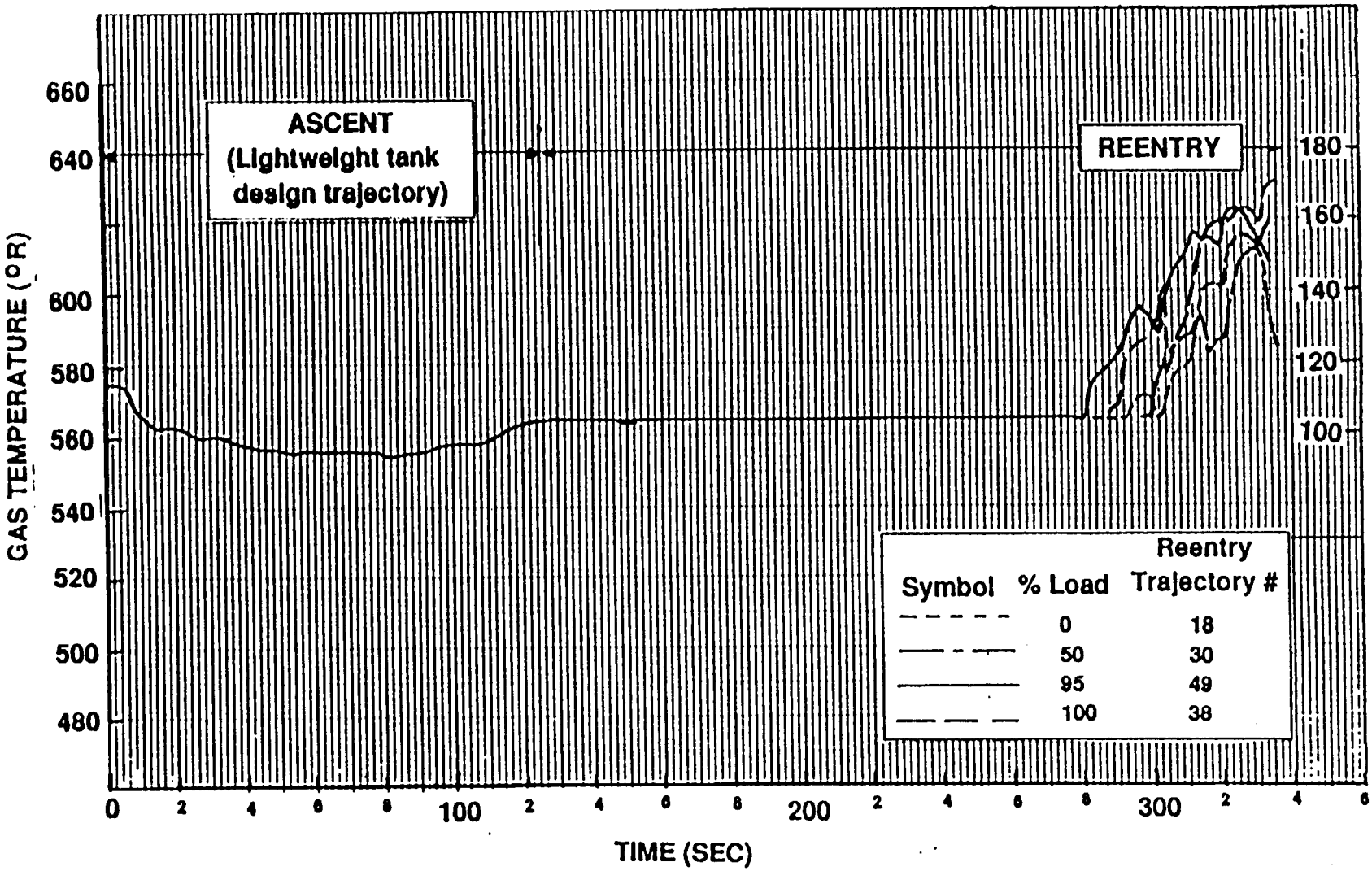

Figure 23: Frustum Combined Ascent and Reentry Design Internal Gas Temperature Summary (Body Point 401)

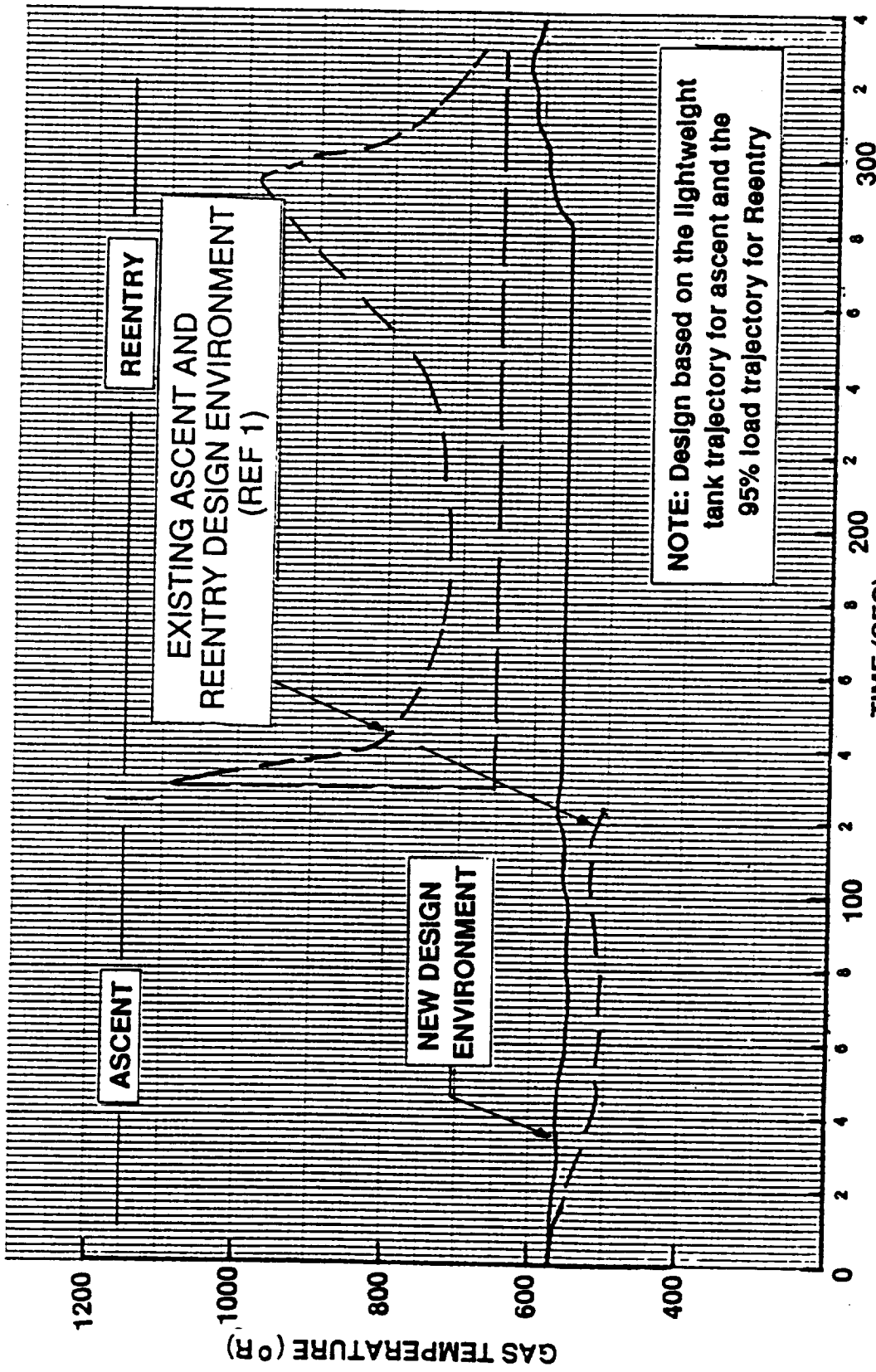

Figure 24: Comparison of Existing and New Frustum Internal Gas Temperature Design Environment

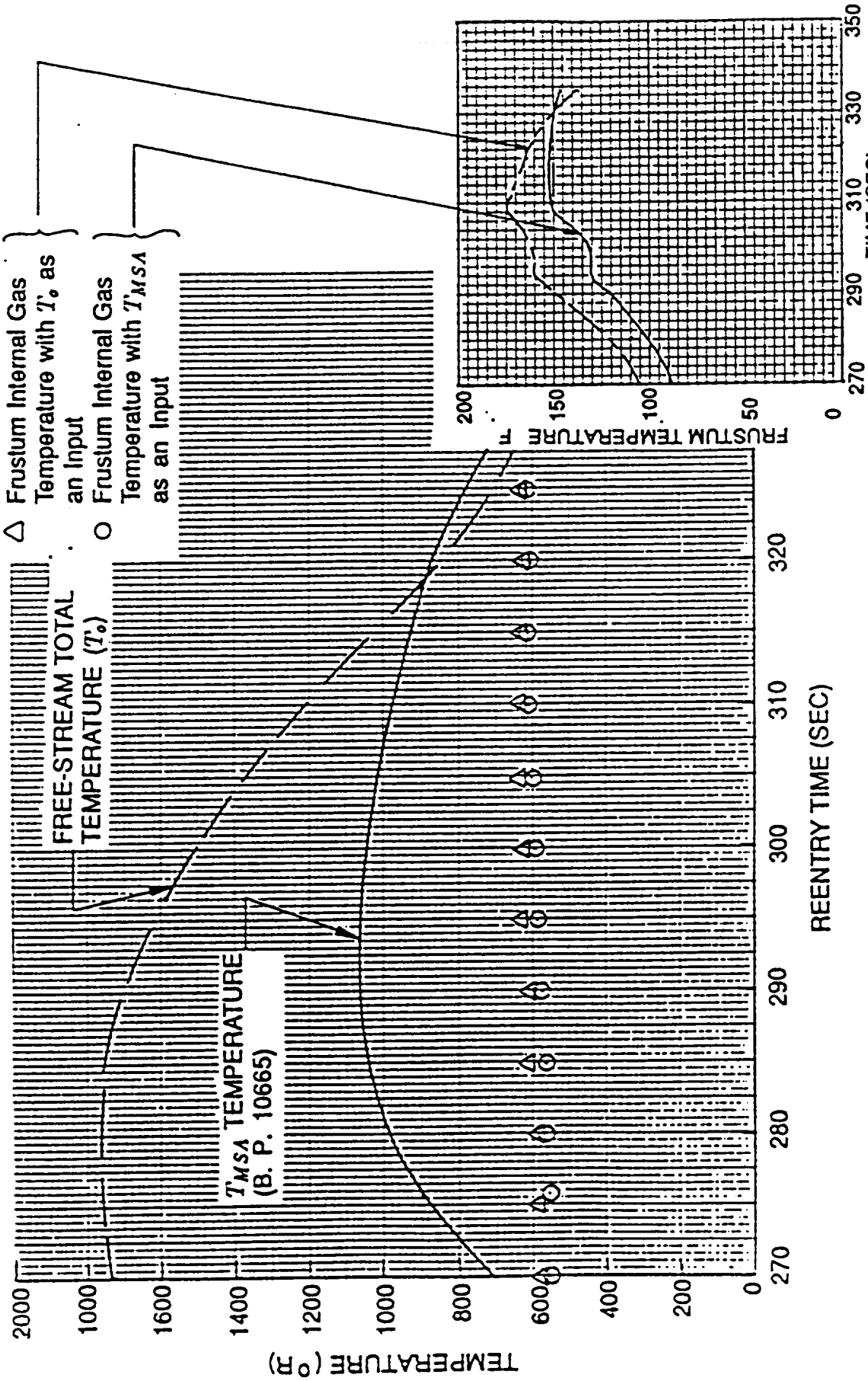

Figure 25: Effect of Using T_o and T_{MSA} as Entry Conditions on Frustum Reentry Calculated Internal Gas Temperature

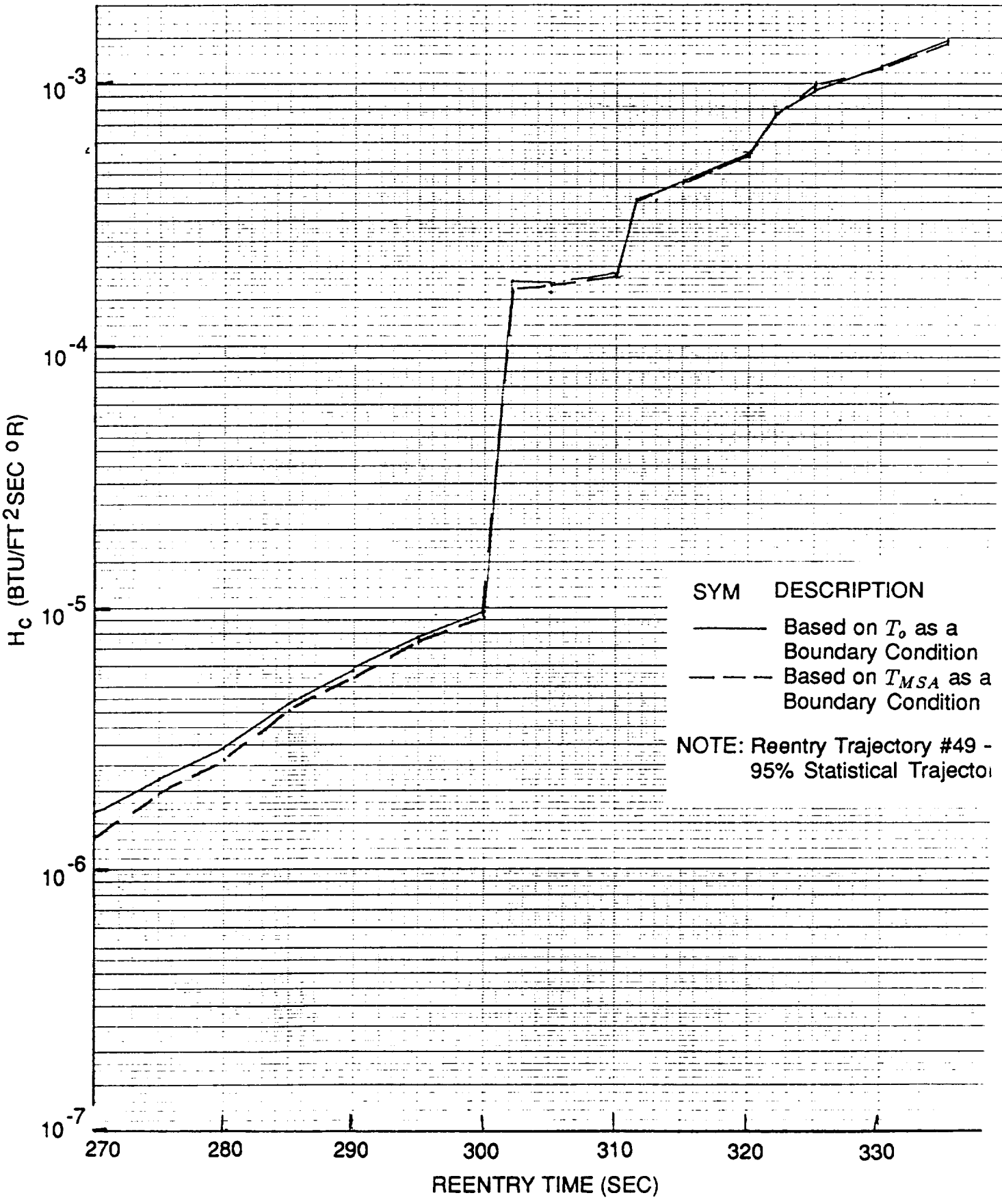

Figure 26: Effect of Using T_o and T_{MSA} as Entry Conditions on Frustum Reentry Internal Heat Transfer Coefficient

Table 1: SRB Nose Cone Ascent Venting Geometry and Assumptions

Component	Weight (lbm)	Diameter ft	Volume ft^3	Air Volume ft^3	Surface Area ft^2
Pilot Chute	42	11.5	1.02	0.15	103
Drogue Chute	1260	54.0	37.50	5.63	2290
Main Chutes (3)	(3)2180	(3)136.0	(3) 71.00	(3) 10.65	3 (14,526)
Nose Cap	—	—	61.37	22.85	100
Frustum	—	—	590.60	377.00	408

Assumption: 15 percent air in packed chutes

Venting Conditions:

Nose Cap — Six 1 1/4″ diameter holes
1 1/2″ gap between drogue chute and frustum rub ring
24″ diameter opening on top of frustum

Frustum — Three vent holes, total exit area = 16.5 in^2

INVENT Code Heat Transfer Assumptions:

438 ft^3 — Total volume of air in nose cone
508 ft^2 — Metal heat transfer area in nose cone
25,000 ft^2 — Chute heat transfer area in nose cone

Natural Convection — Horizontal plate (1 ft)

Forced Convection — 0.715 ft^2 cross sectional area
0.125 ft tube diameter
5.800 ft tube length

Table 2: SRB Nose Cone Reentry Venting Geometry and Assumptions

Component	Weight (lbm)	Diameter ft	Volume ft^3	Air Volume ft^3	Surface Area ft^2
Pilot Chute	42	11.5	1.02	0.15	103
Drogue Chute	1260	54.0	37.50	5.63	2290
Main Chutes (3)	(3)2180	(3)136.0	(3) 71.00	(3) 10.65	3 (14,526)
Nose Cap	—	—	61.37	22.85	100
Frustum	—	—	590.60	377.00	408

Assumption: 15 percent air in packed chutes

Venting Conditions:

Nose Cap — Six 1 1/4″ diameter holes
1 1/2″ gap between drogue chute and frustum rub ring
24″ diameter opening on top of frustum

Frustum — Three vent holes, total exit area = 16.5 in^2

INVENT Code Heat Transfer Assumptions:

438 ft^3 — Total volume of air in nose cone
508 ft^2 — Metal heat transfer area in nose cone
9,000 ft^2 — Chute heat transfer area in nose cone

Natural Convection — Horizontal plate (1 ft)

Forced Convection — 0.715 ft^2 cross sectional area
0.125 ft tube diameter
5.800 ft tube length

Appendix VI

Compilation of SRB DFI Flight Heating Measurements from STS 1-3, 5, 6

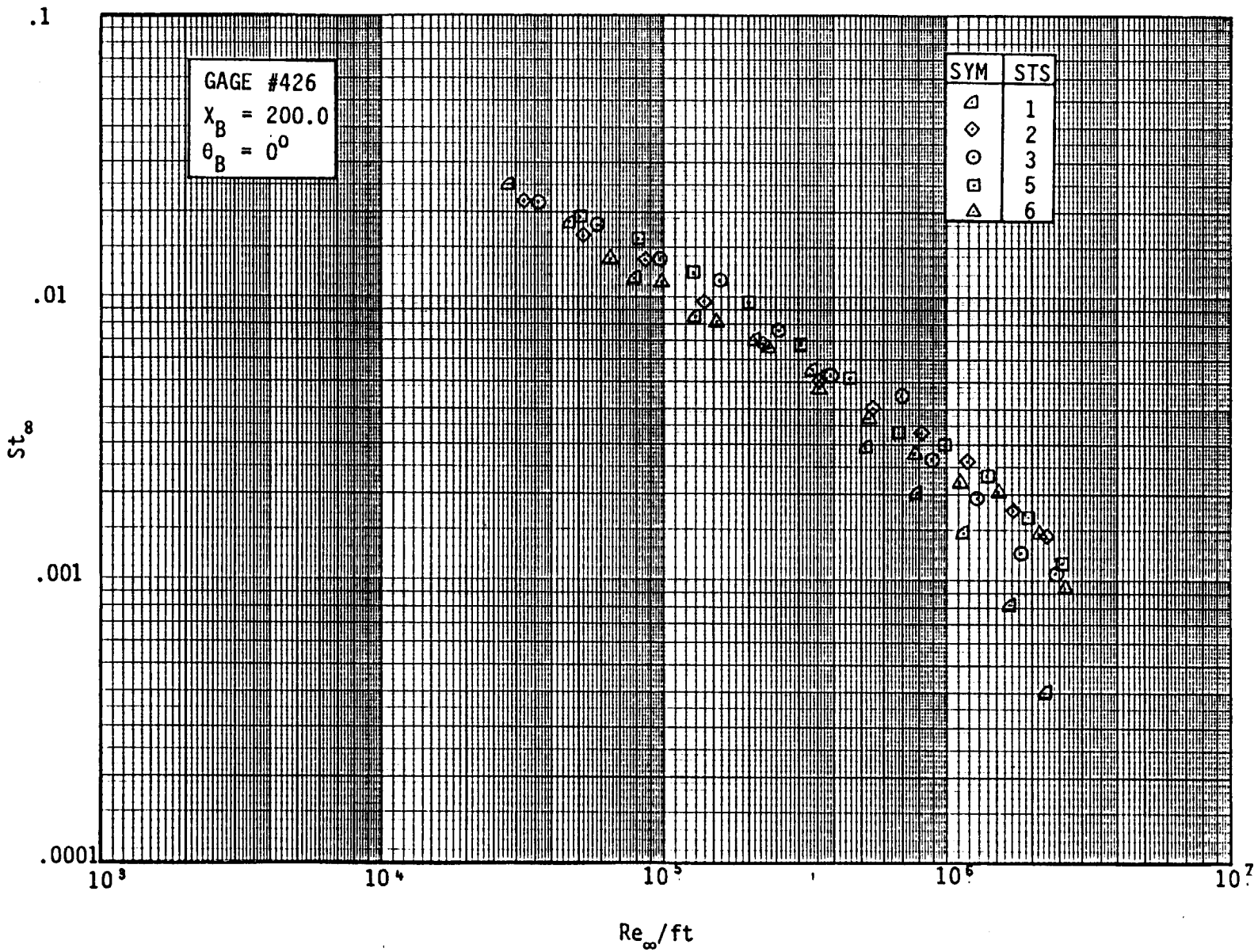

Fig. Stanton Number As A Function Of Reynolds Number For Gage #426

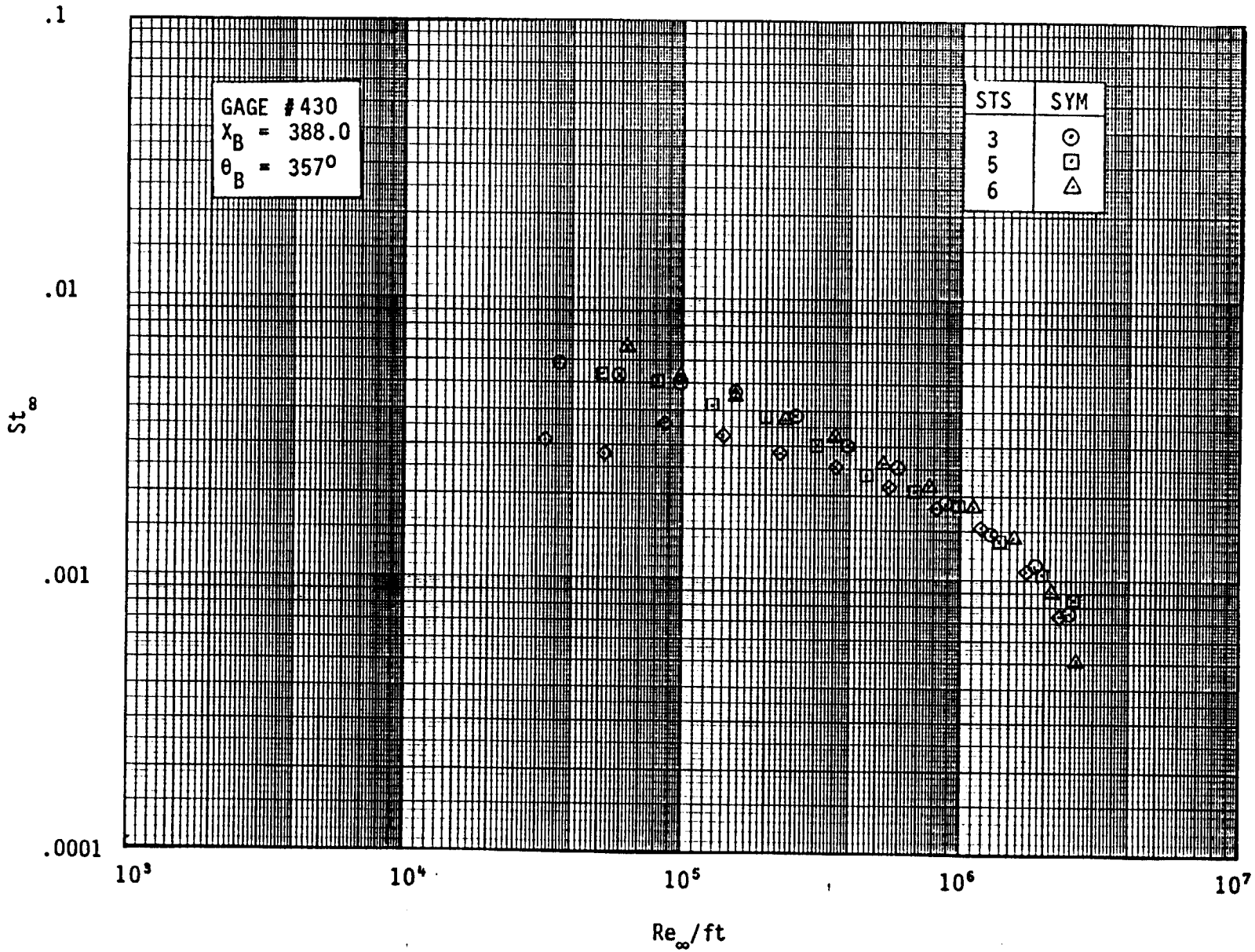

Fig. Stanton Number As A Function Of Reynolds Number For Gage #430

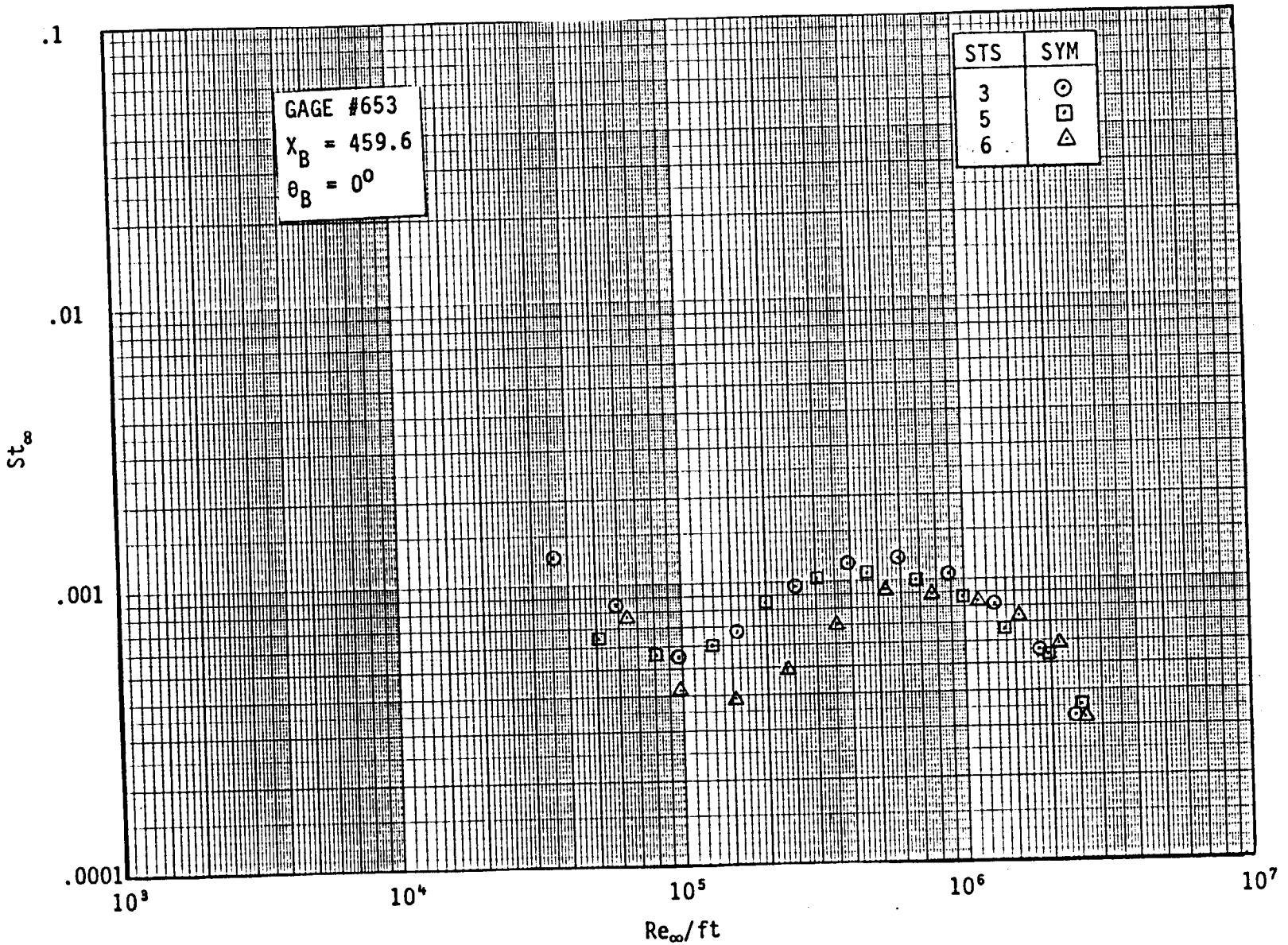

Fig. Stanton Number As A Function Of Reynolds Number For Gage #653

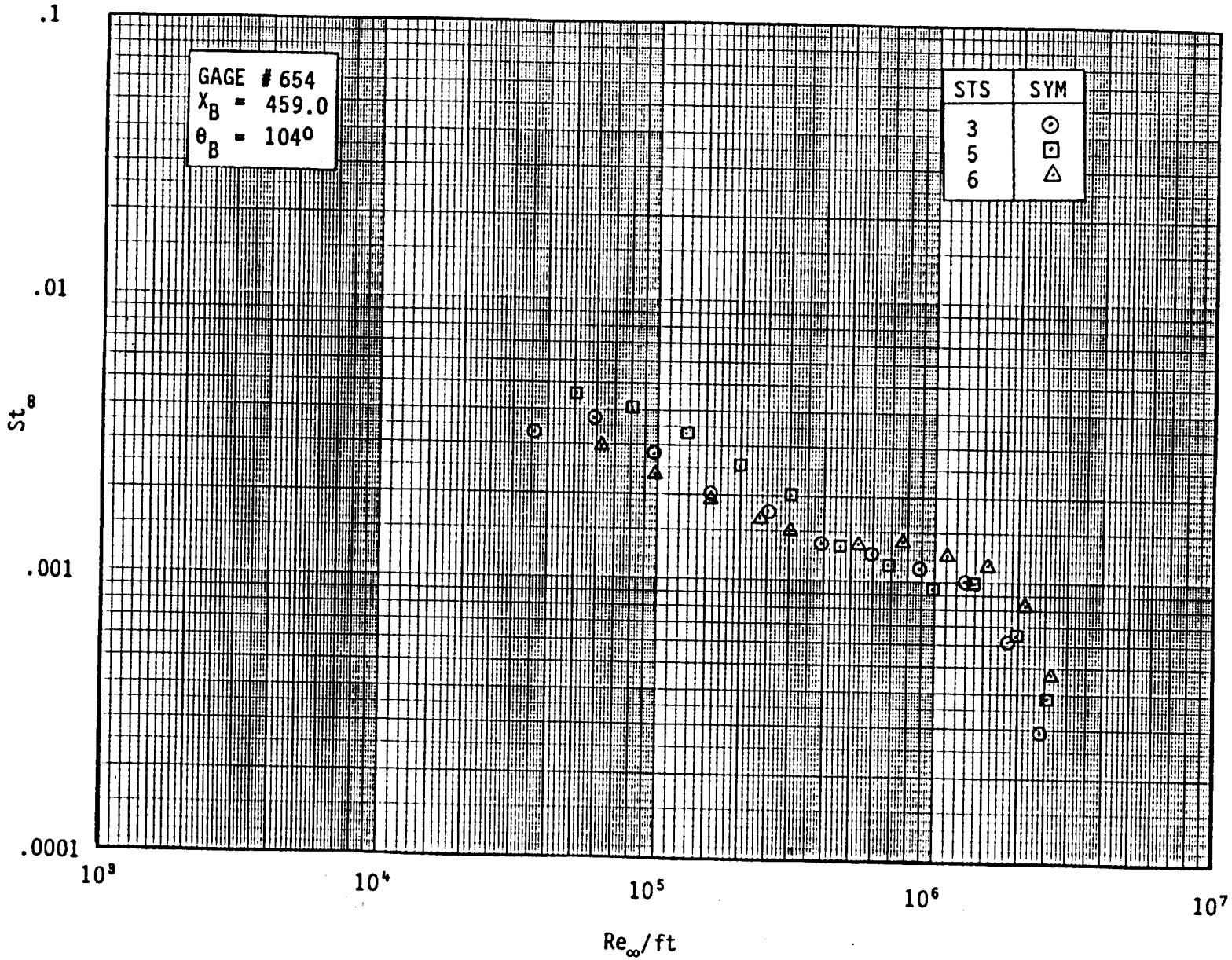

Fig. Stanton Number As A Function Of Reynolds Number For Gage #654

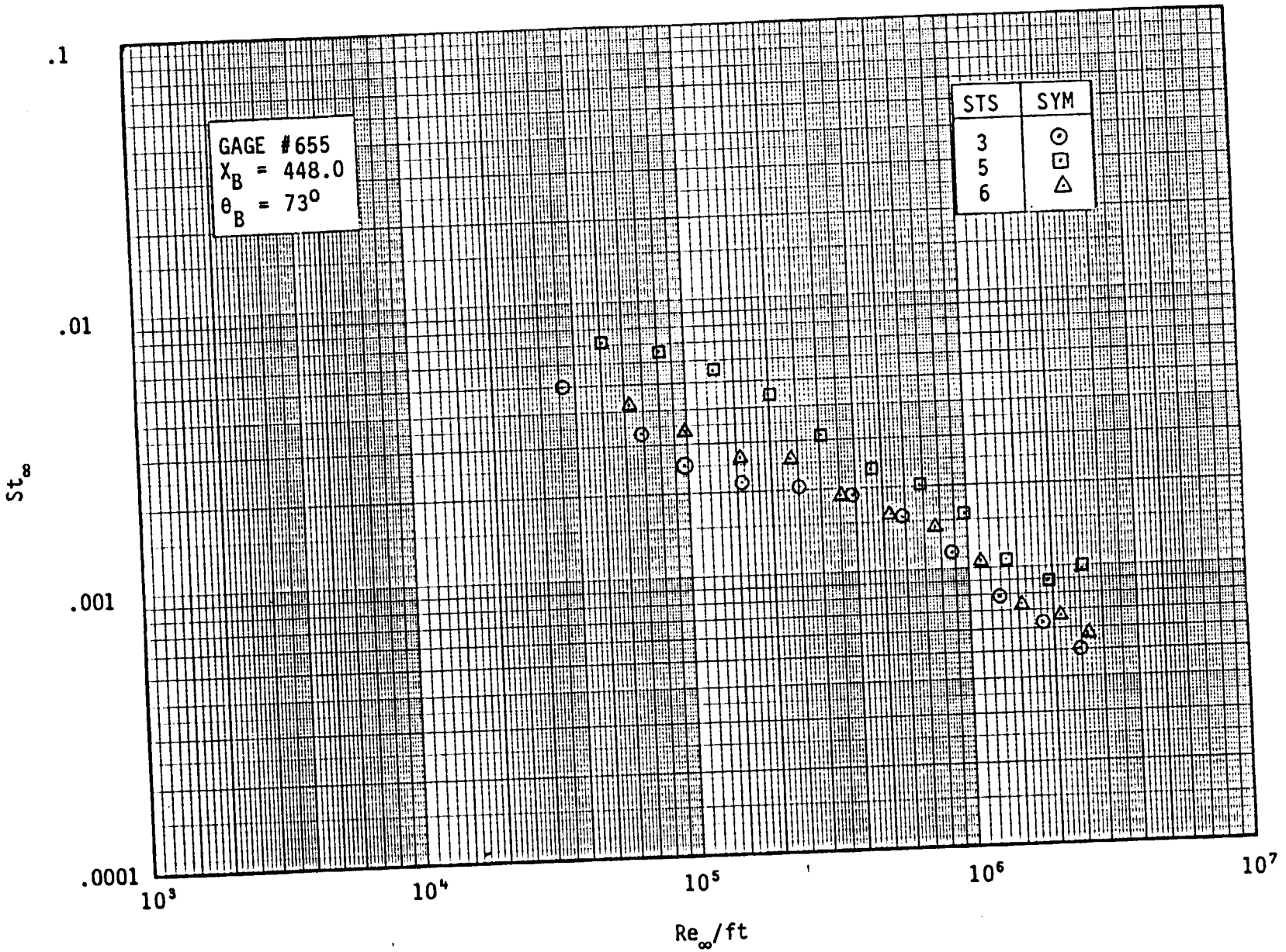

Fig. Stanton Number As A Function Of Reynolds Number For Gage #655

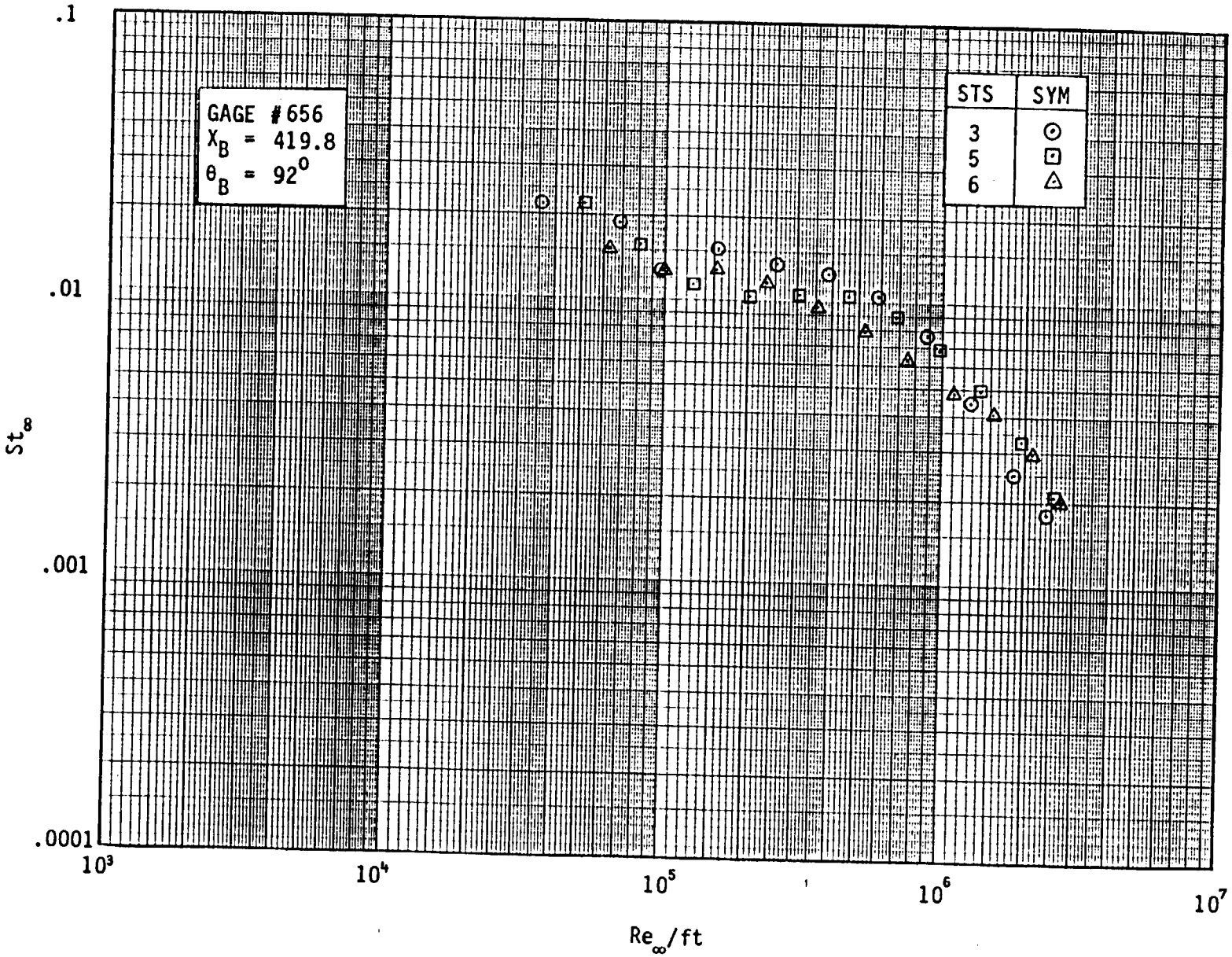

Fig. Stanton Number As A Function Of Reynolds Number For Gage #656

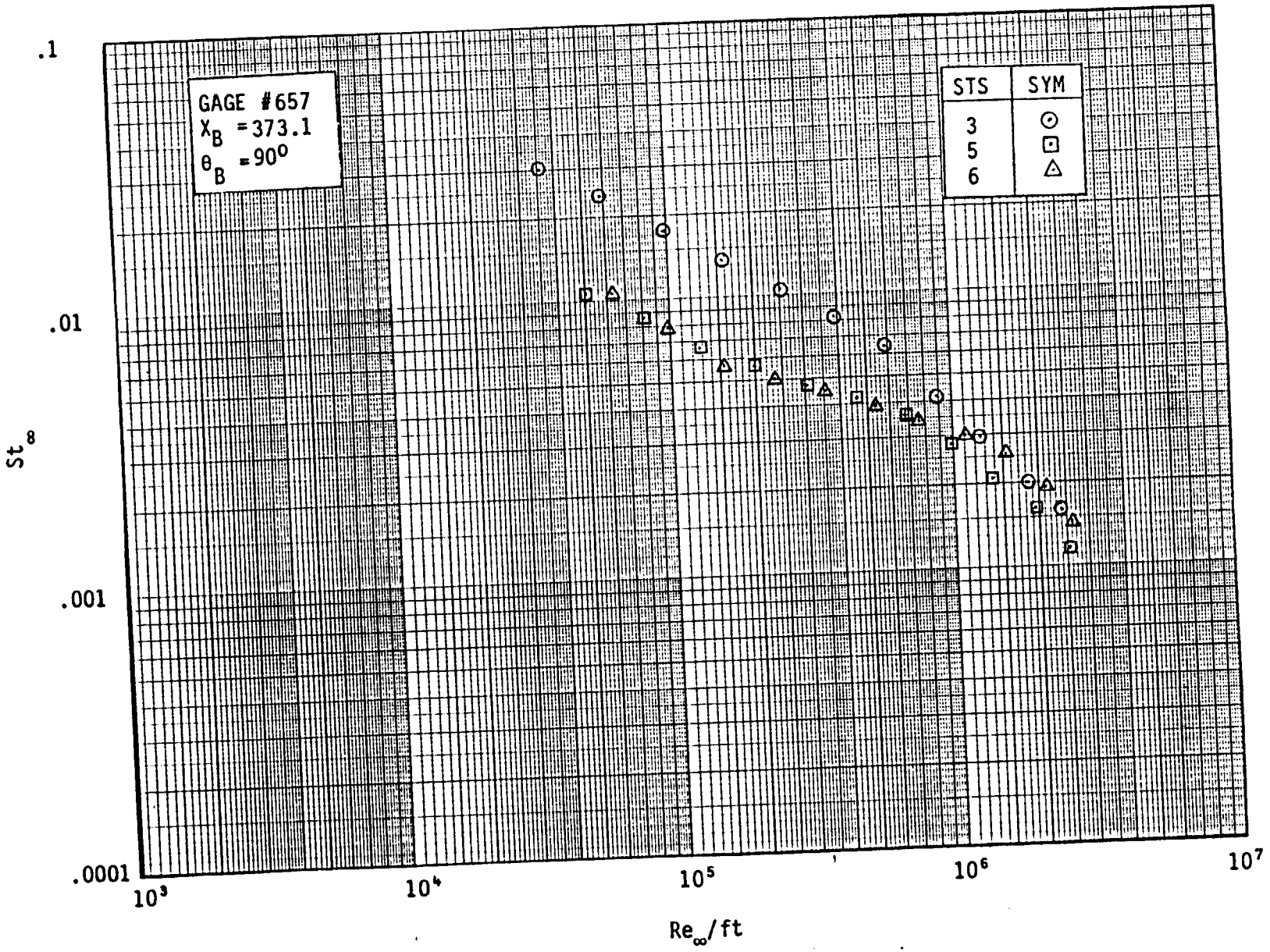

Fig. Stanton Number As A Function Of Reynolds Number For Gage #657

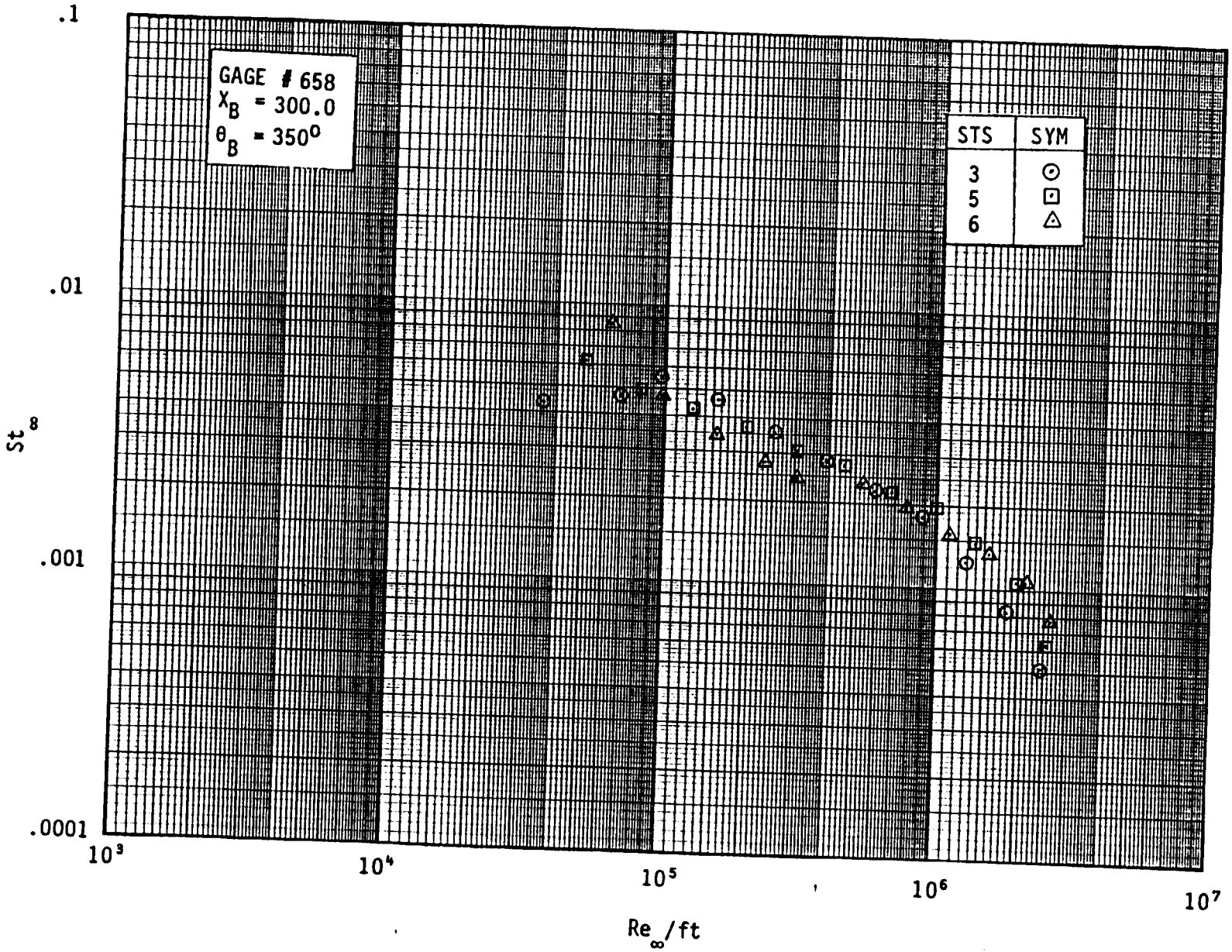

Fig. Stanton Number As A Function Of Reynolds Number For Gage #658

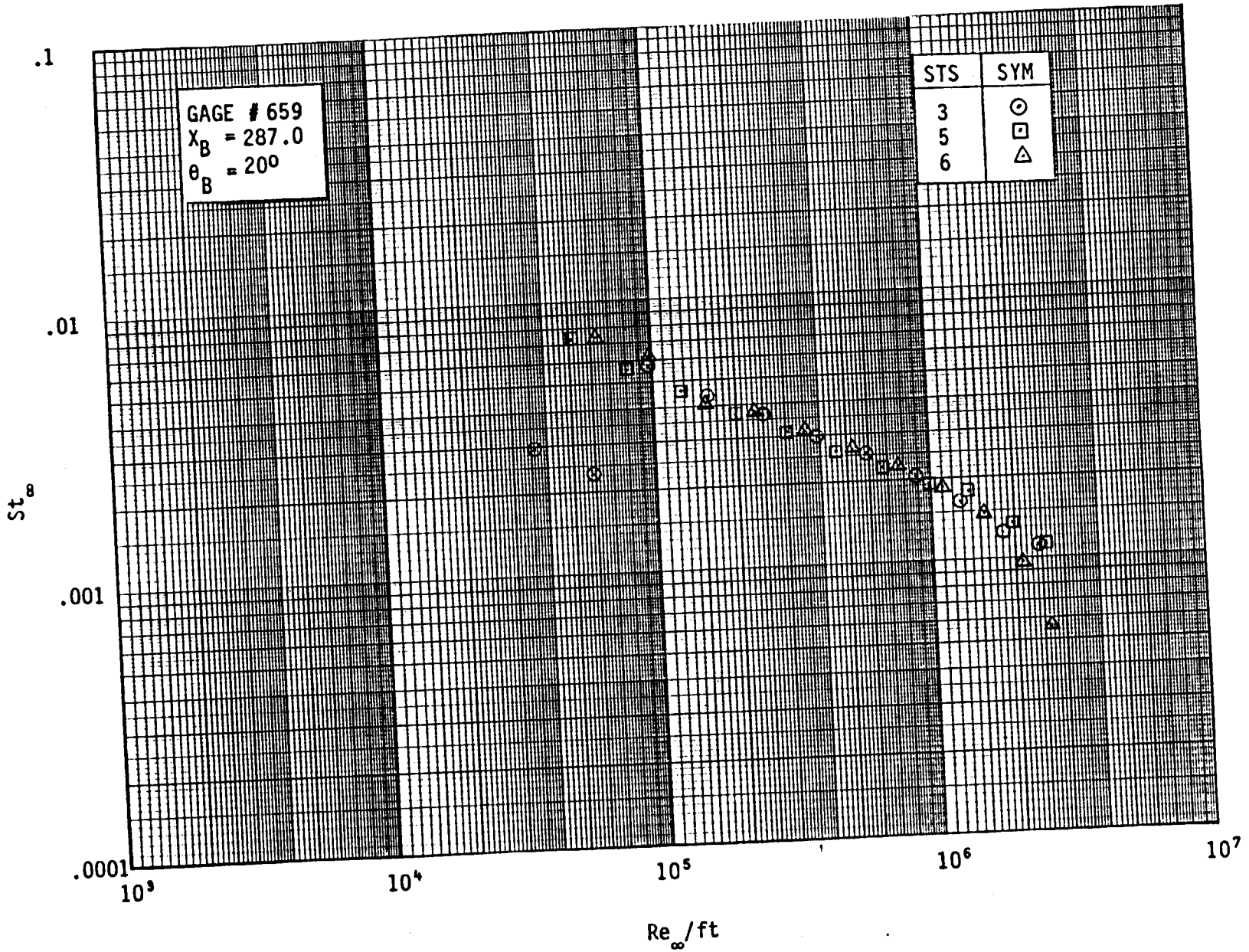

Fig. Stanton Number As A Function Of Reynolds Number For Gage #659

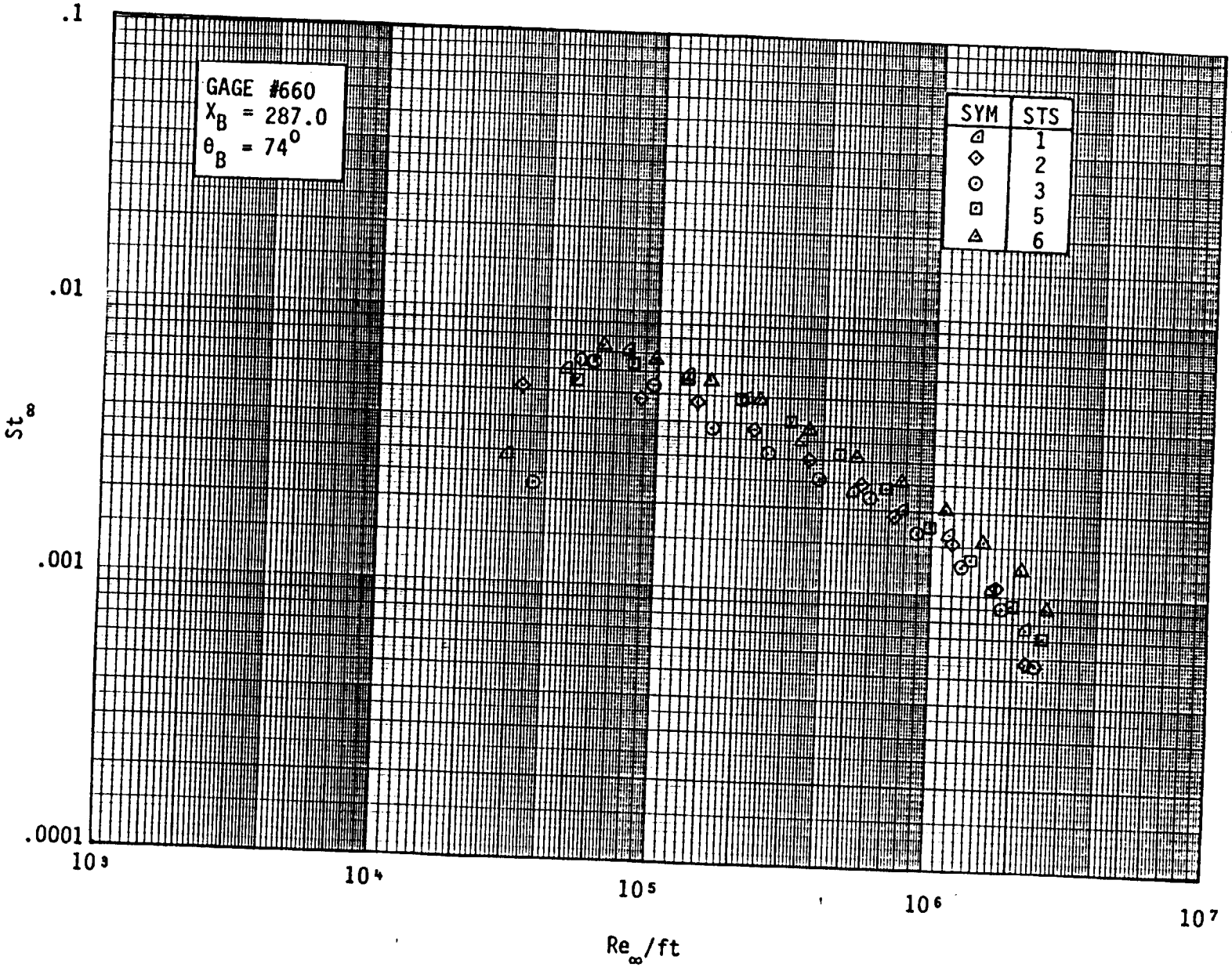

Fig. Stanton Number As A Function Of Reynolds Number For Gage #660

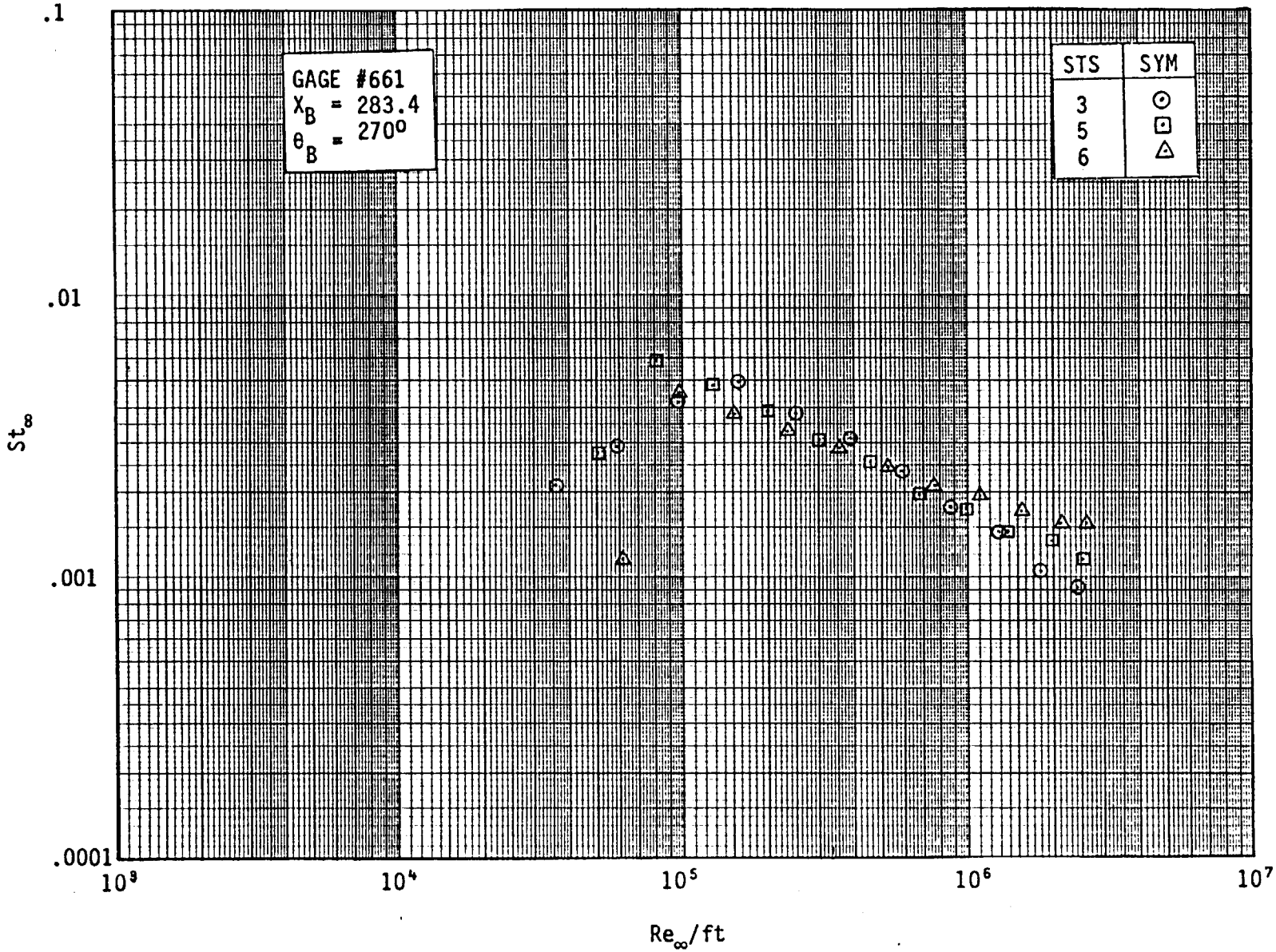

Fig. Stanton Number As A Function Of Reynolds Number For Gage #661